



Earth Resources  
A Continuing  
Bibliography  
with Indexes

NASA SP-7041 (62)  
July 1989

National Aeronautics and  
Space Administration

(NASA-SP-7041(62)) EARTH RESOURCES: A  
CONTINUING BIBLIOGRAPHY WITH INDEXES (ISSUE  
62) (NASA) 146 p C5CL 088

N89-29825

Unclas  
00/43 0228080

es Earth Resources  
s Earth Resources  
Earth Resources  
th Resources Earth  
Resources Earth  
Resources Earth  
Resources Earth

## ACCESSION NUMBER RANGES

Accession numbers cited in this Supplement fall within the following ranges.

STAR (N-10000 Series)    N89-15071 — N89-20085

IAA (A-10000 Series)    A89-20751 — A89-32450

# EARTH RESOURCES

## A CONTINUING BIBLIOGRAPHY WITH INDEXES

### Issue 62

A selection of annotated references to unclassified reports and journal articles that were introduced into the NASA scientific and technical information system and announced between April 1 and June 30 in

- *Scientific and Technical Aerospace Reports (STAR)*
- *International Aerospace Abstracts (IAA)*.



National Aeronautics and Space Administration  
Office of Management  
Scientific and Technical Information Division  
Washington, DC

1989

This supplement is available from the National Technical Information Service (NTIS), Springfield, Virginia 22161, price code A07.



# INTRODUCTION

The technical literature described in this continuing bibliography may be helpful to researchers in numerous disciplines such as agriculture and forestry, geography and cartography, geology and mining, oceanography and fishing, environmental control, and many others. Until recently it was impossible for anyone to examine more than a minute fraction of the Earth's surface continuously. Now vast areas can be observed synoptically, and changes noted in both the Earth's lands and waters, by sensing instrumentation on orbiting spacecraft or on aircraft.

This literature survey lists 544 reports, articles, and other documents announced between April 1 and June 30, 1989 in *Scientific and Technical Aerospace Reports (STAR)*, and *International Aerospace Abstracts (IAA)*.

The coverage includes documents related to the identification and evaluation by means of sensors in spacecraft and aircraft of vegetation, minerals, and other natural resources, and the techniques and potentialities of surveying and keeping up-to-date inventories of such riches. It encompasses studies of such natural phenomena as earthquakes, volcanoes, ocean currents, and magnetic fields; and such cultural phenomena as cities, transportation networks, and irrigation systems. Descriptions of the components and use of remote sensing and geophysical instrumentation, their subsystems, observational procedures, signature and analyses and interpretive techniques for gathering data are also included. All reports generated under NASA's Earth Resources Survey Program for the time period covered in this bibliography are also included. The bibliography does not contain citations to documents dealing mainly with satellites or satellite equipment used in navigation or communication systems, nor with instrumentation not used aboard aerospace vehicles.

The selected items are grouped in nine categories. These are listed in the Table of Contents with notes regarding the scope of each category. These categories were especially chosen for this publication, and differ from those found in *STAR* and *IAA*.

Each entry consists of a standard bibliographic citation accompanied by an abstract. The citations include the original accession numbers from the respective announcement journals.

Under each of the nine categories, the entries are presented in one of two groups that appear in the following order:

*IAA* entries identified by accession number series A89-10,000 in ascending accession number order;

*STAR* entries identified by accession number series N89-10,000 in ascending accession number order.

After the abstract section, there are seven indexes:

subject, personal author, corporate source, foreign technology, contract number, report/accession number, and accession number.

# TABLE OF CONTENTS

	Page
<b>Category 01    Agriculture and Forestry</b> Includes crop forecasts, crop signature analysis, soil identification, disease detection, harvest estimates, range resources, timber inventory, forest fire detection, and wildlife migration patterns.	1
<b>Category 02    Environmental Changes and Cultural Resources</b> Includes land use analysis, urban and metropolitan studies, environmental impact, air and water pollution, geographic information systems, and geographic analysis.	16
<b>Category 03    Geodesy and Cartography</b> Includes mapping and topography.	19
<b>Category 04    Geology and Mineral Resources</b> Includes mineral deposits, petroleum deposits, spectral properties of rocks, geological exploration, and lithology.	20
<b>Category 05    Oceanography and Marine Resources</b> Includes sea-surface temperature, ocean bottom surveying imagery, drift rates, sea ice and icebergs, sea state, fish location.	28
<b>Category 06    Hydrology and Water Management</b> Includes snow cover and water runoff in rivers and glaciers, saline intrusion, drainage analysis, geomorphology of river basins, land uses, and estuarine studies.	48
<b>Category 07    Data Processing and Distribution Systems</b> Includes film processing, computer technology, satellite and aircraft hardware, and imagery.	52
<b>Category 08    Instrumentation and Sensors</b> Includes data acquisition and camera systems and remote sensors.	61
<b>Category 09    General</b> Includes economic analysis.	76
<b>Subject Index .....</b>	<b>A-1</b>
<b>Personal Author Index .....</b>	<b>B-1</b>
<b>Corporate Source Index .....</b>	<b>C-1</b>
<b>Foreign Technology Index .....</b>	<b>D-1</b>
<b>Contract Number Index .....</b>	<b>E-1</b>
<b>Report Number Index .....</b>	<b>F-1</b>
<b>Accession Number Index .....</b>	<b>G-1</b>

## TYPICAL REPORT CITATION AND ABSTRACT

NASA SPONSORED  
 ↓  
 ON MICROFICHE

ACCESSION NUMBER → **N89-14479\*** # Kansas Univ. Center for Research, Inc., Lawrence. ← CORPORATE SOURCE  
 TITLE → **INVESTIGATION OF RADAR BACKSCATTERING FROM SECOND-YEAR SEA ICE**  
 AUTHORS → GUANG-TSAI LEI, RICHARD K. MOORE, and S. P. GOGINENI  
 PUBLICATION DATE → Feb. 1988 67 p  
 CONTRACT NUMBERS → (Contract NASA ORDER W-16712; N00014-85-K-0200)  
 REPORT NUMBERS → (NASA-CR-180986; NAS 1.26:180986; RSL-TR-3311-7) Avail:  
 AVAILABILITY SOURCE → NTIS HC A04/MF A01 CSCL 08L ← COSATI CODE

The scattering properties of second-year ice were studied in an experiment at Mould Bay in April 1983. Radar backscattering measurements were made at frequencies of 5.2, 9.6, 13.6, and 16.6 GHz for vertical polarization, horizontal polarization and cross polarizations, with incidence angles ranging from 15 to 70 deg. The results indicate that the second-year ice scattering characteristics were different from first-year ice and also different from multiyear ice. The fading properties of radar signals were studied and compared with experimental data. The influence of snow cover on sea ice can be evaluated by accounting for the increase in the number of independent samples from snow volume with respect to that for bare ice surface. A technique for calculating the snow depth was established by this principle and a reasonable agreement has been observed. It appears that this is a usable way to measure depth in snow or other snow-like media using radar. Author

## TYPICAL JOURNAL ARTICLE CITATION AND ABSTRACT

NASA SPONSORED  
 ↓  
 ON MICROFICHE

ACCESSION NUMBER → **A89-12756\*** # Michigan State Univ., East Lansing.  
 TITLE → **EVALUATING LANDSAT CLASSIFICATION ACCURACY FROM FOREST COVER-TYPE MAPS**  
 AUTHOR → W. D. HUDSON (Michigan State University, East Lansing) ← AUTHOR'S AFFILIATION  
 JOURNAL TITLE → Canadian Journal of Remote Sensing (ISSN 0008-2821), vol. 13,  
 PUBLICATION DATE → July 1987, p. 39-42. refs  
 CONTRACT NUMBER → (Contract NGL-23-004-083)

The use of complete enumeration in the form of photointerpreted forest cover-type maps to evaluate the accuracy of Landsat classifications was compared with assessments made directly from the aerial photography. A computerized, geographic information system was utilized to compare the Landsat classifications with the cover-type maps on a pixel-by-pixel basis. Error maps of pixels which were similarly misclassified by a variety of algorithms contained a larger number of errors than were verified from the aerial photography. For the two test sites studied, only 67 and 52 percent of the pixels which were originally considered to be in error were substantiated as being in error. Discrepancies between the two results were primarily caused by definitional differences between the cover-type maps and the Landsat classifications, especially with regard to minimum-type size and crown closure estimates of forest land. C.D.

# EARTH RESOURCES

*A Continuing Bibliography (Issue 62)*

JULY 1989

01

## AGRICULTURE AND FORESTRY

Includes crop forecasts, crop signature analysis, soil identification, disease detection, harvest estimates, range resources, timber inventory, forest fire detection, and wildlife migration patterns.

**A89-20752#**

### COMPARATIVE STUDY OF VEGETATION INDEX AND FALSE COLOUR COMPOSITE IMAGE OF NOAA-AVHRR DATA FOR BIO-MASS STUDIES

B. MANIKIAM and TOSHIRO SUGIMURA (ISRO, Bangalore, India) IN: Asian Conference on Remote Sensing, 8th, Jakarta, Indonesia, Oct. 22-27, 1987, Proceedings. Bogor, Indonesia, EXSA International, 1987, p. A-1-1 to A-1-7. refs

Vegetation status maps derived from the NOAA-AVHRR vegetation index (channel 2/channel 1) are compared with FCC images from these two channels to estimate biomass levels for the Southern Indian Peninsula. It is found that a higher level of information is provided by vegetation index maps. These maps provide up to five broad levels of vegetation vigor, whereas FCCs provide three. It is shown that cloud covered areas are more easily distinguished with FCCs than with the vegetation index. It is suggested that the analysis of meteorological parameters derived from FCC images and vegetation index data can be used for broad biomass classification. R.B.

**A89-20753#**

### SPECTRAL REFLECTANCE PROPERTIES OF A LEAF OF SOME MANGROVE SPECIES IN OKINAWA

KAZUHIRO SATO, SHIGEYUKI BABA (University of the Ryukyus, Okinawa, Japan), and TAKASHI HOSHI (Tsukuba, University, Japan) IN: Asian Conference on Remote Sensing, 8th, Jakarta, Indonesia, Oct. 22-27, 1987, Proceedings. Bogor, Indonesia, EXSA International, 1987, p. A-4-1 to A-4-10.

The spectral reflectance properties were determined for mangrove leaves collected at various times from several sites on Okinawa. The spectral reference curves were classified into six shapes. Seasonal changes were determined based on the shapes in the visible wavelength region of the spectral reflectance curve. It is found that the spectral reflectance properties are closely connected with the organomorphological properties of the leaf. The planned use of the results in remote sensing studies of mangrove forests is discussed. R.B.

**A89-20754#**

### THE STUDIES FOR THE COMPUTER CLASSIFICATION AND THE INVESTIGATION OF GRASSLANDS IN TIBET USING SPACE-LAB COLOR INFRARED IMAGE

NING SHU and ZHE-QUN GUAN (Wuhan Technical University of Surveying and Mapping, People's Republic of China) IN: Asian Conference on Remote Sensing, 8th, Jakarta, Indonesia, Oct. 22-27, 1987, Proceedings. Bogor, Indonesia, EXSA International, 1987, p. A-6-1 to A-6-6.

**A89-20755#**

### THE USE OF SPOT IMAGERY IN MEDAN AGRICULTURE AREA FOR MONITORING FEATURES CHANGES

RIADIKA MASTRA and SHUNJI MURAI (Tokyo, University, Japan) IN: Asian Conference on Remote Sensing, 8th, Jakarta, Indonesia, Oct. 22-27, 1987, Proceedings. Bogor, Indonesia, EXSA International, 1987, p. A-8-1 to A-8-9. refs

**A89-20756#**

### DIGITAL IMAGE ANALYSIS OF LANDSAT MSS DATA IN AN ESTATE CROP INVENTORY OF THE ISLAND OF BALI

I. L. SUBADIYASA and U. S. WIRADISASTRA IN: Asian Conference on Remote Sensing, 8th, Jakarta, Indonesia, Oct. 22-27, 1987, Proceedings. Bogor, Indonesia, EXSA International, 1987, p. A-10-1 to A-10-12.

**A89-20757#**

### AIRBORNE MULTISPECTRAL REMOTE SENSING OF FOREST DECLINE IN WEST GERMANY

GERD LANDAUER (DFVLR, Institut fuer Optoelektronik, Oberpfaffenhofen, Federal Republic of Germany) IN: Asian Conference on Remote Sensing, 8th, Jakarta, Indonesia, Oct. 22-27, 1987, Proceedings. Bogor, Indonesia, EXSA International, 1987, p. A-11-1 to A-11-5.

False color IR photography has already proven as a useful tool to detect forest diseases. The use of digital multispectral remote sensing methods to detect and classify the forest decline is investigated. An airborne scanner and methods of digital image processing have been used to successfully detect forest disease.

Author

**A89-20758#**

### SOIL AND VEGETATION MAPPING BY USING SPOT IMAGE

SRI JATNO WIRJOSOEDIRDJO, SRI KUSNO GULARSO, and WIEKE WISNUWARDHANI (National Coordination Agency for Surveys and Mapping, Bogor, Indonesia) IN: Asian Conference on Remote Sensing, 8th, Jakarta, Indonesia, Oct. 22-27, 1987, Proceedings. Bogor, Indonesia, EXSA International, 1987, p. A-12-1 to A-12-5.

The use of SPOT images for soil and vegetation mapping is evaluated, using images of the Jogjakarta area of Indonesia from channels 1, 2, and 3 of the High Resolution Visible sensor. A numerical technique for calibrating SPOT and Landsat MSS radiometric data is presented and used to convert the SPOT data into its equivalent Landsat data. This data is transformed using the method of Kauth and Thomas (1976). A gray map is made from the data using the method of Richardson and Wiegand (1977). R.B.

**A89-20759#**

### FOREST OBSERVATION BY SATELLITE

NASRIL HADJAR (Indonesian National Institute of Aeronautics and Space, Jakarta, Indonesia) IN: Asian Conference on Remote Sensing, 8th, Jakarta, Indonesia, Oct. 22-27, 1987, Proceedings. Bogor, Indonesia, EXSA International, 1987, p. A-16-1 to A-16-13. refs

The computer-assisted interpretation and classification of forest and vegetation in Indonesia using Landsat imagery is discussed. The problems addressed include the forest degradation surround the Toba lake in North Sumatera, damage from volcano induced

## 01 AGRICULTURE AND FORESTRY

forest fires on the island of Sangeang, and tracking forest fires on other islands. It is found that the use of satellite data in conservation studies is inexpensive and effective. R.B.

### **A89-20760# THE FEASIBILITY STUDY OF OIL PALM AREA ESTIMATION IN THE SOUTHERN PART OF THAILAND USING LANDSAT DATA**

SUPAN KARNCHANASUTHAM, CHALIT AMNUAY, THANOMSRI RANGSIKANBHUM, MONTOL JEAMCHARETON, and VICHARN AMARAKUL (Agricultural Economics Office, Bangkok, Thailand) IN: Asian Conference on Remote Sensing, 8th, Jakarta, Indonesia, Oct. 22-27, 1987, Proceedings. Bogor, Indonesia, EXSA International, 1987, p. A-17-1 to A-17-8. refs

### **A89-20761# ON CLASSIFICATION OF FORESTS OF SOME PORTIONS OF CENTRAL INDIA USING SATELLITE IMAGERIES**

V. K. FARKYA (Rani Durgavati University, Jabalpur, India) IN: Asian Conference on Remote Sensing, 8th, Jakarta, Indonesia, Oct. 22-27, 1987, Proceedings. Bogor, Indonesia, EXSA International, 1987, p. A-18-1 to A-18-5. refs

### **A89-20762# RELATIONSHIP OF SPECTRAL DATA AND GRAIN YIELD VARIATION IN RICE (ORYZA SATIVA L.) ADT 31**

M. RAJA, R. PALANIVELU (Anna University, Madras, India), and M. JAYARAMAN (Department of Agriculture, Tamil Nadu, India) IN: Asian Conference on Remote Sensing, 8th, Jakarta, Indonesia, Oct. 22-27, 1987, Proceedings. Bogor, Indonesia, EXSA International, 1987, p. A-19-1 to A-19-13. refs

A field experiment to establish the relationship between spectral parameters and grain yield variation was conducted in India, using rice variety ADT 31 as a test crop. The rice was grown under different nitrogen levels. Spectral measurements were collected using a hand held radiometer in the red and IR portions of reflected light at an interval of 15 days. The spectral data was compared to the final grain yields resulting from different levels of nitrogen. It was found that nitrogen deficiency can be detected spectrally. Good correlations were found between the radiometric data and grain yields. R.B.

### **A89-20763# REMOTE SENSING APPLICATIONS FOR AGRICULTURAL LANDUSE SURVEY IN INDONESIA - ISIMU CASE STUDY**

ARIS PONIMAN KERTOPERMONO (National Coordination Agency for Surveys and Mapping, Indonesia) IN: Asian Conference on Remote Sensing, 8th, Jakarta, Indonesia, Oct. 22-27, 1987, Proceedings. Bogor, Indonesia, EXSA International, 1987, p. B-2-1 to B-2-8. refs

### **A89-20769# APPLICATIONS OF SPOT HRV DATA FOR LAND USE AND SOIL MAPPING IN RAYONG BASIN**

APISIT EIUMNOH (Interdisciplinary Natural Resources Development and Management, Bangkok, Thailand) IN: Asian Conference on Remote Sensing, 8th, Jakarta, Indonesia, Oct. 22-27, 1987, Proceedings. Bogor, Indonesia, EXSA International, 1987, p. B-14-1 to B-14-9.

**A89-20773#  
SOIL SURFACE MOISTURE ESTIMATION - A CASE STUDY  
AREA ON NORTH BANTEN, WEST JAVA, INDONESIA**  
NANIEK SITI MURDJATI and HARIYATNO SOERMANMAN (Ministry of Public Works, Remote Sensing Center, Indonesia) IN: Asian Conference on Remote Sensing, 8th, Jakarta, Indonesia, Oct. 22-27, 1987, Proceedings. Bogor, Indonesia, EXSA International, 1987, p. C-6-1 to C-6-10. refs

The use of Landsat MSS data to estimate soil surface moisture for the North Banten region of West Java in Indonesia is discussed. The soil surface moisture estimates are classified into five groups and the results are compared with a soil map. The model of Fukuhara et al. (1979) is used to make the estimations. R.B.

### **A89-20802# AEROSPACE IMAGERY AND DATA FOR MODELLING EROSION, SEDIMENT YIELD AND CROP YIELD PREDICTION USING GIS, APPLIED TO THE UPPER KOMERING CATCHMENT, SUMATRA**

A. M. MEIJERINK, SHYARIF KOSASIH, C. R. VALENZUELA, and ISMANGUN IN: Asian Conference on Remote Sensing, 8th, Jakarta, Indonesia, Oct. 22-27, 1987, Proceedings. Bogor, Indonesia, EXSA International, 1987, p. H-2-1 to H-2-25. refs

### **A89-20809# THE APPLICATION OF REMOTE SENSING FOR FOREST INVENTORY**

Y. L. ROMBE (Ministry of Forestry, Centre for Forest Inventory, Indonesia) IN: Asian Conference on Remote Sensing, 8th, Jakarta, Indonesia, Oct. 22-27, 1987, Proceedings. Bogor, Indonesia, EXSA International, 1987, p. P-7-1 to P-7-11.

The stand volume of a 38,750 ha forest area in Pulau Laut, Indonesia is estimated using a satellite image and aerial photographs. Research concerned with forest inventory via remote sensing techniques is reviewed. A three-stage sampling technique is used to determine that the area consists of 37,500 ha of forest land and 1250 ha of nonforest land. R.B.

### **A89-20814# ASSESSING EXTENT OF DAMAGE CAUSED BY FLOODING AND DROUGHT IN DOMINANTLY RICE CROPLAND AREA USING LANDSAT DATA**

A. N. SINGH (Remote Sensing Applications Centre, Lucknow, India) IN: Asian Conference on Remote Sensing, 8th, Jakarta, Indonesia, Oct. 22-27, 1987, Proceedings. Bogor, Indonesia, EXSA International, 1987, p. P-14-1 to P-14-9. refs

A program using Landsat MSS and TM imagery to study floods and droughts in eastern Uttar Pradesh, India is discussed. Landsat data for the rice growing season of 1982, 1985, and 1986 were used to observe the effects of floods and droughts on vegetation density. The extent of inundation by flooding in 1985 and the areal extent of drought in 1986 were determined. It is found that correlation of low vegetation density areas delineated from the Landsat data with meteorological data and ground information is a good method for determining the areal extent of drought-affected croplands. R.B.

### **A89-20815# STUDY OF THE MONITORING OF LAND COVER/USE USING REMOTE SENSING DATA BY PERSONAL COMPUTER IN SOUTHERN PART OF BANDUNG AREA, WEST JAVA**

MUH. DIMYATI (Ministry of Public Works, Center for Data Processing and Mapping, Indonesia) and EIJI YAMAJI (Tokyo, University, Japan) IN: Asian Conference on Remote Sensing, 8th, Jakarta, Indonesia, Oct. 22-27, 1987, Proceedings. Bogor, Indonesia, EXSA International, 1987, p. P-20-1 to P-20-6. refs

The use of Landsat MSS data for land cover and land use monitoring in the southern part of the Bandung region of Indonesia is discussed. The techniques and computer programs used in analysis and classification processes are described. The changes in forest areas, settled areas, and vegetation during the 1976-1984 period are determined. R.B.

### **A89-20819# AERIAL REMOTE SENSING TECHNIQUE IN THE IDENTIFICATION AND ACREAGE ESTIMATION OF VARIOUS PLANTATIONS - A CASE STUDY IN GORAKHPUR DISTRICT, UTTAR PRADESH, INDIA**

P. C. GUPTA (Remote Sensing Applications Centre, Lucknow, India) IN: Asian Conference on Remote Sensing, 8th, Jakarta, Indonesia, Oct. 22-27, 1987, Proceedings. Bogor, Indonesia, EXSA International, 1987, p. Q-5-1 to Q-5-6.

Black and white aerial photographs on a 1:15,000 scale are used to identify and assess plantations in the Gorakhpur district of eastern Uttar Pradesh, India. Banana, mango, and guava crops are identified and the acreage of the three crops is estimated for various villages in the regions. Field checks confirm the validity

plantation identification using aerial photography. The possibility of using satellite data for similar applications is considered.

R.B.

**A89-20822#**

**STUDY ON CHANGES OF MANGROVE FOREST IN THAILAND BY USIGN LANDSAT IMAGERY**

THONGCHAI CHARUPPAT (Royal Forest Department, Forest Management Div., Bangkok, Thailand) IN: Asian Conference on Remote Sensing, 8th, Jakarta, Indonesia, Oct. 22-27, 1987, Proceedings. Bogor, Indonesia, EXSA International, 1987, p. Q-9-1 to Q-9-11.

**A89-20826#**

**THE APPLICATIONS OF LANDSAT IMAGERY TO SOIL EROSION STUDY IN NORTHERN THAILAND**

PONGPIT PIYAPONGSE (Department of Agriculture, Soil Science Div., Thailand) IN: Asian Conference on Remote Sensing, 8th, Jakarta, Indonesia, Oct. 22-27, 1987, Proceedings. Bogor, Indonesia, EXSA International, 1987, p. Q-18-1 to Q-18-5. refs

**A89-20923**

**A COMPARISON OF MODELS FOR DERIVING DRY DEPOSITION FLUXES OF O<sub>3</sub> AND SO<sub>2</sub> TO A FOREST CANOPY**

TILDEN P. MEYERS and DENNIS D. BALDOCCHI (NOAA, Air Resources Laboratory, Oak Ridge, TN) Tellus, Series B - Chemical and Physical Meteorology (ISSN 0280-6509), vol. 40B, Sept. 1988, p. 270-284. Research supported by NOAA and DOE. refs

A set of four canopy models, representing the various classes of models that are used to estimate gaseous deposition to plant canopies are present. The predictive capabilities of the models are evaluated with direct eddy correlation measurements of SO<sub>2</sub> and O<sub>3</sub> fluxes to deciduous forest for both well-watered and water-stressed conditions. By increasing the degree of detail of exchange-governing physical processes from the more simple single layer model to the more detailed multi-layer models, the predictions of the deposition rates improved by 40-50 percent as determined from the rms error.

Author

**A89-21612**

**EFFECTIVE PERMITTIVITY OF VEGETATION IN THE MICROWAVE RANGE [OB EFEKTYVNOI DIELEKTRICHESKOI PRONITSAEMOSTI RASTITEL'NOSTI V SVCH-DIAPAZONE]**

A. A. CHUKHLANTSEV Radiotekhnika i Elektronika (ISSN 0033-8494), vol. 33, Nov. 1988, p. 2310-2319. In Russian. refs

**A89-21740\*** National Aeronautics and Space Administration. Goddard Space Flight Center, Greenbelt, MD.

**DEPENDENCE OF SNOW MELTING AND SURFACE-ATMOSPHERE INTERACTIONS ON THE FOREST STRUCTURE**

J. OTTERMAN (NASA, Goddard Space Flight Center, Greenbelt, MD; Tel Aviv University, Israel), K. STAENZ, K. I. ITTEN (Zuerich, Universitaet, Zurich, Switzerland), and G. KUKLA (Lamont-Doherty Geological Observatory, Palisades, NY) Boundary-Layer Meteorology (ISSN 0006-8314), vol. 45, no. 1-2, Oct. 1988, p. 1-8. refs

(Contract NSF ATM-85-05558)

The surface albedo and the surface roughness for forested areas with snow on the ground are expressed in terms of the tree silhouette parameter,  $s$ , the projection on the vertical plane of trees per unit area. The absorption of insolation (direct solar beam) is quantitatively described for a horizontal snow surface with vertical tree trunks, stressing the role of the bark at snow level as triggering the snow melt. Measurement of  $s$  by field sampling in two forested sites in central Switzerland yielded values ranging from 1.8 to 2.1.

Author

**A89-22221**

**BRIGHTNESS OF A LASER-BEAM HALO IN VEGETATION COVER [IARKOST' OREOLA VOKRUG LAZERNOGO LUCHA V RASTITEL'NOM POKROVE]**

A. E. KUUSK (AN ESSR, Institut Astrofiziki i Fiziki Atmosfery, Tyrave, Estonian SSR) Issledovanie Zemli iz Kosmosa (ISSN 0205-9614), Sept.-Oct. 1988, p. 87-93. In Russian. refs

A quantitative theory is presented to explain the formation of a halo around a laser beam in vegetation with elliptically-oriented leaves. Experimental data show that the halo brightness profile is sensitive to variations in the leaf-area density and in the orientation of the leaf's phytoelements, as well as to the optical parameters of the leaves and the soil. It is proposed that these effects can be used for the determination of the vegetation cover parameters such as the leaf-area density and the leaf orientation from data on the halo brightness profile provided by the laser soundings.

I.S.

**A89-22249**

**EFFECTIVENESS OF SOIL MAPPING ON THE BASIS OF SPACE PHOTOGRAPHIC DATA [OB EFEKTYVNOI SOSTAVLENIIA POCHVENNYKH KART NA OSNOVE KOSMICHESKOI FOTOINFORMATSII]**

L. N. KULESHOV Geodeziia i Kartografiia (ISSN 0016-7126), Oct. 1988, p. 28-30. In Russian. refs

**A89-22728**

**DISPERSION PARAMETERS OVER FORESTED TERRAIN**

R. T. PINKER and J. Z. HOLLAND (Maryland, University, College Park) Journal of Applied Meteorology (ISSN 0894-8763), vol. 27, Nov. 1988, p. 1198-1217. refs  
(Contract DAAG29-80-C-0012)

Based on a set of micrometeorological data obtained in 1967-70 for a tropical forest region in Thailand, wind variability parameters are derived, which characterize the dispersion process within and above the forest canopy and over a nearby clearing under different stability conditions. The information required to compute or estimate all the commonly used stability parameters (the Monin-Obukhov length scale, the Richardson number, the bulk Richardson number, and the Pasquill-Turner categories) is presented. Values of turbulence intensity based on wind speed measurements show that dispersion rates within the forest canopy would be larger, relative to the mean transport velocity, than in the free air.

R.B.

**A89-23431\*** Wisconsin Univ., Madison.

**REMOTE SENSING OF CANOPY CHEMISTRY AND NITROGEN CYCLING IN TEMPERATE FOREST ECOSYSTEMS**

CAROL A. WESSMAN, JOHN D. ABER (Wisconsin, University, Madison), DAVID L. PETERSON (NASA, Ames Research Center, Moffett Field, CA), and JERRY M. MELILLO (Woods Hole Oceanographic Institution, MA) Nature (ISSN 0028-0836), vol. 335, Sept. 8, 1988, p. 154-156. Research supported by NASA, NSF, and McIntire/Stennis Program. refs

The use of images acquired by the Airborne Imaging Spectrometer, an experimental high-spectral resolution imaging sensor developed by NASA, to estimate the lignin concentration of whole forest canopies in Wisconsin is reported. The observed strong relationship between canopy lignin concentration and nitrogen availability in seven undisturbed forest ecosystems on Blackhawk Island, Wisconsin, suggests that canopy lignin may serve as an index for site nitrogen status. This predictive relationship presents the opportunity to estimate nitrogen-cycling rates across forested landscapes through remote sensing.

C.D.

**A89-23663**

**AGROMETEOROLOGICAL ASPECTS OF THE UTILIZATION OF REMOTE-SENSING DATA [AGROMETEOROLOGICHESKIE ASPEKTY ISPOL'ZOVANIIA AEROKOSMICHESKOI INFORMATSII]**

A. D. KLESHCHENKO, O. V. VIRCHENKO (Vsesoiuznyi Nauchno-Issledovatel'skii Institut Sel'skokhoziaistvennoi Meteorologii, Obninsk, USSR), P. BOZO, V. VADASZ, and SH. LESTAK (Orszagos Meteorologiai Szolgalat, Kozponti Elorajelzo Intezet, Budapest, Hungary) Meteorologija i Hidrologija (ISSN 0130-2906), Dec. 1988, p. 93-102. In Russian. refs

The development of techniques for the processing and interpretation of remote-sensing (aircraft and satellite) data in the

area of agriculture is discussed. Results of the identification of crops using various algorithms are presented. It is suggested that weather/harvest dynamic models be used in the interpretation of remote-sensing data for the evaluation of crop state and yield.

B.J.

**A89-24873\*** National Aeronautics and Space Administration. Goddard Space Flight Center, Greenbelt, MD.

**GONIOMETRIC OBSERVATIONS OF LIGHT SCATTERED FROM SOILS AND LEAVES**

JOANN M. KESTNER, HENNING W. LEIDECKER, JAMES R. IRONS, JAMES A. SMITH, THOMAS W. BRAKKE (NASA, Goddard Space Flight Center, Greenbelt, MD) et al. IN: Wave propagation and scattering in varied media; Proceedings of the Meeting, Orlando, FL, Apr. 6-8, 1988. Bellingham, WA, Society of Photo-Optical Instrumentation Engineers, 1988, p. 161-169. Research sponsored by the U.S. Army. refs

The laboratory established at NASA-Goddard to measure and model the light-scattering properties of soil samples and individual plant leaves employs two goniometers: one for the measurement of directional reflectance and transmittance from vertically-mounted leaf samples, and the other for measurement of directional reflectance from such horizontal, semiinfinite particulate surfaces as soil samples. Sample observations of various soil minerals and plant leaves are presented; these goniometric data are compared to the results of a reflectance model from particulate surfaces and those of a ray-tracing model of leaf reflectance and transmittance.

O.C.

**A89-27781** Colorado Univ., Boulder.

**THE CHARACTERIZATION OF SOURCES OF ILLUMINATION IN A PONDEROSA PINE (PINUS PONDEROSA) FOREST COMMUNITY USING THE PORTABLE INSTANTANEOUS DISPLAY AND ANALYSIS SPECTROMETER**

BRIAN CURTISS (Cooperative Institute for Research in the Environmental Sciences, Boulder, CO) and SUSAN L. USTIN (California, University, Davis) IN: Recent advances in sensors, radiometry, and data processing for remote sensing; Proceedings of the Meeting, Orlando, FL, Apr. 6-8, 1988. Bellingham, WA, Society of Photo-Optical Instrumentation Engineers, 1988, p. 273-280. Research supported by NASA. refs  
(Contract EPA-CR-814274-01-0)

**A89-27942**

**USE OF SURFACE TEMPERATURE IN AGROMETEOROLOGY**

BERNARD SEGUIN (Institut National de la Recherche Agronomique, Montfavet, France) IN: Applications of remote sensing to agrometeorology; Proceedings of the Course, Ispra, Italy, Apr. 6-10, 1987. Dordrecht, Netherlands, Kluwer Academic Publishers, 1989, p. 221-240. refs

After a short introduction indicating the interest of surface temperatures derived from satellite thermal IR data as compared to ground climatological measurements, a first chapter describes their physical bases resulting from the surface energy balance equation. Possible applications in agrometeorology are then listed, and the specific application of computing evapotranspiration is finally described and discussed.

Author

**A89-27944**

**MICROWAVE REMOTE SENSING OF SOIL MOISTURE**

THOMAS SCHMUGGE (USDA, Hydrology Laboratory, Beltsville, MD) IN: Applications of remote sensing to agrometeorology; Proceedings of the Course, Ispra, Italy, Apr. 6-10, 1987. Dordrecht, Netherlands, Kluwer Academic Publishers, 1989, p. 257-284. refs

The determination of soil moisture content from remotely sensed measurements of variations in the dielectric constant is discussed. The dielectric properties of soils and the interactions between microwave radiation and the atmosphere are reviewed. Both microwave radiometry and active microwave approaches are examined. It is suggested that frequencies below 5 or 6 GHz are most effective and that the process is limited to a surface layer

about 5 cm thick. Also, the effects of surface properties such as roughness and vegetation cover are considered.

R.B.

**A89-27945**

**THE VEGETATION INDEX AND THE STUDY OF VEGETATION DYNAMICS**

J. P. MALINGREAU (CEC, Joint Research Centre, Ispra, Italy) IN: Applications of remote sensing to agrometeorology; Proceedings of the Course, Ispra, Italy, Apr. 6-10, 1987. Dordrecht, Netherlands, Kluwer Academic Publishers, 1989, p. 285-303. refs

The derivation and analysis of vegetation indices from spectral data are reviewed. The relationships between the normalized difference vegetation index and vegetation characteristics are examined, focusing on the dynamic processes related to biomass accumulation. Problems associated with the time and space dimensions of satellite data are considered. A vegetation index analysis of a time-series of NOAA AVHRR data is presented as an example. Also, the perpendicular vegetation index is discussed.

R.B.

**A89-28035**

**DEVELOPMENT OF PRINCIPAL COMPONENT ANALYSIS APPLIED TO MULTITEMPORAL LANDSAT TM DATA**

JIAJU LU (Lund, Universitet, Sweden) International Journal of Remote Sensing (ISSN 0143-1161), vol. 9, Dec. 1988, p. 1895-1907. refs

A method of extracting different crop information more effectively, by applying principal component analysis to a three-dimensional three-date Landsat TM data space, has been developed. Landsat TM data obtained on June 7, July 9 and August 26, 1984 were used to examine the approach, and the results fully demonstrated its advantages over other methods of keeping classification accuracy without any calibrations for multitemporal Landsat data.

Author

**A89-28127\*** Lockheed Engineering and Sciences Co., Houston, TX.

**EXTENSION OF A DROUGHT MONITORING AND VEGETATION CLASSIFICATION METHODOLOGY TO THE WESTERN SAHEL**

ROBERT R. J. MOHLER (Lockheed Engineering and Sciences Co., Houston, TX) and DAVID L. AMSBURY (NASA, Johnson Space Center, Houston, TX) Geocarto International (ISSN 1010-6049), vol. 3, Dec. 1988, p. 29-36. refs

Biomass of growing vegetation over large semiarid regions can be estimated by digital manipulation of data from the AVHRR on NOAA polar-orbiting satellites. Here, the African Sahel is classified using a methodology which incorporates both the normalized difference and CAUSE procedures for the monitoring of vegetation during drought conditions. Preliminary analysis of color IR photographs taken on Space Shuttle missions indicates that such photographs can be digitized, registered to maps and other images, and utilized to fill temporal gaps in the historical record of data from unmanned satellites.

Author

**A89-28128\*** New Mexico State Univ., Las Cruces.

**INTEGRATED NDVI IMAGES FOR NIGER 1986-1987**

JOHN A. HARRINGTON, JR., BRUCE K. WYLIE (New Mexico State University, Las Cruces), and COMPTON J. TUCKER (NASA, Goddard Space Flight Center, Greenbelt, MD) Geocarto International (ISSN 1010-6049), vol. 3, Dec. 1988, p. 37-40. Sponsorship: U.S. Agency for International Development. refs  
(Contract AID-AFR-0242-C-003017-00)

Two NOAA AVHRR images are presented which provide a comparison of the geographic distribution of an integration of the normalized difference vegetation index (NDVI) for the Sahel zone in Niger for the growing seasons of 1986 and 1987. The production of the images and the application of the images for resource management are discussed. Daily large area coverage with a spatial resolution of 1.1 km at nadir were transformed to the NDVI and geographically registered to produce the images.

R.B.

A89-28129

**MAPPING AND INVENTORY OF FOREST FIRES FROM DIGITAL PROCESSING OF TM DATA**

EMILIO CHUVIECO (Alcala de Henares, Universidad, Spain) and RUSSEL G. CONGALTON (California, University, Berkeley) Geocarto International (ISSN 1010-6049), vol. 3, Dec. 1988, p. 41-53. Research supported by the Ministry of Education of Spain. refs

The application of space-borne sensors to forest fire mapping and inventory was evaluated. Digital image processing of Thematic Mapper data was used to study a big forest fire on the Mediterranean coast of Spain. The results showed that image processing techniques cannot discriminate perfectly the area affected by the fire. The main problem was spectral overlapping between burned and unburned vegetation especially caused by the sparseness of shrub and confusion with other cover types such as urban/rural villages. Most of these problems can be solved by using visual analysis for masking the affected area, although this strategy is not completely reliable on studies of small forest fires. An inventory of the damaged area was performed in three levels: total area affected by the fire, area by previous vegetation species, and identification of levels of damage on the burned vegetation. Author

A89-28130

**VISUAL AND DIGITAL CLASSIFICATION OF LANDSAT TM DATA FOR SOIL, PHYSIOGRAPHY AND LAND USE MAPPING IN AXIOS ALLUVIAL PLAIN, THESSALONIKI, GREECE**

SILLEOS NIKOLAOS (Salonika, University, Greece) Geocarto International (ISSN 1010-6049), vol. 3, Dec. 1988, p. 55-65. refs

A89-28131

**AIRBORNE MSS FOR LAND COVER CLASSIFICATION**

PAUL J. CURRAN (Sheffield, University, England) and BABAFEMI OJEDELE (Federal Department of Agriculture, Lagos, Nigeria) Geocarto International (ISSN 1010-6049), vol. 3, Dec. 1988, p. 67-72. refs

A basic methodology for the classification of land cover using airborne MSS imagery is outlined. This methodology includes four stages: waveband selection and radiometric calibration, correction for scan angle and atmosphere, training and classification, and accuracy assessment. Three possible refinements were: (1) the use of a per-field sampling scheme, (2) the inclusion of texture in the classifier, and (3) the use of two dates of imagery. Ten land covers were classified using the basic methodology; the basic methodology with refinement (1); the basic methodology with (1) and (2); and the basic methodology with refinements (1), (2), and (3). The overall levels of accuracy (Kappa index) were 65, 82, 85, and 87 percent respectively. The basic methodology and refinements (1) and (2) were shown to be suitable for land cover classification. Author

A89-28364#

**DETECTION OF PERIODIC CHARACTERISTICS OF RICE FIELD VEGETATION BY MICROWAVE BACKSCATTER MEASUREMENT**

TAKASHI KUROSU, TAKESHI SUITZ, TOSHIKI KOZU, and TOSHIHIKO UMEHARA Communications Research Laboratory, Journal (ISSN 0914-9260), vol. 35, Nov. 1988, p. 229-242. refs

Microwave backscatter from a rice field was measured using X-band FM-CW radar. By analyzing backscattered power fadings, both the interval between ridges and the size of ears can be detected, deriving approximate curves of observed probability densities, autocorrelation functions, and power spectral density functions of power fadings. In this paper, the results of analysis of fading are shown, and the method for detecting periodic characteristics such as ridges or ears is described. Author

A89-29373#

**ANALYSIS AND INTERPRETATION OF SPOT IMAGES OF URBAN AND AGRICULTURAL/FOREST SECTIONS OF THE SHERBROOKE REGION [ANALYSE ET INTERPRETATION D'IMAGES SPOT D'UN SECTEUR URBAIN ET AGRO-FORESTIER DE LA REGION DE SHERBROOKE]**

L. CHARBONNEAU, S. PERRAS, F. BONN, and R. BROCHU (Sherbrooke, Universite, Canada) Canadian Journal of Remote Sensing (ISSN 0008-2821), vol. 14, Dec. 1988, p. 92-103. In French. Research supported by the Ministere de l'Education du Quebec. refs

(Contract NSERC-A-5252)

A89-29374#

**AREA MEASUREMENT OF AGRICULTURAL FIELDS FROM SATELLITE IMAGES**

JOSEF CIHLAR (Canada Centre for Remote Sensing, Ottawa) Canadian Journal of Remote Sensing (ISSN 0008-2821), vol. 14, Dec. 1988, p. 110-116. refs

This paper describes results of a study to determine the feasibility of measuring areas of agricultural fields from satellite images. LANDSAT Thematic Mapper and SPOT High Resolution Visible data were analyzed for agricultural areas typified by small (Quebec) and large (Saskatchewan) fields. Satellite measurements were compared to values obtained from aerial photographs or cadastral maps. The effect of various spatial and spectral preprocessing operations on the accuracy of measurements was tested. Results show that for an average field size, the difference between satellite and ground measurements of 10 percent or less can be achieved if appropriate data source and preprocessing algorithms are used. Very small fields and those obscured by clouds cannot be measured. In this study, these two categories represented 20 to 35 percent of all fields studied. Author

A89-29409\* Delaware Univ., Newark.

**EFFECTS OF SOLAR ANGLE ON REFLECTANCE FROM WETLAND VEGETATION**

M. F. GROSS, V. KLEMAS (Delaware, University, Newark), and M. A. HARDISKY (Scranton, University, PA) Remote Sensing of Environment (ISSN 0034-4257), vol. 26, Dec. 1988, p. 195-212. Research supported by the University of Delaware. refs (Contract NOAA-NA-85AADSG033; NAGW-374)

A hand-held radiometer was used to gather spectral data from wetland vegetation canopies to determine the effects of solar angle on reflectance. The reflectance of leafless and gramineous canopies was highly dependent on solar angle, while broadleaf canopy reflectance was not. The solar angle effects are quantified, and a method to compensate for differences in solar angle at the time of collection of spectral data is described. It was found that adjusting spectral data for solar angle effects substantially improved remote sensing estimates of biomass. Author

A89-29410

**COMPLEMENTARITY OF MIDDLE-INFRARED WITH VISIBLE AND NEAR-INFRARED REFLECTANCE FOR MONITORING WHEAT CANOPIES**

F. BARET, G. GUYOT, A. BEGUE, P. MAUREL (Institut National de la Recherche Agronomique, Montfavet, France), and A. PODAIRE (Laboratoire d'Etudes et de Recherches en Teledetection Spatiale, Toulouse, France) Remote Sensing of Environment (ISSN 0034-4257), vol. 26, Dec. 1988, p. 213-225. Research supported by CNES. refs

Information given by middle-IR (1.3-2.5 microns) spectral bands, in addition to visible (0.4-0.7 microns) and NIR (0.7-1.3 microns) channels, was evaluated for monitoring wheat canopies. Three middle-IR bands, TM5 (1.56-1.68 microns), TM7 (2.03-2.35 microns), and a narrower band (1.66-1.70 microns) were tested. TM5 appeared to be the best band, giving the maximum information with regard to visible and NIR. Results show that the middle-IR provides valuable complementary information on the geometrical structure of the canopy and on the optical properties of the underlying soil. Author



A89-29411

**APPLICATION OF A FLUX ALGORITHM TO A FIELD-SATELLITE CAMPAIGN OVER VEGETATED AREA**

O. TACONET and D. VIDAL-MADJAR (Centre de Recherches en Physique de l'Environnement Terrestre et Planetaire, Issy-les-Moulineaux, France) *Remote Sensing of Environment* (ISSN 0034-4257), vol. 26, Dec. 1988, p. 227-239. refs

Surface energy fluxes obtained from an inversion algorithm are validated using simultaneous Meteosat and AVHRR data of a wheat growing region near Beauce, France obtained in July 1983. The data set soundings are refined by processing the radiative model with radiances measured at two different view angles. The process of validating the inferred fluxes and the evolution of surface parameters towards a dry state of the canopy are discussed. The results suggest that the stability of the deduced parameters would be greater using atmospheric surface layer parameters from a boundary layer model instead of local weather stations. R.B.

A89-29412

**WATER TURBIDITY AND PERPENDICULAR VEGETATION INDICES FOR PADDY RICE FLOOD DAMAGE ANALYSES**

Y. YAMAGATA, T. AKIYAMA, M. SHIBAYAMA (National Institute of Agro-Environmental Sciences, Tsukuba, Japan), and C. WIEGAND (USDA, Agricultural Research Service, Weslaco, TX) *Remote Sensing of Environment* (ISSN 0034-4257), vol. 26, Dec. 1988, p. 241-251. refs

The reflectance factors for paddy rice are obtained from ground measurements for two sites of calibrated Landsat TM images of the Kanto district of Japan for August 6, 1986 (one day after a typhoon) and September 7, 1986. A water turbidity index analogous to soil brightness and the perpendicular vegetation index (PVI) are computed. Ground data of rice yield are in good agreement with the PVI and the reflectance factors. It is shown that the damage to the crop increases with the turbidity of the flood water at the boot stage. R.B.

A89-29415 San Diego State Univ., CA.

**TERSAIL - A NUMERICAL MODEL FOR COMBINED ANALYSIS OF VEGETATION CANOPY BIDIRECTIONAL REFLECTANCE AND THERMAL EMISSIONS**

ALLEN S. HOPE (San Diego State University, CA), SAMUEL N. COWARD, and DONALD E. PETZOLD (Maryland, University, College Park) *Remote Sensing of Environment* (ISSN 0034-4257), vol. 26, Dec. 1988, p. 287-300. Research supported by USDA and NASA. refs

A modification of the Tergra model (Soer, 1977) is presented, which incorporates the scattering from arbitrarily inclined leaves canopy reflectance model (Verhoef and Bunnik, 1981) for the calculation of albedo and canopy resistance. The combined model, known as Tersail, is capable of simulating the relationship between the bidirectional reflectance and the thermal response of a canopy. The accuracy of the model is tested using data over wheat canopies in Phoenix, Arizona, showing that the model is a good simulator of canopy temperatures under a variety of conditions. R.B.

A89-30262

**DELINEATION OF SALT-AFFECTED SOILS THROUGH DIGITAL ANALYSIS OF LANDSAT MSS DATA**

A. N. SINGH (Remote Sensing Applications Centre, Lucknow, India) and R. S. DWIVEDI (National Remote Sensing Agency, Hyderabad, India) *International Journal of Remote Sensing* (ISSN 0143-1161), vol. 10, Jan. 1989, p. 83-92. refs

Landsat MSS digital data over parts of Uttar Pradesh (Northern India) covering an area of 60243 sq km were analyzed on an interactive multispectral data analysis system to delineate salt-affected soils. Based on the spectral response of these soils and subsequent correlation in the field by studying terrain characteristics and soil profiles, two categories of salt-affected soils that require different management practices, namely, Typic Natrustalfs, and an association of Typic Natraqualfs and Aquic Natrustalfs, could be delineated. Both the soils are saline-sodic in nature and occur in 6.15 and 2.75 percent of the whole area,

respectively. Besides these salt-affected soils, other categories, such as normal soils, forests, water bodies, river sand, gullies and ravines, were also mapped. Author

A89-30264\* New York State Univ., Binghamton.

**BIDIRECTIONAL CANOPY REFLECTANCE AND ITS RELATIONSHIP TO VEGETATION CHARACTERISTICS**

NARENDRA S. GOEL and NIKKI E. REYNOLDS (New York, State University, Binghamton) *International Journal of Remote Sensing* (ISSN 0143-1161), vol. 10, Jan. 1989, p. 107-132. Research supported by NASA. refs

A method for determining the relationship between bidirectional canopy reflectance (CR) of a vegetated area and its characteristics (type and growth stage) is presented. In the method, the three-dimensional CR surface is expressed in terms of spherical harmonics which are weighted by appropriate coefficients, and the coefficients are analyzed by a cluster technique. The method is applied to four vegetation types (soybeans, corn, shinnery oak, and orchard grass) at various stages of growth. R.R.

A89-30265

**UNSUPERVISED TRAINING AREA SELECTION IN FORESTS USING A NONPARAMETRIC DISTANCE MEASURE AND SPATIAL INFORMATION**

A. K. SKIDMORE (Australian National University, Canberra, Australia) *International Journal of Remote Sensing* (ISSN 0143-1161), vol. 10, Jan. 1989, p. 133-146. refs

A new unsupervised technique that automatically delineates areas with a similar tone is described. The proposed algorithm grows a region of homogeneous tone around a seed pixel; membership criteria for the region is based upon a nonparametric distance measure. The thematic image output can be used to define training areas for a supervised classifier. Two commonly used unsupervised strategies for delineating training areas (viz., clustering and uniform texture mapping) are compared with the proposed technique using SPOT digital data collected over a multi-aged forest plantation in south-east Australia. Author

A89-30266\* Kansas Univ. Center for Research, Inc., Lawrence.

**FINE RESOLUTION SIGNATURES OF CONIFEROUS AND DECIDUOUS TREES AT C BAND**

R. ZOUGH, J. BREDOW, S. OSMAN, and R. K. MOORE (University of Kansas Center for Research, Inc., Lawrence) *International Journal of Remote Sensing* (ISSN 0143-1161), vol. 10, Jan. 1989, p. 147-169. refs  
(Contract NAG5-271)

A89-30267

**THEORETICAL STUDY OF THE SENSITIVITY OF THE MICROWAVE BACKSCATTERING COEFFICIENT TO THE SOIL SURFACE PARAMETERS**

M. AUTRET, R. BERNARD, and D. VIDAL-MADJAR (Centre de Recherches en Physique de l'Environnement Terrestre et Planetaire, Issy-les-Moulineaux, France) *International Journal of Remote Sensing* (ISSN 0143-1161), vol. 10, Jan. 1989, p. 171-179. refs

The microwave backscattered signal from soil is sensitive to surface parameters and especially to roughness and moisture. The object of this work is to evaluate the optimum operating configuration for a spacecraft radar which would allow the extraction of one of these parameters, minimizing the effect of the other. A theoretical study, using a simulation model based on the scalar approximation, has permitted the estimation of the backscattering coefficient's sensitivity to a relative variation in soil parameters in terms of radar characteristics. The results show that, if a very low incidence angle is not acceptable, the best configuration for a soil moisture measurement requires the simultaneous use of two polarizations (HH and VV) and a large look-angle (greater than 35 deg). For a roughness measurement, the coupling of two incidence angles (20 deg and 40 deg), a low frequency (S or C-band) and the HH polarization seem to give satisfactory results. Author

A89-30268

**ANALYSIS AND REPRESENTATION OF VEGETATION CONTINUA FROM LANDSAT THEMATIC MAPPER DATA FOR LOWLAND HEATHS**

T. F. WOOD and G. M. FOODY (Kingston Polytechnic, Kingston upon Thames, England) *International Journal of Remote Sensing* (ISSN 0143-1161), vol. 10, Jan. 1989, p. 181-191. Research supported by Kingston Polytechnic. refs

The use of ordinary techniques for studying the vegetation types of lowland heathland in Surrey is considered, and problems in the conventional classification of such regions using remotely-sensed data are pointed out. In heathland, spatial variation frequently exists as coenoclines, and the analysis of remotely-sensed images must reflect such changes. Probability mapping can be used to show the likelihood of heath, degrees of similarity to coniferous woodland, and degrees of likelihood of wet heath and bog. R.R.

A89-30269

**VISUAL AND COMPUTER CLASSIFICATIONS OF REMOTELY-SENSED IMAGES - A CASE STUDY OF GRASSLANDS IN CAMBRIDGESHIRE**

R. M. FULLER, R. J. PARSELL (NERC, Institute of Terrestrial Ecology, Huntingdon, England), M. OLIVER, and G. WYATT *International Journal of Remote Sensing* (ISSN 0143-1161), vol. 10, Jan. 1989, p. 193-210. Research supported by the Bedfordshire and Huntingdonshire Wildlife Trust and Manpower Services Commission. refs

Study sites in Cambridgeshire have been used to assess the relative merits of Landsat TM data, airborne TM data, and conventional panchromatic aerial photographs, for surveying the ecology and land uses of lowland Britain, with particular attention to grasslands. Techniques of computer enhancement, classification and measurement are compared with those involving visual interpretation and manual collation of map information and land-use statistics. Comparison include measurements of the accuracy and assessments of general accessibility, ease of use, efficiency and effectiveness of the various techniques. Author

A89-31890

**THE CLASSIFICATION OF LOAMY GROUND IN THE OUTRE-FORET REGION OF ALSACE IN FRANCE USING LANDSAT 5 TM IMAGES [ESSAI DE CLASSIFICATION DE TERRES LIMONEUSES DANS L'OUTRE-FORET /ALSACE, FRANCE/ A L'AIDE DE DONNEES LANDSAT 5 TM]**

T. VOGT (Strasbourg I, Universite, France) *Photo Interpretation* (ISSN 0031-8523), vol. 27, Mar.-Apr. 1988, p. 31-33, 35, 36. In French, English, and Spanish. Research supported by CNES. R.R.

A89-31892

**COMBINING OBLIQUE SPOT-1 IMAGES FOR THE ANALYSIS OF CERTAIN SOIL PROPERTIES [COMBINAISONS D'IMAGES SPOT-1 OBLIQUES POUR L'ANALYSE DE CERTAINES PROPRIETES DES SOLS]**

J. DELEZIR and M. GUY (CNES, Toulouse, France) *Photo Interpretation* (ISSN 0031-8523), vol. 27, May-June 1988, p. 1-3, 5, 7 (6 ff.). In French, English, and Spanish.

SPOT-1 images were obtained to the southwest of the Oued En Namous region in Algeria in order to explore the use of multiple oblique images in determining soil properties. The results of a principal-components analysis show that the components deduced from oblique viewings have a geomorphological interpretation that can be linked to relief types (such as a slope with an eastern exposure) and, often, to the soil properties. It is noted that due to the selection of a desert area for the study, the ground material could not easily be surveyed. R.R.

A89-31893

**DETERMINING THE AGE OF CUT FOREST AREAS IN QUEBEC, CANADA USING THE LANDSAT-5 TM [DETERMINATION DE L'AGE DES COUPES FORESTIERES AVEC TM DE LANDSAT-5 /QUEBEC, CANADA/]**

S. MATEJEK and J. M. M. DUBOIS (Sherbrooke, Universite, Canada) *Photo Interpretation* (ISSN 0031-8523), vol. 27, May-June 1988, p. 15-17, 19, 21, 22. In French, English, and Spanish.

Landsat-5 TM images with a resolution of 10 pixels per hectare are used to survey cutting and regeneration in the Watopeka Forest in Quebec, Canada. A principal component analysis based on values obtained for the TM channels 3, 4, and 5 enabled an accurate classification to be made. The results have been validated by comparison with field data. It is noted that it is more difficult to determine age and density variations for the deciduous trees than for the coniferous trees. R.R.

A89-31894

**MULTITEMPORAL STUDY OF DIFFERENTLY FARMED PERMANENT GRAZING LANDS IN THE LORRAINE REGION OF FRANCE USING SPOT-1 DATA [ETUDE MULTITEMPORELLE DE DIFFERENTS MODES D'EXPLOITATION DES PRAIRIES PERMANENTES EN LORRAINE /FRANCE/, A L'AIDE DE SPOT-1]**

C. M. GIRARD (Institut National Agronomique Paris-Grignon, Thiverval-Grignon, France), M. BENOIT, and E. DE VAUBERNIER (Institut National de la Recherche Agronomique, Mirecourt, France) *Photo Interpretation* (ISSN 0031-8523), vol. 27, May-June 1988, p. 23-25, 27, 29, 31, 32. In French, English, and Spanish. R.R.

A89-32110

**MODELING VEGETATION AS A SET OF SCATTERERS [O MODELIROVANII RASTITEL'NOSTI SOVOKUPNOST'IU RASSEIVATELEI]**

A. A. CHUKHLANTSEV *Radiotekhnika i Elektronika* (ISSN 0033-8494), vol. 34, Feb. 1989, p. 240-244. In Russian. refs

Expressions for calculating the attenuation coefficient and albedo of a unit volume of vegetation are derived, and the relationship between these two parameters and biometric indices is established. Spectral dependences of transmission and reflection coefficients are calculated for a number of vegetation covers. The results are found to agree well with microwave radiometry data. B.J.

A89-32336

**A COMPARISON OF IMAGES FROM A PUSHBROOM SCANNER WITH NORMAL COLOR AERIAL PHOTOGRAPHS FOR DETECTING SCATTERED RECENT CONIFER MORTALITY**

I. D. KNEPPECK (Dendron Resource Surveys, Ltd., Ottawa, Canada) and F. J. AHERN (Canada Centre for Remote Sensing, Ottawa) *Photogrammetric Engineering and Remote Sensing* (ISSN 0099-1112), vol. 55, March 1989, p. 333-337. refs

A89-32432\* National Aeronautics and Space Administration. Langley Research Center, Hampton, VA.

**TRACE GAS EMISSIONS FROM CHAPARRAL AND BOREAL FOREST FIRES**

WESLEY R. COFER, III, JOEL S. LEVINE, DANIEL I. SEBACHER (NASA, Langley Research Center, Hampton, VA), EDWARD L. WINSTEAD (ST Systems Corp., Hampton, VA), PHILIP J. RIGGAN (USDA, Forest Service, Riverside, CA), BRIAN J. STOCKS (Canadian Forestry Service, Great Lakes Forestry Center, Sault Sainte Marie, Canada), JAMES A. BRASS, VINCENT G. AMBROSIA (NASA, Ames Research Center, Moffett Field, CA) et al. *Journal of Geophysical Research* (ISSN 0148-0227), vol. 94, Feb. 20, 1989, p. 2255-2259. refs

Using smoke samples collected during low-level helicopter flights, the mixing ratios of CO<sub>2</sub>, CO, CH<sub>4</sub>, total nonmethane hydrocarbons, H<sub>2</sub>, and N<sub>2</sub>O over burning chaparral in southern California and over a burning boreal forest site in northern Ontario, Canada, were determined. Carbon dioxide-normalized emission ratios were determined for each trace gas for conditions of flaming, mixed, and smoldering combustion. The emission ratios for these trace gases were found to be highest for the smoldering combustion, generally thought to be the least efficient combustion

stage. However, high emission ratios for these gases could be also produced during very vigorous flaming combustion. I.S.

**N89-17339\*#** National Aeronautics and Space Administration. Ames Research Center, Moffett Field, CA.

**ACCURACY ASSESSMENT, USING STRATIFIED PLURALITY SAMPLING, OF PORTIONS OF A LANDSAT CLASSIFICATION OF THE ARCTIC NATIONAL WILDLIFE REFUGE COASTAL PLAIN**

DON H. CARD and LAURENCE L. STRONG (TGS Technology, Inc., Moffett Field, CA.) Jan. 1989 48 p Sponsored by NASA (Contract GSRN-1-7060-0450) (NASA-TM-101042; A-88309; NAS 1.15:101042) Avail: NTIS HC A03/MF A01 CSCL 08B

An application of a classification accuracy assessment procedure is described for a vegetation and land cover map prepared by digital image processing of LANDSAT multispectral scanner data. A statistical sampling procedure called Stratified Plurality Sampling was used to assess the accuracy of portions of a map of the Arctic National Wildlife Refuge coastal plain. Results are tabulated as percent correct classification overall as well as per category with associated confidence intervals. Although values of percent correct were disappointingly low for most categories, the study was useful in highlighting sources of classification error and demonstrating shortcomings of the plurality sampling method.

Author

**N89-17930** Missouri Univ., Columbia.

**SATELLITE DERIVED EARTH SURFACE TEMPERATURES: A CROP ASSESSMENT TOOL Ph.D. Thesis**

CHRISTY LYNN CROSIAR 1987 144 p

Avail: Univ. Microfilms Order No. DA8818929

The data for this research consist of the following: 23 days of NOAA/AVHRR satellite data; AgRISTARS enumerator data (or ground truth data) for 26 counties in three midwestern states and radiosonde observations for nine upper air stations, producing an 8 state coverage. The objectives of this research are threefold: (1) to develop a regression model to estimate maximum shelter temperature, (2) to develop a method to assess crop conditions and (3) to determine the variability within a scan line due to changes in optical depth and/or scan angle. The results from this research is given and discussed.

Dissert. Abstr.

**N89-18708#** Royal Signals and Radar Establishment, Malvern (England).

**A COMPARISON OF CLUTTER TEXTURE PROPERTIES IN OPTICAL AND SAR IMAGES**

J. R. GARSIDE and C. J. OLIVER *In* ESA, Proceedings of the 1988 International Geoscience and Remote Sensing Symposium (IGARSS) '88 on Remote Sensing: Moving Towards the 21st Century, Volume 3 p 1249-1255 Aug. 1988

Avail: NTIS HC A99/MF A01; ESA Publications Division, ESTEC, Noordwijk, Netherlands, \$120 US or 250 Dutch guilders

The theoretical relationship between optical and SAR images in terms of their single-point moments and the intensity autocorrelation function was examined. It is demonstrated that a correlated noise model based on gamma-distributed noise is consistent with both image textures. The incoherent optical image was used to simulate a set of SAR-like textures which are statistically indistinguishable from the original SAR texture. This represents a significant step in the ability to combine information from different sensors.

ESA

**N89-18709#** Wageningen Agricultural Univ. (Netherlands). Dept. of Surveying and Remote Sensing.

**EXTRACTION OF SMALL-SCALE SPATIAL INFORMATION FROM SLAR RAW DATA OF FORESTS THROUGH AN ANALYSIS OF SPECKLE**

D. H. HOEKMAN *In* ESA, Proceedings of the 1988 International Geoscience and Remote Sensing Symposium (IGARSS) '88 on Remote Sensing: Moving Towards the 21st Century, Volume 3 p 1257-1261 Aug. 1988

Avail: NTIS HC A99/MF A01; ESA Publications Division, ESTEC, Noordwijk, Netherlands, \$120 US or 250 Dutch guilders

It is shown that the autocorrelation function of the (subresolution cell) spatial backscatter signature in azimuth of distributed targets can be estimated from the averaged power density spectrum of azimuth (speckle) signals. The (theoretical) accuracy of this estimation can be indicated. Results of experiments with an X-band SLAR over forest plantations show good agreement with theory. The tree row spacing (on the order of several meters) could be estimated accurately (within a few decimeters) using an antenna with an efficient length of 2 m and an azimuth spatial resolution on the order of 25 m.

ESA

**N89-18712\*#** National Aeronautics and Space Administration. Lyndon B. Johnson Space Center, Houston, TX.

**COMPARISON OF MEASURED C-BAND SCATTERING COEFFICIENTS WITH MODEL PREDICTIONS AS A FUNCTION OF LEAF AREA INDEX AND BIOMASS**

D. E. PITTS, G. D. BADHWAR, and A. H. FEIVSON *In* ESA, Proceedings of the 1988 International Geoscience and Remote Sensing Symposium (IGARSS) '88 on Remote Sensing: Moving Towards the 21st Century, Volume 3 p 1271-1275 Aug. 1988

Avail: NTIS HC A99/MF A01; ESA Publications Division, ESTEC, Noordwijk, Netherlands, \$120 US or 250 Dutch guilders CSCL 08B

The backscattering coefficients for black spruce and aspen at an incidence angle of 50 deg obtained using a helicopter mounted C-band scatterometer are related to leaf area index (LAI) and biomass for several dates while leaves are present. These data are compared with estimates obtained from the Fung disk model for aspen. Implications for spacecraft SAR (e.g., SIR-C) systems and their ability to determine biophysical characteristics of forest canopies are discussed. The precision of SAR data is insufficient to provide consistent tests of the relationship of LAI to the scattering coefficient for single polarizations alone. Backscatter models only provide a simulation of part of the canopy, and more attention needs to be placed on collecting field data which support tests of the microwave scattering models.

ESA

**N89-18713#** Massachusetts Univ., Amherst. Microwave Remote Sensing Lab.

**LEAF BACKSCATTERING MEASUREMENTS AND MODELLING AT 94 GHZ**

C. C. BOREL and R. E. MCINTOSH *In* ESA, Proceedings of the 1988 International Geoscience and Remote Sensing Symposium (IGARSS) '88 on Remote Sensing: Moving Towards the 21st Century, Volume 3 p 1277-1278 Aug. 1988

Avail: NTIS HC A99/MF A01; ESA Publications Division, ESTEC, Noordwijk, Netherlands, \$120 US or 250 Dutch guilders

Scattering of leaves at 94 GHz was studied, showing that smooth leaves such as philodendron leaves have scattering patterns which exhibit strong fading characteristics. The fading is due to the superposition and cancelling out of the scattered fields by the spatial variations of the surface, which can be large compared to millimeter wavelengths. This fading of the radar return from a single leaf is not usually taken into account in foliage models. It is found that the average lobe width is proportional to the ratio of wavelength over square root of the leaf area.

ESA

**N89-18714#** Ministry of Posts and Telecommunications, Tokyo (Japan). Communications Research Lab.

**A MEASUREMENT OF MICROWAVE BACKSCATTERING COEFFICIENTS OF RICE PLANTS**

TAKESHI SUITZ, TAKASHI KUROSU, and TOSHIHIKO UMEHARA *In* ESA, Proceedings of the 1988 International Geoscience and Remote Sensing Symposium (IGARSS) '88 on Remote Sensing: Moving Towards the 21st Century, Volume 3 p 1283-1286 Aug. 1988

Avail: NTIS HC A99/MF A01; ESA Publications Division, ESTEC, Noordwijk, Netherlands, \$120 US or 250 Dutch guilders

Microwave backscattering coefficients of rice plants were measured with an FM-CW scatterometer. The scatterometer was moved on a pair of rails along a rice field to observe a selected

area for a given time. The fading characteristics of backscattering signals deviate from the Rayleigh distribution, because rice plants were planted at regular intervals in the field. Properties of rice plants were derived from the probability density distribution, power spectrum, and autocorrelation function of the fading signals. The probability density distribution functions of scattered power is approximated by an expansion in terms of Sonine's normalized orthogonal polynomials. ESA

**N89-18715#** Budapest Science Univ. (Hungary). Dept. of Microwave Telecommunications.

**X-BAND SCATTEROMETRY IN AGRICULTURE**

S. MIHALY and I. BOZSOKI *In* ESA, Proceedings of the 1988 International Geoscience and Remote Sensing Symposium (IGARSS) '88 on Remote Sensing: Moving Towards the 21st Century, Volume 3 p 1287-1290 Aug. 1988 (Contract OMF7-12-0127)

Avail: NTIS HC A99/MF A01; ESA Publications Division, ESTEC, Noordwijk, Netherlands, \$120 US or 250 Dutch guilders

Bare soil backscattering measurements at 10.3 GHz at H and V like polarization are interpreted with in situ gravimetric and pF soil moisture data. Surface roughness and temperature are indicated. A mobile FM-CW scatterometer with flat microstrip cross-polarized antenna and automated data collecting and processing facilities is described, including hardware and software structure. ESA

**N89-18716#** Centre d'Etude Spatiale des Rayonnements, Toulouse (France).

**MULTITEMPORAL AND DUAL POLARIZATION OF AGRICULTURAL CROPS BY X-BAND SAR IMAGES**

T. LETOAN and H. LAUR *In* ESA, Proceedings of the 1988 International Geoscience and Remote Sensing Symposium (IGARSS) '88 on Remote Sensing: Moving Towards the 21st Century, Volume 3 p 1291-1294 Aug. 1988

Avail: NTIS HC A99/MF A01; ESA Publications Division, ESTEC, Noordwijk, Netherlands, \$120 US or 250 Dutch guilders

X-band SAR images on agricultural crops were analyzed, emphasizing the differences between two parallel polarizations HH and VV, observed on cover types at two dates. The most striking feature is the singular behavior of flooded ricefields, which differs from the early to fully growth stage. The behavior, explained by backscattering models on vegetation canopy with highly reflecting underlying surface, suggests the use of the polarization ratio between HH and VV for ricefield monitoring. ESA

**N89-18724#** Institute for Image Processing Computer Mapping, Graz (Austria). Research Center.

**SPECTRAL RESPONSE CHARACTERISTICS OF A METAL-STRESSED CONIFEROUS FOREST AS MEASURED BY THE FLUORESCENCE LINE IMAGER (FLI) AIRBORNE IMAGING SPECTROMETER**

C. BANNINGER *In* ESA, Proceedings of the 1988 International Geoscience and Remote Sensing Symposium (IGARSS) '88 on Remote Sensing: Moving Towards the 21st Century, Volume 3 p 1331-1334 Aug. 1988

Avail: NTIS HC A99/MF A01; ESA Publications Division, ESTEC, Noordwijk, Netherlands, \$120 US or 250 Dutch guilders

Airborne imaging spectrometer data in the visible to near-infrared part of the spectrum (430 to 805 nm) were acquired by fluorescence line imager over a metal-stressed coniferous forest in the southeastern Alps of Austria. They show increases in reflectance in the red and near-infrared, associated with increased levels of copper, lead, and zinc in the underlying soil. No significant changes, however, occur in the wavelength position of the slope of the transition zone between the red absorption well and the near-infrared reflectance plateau (the so-called red-edge shift), nor that of the chlorophyll absorption maximum. This implies that the relative amounts of chlorophyll-a to chlorophyll-b in the canopy foliage are unchanged between stressed and nonstressed trees. ESA

**N89-18725#** Canada Centre for Remote Sensing, Ottawa (Ontario).

**ASSESSMENT OF CLEARCUT MAPPING ACCURACY WITH C-BAND SAR**

F. J. AHERN and J. A. DRIEMAN (INTERA Environmental Consultants Ltd., Ottawa, Ontario) *In* ESA, Proceedings of the 1988 International Geoscience and Remote Sensing Symposium (IGARSS) '88 on Remote Sensing: Moving Towards the 21st Century, Volume 3 p 1335-1338 Aug. 1988

Avail: NTIS HC A99/MF A01; ESA Publications Division, ESTEC, Noordwijk, Netherlands, \$120 US or 250 Dutch guilders

The Canada Center for Remote Sensing C-band SAR was tested for clearcut mapping accuracy in a forested area of central Alberta typical of the boreal forests of Canada. Comparison data was clearcut boundaries plotted at 1:20,000 scale from 1:60,000 panchromatic aerial photography. The average areal error incurred with the SAR data is -11 pct. The average boundary placement error is 30 m. These errors are larger than acceptable for operational forest inventory update in most provinces. However, areas for improvement which may make provincial requirements attainable are identified. ESA

**N89-18726#** Karlsruhe Univ. (Germany, F.R.). Inst. of Plant Physiology.

**CORRELATION OF REFLECTANCE AND CHLOROPHYLL FLUORESCENCE SIGNATURES OF HEALTHY AND DAMAGED FOREST TREES**

C. BUSCHMANN and H. K. LICHTENTHALER *In* ESA, Proceedings of the 1988 International Geoscience and Remote Sensing Symposium (IGARSS) '88 on Remote Sensing: Moving Towards the 21st Century, Volume 3 p 1339-1342 Aug. 1988 Sponsored in part by the Projekt Europaisches Forschungszentrum fuer Massnahmen zur Luftreinhaltung, Karlsruhe, Fed. Republic of Germany

Avail: NTIS HC A99/MF A01; ESA Publications Division, ESTEC, Noordwijk, Netherlands, \$120 US or 250 Dutch guilders

A remote sensor to overcome difficulties in the classification of tree damage by airborne forest inventory, which arose as the reflectance signature of damaged trees with low physiological activity no longer showed the expected decrease of the reflectance signal in the 800 nm region, was developed. The measuring system (VIRAF-spectrometer) makes it possible to detect absorption spectra, fluorescence emission spectra, and Kautsky induction kinetics parallel to the reflection spectra without changing the position of the leaf sample. These additional measurements characterize the physiological activity of one leaf sample, which can be left intact and attached to the plant. The system permits a better interpretation of remotely sensed reflection signatures and can improve forest classification and agricultural field studies. ESA

**N89-18727#** Karlsruhe Univ. (Germany, F.R.). Inst. of Plant Physiology.

**CORRELATION OF RADAR REFLECTIVITY AND CHLOROPHYLL FLUORESCENCE OF FOREST TREES**

U. RINDERLE, M. HAITZ, H. K. LICHTENTHALER, D. H. KAEHNY, Z. SHI, and W. WIESBECK *In* ESA, Proceedings of the 1988 International Geoscience and Remote Sensing Symposium (IGARSS) '88 on Remote Sensing: Moving Towards the 21st Century, Volume 3 p 1343-1346 Aug. 1988 Sponsored by the Projekt Europaisches Forschungszentrum fuer Massnahmen zur Luftreinhaltung, Karlsruhe, Fed. Republic of Germany and Joint Research Center of the European Communities, Ispra, Italy

Avail: NTIS HC A99/MF A01; ESA Publications Division, ESTEC, Noordwijk, Netherlands, \$120 US or 250 Dutch guilders

High resolution wide band complex polarimetric radar cross section (RCS) measurements of cut-off twigs and leaves of forest trees (*Picea glauca*, *Acer platanoides*) were determined parallel to the light-induced in vivo chlorophyll fluorescence in order to possibly correlate changes in radar reflectivity signatures with changes in tree vitality during increasing water stress. The RCS changes considerably with increasing time after abscission of healthy needles and twigs from the tree. Several chlorophyll fluorescence

parameters, e.g., decreasing Rfd-values, decreasing height of the saturating fluorescence spikes (QA-reoxidation capacity) indicate decreasing photosynthesis of the leaves, needles and twigs. The comparative results of the development of radar and fluorescence signals in cut-off plant parts are a promising step towards the aim of creating a link between RCS signatures and tree vitality. ESA

**N89-18728\*#** National Aeronautics and Space Administration, Goddard Space Flight Center, Greenbelt, MD.  
**CHARACTERIZING FOREST ECOSYSTEM DYNAMICS THROUGH MODELLING AND REMOTE SENSING OBSERVATIONS**

K. J. RANSON, J. A. SMITH, and F. G. HALL *In* ESA, Proceedings of the 1988 International Geoscience and Remote Sensing Symposium (IGARSS) '88 on Remote Sensing: Moving Towards the 21st Century, Volume 3 p 1347-1350 Aug. 1988  
 Avail: NTIS HC A99/MF A01; ESA Publications Division, ESTEC, Noordwijk, Netherlands, \$120 US or 250 Dutch guilders USCL 02F

To gain a better understanding of northern/boreal forest dynamics over a range of spatial and temporal scales, an approach to integrate models of forest growth, soil processes and radiative transfer with remote sensing observations was developed. The integrated model and remote sensing can be used to examine descriptors of ecosystem dynamics. To examine the scaling of vegetation pattern from the local to the regional domain, distributions of area and perimeters of vegetation community associations were determined from satellite and aircraft images. Relationships between computed fractal dimensions (1.5 to 1.8) and succession history for managed and unmanaged areas are being explored. ESA

**N89-18729#** Ministere de l'Environnement et du Cadre de Vie, Neuilly (France).

**POSSIBILITIES OF THE SATELLITE IMAGERY TO LOCATE THE FOREST DECLINE AREAS IN THE VOSGES MASSIF (FRANCE)**

M. LENCO and PH. COUR (SFERES Remote Sensing Co., France) *In* ESA, Proceedings of the 1988 International Geoscience and Remote Sensing Symposium (IGARSS) '88 on Remote Sensing: Moving Towards the 21st Century, Volume 3 p 1353-1354 Aug. 1988

Avail: NTIS HC A99/MF A01; ESA Publications Division, ESTEC, Noordwijk, Netherlands, \$120 US or 250 Dutch guilders

Data of the Vosges Massif (France) from LANDSAT TM data were compared with MSS data and SPOT data on 36 test sites representative of the forest according to species, age, health, and ecological situation. It is shown that the normalized vegetation index of the 3 sensors and the difference TM4-TM5 of TM channels are good indicators to study and to locate changing health conditions with time in the coniferous forests and, but only with LANDSAT TM data, to locate forest damage by species and age groups. ESA

**N89-18730#** Laval Univ. (Quebec). Dept. des Sciences Geodesiques et de Teledetection.

**TEXTURE ANALYSIS OF FOREST REGENERATION SITES IN HIGH-RESOLUTION SAR IMAGERY**

G. EDWARDS, R. LANDRY, and K. P. B. THOMPSON *In* ESA, Proceedings of the 1988 International Geoscience and Remote Sensing Symposium (IGARSS) '88 on Remote Sensing: Moving Towards the 21st Century, Volume 3 p 1355-1360 Aug. 1988  
 Avail: NTIS HC A99/MF A01; ESA Publications Division, ESTEC, Noordwijk, Netherlands, \$120 US or 250 Dutch guilders

A procedure for extracting textural information, based on the classic co-occurrence techniques, and for obtaining carefully calibrated estimates of the uncertainty of these texture measurements was developed for forest inventories. This approach gives the control necessary to separate texture due to speckle from natural scene texture, to determine to what accuracy classification of different textures can proceed, and to develop analysis methods appropriate to eventual operational mapping of radar images in forestry. Results in a region containing clear cuts

and regeneration sites show considerable promise: four texture classes corresponding to different stages of forest regeneration; the presence of a minimum contrast threshold due to the speckle, and the presence of texture at scales larger than the window used to sample the texture are detected. ESA

**N89-18731#** New South Wales Univ., Campbell (Australia). Dept. of Electrical Engineering.

**ASSOCIATION OF RADAR BACKSCATTERING WITH BIOPHYSICAL CHARACTERISTICS OF AUSTRALIAN FORESTS**

J. A. RICHARDS and Z. AHMED (New South Wales Univ., Kensington, Australia) *In* ESA, Proceedings of the 1988 International Geoscience and Remote Sensing Symposium (IGARSS) '88 on Remote Sensing: Moving Towards the 21st Century, Volume 3 p 1363-1365 Aug. 1988 Sponsored in part by the Australian Research Council

Avail: NTIS HC A99/MF A01; ESA Publications Division, ESTEC, Noordwijk, Netherlands, \$120 US or 250 Dutch guilders

A simple procedure is used to provide relative calibration of a SIR-B multiple incidence angle data set, leading to backscatter dependence on incidence angle consistent with a double bounce interpretation of forest scattering. A backscatter model based on a dihedral corner reflector is shown to explain the calibrated SIR-B data. To the extent that backscattering from new plantings can be considered to be reasonably Lambertian, the results obtained support to a double bounce interpretation as the dominant scattering mechanism from mature forest stands at L-band. Any rough surface model in general, applied to the data, leads to backscatter dependence on theta also consistent with trunk ground double bounce behavior. It is encouraging however that the calibrated backscatter measurements derived from the Lambertian basis are so well represented with the simple lossy corner reflector model. ESA

**N89-18732#** National Remote Sensing Centre, Farnborough (England).

**LANDSAT TM STUDY OF AFFORESTATION IN NORTHERN SCOTLAND AND ITS IMPACT ON BREEDING BIRD POPULATIONS**

J. M. SMITH *In* ESA, Proceedings of the 1988 International Geoscience and Remote Sensing Symposium (IGARSS) '88 on Remote Sensing: Moving Towards the 21st Century, Volume 3 p 1369-1370 Aug. 1988

Avail: NTIS HC A99/MF A01; ESA Publications Division, ESTEC, Noordwijk, Netherlands, \$120 US or 250 Dutch guilders

An area of actively growing acid bog in Scotland, important physiographically, and for the variety and type of flora and fauna it supports was surveyed by Thematic Mappers (TM). Pool systems which characterize the flatter areas of peatland provide feeding grounds for large numbers of breeding wetland birds. Since 1980, 20 pct of the total area of blanket bog has been afforested, reducing drastically the area of suitable habitat for many moorland birds. Young plantations can be readily identified on LANDSAT TM imagery. During the first year after ploughing, spectral response of exposed, deeply ploughed and drained peat soils contrasts well with that of the surrounding vegetation. Areas of ecologically important pool systems can also be detected, and TM imagery offers the potential to map areas of suitable wader habitat. ESA

**N89-18772#** China Research Inst. of Radiowave Propagation, Xinxiang.

**A SIMULATION TEST FOR SOIL MOISTURE SENSING**

JIANKANG JI *In* ESA, Proceedings of the 1988 International Geoscience and Remote Sensing Symposium (IGARSS) '88 on Remote Sensing: Moving Towards the 21st Century, Volume 3 p 1555-1556 Aug. 1988

Avail: NTIS HC A99/MF A01; ESA Publications Division, ESTEC, Noordwijk, Netherlands, \$120 US or 250 Dutch guilders

The sample-on-plank simulation test for the remote sensing of bare soil moisture by X-band scatterometer during two months is summarized. The process and the general observations of the test are presented. The sample test shows the advantage in

reducing the error which comes from the inhomogeneity of soil moisture and that of soil surface roughness in measuring the backscattering coefficients at different incidence angles in field.

ESA

**N89-18773#** Instituto de Pesquisas Espaciais, Rio de Janeiro (Brazil).

**MICROWAVE X-BAND RADIOMETRIC CHARACTERIZATION OF BRAZILIAN SOILS BY MEASUREMENT OF THE COMPLEX PERMITTIVITY**

U. W. PALME *In* ESA, Proceedings of the 1988 International Geoscience and Remote Sensing Symposium (IGARSS) '88 on Remote Sensing: Moving Towards the 21st Century, Volume 3 p 1557-1561 Aug. 1988

Avail: NTIS HC A99/MF A01; ESA Publications Division, ESTEC, Noordwijk, Netherlands, \$120 US or 250 Dutch guilders

Activities in microwave radiometry for agriculture in Brazil are reviewed. Results regarding measurements of the complex permittivity and estimates of emissivity for soils from tropical areas as a function of soil moisture, at 10.62 GHz, are presented. Difficulties related to the measurement of permittivity of important Brazilian soils (dielectric/ferromagnetic mixture) are highlighted.

ESA

**N89-18774#** Academy of Sciences (USSR), Moscow. Inst. of Radioengineering and Electronics.

**MICROCOMPUTER-BASED RADIOMETER DATA ACQUISITION AND PROCESSING SYSTEM FOR LARGE-AREA MAPPING OF SOIL MOISTURE CONTENT IN THE TOP ONE METER LAYER**

F. A. MKRTCHJAN, E. A. REUTOV, A. M. SHUTKO, K. G. KOSTOV, M. A. MICHALEV, N. M. NEDELTCHEV, A. Y. SPASOV, and B. I. VICHEV (Bulgarian Academy of Sciences, Sofia.) *In* ESA, Proceedings of the 1988 International Geoscience and Remote Sensing Symposium (IGARSS) '88 on Remote Sensing: Moving Towards the 21st Century, Volume 3 p 1563-1564 Aug. 1988

Avail: NTIS HC A99/MF A01; ESA Publications Division, ESTEC, Noordwijk, Netherlands, \$120 US or 250 Dutch guilders

An airborne microcomputer-based radiometer data acquisition and processing system for mapping the soil moisture content in the top 1 m layer is described. The system consists of two radiometers, a microcomputer system for radiometer data preprocessing and recording on board an aircraft, and software for estimating and mapping the water content in the top 1 m layer using radiometer data and a priori information on hydrophysical properties of soils. Test flights show the potential of the system for near real time mapping of the water content in the top 1 m layer with accuracy 0.05 g/cc if the crop biomass is less than 2 kg/sq m, which is quite suitable for many applications.

ESA

**N89-18781#** Sherbrooke Univ. (Quebec). Centre d'Applications et de Recherches en Teledetection.

**OBSERVATIONS OF THE EFFECT OF GEOMETRIC PROPERTIES OF AGRICULTURAL SOILS ON RADAR BACKSCATTER, FROM C-SAR IMAGES**

A. BEAUDOIN, T. LETOAN (Centre d'Etude Spatiale des Rayonnements, Toulouse, France), and Q. H. J. GWYN *In* ESA, Proceedings of the 1988 International Geoscience and Remote Sensing Symposium (IGARSS) '88 on Remote Sensing: Moving Towards the 21st Century, Volume 3 p 1595-1598 Aug. 1988

Avail: NTIS HC A99/MF A01; ESA Publications Division, ESTEC, Noordwijk, Netherlands, \$120 US or 250 Dutch guilders

An analysis of C-band SAR images, concerning the effects of the geometric properties of agricultural surfaces is presented. The multi-image analysis is made possible by a relative calibration method using a natural extended target (dense forest stands). Quantitative results are obtained for the effect of the soil moisture variation induced by a particular large-scale surface pattern, the look angle relative to row crop direction; and the small-scale roughness. The results show that for soil moisture inversion using airborne SAR images, both look angle and small-scale roughness effect must be accounted for. The experimental results can be

used to validate models aiming at simulating the effects of field geometric properties at incidence angles of spaceborne SARs.

ESA

**N89-18822#** Sheffield Univ. (England). Dept. of Geography.  
**OPTIMAL SAMPLING FOR REMOTE SENSING: ESTIMATING THE REGIONAL MEAN**

P. M. ATKINSON *In* ESA, Proceedings of the 1988 International Geoscience and Remote Sensing Symposium (IGARSS) '88 on Remote Sensing: Moving Towards the 21st Century, Volume 3 p 1793-1796 Aug. 1988 Prepared in cooperation with Rothamsted Experimental Station, Harpenden, United Kingdom (Contract NERC-GT4/86/TLS/47)

Avail: NTIS HC A99/MF A01; ESA Publications Division, ESTEC, Noordwijk, Netherlands, \$120 US or 250 Dutch guilders

The advantages of kriging from samples when estimating the mean value of a property over a region are demonstrated. In an agriculture example, up to 1.7-fold gains in precision are obtained by kriging. The problem of sampling across the rows was ignored as it was expected that such short range periodicity would be averaged within the support. If larger scale periodicities are suspected, for example due to tramline patterns, then the practical solution is to orientate the grid so as to avoid such bias. The main drawback is that the semi-variogram must be known before an optimum scheme can be chosen. The cost of deriving the semivariogram could outweigh any saving due to optimal sampling. In these circumstances a crude estimate might be obtained from archive imagery. If no estimate is available then the investigator should sample as intensively as can be afforded on a regular grid. The errors incurred are less than those obtained by sampling randomly unless the random observations are so far apart as to be spatially independent.

ESA

**N89-18825#** Aston Univ., Birmingham (England). Remote Sensing Unit.

**MONITORING OF AGRO-FORESTRY PRODUCTION SYSTEMS IN THE SUDANO-SAHELIAN ZONE OF WEST AFRICA**

J. E. NICHOL and W. G. COLLINS *In* ESA, Proceedings of the 1988 International Geoscience and Remote Sensing Symposium (IGARSS) '88 on Remote Sensing: Moving Towards the 21st Century, Volume 3 p 1809-1811 Aug. 1988

Avail: NTIS HC A99/MF A01; ESA Publications Division, ESTEC, Noordwijk, Netherlands, \$120 US or 250 Dutch guilders

The reflectance properties of semi-arid land cover types and in particular the contribution to pixel brightness of differing proportions of tree canopy cover as an estimate of woody biomass in semi-arid West African farmland is considered. The very high reflectance of dry red sandy loam soils in all wavebands means that vegetation indices for temperate regions have limited success. Principle component transformation of LANDSAT MSS data has the potential for providing a feasible and practicable method for estimating tree stocks and wood fuel resources in farmlands of the West African Sudan and Sahel zones.

ESA

**N89-18843#** Academy of Sciences (USSR), Moscow. Inst. of Radio Engineering and Electronics.

**EXPERIMENTS IN BULGARIA FOR DETERMINATION OF SOIL MOISTURE IN THE TOP ONE-METER LAYER USING MICROWAVE RADIOMETRY AND A PRIORI INFORMATION**

F. A. MKRTCHJAN, E. A. REUTOV, A. M. SHUTKO, K. G. KOSTOV, M. A. MICHALEV, N. M. NEDELTCHEV, A. Y. SPASOV, and B. I. VICHEV (Bulgarian Academy of Sciences, Sofia.) *In* ESA, Proceedings of the 1988 International Geoscience and Remote Sensing Symposium (IGARSS) '88 on Remote Sensing: Moving Towards the 21st Century, Volume 2 p 665-666 Aug. 1988

Avail: NTIS HC A99/MF A01; ESA Publications Div. ESTEC, Noordwijk, Netherlands, \$120 US or 250 Dutch guilders

The results or airborne experiments conducted in April and July over bare and vegetated fields for determination of soil moisture in the top layer are presented. Radiometric measurements were made at wavelengths of 2.25, 18, and 30 cm. Ground-truth soil moisture measurements were also carried out. The experiments confirm that using airborne dual frequency radiometer systems



operating in the dm-band and a priori information on hydrophysical properties of soils, it is possible to determine the soil moisture profile and the water content in the top 1m layer with accuracy 0.05 g/cc, if the crop biomass is less than 1 kg/sqm and (0.05 to 0.08) g/cc if the crop biomass is more than 2 kg/sqm which is suitable for many applications. ESA

**N89-18844#** Tor Vergata Univ., Rome (Italy). Dipt. di Ingegneria Elettronica.

**COMPARISON BETWEEN MICROWAVE EMISSIVITY AND BACKSCATTERING COEFFICIENT OF AGRICULTURAL FIELDS**

P. FERRAZZOLI, G. SCHIAVON, D. SOLIMINI, G. LUZI, P. PAMPALONI, and S. PALOSCIA (Consiglio Nazionale delle Ricerche, Florence, Italy) *In* ESA, Proceedings of the 1988 International Geoscience and Remote Sensing Symposium (IGARSS) '88 on Remote Sensing: Moving Towards the 21st Century, Volume 2 p 667-672 Aug. 1988 Sponsored in part by the Italian Ministry of Public Education, CNR/PSN, Italy and the Joint Research Centre of the European Communities, Ispra, Italy

Avail: NTIS HC A99/MF A01; ESA Publications Div. ESTEC, Noordwijk, Netherlands, \$120 US or 250 Dutch guilders

Definitions and basic relations which are the basis of active and passive microwave remote sensing systems are recalled. The case of a half space of isotropic scatterers, for which a simple relation between emissivity and backscatter coefficient holds, is considered. For real agricultural fields, the isotropic case is taken as a reference to perform comparisons between results of active and passive systems at X-band. Theoretical results are obtained by modeling the vegetation as an ensemble of small disks overlaying the ground; emissivity and backscatter coefficient for different stages of growth are computed and compared. Experimental results from active and passive systems are considered with reference to both ground-based and airborne measurements. ESA

**N89-18845\*#** National Aeronautics and Space Administration. Goddard Space Flight Center, Greenbelt, MD.

**OBSERVED EFFECTS OF SOIL ORGANIC MATTER CONTENT ON THE MICROWAVE INTENSITY OF SOILS**

T. J. JACKSON (Agricultural Research Service, Beltsville, MD.) and P. E. ONEILL *In* ESA, Proceedings of the 1988 International Geoscience and Remote Sensing Symposium (IGARSS) '88 on Remote Sensing: Moving Towards the 21st Century, Volume 2 p 673-676 Aug. 1988

Avail: NTIS HC A99/MF A01; ESA Publications Div. ESTEC, Noordwijk, Netherlands, \$120 US or 250 Dutch guilders CSCL 08M

In order to determine the significance of organic matter content on the microwave emissivity of soils when estimating soil moisture, field experiments were conducted in which 1.4 GHz microwave emissivity data were collected over test plots of sandy loam soil with different organic matter levels (1.8, 4.0, and 6.1 percent) for a range of soil moisture values. Analyses of the observed data show only minor variation in microwave emissivity due to a change in organic matter content at a given moisture level for soils with similar texture and structure. Predictions of microwave emissivity made using a dielectric model for aggregated soils exhibit the same trends and type of response as the measured data when appropriate values for the input parameters were utilized. ESA

**N89-18846\*#** Texas Univ., Arlington. Wave Scattering Research Center.

**THE LEAF-SHAPE EFFECT ON ELECTROMAGNETIC SCATTERING FROM VEGETATED MEDIA**

M. A. KARAM, A. K. FUNG, A. J. BLANCHARD, and G. X. SHEN *In* ESA, Proceedings of the 1988 International Geoscience and Remote Sensing Symposium (IGARSS) '88 on Remote Sensing: Moving Towards the 21st Century, Volume 2 p 677-680 Aug. 1988

(Contract NAG5-486)

Avail: NTIS HC A99/MF A01; ESA Publications Div. ESTEC, Noordwijk, Netherlands, \$120 US or 250 Dutch guilders CSCL 02F

Using the generalized Rayleigh Gans approximation along with the radiative transfer method, a bistatic backscattering model for a layer of randomly oriented, elliptic-shaped leaves is formulated. Following a similar procedure the bistatic scattering model for a layer of needle-shaped leaves is also developed to simulate coniferous vegetation. The differences between the scattering characteristics of the deciduous and coniferous leaves are illustrated numerically for different orientation and incidence angles. It is found that both like and cross polarizations are needed to differentiate the difference in scattering due to the shapes of the scatterers. The calculated backscattering coefficients are compared with measured values from artificial canopies with circular-shaped leaves. ESA

**N89-18848#** Kanagawa Univ (Japan). Inst. of Space and Astronautical Science.

**MEASUREMENTS OF MICROWAVE BACKSCATTER FROM CONIFERS**

H. HIROSAWA, Y. MATSUZAKA, O. KOBAYASHI, Y. TSUKAGOSHI, M. TANABE, and H. TAKAHASHI *In* ESA, Proceedings of the 1988 International Geoscience and Remote Sensing Symposium (IGARSS) '88 on Remote Sensing: Moving Towards the 21st Century, Volume 2 p 683-684 Aug. 1988

Avail: NTIS HC A99/MF A01; ESA Publications Div. ESTEC, Noordwijk, Netherlands, \$120 US or 250 Dutch guilders

Backscattering characteristics of Japanese cedar, Japanese cypress, and Japanese pine, in C-band (4.0 GHz) for linear and circular polarizations, are described. Depolarization observed in two polarizations, and changes of scattering coefficients of cypress when its leaves were removed, are discussed. ESA

**N89-18857#** Joint Research Centre of the European Communities, Ispra (Italy).

**POST-PROCESSING AIRBORNE SAR DATA FOR MULTITEMPORAL LAND-COVER STUDIES**

H. DEGROOF *In* ESA, Proceedings of the 1988 International Geoscience and Remote Sensing Symposium (IGARSS) '88 on Remote Sensing: Moving Towards the 21st Century, Volume 2 p 721-723 Aug. 1988

Avail: NTIS HC A99/MF A01; ESA Publications Div. ESTEC, Noordwijk, Netherlands, \$120 US or 250 Dutch guilders

The quality analysis and postprocessing chain for Agrisar'86, VARAN-S data is presented. Potential use of the Agrisar'86 data for multitemporal landcover studies was evaluated. Problems on radiometric and geometric quality are addressed and the results of applied restoration and correction procedures presented. The limited use of the data, especially if target characterization by absolute sigma-nought values is demanded, is highlighted. ESA

**N89-18862#** Durham Univ. (England). Dept. of Geological Sciences.

**PREPROCESSING AND ANALYSIS OF AIRBORNE VISIBLE NEAR AND SHORTWAVE INFRARED DATA FOR THE DETECTION OF ALTERATION IN WEATHERED VEGETATED TERRAIN**

S. J. HOOK and T. J. MUNDAY *In* ESA, Proceedings of the 1988 International Geoscience and Remote Sensing Symposium (IGARSS) '88 on Remote Sensing: Moving Towards the 21st Century, Volume 2 p 753-758 Aug. 1988 (Contract NERC-GST/02/126)

Avail: NTIS HC A99/MF A01; ESA Publications Div. ESTEC, Noordwijk, Netherlands, \$120 US or 250 Dutch guilders

The ability of broadband multispectral data obtained using the NS-001 airborne scanner to detect areas of hydrothermal alteration in weathered, vegetated terrain was evaluated. Four techniques developed to enhance alteration in this context were examined: band ratios, log residuals, least-squares residuals, and directed principal components analysis. The first two enhancements which reduce brightness variations due to topography and atmospheric effects are of limited use due to numerous false anomalies resulting

from vegetation. The latter two techniques which attempt to separate vegetation effects from alteration prove more effective enabling the discovery of an area of predominantly agrilic alteration. However, another area of silicic alteration is not detectable.

ESA

**N89-18876#** Department of Agriculture, Beltsville, MD. Remote Sensing Research Lab.

**ESTIMATING ABSORBED RADIATION AND PHYTOMASS FROM MULTISPECTRAL REFLECTANCE OF CORN AND SOYBEANS**

C. S. T. DAUGHTRY /in ESA, Proceedings of the 1988 International Geoscience and Remote Sensing Symposium (IGARSS) '88 on Remote Sensing: Moving Towards the 21st Century, Volume 2 p 821-824 Aug. 1988

Avail: NTIS HC A99/MF A01; ESA Publications Div. ESTEC, Noordwijk, Netherlands, \$120 US or 250 Dutch guilders

Spectral reflectance data of corn and soybeans were highly correlated with leaf area index and absorbed photosynthetically active radiation (PAR). Above ground phytomass and grain yields were predicted with absorbed PAR cumulated during the growing season. The concept of merging spectral and meteorological data represents a viable approach for assessing vegetation and forecasting phytomass and grain production.

ESA

**N89-18878#** Southampton Univ. (England). Dept. of Geography.

**THE DIRECTIONAL REFLECTANCE OF HEATHER CANOPIES: TOWARDS A DESCRIPTIVE MODEL**

E. J. MILTON and E. M. ROLLIN /in ESA, Proceedings of the 1988 International Geoscience and Remote Sensing Symposium (IGARSS) '88 on Remote Sensing: Moving Towards the 21st Century, Volume 2 p 829-832 Aug. 1988 (Contract NERC-GST/02/123)

Avail: NTIS HC A99/MF A01; ESA Publications Div. ESTEC, Noordwijk, Netherlands, \$120 US or 250 Dutch guilders

A simplified model of the angular reflectance of shrub canopies based on field data from a multiband radiometer and a spectroradiometer is presented. Directional reflectance observed at the solar zenith angle for a range of azimuth angles was studied. A marked minimum in reflectance relative to nadir when viewing up-Sun and a localized peak (in visible wavelengths especially), when viewing down-Sun are features characteristic of the heather (*Calluna vulgaris*) canopies studied. These relationships are encapsulated in a simple graphic device, that of an imaginary landscape.

ESA

**N89-18879#** Tokyo Univ. (Japan). Faculty of Engineering.

**A MATHEMATICAL MODEL OF REFLECTANCE AND TRANSMITTANCE OF PLANT LEAVES AS A FUNCTION OF CHLOROPHYLL PIGMENT CONTENT**

N. YAMADA and S. FUJIMURA /in ESA, Proceedings of the 1988 International Geoscience and Remote Sensing Symposium (IGARSS) '88 on Remote Sensing: Moving Towards the 21st Century, Volume 2 p 833-834 Aug. 1988

Avail: NTIS HC A99/MF A01; ESA Publications Div. ESTEC, Noordwijk, Netherlands, \$120 US or 250 Dutch guilders

Reflectance and transmittance of plant leaves were modeled as a function of their chlorophyll pigment content, based on the Kubelka-Munk theory, and modeling of multiple-reflection of light in a leaf which is assumed to be composed of a pile of four layers. The model assumes that the scattering coefficient and the absorption coefficient of Kubelka-Munk theory can be expressed as a linear function of pigment content of a plant leaf. Spectral reflectance and transmittance calculated with this model show very good agreement with measured values. Unmeasurable constants necessary in the calculation were determined by a least squares method. Results are consistent with known botanical data.

ESA

**N89-18880#** New South Wales Univ., Kensington (Australia). Center for Remote Sensing.

**SOIL INFLUENCES ON VEGETATION REFLECTANCE OF A SEMI-ARID SHRUBLAND**

H. D. WILLIAMSON /in ESA, Proceedings of the 1988 International Geoscience and Remote Sensing Symposium (IGARSS) '88 on Remote Sensing: Moving Towards the 21st Century, Volume 2 p 837-840 Aug. 1988 Sponsored in part by Adelaide Univ., Australia

Avail: NTIS HC A99/MF A01; ESA Publications Div. ESTEC, Noordwijk, Netherlands, \$120 US or 250 Dutch guilders

Reflectance data were recorded from nine vegetation species and nine terrain units using a radiometer in a semi-arid shrubland. Many of the vegetation species show distinct spectral responses. Reflectance from vegetation is affected significantly by changes in soil background. No single soil line is applicable for use in vegetation indices which allow for soil background influences, but a perpendicular vegetation index calculated using reflectance data from each soil type reduces the soil background effects significantly.

ESA

**N89-18881#** Edinburgh Univ. (Scotland).

**PROBLEMS IN THE ESTIMATION OF BARLEY YIELDS BY REMOTE SENSING**

G. RUSSELL /in ESA, Proceedings of the 1988 International Geoscience and Remote Sensing Symposium (IGARSS) '88 on Remote Sensing: Moving Towards the 21st Century, Volume 2 p 841-842 Aug. 1988

Avail: NTIS HC A99/MF A01; ESA Publications Div. ESTEC, Noordwijk, Netherlands, \$120 US or 250 Dutch guilders

Grain yield was predicted using only information potentially obtainable from satellite imagery. Above-ground biomass at 20 day intervals, latitude, mean thermal time (above 0 C) from February till June and yield were abstracted from studies on barley. The data cover a wide range of varieties, sowing date (September till May), nitrogen and water status and represent the range of conditions in Europe. Results show that predictions can be seriously in error because biomass on a given date is not a good predictor unless sowing date, date of maturity and growth rate are known. Predictions made using remotely sensed data are further complicated because the timing of development changes with geographical location and variety of crop and because biomass estimates can be inaccurate. Knowledge of the physiology of the crop may allow estimates to be improved.

ESA

**N89-18882#** Roskilde Univ. (Denmark). Inst. of Geography and Computer Science.

**ASSESSMENT OF LAND/SOIL DEGRADATION IN NORTHERN BURKINA FASO**

S. FOLVING /in ESA, Proceedings of the 1988 International Geoscience and Remote Sensing Symposium (IGARSS) '88 on Remote Sensing: Moving Towards the 21st Century, Volume 2 p 843-846 Aug. 1988

Avail: NTIS HC A99/MF A01; ESA Publications Div. ESTEC, Noordwijk, Netherlands, \$120 US or 250 Dutch guilders

Data from LANDSAT MSS were used together with field measurements of spectral reflectance from various surface types to develop a method with which assessment of especially irreversible land degradation can be mapped. Field reconnaissance mappings were carried out and development from 1972 was studied. Principal component analysis was used and there seems to be a very good accordance between the results of the field measurements and the results from LANDSAT data.

ESA

**N89-18883#** New South Wales Univ., Kensington (Australia). Center for Remote Sensing.

**VEGETATION SAMPLING FOR STUDIES USING REMOTELY SENSED DATA**

H. D. WILLIAMSON /in ESA, Proceedings of the 1988 International Geoscience and Remote Sensing Symposium (IGARSS) '88 on Remote Sensing: Moving Towards the 21st Century, Volume 2 p 849-852 Aug. 1988



Avail: NTIS HC A99/MF A01; ESA Publications Div. ESTEC, Noordwijk, Netherlands, \$120 US or 250 Dutch guilders

The requirements of ground vegetation data used in calibrating remotely sensed data and checking the accuracy of the final products of remotely sensed data in vegetation studies are considered. Methods of collecting vegetation samples via a double sampling procedure which involves the training of observers in visual estimation and the calibration of their results are reviewed. The use of reference photographs as an aid in the visual estimation of grassland biomass was tested in the field. This method enables a rapid collection of a large number of samples to be made providing accurate ground data for use in remote sensing studies. The biomass estimates obtained via the double sampling technique are significantly correlated with biomass estimates from clipped samples at the 99 percent confidence level. ESA

**N89-18895#** Joint Research Centre of the European Communities, Ispra (Italy). Lab. for Image Processing.

**IMAGE-BASED ATMOSPHERIC CORRECTION OF MULTITEMPORAL THEMATIC MAPPING DATA FOR AGRICULTURAL LAND COVER CLASSIFICATION**

J. HILL and B. STURM *In* ESA, Proceedings of the 1988 International Geoscience and Remote Sensing Symposium (IGARSS) '88 on Remote Sensing: Moving Towards the 21st Century, Volume 2 p 895-899 Aug. 1988

Avail: NTIS HC A99/MF A01; ESA Publications Div. ESTEC, Noordwijk, Netherlands, \$120 US or 250 Dutch guilders

An approach to the atmospheric correction of Thematic Mapper data is presented, which is based solely on the evaluation of scene information and may, therefore, be considered operational. The method is based on the determination of aerosol optical thickness from histogram minima and/or clear water targets. Atmospheric conditions are assumed constant over the scene, but variation with the Sun-to-satellite scattering angle is accounted for. The environment effect is corrected for each pixel. The accuracy of the method is analyzed with respect to ground measurements and a between-scene comparison of derived target signatures. Results indicate a precision of 10 percent in terms of retrieved inherent target reflectances. Potential applications to the monitoring and classification of agricultural crop systems are outlined. ESA

**N89-18899#** Ghent Univ. (Belgium). Satellite Remote Sensing Research Project.

**THE USE OF SPOT-1 IMAGERY FOR FOREST CLASSIFICATION IN FLANDERS (BELGIUM)**

F. BORRY, B. DEROOVER, R. DEWULF, and R. GOOSSENS *In* ESA, Proceedings of the 1988 International Geoscience and Remote Sensing Symposium (IGARSS) '88 on Remote Sensing: Moving Towards the 21st Century, Volume 2 p 913-916 Aug. 1988

Avail: NTIS HC A99/MF A01; ESA Publications Div. ESTEC, Noordwijk, Netherlands, \$120 US or 250 Dutch guilders

Performance of digital classification and visual interpretation of digitally enhanced monotemporal SPOT images, for identification of tree species is compared. The accuracy of visual interpretation is rarely significantly influenced by enhancement procedure. The only significant effect is attributed to recording date. Interaction between recording date and enhancement procedure is usually not significant. The results indicate that images dating from the beginning of the vegetation period are best suited for forest classification. No significant difference is found between digital classification and visual interpretation accuracies, provided that for each method the images from the best recording are used. The level of classification detail as required for forest management purposes cannot be obtained using monotemporal images. However with the monotemporal approach acceptable results can be obtained for general purposes, e.g., forest area updating. The results of a layered classification procedure indicate the usefulness of multitemporal satellite imagery with high spatial resolution for forest management practice. ESA

**N89-18901#** Roskilde Univ. (Denmark). Dept. of Geography and Computer Science.

**MAPPING OF NATURAL VEGETATION IN NORTH-EAST ZIMBABWE BY MEANS OF LANDSAT THEMATIC MAPPER DATA**

P. ANDERSEN *In* ESA, Proceedings of the 1988 International Geoscience and Remote Sensing Symposium (IGARSS) '88 on Remote Sensing: Moving Towards the 21st Century, Volume 2 p 923-926 Aug. 1988 Sponsored in part by the Danish Research Council of Natural Sciences

Avail: NTIS HC A99/MF A01; ESA Publications Div. ESTEC, Noordwijk, Netherlands, \$120 US or 250 Dutch guilders

Field registrations of 70 stands of natural vegetation were used to determine phytosociological communities, cover abundance, and ecological conditions. Communities were classified with the Two-Way Indicator Species Analysis program. Spectral signatures derived from LANDSAT TM imagery were compared with species composition, cover abundance, pedology, and drainage. Data processing included classifications, principal component analysis, and calculation of vegetation indices. The overall results are poor due to the complex nature of the object and the large area covered. Major factors affecting spectral signatures are variations in species composition, structure, and phenology and shade effects, soil color differences, and algae layers. ESA

**N89-18902#** Hydrological Research Inst., Pretoria (South Africa). Dept. of Water Affairs.

**ESTIMATING THE EXTENT OF IRRIGATED CROPLAND IN A LARGE CATCHMENT USING LANDSAT MSS DATA**

U. LOURENS, B. BROWN, and A. SEED *In* ESA, Proceedings of the 1988 International Geoscience and Remote Sensing Symposium (IGARSS) '88 on Remote Sensing: Moving Towards the 21st Century, Volume 2 p 931-932 Aug. 1988

Avail: NTIS HC A99/MF A01; ESA Publications Div. ESTEC, Noordwijk, Netherlands, \$120 US or 250 Dutch guilders

A training area of 2000 ha, representative of the agriculture in a large catchment was used to generate chromatic signatures. A combination of unsupervised and supervised clustering was applied in different ways to generate and select the set of signatures which best classified irrigated cropland in the training area. The set of signatures chosen was used to classify the entire catchment. The classification was validated by comparing the classified result, obtained in six areas of the catchment, with a ground survey undertaken close to the time of image capture. The extent of irrigated cropland was estimated, per drainage region, and the numerical and spatial accuracies of the classification were determined. ESA

**N89-18917#** Massachusetts Univ., Amherst. Microwave Remote Sensing Lab.

**RADAR BACKSCATTER CHARACTERISTICS OF TREES AT 215 GHZ**

R. M. NARAYANAN, C. C. BOREL, and R. E. MCINTOSH *In* ESA, Proceedings of the 1988 International Geoscience and Remote Sensing Symposium (IGARSS) '88 on Remote Sensing: Moving Towards the 21st Century, Volume 2 p 997-998 Aug. 1988

(Contract DAAG29-85-K-0227)

Avail: NTIS HC A99/MF A01; ESA Publications Div. ESTEC, Noordwijk, Netherlands, \$120 US or 250 Dutch guilders

Millimeter wave backscattering measurements of various tree types during the growing season are presented. A simple model based on geometrical optics shows that the backscatter of deciduous trees can be characterized in terms of three ground truth parameters. The data indicate that the millimeter-wave backscatter increases as deciduous trees become fully foliated, and decreases as leaves drop off during the fall season. Coniferous needle trees are seen to have almost constant backscatter. ESA

**N89-18918#** Texas Univ., Arlington. Wave Scattering Research Center.

**THE EXTINCTION PROPERTIES OF FOREST COMPONENTS**

M. A. KARAM, A. K. FUNG, A. J. BLANCHARD, and C. E. NANCE /in ESA, Proceedings of the 1988 International Geoscience and Remote Sensing Symposium (IGARSS) '88 on Remote Sensing: Moving Towards the 21st Century, Volume 2 p 999-1002 Aug. 1988  
(Contract NAG5-486)  
Avail: NTIS HC A99/MF A01; ESA Publications Div. ESTEC, Noordwijk, Netherlands, \$120 US or 250 Dutch guilders CSCL 02F

The effect of each forest component on the extinction of electromagnetic waves is investigated by modeling the branches with finite cylinders, deciduous leaves with elliptic disks, and coniferous leaves with needles. The inner field is estimated by the field inside an infinitely long cylinder of similar properties for the branches, and by the Shifrin approximation for the leaves. For each forest component analytic expressions were derived for the extinction cross section via the forward scattering theorem and for ohmic and scattered losses. For branches, the variation of the extinction cross section obtained via the forward scattering theorem is illustrated numerically as a function of the branch radius and the imaginary part of its dielectric constant. It is compared with the measurements from a single branch. For the leaves, the forward scattering theorem gives value for the extinction cross section equal to the ohmic cross section. ESA

**N89-18919\*** Jet Propulsion Lab., California Inst. of Tech., Pasadena.

#### APPLICATION OF RADAR POLARIMETRY TO FORESTRY

S. L. DURDEN, H. A. ZEBKER, and J. J. VANZYL /in ESA, Proceedings of the 1988 International Geoscience and Remote Sensing Symposium (IGARSS) '88 on Remote Sensing: Moving Towards the 21st Century, Volume 2 p 1003-1004 Aug. 1988  
Avail: NTIS HC A99/MF A01; ESA Publications Div. ESTEC, Noordwijk, Netherlands, \$120 US or 250 Dutch guilders CSCL 02F

In order to understand L-band multipolarization radar measurements of forested areas, a model for the forest polarization signature was developed. The model is based on backscatter from dielectric cylinders which represent branches and trunks. In the model the Stokes matrices corresponding to several different scattering mechanisms is calculated, combining the results to get the total Stokes matrix. Comparison of model predictions with radar measurements shows that the model can accurately predict the forest polarization signature. ESA

#### **N89-18920#** Michigan Univ., Ann Arbor. Radiation Lab. RADAR POLARIMETRIC OBSERVATIONS OF A TREE CANOPY

F. T. ULABY, M. W. WHITT, and M. C. DOBSON /in ESA, Proceedings of the 1988 International Geoscience and Remote Sensing Symposium (IGARSS) '88 on Remote Sensing: Moving Towards the 21st Century, Volume 2 p 1005-1008 Aug. 1988  
Avail: NTIS HC A99/MF A01; ESA Publications Div. ESTEC, Noordwijk, Netherlands, \$120 US or 250 Dutch guilders

A technique for characterizing the propagation properties of a forest canopy is described. The technique requires the use of a polarimetric scatterometer. A truck-mounted 1.6 GHz polarimetric scatterometer was used from a 19 m high platform to measure the backscattering from a dense canopy of pine trees at an incidence angle of 40 deg. Two sets of measurements were made at each of many spatial locations, one set with and the other without a trihedral corner reflector present on the ground surface underneath the canopy. From the two sets of polarimetric measurements, it was possible to determine the mean values and the statistical distributions of the canopy attenuation factors for horizontal and vertical polarizations. The mean values of the one-way attenuation factors are 9.31 dB for horizontal polarization and 9.16 dB for vertical polarization. ESA

**N89-18947#** Telespazio, S.p.A., Rome (Italy).  
**CROPS RADAR RESPONSES ANALYSIS BASED ON AGRISAR '86 DATA**  
A. FIUMARA, N. PIERDICCA, and M. RICOTTILLI /in ESA,

Proceedings of the 1988 International Geoscience and Remote Sensing Symposium (IGARSS) '88 on Remote Sensing: Moving Towards the 21st Century, Volume 2 p 1131-1132 Aug. 1988  
Sponsored in part by CNR/PNR, Italy  
Avail: NTIS HC A99/MF A01; ESA Publications Div. ESTEC, Noordwijk, Netherlands, \$120 US or 250 Dutch guilders

The utility of multistate and multipolarization synthetic aperture radar (SAR) data for agricultural crops classification is assessed. Divergence as a separability index is used over X-band SAR airborne data to identify class pairs that have poor separability, and to single out the set of channels that will produce acceptable classification results. A discriminant analysis is carried out over the same set of data, and K coefficient is used to evaluate final classification accuracy. Multitemporal observation at VV polarization gives the best classification. ESA

**N89-18948#** Freiburg Univ. (Germany, F.R.). Inst. for Physical Geography and Hydrology.

#### EXTRACTION OF AGRICULTURAL PLANT PARAMETERS FROM MULTITEMPORAL THEMATIC MAPPER (TM) AND X-SAR DATA

W. MAUSER and A. RIEG /in ESA, Proceedings of the 1988 International Geoscience and Remote Sensing Symposium (IGARSS) '88 on Remote Sensing: Moving Towards the 21st Century, Volume 2 p 1133-1137 Aug. 1988  
(Contract BMFT-01-QS-86090; BMFT-01-QS-87033)  
Avail: NTIS HC A99/MF A01; ESA Publications Div. ESTEC, Noordwijk, Netherlands, \$120 US or 250 Dutch guilders

Within the AGRISAR'86 campaign, 4 SAR images were produced of an agricultural area using the VARAN-S X-band SAR. Three TM-scenes were analyzed. Ground truth was gathered on an area of 48 sqkm and the field boundaries were digitized to produce images of the measured plant parameters. After geometric registration, regressions were calculated between sensor data and measured biomass, plant height, and water content of different plant species. Land use classifications were carried out. Results show strong correlations between plant parameters and the ratio between bands 4 and 5 of TM. For the SAR data a separation between cereals and corn is possible using a multitemporal approach. ESA

**N89-18949#** Sheffield Univ. (England).

#### CHANGE DETECTION IN AGRISAR IMAGES

S. QUEGAN, C. YANASSE, S. BLACK, and M. DANSON /in ESA, Proceedings of the 1988 International Geoscience and Remote Sensing Symposium (IGARSS) '88 on Remote Sensing: Moving Towards the 21st Century, Volume 2 p 1139-1140 Aug. 1988  
Avail: NTIS HC A99/MF A01; ESA Publications Div. ESTEC, Noordwijk, Netherlands, \$120 US or 250 Dutch guilders

Synthetic aperture radar (SAR) data at four dates spanning the growing season over a UK site was used to derive multitemporal crop radar cross section signatures. This involves measuring and correcting variations due to the SAR system within single images, and calibrating images gathered at different times. Calibration based on use of point targets, fields of particular crop types, and global measures assuming statistical homogeneity are evaluated. No basis for multitemporal calibration is apparent. ESA

**N89-18950#** European Space Agency. European Space Research and Technology Center, ESTEC, Noordwijk (Netherlands).

#### RADAR SIGNATURE MEASUREMENTS DURING THE AGRISCATT CAMPAIGNS

E. ATTEMA /in its Proceedings of the 1988 International Geoscience and Remote Sensing Symposium (IGARSS) '88 on Remote Sensing: Moving Towards the 21st Century, Volume 2 p 1141-1144 Aug. 1988  
Avail: NTIS HC A99/MF A01; ESA Publications Div. ESTEC, Noordwijk, Netherlands, \$120 US or 250 Dutch guilders

During AGRISCATT, airborne radar campaigns measured the radar echo from agricultural crops, bare soils, and forests as a function of radar frequency, polarization, and incidence angle during

the growing season on several test sites in Europe. During radar coverage, comprehensive ground data collection was carried out. Complementary deployment of airborne scatterometers and imaging radars during AGRISCATT, as well as the ground data collection, are described. ESA

**N89-18951#** Freiburg Univ. (Germany, F.R.). Inst. of Physical Geography and Hydrology.

**CORRELATIONS BETWEEN AGRICULTURAL PLANT PARAMETERS AND MULTITEMPORAL RADAR SCATTEROMETER DATA: FIRST RESULTS FROM THE EUROPEAN AGRISCATT 87 CAMPAIGN**

W. MAUSER and T. GREICHGAUER /in ESA, Proceedings of the 1988 International Geoscience and Remote Sensing Symposium (IGARSS) '88 on Remote Sensing: Moving Towards the 21st Century, Volume 2 p 1145-1149 Aug. 1988  
Avail: NTIS HC A99/MF A01; ESA Publications Div. ESTEC, Noordwijk, Netherlands, \$120 US or 250 Dutch guilders

In the European AGRISCATT 87 campaign ground truth was gathered on plant parameters of several crops. Radar measurements with an airborne multiband scatterometer gave sigma-0 values for 6 frequencies, 4 incidences angles, and 2 polarizations. Correlation calculations between biomass and soil moisture of wheat and corn and the backscatter signals were carried out. For steep incidence angles and several frequencies good correlations with high regression coefficients are found. The measured backscatter values for the different crop types enable, together with a digitized map of the field boundaries and the land use, the production of a synthetic radar image of the area. ESA

**N89-18961#** National Electric Reliability Council, Bangor (Wales). Remote Sensing Application Centre.

**ALTERNATIVE APPROACHES TO THE CLASSIFICATION OF UPLAND SEMI-NATURAL VEGETATION**

B. WYATT, A. JONES, J. SETTLE, and N. DRAKE (Reading Univ., England) /in ESA, Proceedings of the 1988 International Geoscience and Remote Sensing Symposium (IGARSS) '88 on Remote Sensing: Moving Towards the 21st Century, Volume 2 p 1195-1198 Aug. 1988

Avail: NTIS HC A99/MF A01; ESA Publications Div. ESTEC, Noordwijk, Netherlands, \$120 US or 250 Dutch guilders

Visual interpretation of data derived from sensors onboard Earth observation satellites was used quite successfully to identify and map broad units of seminatural upland vegetation. However, when standard supervised classification techniques are applied to such data sets, their overall performance is much worse than results obtained in the lowlands. The use of digital elevation data to suppress the effects of relief allows more efficient information extraction, but overall accuracies are still not very high. Analysis of ecological knowledge-based classifiers shows great potential. The use of spectral mixture modeling differs from traditional classification techniques in producing percentage proportion maps as opposed to regimented class maps where all pixels must belong in a given class. This approach appears well-suited in applications such as the mapping of seminatural vegetation, where boundaries may be arbitrary and where ground cover often approximates to a continuum of different types. ESA

**N89-18966#** Instituut voor Cultuurtechniek en Waterhuishouding, Wageningen (Netherlands).

**THE EFFECT OF SOIL MOISTURE ON REFLECTANCE CHARACTERISTICS OF SALT CRUSTS**

P. B. ROETERS /in ESA, Proceedings of the 1988 International Geoscience and Remote Sensing Symposium (IGARSS) '88 on Remote Sensing: Moving Towards the 21st Century, Volume 2 p 1225-1227 Aug. 1988

Avail: NTIS HC A99/MF A01; ESA Publications Div. ESTEC, Noordwijk, Netherlands, \$120 US or 250 Dutch guilders

In the Western Desert of Egypt small lakes were studied by remote sensing techniques in order to determine groundwater losses by evaporation. Identification of areas where changes in groundwater level occurred; and the combination of LANDSAT TM bands that is most suitable for mapping wet soils in (semi-)arid

areas are also studied. Black and white transparencies in a negative format were used in a color additive viewing system. The color composite of bands 3 (green), 4 (blue) and 7 (red) is described. Digital processing of LANDSAT TM CCT results in spectral absorbance patterns of various soil types that could be used for indicating the relative height of the terrain. Comparison of results obtained with the color additive viewer and through digital image processing shows that for qualitative mapping of soil moisture conditions in playas, the former technique is satisfactory. When the mineral composition of crusts has to be taken into account digital analysis is mandatory. ESA

**N89-19734#** Begeleidingscommissie Remote Sensing, Delft (Netherlands).

**SALINITY MAPPING BASED ON SPOT IMAGES OF THE PUNJAB, PAKISTAN Final Report [ZOUTKARTERING MET BEHULP VAN SPOT-BEELDEN IN DE PUNJAB, PAKISTAN]**

Feb. 1988 48 p In DUTCH Prepared in cooperation with EUROCONSULT B.V., Arnhem, Netherlands Original contains color illustrations

(Contract BCRS-PROJ. CO-1.6)

(BCRS-88-03; ETN-89-93874) Avail: NTIS HC A03/MF A01

Water logging and salinity in an irrigated agriculture area to the west of the Indus were inventoried using satellite images. Advanced image processing apparatus was used for the analysis of multispectral information and texture. Enlargements of false color images allowed a classification resulting in a salinity map. The combination of detailed panchromatic images and multispectral images proves to be very successful. ESA

**N89-19735#** Begeleidingscommissie Remote Sensing, Delft (Netherlands).

**STUDY OF THE USE OF RADAR X-BAND DATA OF BARE SOIL IN A RADAR SCATTERING MODEL [ONDERZOEK NAAR DE TOEPASSING VAN RADAR X-BAND GEGEVENS VAN KALE GROND IN EEN RADARVERSTROOIINGSMODEL]**

M. A. P. VISSERS and J. STOLP Mar. 1988 28 p In DUTCH Original contains color illustrations

(Contract BCRS-PROJ. AO-2.1)

(BCRS-88-04; REPT-2021; ETN-89-93875) Avail: NTIS HC A03/MF A01

The combination of soil data and X-band side looking airborne radar data via a radar scattering was investigated. The radar reflection from the mainly bare soil of a test farm was measured, and samples of the moisture content of the top layer and of the soil roughness were determined. The calibrated radar data and soil data were coupled using a radar scattering model which describes the interaction mechanism radar-bare soil. It is shown that the standard deviation of the differences in height of the surface (i.e., as measure of the roughness) does not provide a correct adaptation in the correlation between radar backscatter and incidence angle of the scatter. A model parameter value of the soil roughness was deduced. The introduction of this value in the model provides a relation between radar backscatter and moisture content via regression, in agreement with previous experiments. ESA

## 02

### ENVIRONMENTAL CHANGES AND CULTURAL RESOURCES

Includes land use analysis, urban and metropolitan studies, environmental impact, air and water pollution, geographic information systems, and geographic analysis.

**A89-20766#**

**LAND USE SUITABILITY CLASSIFICATION USING REMOTE SENSING DATA AND GEOGRAPHIC INFORMATION FOR VOLCANIC REGIONS**

MASAHIRO SETOJIMA, YUKIO AKAMATSU, YASUHIRO UCHIDA (Kokusai Kogyo Co., Ltd., Hino, Japan), and MASAKATSU HORINO (National Land Agency, Tokyo, Japan) IN: Asian Conference on Remote Sensing, 8th, Jakarta, Indonesia, Oct. 22-27, 1987, Proceedings. Bogor, Indonesia, EXSA International, 1987, p. B-6-1 to B-6-13. refs

Land use suitability classification was made by considering volcanic hazard for active volcanic regions of Japan by means of remote sensing data analysis and the overlay processing of various geographic information. Results of the analysis have clarified the optimum forms of land use in the object regions and have provided effective data for formulating land use plans in future. Author

**A89-20792#**

**THE ROLE OF REMOTE SENSING IN GEOGRAPHIC INFORMATION SYSTEMS USING COMPUTER**

MUH. DIMYATI (Ministry of Public Works, Indonesia) and YOSHIO MATSUO (Kyoto University, Japan) IN: Asian Conference on Remote Sensing, 8th, Jakarta, Indonesia, Oct. 22-27, 1987, Proceedings. Bogor, Indonesia, EXSA International, 1987, p. F-8-1 to F-8-7. refs

The role of remote sensing data and remote sensing techniques in a geographic information system (GIS) is discussed, focusing on GISs which use personal computers. The data acquisition, data base management, regional analysis, and mapping systems of a GIS are described. Examples of GIS applications in Indonesia are presented, including critical land estimates in the Toba River Basin and land cover/land use monitoring of the Bandung area. R.B.

**A89-20813#**

**LAND USE AND LAND COVER APPLICATIONS OF LANDSAT MSS DATA**

GAIL D. KELLY (Department of Mapping and Surveying, Brisbane, Australia) and GREG J. E. HILL (Queensland, University, Brisbane, Australia) IN: Asian Conference on Remote Sensing, 8th, Jakarta, Indonesia, Oct. 22-27, 1987, Proceedings. Bogor, Indonesia, EXSA International, 1987, p. P-13-1 to P-13-7. refs

The use of Landsat MSS and TM data for land assessment and management in rural zones is examined. The benefits of remote sensing technology are reviewed. A program to assess the capabilities of Landsat data for mapping land cover and land use patterns across the Waggamba Shire in southern Queensland, Australia is discussed (Hill and Kelly, 1986, 1987). Image processing strategies which make the satellite data more useful for land use and cover mapping are described. R.B.

**A89-20824#**

**SPOT IMAGE INTERPRETATION FOR INFORMATION ON HUMAN SETTLEMENT GROWTH**

VICTOR F. L. POLLE (International Institute for Aerospace Survey and Earth Sciences, Enschede, Netherlands) IN: Asian Conference on Remote Sensing, 8th, Jakarta, Indonesia, Oct. 22-27, 1987, Proceedings. Bogor, Indonesia, EXSA International, 1987, p. Q-14-1 to Q-14-8.

SPOT imagery is used to study the development and population growth of two sections of Bandung, Indonesia and the Almelo/Wierden region of the Netherlands. Methods to prepare SPOT data for interpretation, the use of topographical maps for point selection, and image processing techniques to improve the quality of data are discussed. The results of the experiments are presented and recommendations are made for future research topics. R.B.

**A89-21250**

**CONTRIBUTION OF SECOND-GENERATION LANDSAT TM AND SPOT HRV SATELLITES TO URBAN ANALYSIS (RENNES, FRANCE) [APPORT DES SATELLITES DE DEUXIEME GENERATION LANDSAT TM ET SPOT HRV A L'ANALYSE URBAINE /RENNES, FRANCE/]**

R. BARIOU, L. HUBERT, and F. LE HENAFF (Rennes II, Universite, France) Photo Interpretation (ISSN 0031-8523), vol. 27, Jan.-Feb. 1988, p. 33-35, 37, 39 (7 ff.). In French, English, and Spanish.

**A89-21892\*** National Aeronautics and Space Administration. Langley Research Center, Hampton, VA.

**COMPARISON OF SATELLITE TOTAL OZONE MEASUREMENTS WITH THE DISTRIBUTION OF TROPOSPHERIC OZONE OBTAINED BY AN AIRBORNE UV-DIAL SYSTEM OVER THE AMAZON BASIN**

JACK FISHMAN and EDWARD V. BROWELL (NASA, Langley Research Center, Hampton, VA) (IAMAP, Commission for Atmospheric Chemistry and Global Pollution, International Symposium on Global Atmospheric Chemistry, 6th, Peterborough, Canada, Aug. 23-29, 1987) Tellus, Series B - Chemical and Physical Meteorology (ISSN 0280-6509), vol. 40B, Nov. 1988, p. 393-407. refs

**A89-21931**

**LONG-RANGE TRANSPORT OF GIANT MINERAL AEROSOL PARTICLES**

P. R. BETZER, K. L. CARDER (South Florida, University, Saint Petersburg, FL), R. A. DUCE, J. T. MERRILL, N. W. TINDALE (Rhode Island, University, Narragansett) et al. Nature (ISSN 0028-0836), vol. 336, Dec. 8, 1988, p. 568-571. Research supported by NSF and NOAA. refs

In March 1986 a major dust outbreak in China moved over the North Pacific Ocean and was detected downstream by the Asian Dust Input to the Oceanic System (ADIOS) experiment using changes in particle number, size, and composition. Most striking was the presence of 'giant' silica minerals found in the atmospheric as well as water-column samples at the ADIOS sampling site. Their appearance more than 10,000 km from their source cannot be explained using currently acknowledged atmospheric transport mechanisms. Furthermore, the large wind-blown minerals that dominate the samples are extremely rare in the long-term sedimentary record in the North Pacific. C.D.

**A89-22066**

**LASER SOUNDING OF THE TROPOSPHERE AND THE UNDERLYING SURFACE [LAZERNOE ZONDIROVANIE TROPOSFERY I PODSTILAIUSHCHIEI POVERKHNOSTI]**

V. E. ZUEV, ED. Novosibirsk, Izdatel'stvo Nauka, 1987, 264 p. In Russian. No individual items are abstracted in this volume.

The use of remote laser sounding techniques for the monitoring of the environment is examined. Particular attention is given to the remote measurement of atmospheric-aerosol characteristics; the differential-absorption lidar sounding of meteorological-parameter fields; the use of absorption and Raman spectroscopy techniques to investigate the gas composition of the atmosphere; remote-sensing methods based on nonlinear and coherent optical effects; and the use of lasers to investigate the characteristics of aqueous environments. B.J.

**A89-22213**

**A MODEL FOR THE PROPAGATION OF INDUSTRIAL ATMOSPHERIC POLLUTION REGISTERED ON MULTISPECTRAL EARTH IMAGES [MODEL' RASPROSTRANENIIA PROMYSHLENNYKH ZAGRIAZNENII ATMOSFERY, REGISTRIRUEMYKH NA MNOGOZONAL'NYKH SNIMKAKH ZEMLI]**

T. Z. DVORAK (Akademia Gorniczo-Hutnicza, Krakow, Poland) Issledovanie Zemli iz Kosmosa (ISSN 0205-9614), Sept.-Oct. 1988, p. 35-43. In Russian. refs

This paper describes the results of space imagery interpretation of measurements obtained for a territory near Krakow, Poland, in two spectral bands of the Landsat scanner along the cone axis of smoke plume propagation and also at a right angle to the satellite groundtrack. Densitometry profiles were analyzed to demonstrate the effects of terrain on the propagation of factory-stack smoke. A semiempirical model for pollution propagation cones was developed to illustrate the qualitative interpretation of data. I.S.

**A89-24651#**

**A PROCEDURE FOR LAND AREA CLASSIFICATION USING LANDSAT TM DIGITAL IMAGERY**

SYED GUL MOHAMMED NAQVI, TSUTOMU SUZUKI, IKUO ARAI, and KAZUMA MOTOMURA (University of Electro-Communications, Tokyo, Japan) University of Electro-Communications, Bulletin (ISSN 0493-4253), vol. 1, June 1988, p. 1-9, 11. refs

The categorization and determination of urbanization regions has been studied using Landsat TM data of Chofu city and its surroundings in Japan. The stepwise procedure used for subscene analysis of raw satellite data is explained in this paper. The data are first made geometrically registerable within the UTM mapping coordinate system. The resulting residual error is less than + or - 0.5 pixel. An improved categorization technique for urban land usage and region determination using color composites is described. C.D.

**A89-24849**  
**SOME ASPECTS OF SPACE APPLICATIONS FOR DISASTER MANAGEMENT - THE USE OF SPACE TECHNOLOGY FOR DISASTER WARNING AND FOR DETERMINING THE EFFECTS OF NATURAL DISASTERS**

CHARLES KERPELMAN (UN, Geneva, Switzerland) IN: Space safety and rescue 1986-1987. San Diego, CA, Univelt, Inc., 1988, p. 117-129. (IAF PAPER 86-426)

**A89-27630**  
**USING A TOP-DOWN AND BOTTOM-UP STRATEGY TO ANALYZE HIGH RESOLUTION AERIAL PHOTOGRAPHS OF URBAN AREAS**

DWAYNE PHILLIPS (Louisiana State University, Baton Rouge) IN: International Conference on Industrial and Engineering Applications of Artificial Intelligence and Expert Systems, 1st, Tullahoma, TN, June 1-3, 1988, Proceedings. Volume 2. Tullahoma, TN, University of Tennessee, 1988, p. 1139-1145. refs

**A89-27785**  
**INTERACTIVE IMAGE FEATURE COMPILATION FOR GEOGRAPHIC INFORMATION SYSTEMS**

ROBERT A. SCHOWENGERDT (Arizona, University, Tucson) and RICHARD A. PRIES (Bonneville Power Administration, Portland, OR) IN: Recent advances in sensors, radiometry, and data processing for remote sensing; Proceedings of the Meeting, Orlando, FL, Apr. 6-8, 1988. Bellingham, WA, Society of Photo-Optical Instrumentation Engineers, 1988, p. 305-311. refs

Image processing techniques are described that assist an operator in delineating planimetric features in digital imagery. The techniques are simple, robust and highly efficient, allowing the processing to occur at interactive rates. The operator defines a general path for the feature, for example a road, by moving a cursor along the road. Simultaneously, the computer processes a moving window of pixel data along the direction defined by the operator and produces a centerline for the road. These data are converted into vector form and entered into line sets for subsequent GIS Processing or mapping applications. By combining manual and computer-assisted feature delineation, an efficient, less labor-intensive, more objective feature extraction approach results. An example application of this approach to road mapping in a rural area is presented. Author

**A89-27788**  
**DEFINITION AND DESIGN OF AN OPERATIONAL ENVIRONMENT-MONITORING SYSTEM**

J. C. VENEMA and H. A. VAN INGEN SCHENAU (Nationaal Lucht-en Ruimtevaartlaboratorium, Amsterdam, Netherlands) IN: Recent advances in sensors, radiometry, and data processing for remote sensing; Proceedings of the Meeting, Orlando, FL, Apr. 6-8, 1988. Bellingham, WA, Society of Photo-Optical Instrumentation Engineers, 1988, p. 328-331. Research supported by UN and Ministry of Foreign Affairs of the Netherlands. refs

The definition and design of an operational environment-monitoring system are described. The system supports the principal information demands of the Food and Agriculture Organization of the United Nations by monitoring ecological conditions in Africa. Author

**A89-29371#**  
**MULTISPECTRAL CLASSIFICATION OF LAND USE AT THE RURAL-URBAN FRINGE USING SPOT DATA**

LARRY R. G. MARTIN, PHILIP J. HOWARTH, and GLENN H. HOLDER (Waterloo, University, Canada) Canadian Journal of Remote Sensing (ISSN 0008-2821), vol. 14, Dec. 1988, p. 72-79. refs (Contract NSERC-A-0766)

Municipal authorities and companies providing socio-economic data require information on urban expansion. A study has been undertaken for part of Metropolitan Toronto to determine to what extent information on rural-to-urban land conversion can be obtained through supervised and unsupervised classification of SPOT multispectral data. Results indicate that SPOT imagery does not provide increased classification accuracy over LANDSAT MSS data. Even for an aggregation into the three major land-use groups of under-development, urban, and vegetation, overall classification accuracy for the SPOT imagery is only about 80 percent. Confusion between land-use classes results from the fact that the land-cover classes encountered at the rural-urban fringe are not unique to the different land-use classes. However, visual interpretation of either the image or the classifications shows that the different land uses are clearly delimited. In addition, smaller individual parcels of land can be identified with a greater spatial precision than can be achieved with the LANDSAT imagery. Author

**A89-29437**  
**ACCURACY ASSESSMENT OF LANDSAT-BASED VISUAL CHANGE DETECTION METHODS APPLIED TO THE RURAL-URBAN FRINGE**

LARRY R. G. MARTIN (Waterloo, University, Canada) Photogrammetric Engineering and Remote Sensing (ISSN 0099-1112), vol. 55, Feb. 1989, p. 209-215. Research supported by the Central Mortgage and Housing Corp., University of Waterloo, SSHRC, and NSERC. refs

**A89-30263**  
**WASTELAND IDENTIFICATION IN INDIA USING SATELLITE REMOTE SENSING**

L. R. A. NARAYAN, D. P. RAO, and N. C. GAUTAM (National Remote Sensing Agency, Hyderabad, India) International Journal of Remote Sensing (ISSN 0143-1161), vol. 10, Jan. 1989, p. 93-106. refs

MSS data were used to study wasteland categories in India including salt-affected land, gullied or ravined land, water-logged or marshy land, sandy areas, and snow-covered or glacial areas. Comparing the results to ground survey data, it is shown that the wastelands were identified and mapped with 80-90 percent accuracy. Based on the study, wasteland types in 146 districts have been mapped at 1:50,000 scale using Landsat TM FCC prints made from bands 2, 3, and 4. R.R.

**A89-31891**  
**INTEGRATION OF SPOT DATA IN AN URBAN DATA BANK - LOCATING WORK SITES [INTEGRATION DES DONNEES SPOT DANS UNE BANQUE DE DONNEES URBAINES - LA LOCALISATION DES CHANTIERS]**

C. PEDRON (Toulouse, Mairie, Service Informatique, France) Photo Interpretation (ISSN 0031-8523), vol. 27, Mar.-Apr. 1988, p. 47-49, 51, 52. In French, English, and Spanish.

SPOT-1 images of Toulouse in France obtained on September 23, 1986 and on December 5, 1986 were used to extract information on work sites. Comparison of the images allowed changes (occurring between the dates) in the states of work sites to be determined. It is noted that work sites with areas of less than the 100 sq m pixel size could be correctly detected if the work site environment had sufficient contrast (as in the case of a vegetative area surrounding bare ground). R.R.

**N89-18833\*#** National Aeronautics and Space Administration, Washington, DC.

**REMOTE SENSING OF LAND PROCESSES: SPONSORED PROGRAMS OF STUDY BY THE NATIONAL AERONAUTICS AND SPACE ADMINISTRATION**

G. ASRAR, D. E. WICKLAND, M. BALTUCK, M. J. RUZEK, and R. E. MURPHY *In* ESA, Proceedings of the 1988 International Geoscience and Remote Sensing Symposium (IGARSS) '88 on Remote Sensing: Moving Towards the 21st Century, Volume 3 p 1855-1858 Aug. 1988

Avail: NTIS HC A99/MF A01; ESA Publications Division, ESTEC, Noordwijk, Netherlands, \$120 US or 250 Dutch guilders CSDL 08G

The NASA Land Processes Program consists of four interrelated disciplines which support studying the terrestrial geology, ecology, hydrology, and remote sensing science. The first three represent the space based components of classical science disciplines, while the last discipline is the study of the physics, biology, and chemistry of the land surface as it relates to the interaction of electromagnetic energy with the land surface. ESA

## 03

## GEODESY AND CARTOGRAPHY

Includes mapping and topography.

**A89-22316**

**THE GEOSAT ORBIT ADJUST**

BRUCE SHAPIRO (Ford Aerospace Corp., Seabrook, MD) *Journal of the Astronautical Sciences* (ISSN 0021-9142), vol. 36, Oct.-Dec. 1988, p. 407-424. refs

Geosat is a U.S. Navy gravity gradient stabilized spacecraft which aids geodetics and oceanographic researchers by mapping the earth's shape with a radar altimeter. The transition from the geodetic phase of the mission to the oceanographic phase required modifications of the spacecraft's orbit. The orbital change, implemented as a series of 239 maneuvers comprising over 170,000 seconds of thrusting, was performed during a 37-day period starting October 1, 1986. The subsequent Exact Repeat Mission has, to date, maintained a repeat ground track (+ or - 1 km) for over a year with sigma = 490 meters. Author

**A89-22639#**

**DISPLACEMENT CALCULATIONS FROM GEODETIC DATA AND THE TESTING OF GEOPHYSICAL DEFORMATION MODELS**

P. SEGALL and M. V. MATTHEWS (USGS, Menlo Park, CA) *Journal of Geophysical Research* (ISSN 0148-0227), vol. 93, Dec. 10, 1988, p. 14954-14966. refs

Solutions of the inverse problem of estimating displacements on the earth's surface from repeated geodetic measurements by constrained optimization, its connection with generalized matrix inverses, and current methods such as 'inner coordinate' and 'outer coordinate' are reviewed. In the context of fitting deformation models to geodetic data, a 'model coordinate' solution is introduced that fixes the indeterminate components of the displacement field by minimizing the difference between the computed displacements and those predicted by a geophysical model. This gives an appropriate solution for model assessment. A means to exploit the overdetermination of some geodetic data by decomposing the model residuals from a geometrically redundant network into two orthogonal components is also proposed. This decomposition is also useful in a model assessment. C.D.

**A89-24442#**

**ERRORS OF THE GRAVITATIONAL FIELD DETERMINED BY THE SATELLITE**

RUEY-GANG CHANG (Chung Cheng Institute of Technology, Taoyuan, Republic of China) and CHUN-SUNG CHEN (National

Chiao Tung University, Hsinchu, Republic of China) *Chinese Institute of Engineers, Journal* (ISSN 0253-3839), vol. 11, Nov. 1988, p. 693-700. refs

This paper intends to deal with the needs and requirements that determine the earth's gravitational field with an emphasis on the errors in satellite-derived gravitational fields. An attempt was made to compare the most precise satellite model (GEM-L2) with other models and independent data. A general survey of future satellite missions (GRM, GGM, TSS) is presented with an evaluation of the expected results. Author

**N89-15476\*#** Massachusetts Inst. of Tech., Cambridge. Dept. of Earth, Atmospheric, and Planetary Sciences.

**GEODETIC MEASUREMENT OF DEFORMATION IN CALIFORNIA Ph.D. Thesis**

JEANNE MARIE SAUBER Nov. 1988 219 p

(Contract NAG5-814; NGT-50103; NAG5-459)

(NASA-CR-184604; NAS 1.26:184604) Avail: NTIS HC A10/MF A01 CSDL 08G

The very long baseline interferometry (VLBI) measurements made in the western U.S. since 1979 as part of the NASA Crustal Dynamics Project provide discrete samples of the temporal and spatial deformation field. The interpretation of the VLBI-derived rates of deformation requires an examination of geologic information and more densely sampled ground-based geodetic data. In the first two of three related studies embodying this thesis triangulation and trilateration data measured on two regional networks are processed, one in the central Mojave Desert and one in the Coast Ranges east of the San Andreas fault. At the spatial scales spanned by these local geodetic networks, auxiliary geologic and geophysical data have been utilized to examine the relation between measured incremental strain and the accommodation of strain seen in local geological structures, strain release in earthquakes, and principal stress directions inferred from in situ measurements. In the third study, VLBI data from stations distributed across the Pacific - North American plate boundary zone in the western United States are processed. The VLBI data have been used to constrain the integrated rate of deformation across portions of the continental plate boundary in California and to provide a tectonic framework to interpret regional geodetic and geologic studies. Author

**N89-16207\*#** Ohio State Univ., Columbus. Dept. of Geodetic Science and Surveying.

**REFERENCE COORDINATE SYSTEMS: AN UPDATE. SUPPLEMENT 11**

IVAN I. MUELLER Nov. 1988 63 p

(Contract NSG-5265; RF PROJ. 761054/711055)

(NASA-CR-184764; NAS 1.26:184764) Avail: NTIS HC A04/MF A01 CSDL 08B

A common requirement for all geodetic investigations is a well-defined coordinate system attached to the earth in some prescribed way, as well as a well-defined inertial coordinate system in which the motions of the terrestrial frame can be monitored. The paper deals with the problems encountered when establishing such coordinate systems and the transformations between them. In addition, problems related to the modeling of the deformable earth are discussed. This paper is an updated version of the earlier work, Reference Coordinate Systems for Earth Dynamics: A Preview, by the author. Author

**N89-17371#** Technische Univ., Delft (Netherlands). Dept. of Geodesy.

**AN ALGORITHM FOR ANALYSIS OF PLATE MOTIONS IN CRUST DYNAMICS PROJECT (CDP) NETWORKS Thesis**

R. VANGEIN May 1988 71 p

(B8821606; ETN-89-93326) Avail: NTIS HC A04/MF A01

An algorithm is developed to analyze the motion of rigid lithospheric plates. This algorithm is important for the analysis of the satellite laser ranging network in the east Mediterranean region. In a spherical representation, angular velocity vectors of plates are estimated using baseline extension rates derived from a kinematical plate motion model and baseline extension rates



derived from satellite laser ranging observations. Both covariance matrices are singular due to a loss of rank. A least squares adjustment is used to obtain the angular velocity vectors. Based on the algorithm a program was developed and applied to a worldwide network. ESA

**N89-17935#** Institut fuer Angewandte Geodaesie, Frankfurt am Main (Germany, F.R.).  
**REPORTS ON CARTOGRAPHY AND GEODESY, SERIES 1, NUMBER 100 [NACHRICHTEN AUS DEM KARTEN- UND VERMESSUNGSWESEN, REIHE 1, HEFT NR. 100]**  
 1988 86 p In GERMAN; ENGLISH summary  
 (ISSN-0469-4236; ETN-89-93778) Avail: NTIS HC A05/MF A01

The proximity relations between spatially distributed points in a three-dimensional lattice were established using raster data processing. A digital terrain model was created using triangulation in the raster. A basis for the optimal visual perception of television weather forecast maps was established. A system for the automated construction of panoramic views from digital terrain models was developed. ESA

**N89-19731#** Naval Postgraduate School, Monterey, CA.  
**LOCAL GEOID DETERMINATION USING THE GLOBAL POSITIONING SYSTEM M.S. Thesis**  
 WEI-MING MA Sep. 1988 94 p  
 (AD-A202220) Avail: NTIS HC A05/MF A01 CSCL 08E

A local geoid model to predict the geoid heights in the vicinity of Monterey Bay, California, was developed to use Global Position System (GPS) differential positions and known Mean Sea Level (MSL) with the method of collocation. The local geoid models were based on Rapp's 360 degree x 360 order global geoid model determined from gravity measurements. Control data were adjusted by least squares to solve the parameters in the local geoid model. Also studied were factors that affected the GPS-measured ellipsoid height differences. These included: (1) comparing GPS differencing solutions; (2) standard error of GPS observations; (3) corrections for surface meteorological values; and (4) observation durations for GPS. The data used in this research were taken from GPS measurements on the campus of the Naval Postgraduate School (NPS), an area about 100 m x 630 m, and in an area approximately 15 km x 33 km near Monterey, CA. The time period was from February 5, 1988, to May 12, 1988. The accuracy of the predicted geoid heights is + or - 2 cm if a six-parameter model is used for the larger area, and + or - 2 to 10 mm if a five-parameter model is used for the NPS campus. GRA

**N89-19736#** Technische Univ., Delft (Netherlands).  
**THE GEOMETRY OF GEODETIC INVERSE LINEAR MAPPING AND NONLINEAR ADJUSTMENT Ph.D. Thesis**  
 PETER J. G. TEUNISSEN 1988 188 p Sponsored by The Netherlands Organization for the Advancement of Pure Research (ETN-89-93900) Avail: NTIS HC A09/MF A01

It is shown that every inverse B of a linear map A can be uniquely characterized through the choice of three subspaces, S, C and D. Each of these three subspaces has an interesting interpretation of its own. The consequences of the inverse mapping problem for two- and three-dimensional geodetic networks are shown. The problem of nonlinear adjustment is considered, using a differential geometric approach throughout. Gauss method is analyzed, showing how the extrinsic curvatures of submanifold N affects its local behavior. It is also shown how in some cases the geometry of the problem suggests important simplifications. Typical examples are generalizations of the classical Helmert transformation. ESA

## GEOLOGY AND MINERAL RESOURCES

Includes mineral deposits, petroleum deposits, spectral properties of rocks, geological exploration, and lithology.

**A89-20779#**  
**APPLICATIONS OF IMAGE SCANNING AND PROCESSING IN ROCK SHEAR SURFACE STUDY**  
 SCOTT L. HUANG and ROBERT C. SPECK (Alaska, University, Fairbanks) IN: Asian Conference on Remote Sensing, 8th, Jakarta, Indonesia, Oct. 22-27, 1987, Proceedings. Bogor, Indonesia, EXSA International, 1987, p. D-11-1 to D-11-11. Research supported by the University of Alaska. refs

The possible applications of digital image scanning and processing to rock joint surface studies, including joint surface roughness, are discussed. Rock joint surfaces were artificially created by loading three rock samples uniaxially in a compression testing machine. The image scanning and processing devices used in the study are described. Several image processing functions were tested. It is shown that image scanning techniques may be used to digitize the fine details of joint surfaces created during the deformation of rock or other solid materials. Of the methods tested, it is found that image ratioing is the best technique for automatizing the identification of joint asperity and mineral distribution. The filtering process is best for identifying fracture patterns. R.B.

**A89-20780#**  
**RADAR IMAGERY AS A TOOL FOR MINERAL EXPLORATION - A CASE STUDY OF GOLD MINERALIZATION IN EAST KALIMANTAN**

SUWI JANTO and R. DELINOM (Indonesian Institute of Sciences, Center for Geotechnological Research and Development, Bandung, Indonesia) IN: Asian Conference on Remote Sensing, 8th, Jakarta, Indonesia, Oct. 22-27, 1987, Proceedings. Bogor, Indonesia, EXSA International, 1987, p. D-13-1 to D-13-11. refs

**A89-20781#**  
**THE GEOLOGY OF THE AREA SURROUNDING LAKE KERINCI, INDONESIA AS INTERPRETED THROUGH SIR-B IMAGERIES**

S. HARDJOPRAWIRO and SIDARTO (Geological Research and Development Centre, Bandung, Indonesia) IN: Asian Conference on Remote Sensing, 8th, Jakarta, Indonesia, Oct. 22-27, 1987, Proceedings. Bogor, Indonesia, EXSA International, 1987, p. D-15-1 to D-15-11. refs

**A89-20783#**  
**VOLCANIC ERUPTION MONITORING USING SATELLITE PLATFORM**

ADJAT SUDRADJAT (Directorate General of Geology and Mineral Resources, Indonesia) IN: Asian Conference on Remote Sensing, 8th, Jakarta, Indonesia, Oct. 22-27, 1987, Proceedings. Bogor, Indonesia, EXSA International, 1987, p. D-19-1 to D-19-17.

Remotely sensed imagery is used to monitor the eruptions of the Colo and Galunggung volcanoes in Indonesia. The data and methods used to monitor each volcano are described. A variety of satellite imagery is used in the study, including data from Landsat, the Japanese Geometeorologic satellite (GMS), GOES, NOAA-6, and NOAA-7. It is found that weather satellites, such as NOAA-7 and GMS, are particularly useful for volcano monitoring. R.B.

**A89-20784#**  
**THE USE OF AERIAL PHOTOGRAPHS IN QUATERNARY-VOLCANIC TERRAINS MAPPING**

U. HARTONO and A. BAHARUDDIN (Geological Research and Development Centre, Bandung, Indonesia) IN: Asian Conference on Remote Sensing, 8th, Jakarta, Indonesia, Oct. 22-27, 1987, Proceedings. Bogor, Indonesia, EXSA International, 1987, p. D-23-1 to D-23-15. refs

The use of aerial photography for the stratigraphic classification of the Quaternary Willis volcanic complex in East Java is discussed. The classification is based on the morphostratigraphic concept. The aerial photographs are used to identify the characteristics of the three basic units, or morphocets, in the rocks of the Willis complex. The three morphocets are broken down into eight subdivisions. Geological field mapping is used to support the classification of these subdivisions. R.B.

**A89-20808#**  
**ON GEOLOGY OF SOME DISTRICTS IN CENTRAL INDIA USING LANDSAT IMAGERIES**

V. K. VARKYA (Rani Durgawati University, Jabalpur, India) IN: Asian Conference on Remote Sensing, 8th, Jakarta, Indonesia, Oct. 22-27, 1987, Proceedings. Bogor, Indonesia, EXSA International, 1987, p. P-4-1 to P-4-4. refs

**A89-20817#**  
**CORRELATION OF LANDSAT TM AND AEROMAGNETIC DATA ALONG THE EASTERN MARGIN OF THE CUDDAPAH BASIN, SOUTH INDIA**

K. V. RAVINDRAN (ISRO, Dehra Dun, India) IN: Asian Conference on Remote Sensing, 8th, Jakarta, Indonesia, Oct. 22-27, 1987, Proceedings. Bogor, Indonesia, EXSA International, 1987, p. Q-1-1 to Q-1-8. refs

**A89-20820#**  
**IDENTIFICATION OF GEOLOGICAL FEATURES FROM THEIR SURFACE TEXTURAL PROPERTIES USING OPS MEASUREMENTS**

B. L. DEEKSHATHULU, R. RAMACHANDRAN, K. SRINATH, KIRON K. RAO, R. N. BERA (National Remote Sensing Agency, Hyderabad, India) et al. IN: Asian Conference on Remote Sensing, 8th, Jakarta, Indonesia, Oct. 22-27, 1987, Proceedings. Bogor, Indonesia, EXSA International, 1987, p. Q-6-1 to Q-6-6. refs

The classification of geological surfaces based on differences in the optical power spectra of the surfaces is discussed. The power spectra are sampled to obtain the power spectral energy in different spatial frequency intervals. These data are used as textural features for geological classification. It is found that optical power spectra measurements may be used to separate different surface textures to identify different geological surfaces. R.B.

**A89-20823#**  
**INTEGRATED STUDY OF LANDSAT, AEROMAGNETIC AND BOUGUER GRAVITY ANOMALY DATA FOR GEOLOGICAL APPRAISAL - A CASE STUDY FROM TAMIL NADU, INDIA**

T. V. RAMACHANDRAN (Geological Survey of India, Bangalore) IN: Asian Conference on Remote Sensing, 8th, Jakarta, Indonesia, Oct. 22-27, 1987, Proceedings. Bogor, Indonesia, EXSA International, 1987, p. Q-11-1 to Q-11-6. refs

**A89-20825#**  
**APPLICATION OF REMOTE SENSING FOR HYDROCARBON EXPLORATION ON TIMOR ISLAND, INDONESIA**

ATIK SUARDHY, MULHADIONO (National Indonesian Oil and Gas Co., Jakarta, Indonesia), and F. HEJUWAT (Indonesian Institute of Sciences, Indonesia) IN: Asian Conference on Remote Sensing, 8th, Jakarta, Indonesia, Oct. 22-27, 1987, Proceedings. Bogor, Indonesia, EXSA International, 1987, p. Q-17-1 to Q-17-15. refs

False color IR aerial photography, Landsat data, and a limited amount of field study have been used for geological reconstruction and hydrocarbon exploration on Timor Island in Indonesia. The performance of Landsat data and aerial photographs are compared, focusing on their ability to discriminate between various lithologic units and to identify the nature and magnitude of geologic structures. The benefits of using Landsat data are examined. R.B.

**A89-20827#**  
**STAR-1 HIGH RESOLUTION SYNTHETIC APERTURE RADAR IMAGERY FOR PRECIOUS METAL EXPLORATION**  
 DAVID F. GRANT, WILLIAM C. JEFFERIES, RAYMOND T. LOWRY

(INTERA Technologies, Ltd., Ottawa, Canada), and LAURIE WHITEHOUSE (Pelsart International, Australia) Asian Association on Remote Sensing, Asian Conference on Remote Sensing, 8th, Jakarta, Indonesia, Oct. 22-27, 1987, Paper. 9 p.

SAR data from the STAR-1 system is used to assist in the search for precious metals in Indonesia and Papua New Guinea. The preparation and analysis of the radar images is discussed. The creation of an accurate base image map and the geological evaluation of the region area examined. The process of planning the search for resources and the economic benefits of remote sensing techniques for precious metal exploration are considered. R.B.

**A89-20828#**  
**USEFULNESS OF REMOTE SENSING IN URANIUM EXPLORATION PROGRAMME IN PARTS OF KARNATAKA STATE, INDIA**

S. N. KAK, V. J. KATTI, K. K. ACHAR, N. V. A. S. PERUMAL, and A. C. SARASWAT (Department of Atomic Energy, Atomic Minerals Div., Hyderabad, India) Asian Association on Remote Sensing, Asian Conference on Remote Sensing, 8th, Jakarta, Indonesia, Oct. 22-27, 1987, Paper. 12 p. refs

Landsat and aerial photography images of areas of the Karnataka region of India are used to delimit the target area for high sensitivity airborne gamma-ray spectrometric and magnetic surveys to explore for uranium in the region. The integration of data sets to locate extension zones of geological occurrences is discussed. The Landsat data was analyzed by directional lineament extraction through convolution techniques. Faults, fractures and folds which have significant bearing on mineralizations were isolated through stretching, band ratioing, and color coding. Also, the relationship between structural elements and mineralization is examined. R.B.

**A89-20829#**  
**AIRBORNE GRAVITY AS A SUPPORTING TOOL FOR HYDROCARBON EXPLORATION IN INDONESIA**

B. SIMBOLON, MARWADI ANWAR, and SUDARNO AMRIN (National Indonesian Oil and Gas Co., Jakarta, Indonesia) Asian Association on Remote Sensing, Asian Conference on Remote Sensing, 8th, Jakarta, Indonesia, Oct. 22-27, 1987, Paper. 25 p. refs

This paper reports the results of using an airborne gravity system for hydrocarbon exploration in Indonesia. The measurements were conducted using a modified air gravimeter mounted on a fixed-wing aircraft which flew at 2500-ft height at 90-knot speed. The gravity measurements could be made at every second at any position along the flight line and be tied to known reference stations. Although this method is less accurate than the conventional land-gravity method, the airborne-gravity measurements demand shorter time than the conventional ones, can be used in inaccessible areas of regional scale. The measurements can be used to delineate structural highs and lows which represent sedimentary thickness, an important aspect in hydrocarbon exploration. I.S.

**A89-22215**  
**NEOTECTONIC ZONING OF BELORUSSIA ON THE BASIS OF SPACE DATA [NEOTEKTONICHESKOE RAIONIROVANIE TERRITORII BELORUSSII NA OSNOVE KOSMICHESKOI INFORMATSII]**

V. N. GUBIN, E. A. LEVKOV, and A. K. KARABANOV (Belorusskii Nauchno-Issledovatel'skii Geologorazvedochnyi Institut; AN BSSR, Institut Geokhimii i Geofiziki, Minsk, Belorussian SSR) Issledovanie Zemli iz Kosmosa (ISSN 0205-9614), Sept.-Oct. 1988, p. 50-56. In Russian. refs

The interpretation of space imagery taken over the territory of Belorussia helps to identify earth crust megablocks that were in differentiated motion throughout the neotectonic stage (with net amplitudes of 150-170 m) and smaller blocks that went into motion in the Late Quaternary. Recent vertical movements in Belorussia are only about 2-3 mm per year, and they match the distribution of neotectonic structures. I.S.



## 04 GEOLOGY AND MINERAL RESOURCES

**A89-22216**

**FAULT CLASSIFICATION FOR THE GEOLOGICAL SUPPORT OF THE TUNNEL CONSTRUCTION PROJECT FOR THE CAUCASUS MOUNTAIN-PASS RAILROAD, USING SPACE IMAGES [KLASSIFIKATSIIA RAZLOMOV DLIA INZHENERNO-GEOLOGICHESKOGO OBOSNOVANIIA PROEKTIROVANIIA TUNNELI KAVKAZSKOI PEREVAL'NOI ZHELEZNOI DOROZI S ISPOL'ZOVANIEM S'EMKI IZ KOSMOSA]**

A. P. BGATOV (Vsesoiuznyi Nauchno-Issledovatel'skii Institut Transportnogo Stroitel'stva, Moscow, USSR) Issledovanie Zemli iz Kosmosa (ISSN 0205-9614), Sept.-Oct. 1988, p. 57-63. In Russian. refs

**A89-22217**

**THE PROCEDURE FOR AND THE RESULTS OF THE GEOLOGICAL INTERPRETATION OF PHOTOGRAPHIC IMAGES OF THE BUKHTARMA LINEAMENT ZONE [METODIKA I REZULTATY GEOLOGICHESKOGO DESHIFRIROVANIIA FOTOSNIMKOV BUKHTARMINSKOI LINEAMENTNOI ZONY]**

B. M. CHIKOV, O. A. BAKLANOVA, V. P. GORBENKO, V. N. DEMENT'EV, and V. A. ZABELIN (AN SSSR, Institut Geologii i Geofiziki and Vychislitel'nyi Tsent, Novosibirsk, USSR) Issledovanie Zemli iz Kosmosa (ISSN 0205-9614), Sept.-Oct. 1988, p. 64-70. In Russian.

This paper describes a procedure for geological interpretation of remote images, based on independent multistage decoding of different-scale photographs of a region. The results of geological interpretation of photographic images of the Bukhtarma river basin, Altai, are presented, demonstrating that it was possible to single out the Bukhtarma lineament zone among the tectonic zones of the southwestern Altai. Using this procedure, it was also possible to distinguish subzones of this lineament, characterized by specific geological features. I.S.

**A89-22218**

**DETERMINATION OF RELATIVE CROP AREAS FROM SPECTROMETRIC DATA [OPREDELЕНИЕ OTNOSITEL'NOI PLOSHCHADI, ZANIMAEMOI POSEVOM, PO DANNYM SPEKTROMETRICHESKIKH IZMERENII]**

D. N. MISHEV and R. KH. K'NCHEVA (B'lgarska Akademiia na Naukite, Tsentralna Laboratoria za Kosmicheski Izsledvaniia, Sofia, Bulgaria) Issledovanie Zemli iz Kosmosa (ISSN 0205-9614), Sept.-Oct. 1988, p. 71-75. In Russian. refs

This paper describes a procedure for estimating the percentage of area covered by different crops from spectral reflectance data on a cultivated area. The algorithms that were developed were applied to the chernozem/winter wheat system, demonstrating the validity of the method. The method is accurate and is relatively insensitive to environmental conditions. I.S.

**A89-22223**

**A TOMOGRAPHIC APPROACH TO LINEAMENT IDENTIFICATION ON AERIAL AND SPACE IMAGES [TOMOGRAFICHESKII PODKHOD K VYDELENIU LINEAMENTOV NA AEROKOSMICHESKIKH IZOBRAZHENIIAKH]**

A. S. ALEKSEEV, I. G. KAZANTSEV, and V. P. PIATKIN (AN SSSR, Vychislitel'nyi Tsent, Novosibirsk, USSR) Issledovanie Zemli iz Kosmosa (ISSN 0205-9614), Sept.-Oct. 1988, p. 99-103. In Russian. refs

This paper describes a tomographic procedure, based on a projection optimality criterion, for automatic identification of lineaments on aerial and space images. The lineament-identification software, developed for the SM-4 Omega interactive image processing system, was tested in the processing of real-world imagery. I.S.

**A89-22632**

**EROSIONAL FURROWS FORMED DURING THE LATERAL BLAST AT MOUNT ST. HELENS, MAY 18, 1980  
SUSAN WERNER KIEFFER (USGS, Flagstaff, AZ) and BRADFORD**

STURTEVANT (California Institute of Technology, Pasadena) Journal of Geophysical Research (ISSN 0148-0227), vol. 93, Dec. 10, 1988, p. 14793-14816. Research supported by USGS. refs (Contract NSF EAR-85-12724)

The erosional furrows formed during the lateral blast at Mount St. Helens are addressed here as an example of enhanced erosion by large-scale vortices in a volcanic setting. These erosional features are attributed to scouring by longitudinal vortices resulting from flow instabilities induced by complex topography. The Reynolds number, Mach number, Goertler number, and erosional efficiency of the blast are estimated. C.D.

**A89-22647\*** Jet Propulsion Lab., California Inst. of Tech., Pasadena.

**RELATIVE DATING OF HAWAIIAN LAVA FLOWS USING MULTISPECTRAL THERMAL INFRARED IMAGES - A NEW TOOL FOR GEOLOGIC MAPPING OF YOUNG VOLCANIC TERRANES**

ANNE B. KAHLE, ALAN R. GILLESPIE, ELSA A. ABBOTT, MICHAEL J. ABRAMS, RICHARD E. WALKER (California Institute of Technology, Jet Propulsion Laboratory, Pasadena) et al. Journal of Geophysical Research (ISSN 0148-0227), vol. 93, Dec. 10, 1988, p. 15239-15251. refs

The weathering of Hawaiian basalts in arid and semiarid environments is accompanied by changes in their thermal infrared emittance spectra. The spectral differences can be measured and mapped with multispectral imaging systems. The differences appear to be related to the degree of development, preservation, and alteration of glassy crusts; the oxidation of iron; and the accretion of silica-rich surface veneers. Because the measurements are quantitative and in image format, they are useful for estimating relative ages in geologic mapping of lava flows. In Hawaii this technique is most diagnostic for distinguishing among sparsely vegetated flows less than 1.5 ka in age. Author

**A89-22877**

**THE CRUSTAL FIELD**

C. G. A. HARRISON IN: Geomagnetism. Volume 1. London, Academic Press, Ltd., 1987, p. 513-610. Research supported by NSF, U.S. Navy, and NASA. refs

Studies of the crustal geomagnetic field and magnetic anomalies are reviewed. The instruments used to study magnetic anomalies and the problem of separating the crustal field from the core field are considered. The lineated magnetic anomalies over ocean basins, deep-towed observations of the crustal field made in ocean basins, studies of unlineated magnetic anomalies in ocean basins, and the seamount problem are examined. Continental magnetic anomalies, satellite observations of the earth's magnetic field, and the relation of magnetic properties to the source of the crustal field are discussed. R.B.

**A89-26397#**

**APPLICATION OF LANDSAT MSS AND TM DATA TO GEOLOGICAL RESOURCE EXPLORATION**

KEN M. MORGAN, DAVID G. KOGER (Texas Christian University, Fort Worth), and DONALD R. MORRIS-JONES (Kodak, Inc., Landover, MD) IN: Commercial opportunities in space; Symposium, Taipei, Republic of China, Apr. 19-24, 1987, Technical Papers. Washington, DC, American Institute of Aeronautics and Astronautics, Inc., 1988, p. 361-372. refs

Methods are discussed for using Landsat MSS and TM data with geophysical information producing maps and geochemical studies to delineate structural and geochemical information for hydrocarbon and mineral exploration. MSS and TM data are compared and image processing and interpretation techniques are examined. The process of mapping various geologic features is analyzed, including lithology, lineaments, structures, and tonal anomalies. The importance of selecting the appropriate resolution and enhancement technique for mapping surface indications of subsurface geologic features is emphasized. R.B.

A89-28126

**APPLICATION OF LANDSAT IMAGERY AND SURFICIAL GEOCHEMISTRY TO THE DISCOVERY OF TUNGSTEN SKARN DEPOSITS ASSOCIATED WITH BURIED PLUTONS, YUKON AND NORTHWEST TERRITORIES, CANADA**

W. D. GOODFELLOW (Geological Survey of Canada, Ottawa) and S. ARONOFF (WDL Consultants, Ottawa, Canada) *Geocarto International* (ISSN 1010-6049), vol. 3, Dec. 1988, p. 3-16. refs

A89-29301\* Jet Propulsion Lab., California Inst. of Tech., Pasadena.

**MAPPING IN THE OMAN OPHIOLITE USING ENHANCED LANDSAT THEMATIC MAPPER IMAGES**

M. J. ABRAMS (California Institute of Technology, Jet Propulsion Laboratory, Pasadena), D. A. ROTHERY, and A. PONTUAL (Open University, Milton Keynes, England) *Tectonophysics* (ISSN 0040-1951), vol. 151, 1988, p. 387-401. refs  
(Contract NERC-GR/3/6388)

The level of apparent lithological discrimination possible with Landsat TM images in the Oman are discussed. It is found that by using parts of the short-wavelength IR spectrum, the discrimination revealed by the TM data is sufficiently uniform throughout the Oman ophiolite to produce lithological maps at 1:100,000 scale. Decorrelation stretching of the data produces images in which allows for the recognition of variations in gabbro composition, the identification of small acidic, gabbroic, and ultramafic intrusions, the discrimination of the uppermost mantle from the deeper mantle, the precise location of the Moho, and the delineation of gossans and areas subject to choritic-epidiotic alteration.

R.B.

A89-30116

**DIGITAL PROCESSING OF A LINEAMENT GRID WITH THE AIM OF ANALYZING REGIONAL TECTONIC STRUCTURES OF THE WESTERN HIMALAYAS IN INDIA [TSIFROVAIA OBRABOTKA LINEAMENTNOI SETI S TSEL'IU ANALIZA REGIONAL'NYKH TEKTONICHESKIKH STRUKTUR ZAPADNYKH GIMALAEV V INDII]**

D. K. MISRA (Institut Geologii Gimalaev, Dehra Dun, India), V. M. MORALEV, and O. G. SHEREMET (AN SSSR, Institut Litofery, Moscow, USSR) *Issledovanie Zemli iz Kosmosa* (ISSN 0205-9614), Nov.-Dec. 1988, p. 41-50. In Russian. refs

A89-30118

**RING STRUCTURES OF BURIED PLATFORM AREAS AND THE EVALUATION OF THEIR TECTONIC ACTIVITY ON THE BASIS OF GEOMORPHOLOGICAL DATA [KOL'TSEVYE STRUKTURY ZAKRYTYKH PLATFORMENNYKH TERRITORII I OTSENKA IKH TEKTONICHESKOI AKTIVNOSTI PO GEOMORFOLOGICHESKIM DANNYM]**

O. T. KROTKOVA (Moskovskii Gosudarstvennyi Universitet, Moscow, USSR) *Issledovanie Zemli iz Kosmosa* (ISSN 0205-9614), Nov.-Dec. 1988, p. 57-65. In Russian. refs

A89-30119

**FEATURES OF THE GEOLOGICAL STRUCTURE OF THE POLAR URALS AND THE DISTRIBUTION OF CERTAIN MINERALS, AS EVALUATED ON THE BASIS OF THE INTERPRETATION OF AERIAL AND SPACE PHOTOGRAPHS [OSOBENNOSTI GEOLOGICHESKOGO STROENIIA POLIARNOGO URALA I ZAKONOMERNOSTI RAZMESHCHENIIA NEKOTORYKH POLEZNYKH ISKOPAEMYKH, USTANOVLENNYE S POMOSHCH'IU DESHIFIROVANIYA KOSMICHESKIKH I AEROFOTOSNIMKOV]**

E. V. KUZNETSOV (Vsesoiuznyi Nauchno-Issledovatel'skii Institut Kosmoaerogeologicheskikh Metodov, Leningrad, USSR) *Issledovanie Zemli iz Kosmosa* (ISSN 0205-9614), Nov.-Dec. 1988, p. 66-71. In Russian.

A89-30271\* Open Univ., Milton (England).

**REMOTE SENSING OF EVAPORITE MINERAL ZONATION IN SALT FLATS (SALARS)**

J. E. CHAPMAN, D. A. ROTHERY, A. PONTUAL (Open University, Milton Keynes, England), and P. W. FRANCIS (Lunar and Planetary Institute, Houston, TX) *International Journal of Remote Sensing* (ISSN 0143-1161), vol. 10, Jan. 1989, p. 245-255. Research supported by the Nuffield Foundation. refs  
(Contract NASW-4066)

Compositional zoning within Salar de Atacama and Salar de Llulliallaco has been mapped from Landsat Thematic Mapper (TM) data. The data were enhanced using decorrelation stretching of TM bands 7, 5, and 4, which were considered to possess the majority of the mineralogical information. The resulting 7, 5, 4 (red, green, blue) color composites provide excellent discrimination of evaporite mineral zones within the salar. The interpretation is supported by fieldwork at the Salar de Atacama and spectral considerations. A strong relationship between the mineralogy of a unit and surface roughness was observed in the field, hence there is potential for imaging radar to provide complementary zonal data.

Author

A89-31755

**LARGE-SCALE, LOW-AMPLITUDE BEDFORMS (CHEVRONS) IN THE SELIMA SAND SHEET, EGYPT**

TED A. MAXWELL (Smithsonian Institution, Washington, DC) and C. VANCE HAYNES, JR. (Arizona, University, Tucson) *Science* (ISSN 0036-8075), vol. 243, March 3, 1989, p. 1179-1182. Research supported by the National Geographic Society, and Smithsonian Institution. refs

(Contract NSF EAR-83-12651; NSF EAR-86-07479)

Landsat images of the Selima sand sheet in southwestern Egypt display alternating light and dark chevron-shaped patterns that occur downwind from low scarps and major dune fields. Images acquired between 1972 and 1988 indicate that these features move as discrete bedforms at a rate of up to 500 meters per year. Extremely long-wavelength (130 to 1200 meters), low-amplitude (10 to 30 centimeters) bedforms were measured in the field; the light chevrons seen in the orbital data may be thin accumulations of active sand sheet deposits in the lee of these bedforms. Dark chevrons contain an admixture of coarse-granule lag deposits that are continually winnowed by aeolian erosion on the windward sides of the large bedforms. Sediment transport budgets derived from orbital and field analyses suggest net movement of up to 83,000 cubic meters per year for a single light chevron; such measurements can be used as a check on similar calculations from dunes and other smaller scale features to determine sand transport budgets for large areas of the eastern Sahara.

Author

A89-31887

**GEOLOGICAL MAPPING AND ANALYSIS OF FRACTURING IN THE SOUTH PART OF THE CENTRAL ANTI-ATLAS IN MOROCCO USING A LANDSAT MSS IMAGE [CARTOGRAPHIE GEOLOGIQUE ET ANALYSE DE LA FRACTURATION DU SUD DE L'ANTI-ATLAS CENTRAL /MAROC/ A PARTIR D'UNE IMAGE LANDSAT MSS]**

A. EMRAN, J. CHOROWICZ, B. CERVELLE, N. LYBERIS, G. TAMAIN (Paris VI, Universite, France) et al. *Photo Interpretation* (ISSN 0031-8523), vol. 27, Mar.-Apr. 1988, p. 1-3, 5, 7, 9, 10. In French, English, and Spanish.

R.R.

N89-15439 Purdue Univ., West Lafayette, IN.

**THE APPLICATION OF REMOTE SENSING TO GEOMORPHOLOGICAL MAPPING AND MASS MOVEMENT STUDY IN THE VICINITY OF PROVO, UTAH Ph.D. Thesis**

NABIL SUBHI AL-DAGHASTANI 1987 414 p  
Avail: Univ. Microfilms Order No. DA8807580

Analysis of National High Altitude Photography (NHAP) and LANDSAT Thematic Mapper data on the central Wasatch Range was used to evaluate the relative effectiveness of these products for geomorphological and structural mapping, and to determine the mass movement susceptibility of different landforms. The study area includes portions of the Basin and Range and Middle Rocky Mountains physiographic provinces near Provo, UT, as defined and subdivided into formal sections based on internal

physiographic, structural, and geological elements. The present study subdivides these sections into smaller, discrete sectors and discriminates mappable geomorphological units within each sector. The geomorphic analysis is based on the premise that the land surface consists of units which are convexo-concave and convex-rectilinear in plan; each unit is bounded by slope discontinuities. Geomorphological maps at 1:250,000 and 1:100,000 scale made from LANDSAT TM data and Infrared Aerial Photographs provide basic information on distribution of unstable slopes and sites of previous slope failure. The NHAP aerial photographs provide the most accurate, complete portrayal of terrain, and better mass movement susceptible landforms than does TM data. Dissert. Abstr.

**N89-15446#** Instituto de Pesquisas Espaciais, Sao Jose dos Campos (Brazil). Ministerio da Ciencia e Tecnologia.

**KNOWLEDGE RELATED ASPECTS OF LINEATION AND LINEAMENT EXTRACTION**

PAULO OUVÉRASIMONI, VALTER RODRIGUES, and PEDRO PAULO BDEOLIVEIRA Sep. 1988 14 p Presented at the 5th Simposio Brasileiro de Inteligencia Artificial, Natal, Brazil, 7-11 Nov. 1988 Submitted for publication  
(INPE-4709-PRE/1391) Avail: NTIS HC A03/MF A01

The problem of linear feature extraction from remote sensing images for structural geology analysis is discussed. The linear features extracted give valuable clues to geologists in the identification of the internal structure of the lithosphere. A number of factors may influence the extraction process besides the identification of small textural elements. A knowledge-based approach to develop a vision system for linear feature extraction is proposed for integrating these factors. Author

**N89-15447#** Instituto de Pesquisas Espaciais, Sao Jose dos Campos (Brazil). Lab. Associado de Computacao e Matematica Aplicada.

**USING DIFFERENT SOURCES OF INFORMATION IN AUTOMATED LINEAR FEATURE EXTRACTION FROM REMOTE SENSING DATA**

PAULO OUVÉRASIMONI, VALTER RODRIGUES, and PEDRO PAULO BDEOLIVEIRA Sep. 1988 11 p Presented at the 5th Simposio Brasileiro de Sensoriamento Remoto, Natal, Brazil, 11-15 Oct. 1988  
(INPE-4708-PRE/1390) Avail: NTIS HC A03/MF A01

The extraction of linear features from LANDSAT satellite images for structural geology applications is analyzed. Also discussed is the influence of a number of factors such as sensor type, position of the observer, shadowing and knowledge about dominant structures, over the inference of relief convexity, the detection of linear features and the type of feature. The integration of these factors is then studied in the context of an automated linear feature extraction process under specification and the desirability of a knowledge representation model for combining all the available sources of information that are important for the extraction process is argued. Author

**N89-16199\*#** California Inst. of Tech., Pasadena.  
**COMPARISON OF GPS SURVEYS WITH HISTORICAL TRIANGULATION SURVEYS IN THE SOUTHERN CALIFORNIA BORDERLAND**

FRANK H. WEBB, BRADFORD H. HAGER, and DUNCAN C. AGNEW 1988 13 p

(Contract NAG5-842)  
(NASA-CR-183405; NAS 1.26:183405) Avail: NTIS HC A03/MF A01 CSCL 08B

Global plate models predict about 56 mm/yr of motion between the North American and Pacific plates along the plate boundary in southern California, while geodetic and Holocene geological data suggest only 34 mm/yr on the San Andreas fault. Deformation in the Great Basin does not explain this discrepancy, and it has been suggested that faulting in the offshore of southern California could account for some of the discrepancy. Evidence of deformation in the offshore region of southern California is most abundant in the Santa Barbara Channel. Geological investigations of folding

and faulting in this region, as well as earthquake investigations, indicate north-south shortening across the channel on the order of 10 to 20 mm/yr. The most rapid rates occur to the east of the channel in the Ventura Basin. South of the Santa Barbara Channel, though, evidence for deformation is limited to seismicity studies which are sparse. Seismic events are abundant in this area, but their implication for the amount of deformation in the offshore is unclear. GPS measurements made between June 1986 and May 1988 have been used to obtain vector positions for several stations at which historical first order triangulation observations were performed between the late 1800's and the mid 1900's between the coast of southern California and the nearby offshore islands. By comparing the spheroidal angles obtained from the GPS positions with the the previously observed triangulation data, shear strain rates can be calculated for the region using Frank's method. These results seem to suggest that shear strain deformation occurs in the offshore of southern California as a result of north to north-west shortening. That deformation is most active in the Santa Barbara Channel region and least active between Catalina and San Nicholas islands. Just how much of the missing plate motion can be accounted for by this deformation is not known at this time and will have to await further analysis. Author

**N89-16208#** Geological Survey, Reston, VA. National Mapping Div.

**RESEARCH, INVESTIGATIONS AND TECHNICAL DEVELOPMENTS. NATIONAL MAPPING PROGRAM, 1985-1986**  
SHEILA E. MARTIN, CYNTHIA L. CUNNINGHAM, and MARY E. GRAZIANI 1988 149 p

(USGS-OPEN-FILE-REPT-87-315) Avail: NTIS HC A07/MF A01

This report provides general information on the research, investigations, and technical developments conducted by the U.S. Geological Survey's National Mapping Division. The Division collects, processes, and disseminates geographic, cartographic, and remote sensing information, digital data, and maps for the Nation. It also provides scientific and technical assistance and conducts research in the disciplines of cartography, geography, photogrammetry, remote sensing, surveying, and geodesy. Summaries of selected R and D projects conducted in the Survey's National Mapping Division during 1985 and 1986 are contained in this report, and several longer term research projects reported in the 1983 and 1984 report are brought up to date. The selected bibliography includes citations of papers and reports produced during 1985 and 1986. Primary responsibility for the generation of this report was undertaken by the Office of Research. The report is organized into major subject areas of digital cartography, geodetic surveys, image mapping, image processing, remote sensing, and geographic information systems. It has become evident that the application of digital cartographic concepts leads not only to automated map production, but to the merging and analysis of cartographic and other earth science data in digital form -- the essence of modern geographic information systems. F.M.R.

**N89-17910#** Joint Publications Research Service, Arlington, VA.  
**PRINCIPAL PROBLEMS IN UPGRADING QUALITY AND EFFICIENCY OF GEOLOGICAL SURVEY WORK Abstract Only**  
D. S. BULAYEVSKIY, V. A. VELIKANOV, D. F. VOLODIN, A. S. DRANNIK, V. N. SOLOVITSKIY, and A. A. FRAYBERGER *In its* JPRS Report: Science and Technology. Science and Technology. USSR: Earth Sciences p 2 8 Sep. 1988 Transl. into ENGLISH from *Geologicheskii Zhurnal* (Kiev, USSR), no. 2, Feb. 1988 p 3-12

Avail: NTIS HC A03/MF A01

In many areas the upper horizons have been studied to a much better degree than the deeper horizons, although the latter afford the best possibilities for detecting new mineral deposits. Materials collected during the last 13 years on geological survey work done in the Ukrainian SSR is summarized. This includes the work of 80 survey parties and detachments. The types of work done and its adequacy are discussed in detail. This is followed by a discussion of some of the gaps and inadequacies in this work. Author

**N89-17915#** Joint Publications Research Service, Arlington, VA.  
**ANNULAR AND BLOCK-FOLDED STRUCTURES ON SPACE  
 AND AERIAL PHOTOGRAPHS**

A. A. BAYRAMOV, KH. S. MIRZABEKOV, and A. Z. ABDULLAYEV *In its* JPRS Report: Science and Technology. Science and Technology. USSR: Earth Sciences p 7-8 8 Sep. 1988 Transl. into ENGLISH from Razvedka i Okhrana Nedr (Moscow, USSR), no. 6, Jun. 1988 p 17-20  
 Avail: NTIS HC A03/MF A01

The basin of the middle course of the Terter River, where the Kyzylbulakh ore field is located, is one of the regions in the Lesser Caucasus which has been studied in detail. According to the concepts of most researchers, the basin of the middle course of the Terter River is the point of joining of the Agdam anticlinorium and the northwestern part of the Martunin and Toragaychay synclinoriums. On the basis of geological observations and also a detailed study of space photographs and aerial photographs at different scales, a great many large fragments of Upper Jurassic limestones were detected, displaced in the direction of the Terter River floodplain, and thick alluvial-talus formations filling the Aterk accumulative basin. A study of the blocks and folded structures detected on the photographs shows that the first are a component part of the second. A block structure is expressed quite clearly in the Middle Jurassic formations, cut by longitudinal and transverse faults. Other structures are discussed in detail. Author

**N89-17933#** Harvard Coll. Observatory, Cambridge, MA.  
**RESEARCH IN GEODESY AND GEOPHYSICS BASED UPON  
 RADIO INTERFEROMETRIC OBSERVATIONS OF  
 EXTRAGALACTIC RADIO SOURCES Final Report, 3 Apr. 1988  
 - 15 Jun. 1988**

T. A. HERRING 1 Oct. 1988 80 p  
 (Contract F19628-86-K-0025)  
 (AD-A200958; AFGL-TR-88-0204) Avail: NTIS HC A05/MF A01  
 CSDL 08E

Data is used from the Mark 3 Very-Long-Baseline Interferometry (VLBI) system to study the relative motions of radiotelescopes on the Pacific, North American, and Eurasian plates, and in the deformation zone between the North American and Pacific plates in the California region. These results are in accord with recent geologic plate motion models, and a distributed deformation zone between the North American and Pacific plates. We have carried out a number of studies on the accuracy of the results being obtained with VLBI. The most notable of these studies are of the repeatability of the estimates of 3-D coordinates of the sites for long baselines (approx. 4,000 km), and the effects of calibrations of the wet tropospheric delays using water-vapor radiometers. We have also been studying the usefulness of observations made at very low elevation angles (approx. 4 deg.) for improving the accuracy of VLBI baseline determinations. We have also studied the forced nutations of the Earth which yielded results consistent with the flattening of the core-mantle boundary being about 5 percent greater than that predicted by the assumption of hydrostatic equilibrium within the Earth. The effects of ocean tides and the anelasticity of the mantle on the the forced nutations are not clearly evident in the results, and are still being investigated.

GRA

**N89-18791#** Consiglio Nazionale delle Ricerche, Frascati (Italy).  
**A QUANTITATIVE GEOMORPHOLOGY STUDY OF MAIN  
 CARBONATE MASSIFS OF CENTRAL AND SOUTHERN  
 APENNINES (ITALY) BASED ON A DIGITAL ELEVATIONS  
 ARCHIVE**

M. POSCOLIERI and G. ONORATI (Servizio Geologico d'Italia, Rome.) *In* ESA, Proceedings of the 1988 International Geoscience and Remote Sensing Symposium (IGARSS) '88 on Remote Sensing: Moving Towards the 21st Century, Volume 3 p 1653-1654 Aug. 1988

Avail: NTIS HC A99/MF A01; ESA Publications Division, ESTEC, Noordwijk, Netherlands, \$120 US or 250 Dutch guilders

Thirty-one Apennines carbonate massifs were analyzed using the mean heights archive. The elevation data were obtained from the 1:25,000 scale topographic maps with a grid cell size of 7.5

arc sec longitude, and 10 deg latitude. The data were assembled as digital elevation models and processed in order to compute slope and aspect values and to create derived pictures (filtered images, anaglyphs, block diagrams, etc). The digital images were displayed as false color composites, enhancing the carbonate structures boundaries. For outlined landforms 21 morphometric parameters were calculated and their correlation coefficients matrix was computed. A classification of the 31 structures was carried out by applying a hierarchical cluster analysis method. Two main clusters, relative to the central Apennines large carbonate units and to the southern Apennines massifs, are obtained. Subsets are also identified, including landforms with analogous tectonic setting with respect to the Apennine mounts. ESA

**N89-18792#** New Brunswick Univ., Fredericton. Dept. of Surveying Engineering.

**INTEGRATION OF DIGITAL SATELLITE AND GEOPHYSICAL  
 DATA, HEATH STEELE MINES, NEW BRUNSWICK, CANADA**

M. LODIN and J. G. TORRANCE *In* ESA, Proceedings of the 1988 International Geoscience and Remote Sensing Symposium (IGARSS) '88 on Remote Sensing: Moving Towards the 21st Century, Volume 3 p 1655-1658 Aug. 1988 Sponsored in part by the Canada-New Brunswick Mineral Development Agreement  
 Avail: NTIS HC A99/MF A01; ESA Publications Division, ESTEC, Noordwijk, Netherlands, \$120 US or 250 Dutch guilders

Multidate LANDSAT MSS, LANDSAT TM, and airborne magnetic data were acquired and analyzed in order to augment knowledge of the spatial distribution of sulfide deposits in the Heath Steele Mines area of New Brunswick, Canada. Lineament extraction of the infrared spectral bands was performed using multistep directional filtering procedures. Computer search for multispectral characteristics (signatures) similar to those of mapped rock outcrops were conducted using discrete pixel and areal parameters. Lineament extraction and signature search results were digitally integrated with rasterized magnetic data. Results were used in the creation of fully annotated, continuous tone, MSS and TM base maps; binary color image TM lineament plots; and rock occurrence probability maps. ESA

**N89-18793#** National Remote Sensing Centre, Farnborough (England).

**IMAGE PROCESSING METHODS FOR THE PRESENTATION  
 OF MULTIPLE GEOLOGICAL DATASETS FROM THE ENGLISH  
 LAKE DISTRICT**

A. E. HARDING and M. D. FORREST (Natural Environmental Research Council, London, England) *In* ESA, Proceedings of the 1988 International Geoscience and Remote Sensing Symposium (IGARSS) '88 on Remote Sensing: Moving Towards the 21st Century, Volume 3 p 1659-1662 Aug. 1988 Sponsored in part by the Department of Trade and Industry, London, United Kingdom

Avail: NTIS HC A99/MF A01; ESA Publications Division, ESTEC, Noordwijk, Netherlands, \$120 US or 250 Dutch guilders

Geological datasets for the English Lake District were coregistered and converted to image format. Image enhancement and integration techniques for analyzing the datasets and studying spatial correlations within the database are described. Multispectral LANDSAT TM data over the area is of limited use for lithological discrimination. Single band (TM 5) data however, yields much structural information, and enhancement using directional spatial filtering allows recognition of previously unmapped structures. The TM band 5 imagery and its first order filter derivatives were combined with regional survey data using IHS transforms and stereoscopic view generation techniques, and overlaid with line and polygon information from other exploration datasets. Datasets were combined in a manner which maintains identity of each dataset and the imagery produced demonstrates the power of image presentation for efficient multidata analysis. ESA

**N89-18794#** Open Univ., Milton (England). Dept. of Earth Sciences.

**INTEGRATION OF GEOLOGICAL, GEOPHYSICAL AND REMOTELY SENSED DATA FOR THE SOLWAY BASIN, ENGLAND**

S. A. DRURY and A. S. D. WALKER (Natural Environmental Research Council, Keyworth, England) *In* ESA, Proceedings of the 1988 International Geoscience and Remote Sensing Symposium (IGARSS) '88 on Remote Sensing: Moving Towards the 21st Century, Volume 3 p 1663-1666 Aug. 1988

Avail: NTIS HC A99/MF A01; ESA Publications Division, ESTEC, Noordwijk, Netherlands, \$120 US or 250 Dutch guilders

The synergistic use of low-cost data sets in a common raster format for structural analysis of a small onshore basin in England is discussed. Most useful information stems from aeromagnetic and gravity data, expressed as images enhanced by a variety of image processing methods aimed at expressing the data in a form most readily appreciated by human vision. This involved side-illumination of the geophysical data and pseudo-coloring based on look-up table techniques. The principal data handling method was trend-surface analysis and calculation of nth-order residual images. Most of the known structural attributes of the basin are resolved, together with many previously unknown features affecting the basin's deep architecture. ESA

**N89-18796#** National Remote Sensing Centre, Farnborough (England).

**MONITORING SURFACE MINERAL WORKINGS USING TM AND SPOT**

A. E. HARDING *In* ESA, Proceedings of the 1988 International Geoscience and Remote Sensing Symposium (IGARSS) '88 on Remote Sensing: Moving Towards the 21st Century, Volume 3 p 1671-1673 Aug. 1988

Avail: NTIS HC A99/MF A01; ESA Publications Division, ESTEC, Noordwijk, Netherlands, \$120 US or 250 Dutch guilders

Use of SPOT and TM data for study of mineral workings was assessed using sand and gravel sites. Identification of sand and gravel sites is not feasible because of similarity between within site features and surrounding land covers. Thus to study sites it is necessary to predefine site boundaries. For regional objective study it appears that discrimination of operations within sites is restricted to basic land cover types. If however interpretation of imagery is performed by Mineral Officers with responsibility for the relevant sites much improved discrimination of site operations is possible. Suitable imagery for use by Local Mineral Officers can be produced by combining SPOT panchromatic data with multispectral TM or SPOT XS data through an IHS transform and offers the potential for operational monitoring of mineral sites. ESA

**N89-18818#** Reading Univ. (England). NERC Unit for Thematic Information Systems.

**GEOLOGICAL LINEAMENT DETECTION USING THE HOUGH TRANSFORM**

A. CROSS and G. WADGE *In* ESA, Proceedings of the 1988 International Geoscience and Remote Sensing Symposium (IGARSS) '88 on Remote Sensing: Moving Towards the 21st Century, Volume 3 p 1779-1782 Aug. 1988 (Contract NERC-F60/G6/12)

Avail: NTIS HC A99/MF A01; ESA Publications Division, ESTEC, Noordwijk, Netherlands, \$120 US or 250 Dutch guilders

A system for automatic linear detection based on the Hough transform is described, and its performance when applied to LANDSAT MSS imagery of the East African Rift Valley reported. The method succeeds in detecting the majority of faults with a visual expression in the image, but with a very high rate of commission error. Omission errors are fewer than those resulting from photointerpretation. ESA

**N89-18859#** Dames and Moore International, Twickenham (England).

**ENHANCEMENT OF GLACIAL FRACTURES BY ANALYSIS OF THEMATIC MAPPER DATA: GLEN ROY, SCOTLAND**

P. S. RINGROSE and C. A. DAVENPORT (Strathclyde Univ., Glasgow, Scotland) *In* ESA, Proceedings of the 1988 International Geoscience and Remote Sensing Symposium (IGARSS) '88 on Remote Sensing: Moving Towards the 21st Century, Volume 2 p 741-743 Aug. 1988 Sponsored by the Natural Environment Research Council, London, United Kingdom

Avail: NTIS HC A99/MF A01; ESA Publications Div. ESTEC, Noordwijk, Netherlands, \$120 US or 250 Dutch guilders

Analysis of LANDSAT Thematic Mapper (TM) imagery resulted in the resolution of unidentified features within the glaciated terrain of the Glen Roy area, Scotland. Basement faults and more recent fractures are enhanced best by the processing of Band 4 data (near infrared). A glacial fracture set becomes evident when the dominant structural grain (NE-SW trending lineaments of Caledonian age) is removed by the elimination of the 1st and 2nd principal components of TM bands 2, 3, 4, 5 and 7. The images indicate the location of a NNW-SSE trending lineament across Glen Roy. This feature is identified as a surface fault rupture within glaciated metamorphic bedrock, having moved during glacial and post-glacial times. The trace of this feature (on the imagery) is found to extend beyond the portion which exhibits clear field evidence, and is associated with other similar lineaments not previously identified. The results are discussed in terms of fault activity during late and postglacial times and in terms of present-day seismic hazard. ESA

**N89-18860#** Dundee Univ. (Scotland). Dept. of Applied Physics and Electronic and Manufacturing Engineering.

**INTERPRETING THE GEOLOGY OF GLEN COE USING LANDSAT MSS DATA AND AERIAL PHOTOGRAPHS**

G. A. A. ABDELHAMID and R. A. VAUGHAN *In* ESA, Proceedings of the 1988 International Geoscience and Remote Sensing Symposium (IGARSS) '88 on Remote Sensing: Moving Towards the 21st Century, Volume 2 p 745-746 Aug. 1988

Avail: NTIS HC A99/MF A01; ESA Publications Div. ESTEC, Noordwijk, Netherlands, \$120 US or 250 Dutch guilders

The area around Glen Coe in Scotland was surveyed using LANDSAT MSS and aerial photography. The area exhibits a number of obvious structural features and lithologic units and, even in the presence of considerable vegetation cover and surficial deposits, many linear structures can be observed on the satellite imagery. Structural details can also be delineated on the stereo airphotos and lithologic units and vegetation types can be identified. Field work identified the rock-type distributions, the degree of direct exposure, the variation of plant and peat cover, and the distribution of morainic drift deposits. This area is a classic example of cauldron subsidence and its influence, together with that of several dykes which cut through the older metamorphic rock and the early fault intrusions, show up quite well on enhanced composite images, although little of the ring fault itself can be discerned because of lack of geomorphic expression and the presence of shadows. ESA

**N89-18861#** Terra Investigations and Imaging Ltd., Surrey (England).

**MAJOR CRUSTAL LINEAMENTS ON SEASAT SAR AND THEIR OFF-SHORE EXTENSIONS IN THE UK**

R. L. BEDELL, N. KENYON, and A. SCOON (Institute of Oceanographic Sciences, Wormley, England) *In* ESA, Proceedings of the 1988 International Geoscience and Remote Sensing Symposium (IGARSS) '88 on Remote Sensing: Moving Towards the 21st Century, Volume 2 p 747-750 Aug. 1988

Avail: NTIS HC A99/MF A01; ESA Publications Div. ESTEC, Noordwijk, Netherlands, \$120 US or 250 Dutch guilders

Geological investigations of Seasat synthetic aperture radar (SAR) data delineated rock structures within Britain which have detectable off-shore extensions. The on-shore and off-shore SAR expression of various lineaments are described and criteria for distinguishing hard rock features off-shore from sediments are provided. Guidelines for choosing the appropriate imagery to detect ocean floor features are included. ESA

**N89-18863#** Open Univ., Milton (England). Dept. of Earth Sciences.

**APPLICATIONS OF LANDSAT THEMATIC MAPPER IMAGERY TO THE STUDY OF SUBTLE VARIATIONS IN LITHOLOGY**

A. PONTUAL *In* ESA, Proceedings of the 1988 International Geoscience and Remote Sensing Symposium (IGARSS) '88 on Remote Sensing: Moving Towards the 21st Century, Volume 2 p 761-762 Aug. 1988 Sponsored in part by the Natural Environment Research Council, London, United Kingdom  
 Avail: NTIS HC A99/MF A01; ESA Publications Div. ESTEC, Noordwijk, Netherlands, \$120 US or 250 Dutch guilders

Study of enhanced LANDSAT TM images of several localities in semi-arid to arid regions revealed subtle variations within lithologies the reasons for which were not directly evident in the field. Samples were collected during fieldwork, and laboratory spectra (in the VIS-NIR-SWIR) of fresh and weathered surfaces were studied. Examples from two areas show that, though weathering is ubiquitous, it does not entirely mask real lithological variations due to the primary rock mineralogy. ESA

**N89-18929#** Deutsche Forschungs- und Versuchsanstalt fuer Luft- und Raumfahrt, Oberpfaffenhofen (West Germany). Inst. for Optoelectronics.

**RESULTS OF TECTONIC AND SPECTRAL INVESTIGATIONS IN THE COAST RANGE OF NORTHERN CHILE USING SPECIAL PROCESSED THEMATIC MAPPER (TM) DATA**

M. HAUCK and K. HILLER *In* ESA, Proceedings of the 1988 International Geoscience and Remote Sensing Symposium (IGARSS) '88 on Remote Sensing: Moving Towards the 21st Century, Volume 2 p 1043-1047 Aug. 1988  
 Avail: NTIS HC A99/MF A01; ESA Publications Div. ESTEC, Noordwijk, Netherlands, \$120 US or 250 Dutch guilders

An image processing concept for tectonic and lithological investigations carried out in a desert region using LANDSAT Thematic Mapper and MOMS-01-data was developed. Beside the problems of an enormous alteration zone, caused by temperature and hydrothermal activities, the applicability of processed data for registration of various magmatic series (due to different Fe content) and sedimentary series (due to different CaO and clay content) could be demonstrated. ESA

**N89-18930#** Open Univ., Milton (England). Dept. of Earth Sciences.

**INVESTIGATIONS OF THE CERRO COLORADO PLUTON, NORTHERN CHILE, USING ENHANCED LANDSAT THEMATIC MAPPER IMAGES**

A. PONTUAL *In* ESA, Proceedings of the 1988 International Geoscience and Remote Sensing Symposium (IGARSS) '88 on Remote Sensing: Moving Towards the 21st Century, Volume 2 p 1049-1052 Aug. 1988 Sponsored in part by the Natural Environment Research Council, London, United Kingdom  
 Avail: NTIS HC A99/MF A01; ESA Publications Div. ESTEC, Noordwijk, Netherlands, \$120 US or 250 Dutch guilders

Digitally enhanced Thematic Mapper images of the Cerro Colorado pluton, northern Chile, were studied in conjunction with fieldwork. The imagery displays many internal features which suggest that the intrusion is more complex than previously noted. The bulk of the intrusion is magnetite-rich and laboratory spectra of the fresh surfaces of field samples are severely quenched. Weathering and oxidation of the magnetite reduced the quenching effects thus allowing features due to the primary mineralogy of the rock to be observed in the spectra of the weathered surfaces. ESA

**N89-18931\*#** Jet Propulsion Lab., California Inst. of Tech., Pasadena.

**AUTOMATIC MINERAL MAP GENERATION PROCEDURE FROM IMAGING SPECTROMETER DATA**

M. LEE *In* ESA, Proceedings of the 1988 International Geoscience and Remote Sensing Symposium (IGARSS) '88 on Remote Sensing: Moving Towards the 21st Century, Volume 2 p 1055-1058 Aug. 1988

Avail: NTIS HC A99/MF A01; ESA Publications Div. ESTEC, Noordwijk, Netherlands, \$120 US or 250 Dutch guilders CSDL 08B

An airborne imaging spectrometer collected data for 128 wave length channels covering from near to short wavelength infrared across a 320 m swath, to help obtain a mineral map of an area based on reflectance spectral signatures of the area. Minerals have distinctive crystal structures and chemical contents which can be identified by their light absorption characteristics, and an optimized automatic mineral map generation procedure for imaging spectrometer data was developed. The procedure generates two types of mineral maps, a mineral distribution map showing spatial layout of various minerals and a mineral composition map showing the percentage composition of a selected mineral. ESA

**N89-18932#** Dundee Univ. (Scotland). Dept. of Applied Physics and Electronic and Manufacturing Engineering.

**GEOLOGICAL APPLICATIONS OF THERMAL INFRARED CHARACTERISTICS OF VEGETATION**

A. K. SARAF and A. P. CRACKNELL *In* ESA, Proceedings of the 1988 International Geoscience and Remote Sensing Symposium (IGARSS) '88 on Remote Sensing: Moving Towards the 21st Century, Volume 2 p 1059-1060 Aug. 1988  
 Avail: NTIS HC A99/MF A01; ESA Publications Div. ESTEC, Noordwijk, Netherlands, \$120 US or 250 Dutch guilders

The effect of stress on vegetation and its relationship to the underlying geology was investigated for an area of north-west Scotland using data obtained from an airborne thermal scanner. Stress effects resulting from high concentrations of heavy metals, arising from natural sources, are identified. It is shown that temperature differences in a plant canopy can be used to detect stressed vegetation. ESA

**N89-18933#** Open Univ., Milton (England). Earth Science Dept.  
**IMPROVEMENTS IN THE FORWARD AND INVERSE PRINCIPAL COMPONENT TRANSFORMATIONS FOR GEOLOGICAL MAPPING IN A SEMI-ARID TERRAIN**

G. A. HUNT *In* ESA, Proceedings of the 1988 International Geoscience and Remote Sensing Symposium (IGARSS) '88 on Remote Sensing: Moving Towards the 21st Century, Volume 2 p 1061-1062 Aug. 1988

Avail: NTIS HC A99/MF A01; ESA Publications Div. ESTEC, Noordwijk, Netherlands, \$120 US or 250 Dutch guilders

Methods of principal component analysis (PCA) applied to thematic infrared multispectral scanner and airborne thematic mapper data to aid and improve geological mapping over a complexly folded, heavily lateritized, Archaean peneplain in Western Australia are described. Statistic generation from the entire scene rather than a canonical approach is favored in doing the forward (principal component) transformation. Correlation statistics produce better quality imagery with a greater signal to noise ratio particularly in the lower order PCs, than the covariance-variance statistical method, and works best of all for extremely correlated data. ESA

**N89-18934#** Durham Univ. (England). Dept. of Geological Sciences.

**AN EVALUATION OF SURFACE EMITTANCE AND TEMPERATURE DATA DERIVED FROM THERMAL INFRARED MULTISPECTRAL SCANNER (TIMS) FOR LITHOLOGICAL MAPPING IN WEATHERED VEGETATED TERRAIN: N. QUEENSLAND, AUSTRALIA**

S. J. HOOK, T. J. MUNDAY, A. A. GREEN, and A. R. GABELL *In* ESA, Proceedings of the 1988 International Geoscience and Remote Sensing Symposium (IGARSS) '88 on Remote Sensing: Moving Towards the 21st Century, Volume 2 p 1063-1068 Aug. 1988

(Contract NERC-GST/02/126)

Avail: NTIS HC A99/MF A01; ESA Publications Div. ESTEC, Noordwijk, Netherlands, \$120 US or 250 Dutch guilders

The NASA airborne thermal infrared multispectral scanner (TIMS) was flown over a test site, and data were calibrated and atmospherically corrected. The data were analyzed by two methods



which attempt to separate temperature information from emittance information. The two methods used were the model emittance calculation and thermal log residuals (TLR's). Results suggest that TLR's provide emittance equivalent information in all six TIMS bands compared to the model emittance calculation which only provides emittance information in five bands. The data derived using both methods were geometrically corrected and evaluated for lithological discrimination on the weathered vegetated terrain of the test site. Data from both methods enable mapping of known contacts. ESA

**N89-18935\*#** Carnegie Museum of Natural History, Pittsburgh, PA. Section of Vertebrate Fossils.

**GEOLOGICAL REMOTE SENSING OF PALAEOGENE ROCKS IN THE WIND RIVER BASIN, WYOMING, USA**

L. KRISHTALKA, R. K. STUCKY, and A. D. REDLINE *In* ESA, Proceedings of the 1988 International Geoscience and Remote Sensing Symposium (IGARSS) '88 on Remote Sensing: Moving Towards the 21st Century, Volume 2 p 1069-1072 Aug. 1988 (Contract NAGW-949; NSF BSR-87-09242)

Avail: NTIS HC A99/MF A01; ESA Publications Div. ESTEC, Noordwijk, Netherlands, \$120 US or 250 Dutch guilders CSCL 08G

Remote sensing studies of Palaeogene sediments in the Wind River Basin (Wyoming) were used for mapping stratigraphic units, sedimentary features and facies, and structural patterns. Thematic Mapper principal component images for the central and eastern Wind River Basin along with geological investigations and spectral analyses allowed: mapping of the Fort Union, Wind River, and Wagon Bed formations (Fm) and their subunits; recognition of two subunits in the Wind River Fm, one of which can be traced for 75 km; determination of sediment source and depositional environment of units within the Wind River Fm; correlation of the Wagon Bed Fm across the basin; and apparent confirmation of different sources of volcanic debris in the western and southeastern exposures of the Wagon Bed Fm. ESA

**N89-18936#** Aston Univ., Birmingham (England). Remote Sensing Unit.

**THE USE OF COREGISTERED LANDSAT MSS, TM AND SIR-A IMAGERY FOR LITHOLOGICAL MAPPING**

R. B. OLDFIELD, J. ELGY, and J. A. MORTON *In* ESA, Proceedings of the 1988 International Geoscience and Remote Sensing Symposium (IGARSS) '88 on Remote Sensing: Moving Towards the 21st Century, Volume 2 p 1073-1074 Aug. 1988  
Avail: NTIS HC A99/MF A01; ESA Publications Div. ESTEC, Noordwijk, Netherlands, \$120 US or 250 Dutch guilders

The ways in which coregistered radar and multispectral data can be used for lithological mapping are discussed. A problem with such data sets is handling their large dimensionality. A spectral shape classifier which can efficiently classify highly dimensioned data sets is described. The study area is the La Rioja province of northwest Argentina which is a semi-arid environment with relatively good lithological exposure. ESA

**N89-18973\*#** Cornell Univ., Ithaca, NY. Inst. for the Study of the Continents.

**TECTONICS OF THE CENTRAL ANDES Final Report**

ARTHUR L. BLOOM, BRYAN L. ISACKS, ERIC J. FIELDING, ANDREW N. FOX, and TIMOTHY L. GUBBELS 30 Jan. 1989 13 p

(Contract NAS5-28767)  
(NASA-CR-184683; NAS 1.26:184683) Avail: NTIS HC A03/MF A01 CSCL 08G

Acquisition of nearly complete coverage of Thematic Mapper data for the central Andes between about 15 to 34 degrees S has stimulated a comprehensive and unprecedented study of the interaction of tectonics and climate in a young and actively developing major continental mountain belt. The current state of the synoptic mapping of key physiographic, tectonic, and climatic indicators of the dynamics of the mountain/climate system are briefly reviewed. Author

**OCEANOGRAPHY AND MARINE RESOURCES**

Includes sea-surface temperature, ocean bottom surveying imagery, drift rates, sea ice and icebergs, sea state, fish location.

**A89-20785#**

**SUSPENDED SOLID CLASSIFICATION OF THE JAKARTA BAY**  
ADI SASUTJI (Ministry of Public Works, Remote Sensing Center, Indonesia) *IN:* Asian Conference on Remote Sensing, 8th, Jakarta, Indonesia, Oct. 22-27, 1987, Proceedings. Bogor, Indonesia, EXSA International, 1987, p. E-2-1 to E-2-8. refs

Landsat MSS data were classified using the MLM to analyze suspended solids at the sea surface. The classification was performed on the basis of brightness or 'color' classes. This type of study can be used to assess the degree of erosion, the sediment distribution, upstream conditions, and water quality. K.K.

**A89-20786#**

**THE EXTRACTION OF SEA FISHERY POTENTIAL AREA FROM AIRBORNE OCEAN COLOR RADIOMETER DATA**

SRI UTAMININGSIH NUGROHO (Indonesian National Institute of Aeronautics and Space, Remote Sensing Div., Indonesia) *IN:* Asian Conference on Remote Sensing, 8th, Jakarta, Indonesia, Oct. 22-27, 1987, Proceedings. Bogor, Indonesia, EXSA International, 1987, p. E-4-1 to E-4-16. refs

Airborne Ocean Color Radiometer sea surface reflectance data is used to define the potential area of a sea fishery near Jakarta Bay in Indonesia. The ratio of data at wavelengths of 0.548 and 0.446 microns is used to determine sea surface chlorophyll concentration. Simultaneously collected seatruth data is used with the airborne data to plot the potential sea fishery area. The results are compared to the fish catch rates determined from discussions with fishermen in the region. It is concluded that remote sensing technique can be effectively used to define sea fishery potential areas. R.B.

**A89-20787#**

**THE RETRIEVAL OF SEA SURFACE TEMPERATURE FROM NOAA/AVHRR SATELLITE DATA - COMPARISON BETWEEN SINGH'S AND MCCLAIN'S METHODS**

P. MARDIO, M. KARTASAMITA, A. S. HAPIP, and B. UNTORO (Indonesian National Institute of Aeronautics and Space, Jakarta, Indonesia) *IN:* Asian Conference on Remote Sensing, 8th, Jakarta, Indonesia, Oct. 22-27, 1987, Proceedings. Bogor, Indonesia, EXSA International, 1987, p. E-6-1 to E-6-9. refs

Sea surface temperature near Indonesia is obtained from the thermal IR bands (channel 4 and 5) of NOAA/AVHRR data using the methods of Singh (1984) and McClain (Robinson, 1984, Maul, 1985). The atmospheric correction approaches, computational complexities, and experimental results of the two methods are compared. It is found that although the computations of Singh's method are more complex, it is more useful for Indonesian applications than McClain's method because it includes atmospheric transmittance. Also, Singh's method makes it possible to observe the theoretical water vapor contents of the atmosphere. R.B.

**A89-20788#**

**WATER QUALITY ESTIMATION FROM LANDSAT DATA WITH SPECTRAL AND SEA TRUTH DATA BASE SYSTEM**

ATSUSHI RIKIMARU, TAICHI OSHIMA (Hosei University, Tokyo, Japan), KEISHIN MATSUSHITA, MINORU NAKAJIMA (Omdec Corp., Tokyo, Japan), and HARUTO OKAMOTO (PASCO Corp., Tokyo, Japan) *IN:* Asian Conference on Remote Sensing, 8th, Jakarta, Indonesia, Oct. 22-27, 1987, Proceedings. Bogor, Indonesia, EXSA International, 1987, p. E-7-1 to E-7-8.

Temporal estimates of the water quality of Lake Biwa in the western part of Japan are made using Landsat MSS and sea truth data. The water quality field data and spectral data were

coupled and multiple regression analysis was performed. Highly correlated estimation factors were obtained. The possible applications of this method are discussed. R.B.

**A89-20789#****APPLICATION OF AIRBORNE SCANNERS IN REMOTE SENSING OF SEA**

MINGMING SHEN, PEIFEN MAO, and YONGQI XUE (Chinese Academy of Sciences, Shanghai Institute of Technical Physics, People's Republic of China) IN: Asian Conference on Remote Sensing, 8th, Jakarta, Indonesia, Oct. 22-27, 1987, Proceedings. Bogor, Indonesia, EXSA International, 1987, p. E-8-1 to E-8-7.

The design and maritime applications of a multispectral scanner and an IR/UV scanner developed in China are discussed. The airborne, ground processing, and optical systems of the scanners are described and the main specifications of the scanners are listed. Case studies are presented for the aerial surveillance of sea ice and oil pollution monitoring. R.B.

**A89-20803#****CIRCULATION IN THE EAST ASIAN SEAS FROM SATELLITE AND SHIP DATA**

ABSORNSUDA SIRIPONG (Chulalongkorn University, Bangkok, Thailand) IN: Asian Conference on Remote Sensing, 8th, Jakarta, Indonesia, Oct. 22-27, 1987, Proceedings. Bogor, Indonesia, EXSA International, 1987, p. H-3-1 to H-3-14. refs

During the 1982-1983 peak El Nino/Southern Oscillation episode, sea surface temperature in the western Pacific and East Asian seas regions revealed the eastward expansion of the warm current from western Pacific region. This expansion is observed, using sea surface temperature images from the Geostationary Meteorological satellite from March 1983 to January 1984.

Author

**A89-20804#****COASTLINE MONITORING IN MADURA STRAIT, INDONESIA ON 1972-1985**

IBNU KATAMSI and SRI YUMADIATI (Ministry of Public Works, Remote Sensing Center, Indonesia) IN: Asian Conference on Remote Sensing, 8th, Jakarta, Indonesia, Oct. 22-27, 1987, Proceedings. Bogor, Indonesia, EXSA International, 1987, p. H-9-1 to H-9-8. refs

Landsat MSS color composite images from 1972 and 1985 are used to monitor the coastline of the Madura Strait in Indonesia. Suspended solid estimates are made for both images and the suspended solid components are classified. The results are used to describe geomorphology of the region, focusing on coastal deltaic sediments and slightly eroded coastal escarpment. R.B.

**A89-20805#****THE PRELIMINARY STUDY ON CORRELATION BETWEEN SATELLITE INFORMATION AND BOTTOM TRAWLING GROUND IN THE EAST CHINA SEA AND THE YELLOW SEA**

SHIXING HAN and JIANHUA SHEN (East China Sea Fisheries Research Institute, Shanghai, People's Republic of China) IN: Asian Conference on Remote Sensing, 8th, Jakarta, Indonesia, Oct. 22-27, 1987, Proceedings. Bogor, Indonesia, EXSA International, 1987, p. H-11-1 to H-11-12.

**A89-20810#****NEW TECHNOLOGY FOR DISPLAYING OF NOAA AVHRR THERMAL BAND IMAGE**

TSUKASA HOSOMURA and RYOSHI NAKANO (Tokai University, Tokyo, Japan) IN: Asian Conference on Remote Sensing, 8th, Jakarta, Indonesia, Oct. 22-27, 1987, Proceedings. Bogor, Indonesia, EXSA International, 1987, p. P-8-1 to P-8-5.

A method for extracting and displaying sea surface temperature from NOAA/AVHRR imagery is presented. A three-dimensional displaying technique is used to produce a pseudocolor display in which the fine structures of sea currents are clearly visible. Examples of images produced by the method are presented.

R.B.

**A89-20925****DISTRIBUTION AND VARIATIONS OF OCEANIC CARBON DIOXIDE IN THE WESTERN NORTH PACIFIC, EASTERN INDIAN, AND SOUTHERN OCEAN SOUTH OF AUSTRALIA**

HISAYUKI INOUE and YUKIO SUGIMURA (Meteorological Research Institute, Tsukuba, Japan) Tellus, Series B - Chemical and Physical Meteorology (ISSN 0280-6509), vol. 40B, Sept. 1988, p. 308-320. refs

The partial pressure of CO<sub>2</sub> in surface seawater was measured to determine its time and space variation in the western North Pacific, eastern Indian, and Southern Ocean south of Australia during 1968-69, 1983, 1984, and 1987. It was found that the partial pressure of CO<sub>2</sub> was high in high latitudes, coastal, and equatorial regions, and low in the subtropics. Periodicities during the annual cycles were found off the coast of Japan, caused by variations in seawater temperature, vertical mixing, and biological activities. The measurements obtained in the boreal winters of 1969 and 1984 suggest an increase in the partial pressure of CO<sub>2</sub>, due to the enhancement of CO<sub>2</sub> flux from air to sea. R.B.

**A89-21798****A SURFACE-WAVE STUDY OF THE PACIFIC OCEAN BASIN**

TA-LIANG TENG and CHUNG-HUEI CHAO (Southern California, University, Los Angeles, CA) Geophysical Journal (ISSN 0952-4592), vol. 95, Dec. 1988, p. 503-521. refs (Contract NSF EAR-80-25723; NSF EAR-83-13678; F19628-85-K-0018)

The crustal and upper-mantle structure beneath the Pacific Ocean basin is mapped using group velocity dispersion data from Rayleigh waves. The data is from the Global Digital Seismic Network, and provides dispersion information of a period range from 15 to 300 s. The method of Feng and Teng (1983) for subdividing the medium into geometric grids that permit objective inversion. A stochastic inversion is performed on the measured mixed-path dispersion data to provide pure-path data for each grid element. A second generalized inversion is applied to the pure-path data, yielding the velocity structure of the crust and upper mantle for each grid element. The velocity structures are combined to provide a three-dimensional view. The structure of the basin is described in detail and maps of the structure are presented. R.B.

**A89-22000\***

Jet Propulsion Lab., California Inst. of Tech., Pasadena.

**SEASAT - RESULTS OF THE MISSION**

ROBERT H. STEWART (California Institute of Technology, Jet Propulsion Laboratory, Pasadena; California, University, La Jolla) American Meteorological Society, Bulletin (ISSN 0003-0007), vol. 69, Dec. 1988, p. 1441-1447. refs

The scientific results of the Seasat mission are reviewed, including altimeter, scatterometer, microwave radiometer, and imaging radar studies. The analyses of Seasat data showed that global calibrations of satellite observations are much more accurate than measurements made at points on the ocean. It is found that the accuracy of satellite measurements of a particular variable are improved if the variable is measured by different instruments on the same satellite. The results suggest that important oceanographic variables can be mapped from space with accuracies required by climatological and scientific studies. R.B.

**A89-22210****DETERMINATION OF THE SPECTRUM OF ENERGY-CONTAINING SURFACE WAVES FROM A SUN-GLITTER IMAGE [OPREDELENIE SPEKTRA ENERGOESUSHCHIKH POVERKHNOSTNYKH VOLN PO IZOBRAZHENIIU SOLNECHNOGO BLIKA]**

A. N. BOL'SHAKOV, V. M. BURDIUGOV, S. A. GRODSKII, and V. N. KUDRIAVTSEV (AN USSR, Morskoi Gidrofizicheskii Institut, Sevastopol, Ukrainian SSR) Issledovanie Zemli iz Kosmosa (ISSN 0205-9614), Sept.-Oct. 1988, p. 11-18. In Russian. refs

A procedure is described for calculating the spectrum of energy-containing sea-surface waves from the radiance variations in a sun-glitter image. The equation makes it possible to retrieve



the spectrum of surface elevations from the radiance variations, using the characteristics of the radiance trend in a remote-image fragment. An example is presented in which the elevation spectrum was derived from an aerial photograph obtained at a height of 3120 m. I.S.

**A89-22224**  
**PROCEDURES FOR THE DETERMINATION OF GEOPHYSICAL PARAMETERS FROM SPACEBORNE MICROWAVE POLARIMETER MEASUREMENTS [METODY OPREDELENIIA GEOFIZICHESKIKH PARAMETROV PO SVCH-RADIOMETRICHESKIM POLIARIZATSIONNYM IZMERENIAMI SO SPUTNIKOV]**

A. A. VLASOV, S. T. EGOROV, and V. A. PLIUSHCHEV  
 Issledovanie Zemli iz Kosmosa (ISSN 0205-9614), Sept.-Oct. 1988, p. 104-110. In Russian. refs

This paper describes procedures for estimating such geophysical parameters as the sea surface emissivity, integral cloud absorptivity, mean slope of a rugged terrain, and complex permittivity of the underlying surface from brightness temperature measurements by a microwave polarimeter. Using digitally processed Cosmos-1151 microwave polarization measurements, these geophysical constants were estimated and compared with literature data. The accuracies of these estimates are given. I.S.

**A89-22583**  
**OCEAN WAVE SPECTRA DERIVED FROM SHUTTLE IMAGING RADAR-B IMAGERY AND SURFACE MEASUREMENTS**

TOSHIO IGUCHI (Okinawa Radio Wave Observatory, Japan), HIDEYUKI INOMATA, HARUNOBU MASUKO, and NOBUYOSHI FUGONO (Ministry of Posts and Telecommunications, Communications Research Laboratory, Tokyo, Japan) Journal of Geophysical Research (ISSN 0148-0227), vol. 93, Dec. 15, 1988, p. 15367-15373. refs

During the Shuttle Imaging Radar-B (SIR-B) mission in October 1984, synthetic aperture radar (SAR) images were taken off the coast of Japan. Wave spectra derived from SIR-B imagery were compared with simultaneous wave buoy observations. Waves at the time of flight were nearly perpendicular to the SAR flight direction and were composed of two major systems: a swell of about 200-m wavelength and wind waves with 70-m wavelength. Both the swell and wind wave peaks were identifiable in the SAR image spectrum after stationary response correction. Peak frequencies derived from SIR-B images and from the wave gauge agreed satisfactorily. However, the relative magnitudes of the peaks are not in accordance with the surface measurements. Possible reasons for the disagreement are discussed. Author

**A89-22584** Johns Hopkins Univ., Laurel, MD.  
**COMPARISON OF SHUTTLE IMAGING RADAR-B OCEAN WAVE IMAGE SPECTRA WITH LINEAR MODEL PREDICTIONS BASED ON AIRCRAFT MEASUREMENTS**

FRANK M. MONALDO (Johns Hopkins University, Laurel, MD) and DAVID R. LYZENGA (Delaware University, Newark) Journal of Geophysical Research (ISSN 0148-0227), vol. 93, Dec. 15, 1988, p. 15374-15388. Research supported by NASA and U.S. Navy. refs

During October 1984, coincident Shuttle Imaging Radar-B synthetic aperture radar (SAR) imagery and wave measurements from airborne instrumentation were acquired. The two-dimensional wave spectrum was measured by both a radar ocean-wave spectrometer and a surface-contour radar aboard the aircraft. In this paper, two-dimensional SAR image intensity variance spectra are compared with these independent measures of ocean wave spectra to verify previously proposed models of the relationship between such SAR image spectra and ocean wave spectra. The results illustrate both the functional relationship between SAR image spectra and ocean wave spectra and the limitations imposed on the imaging of short-wavelength, azimuth-traveling waves. Author

**A89-22585\*** Saint John's Coll., Annapolis, MD.  
**OCEAN WAVE DIRECTIONAL SPECTRA AND WAVE-CURRENT INTERACTION IN THE AGULHAS FROM THE SHUTTLE IMAGING RADAR-B SYNTHETIC APERTURE RADAR**

D. E. IRVINE (Saint John's College, Annapolis, MD) and D. G. TILLEY (Johns Hopkins University, Laurel, MD) Journal of Geophysical Research (ISSN 0148-0227), vol. 93, Dec. 15, 1988, p. 15389-15401. Research supported by NASA. refs

SIR-B synthetic aperture radar ocean-wave spectra for a 200-km pass crossing the Agulhas current off the coast of Africa are analyzed. A significant enhancement of one spectral peak along the northern edge of the current is attributed both to amplification of the waves by refraction-dominated wave-current interaction and to transient specular backscatter contributions spatially correlated to the waves. Author

**A89-22586**  
**VALIDATION OF A SYNTHETIC APERTURE RADAR OCEAN WAVE IMAGING THEORY BY THE SHUTTLE IMAGING RADAR-B EXPERIMENT OVER THE NORTH SEA**

CLAUS BRUENING (European Centre for Medium Range Weather Forecasts, Reading, England), WERNER ALPERS (Bremen, Universitaet, Federal Republic of Germany), LIANA F. ZAMBRESKY (European Centre for Medium Range Weather Forecasts, Reading, England; GKSS-Forschungszentrum Geesthacht GmbH, Federal Republic of Germany), and DAVID G. TILLEY (Johns Hopkins University, Laurel, MD) Journal of Geophysical Research (ISSN 0148-0227), vol. 93, Dec. 15, 1988, p. 15403-15425. refs (Contract BMFT-01-QS-86174; N00014-83-G-0126)

SAR image intensity spectra measured during the SIR-B mission (October 6 and October 8, 1984) over the North Sea were compared with an ocean wave spectra hindcast by a third-generation wave prediction model (WAMODEL). It was found that, while the hindcast ocean wave spectra had only single peaks, most of the measured SAR image spectra of October 6 showed double peaks. It is shown that the double peaks are generated by the SAR imaging mechanism, when the SAR MTF consisting of the sum of the complex real aperture radar (RAR) MTF and the velocity bunching MTF has a strong minimum near the range direction, by which the wave spectrum is cut into two. The azimuth angle at which this minimum occurs depends strongly on the phase of the RAR MTF. I.S.

**A89-22591#**  
**UPWELLING OFF THE GULFS OF PANAMA AND PAPAGAYO IN THE TROPICAL PACIFIC DURING MARCH 1985**

RICHARD LEGECKIS (NOAA, National Environmental Satellite, Data and Information Service, Washington, DC) Journal of Geophysical Research (ISSN 0148-0227), vol. 93, Dec. 15, 1988, p. 15485-15489. Research supported by NOAA. refs

**A89-22592**  
**INERTIAL WIND PATH AND SEA SURFACE TEMPERATURE PATTERNS NEAR THE GULF OF TEHUANTEPEC AND GULF OF PAPAGAYO**

ALLAN J. CLARKE (Florida State University, Tallahassee) Journal of Geophysical Research (ISSN 0148-0227), vol. 93, Dec. 15, 1988, p. 15491-15501. refs (Contract NSF OCE-85-15979; NSF OCE-85-00669)

**A89-22593**  
**A SIMULATION OF THE GLOBAL OCEAN CIRCULATION WITH RESOLVED EDDIES**

ALBERT J. SEMTNER, JR. (U.S. Naval Postgraduate School, Monterey, CA) and ROBERT M. CHERVIN (National Center for Atmospheric Research, Boulder, CO) Journal of Geophysical Research (ISSN 0148-0227), vol. 93, Dec. 15, 1988, p. 15502-15522. Research supported by DOE. refs (Contract NSF ATM-87-05980)

This paper describes a multilevel primitive-equation model for simulating global ocean circulation, designed to take advantage of faster clock speeds, increased numbers of processors, and

enlarged memories of supercomputers expected to be available over the next decade. The model represents the first global ocean simulation with resolution fine enough to simulate spontaneous formation of mesoscale eddies. A 20-year integration of a global ocean model with 1/2-deg grid spacing and 20 vertical levels was carried out with realistic geometry and annual mean wind forcing. I.S.

A89-22594

**SATELLITE SEA SURFACE TEMPERATURE AT THE NORTH ATLANTIC POLAR FRONT RELATED TO HIGH-RESOLUTION TOWED CONDUCTIVITY-TEMPERATURE-DEPTH DATA**

T. VIEHOFF (Alfred-Wegener-Institut fuer Polar- und Meeresforschung, Bremerhaven, Federal Republic of Germany) and J. FISCHER (Kiel, Universitaet, Federal Republic of Germany) *Journal of Geophysical Research* (ISSN 0148-0227), vol. 93, Dec. 15, 1988, p. 15551-15560. refs (Contract DFG-SFB-133)

A meander structure of the North Atlantic Polar Front has been observed by satellite and towed undulating conductivity-temperature-depth probe (CTD) during the summer 1981. The high resolution of the CTD data allowed a comparison at the resolution of the satellite images (1.2 km). The average surface temperature differences of the independently calibrated CTD and satellite data were less than 0.2 K for those mixed-layer CTD data measured within 1 day of the satellite images. A strong decline of the temporal cross correlations between mixed-layer temperatures and sea surface temperature (SST) was observed shortly after the transition of an atmospheric front. A comparison of the SST with the isopycnic temperature distribution revealed the longer persistence of the structures in the stably stratified layers just beneath the mixed layer. The slow decline of the cross correlation between SST maps and the isopycnic temperature showed that the towed-fish survey was a synoptic measurement of the thermohaline field in the seasonal thermocline. Author

A89-22596

**LOOP CURRENT BOUNDARY VARIATIONS**

FRED M. VUKOVICH (Research Triangle Institute, Research Triangle Park, NC) *Journal of Geophysical Research* (ISSN 0148-0227), vol. 93, Dec. 15, 1988, p. 15585-15591. Research supported by Science Applications International Corp. refs

The periodicity of warm ring separation from the Loop Current and the characteristics of cold perturbations found along the Loop Current boundary were studied using a long-term data set made up of NOAA satellite infrared images. The results showed that the period between the separation of warm rings from the Loop Current was highly variable. The average period was about 10.9 months. The minimum period was 6 months, and the maximum period was 17 months. For the data set used, ring separations occurred most often in the winter. The study of the cold perturbations indicated that these perturbations were most pronounced along the northern and eastern portions of the Loop Current boundary and were less pronounced south of 27 N along the western boundary. The data suggested that the perturbations either formed or intensified in the northwestern portions of the boundary. The large effects along the eastern boundary of the Loop Current were thought to be associated with the movement of the intense perturbations that are initially found along the northwestern portions of the boundary. Author

A89-22597#

**A TIDE-GENERATED INTERNAL WAVEFORM IN THE WESTERN APPROACHES TO THE STRAIT OF GIBRALTAR**

PAUL E. LA VIOLETTE and ROBERT A. ARNONE (U.S. Navy, Naval Ocean Research and Development Activity, Bay Saint Louis, MS) *Journal of Geophysical Research* (ISSN 0148-0227), vol. 93, Dec. 15, 1988, p. 15653-15667. refs

Aircraft expendable bathythermograph, radar, infrared scanner, and visual data collected in October 1982, 1984, and 1985, as well as Space Shuttle photographs, indicate that an internal waveform (depending on flow conditions, either in internal hydraulic jump or a lee wave) is a semipermanent feature over the Camarinal

Sill in the western approaches to the Strait of Gibraltar. Comparison of these data with both historic and recent current meter mooring data indicates that the waveform, generated at the interface between the Atlantic and Mediterranean waters, undergoes periodic changes wrought by interaction of the tidal current and the flow of the Atlantic and Mediterranean waters. It is believed that the waveform is a major mixing mechanism between the two water masses. Author

A89-22598

**SATELLITE DETERMINATION OF THE CARBON DIOXIDE EXCHANGE COEFFICIENT AT THE OCEAN-ATMOSPHERE INTERFACE - A FIRST STEP**

J. ETCHETO and L. MERLIVAT (Paris VI, Universite, France) *Journal of Geophysical Research* (ISSN 0148-0227), vol. 93, Dec. 15, 1988, p. 15669-15678. Research supported by PIROCEAN. refs (Contract CNES-86-1227)

The coefficient for the exchange of CO<sub>2</sub> between air and sea was deduced from wind determinations derived from Seasat scatterometer data, using the relationship between the wind speed and the transfer velocity measured by Liss and Merlivat (1986). Global maps of the exchange coefficient, with a 10 x 10 deg resolution, were constructed, neglecting the temperature dependence due to the Schmidt number and solubility temperature variations. The map was then combined with the global map of partial pressure gradient of CO<sub>2</sub> by Broecker et al. (1986) to make an estimation of the net flux on a worldwide scale. I.S.

A89-22876\* Miami Univ., FL.

**THE SOURCE OF MARINE MAGNETIC ANOMALIES**

CHRISTOPHER G. A. HARRISON (Miami, University, FL) IN: *Marine geophysics: A Navy Symposium*, University of California, La Jolla, Oct. 16, 1986, Proceedings. San Diego, CA, Marine Physical Laboratory, 1987, p. 52-60. refs (Contract NAG5-414) (MPL-U-42/87)

The Vine-Matthews hypothesis (1963) is examined. This hypothesis suggests that oceanic rocks become polarized in the direction of the magnetic field at the time of their formation, thus recording the polarity history of the earth's magnetic field. This produces the lineated magnetic anomalies on either side of the midoceanic ridge crests. The strength of these magnetic anomalies is studied to determine the strength of magnetization. Indirect determinations of the magnetization intensity of the oceanic crust and direct observations of the oceanic crust are compared. It is found that the average magnetization of a 6-km thick oceanic crust is 1.18 A/m. R.B.

A89-23433

**A NEW VIEW OF THE MID-OCEAN RIDGE FROM THE BEHAVIOUR OF RIDGE-AXIS DISCONTINUITIES**

KEN C. MACDONALD, L. J. PERRAM, R. M. HAYMON (California, University, Santa Barbara), P. J. FOX, M. F. EISEN (Rhode Island, University, Narragansett) et al. *Nature* (ISSN 0028-0836), vol. 335, Sept. 15, 1988, p. 217-225. Research supported by the U.S. Navy and NSF. refs

High-resolution images covering large areas of the seafloor reveal numerous discontinuities along the midocean ridge. These discontinuities occur at a range of scales (10-1,000 km) and define a fundamental segmentation of seafloor spreading centers. Some are transient; others persist for millions of years, migrating along the midocean ridge and disrupting the structural and geochemical character of approximately 20 percent of the oceanic lithosphere. Author

A89-23438\* National Aeronautics and Space Administration. John C. Stennis Space Center, Bay Saint Louis, MS.

**SATELLITE DETECTION OF TRANSIENT ENHANCED PRIMARY PRODUCTION IN THE WESTERN MEDITERRANEAN SEA**

STEVEN E. LOHRENZ, ROBERT A. ARNONE, DENIS A. WIESENBURG, and IRENE P. DEPALMA (NASA, Stennis Space

## 05 OCEANOGRAPHY AND MARINE RESOURCES

Center; U.S. Navy, Oceanography Div., Bay Saint Louis, MS) Nature (ISSN 0028-0836), vol. 335, Sept. 15, 1988, p. 245-247. Research supported by the U.S. Navy. refs

Extensive ship sampling of chlorophyll a and primary production of CO<sub>2</sub> in the western Mediterranean Sea was conducted contemporaneous with Nimbus-7 coastal zone color scanner imagery. This approach resulted in an empirical model for estimating integrated water-column primary production from satellite imagery. Precision was adequate to resolve short-term fluctuations in primary production associated with a mesoscale circulation feature. C.D.

**A89-23590**

### MOTION CHARACTERISTICS OF SEA WAVES

#### [ZAKONOMERNOSTI DVIZHENIIA MORSKIKH VOLN]

IU. V. GLIBIN, E. O. ZHILKO, A. A. ZAGORODNIKOV, and S. I. MIROSHNICHENKO (Glavnaia Geofizicheskaiia Observatoriia, Leningrad, USSR; Kievskoe Vysshie Voennoe Aviatsionnoe Inzhenernoe Uchilishche, Kiev, Ukrainian SSR) Akademiia Nauk SSSR, Doklady (ISSN 0002-3264), vol. 303, no. 3, 1988, p. 729-732. In Russian.

Airborne radar studies of sea waves in the Bering experiment have shown that moving waves preserve an invariant position with respect to one another in the course of several minutes. The observed period amounted to 6-87 sec, but the time of existence of individual waves was found to significantly exceed 20 sec. In order to clarify this phenomenon, a series of experiments was carried out over the Black Sea using shore-based 3-cm-wave radar facilities. The results point to the prolonged existence of wave packets; on the 6-7 wave turbulence scale, the packets last up to 35 minutes and move with group velocity over a distance up to 15 km. B.J.

**A89-23646**

### FEATURES OF THE CALCULATION OF THE MAIN CHARACTERISTICS OF AN OCEANOGRAPHIC RADAR ALTIMETER [OSOBENOSTI RASCHETA OSNOVNYKH KHARAKTERISTIK OKEANOGRAFICHESKOGO RADIOVYSOTOMERA]

A. I. BASKAKOV (Moskovskii Energeticheskii Institut, Moscow, USSR) Radiotekhnika (ISSN 0033-8486), Nov. 1988, p. 66-71. In Russian. refs

An algorithm is obtained for the operation of the optimal detector and optimal discriminator in an oceanographic radar altimeter with a nanosecond sounding pulse. The measurement accuracy is assessed as a function of the degree of agitation of the sea surface and the signal/noise ratio. B.J.

**A89-24872\*** Jet Propulsion Lab., California Inst. of Tech., Pasadena.

### FRACTAL FEATURES OF SEA SURFACE MANIFESTED IN MICROWAVE REMOTE SENSING SIGNATURES

ROMAN E. GLAZMAN (California Institute of Technology, Jet Propulsion Laboratory, Pasadena) IN: Wave propagation and scattering in varied media; Proceedings of the Meeting, Orlando, FL, Apr. 6-8, 1988. Bellingham, WA, Society of Photo-Optical Instrumentation Engineers, 1988, p. 150-153. refs

The wave number spectrum of a well developed sea includes a broad range of wavenumbers (the equilibrium range) where the spectral density is governed by a power law,  $k \exp p$ . In the approximation of a Gaussian surface, the exponent  $p$  is related to the Hausdorff dimension. For  $p$  less than 4 the Hausdorff dimension is greater than 2 and the surface is characterized by an increased number of steep and breaking wavelets and by an increased number of specular points at near vertical incidence. The former results in the so-called spike component in the total return at oblique incidence, whereas the latter leads to an increased backscatter at nadir and near-nadir angles. Theory for both cases is reviewed and implications for satellite scatterometer and altimeter measurements of surface winds are discussed. Author

**A89-24875#**

### EFFECTIVENESS OF SATELLITE REMOTE SENSING ON MONITORING OF MARINE ENVIRONMENT

HIROAKI OCHIAI (Toba Merchant Marine College, Japan) IAF, International Astronautical Congress, 39th, Bangalore, India, Oct. 8-15, 1988.

(IAF PAPER 88-153)

The use of remote sensing to monitor the marine environment is evaluated using GMS, NOAA, MOS-1, and Landsat data. It is found that the visible and IR bands of NOAA VISSR and AVHRR are effective for monitoring sea ice, with the IR band of AVHRR providing the best results. In addition, the effectiveness of remote sensing techniques for monitoring sea surface temperature, currents, and pollution is discussed. Examples demonstrating these applications for sea regions near Japan are presented. R.B.

**A89-26181**

### OPTICAL METHODS OF SATELLITE HYDROPHYSICS.

#### INVESTIGATION OF THE ENVIRONMENT FROM MANNED ORBITAL STATIONS [OPTICHESKIE METODY SPUTNIKOVOI GIDROFIZIKI. ISSLEDOVANIE OKRUZHAIUSHCHEI SREDY S PILOTIRUEMYKH ORBITAL'NYKH STANTSII]

BORIS A. NELEPO, GENNADII A. GRISHIN, IURII P. KIENKO, and ALEKSANDR D. KOVAL' Kiev, Izdatel'stvo Naukova Dumka, 1987, 144 p. In Russian. refs

Aspects of the remote sensing of the ocean from manned satellites and orbital stations are discussed. The analog and digital processing of satellite data is described, and examples of the analysis of Salyut data are examined. Particular attention is given to the study of frontocyclogenesis in the ocean and atmosphere, the wave dynamics of the ocean, and observations of coastal regions. An atlas of space photographs is presented. B.J.

**A89-26438\*** California Univ., La Jolla.

### GEOSAT CROSSOVER ANALYSIS IN THE TROPICAL PACIFIC. II - VERIFICATION ANALYSIS OF ALTIMETRIC SEA LEVEL MAPS WITH EXPENDABLE BATHY THERMOGRAPH AND ISLAND SEA LEVEL DATA

CHANG-KOU TAI, WARREN B. WHITE, and STEPHEN E. PAZAN (California, University, La Jolla) Journal of Geophysical Research (ISSN 0148-0227), vol. 94, Jan. 15, 1989, p. 897-908. Research supported by NASA. refs (Contract NSF OCE-86-07962)

Altimetric sea level time series for the tropical Pacific have been generated from the Geosat crossover differences during the classified era of the Geosat mission from April 1985 to September 1986. These are compared with the expendable bathythermograph (XBT)-derived dynamic height and island sea level observations, yielding good agreement. A complex empirical orthogonal function analysis is also applied to the altimetric and XBT results. The analysis demonstrates the dominance of the annual signal in this relatively short time series and the westward propagation of major features away from the equator. C.D.

**A89-26442**

### HINDCASTS AND DATA ASSIMILATION STUDIES WITH THE WAM MODEL DURING THE SEASAT PERIOD

PETER A. E. M. JANSSEN, PIERO LIONELLO, MAGNAR REISTAD, and ANTHONY HOLLINGSWORTH (European Centre for Medium Range Weather Forecasts, Reading, England) Journal of Geophysical Research (ISSN 0148-0227), vol. 94, Jan. 15, 1989, p. 973-993. Research supported by EEC. refs (Contract ESRIN-6297/86/HGE-I(SC); NATO-SA-9-9-03-0523/85)

The results are presented of a study of the feasibility of using altimeter wave height data from a satellite in a real-time wave data assimilation scheme. The Wave Model (WAM) is used to show how to cross-validate altimeter wave height with scatterometer data and how to construct an analyzed wave model spectrum from the altimeter wave height. The analyzed wave spectrum may be cross-validated with the synthetic aperture radar spectrum. The implications for improving the Seasat scatterometer algorithm are pointed out. C.D.

A89-26443

**SIMULATED EFFECTS OF BAROMETRIC PRESSURE AND OZONE CONTENT UPON THE ESTIMATE OF MARINE PHYTOPLANKTON FROM SPACE**

JEAN-MICHEL ANDRE and ANDRE MOREL (Paris VI, Universite, Villefranche-sur-Mer, France) *Journal of Geophysical Research* (ISSN 0148-0227), vol. 94, Jan. 15, 1989, p. 1029-1037. refs

Barometric pressure and total ozone content may significantly depart from their mean climatology values; these values, however, are used when processing visible remote sensing (VRS) data in order to estimate phytoplanktonic pigment concentration within the upper ocean. In this paper, the effect of ignoring such departures upon the retrieved concentration is simulated for typical VRS situations when information about the variable aerosol is not available when entering processing or, conversely, when such information has been separately obtained. The result for both these cases is that the use of mean climatology values leads to variable misestimates of the pigment content, by a factor of up to two in many common VRS situations and above two for very low or high actual pigment content. It is concluded that actual values of the barometric pressure and of ozone content will have to be introduced in processing future visible sensor data in order to preserve expected accuracy. C.D.

A89-26643

**FRONTAL SIGNALS EAST OF ICELAND FROM THE GEOSAT ALTIMETER**

A. R. ROBINSON, L. J. WALSTAD, D. W. DENBO (Harvard University, Cambridge, MA), J. CALMAN, E. B. DOBSON (Johns Hopkins University, Laurel, MD) et al. *Geophysical Research Letters* (ISSN 0094-8276), vol. 16, Jan. 1989, p. 77-80. Research supported by NOAA. refs (Contract N00039-87-C-5301)

Geosat satellite radar altimeter data are used to identify and analyze frontal signals in sea surface height in the region between Iceland and the Faeroe Islands from three satellite passes over the region during a five-day period starting July 9, 1987. The data are verified and combined with in situ measurements for an improved and synoptic estimate of frontal location. The data assimilation context makes weak signals quantitatively useful. C.D.

A89-26844#

**EDGE DETECTION APPLIED TO SATELLITE IMAGERY OF THE OCEANS**

RONALD J. HOLYER and SARAH H. PECKINPAUGH (U.S. Navy, Naval Ocean Research and Development Activity, Bay Saint Louis, MS) *IEEE Transactions on Geoscience and Remote Sensing* (ISSN 0196-2892), vol. 27, Jan. 1989, p. 46-56. Research supported by the U.S. Navy. refs

A computer edge-detection algorithm for automatic delineation of mesoscale structure in digital satellite IR (infrared) images of the ocean is developed. The popular derivative-based edge operators are shown to be too sensitive to edge fine-structure and to weak gradients to be useful in this application. The edge-detection algorithm is based on the gray level cooccurrence (GLC) matrix, which is commonly used in image texture analysis. The cluster shade texture measure derived from the GLC matrix is found to be an excellent edge detector that exhibits the characteristic of fine-structure rejection while retaining edge sharpness. This characteristic is highly desirable for analyzing oceanographic satellite images. The method is evaluated on an advanced very-high-resolution radiometer (AVHRR) image of the Gulf Stream region. I.E.

A89-26846

**A SIMULATION FOR SPACEBORNE SAR IMAGERY OF A DISTRIBUTED, MOVING SCENE**

PARIS W. VACHON (Canada Centre for Remote Sensing, Ottawa), R. KEITH RANEY (Radarsat Project Office, Ottawa, Canada), and WILLIAM J. EMERY (Colorado, University, Boulder) *IEEE Transactions on Geoscience and Remote Sensing* (ISSN 0196-2892), vol. 27, Jan. 1989, p. 67-78. refs

A computer simulation that is designed to represent aspects of spaceborne synthetic-aperture radar (SAR) imagery of the ocean surface is presented. The simulation is unique in that a scatterer density (per resolution cell) is explicitly included, thus allowing the incorporation of various scattering natures, from purely specular to purely diffuse. The simulation may be applied to ocean surface wave imaging since velocity bunching and scene coherence times are also included. Certain assumptions inherent in the velocity bunching formulation limit the applicability of the simulation in its present form to spaceborne SAR systems only. Two experiments based on this simulation are considered: (1) the effect of varying the target density; and (2) the effect of the mean scene coherence time in the imaging of a ocean swell system. In each case, the simulation outputs are compared with actual SEASAT SAR imagery. On the basis of certain statistics derived from the simulated scenes, it is shown that specular statistics are quantitatively correct for scenes that may appear diffuse in hard copy form. This observation suggests that quantitative norms be used (rather than intuitive opinion or appearance) for investigating ocean scattering statistics, for example. I.E.

A89-27941

**EXTRACTION OF SURFACE TEMPERATURE FROM SATELLITE DATA**

HARTMUT GRASSL (GKSS-Forschungszentrum Geesthacht GmbH, Federal Republic of Germany) IN: *Applications of remote sensing to agrometeorology; Proceedings of the Course, Ispra, Italy, Apr. 6-10, 1987*. Dordrecht, Netherlands, Kluwer Academic Publishers, 1989, p. 199-220. refs

Problems in extracting surface temperature from satellite data are discussed, focusing on the possible influences of water vapor content, near surface thermal structure, aerosol particles, thin clouds, slant paths, and surface emissivity on the correction of atmospheric masking. A procedure for land surface temperature determination for the NOAA 7, 9 satellite data is presented. The steps of the procedure are derivation of water surface temperature, interpolation of the water surface correction, correction due to heated or cooled surfaces, and choice of the highest temperature from the three thermal IR channels. An example is presented applying the procedure to a daytime and a nighttime scene covering the Alps. R.B.

A89-27976

**OCEAN OPTICS IX; PROCEEDINGS OF THE MEETING, ORLANDO, FL, APR. 4-6, 1988**

MARVIN A. BLIZARD, ED. (U.S. Navy, Office of Naval Research, Arlington, VA) Meeting sponsored by SPIE, Bellingham, WA, Society of Photo-Optical Instrumentation Engineers (SPIE Proceedings, Volume 925), 1988, 447 p. For individual items see A89-27977 to A89-28003. (SPIE-925)

Recent advances in optical techniques and instruments for applications to oceanography and related fields are discussed in reviews and reports. Topics addressed include basic concepts and theoretical models, the optical properties of the oceans, optical instrumentation, laser bathymetry, particle optics, imaging, remote sensing, and animal vision. Extensive diagrams, drawings, graphs, photographs, and sample images are provided. T.K.

A89-27980

**SIMULATION OF RADIOMETRIC OCEAN IMAGES RECORDED FROM HIGH-ALTITUDE PLATFORMS**

J. C. ERDMANN and J. M. SAINT CLAIR (Boeing Aerospace Co., Seattle, WA) IN: *Ocean optics IX; Proceedings of the Meeting, Orlando, FL, Apr. 4-6, 1988*. Bellingham, WA, Society of Photo-Optical Instrumentation Engineers, 1988, p. 36-49. refs

The generation of simulated multispectral ocean scenes, as affected by the presence of phytoplankton under varying insolation, is reported. Both the 1-dimensional radiative transfer model and a probabilistic method are applied. The former is simple, but does not account explicitly for sun angle and observation angle dependence. The latter is based on the analysis of expected Monte Carlo results and allows the rendering of radiometric images of a

spherical ocean. Also included is the stochastic subdivision of a nonuniform ocean, resulting in simulations of random biomass distribution. Simulated multispectral images obtained at varying wavelength can be processed like real records and by means of scatterplots yield similar results for the phytoplankton concentration. Author

**A89-27995**

**BATHYMETRY USING THEMATIC MAPPER IMAGERY**

R. KENT CLARK (South Alabama, University, Mobile, AL), TEMPLE H. FAY (Southern Mississippi, University, Hattiesburg, MS), and CHARLES L. WALKER (U.S. Navy, Naval Ocean Research and Development Activity, Bay Saint Louis, MS) IN: Ocean optics IX; Proceedings of the Meeting, Orlando, FL, Apr. 4-6, 1988. Bellingham, WA, Society of Photo-Optical Instrumentation Engineers, 1988, p. 229-231. Research sponsored by the U.S. Navy. refs

Remotely sensed bathymetry in the vicinity of Vieques Island and Key West, Florida is performed using Landsat Thematic Mapper imagery and a multiband model. Previous bathymetric algorithms using a single band or a ratio of bands assumed a constant bottom reflectance and thus required a bottom-type classification to isolate areas of uniform reflectance. The multiband model described in this paper does not require homogeneous bottom-types and yields somewhat improved results over older methods. Depths to 16 m are measured with RMS residuals of less than 2 m. Results using other algorithms will be compared to the results from the multiband model. Author

**A89-28003**

**REMOTE SENSING OF OCEAN PHYSICAL PROPERTIES - A COMPARISON OF RAMAN AND BRILLOUIN TECHNIQUES**

DONALD A. LEONARD and HAROLD E. SWEENEY (GTE Government Systems Corp., Mountain View, CA) IN: Ocean optics IX; Proceedings of the Meeting, Orlando, FL, Apr. 4-6, 1988. Bellingham, WA, Society of Photo-Optical Instrumentation Engineers, 1988, p. 407-414. refs

The fundamental principles and practical feasibility of optical ocean remote-sensing methods based on Raman and Brillouin scattering are discussed. The ocean properties to be measured and the capabilities of the instruments available are reviewed; the basic physics of the processes is explained and illustrated with diagrams; field-test results for various methods are listed in tables; and it is concluded that temperature accuracy of order 0.1 C should be obtainable over water path lengths equal to 2-3 diffuse attenuation lengths using either Raman or Brillouin methods. T.K.

**A89-28034**

**DETERMINATION OF ATMOSPHERIC TURBIDITY FROM REMOTELY-SENSED DATA - A CASE STUDY**

G. ZIBORDI (CNR, Istituto per lo Studio delle Metodologie Geofisiche-Ambientali, Modena, Italy) and G. MARACCI (CEC, Joint Research Centre, Ispra, Italy) International Journal of Remote Sensing (ISSN 0143-1161), vol. 9, Dec. 1988, p. 1881-1894. refs

A model developed for radiative transfer in the atmosphere-sea system is applied to remotely-sensed radiances to evaluate its applicability in the determination of atmospheric turbidity. Data measured at different atmospheric turbidities over clear sea water by a multispectral scanner installed on an aeroplane have been used. Comparisons of aerosol optical thicknesses obtained from remotely-sensed data and from ground-based atmospheric transmittance measurements are given and discussed. Author

**A89-28290**

**POLARIZATION OF MICROWAVE EMISSION OF A WATER SURFACE IN A WIDE RANGE OF ANGLES OF SIGHT [POLIARIZATSIIA SOBSTVENNOGO MIKROVOLNOVOGO IZLUCHENIIA VODNOI POVERKHNOSTI V SHIROKOM DIAPAZONE UGLOV VIZIROVANIIA]**

ZHIUL'VERN B. KHACHATRIAN (Erevanskii Gosudarstvennyi

Universitet, Yerevan, Armenian SSR) Zeitschrift fuer Meteorologie (ISSN 0084-5361), vol. 38, no. 4, 1988, p. 212-218. In Russian. refs

Results of simultaneous measurements at 0.8 and 3.2 cm are presented for the microwave emission field of the atmosphere/ocean surface system. Measurements are analyzed for a wide range of angles of sight. The introduction of an effective radiation coefficient makes the interpretation of the experimental data substantially easier. It is shown that the vertical component of the radiation increases in the Bragg reflection angle range of 85-88 deg. B.J.

**A89-28305**

**THE IMPACT OF SATELLITE ALTIMETRY DATA ON NUMERICAL SIMULATIONS OF GENERAL MIDLATITUDE OCEANIC CIRCULATION [IMPACTS DE DONNEES D'ALTIMETRIE SATELLITAIRE SUR LES SIMULATIONS NUMERIQUES DES CIRCULATIONS GENERALES OCEANIQUES AUX LATITUDES MOYENNES]**

JACQUES VERRON and WILLIAM R. HOLLAND (National Center for Atmospheric Research, Boulder, CO) Annales Geophysicae (ISSN 0980-8752), vol. 7, Feb. 1989, p. 31-46. In French. refs

Tests of altimeter data assimilation are conducted into a quasi-geostrophic eddy-resolving three-layer model, in an effort to study the dynamical behavior of the model under the data constraints. When the data is expressed in the form of the vorticity field and assimilated with the simple technique of nudging, the subsurface transfer of information is rather efficient, and the model is brought into agreement with the observations even in the deep layers. It is shown that truncation of the vorticity data along any horizontal direction does not affect the efficiency of the assimilation process. Author

**A89-28365#**

**STEP FREQUENCY RADAR EXPERIMENTS ON THE ANTARCTIC SEA ICE**

HITOSHI MINENO (Telecommunication Satellite Corporation of Japan, Tokyo), FUMIHIKO NISHIO (National Institute of Polar Research, Tokyo, Japan), SHINJI MAE (Hokkaido University, Sapporo, Japan), SEIHO URATSUKA, and KEN'ICHI OKAMOTO (Communications Research Laboratory, Journal (ISSN 0914-9260), vol. 35, Nov. 1988, p. 251-258. refs

UHF step-frequency radar experiments have been carried out on sea ice near Syowa Station (as part of the 27th Japanese Antarctic Research Expedition) to develop an airborne sensor for measuring vertical sea-ice structures. The radar transmits 32 different frequencies in a stepwise-fashion between 300 and 796 MHz and measures the amplitude and phase of reflected waves at each frequency. The discrete Fourier transform of the 32 complex values of signals indicates the distance of vertical sea ice structures. The range resolution is about 15 cm in sea ice. Author

**A89-29075**

**PROCESSING SATELLITE INFRARED AND VISIBLE IMAGERY FOR OCEANOGRAPHIC ANALYSES**

PAUL E. LA VIOLETTE (U.S. Navy, Naval Ocean Research and Development Activity, Bay Saint Louis, MS) IN: Digital image processing in remote sensing. London and Philadelphia, PA, Taylor and Francis, 1988, p. 213-241. refs

The most important of the basic techniques that must be applied to satellite data in order to obtain reliable and quantifiable oceanographic information are proper registration and atmospheric correction, especially in the case of visible-range data. Registration to a set graphic projection can be extremely useful in allowing several days of data to be studied as temporal, as well as spatial, continuity. It is also noted that, when the data are accurately calibrated and atmospherically corrected, the usefulness of the data can be substantially expanded through coregistry with other data sets; they can then be used as part of an overall analysis of the data available for the given study region. O.C.

A89-29726

**OCEANIC REMOTE SENSING**

F. V. BUNKIN, ED. and K. I. VOLIAK, ED. Commack, NY, Nova Science Publishers, 1987, 234 p. Translation. For individual items see A89-29727 to A89-29733.

Topics related to oceanic remote sensing are examined, focusing on laser methods for measuring sea surface conditions, the nonlinear dynamics of surface waves, and laser methods of sound generation in free boundary fluid theory of oceanic acoustic propagation. The laser studies include measuring sea waves by reflected laser emission statistics, laser airborne sensing field experiments, mapping the surface distribution of chlorophyll and organic solute, measuring the temporal structure of an echo signal, the effects of round trip laser emission propagation through a turbulent surface, the capabilities of nonlinear Raman spectroscopy for remote diagnostics of water bodies. Other topics include the detection of ocean bottom relief by local geoid, the remote sensing of surface wave interaction, the parametric generation of edge waves, laser-induced sound generation in conditions of fluid surface turbulence for application to optoacoustic profilometry, and methods of acoustic propagation theory in stratified horizontally-inhomogeneous absorbing boundary waveguides. R.B.

A89-29728

**LASER AIRBORNE SENSING FIELD EXPERIMENTS USING THE 'CHAIKA' ASSEMBLY**

A. G. ABROSKIN, A. F. BUNKIN, D. V. VLASOV, A. L. GORVUNOV, and D. M. MIRKAMILOV IN: Oceanic remote sensing. Commack, NY, Nova Science Publishers, 1987, p. 27-48. refs

This study gives results from field experiments on the remote laser airborne probing of water bodies using a Soviet assembly on the An-30 aircraft. The surface and depth distributions of phytoplankton chlorophyll 'a', organic solute, and suspensions were measured. The influence of surface wave activity on the waveform of the received echo signal is discussed. Author

A89-29729

**EFFECTS OF ROUND TRIP LASER EMISSION PROPAGATION THROUGH A TURBULENT SURFACE FOR LASER AIRBORNE OCEANIC SENSING**

D. V. VLASOV, V. N. STREL'TSOV, and V. P. SLOBODIANIN IN: Oceanic remote sensing. Commack, NY, Nova Science Publishers, 1987, p. 49-73. refs

The propagation of a laser beam through the sea surface and its subsequent reflection or scattering in the water column with developed surface wind wave turbulence are examined. The dependence of the reflected echo signal intensity for a stationary probe beam on the probe depth and the parameters of surface turbulence is investigated. The temporal structure of the echo signal is examined in pulsed probing conditions. The problem of identifying the parameters of a recorded echo signal with the measured physical parameters of the water body is discussed. Author

A89-29730

**THE CAPABILITIES OF NONLINEAR RAMAN SPECTROSCOPY FOR REMOTE DIAGNOSTICS OF WATER BODIES**

A. F. BUNKIN, D. V. VLASOV, A. S. GALUMIAN, and K. O. SURSKII IN: Oceanic remote sensing. Commack, NY, Nova Science Publishers, 1987, p. 74-88. refs

The possibilities for using a variety of nonlinear Raman spectroscopy techniques for ocean water diagnostics are examined. Polarization coherent anti-Stokes spectroscopy is used to resolve the structure of the valence band of the OH bond of water molecules, and temperature deformations in the derived spectra are studied. Author

A89-29731

**DETECTION OF OCEAN BOTTOM RELIEF BY LOCAL GEOID**

I. A. MASLOV IN: Oceanic remote sensing. Commack, NY, Nova Science Publishers, 1987, p. 89-106. refs

The correlation relations between medium-scale deviations in

the geoid and the ocean bottom relief based on satellite data are examined. The possibility for determining the local geoid by airborne observations that measure deviations of the vertical is demonstrated. The possibility for converting the measured quantities from the flight altitude to the sea surface is demonstrated. Author

A89-29732

**SURFACE WAVE INTERACTION - THEORY AND CAPABILITY OF OCEANIC REMOTE SENSING**

K. I. VOLIAK, G. A. LIAKHOV, and I. V. SHUGAN IN: Oceanic remote sensing. Commack, NY, Nova Science Publishers, 1987, p. 107-145. refs

The experimental capabilities for RF oceanographic methods of studying the sea surface layer and the water atmosphere are examined, focusing on the radar method of observing nonlinear wave interactions. A theory of cubic interaction of nonsynchronized gravity waves is developed using the averaged Lagrangian method. The theory is used to analyze the quasi-synchronous cubic interaction of randomly modulated waves. The increments and intensities of the interacting waves are calculated. Airborne RF images are used to determine the kinematic parameters of interacting waves systems and to estimate the energy transfer between systems. R.B.

A89-29763#

**UV LASER FLUOROSENSOR FOR REMOTE SENSING**

V. N. SAXENA (Institute of Armament Technology, Poona, India) Defence Science Journal (ISSN 0011-748X), vol. 38, July 1988, p. 315-320. refs

It is shown how the spectral analysis of fluorescence can be used to detect, monitor, and even quantify oil spills in the ocean. On the basis of the concentration of chlorophyll in water, it is possible to assess environmental conditions. Since chlorophyll in green plants fluoresces in the wavelength range of 650-750 nm, the best excitation is achieved by a laser in the 400-500 nm range. K.K.

A89-30019

**WAVENUMBER SPECTRA OF SHORT GRAVITY WAVES**

M. L. BANNER, J. C. TRINDER (New South Wales, University, Kensington, Australia), and IAN S. F. JONES (Royal Australian Navy, Research Laboratory, Darlinghurst, Australia) Journal of Fluid Mechanics (ISSN 0022-1120), vol. 198, Jan. 1989, p. 321-344. Research supported by the Australian Marine Science and Technology Grants Scheme. refs

The paper presents the results of an experimental determination of the wavenumber spectrum for the wavelength range of 0.1-1.6 m. They are based on stereophotogrammetric determinations from an oil platform under open ocean conditions. The observations are consistent with the radar reflectivity dependence on wind direction and wind speed under Bragg scattering conditions within this wavenumber range. K.K.

A89-30114

**REMOTE SENSING OF SURFACE MANIFESTATIONS OF SHORT-PERIOD INTERNAL WAVES IN THE OCEAN [K ISSLEDOVANIU POVERKHNOSTNYKH PROIAVLENIU KOROTKOPRIODNYKH VNUTRENNIKH VOLN V OKEANE DISTANTSIONNYMI METODAMI]**

V. E. GERSHENZON (AN SSSR, Institut Kosmicheskikh Issledovaniy, Moscow, USSR) Issledovanie Zemli iz Kosmosa (ISSN 0205-9614), Nov.-Dec. 1988, p. 27-32. In Russian. refs

The feasibility of remote sensing from different platforms (aircraft, ships, and satellites) to study short-period internal waves in the ocean from their surface manifestations is examined. An examination of the typical dispersion characteristics of the process considered shows that the optimal study technique is time analysis, while the optimal platform is an aerospace system capable of acquiring frequent images over the ocean. B.J.



A89-30120

**RADIATION MODELS OF MESOTROPHIC AND EUTROPHIC BODIES OF WATER [RADIATIONNYE MODELI MEZOTROFNYKH I EVTROFNYKH VODNYKH OB'EKTOV]**

A. A. GITEL'SON (Gidrokhimicheskii Institut, Rostov-on-Don, USSR) and F. SYILAGGI (Tsentr Vodnogo Khoziaistva Vengerskoi Narodnoi Respubliki, Budapest, Hungary) *Issledovanie Zemli iz Kosmosa* (ISSN 0205-9614), Nov.-Dec. 1988, p. 72-82. In Russian. refs

Radiation models relating water quality and reflectance are developed, and tested for mesotrophic and eutrophic water bodies for suspended-mineral concentrations ranging from 3 to 40 mg/l and chlorophyll a concentration ranging from 1.3 to 400 mg/cu m. It is shown that these models permit space remote sensing (multispectral) measurements of chlorophyll a with an error less than 3 mg/cu m and measurements of suspended minerals with an error less than 4 mm/cu m. B.J.

A89-30122

**A METHOD FOR PROCESSING AND RESULTS OF MICROWAVE RADIOMETER STUDIES OF THE EARTH FROM THE INTERCOSMOS 20 AND 21 SATELLITES [METODIKA OBRABOTKI I REZULTATY SVCH-RADIOMETRICHESEKIKH ISSLEDOVANII ZEMLI SO SPUTNIKOV 'INTERKOSMOS-20, -21']**

A. B. AKVILONOVA, M. S. KRYLOVA, B. G. KUTUZA, V. P. SAVORSKII, and M. T. SMIRNOV (AN SSSR, Institut Radiotekhniki i Elektroniki, Moscow, USSR) *Issledovanie Zemli iz Kosmosa* (ISSN 0205-9614), Nov.-Dec. 1988, p. 88-94. In Russian. refs

The data-acquisition capabilities provided by polarization measurements of thermal emission from the ocean-atmosphere system at 2.25 cm by the R-22.5 microwave radiometer is assessed. A procedure for identifying precipitation zones over the ocean is examined. Sea surface temperature estimates are presented along with a polarized-radiation map of Africa compiled from Intercosmos-21 measurements. B.J.

A89-30257

**TECHNOLOGICAL LIMITATIONS TO SATELLITE GLACIOLOGY**

W. G. REES (Cambridge University, England) and V. A. SQUIRE (Otago, University, Dunedin, New Zealand) *International Journal of Remote Sensing* (ISSN 0143-1161), vol. 10, Jan. 1989, p. 7-22. refs

Satellite observations of the most important geophysical parameters measured in the investigation of land-ice and sea-ice glaciology are discussed. Passive microwave radiometry and synthetic aperture radar are used to study ice type, ice kinematics, swell and waves in ice, ice roughness, and ice thickness. The radar altimeter can be used to measure land-ice-surface topography to an accuracy of 0.5 m or better. Visible radar images may be used to locate and track land-ice surface features. R.R.

A89-30258

**CAN BETTER ENVIRONMENTAL INPUTS IMPROVE SEA CLUTTER ESTIMATION? A NUMERICAL EXPERIMENT**

TAK KEE CHEUNG (U.S. Navy, Naval Environmental Prediction Research Facility, Monterey, CA) *International Journal of Remote Sensing* (ISSN 0143-1161), vol. 10, Jan. 1989, p. 23-35. refs

The effect of applying better environmental inputs to an existing sea clutter model which has proved to be adequate for small grazing angles is investigated. Various scattering models, ocean-wave models, and hybrid models are considered. It is shown that even a simple choice in direction can make a large difference in the sea clutter signal. Other factors which should be taken into account include the discrepancy in propagation direction between swell and gravity waves, the spectral content of the waves, and the whitecap coverage. R.R.

A89-30259

**COMPARISON OF NOAA/AVHRR-2 SEA SURFACE TEMPERATURES WITH SURFACE MEASUREMENTS IN COASTAL WATERS**

A. F. PEARCE, C. R. MANNING (CSIRO, Marine Laboratories, North Beach, Australia), and A. J. PRATA (CSIRO, Div. of Atmospheric Research, Mordialloc, Australia) *International Journal of Remote Sensing* (ISSN 0143-1161), vol. 10, Jan. 1989, p. 37-52. refs

Sea surface temperatures (SSTs) derived from the Advanced Very High Resolution Radiometer (AVHRR-2) on the NOAA-7 and NOAA-9 satellites are compared with measurements taken from a boat in coastal waters off Fremantle, Western Australia. The satellite temperatures have been corrected for atmospheric water vapor, using seven published algorithms. The two most appropriate algorithms for the data set result in 'boat-minus-satellite' biases of about 0.2 deg C and -0.1 deg C, with rms errors of about 0.6 deg C. The satellite temperature transects are shown to reproduce satisfactorily the seasonally reversing cross-shelf gradients as well as the finer thermal structure, demonstrating the value of high-resolution satellite SST measurements in continental shelf regions. Author

A89-30260

**REMOTE SENSING OF MACROPHYTIC ALGAE OF THE MOLENE ARCHIPELAGO IN FRANCE - TERRAIN RADIOMETRY AND APPLICATION TO SPOT SATELLITE DATA [TELEDETECTION DES ALGUES MACROPHYTES DE L'ARCHIPEL DE MOLENE (FRANCE) - RADIOMETRIE DE TERRAIN ET APPLICATION AUX DONNEES DU SATELLITE SPOT]**

H. BEN MOUSSA, T. BELSHER, and M. VIOLLIER (Institut Francais de Recherches pour l'Exploitation de la Mer, Brest, France) *International Journal of Remote Sensing* (ISSN 0143-1161), vol. 10, Jan. 1989, p. 53-69. In French. refs

A89-30900

**AN EXPERIMENT TO INVERT SEASAT ALTIMETRY FOR THE MEDITERRANEAN AND BLACK SEA MEAN SURFACES**

P. MAZZEGA and S. HOURY (CNES, Groupe de Recherches de Geodesie Spatiale, Toulouse, France) (Colloque National sur la Localisation en Mer, 3rd, Rueil-Malmaison, France, Sept. 28-Oct. 1, 1987) *Geophysical Journal* (ISSN 0955-419X), vol. 96, Feb. 1989, p. 259-272. refs  
(Contract CNRS-ATP-0693)

Numerical experiments are performed to obtain the Mediterranean and Black Sea mean sea surfaces (MSS) by least squares inversion of Seasat altimeter data. The data editing and the starting maps are described. A discussion is presented of the choice of the various covariance functions, and an insight of their geometrical properties for the space-time sampling of the sea by the orbiting altimeter is given. A reconstruction is performed of the inverse solutions for the MSS and the gravity anomalies from the previous information. The main numerical difficulties are dealt with, and nominal solutions with their formal errors are presented. Because the a priori statistics of the residual MSS, built globally, can be refined, the present solution must not be considered as definitive. S.A.V.

A89-32108

**THE SOLID OCEANIC CRUST (THE LITHOS PROJECT) [TVERDAIA KORA OKEANOV /PROEKT 'LITOS']**

IU. M. PUSHCHAROVSKII, ED. and A. A. PEIVE, ED. Moscow, *Izdatel'stvo Nauka*, 1987, 192 p. In Russian. No individual items are abstracted in this volume.

Results from the Lithos project are reported in a series of papers. Particular attention is given to oceanic basalts and the problem of mantle heterogeneity; upper-mantle heterogeneities in ultrabasite compositions of ophiolites of continents and oceans; the Pacific basaltic magmatism and the problem of petrogeochemical heterogeneities of the tectonosphere; the spatial and temporal distribution of petrochemical types of oceanic magmatic rocks; isotopic and geochemical evidence for lateral and vertical heterogeneities of the oceanic upper mantle; and the origin of deep-sea basins in active continental margins. B.J.



A89-32434

**PHYSICAL RETRIEVAL OF RAINFALL RATES OVER THE OCEAN BY MULTISPECTRAL MICROWAVE RADIOMETRY - APPLICATION TO TROPICAL CYCLONES**WILLIAM S. OLSON (Wisconsin, University, Madison) *Journal of Geophysical Research* (ISSN 0148-0227), vol. 94, Feb. 20, 1989, p. 2267-2280. refs

(Contract NOAA-MO-A01-78-00-4320; N00014-86-K-2001)

Brightness temperature data from the SMMR channels were inverted to yield quantitative estimates of tropical cyclone, based upon a detailed physical model developed for the sensor response in all channels. Since the spatial response of the SMMR varies with channel frequency, antenna response functions were estimated to enable multispectral rain retrievals near optimal resolution. A further advantage of this model-based retrieval approach is that new knowledge concerning atmospheric structure/physics or sensor response can be logically introduced into the retrieval method to improve rain rate estimates. The rain patterns retrieved using SMMR hurricane data appear reasonable in comparison to radar, with a mean retrieval error of 57 percent.

I.S.

**N89-15309# Naval Research Lab., Washington, DC. SEGMENTATION OF SYNTHETIC APERTURE RADAR (SAR) IMAGES OF OCEAN SURFACE BY THE TEXTURE ENERGY TRANSFORM METHOD Interim Report**

LI-JEN DU 17 Aug. 1988 22 p

(AD-A199536; NRL-MR-6259) Avail: NTIS HC A03/MF A01 CSCL 17E

A texture energy transform approach has been chosen for the study of texture analysis and classification in digital images. It is based on the idea of detecting the degree of similarity between the spatial variation of image pixels and a set of chosen mask filters. Feature measures which characterize the texture are simpler to compute as compared with other approaches based on auto-correlation functions, digital transform methods, spatial gray tone co-occurrence probabilities, auto-regression models, etc. An algorithm was developed for the segmentation of SAR ocean surface images into regions with and without directional streaks. Excellent results are obtained in which surface areas with relatively rough and calm water are identified. GRA

**N89-15444\*# Scripps Institution of Oceanography, San Diego, CA.****A MULTI-SENSOR REMOTE SENSING APPROACH FOR MEASURING PRIMARY PRODUCTION FROM SPACE Final Technical Report**

CATHERINE GAUTIER 10 Jan. 1989 62 p

(Contract NAGW-0851)

(NASA-CR-184662; NAS 1.26:184662) Avail: NTIS HC A04/MF A01 CSCL 08C

It is proposed to develop a multi-sensor remote sensing method for computing marine primary productivity from space, based on the capability to measure the primary ocean variables which regulate photosynthesis. The three variables and the sensors which measure them are: (1) downwelling photosynthetically available irradiance, measured by the VISSR sensor on the GOES satellite, (2) sea-surface temperature from AVHRR on NOAA series satellites, and (3) chlorophyll-like pigment concentration from the Nimbus-7/CZCS sensor. These and other measured variables would be combined within empirical or analytical models to compute primary productivity. With this proposed capability of mapping primary productivity on a regional scale, we could begin realizing a more precise and accurate global assessment of its magnitude and variability. Applications would include supplementation and expansion on the horizontal scale of ship-acquired biological data, which is more accurate and which supplies the vertical components of the field, monitoring oceanic response to increased atmospheric carbon dioxide levels, correlation with observed sedimentation patterns and processes, and fisheries management. Author

**N89-17357# Applied Science Associates, Inc., Narragansett, RI. EVALUATION OF SATELLITE-TRACKED SURFACE DRIFTING BUOYS FOR SIMULATING THE MOVEMENT OF SPILLED OIL IN THE MARINE ENVIRONMENT. VOLUME 1: EXECUTIVE SUMMARY Report, 1986 - 1988**

MARK REED, CHRIS TURNER, MALCOLM SPAULDING, KATHERINE JAYKO, DONALD DORSON, and OISTEIN JOHANSEN (Oceanographic Center, Trondheim, Norway) 15 Mar. 1988 19 p

(Contract DI-14-12-0001-30340)

(PB88-226048; OCS/MMS-87/0071-VOL-1) Avail: NTIS HC A03/MF A01 CSCL 13B

Satellite tracked surface drifters were studied to evaluate the simulation of movement of spilled crude oil and assessing the skill of the Oil Spill Risk Analysis model. Review of the oil spill literature since 1980 shows that the most significant advance relative to surface transport processes relates to the effect of temporary submergence and surface shear on the distribution of oil behind the downwind leading edge of a surface slick. Dynamic analyses of three basic buoy shapes, the sphere, the spar or cylinder, and the disk or flattened spheroid, were undertaken using a numerical model. Results are given. Author

**N89-17358# Applied Science Associates, Inc., Narragansett, RI. EVALUATION OF SATELLITE-TRACKED SURFACE DRIFTING BUOYS FOR SIMULATING THE MOVEMENT OF SPILLED OIL IN THE MARINE ENVIRONMENT, VOLUME 2 Final Report**

MARK REED, CHRIS TURNER, MALCOLM SPAULDING, KATHERINE JAYKO, DONALD DORSON, and OISTEIN JOHANSEN (Oceanographic Center, Trondheim, Norway) 15 Mar. 1988 166 p

(Contract DI-14-12-0001-30340)

(PB88-226055; OCS/MMS-87/0071-VOL-2) Avail: NTIS HC A08/MF A01 CSCL 13B

Satellite tracked surface drifters were evaluated for use in simulating the movement of spilled crude oil and assessing the skill of the Oil Spill Risk Analysis (OSRA) model. Review of the literature since 1980 shows that the most significant advance relative to surface transport processes relates to the effect of temporary submergence and surface shear on the distribution of oil behind the downwind leading edge of a surface slick. The results of dynamic analyses suggests that, two existing drifters, a sphere and a disk, represent the most promising available surface drifters for simulating the movement of spilled crude oil. Author

**N89-18706# Canada Centre for Remote Sensing, Ottawa (Ontario). Radarsat Project Office.****ESTIMATION OF THE SAR SYSTEM TRANSFER THROUGH PROCESSOR DEFOCUS**P. W. VACHON and R. K. RANEY *In* ESA, Proceedings of the 1988 International Geoscience and Remote Sensing Symposium (IGARSS) '88 on Remote Sensing: Moving Towards the 21st Century, Volume 3 p 1239-1242 Aug. 1988

Avail: NTIS HC A99/MF A01; ESA Publications Division, ESTEC, Noordwijk, Netherlands, \$120 US or 250 Dutch guilders

An approach for estimating SAR system transfer function (STF) based on the observation that system defocus, to first order, does not impact speckle statistics, is shown. A speckle pattern suitable for STF estimation may be produced from ocean wave SAR data by operating the processor out of focus, irrespective of the presence of waves in the image. ESA

**N89-18707# Kings Coll., London (England). Dept. of Physics. SPECKLE CORRELATION IN SAR IMAGES OF DYNAMIC DISCRETE SCATTERERS**K. OUCHI and R. E. BURGE *In* ESA, Proceedings of the 1988 International Geoscience and Remote Sensing Symposium (IGARSS) '88 on Remote Sensing: Moving Towards the 21st Century, Volume 3 p 1243-1247 Aug. 1988 Sponsored in part by the Royal Signals and Radar Establishment, Malvern, United Kingdom and the Ministry of Defence, London, United Kingdom

Avail: NTIS HC A99/MF A01; ESA Publications Division, ESTEC, Noordwijk, Netherlands, \$120 US or 250 Dutch guilders

The autocorrelation functions of speckle intensity in the SAR images of ocean surfaces that consist of discrete scatterers in uniform and random motions are discussed. Three types of motions are considered, namely random motion, azimuth velocity, and range acceleration. The speckle autocovariance functions are found to have a sharp central spike followed by a slow decaying long tail. The spike arising from the Gaussian contribution is proportional to the impulse response from a static point scatterer and unaffected by the motions. The slow decay is the non-Gaussian contribution, which is proportional to the impulse response degraded by the motions. The width of this decay, therefore, increases with increasing amount of degradation. The magnitude of the motion is found to be within the range of dynamic ocean surfaces for the effect to be observed. ESA

**N89-18717#** Ecole Nationale Supérieure des Telecommunications, Brest (France). Groupe Traitement d'Images.

**STATISTICAL EVALUATION OF THE INTENSITY DISTRIBUTION OF SEA SURFACE RADAR IMAGES**

J. M. SENECHAL, R. GARELLO, and A. HILLION *In* ESA, Proceedings of the 1988 International Geoscience and Remote Sensing Symposium (IGARSS) '88 on Remote Sensing: Moving Towards the 21st Century, Volume 3 p 1301-1302 Aug. 1988 Avail: NTIS HC A99/MF A01; ESA Publications Division, ESTEC, Noordwijk, Netherlands, \$120 US or 250 Dutch guilders

The relation  $I = S.Z$  is taken as a model for the intensity of the image:  $S$  is the reflectivity (of unknown law) and  $Z$  a multiplicative noise (of known law). Two possible probability distributions are considered (namely Dirac and uniform distribution) for the sea reflectivity and the two (theoretical) probability laws of the image intensity are derived. Statistical tests are performed from the observed data and a probabilistic model for the reflectivity coefficients in the case of particular SEASAT images is deduced. ESA

**N89-18718#** Rijkswaterstaat, The Hague (Netherlands). Tidal Waves Div.

**SEA BOTTOM TOPOGRAPHY WITH X-BAND SLAR: EVALUATION OF EXISTING MODELS**

J. VOGELZANG, G. J. WENSINK, G. P. DELOOR, H. C. PETERS, and H. POUWELS (National Aerospace Lab., Amsterdam, Netherlands) *In* ESA, Proceedings of the 1988 International Geoscience and Remote Sensing Symposium (IGARSS) '88 on Remote Sensing: Moving Towards the 21st Century, Volume 3 p 1303-1307 Aug. 1988 Sponsored in part by the Begeleidingscommissie Remote Sensing, Delft, Netherlands Avail: NTIS HC A99/MF A01; ESA Publications Division, ESTEC, Noordwijk, Netherlands, \$120 US or 250 Dutch guilders

The possibility of mapping bottom topography with imaging radar for cartography was assessed. Experimental results are compared with predictions of theories of the imaging mechanism. The experiment was carried out in an area off the Dutch coast where the bottom topography is dominated by sand waves with a crest-to-crest distance of typically 500 m. Images are to be compared with a digitized bathymetric map. ESA

**N89-18719\*#** Johns Hopkins Univ., Laurel, MD. Applied Physics Lab.

**MODELLING THE SIR-B IMAGE RESPONSE TO PARTIALLY COHERENT SEAS**

D. G. TILLEY *In* ESA, Proceedings of the 1988 International Geoscience and Remote Sensing Symposium (IGARSS) '88 on Remote Sensing: Moving Towards the 21st Century, Volume 3 p 1309-1312 Aug. 1988 Sponsored by the NASA, Washington, DC

Avail: NTIS HC A99/MF A01; ESA Publications Div., ESTEC, Noordwijk, Netherlands, \$120 US or 250 Dutch guilders CSCL 08C

A mathematical model of transient seas modulated by coherent swells is developed as a Rayleigh-Poisson random process subject to deterministic correlations of scattering sites, as they appear in a time window defined by a SAR's range-Doppler measurements

of the surface coordinates. This model of SAR response to sea surface dynamics is discussed as a Fourier domain predictor/corrector of a dynamic motion blur. ESA

**N89-18720#** Johns Hopkins Univ., Laurel, MD. Applied Physics Lab.

**RESULTS OF SOFTWARE SIMULATION OF A REAL-TIME SAR PROCESSOR CAPABLE OF PROVIDING OCEAN WAVE SPECTRA**

F. MONALDO *In* ESA, Proceedings of the 1988 International Geoscience and Remote Sensing Symposium (IGARSS) '88 on Remote Sensing: Moving Towards the 21st Century, Volume 3 p 1313-1315 Aug. 1988

Avail: NTIS HC A99/MF A01; ESA Publications Division, ESTEC, Noordwijk, Netherlands, \$120 US or 250 Dutch guilders

Hardware computations of a real-time, on-board SAR processor, capable of calculating SAR image spectra, scheduled to be carried aboard the shuttle during the SIR-C mission, were simulated. Results confirm the SAR image spectra generation capacity of the on-board processor. ESA

**N89-18721#** Bulgarian Academy of Sciences, Sofia. Inst. of Electronics.

**DISTRIBUTION OF SPECULAR POINTS ON THE OCEAN SURFACE: BISTATIC SCATTERING**

O. I. YORDANOV and M. A. MICHALEV *In* ESA, Proceedings of the 1988 International Geoscience and Remote Sensing Symposium (IGARSS) '88 on Remote Sensing: Moving Towards the 21st Century, Volume 3 p 1317-1318 Aug. 1988

Avail: NTIS HC A99/MF A01; ESA Publications Division, ESTEC, Noordwijk, Netherlands, \$120 US or 250 Dutch guilders

Assuming the validity of geometric optics, the distribution of specular points (DSP) on a non-Gaussian random rough surface is derived, in the case of bistatic scattering. The surface slope probability density function is taken to be the Edgeworth series in two dimensions. The form of the DSP is obtained for various positions and altitudes of the source and receiver. The knowledge of the DSP allows criteria for discriminating Fraunhofer and Fresnel type scattering to be examined. It is concluded that for source and receiver altitudes small compared to the distance between them, the scattering cannot be adequately described as a Fraunhofer one. The DSP patterns show that for small rms slopes the frequently used cylindrical surfaces are a conceivable approximation to the natural surfaces. ESA

**N89-18722#** Kings Coll., London (England). Dept. of Physics. **COMPUTER SIMULATION OF MULTIPATH SEA ECHO NEAR GRAZING INCIDENCE**

K. OUCHI and R. E. BURGE *In* ESA, Proceedings of the 1988 International Geoscience and Remote Sensing Symposium (IGARSS) '88 on Remote Sensing: Moving Towards the 21st Century, Volume 3 p 1319-1325 Aug. 1988 Sponsored in part by the Royal Signals and Radar Establishment, Malvern, United Kingdom and the Ministry of Defence, London, United Kingdom Avail: NTIS HC A99/MF A01; ESA Publications Division, ESTEC, Noordwijk, Netherlands, \$120 US or 250 Dutch guilders

Results for a computer simulation of multipath radar returns from a small target above the sea surface at near grazing incidence are presented. A radio wave directly reflected by the target is considered to interfere with many multipath radio waves reflected by the undulating sea waves and by the target. The temporal autocorrelation function of the detected signal intensity is found to consist of a sharp central spike followed by a damped oscillation. The spike, having very short decorrelation times, arises from fast fluctuating small-scale sea waves. The oscillation has the same period as the large-scale swell wave and the damping is caused by the random fluctuations of amplitude, wavelength and/or phase velocity of the swell wave. For certain values of radar and sea wave parameters, the oscillation reduces, enhances, or it contains frequencies higher than the sea wave frequency. ESA

**N89-18723#** Indian Space Research Organization, Ahmedabad. Space Applications Center.

**SPECULAR SCATTERING WITH EFFECTIVE REFLECTION COEFFICIENT**

R. KUMAR and A. SARKAR *In* ESA, Proceedings of the 1988 International Geoscience and Remote Sensing Symposium (IGARSS) '88 on Remote Sensing: Moving Towards the 21st Century, Volume 3 p 1327-1328 Aug. 1988

Avail: NTIS HC A99/MF A01; ESA Publications Division, ESTEC, Noordwijk, Netherlands, \$120 US or 250 Dutch guilders

The relationship between backscattering coefficient and wind speed for microwave frequencies at normal incidence angle was examined. The quasi-specular scattering theory for rough dielectric surfaces was applied with effective reflection coefficient and refined sea spectrum. The results show improvements compared with previous ones. ESA

**N89-18734#** Joint Research Centre of the European Communities, Ispra (Italy).

**OPTICAL PROPERTIES OF SEA WATER BODIES: MEASUREMENTS WITH AN UNDERWATER RADIOMETER AND A HIGH-RESOLUTION SPECTRORADIOMETER**

G. MARACCI and M. OOMS *In* ESA, Proceedings of the 1988 International Geoscience and Remote Sensing Symposium (IGARSS) '88 on Remote Sensing: Moving Towards the 21st Century, Volume 3 p 1379-1380 Aug. 1988

Avail: NTIS HC A99/MF A01; ESA Publications Division, ESTEC, Noordwijk, Netherlands, \$120 US or 250 Dutch guilders

Two different instruments, one for the determination of underwater downwelling and upwelling radiation, one for the measurement of the water-leaving radiance are described. The immersible instrument allows the determination of the light attenuation coefficient and the reflectance as a function of depth for 4 different wavelengths, corresponding to the Coastal Zone Color Scanner channels. Water leaving radiance is measured in 256 channels in the range of 380 to 1100 nm. The high resolution constitutes the state of the art of radiometer technology. Narrow band measurements of single channels and integration of measurements over selected ranges are possible. Examples of different water bodies are shown. Results are confronted with *in situ* data of chlorophyll. Optical *in situ* data are in good agreement with analytical results of chlorophyll determination. ESA

**N89-18737#** Institute of Ocean Sciences, Sidney (British Columbia).

**MAPPING OF PHYTOPLANKTON FLUORESCENCE WITH THE FLUORESCENCE LINE IMAGER (FLI) IMAGING SPECTROMETER**

J. F. R. GOWER and G. A. BORSTAD (Borstad Associates Ltd., Sidney, British Columbia) *In* ESA, Proceedings of the 1988 International Geoscience and Remote Sensing Symposium (IGARSS) '88 on Remote Sensing: Moving Towards the 21st Century, Volume 3 p 1391-1394 Aug. 1988

Avail: NTIS HC A99/MF A01; ESA Publications Division, ESTEC, Noordwijk, Netherlands, \$120 US or 250 Dutch guilders

The FLI (Fluorescence Line Imager) airborne imaging spectrometer is discussed. The value of high spectral resolution imaging over a variety of targets on land and water is underlined. The FLI was originally designed for a particular water application that influenced its technical specifications. These result, for example, in the instrument now having a higher spectral resolution than similar existing or planned instruments, while covering a narrower spectral range. An example of imagery over water where the effects of chlorophyll fluorescence can be clearly seen is shown. ESA

**N89-18738#** Johns Hopkins Univ., Laurel, MD. Applied Physics Lab.

**VARIABILITY OF THE DIFFUSE ATTENUATION COEFFICIENT IN WATERS OFF THE US EAST COAST**

J. A. GIANNINI *In* ESA, Proceedings of the 1988 International Geoscience and Remote Sensing Symposium (IGARSS) '88 on Remote Sensing: Moving Towards the 21st Century, Volume 3 p

1395-1397 Aug. 1988

Avail: NTIS HC A99/MF A01; ESA Publications Division, ESTEC, Noordwijk, Netherlands, \$120 US or 250 Dutch guilders

The seasonal variability of ocean color is examined using Coastal Zone Color Scanner (CZCS) data. The CZCS provided direct measurement of the upwelled radiance at wavelengths in the visible regime, from which the diffuse attenuation coefficient,  $K$ , at 490 nm was derived. Thirteen scenes are chosen from the mid-Atlantic Bight region off the east coast of the United States (38 N and 70 W) from 1979 to 1982, showing the seasonal variability in the ocean color on scales of 30,000 sq km. The distributions show a shift in the peak  $K$  value and a change in their width as functions of season. ESA

**N89-18739#** Bedford Inst. of Oceanography, Dartmouth (Nova Scotia). Dept. of Fisheries and Oceans.

**MONITORING OFFSHORE WATER QUALITY FROM SPACE**

B. J. TOPLISS and P. C. F. HURLEY *In* ESA, Proceedings of the 1988 International Geoscience and Remote Sensing Symposium (IGARSS) '88 on Remote Sensing: Moving Towards the 21st Century, Volume 3 p 1399-1402 Aug. 1988

Avail: NTIS HC A99/MF A01; ESA Publications Division, ESTEC, Noordwijk, Netherlands, \$120 US or 250 Dutch guilders

Images from the Coastal Zone Color Scanner (CZCS) onboard Nimbus-7 were compared to survey data taken by fisheries vessels off the east coast of Canada. A significant relationship between the corrected satellite radiance ratio and the Secchi disk depth is found although no significant relationship is determined for chlorophyll-a concentrations. It is shown that increased water turbidity can shift the water leaving optical signal out of the spectral range of a given satellite system and into the spectral range of another system. Visible satellite sensors were ranked for their ability to record coastal water turbidity. The SPOT and MOS-1 systems probably have better spectral capabilities for monitoring in-shore water quality than CZCS. ESA

**N89-18741#** State Oceanic Administration, Zhejiang (China). Second Inst. of Oceanography.

**QUICK REPORTING STATE OF FISHERY AND SEA ON THE EAST CHINA SEA AND THE YELLOW SEA WITH NOAA**

XINGWEI SHA and BAIDE XU *In* ESA, Proceedings of the 1988 International Geoscience and Remote Sensing Symposium (IGARSS) '88 on Remote Sensing: Moving Towards the 21st Century, Volume 3 p 1405-1408 Aug. 1988

Avail: NTIS HC A99/MF A01; ESA Publications Division, ESTEC, Noordwijk, Netherlands, \$120 US or 250 Dutch guilders

The quick reporting of the state of fishery and sea on the East China Sea and the Yellow Sea from 25 to 40 N, 120 to 130 E is introduced. The quick report chart contains sea surface temperature (SST), nearshore water color results from nearshore sediment, current state, and central fishing ground. By comparison with the value of observation on the spot, accuracy of SST on chart is within 0.4 C (rms). ESA

**N89-18742#** State Oceanic Administration, Zhejiang (China). Second Inst. of Oceanography.

**THE PRELIMINARY STUDY OF CURRENT SHIFTING STATE BY THE USE OF INFRARED IMAGES OF NOAA-9**

FU LE HUA *In* ESA, Proceedings of the 1988 International Geoscience and Remote Sensing Symposium (IGARSS) '88 on Remote Sensing: Moving Towards the 21st Century, Volume 3 p 1409-1412 Aug. 1988

Avail: NTIS HC A99/MF A01; ESA Publications Division, ESTEC, Noordwijk, Netherlands, \$120 US or 250 Dutch guilders

During the quick report state of fisheries and sea on East China Sea and Yellow Sea, the fourth channel infrared images of NOAA-9 satellite were utilized. Current shifting states and dividing points of warm Yellow Sea current and Tsushima current were analyzed. Results were compared with historical information and show a similar tendency. The dividing point of the Yellow Sea warm current can be determined at longitude 128 and latitude 32. The Tsushima shifting states coincide with the historical data. The warm current shifting states can be determined according to the

change in temperature of NOAA infrared images in winter. Space remote sensing provides a large number of continuous ocean data in a short time. ESA

**N89-18743#** State Oceanic Administration, Zhejiang (China). Second Inst. of Oceanography.

**A PRELIMINARY STUDY ON NEARSHORE WATER IN CHINA WITH NOAA SATELLITE IMAGES**

BAIDE XU and XINGWEI SHA /n ESA, Proceedings of the 1988 International Geoscience and Remote Sensing Symposium (IGARSS) '88 on Remote Sensing: Moving Towards the 21st Century, Volume 3 p 1413-1416 Aug. 1988  
Avail: NTIS HC A99/MF A01; ESA Publications Division, ESTEC, Noordwijk, Netherlands, \$120 US or 250 Dutch guilders

The distributions of nearshore water surface temperature (ST) on Northern Jiangsu and Southern Bohai Sea were obtained using data from channel 4 of AVHRR on NOAA satellites. It is clear that one on Northern Jiangsu appears in radiant pattern, one on Southern Bohai Sea appears in clockwise whirl in the vicinity of Shidao. The relationship between nearshore water ST shown to be radiant and the topography of the shallow marine bottom was assessed. The causes for such a topography are discussed according to material and hydrodynamical conditions. ESA

**N89-18744\*#** Environmental Research Inst. of Michigan, Ann Arbor. Radar Science Lab.

**INTERCOMPARISON OF SYNTHETIC- AND REAL-APERTURE RADAR OBSERVATIONS OF ARCTIC SEA ICE DURING WINTER MIZEX '87**

R. A. SCHUCHMANN, R. G. ONSTOTT, L. L. SUTHERLAND, and C. C. WACKERMAN /n ESA, Proceedings of the 1988 International Geoscience and Remote Sensing Symposium (IGARSS) '88 on Remote Sensing: Moving Towards the 21st Century, Volume 3 p 1419-1422 Aug. 1988 Sponsored in part by NASA, Washington, DC

(Contract N00014-81-C-0295; N00014-86-C-0469)  
Avail: NTIS HC A99/MF A01; ESA Publications Division, ESTEC, Noordwijk, Netherlands, \$120 US or 250 Dutch guilders CSCL 08L

Active microwave measurements were made of various sea ice forms in March and April 1987 during the Marginal Ice Zone Experiment, at 1, 5, 10, 18, and 35 GHz using a synthetic aperture radar (SAR) and helicopter and ship-based scatterometers. The X-band (9.8 GHz) SAR data were compared to the scatterometer data and it was determined that for 5 GHz and higher frequencies both the SAR and scatterometers can differentiate open water, new ice (5 to 30 cm), first-year ice with rubble (0.60 -1.5 m), and multiyear ice. The analysis further confirmed that the C-band (5 GHz) SAR's flying on ESA ERS-1 and Radarsat will differentiate the mentioned ice types. ESA

**N89-18745#** Canada Centre for Remote Sensing, Ottawa (Ontario).

**SAR IMAGERY OF THE GRAND BANKS (NEWFOUNDLAND) PACK ICE PACK AND ITS RELATIONSHIP TO SURFACE FEATURES**

S. D. ARGUS and F. D. CARSEY (Jet Propulsion Lab., California Inst. of Tech., Pasadena.) /n ESA, Proceedings of the 1988 International Geoscience and Remote Sensing Symposium (IGARSS) '88 on Remote Sensing: Moving Towards the 21st Century, Volume 3 p 1425-1428 Aug. 1988  
Avail: NTIS HC A99/MF A01; ESA Publications Division, ESTEC, Noordwijk, Netherlands, \$120 US or 250 Dutch guilders

Synthetic Aperture Radar (SAR) data and aerial photographs were obtained over pack ice off the East Coast of Canada in March 1987 as part of the Labrador Ice Margin Experiment (LIMEX) pilot project. Examination of this data shows that although the pack ice off the Canadian East Coast appears essentially homogeneous to visible light imagery, two clearly defined zones of ice are apparent on C-band SAR imagery. To identify factors that create the zones seen on the radar image, aerial photographs were compared to the SAR imagery. Floe size data from the aerial photographs was compared to digital number values taken

from SAR imagery of the same ice. The SAR data of the inner zone acquired three days apart over the melt period was also examined. The studies indicate that the radar response is governed by floe size and meltwater distribution. ESA

**N89-18746#** Jet Propulsion Lab., California Inst. of Tech., Pasadena.

**USE OF SAR IMAGERY AND OTHER REMOTELY-SENSED DATA IN DERIVING ICE INFORMATION DURING A SEVERE ICE EVENT ON THE GRAND BANKS (NEWFOUNDLAND)**

F. D. CARSEY and S. D. ARGUS (Canada Centre for Remote Sensing, Ottawa, Ontario ) /n ESA, Proceedings of the 1988 International Geoscience and Remote Sensing Symposium (IGARSS) '88 on Remote Sensing: Moving Towards the 21st Century, Volume 3 p 1431-1433 Aug. 1988 Sponsored by the Office of Energy Research and Development, Canada  
Avail: NTIS HC A99/MF A01; ESA Publications Division, ESTEC, Noordwijk, Netherlands, \$120 US or 250 Dutch guilders

Image data from synthetic aperture radar (SAR) are used to observe an ice compaction event off the East Coast of Newfoundland in spring, 1987. The information developed from sequential SAR observations is shown to do a remarkably effective job of describing the ice conditions; the difficult variable is the ice thickness which is found to be surprisingly large (2 to 4 times the thickness predictable from thermodynamic growth alone). It may be possible to model the ice thickness using SAR-derived ice motion. ESA

**N89-18747#** Environmental Research Inst. of Michigan, Ann Arbor. Radar Science Lab.

**SAR IMAGING OF OCEAN WAVES IN THE MARGINAL ICE ZONE**

J. LYDEN, R. A. SHUCHMAN, C. ZAGO, P. ROTTIER, P. WADHAMS, and O. JOHANNSEN (Nansen Ocean and Remote Sensing Center, Solheimsvik, Norway ) /n ESA, Proceedings of the 1988 International Geoscience and Remote Sensing Symposium (IGARSS) '88 on Remote Sensing: Moving Towards the 21st Century, Volume 3 p 1435-1437 Aug. 1988  
(Contract N00014-18-C-0295)

Avail: NTIS HC A99/MF A01; ESA Publications Division, ESTEC, Noordwijk, Netherlands, \$120 US or 250 Dutch guilders

The utility of a frequently observed phenomenon in SAR imagery of the marginal ice zone (MIZ) i.e., ocean gravity waves entering the pack ice is discussed. They provide information on the wave activity in the MIZ. The presence or absence of waves may also indicate differences in surface ice conditions. Measurement of wavelengths and directions from the SAR data may indicate refraction due to a surface current field such as that associated with mesoscale oceanic eddies. These waves also provide a unique test of SAR ocean wave imaging theories. ESA

**N89-18749#** Florida International Univ., Miami.  
**TECHNOLOGY TRANSFER FOR DEVELOPMENT OF COASTAL ZONE RESOURCES: CARIBBEAN EXPERTS EXAMINE CRITICAL ISSUES**

C. SPECTER and D. GAYLE /n ESA, Proceedings of the 1988 International Geoscience and Remote Sensing Symposium (IGARSS) '88 on Remote Sensing: Moving Towards the 21st Century, Volume 3 p 1449-1452 Aug. 1988  
Avail: NTIS HC A99/MF A01; ESA Publications Division, ESTEC, Noordwijk, Netherlands, \$120 US or 250 Dutch guilders

Remote sensing utilization by developing countries for the exploration, development, and conservation of their marine/coastal zone resources is discussed. This technology is not being applied to development activities to the extent that it could be. Technological factors, as well as other significant factors in the transfer process, such as political and economic constraints, that hinder the flow of technology to the Caribbean area are assessed. Recommendations that may be useful to policy-makers and managers concerned with this technology transfer problem are considered. ESA

**N89-18765#** Norwegian Defence Research Establishment, Kjeller.

**SIMULATION OF SAR IMAGING OF SHIP WAKES**

A. SKOELV, T. WAHL, and S. ERIKSEN *In* ESA, Proceedings of the 1988 International Geoscience and Remote Sensing Symposium (IGARSS) '88 on Remote Sensing: Moving Towards the 21st Century, Volume 3 p 1525-1528 Aug. 1988  
 Avail: NTIS HC A99/MF A01; ESA Publications Division, ESTEC, Noordwijk, Netherlands, \$120 US or 250 Dutch guilders

A numerical simulation scheme that is able to model the SAR imaging of different current-induced ocean phenomena is applied to SAR imaging of ship wakes. Ship wake simulations are performed in L- and C-band comparing two different imaging models. Weather state and ship parameters are varied, and results are compared with empirical wake data obtained from Seasat SAR images. The naive Bragg model may not fully describe the radar backscatter mechanisms. In L-band, however, there seems to be no qualitative differences between the wake cross sections predicted by the Bragg and HSW models, although the HSW model gives larger maximum positive and negative modulations. For the C-band case, the wake should not be visible, according to the Bragg model. The HSW model, on the other hand, predicts that the wake should be visible from satellites like ERS-1. The vortex and wake model has shortcomings, including no axial flow, and the initial circulation is uncertain. The vortex decay model is based upon results from aerodynamics, and does not consider the physical properties of the sea surface (presence of organic materials, films of oil, water temperature differences, etc.). In a complete model such effects should be taken into account. ESA

**N89-18766#** Norwegian Defence Research Establishment, Kjeller.

**AUTOMATIC SHIP AND SHIP WAKE DETECTION IN SPACEBORNE SAR IMAGES FROM COASTAL REGIONS**

K. ELDHUSET *In* ESA, Proceedings of the 1988 International Geoscience and Remote Sensing Symposium (IGARSS) '88 on Remote Sensing: Moving Towards the 21st Century, Volume 3 p 1529-1533 Aug. 1988  
 Avail: NTIS HC A99/MF A01; ESA Publications Division, ESTEC, Noordwijk, Netherlands, \$120 US or 250 Dutch guilders

Methods for automatic detection of ships and ship wakes in digital SAR images were developed. Accurate pixel location algorithms with digital maps are used to distinguish sea from land. A Wiener filter and a high pass filter are employed to enhance potential ship targets. With an appropriate choice of threshold, all ships visible to the human eye are detected. More rapid filters using statistics were also developed. By analyzing the statistics of the backscatter scan around each ship candidate, the various types of wakes may be detected with a very high probability. ESA

**N89-18782\*#** Jet Propulsion Lab., California Inst. of Tech., Pasadena.

**STUDIES OF THE DEPENDENCE OF THE MICROWAVE RADAR CROSS SECTION ON OCEAN SURFACE VARIABLES DURING THE FASINEX EXPERIMENT**

D. A. WEISSMAN (Hofstra Coll., Hempstead, NY.) and FUK LI *In* ESA, Proceedings of the 1988 International Geoscience and Remote Sensing Symposium (IGARSS) '88 on Remote Sensing: Moving Towards the 21st Century, Volume 3 p 1603-1608 Aug. 1988  
 Avail: NTIS HC A99/MF A01; ESA Publications Division, ESTEC, Noordwijk, Netherlands, \$120 US or 250 Dutch guilders CSLC 171

The ability of theoretical radar cross section (RCS) models to predict the absolute magnitude of the ocean radar cross section under a wide variety of sea and atmospheric conditions was studied using experimental data from the FASINEX Experiment. This consists of RCS data from a Ku-band scatterometer mounted on an aircraft (10 separate flights were conducted), a wide variety of atmospheric measurements (including stress) and sea conditions. Theoretical models are tested. Where discrepancies are observed, revisions are hypothesized and evaluated. ESA

**N89-18783#** Johns Hopkins Univ., Laurel, MD. Applied Physics Lab.

**THE EFFECT OF INTERNAL WAVES ON THE DOPPLER SPECTRUM OF MICROWAVES SCATTERED FROM THE OCEAN SURFACE**

D. R. THOMPSON *In* ESA, Proceedings of the 1988 International Geoscience and Remote Sensing Symposium (IGARSS) '88 on Remote Sensing: Moving Towards the 21st Century, Volume 3 p 1609-1613 Aug. 1988

Avail: NTIS HC A99/MF A01; ESA Publications Division, ESTEC, Noordwijk, Netherlands, \$120 US or 250 Dutch guilders

A composite model, derived from the Kirchhoff approximation for computing the microwave backscatter cross section from the ocean surface, was extended to include surface-motion effects. This extension enables one to calculate the autocovariance of the backscattered field and the associated Doppler spectrum. Such a time-dependent composite model is used to examine the variation of the Doppler spectrum produced by modulations in the surface-wave spectrum induced by internal waves. It is found that the computed Doppler spectra reflect the modulation structure found in direct measurements of the 2-D surface-wave spectrum. The results suggest that Doppler spectra can provide a useful probe of the ocean surface structure especially when direct measurements are not available. ESA

**N89-18784#** Jet Propulsion Lab., California Inst. of Tech., Pasadena.

**FRACTAL PROPERTIES OF THE SEA SURFACE MANIFESTED IN MICROWAVE REMOTE SENSING SIGNATURES**

R. E. GLAZMAN *In* ESA, Proceedings of the 1988 International Geoscience and Remote Sensing Symposium (IGARSS) '88 on Remote Sensing: Moving Towards the 21st Century, Volume 3 p 1623-1624 Aug. 1988

Avail: NTIS HC A99/MF A01; ESA Publications Division, ESTEC, Noordwijk, Netherlands, \$120 US or 250 Dutch guilders

The wave spectrum of a well developed sea is discussed. It includes a broad range of wavenumbers where the spectral density is governed by a power law of the form  $k \text{ sup-} p$ . When  $p$  is less than or = 4, the surface exhibits properties, such as an increased surface number density of steep and breaking wavelet events and an increased number of specular points for vertical incidence, due to the cascade (fractal) pattern in its geometry. These properties manifest themselves in error trends in wind speed measurements by scatterometer and altimeter. ESA

**N89-18785#** Tromsø Univ. (Norway).

**REMOTE STUDIES OF THE OCEAN SURFACE BY A TOWER-BASED MULTIFREQUENCY MICROWAVE RADAR**

T. ELTOFT, S. E. HAMRAN, and E. AARHOLT (Royal Norwegian Council for Scientific and Industrial Research, Kjeller.) *In* ESA, Proceedings of the 1988 International Geoscience and Remote Sensing Symposium (IGARSS) '88 on Remote Sensing: Moving Towards the 21st Century, Volume 3 p 1625-1629 Aug. 1988

Avail: NTIS HC A99/MF A01; ESA Publications Division, ESTEC, Noordwijk, Netherlands, \$120 US or 250 Dutch guilders

A tower-based multifrequency C-band radar was used to infer ocean surface waves and current characteristics. The wave spectrum was estimated from the cross-product signal spectra by dividing the power of the resonance lines with the squared modulus of the modulation transfer function. The resulting spectra are in good agreement with other measurements of the waves. The current was obtained from the frequency locations of the resonance lines, and the radar measurements compare well to the current measured by traditional instruments. ESA

**N89-18786#** Bulgarian Academy of Sciences, Sofia. Inst. of Electronics.

**STUDY ON DIRECTIONAL SPECTRUM CHARACTERISTICS OF MARINE RADAR IMAGES OF OCEAN WAVES**

V. ATANASSOV and L. MLADENOV *In* ESA, Proceedings of the 1988 International Geoscience and Remote Sensing Symposium (IGARSS) '88 on Remote Sensing: Moving Towards the 21st

Century, Volume 3 p 1631-1632 Aug. 1988

Avail: NTIS HC A99/MF A01; ESA Publications Division, ESTEC, Noordwijk, Netherlands, \$120 US or 250 Dutch guilders

A numerical scheme to compute integral characteristics of the 2-D wavenumber spectrum of radar ocean wave images collected in polar coordinates (range and azimuth) is developed. The directional spectrum characteristics include mean wavenumber, mean direction, minimum and maximum rms wavenumbers, and principal direction. The method exploits the fundamental relations between the moments of the 1-D wavenumber spectrum in a given direction and those of the 2-D wavenumber spectrum; a least square technique fits these relations with radar data. The numerical procedure was checked with artificially created images. It was also successfully applied to obtain integral characteristics of radar ocean wave images in natural conditions. ESA

**N89-18787#** Kansas Univ., Lawrence. Radar Systems and Remote Sensing Lab.

**ANALYSIS OF OCEAN BACKSCATTER DATA OBTAINED BY THE UNIVERSITY OF KANSAS DURING TOWARD 84/85**

R. K. MOORE, J. C. HOLTZMAN, J. C. WEST, R. LAWNER, V. HESANY, and S. JORDAN *In* ESA, Proceedings of the 1988 International Geoscience and Remote Sensing Symposium (IGARSS) '88 on Remote Sensing: Moving Towards the 21st Century, Volume 3 p 1633-1635 Aug. 1988

Avail: NTIS HC A99/MF A01; ESA Publications Division, ESTEC, Noordwijk, Netherlands, \$120 US or 250 Dutch guilders

Tower-based radar scatterometer measurements of the ocean surface were made. Plots of the backscattering coefficient ( $\sigma_0$ ) versus the neutral stability windspeed (NSW) are comparable to earlier results.  $\sigma_0$  is proportional to NSW sup  $\epsilon$ ,  $\epsilon$  is found to be between 1.5 and 3.0 at C, X, and Ku-bands and lower at L-band at the low wind speeds typical during the experiment. An improved method for detection of sea spikes was developed and is used to help identify their source. Predictions of the instantaneous radar backscatter are made from direct measurements of the small-scale wave spectrum and are compared with simultaneous radar measurements. Inclusion of hydrodynamic effects in the backscattering model gives a better prediction of the backscatter than just using tilt effects alone. The cross-correlation between the radar backscatter and wave height time series was calculated. This provides a measure of where on the long gravity waves the maximum backscatter occurs and does not depend on a linear relationship between the two time series. ESA

**N89-18789#** Tubitak, Kocaeli (Turkey). Dept. of Geosciences.

**WIGNER DISTRIBUTION ANALYSIS OF SURFACE WAVES**

M. AKTAR, S. ERGINTAV, and N. CAMTEZ (Technical Univ. of Istanbul, Turkey) *In* ESA, Proceedings of the 1988 International Geoscience and Remote Sensing Symposium (IGARSS) '88 on Remote Sensing: Moving Towards the 21st Century, Volume 3 p 1643-1646 Aug. 1988

Avail: NTIS HC A99/MF A01; ESA Publications Division, ESTEC, Noordwijk, Netherlands, \$120 US or 250 Dutch guilders

An approach for the analysis of dispersion in seismic surface waves is proposed. The Wigner Distribution concept is applied. The performance characteristics are investigated analytically and experimentally. The analysis is restricted to the continuous signal. Results reveal the overwhelming superiority of this method over currently utilized ones. The major advantages of Wigner distribution appear in the improved spectral resolution and the nonrequirement of an external parameter which introduces bias in the final results. The theoretical inferences are confirmed with experimental results. ESA

**N89-18797#** Washington Univ., Seattle. Polar Science Center. **ESTIMATING SEA ICE CONCENTRATION FROM SATELLITE PASSIVE MICROWAVE DATA AND A PHYSICAL MODEL**

D. A. ROTHROCK and D. R. THOMAS *In* ESA, Proceedings of the 1988 International Geoscience and Remote Sensing Symposium (IGARSS) '88 on Remote Sensing: Moving Towards the 21st Century, Volume 3 p 1677-1683 Aug. 1988 Sponsored

in part by NASA, Washington, DC, NSF, Washington, DC and ONR, Washington, DC

Avail: NTIS HC A99/MF A01; ESA Publications Division, ESTEC, Noordwijk, Netherlands, \$120 US or 250 Dutch guilders

Sea ice remote sensing and estimation of concentrations of each of several ice types from passive microwave satellite data is described. The approach is based on the Kalman filter; it incorporates surface temperature, ice advection, and ice deformation data derived from drifting buoys and uses the whole temporal microwave record to make a smoothed estimate of ice concentration. The method allows resolution of previously ambiguous surface types. An example using time histories of two SMMR measurements to resolve the fractional areas of four surface types: open water, first-year, second-year and older multiyear ice is shown. ESA

**N89-18799#** York Univ., Downsview (Ontario). Center for Research in Experimental Space Science.

**SHIPBORNE PASSIVE MICROWAVE SEA ICE EXPERIMENT IN THE EAST GREENLAND SEA: MAY-JULY 1987**

C. GARRITY *In* ESA, Proceedings of the 1988 International Geoscience and Remote Sensing Symposium (IGARSS) '88 on Remote Sensing: Moving Towards the 21st Century, Volume 3 p 1691-1692 Aug. 1988

Avail: NTIS HC A99/MF A01; ESA Publications Division, ESTEC, Noordwijk, Netherlands, \$120 US or 250 Dutch guilders

It is shown that multiyear (MY), first year (FY) and thinner ice types may be classified from their polarization in the spring using a dual-polarized 37 GHz radiometer if a large number of measurements are averaged for a particular month. Brightness temperature (TB) for MY and FY ice approaches each other during the spring. By the end of June, MY ice shows a larger polarization than FY ice, which is opposite in the early spring. In mid-spring, the TB of FY ice is 10 K higher than for MY ice, yet the polarization can be very similar. At this time, these ice types can be classified based on their TB, irrespective of their polarization. Using data from a passive microwave sensor on a satellite may provide a good average TB for each sea ice type, however, mixed ice types could cause a problem. Further studies to learn more about sea ice signatures using a shipborne radiometer would be beneficial due to the higher resolution as well as the capability of correlating snow plus ice properties with the measured TB's. ESA

**N89-18800\*#** National Aeronautics and Space Administration. Goddard Space Flight Center, Greenbelt, MD.

**PRELIMINARY OBSERVATIONS OF POLAR SEA ICE WITH THE SPECIAL SENSOR MICROWAVE IMAGER**

D. J. CAVALIERI *In* ESA, Proceedings of the 1988 International Geoscience and Remote Sensing Symposium (IGARSS) '88 on Remote Sensing: Moving Towards the 21st Century, Volume 3 p 1693-1694 Aug. 1988

Avail: NTIS HC A99/MF A01; ESA Publications Division, ESTEC, Noordwijk, Netherlands, \$120 US or 250 Dutch guilders CSCL 08L

The Special Sensor Microwave Imager (SSM/I) was launched as part of the Defense Meteorological Satellite Program. The SSM/I operates at 19.4, 22.2, 37.0, and 85.5 GHz with horizontal and vertical polarizations measured at each frequency except 22 GHz which has only a vertical polarization channel. Examination of polarization and spectral gradient ratios derived from the SSM/I radiances for open ocean, first-year, and multiyear Arctic sea ice reveals striking differences between the ratios calculated using lower frequencies and those ratios using the 85 GHz channels. These differences may serve as the basis for deriving sea ice information. ESA

**N89-18801#** Bar-Ilan Univ., Ramat-Gan (Israel). Dept. of Geography.

**A METHOD TO FORECAST OPEN PACK ICE SPEED OF MOTION USING REMOTELY-SENSED DATA**

U. FELDMAN *In* ESA, Proceedings of the 1988 International Geoscience and Remote Sensing Symposium (IGARSS) '88 on Remote Sensing: Moving Towards the 21st Century, Volume 3 p



1695-1702 Aug. 1988

Avail: NTIS HC A99/MF A01; ESA Publications Division, ESTEC, Noordwijk, Netherlands, \$120 US or 250 Dutch guilders

A reduced form of the general equation of motion for drifting pack ice is employed to forecast these motions. In this equation wind, water, and Coriolis stresses are assumed to be at equilibrium. By resolving these vectors two equations, consisting of eight variables, are derived. Ice location and speed of motion are obtained from two-day sequences of sidelapping LANDSAT-1 MSS images. Air density and geostrophic wind speed are obtained from three-day sequences of surface weather charts. The remaining four variables are estimated from these data and from previous observations on minima and maxima of ice thickness and drag coefficients at the air/ice and the water/ice interfaces. The method is tested by six groups of open pack ice floes which drifted in the marginal ice zone of the south-east Beaufort Sea. ESA

**N89-18802#** Ministry of Posts and Telecommunications, Tokyo (Japan). Communications Research Lab.

**STEP FREQUENCY RADAR EXPERIMENTS ON THE ANTARCTIC SEA ICE**

S. URATSUKA, K. OKAMOTO, F. NISHIO, H. MINENO, and S. MAE (Hokkaido Univ., Sapporo, Japan) *In* ESA, Proceedings of the 1988 International Geoscience and Remote Sensing Symposium (IGARSS) '88 on Remote Sensing: Moving Towards the 21st Century, Volume 3 p 1703-1706 Aug. 1988

Avail: NTIS HC A99/MF A01; ESA Publications Division, ESTEC, Noordwijk, Netherlands, \$120 US or 250 Dutch guilders

Ultrahigh frequency step frequency radar experiments were carried out on the sea ice in Antarctica in order to develop the sensor for measurement of sea ice thickness remotely. The radar system transmits 32 different frequencies in a stepwise fashion between 300 and 796 MHz. The distances to the targets are given through the discrete Fourier transform with frequency of complex received signal (amplitude with phase). The range resolution is 15 cm in sea ice. Experimental results show that the depth of the snow on the sea ice is measured clearly by this radar system. Sea ice thickness is accurately measured. ESA

**N89-18803#** Ice Centre Environment Canada, Ottawa (Ontario). **REAL-TIME PROCESSING OF DIGITAL IMAGE DATA IN SUPPORT OF THE CANADIAN SEA ICE ANALYSIS AND PREDICTION PROGRAM**

B. RAMSAY, D. HENDERSON, and L. CARSON (MacDonald, Detwiler and Associates Ltd., Richmond, British Columbia) *In* ESA, Proceedings of the 1988 International Geoscience and Remote Sensing Symposium (IGARSS) '88 on Remote Sensing: Moving Towards the 21st Century, Volume 3 p 1707-1711 Aug. 1988

Avail: NTIS HC A99/MF A01; ESA Publications Division, ESTEC, Noordwijk, Netherlands, \$120 US or 250 Dutch guilders

A computer-based system to enable ice forecasters and technicians to display, process, and integrate both geocoded digital imagery and overlaid chart graphics is presented. The hardware and software architecture is described. The processing and enhancement of digital image data sets are emphasized. ESA

**N89-18804#** Canada Centre for Remote Sensing, Ottawa (Ontario).

**TOWARD THE AUTOMATED USE OF REMOTE SENSING DATA IN OPERATIONAL ICE FORECASTING**

L. MCNUTT, T. MULLANE, and T. HIROSE (Noetix Research Ltd., Ottawa, Ontario) *In* ESA, Proceedings of the 1988 International Geoscience and Remote Sensing Symposium (IGARSS) '88 on Remote Sensing: Moving Towards the 21st Century, Volume 3 p 1713-1715 Aug. 1988

Avail: NTIS HC A99/MF A01; ESA Publications Division, ESTEC, Noordwijk, Netherlands, \$120 US or 250 Dutch guilders

The relationship between the size of ice features and the coverage and resolution provided by different remote sensing instruments is considered. The parameters used in ice models, and which data sources can provide information to drive the model calculations are examined. Remote sensing sources will provide

most of the ice-related information necessary to operational ice forecast models. Oceanographic and atmospheric information will also be available from other model results and remote sensing. Operational models will rely heavily on these data sources for information to initialize and update the models. Changes are being made to the operational environment which will result in the routine use of digital remote sensing information and auxiliary data sources in the ice information system. This means that efficient use of these data sources may require that operational models be modified or rewritten to suit the environment in which they run. ESA

**N89-18805#** Jet Propulsion Lab., California Inst. of Tech., Pasadena.

**SEA-ICE SOFTWARE: ICEMAN**

MEEMONG LEE *In* ESA, Proceedings of the 1988 International Geoscience and Remote Sensing Symposium (IGARSS) '88 on Remote Sensing: Moving Towards the 21st Century, Volume 3 p 1717-1720 Aug. 1988

Avail: NTIS HC A99/MF A01; ESA Publications Division, ESTEC, Noordwijk, Netherlands, \$120 US or 250 Dutch guilders

An oceanographer's work bench which provides tools for ice data display, ice type classification, global and local ice motion analysis, and data enhancing is presented. The user interface; ice texture analysis; and ice motion analysis are described. ESA

**N89-18817#** Copenhagen Univ. (Denmark). Inst. of Geophysics.

**AN ERDAS MODULE FOR ROUTINE PROCESSING OF AVHRR DATA**

L. VANCAMP *In* ESA, Proceedings of the 1988 International Geoscience and Remote Sensing Symposium (IGARSS) '88 on Remote Sensing: Moving Towards the 21st Century, Volume 3 p 1771-1775 Aug. 1988

Avail: NTIS HC A99/MF A01; ESA Publications Division, ESTEC, Noordwijk, Netherlands, \$120 US or 250 Dutch guilders

A software package for routine processing of AVHRR data into sea surface temperature and vegetation index maps was developed. The technical requirements of this AVHRR/ERDAS software package are described. Advantages are its transportability and extended user interface; the suitability of the software for extensions at a later stage to incorporate new functions, options, data formats, etc; good performance; the capability to upgrade the software package with future upgrades of the ERDAS system; and the possibility to obtain an image database that may be integrated with data from other sources in marine geographic information system. ESA

**N89-18837#** Johns Hopkins Univ., Laurel, MD. Applied Physics Lab.

**DYNAMIC TOPOGRAPHY AS MEASURED BY THE GEOSAT ALTIMETER IN REGIONS OF SMALL SURFACE HEIGHT SIGNATURES**

E. B. DOBSON *In* ESA, Proceedings of the 1988 International Geoscience and Remote Sensing Symposium (IGARSS) '88 on Remote Sensing: Moving Towards the 21st Century, Volume 2 p 635-638 Aug. 1988

(Contract N00039-87-C-5301)

Avail: NTIS HC A99/MF A01; ESA Publications Div. ESTEC, Noordwijk, Netherlands, \$120 US or 250 Dutch guilders

Geosat measurements of surface height signatures were used in an attempt to locate the positions of the front in the vicinity of the Iceland-Faroe ridge, where surface signatures are 1/10 to 1/3 of those in the Gulf Stream (already detected by the Geosat altimeter) using along track differences from the mean height and historical boundaries as measured from in situ data. While there is no way of knowing whether the interpretations of the signals position the front in its proper location, there are signals within the indicated boundaries, and the patterns are consistent. ESA

**N89-18838#** Imperial Coll. of Science and Technology, London (England).

**ASSIMILATION OF ALTIMETER DATA INTO NUMERICAL OCEAN MODELS**



P. J. BERRY *In* ESA, Proceedings of the 1988 International Geoscience and Remote Sensing Symposium (IGARSS) '88 on Remote Sensing: Moving Towards the 21st Century, Volume 2 p 639-642 Aug. 1988

Avail: NTIS HC A99/MF A01; ESA Publications Div. ESTEC, Noordwijk, Netherlands, \$120 US or 250 Dutch guilders

By simulating the assimilation of altimeter data into ocean models, it is shown that data from 1 altimeter in a 14 day repeat orbit can constrain the upper level circulation in a nonlinear two-layer model. The subsurface flow can be determined over a period of several months assimilation, the time scale for the decrease in deep circulation errors being given by the coefficient of bottom (Ekman) friction. ESA

**N89-18839#** Johns Hopkins Univ., Laurel, MD. Applied Physics Lab.

**THE INFLUENCE OF WATER VAPOR ON THE DETECTION OF OCEAN MESOSCALE FRONTS AND EDDIES BY THE GEOSAT ALTIMETER**

F. MONALDO *In* ESA, Proceedings of the 1988 International Geoscience and Remote Sensing Symposium (IGARSS) '88 on Remote Sensing: Moving Towards the 21st Century, Volume 2 p 643-646 Aug. 1988

Avail: NTIS HC A99/MF A01; ESA Publications Div. ESTEC, Noordwijk, Netherlands, \$120 US or 250 Dutch guilders

The spatial variability of water vapor as measured by the Seasat Scanning Multichannel Microwave Radiometer over a 30 day period was examined. It is demonstrated that water vapor generally varies on horizontal spatial scales greater than a few hundred kilometers. As such, it is unlikely that water vapor induced changes in altimeter measured heights will be misinterpreted as mesoscale ocean circulation features. ESA

**N89-18840#** Royal Aerospace Establishment, Farnborough (England). British National Space Center.

**A STUDY OF THE EFFECT OF RAIN ON SEASAT RADAR ALTIMETER DATA**

M. A. SROKOSZ and T. H. GUYMER (Institute of Oceanographic Sciences, Wormley, England) *In* ESA, Proceedings of the 1988 International Geoscience and Remote Sensing Symposium (IGARSS) '88 on Remote Sensing: Moving Towards the 21st Century, Volume 2 p 651-654 Aug. 1988

Avail: NTIS HC A99/MF A01; ESA Publications Div. ESTEC, Noordwijk, Netherlands, \$120 US or 250 Dutch guilders

The effect of rain on radar altimeter returns from the sea surface is studied using data from the Seasat mission. Passive microwave estimates of rain-rate are used to identify rainfall areas and the corresponding altimeter waveform and backscattered power data are examined to assess the effects of the rain. Results indicate that the presence of rain significantly affects the power of the backscattered return and that attenuation of the signal by the rain does not completely explain the phenomena observed. The presence of rain can affect the altimeter waveform. The cases examined indicate that light or moderate rainfall has little effect on the waveform, but heavy rain (rain rate over 15 mm/hr) can distort the shape of the waveform. These results, which are consistent with theoretical predictions, are shown to have implications for the retrieval of wind and wave parameters from radar altimeter data. ESA

**N89-18841#** Chalmers Univ. of Technology, Goeteborg (Sweden). Dept. of Radio and Space Science.

**OBSERVATIONS OF ICE TYPES IN SATELLITE ALTIMETER DATA**

L. ULANDER *In* ESA, Proceedings of the 1988 International Geoscience and Remote Sensing Symposium (IGARSS) '88 on Remote Sensing: Moving Towards the 21st Century, Volume 2 p 655-658 Aug. 1988 Sponsored in part with the Swedish Board for Space Activities, Solna

(Contract ESA-6617/85-F-FL(SC))

Avail: NTIS HC A99/MF A01; ESA Publications Div. ESTEC, Noordwijk, Netherlands, \$120 US or 250 Dutch guilders

Data acquired by the Seasat and Geosat radar altimeters over

sea ice were analyzed. The normal-incidence backscatter coefficient ( $\sigma_0$ ) is observed to separate different ice types. Seasat data from October in the Beaufort Sea show that 3 ice types could be separated; new ice ( $\sigma_0 = 33.0 \pm 2.8$  dB) and two types of multi-year ice, one consisting of small and deformed floes ( $24.1 \pm 3.2$  dB) and the other consisting of larger floes with ridge features ( $16.6 \pm 1.3$  dB). Geosat data from April in the brackish Bothnian Sea show that fast ice ( $37.8 \pm 2.8$  dB) and thin first-year ice ( $32.5 \pm 2.1$  dB) could be separated. ESA

**N89-18869#** Helsinki Univ. of Technology, Espoo (Finland). Dept. of Space Technology.

**BACKSCATTER BEHAVIOR OF LOW-SALINITY SEA ICE AT C AND X-BAND**

M. T. HALLIKAINEN, J. M. HYYPPA, M. V. O. TOIKKA, J. A. E. HAAPANEN, T. I. TARES, and P. J. AHOLA *In* ESA, Proceedings of the 1988 International Geoscience and Remote Sensing Symposium (IGARSS) '88 on Remote Sensing: Moving Towards the 21st Century, Volume 2 p 791-792 Aug. 1988

Avail: NTIS HC A99/MF A01; ESA Publications Div. ESTEC, Noordwijk, Netherlands, \$120 US or 250 Dutch guilders

A helicopter-borne dual-frequency scatterometer was used to investigate the backscattering behavior of low-salinity sea ice at 5.4 and 9.8 GHz in the Gulf of Bothnia. The backscattering properties of sea ice types were examined at the two frequencies, using HH, VV, HV, and VH polarization. Results for the like-polarized case suggest that discrimination of sea ice types is difficult due to the relatively large scatter in the results for each ice type. The scatter is largest for thick sea ice which may be caused by the presence of slush between the snow cover and the ice sheet in several areas. The presence of slush could not be confirmed from the helicopter, so the results for the two categories (slush/no slush) could not be identified. Using like-polarization, only two categories can be distinguished: open water and new ice; and thick ice, hummocks, and ice ridges. The backscattering coefficient for the cross-polarized case varies strongly with the ice type. The results suggest that three categories can be discriminated: hummocks and ice ridges; thick sea ice; and new sea ice and open water. ESA

**N89-18870#** Jet Propulsion Lab., California Inst. of Tech., Pasadena.

**IMPORTANT CHANGES IN MICROWAVE SCATTERING PROPERTIES OF YOUNG SNOW-COVERED SEA ICE AS INDICATED FROM DIELECTRIC MODELLING**

M. R. DRINKWATER *In* ESA, Proceedings of the 1988 International Geoscience and Remote Sensing Symposium (IGARSS) '88 on Remote Sensing: Moving Towards the 21st Century, Volume 2 p 793-797 Aug. 1988 Sponsored in part by the Natural Environment Research Council, London, United Kingdom

Avail: NTIS HC A99/MF A01; ESA Publications Div. ESTEC, Noordwijk, Netherlands, \$120 US or 250 Dutch guilders

Winter measurements of the properties of young snow-covered fast ice are input into a mixture model to calculate the complex dielectric constant. Large changes in the electromagnetic properties of the medium occur over the 46 day period of measurements. This early evolution of the surface is shown to have an important impact upon predicted radar backscattering properties at GHz frequencies. This has consequences for the unambiguous identification of young ice forms from synthetic aperture or side-looking airborne radar images. ESA

**N89-18871#** Centre National de Recherche Scientifique, Saint Martin d'Heres (France). Lab. de Glaciologie et Geophysique de l'Environnement.

**MEASURING LEAD AREA CHANGES IN SEA ICE IMAGERY**

M. FILY and D. A. ROTHROCK (Washington Univ., Seattle) *In* ESA, Proceedings of the 1988 International Geoscience and Remote Sensing Symposium (IGARSS) '88 on Remote Sensing: Moving Towards the 21st Century, Volume 2 p 799-800 Aug.

1988

Avail: NTIS HC A99/MF A01; ESA Publications Div. ESTEC, Noordwijk, Netherlands, \$120 US or 250 Dutch guilders

An algorithm for measuring the opening and the closing of sea ice leads by comparing two sequential digital images is described. Inputs to the algorithm are displacements measured on a fine grid over the entire scene, and a segmentation of both images into ice and lead pixels. The opening and closing estimates are within 10 percent of values obtained independently by a manual procedure. Automated ice tracking algorithms would provide ideal kinematic inputs. For the scenes studied, a 2 km spacing between displacements is adequate. ESA

**N89-18872#** Chalmers Univ. of Technology, Goeteborg (Sweden).

#### ICE RIDGE OBSERVATIONS BY MEANS OF SAR

J. ASKNE and R. JOHANSSON *In* ESA, Proceedings of the 1988 International Geoscience and Remote Sensing Symposium (IGARSS) '88 on Remote Sensing: Moving Towards the 21st Century, Volume 2 p 801-803 Aug. 1988 Sponsored in part by the Swedish National Board for Space Research, Stockholm  
Avail: NTIS HC A99/MF A01; ESA Publications Div. ESTEC, Noordwijk, Netherlands, \$120 US or 250 Dutch guilders

A SAR-model for a sea ice ridge is suggested and conclusions drawn, for example with regard to look angle and incidence angle dependence. Although ice ridges show up most clearly at large angles of incidence it is suggested that important information about the ridge properties like the repose angle can be found at an incidence angle typical for ERS-1. A Lee filter is used to discriminate ice ridge pixels in SAR images and to determine a characteristic measure of ice ridge density. ESA

**N89-18874#** Bercha (F. G.) and Associates Ltd., Calgary (Alberta).

#### AUTO AND CROSS CORRELATION ANALYSIS OF ENVIRONMENT, SYSTEM AND TARGET PARAMETERS FOR ICEBERG DETECTION USING AIRBORNE RADAR

V. L. SHAW, F. G. BERCHA, and W. H. MCRUER (Ice Centre Environment Canada, Ottawa, Ontario) *In* ESA, Proceedings of the 1988 International Geoscience and Remote Sensing Symposium (IGARSS) '88 on Remote Sensing: Moving Towards the 21st Century, Volume 2 p 809-816 Aug. 1988 Sponsored in part by the Atmospheric Environment Service, Ottawa, Ontario  
Avail: NTIS HC A99/MF A01; ESA Publications Div. ESTEC, Noordwijk, Netherlands, \$120 US or 250 Dutch guilders

Analysis of real aperture airborne radar data of icebergs, and comparison with corresponding ground truth data describing iceberg characteristics and environmental conditions are summarized. From the 117 SLAR acquisition missions, 1011 icebergs with associated ground truth information were identified as being in the study area during the SLAR overflights. The statistical analysis included autocorrelation and cross correlation analysis of iceberg characteristics, environmental conditions, and radar system imaging variables to determine the effect of each on iceberg detection using SLAR. ESA

**N89-18875#** Chalmers Univ. of Technology, Goeteborg (Sweden). Dept. of Radio and Space Science.

#### EVALUATION OF VARAN-S SAR DATA FROM THE BEPERS STUDY PROJECT

R. JOHANSSON *In* ESA, Proceedings of the 1988 International Geoscience and Remote Sensing Symposium (IGARSS) '88 on Remote Sensing: Moving Towards the 21st Century, Volume 2 p 817-818 Aug. 1988 Sponsored in part by the Swedish Board for Space Activities, Solna  
Avail: NTIS HC A99/MF A01; ESA Publications Div. ESTEC, Noordwijk, Netherlands, \$120 US or 250 Dutch guilders

Relative calibration of four different VARAN-S SAR images, acquired in the Baltic Sea, was performed. Based on this the backscattering coefficient for 3 different ice types was determined as a function of incidence angle (28 to 65 deg). Thin first-year ice is compared with snow covered fast ice, and level thin first-year ice is compared with ridged thin first-year ice. It is shown that the

first-year ice can be separated from the fast ice over the full incidence angle range. It is suggested that the SAR might give the possibility of retrieving the number of ridges per kilometer by means of the backscattering coefficient. ESA

**N89-18909#** Johns Hopkins Univ., Laurel, MD. Applied Physics Lab.

#### THE NAVY GEOSAT RADAR ALTIMETER SATELLITE MISSION

C. C. KILGUS *In* ESA, Proceedings of the 1988 International Geoscience and Remote Sensing Symposium (IGARSS) '88 on Remote Sensing: Moving Towards the 21st Century, Volume 2 p 965-967 Aug. 1988

Avail: NTIS HC A99/MF A01; ESA Publications Div. ESTEC, Noordwijk, Netherlands, \$120 US or 250 Dutch guilders

Geosat altimeter sea surface topography data were validated by comparison with in situ data. An rms precision equal to or better than 20 percent of the peak topography being measured, and 3 cm noise floor are attained. The sea level time series data product measures 20 cm Kelvin wave sea surface anomalies with an rms precision of 4 cm (or better). The colinear track difference data product measures the 51-day change in the 1 m Gulf Stream front with an rms precision of 20 cm (or better). ESA

**N89-18910#** British Aerospace Public Ltd. Co., Bristol (England).

#### AN ADVANCED TERRAIN TRACKING ALTIMETER

R. ANDREWARTHA, R. DURRANT, H. D. GRIFFITHS, D. J. WINGHAM, W. CUDLIP, M. A. J. GUZKOWSKA, C. G. RAPLEY, J. RIDLEY, J. BRADFORD, R. J. POWELL (Rutherford High Energy Lab., Chilton, England) et al. *In* ESA, Proceedings of the 1988 International Geoscience and Remote Sensing Symposium (IGARSS) '88 on Remote Sensing: Moving Towards the 21st Century, Volume 2 p 969-972 Aug. 1988 Prepared in cooperation with Ericsson Radar Electronics A.B., Molndal, Sweden (Contract ESTEC-6483/85-NL-BI)

Avail: NTIS HC A99/MF A01; ESA Publications Div. ESTEC, Noordwijk, Netherlands, \$120 US or 250 Dutch guilders

The results of a feasibility study into a radar altimeter capable of operation over all global terrain types are presented. Adaptive processing is used to allow the instrument to maintain maximum resolution over the ocean while adopting coarser resolution over topographic surfaces. The possible data products and applications are summarized, together with the operation of the tracking algorithms required. An experimental synthetic aperture mode of operation is assessed. The instrument has a built-in radiometer to estimate the wet tropospheric delay correction and a dual frequency altimeter to provide for ionospheric delay corrections. For 5 m significant waveheight, height error including tropospheric correction variance, mispointing, and calibration errors is less than 5 cm. Waveheight measurement error is 4 cm, and backscatter measurement error is 0.25 dB. ESA

**N89-18938#** Karlsruhe Univ. (Germany, F.R.). Inst. fuer Hoehstfrequenztechnik.

#### A STUDY OF PASSIVE MICROWAVE REMOTE SENSING

SHI ZHIFU and W. WIESBECK *In* ESA, Proceedings of the 1988 International Geoscience and Remote Sensing Symposium (IGARSS) '88 on Remote Sensing: Moving Towards the 21st Century, Volume 2 p 1091-1094 Aug. 1988

Avail: NTIS HC A99/MF A01; ESA Publications Div. ESTEC, Noordwijk, Netherlands, \$120 US or 250 Dutch guilders

An airborne millimeter wave imaging radiometer was installed on an aircraft for monitoring the oil pollution on the sea surface. False color images are shown. The oil spill volume can be estimated due to the evident interrelation between the oil slick thickness and the brightness temperature. The distinctive advances of microwave radiometer and the obtained data analysis indicate that passive microwave remote sensing will play an important role in the Earth Observation System. ESA

**N89-18939#** Copenhagen Univ. (Denmark). Inst. of Geophysics.

**THE STRUCTURE AND VARIABILITY OF A FILAMENT IN THE NORTHWEST AFRICAN UPWELLING AREA AS OBSERVED FROM AVHRR AND CXCS IMAGES**

C. NYKJAER, L. VANCAMP, and P. SCHLITTENHARDT (Joint Research Centre of the European Communities, Ispra, Italy) *In* ESA, Proceedings of the 1988 International Geoscience and Remote Sensing Symposium (IGARSS) '88 on Remote Sensing: Moving Towards the 21st Century, Volume 2 p 1097-1100 Aug. 1988

Avail: NTIS HC A99/MF A01; ESA Publications Div. ESTEC, Noordwijk, Netherlands, \$120 US or 250 Dutch guilders

Off Cap Ghir at 30.5 N in the northwest African upwelling area a filament of cold, phytoplankton-rich coastal water extending offshore and beyond the coastal zone was identified in satellite images of sea surface temperature from the Advanced Very High Resolution Radiometer and in images of phytoplankton pigment concentration derived from the Coastal Zone Color Scanner onboard Nimbus-7. The most salient characteristics of the filament as observed in satellite images, i.e., geographic location, length and width scale, and water masses are summarized. ESA

**N89-18940#** Joint Research Centre of the European Communities, Ispra (Italy). Physics Div.

**RADIOMETRIC PROBLEMS IN THE USE OF THE THEMATIC MAPPER FOR MARINE RESEARCH**

S. TASSAN *In* ESA, Proceedings of the 1988 International Geoscience and Remote Sensing Symposium (IGARSS) '88 on Remote Sensing: Moving Towards the 21st Century, Volume 2 p 1101-1103 Aug. 1988

Avail: NTIS HC A99/MF A01; ESA Publications Div. ESTEC, Noordwijk, Netherlands, \$120 US or 250 Dutch guilders

Radiometric problems in using the LANDSAT Thematic Mapper (TM) for marine survey are reviewed. Experience gained from test sites in the Adriatic Sea and in the Gulf of Naples indicates that, provided procedures tailored to the specific features of the sensor are applied, the interpretations of TM data can provide information on water quality parameters (chlorophyll and sediment concentrations) of satisfactory standard. ESA

**N89-18941#** Office of Naval Research, Arlington, VA.

**REMOTE SENSING IN A MARGINAL ICE ZONE: A BRIEF OVERVIEW**

C. A. LUTHER *In* ESA, Proceedings of the 1988 International Geoscience and Remote Sensing Symposium (IGARSS) '88 on Remote Sensing: Moving Towards the 21st Century, Volume 2 p 1107-1109 Aug. 1988

Avail: NTIS HC A99/MF A01; ESA Publications Div. ESTEC, Noordwijk, Netherlands, \$120 US or 250 Dutch guilders

The overall purpose of the series of Marginal Ice Zone Experiments (MIZEX), the disciplines involved, and the role of remote sensing are introduced. The MIZEX denotes a series of multinational, interdisciplinary experiments to study the mesoscale air-ice-ocean interactions in the shallow and deep water regimes of the Arctic marginal ice zone. Remote sensing served a dual role: as a tool to provide synoptic imagery of the experiment area for site location and sensor deployment strategy; and as a research discipline to provide knowledge and understanding of the capabilities and limitations of remote sensors operating in the marginal ice zone environment. ESA

**N89-18942#** Environmental Research Inst. of Michigan, Ann Arbor. Radar Science Lab.

**GEOPHYSICAL INFORMATION ON THE WINTER MARGINAL ICE ZONE OBTAINED FROM SAR**

R. A. SHUCHMAN, L. L. SUTHERLAND, O. M. JOHANNESSEN, and E. D. LEAVITT (INTERA Technologies Ltd., Calgary, Alberta) *In* ESA, Proceedings of the 1988 International Geoscience and Remote Sensing Symposium (IGARSS) '88 on Remote Sensing: Moving Towards the 21st Century, Volume 2 p 1111-1114 Aug. 1988

(Contract N00014-87-C-0418; N00014-81-C-0915)

Avail: NTIS HC A99/MF A01; ESA Publications Div. ESTEC, Noordwijk, Netherlands, \$120 US or 250 Dutch guilders

During the Winter 1987 Marginal Ice Zone Experiment synthetic aperture radar (SAR) data was collected on a daily basis. Each mission covered a 200 x 200 km area surrounding the ice-strengthened vessel Polar Circle. The SAR data were processed in real-time on-board the aircraft and downlinked to Polar Circle. Interpretation of the real-time imagery enabled scientists on-board Polar Circle to locate areas of special geophysical interest in order to facilitate ground truth. The SAR data are shown to be useful in detecting the ice edge, eddies within the ice, floe size distributions, ice types, ice concentration, and kinematics. ESA

**N89-18943\*#** Environmental Research Inst. of Michigan, Ann Arbor. Radar Science Lab.

**RADAR BACKSCATTER OF SEA ICE DURING WINTER**

R. G. ONSTOTT and R. A. SHUCHMAN *In* ESA, Proceedings of the 1988 International Geoscience and Remote Sensing Symposium (IGARSS) '88 on Remote Sensing: Moving Towards the 21st Century, Volume 2 p 1115-1118 Aug. 1988 Sponsored in part by NASA, Washington, DC

(Contract N00014-86-C-0469)

Avail: NTIS HC A99/MF A01; ESA Publications Div. ESTEC, Noordwijk, Netherlands, \$120 US or 250 Dutch guilders CSCL 08L

Active microwave measurements were made during the 1987 Marginal Ice Zone Experiment. Backscatter data were acquired at frequencies from 1.25 to 35 GHz, at incidence angles from 0 to 80 deg, and with linear antenna polarizations. The objective was to describe the scattering coefficients of the major ice types in the region and to study the winter conditions and their influence on the microwave response. Results show that multiyear and pancake ice produce strong backscatter, while returns from open water between floes and new ice are weak. First-year ice has a wide range of returns; when the surface is smooth returns are weak, and if roughened, i.e., like pancake ice, the returns increase substantially. ESA

**N89-18944#** Army Cold Regions Research and Engineering Lab., Hanover, NH.

**PHYSICAL PROPERTIES OF SNOW AND ICE IN THE WINTER MARGINAL ICE ZONE OF FRAM STRAIT**

D. K. PEROVICH, A. J. GOW, and W. B. TUCKER, III *In* ESA, Proceedings of the 1988 International Geoscience and Remote Sensing Symposium (IGARSS) '88 on Remote Sensing: Moving Towards the 21st Century, Volume 2 p 1119-1123 Aug. 1988 Sponsored in part by ONR, Washington, DC

Avail: NTIS HC A99/MF A01; ESA Publications Div. ESTEC, Noordwijk, Netherlands, \$120 US or 250 Dutch guilders

During the 1987 Marginal Ice Zone Experiment (MIZEX) the physical properties of ice and snow in the Fram Strait were examined under winter conditions. Snow and ice cover properties at 35 individual floes were determined. Snow thicknesses are significantly greater on multiyear floes, averaging 0.47 m, compared to 0.11 m for first-year floes. The texture of first-year and multiyear floes is predominantly columnar with granular ice comprising only 20 percent of total core length. The ice composition is comparable to that observed during MIZEX 84. The mean bulk salinity of first-year floes (7.7 0/00) is 3 times greater than that of the multiyear floes (2.5 0/00). In 5 of the 17 multiyear floes, profiles in the upper half meter exhibit first-year characteristics with salinities as high as 9 0/00. Below 0.5 m salinities are comparable to standard multiyear values. ESA

**N89-18945#** Naval Ocean Research and Development Activity, Bay Saint Louis, MS.

**INVESTIGATIONS OF SEA ICE USING COINCIDENT GEOSAT ALTIMETRY AND SYNTHETIC APERTURE RADAR DURING MIZEX-87**

F. FETTERER, D. JOHNSON, J. HAWKINS, and S. LAXON (Mullard Space Science Lab., Dorking, England) *In* ESA, Proceedings of the 1988 International Geoscience and Remote Sensing

Symposium (IGARSS) '88 on Remote Sensing: Moving Towards the 21st Century, Volume 2 p 1125-1126 Aug. 1988  
 Avail: NTIS HC A99/MF A01; ESA Publications Div. ESTEC, Noordwijk, Netherlands, \$120 US or 250 Dutch guilders

As part of the winter Marginal Ice Zone Experiment an aircraft with Synthetic Aperture Radar (SAR) flew under a concurrent Geosat track across the pack ice east of Greenland. Results from a comparison of cluster analysis of the SAR image with altimeter echo components are interpreted. Both SAR and altimeter are shown to discriminate distinct zones of ice characteristics within the pack ice. ESA

**N89-18946#** Sverdrup Technology, Inc., Middleburg Heights, OH.

**ESTIMATION OF SEA-ICE TYPE AND CONCENTRATION BY LINEAR UNMIXING OF GEOSAT ALTIMETER WAVEFORMS**

J. R. CHASE and R. J. HOLYER (Naval Ocean Research and Development Activity, Bay Saint Louis, MS.) *In* ESA, Proceedings of the 1988 International Geoscience and Remote Sensing Symposium (IGARSS) '88 on Remote Sensing: Moving Towards the 21st Century, Volume 2 p 1127-1128 Aug. 1988  
 Avail: NTIS HC A99/MF A01; ESA Publications Div. ESTEC, Noordwijk, Netherlands, \$120 US or 250 Dutch guilders

Given that an altimeter waveform may be a mixture of returns from two or more ice types within the footprint, linear unmixing theory was applied for analysis of waveform data. The mixing model assumes that data samples are linear combinations of a limited number of end members. Unmixing analysis therefore consists of identifying the number and nature of the end members followed by an interpretation of the data set in terms of combinations of these end members. Estimates of ice type and concentration obtained by linear unmixing are compared with passive microwave imagery collected coincident with Geosat overpass during MIZEX'87. Interesting characteristics of the Geosat ice index are revealed as a result of two end member unmixing of the waveform data. ESA

**N89-18972#** Department of Energy, Washington, DC. Office of Health and Environmental Research.

**COASTAL OCEAN MARGINS PROGRAM**

Dec. 1988 44 p  
 (DE89-005937; DOE/ER-0402) Avail: NTIS HC A04/MF A01

The marine research program supported by the Office of Energy Research, Ecological Research Division, provides scientific information on major environmental issues facing development and expansion of most energy technologies and energy policy. These issues include waste disposal, siting/operations, and possible long term effects on global systems. The research is concentrated along the United States coastal margins where marine waters provide abundant food and resources while assimilating discharges from atmospheric, terrestrial, and aquatic sources. The program focuses on the formation and transport of particles within the waters of the continental shelf and the fate of these particles, whether on the shelf, on the slope, or in the open ocean. The program is conducted with multidisciplinary teams of researchers who investigate water mass movements, biological productivity, and naturally forming particles, as well as contaminant transport, to develop a clear understanding of the exchanges of contaminants and other materials that take place between continental shelf and open ocean waters. DOE

**N89-19102\*#** Lamont-Doherty Geological Observatory, Palisades, NY.

**ANTARCTIC OCEAN POLYNYAS Semiannual Status Report, 1 Jul. 1988 - 1 Jan. 1989**

STANLEY S. JACOBS, ARNOLD L. GORDON, and JOSEPH C. COMISO (National Aeronautics and Space Administration, Goddard Space Flight Center, Greenbelt, MD.) 1989 8 p  
 (Contract NAGW-1344)  
 (NASA-CR-184805; NAS 1.26:184805) Avail: NTIS HC A02/MF A01 CSCL 08C

The spatial and temporal variability of sea ice concentrations derived from Nimbus-7 Scanning Multichannel Microwave

Radiometer (SMMR) brightness temperatures are presented. Emphasis is on the continental shelf region of the Ross Sea during 1984, when supporting data were obtained from oceanographic stations and moored instruments. The effects of the large spring polynya in the Ross Sea on summer insolation, surface heat layer storage, and late autumn ice formation are described. NASA

**N89-19792#** Massachusetts Inst. of Tech., Cambridge. Research Lab. of Electronics.

**ACTIVE AND PASSIVE REMOTE SENSING OF ICE Semiannual Report, 1 Feb. - 31 Jul. 1988**

JIN AU KONG 1 Nov. 1988 54 p  
 (Contract N00014-83-K-0258)

(AD-A201915) Avail: NTIS HC A04/MF A01 CSCL 20N

Fully polarimetric scattering properties of earth terrain media are studied with three-layer random medium model. The top scattering layer is modeled as an isotropic random medium which is characterized by a scalar permittivity. The middle scattering layer is modeled as an anisotropic random medium with a symmetric permittivity tensor whose optic axis can be tilted depending on the preferred alignment of the embedded scatters. The bottom layer is considered as a homogeneous half-space. Volume scattering effects of both random media are described by three-dimensional correlation functions with variances and correlation lengths corresponding to the strengths of the permittivity fluctuations and the physical sizes of the inhomogeneities, respectively. The strong fluctuations theory is used to derive the mean fields in the random media under the bilocal approximation with singularities of the dyadic Green's functions properly taken into consideration. With the discrete scatterer concept, effective permittivities of the random media are calculated by two-phase mixing formulas. Then, the distorted Born approximation is used to calculate the covariance matrix which describes the fully polarimetric scattering properties of the remotely sensed media. The polarimetric information is useful in the identification, classification, and radar image simulation of earth terrain media. GRA

**N89-19793#** Institute of Oceanographic Sciences, Wormley (England). Deacon Lab.

**DIRECTIONAL WAVE DATA RECORDED IN THE SOUTHERN NORTH SEA**

C. H. CLAYSON and J. A. EWING 1988 69 p  
 (Contract DEN-E/5B/CON/935/2043)

(IOS-258; ETN-89-93711) Avail: NTIS HC A04/MF A01; Institute of Oceanographic Sciences, Deacon Lab., Wormley, Godalming, Surrey GU8 5UB, United Kingdom, 19 pounds

A directional wave buoy was deployed 11 nm north-east of Cromer, in the southern North Sea during the period from December 1985 to June 1987, in an area which includes gas fields. The techniques used and results obtained are summarized. The basic nondirectional information consists of measurements of the frequency spectrum from which wave height and period statistics were computed. The buoy provides estimates of the directional spectrum from which the mean wave direction and directional spread are calculated. The results are presented in tables and figures which, in addition to wave height and period statistics, provide statistics of the joint occurrence of wave height, wave period, and wave direction. Information for each of four seasons and for the whole data set is given. ESA

## HYDROLOGY AND WATER MANAGEMENT

Includes snow cover and water runoff in rivers and glaciers, saline intrusion, drainage analysis, geomorphology of river basins, land uses, and estuarine studies.

**A89-20768#****MONITORING INUNDATION AREA OF ALIRAN SUNGAI BENGAWAN SOLO JAWA TIMUR WITH LANDSAT IMAGES**

TUTI GANTINI (Indonesian National Institute of Aeronautics and Space, Jakarta, Indonesia) IN: Asian Conference on Remote Sensing, 8th, Jakarta, Indonesia, Oct. 22-27, 1987, Proceedings. Bogor, Indonesia, EXSA International, 1987, p. B-9-1 to B-9-15. refs

**A89-20770\*#** Alabama Univ., Huntsville.**SATELLITE REMOTE SENSING OF CLOUD DISTRIBUTION AND AMOUNT OF RAINFALL OVER THE TIBET PLATEAU AREA OF CHINA**

R. J. HUNG (Alabama, University, Huntsville) and JAMES C. DODGE (NASA, Washington, DC) IN: Asian Conference on Remote Sensing, 8th, Jakarta, Indonesia, Oct. 22-27, 1987, Proceedings. Bogor, Indonesia, EXSA International, 1987, p. C-1-1 to C-1-12. refs

(Contract NAS8-33726)

The use of images from the GOES-1 satellite to study mesoscale convective clouds over the Tibet Plateau region in China is discussed. The correlation between the quantity of rainfall observed at the ground and the cloud volume dissipation per unit area as determined from satellite IR imagery is examined. It is shown that this relationship is almost linear for the rainfall rate exceeding 8 mm/day. R.B.

**A89-20771\*#** Alabama Univ., Huntsville.**VHF RADAR REMOTE SENSING OF VERTICAL PROFILE OF LIQUID WATER CONTENT AND RAINFALL RATE OVER TAIWAN DURING THE TIME PERIOD OF TYPHOON WAYNE**

R. J. HUNG, Y. D. TSAO (Alabama, University, Huntsville), D. L. JOHNSON (NASA, Marshall Space Flight Center, Huntsville, AL), A. J. CHEN, and C. H. LIN (National Central University, Chung-Li, Republic of China) IN: Asian Conference on Remote Sensing, 8th, Jakarta, Indonesia, Oct. 22-27, 1987, Proceedings. Bogor, Indonesia, EXSA International, 1987, p. C-2-1 to C-2-11. Sponsorship: National Science Council of the Republic of China. refs

(Contract NSC-75-0202-M008-21; NSC-76-0202-M008-23; NAG8-063; NAGW-1165)

**A89-20772#****RECONNAISSANCE GROUNDWATER APPRAISAL OF BOHOL ISLAND, PHILIPPINES, BY SATELLITE DATA ANALYSIS**

C. TRAVAGLIA, R. PEBBLES (UN, Food and Agriculture Organization, Rome, Italy), E. BATE, and A. FERRER (Ministry of Natural Resources, Natural Resources Management Center, Philippines) IN: Asian Conference on Remote Sensing, 8th, Jakarta, Indonesia, Oct. 22-27, 1987, Proceedings. Bogor, Indonesia, EXSA International, 1987, p. C-4-1 to C-4-21. refs

**A89-20774#****FLOODED AND INUNDATION DANGEROUS AREA PREDICTION AND ITS VISUALISATION - A CASE STUDY ON THE PEMALI-COMAL RIVER BASIN, CENTRAL JAVA, INDONESIA**

SRI SARWOASIH (Ministry of Public Works, Remote Sensing Center, Indonesia) IN: Asian Conference on Remote Sensing, 8th, Jakarta, Indonesia, Oct. 22-27, 1987, Proceedings. Bogor, Indonesia, EXSA International, 1987, p. C-7-1 to C-7-7. refs

The use of the Planning Assistance Through Technical Evaluation of Relevant Number method for the prediction of flooded and inundated dangerous areas is discussed. The input data consist

of Landsat MSS data and thematic maps. Digital analysis is used to produce FC, land cover, vegetation density, soil surface moisture, and flooded and inundated dangerous area analysis images for a region in Central Java. Flooded dangerous areas, flooded inundation areas, and areas of potentially dangerous flooding are determined. R.B.

**A89-20776#****AN ESTIMATION OF AREAL EVAPOTRANSPIRATION USING LANDSAT AND ELEVATION DATA**

TAKASHI HOSHI and SATOSHI UCHIDA (Tsukuba, University, Sakura, Japan) IN: Asian Conference on Remote Sensing, 8th, Jakarta, Indonesia, Oct. 22-27, 1987, Proceedings. Bogor, Indonesia, EXSA International, 1987, p. C-9-1 to C-9-7. refs

A method for estimating areal evapotranspiration is presented, based on the method of Kotoda et al. (1984). The method uses Landsat imagery and elevation data, and can estimate monthly evapotranspiration corresponding to an area that is tens to hundreds of sq km in size. Case studies demonstrating the method is presented for three areas in the western part of Japan. The results suggest that the method is reliable. R.B.

**A89-20777#****IDENTIFICATION OF SURFACE-GROUNDWATER INTERACTION ZONES IN THE BOGOR VOLCANIC FAN**

P. E. HEHANUSSA and MUNASRI (Indonesian Institute of Sciences, Bandung, Indonesia) IN: Asian Conference on Remote Sensing, 8th, Jakarta, Indonesia, Oct. 22-27, 1987, Proceedings. Bogor, Indonesia, EXSA International, 1987, p. C-10-1 to C-10-13.

Remote sensing techniques were used to identify the surface-groundwater interaction zones in the Bogor volcanic fan in West Java. First, groundtruth measurements were performed to determine the geohydrological features of the area. Landsat data were analyzed to delineate dry and wet areas and to confirm the groundtruth studies. The features determined and the geohydrology of the region are examined. R.B.

**A89-20778#****DRAINAGE PATTERN ANALYSIS WITH THE AID OF LANDSAT MSS DATA OF THE CITARIUM RIVER BASIN, WEST JAVA, INDONESIA**

JOKO SETIYONO HARDJOSUWARNO (Ministry of Public Works, Remote Sensing Center, Indonesia) IN: Asian Conference on Remote Sensing, 8th, Jakarta, Indonesia, Oct. 22-27, 1987, Proceedings. Bogor, Indonesia, EXSA International, 1987, p. C-14-1 to C-14-6.

**A89-20818#****PRIORITIZATION OF WATERSHED WITH REGARD TO SILT YIELD POTENTIAL THROUGH DATA INTEGRATION TECHNIQUE**

P. MANAVALAN and B. MANIKIAM (ISRO, Bangalore, India) IN: Asian Conference on Remote Sensing, 8th, Jakarta, Indonesia, Oct. 22-27, 1987, Proceedings. Bogor, Indonesia, EXSA International, 1987, p. Q-2-1 to Q-2-7. refs

Landsat TM data, topographic maps, and land survey data are integrated to create a data based for studying a watershed of the Tungabhadra, India river catchment. A grid analysis method is used to demarcate the priority areas of the watershed. Maps of relative slope, drainage, land cover, soil cover, and silt yield potential are produced. The watershed management applications of the research are discussed. R.B.

**A89-24649****THE RELATIONSHIP BETWEEN SUSPENDED SEDIMENT CONCENTRATION AND REMOTELY SENSED SPECTRAL RADIANCE - A REVIEW**

P. J. CURRAN (Sheffield, University, England) and E. M. M. NOVO (Instituto de Pesquisas Espaciais, Sao Jose dos Campos, Brazil) Journal of Coastal Research (ISSN 0749-0208), vol. 4, Summer 1988, p. 351-368. refs

The key to the successful remote sensing of suspended sediment concentration (SSC) in coastal waters is the strong

positive relationship that exists between SSC and remotely sensed spectral radiance (SR). This review provides an introduction to the SSC/SR relationship, with attention given to its physical basis, its robustness under a range of environmental conditions, and its usefulness as a tool for estimation. B.J.

A89-27946

**SATELLITE REMOTE SENSING OF RAINFALL**

ERIC C. BARRETT (Bristol, University, England) IN: Applications of remote sensing to agrometeorology; Proceedings of the Course, Ispra, Italy, Apr. 6-10, 1987. Dordrecht, Netherlands, Kluwer Academic Publishers, 1989, p. 305-326. refs

Techniques for satellite-assisted rainfall monitoring are reviewed, including manual, interactive, and objective methods. The use of visible, IR, and passive microwave satellite imagery is considered. The Bristol method (Barrett, 1983), the Bristol/NOAA interactive scheme (Barrett, 1986), a polar orbiter rainfall monitoring technique, an agricultural drought monitoring technique, and passive microwave techniques are examined. Also, suggestions for future strategies for operational rainfall monitoring are given. R.B.

A89-28033\* Alaska Univ., Fairbanks.

**BUOYANT SURFACE JET ANALYSIS OF THE YUKON RIVER**

J. P. GOSINK (Alaska, University, Fairbanks) International Journal of Remote Sensing (ISSN 0143-1161), vol. 9, Dec. 1988, p. 1873-1880. refs

(Contract NAS5-28769)

Thermal infrared satellite imagery of the discharge from the Yukon River obtained on July 5, 1985 was compared with hydraulic theory for the dilution of buoyant surface jets. In a crossflow, the theory predicts that the plume will follow an  $x \exp 1/3$  trajectory where  $x$  is distance alongshore, and that the plume temperature will decay according to  $x \exp -1/6$  due to mixing with the receiving water. Measurements of the Yukon River discharge indicate very good agreement with the predicted trajectory, and less, but acceptable, agreement with the predicted dilution. Large scale thermal fronts are also observable in the thermal imagery; the fronts may be associated with excursions of the plume due to tidal currents. Author

A89-30121

**VARIATIONS OF THE INFRARED EMISSION OF SNOW AND ICE COVER [O VARIATSIIAKH INFRAKRASNOGO IZLUCHENIIA SNEZHNO-LEDIANOGO POKROVA]**

G. S. BORDONSKI, S. D. KRYLOV, S. V. POLIAKOV, and L. D. RIABOVA (AN SSSR, Institut Prirodnykh Resursov, Chita, USSR) Issledovanie Zemli iz Kosmosa (ISSN 0205-9614), Nov.-Dec. 1988, p. 83-87. In Russian.

The paper presents results of an experimental study of 7-14-micron emission from lake snow and ice cover. An anomalous temperature drop down to 20 K was detected. It is suggested that the observed decrease of radiative temperature may be connected with the presence of water-soluble impurities in the thin surface layer of the snow. The results are pertinent to the remote radiometric sensing of ice and snow cover contaminated with pollutants. B.J.

A89-30252

**ESTIMATION OF THE WATER EXCHANGE AND CONTAMINATION ZONES OF BASINS FROM SATELLITE IMAGERY [OTSENKA VODOBMENA I ZON ZAGRIAZNENIIA VODOEMOV PO DANNYM KOSMICHESKOI S'EMKI]**

K. IA. KONDRATEV, N. N. FILATOV, and L. V. ZAITSEV Akademiia Nauk SSSR, Doklady (ISSN 0002-3264), vol. 304, no. 4, 1989, p. 829-832. In Russian. refs

Calculations based on mathematical and physical models of water exchange between the Neva inlet and the Gulf of Finland had indicated that the construction of a dam would reduce the water exchange only by 20 percent, which would guarantee sufficiently good quality of water in the inlet. The construction of the dam, however, has already resulted in a significant deterioration of water quality in the inlet due to the formation of local circulation

and stagnation zones. Here, the hydrodynamic processes and transformations occurring in the inlet and changes in the water exchange between the Gulf and the inlet and water contamination are examined by analyzing Meteor-30 and Cosmos-1939 satellite imagery in the bands 0.5-0.6, 0.6-0.7, and 0.8-0.9 microns and multispectral ERTS-1 satellite imagery. V.L.

A89-30261

**INVESTIGATION OF WATER CONTENT FROM AIRBORNE MSS DATA**

YOSHIRO SUZUKI (Nihon University, Tokyo, Japan) International Journal of Remote Sensing (ISSN 0143-1161), vol. 10, Jan. 1989, p. 71-82. refs

An image analysis of MSS data was performed in order to obtain ground truth data for a zone of instability (one in which a landslide is likely to occur) within a road construction site. In the near-infrared, a correlation is found between water content and the reflectance ratio. Stereoscopic interpretation of the photographs were useful in studying the drainage pattern. Image processing of the MSS data was employed to read the vegetation and land utilization classifications. R.R.

A89-31948

**PASSIVE MICROWAVE REMOTE SENSING SYSTEM FOR SOIL MOISTURE - SOME SUPPORTING RESEARCH**

THOMAS J. JACKSON and THOMAS J. SCHMUGGE (USDA, Hydrology Laboratory, Beltsville, MD) IEEE Transactions on Geoscience and Remote Sensing (ISSN 0196-2892), vol. 27, March 1989, p. 225-235. refs

A review of the current understanding of passive microwave remote sensing of soil moisture and examples of potential applications are presented. The potential platforms for such a system are the Earth Observing System (EOS) platforms planned for the late 1990s. Some of the relevant results supporting the implementation of a soil moisture microwave sensor are discussed. These results include data interpretation, the minimal requirements for sensor system design, and applications in hydrology and water management. I.E.

A89-32338\* National Aeronautics and Space Administration. Ames Research Center, Moffett Field, CA.

**MONITORING WATER QUALITY AND RIVER PLUME TRANSPORT IN GREEN BAY, LAKE MICHIGAN WITH SPOT-1 IMAGERY**

RICHARD G. LATHROP, JR. (NASA, Ames Research Center; TGS Technology, Inc., Moffett Field, CA; Wisconsin, University, Madison) and THOMAS M. LILLESAND (Wisconsin, University, Madison) Photogrammetric Engineering and Remote Sensing (ISSN 0099-1112), vol. 55, March 1989, p. 349-354. Research supported by the University of Wisconsin and William and Flora Hewlett Foundation. refs

(Contract NOAA-NA-84AAD00065)

N89-17340# World Meteorological Organization, Geneva (Switzerland).

**HYDROLOGICAL ASPECTS OF COMBINED EFFECTS OF STORM SURGES AND HEAVY RAINFALL ON RIVER FLOW 1988 85 p**

(WMO-704; OH-30; ISBN-92-63-10704; ETN-89-92880) Avail: MF A01; print copy available at WMO, Case Postale no. 5, CH-1211 Geneva 20, Switzerland

Storm-surge data, stages and discharges in rivers, precipitation and its areal and temporal variation, and methods of observation are reviewed. The deterministic approach to flood modeling in tidal areas including model structure, open sea models, bays and estuaries, and river models is discussed. The empirical approach to flood modeling in tidal areas, empirical models for coastal surge calculation, river surges, physically based formulas, and regression formulas are considered. Risk evaluation of storm surges in rivers and surge frequency at an open coast, flood frequency in tidal rivers, probable maximum floods, damage assessment, and flood insurance are treated. Forecasting centers, their location, choice



## 06 HYDROLOGY AND WATER MANAGEMENT

of model and communication equipment, and dissemination of forecasts and warnings are presented. Case studies are given.

ESA

**N89-17932#** South Carolina Univ., Columbia. Dept. of Geography.

### **A COMPARISON OF ORIGINAL AIRCRAFT MSS AND GENERATED SURFACE WATER REFLECTANCE IMAGES AS PREDICTORS OF LAKE WATER QUALITY INDICATORS**

ELIJAH W. RAMSEY, III and JOHN R. JENSEN 1988 13 p  
Presented at the Fall Technical Meeting of the American Society of Photogrammetry and Remote Sensing, Virginia Beach, VA, 11 Sep. 1988

(Contract DE-AC09-76SR-00001)

(DE89-004882; DP-MS-88-152; CONF-8809220-1) Avail: NTIS HC A03/MF A01

Generated reflectance and original MSS images were compared at six blue to near infrared wavelengths at thirty-eight (38) field locations in three different lakes. Both sets of images were evaluated in terms of their importance in explaining the variance of measured reflectances. Subsequently, the generated reflectance images were related to measured chlorophyll a and total suspended solids using a statistical analysis that uncovered the simplest relationships explaining the greatest amount of each water variables variance. Applying this methodology resulted in predictor equations explaining 82 percent of the chlorophyll a variance and 92 percent of the total suspended solids variance within the thirty-two (32) water samples analyzed. Maps were produced of L Lake depicting the distributions of two water quality indicators: chlorophyll a and total suspended particles. DOE

**N89-18733#** Institute of Karst Geology, Guilin (China).

### **QUANTITATIVE REMOTE DETECTION OF SUSPENDED SEDIMENT CONTENT AND CHLOROPHYLL CONCENTRATION OF WATER IN DIFFERENT DEPTHS**

SHOURONG SHU and JIAN CHEN (Guangzhou Inst. of Geography, China) *In* ESA, Proceedings of the 1988 International Geoscience and Remote Sensing Symposium (IGARSS) '88 on Remote Sensing: Moving Towards the 21st Century, Volume 3 p 1373-1377 Aug. 1988 Sponsored by the Chinese Academy of Sciences  
Avail: NTIS HC A99/MF A01; ESA Publications Division, ESTEC, Noordwijk, Netherlands, \$120 US or 250 Dutch guilders

A method to measure suspended sediment concentration (SC) and chlorophyll concentration (CC) in different depths of water is described. Using a specially designed device, the suspended solid concentration determination, water samples from different depths can be pumped into the device and then their spectral characteristics can be measured by a spectroradiometer. Multivariate regression analysis shows a significant correlation between the reflectance and the concentrations of suspended sediment or chlorophyll. Sediment and chlorophyll concentrations are estimated from spectral reflectance by using regression models with average relative errors of 3.6 pct and 3.4 pct, respectively. It takes only 4 min for measuring SC and CC from a water body. Such a method is effective for water quality monitoring, and when satellite imagery is used to estimate the CC and SC of water, this spectral method can be used in ground truth investigations to calculate satellite measurements. ESA

**N89-18735#** Instituto de Pesquisas Espaciais, Sao Jose dos Campos (Brazil).

### **THE IMPACT OF MULTIVIEWING REFLECTANCE DATA ON THE ESTIMATION OF SUSPENDED SEDIMENT CONCENTRATION**

EVLYN MARCIALEAODEMORAESNOVO *In* ESA, Proceedings of the 1988 International Geoscience and Remote Sensing Symposium (IGARSS) '88 on Remote Sensing: Moving Towards the 21st Century, Volume 3 p 1381-1384 Aug. 1988 Sponsored in part by Sheffield Univ. United Kingdom and the Fundacao de Amparo a Pesquisa do Estado de Sao Paulo, Brazil  
Avail: NTIS HC A99/MF A01; ESA Publications Division, ESTEC, Noordwijk, Netherlands, \$120 US or 250 Dutch guilders

The suitability of using reflectance data measured at different

viewing geometries to improve the estimation of suspended sediment concentration (SSC) was tested. Laboratory simulation of 35 suspended sediment concentrations and 14 different sensing geometries was carried out to derive the SSC reflectance relationship. The results from stepwise regression support the idea that multiviewing algorithms provide better estimates of suspended sediment concentration from water reflectance. The standard error of estimate decreases from 89.00 mg/l with the multispectral model to 24.39 mg/l with the multiviewing model. The explanatory power of viewing variables, however, varies with wavebands. ESA

**N89-18736#** Freiburg Univ. (Germany, F.R.). Inst. for Physical Geography.

### **DATA PROCESSING FOR THE DETERMINATION OF PIGMENTS AND SUSPENDED SOLIDS FROM THEMATIC MAPPER DATA**

B. GRUNWALD, W. MAUSER, and K. SCHNEIDER *In* ESA, Proceedings of the 1988 International Geoscience and Remote Sensing Symposium (IGARSS) '88 on Remote Sensing: Moving Towards the 21st Century, Volume 3 p 1385-1389 Aug. 1988 Sponsored in part by the Bundesministerium fuer Forschung und Technologie, Bonn, Fed. Republic of Germany  
Avail: NTIS HC A99/MF A01; ESA Publications Division, ESTEC, Noordwijk, Netherlands, \$120 US or 250 Dutch guilders

The use of Thematic Mapper data for determination of chlorophyll and suspended solids in fresh water is shown. Data processing, an atmospheric correction model, and a multiple regression model for chlorophyll-a are presented. It is shown that it is possible to use Thematic Mapper data as a source for chlorophyll-a mapping in fresh-water bodies. The regression model for chlorophyll is found to be significant up to the 90 pct level with a regression coefficient of 0.659. ESA

**N89-18740#** Delft Hydraulics Lab. (Netherlands).

### **MONITORING OF SUSPENDED SEDIMENTS IN JATILUHUR RESERVOIR USING SATELLITE IMAGES**

J. R. MOLL *In* ESA, Proceedings of the 1988 International Geoscience and Remote Sensing Symposium (IGARSS) '88 on Remote Sensing: Moving Towards the 21st Century, Volume 3 p 1403-1404 Aug. 1988 Prepared in cooperation with Pusat Penelitian Dan Pengembangan, Pengairan, Indonesia and Technische Hogeschool, Delft, Netherlands  
(Contract BCRS-4532/T0-2.7)  
Avail: NTIS HC A99/MF A01; ESA Publications Division, ESTEC, Noordwijk, Netherlands, \$120 US or 250 Dutch guilders

An approach to monitor erosion using remote sensing data was developed. The approach focuses on the measurement of sedimentation in reservoirs. Concentrations of suspended sediments in a reservoir are related to functions of SPOT and LANDSAT-measured digital photon counts. Jatiluhur reservoir on West Java was selected as a case-study. Ground truth data are computed using the mathematical model SERES-1 (Sedimentation in Reservoirs) as ground measurements are not available at the time of the satellites overpasses. The results are promising. ESA

**N89-18768#** University Coll., Cardiff (Wales). Dept. of Civil and Structural Engineering.

### **IMPROVEMENTS IN GROUND WATER RECHARGE ESTIMATION USING SATELLITE REMOTE SENSING**

R. S. DRAYTON, MD AZLIN MD SAID, and N. J. CARTER *In* ESA, Proceedings of the 1988 International Geoscience and Remote Sensing Symposium (IGARSS) '88 on Remote Sensing: Moving Towards the 21st Century, Volume 3 p 1541-1542 Aug. 1988

Avail: NTIS HC A99/MF A01; ESA Publications Division, ESTEC, Noordwijk, Netherlands, \$120 US or 250 Dutch guilders

Modeling of ground water flows and the difficulties encountered in estimating recharge are discussed. It was thought that remote sensing might provide useful information with regard to the land cover and the distribution of glacial drift in recharge areas. A model of an important aquifer in England was used to check the sensitivity of ground water predictions to changes in land cover



and drift, and numerical results of the sensitivity analysis are presented. A methodology for improving recharge estimation using remote sensing is given, and the improvements in the model results are quantified. ESA

**N89-18769#** University Coll., Cardiff (Wales). Dept. of Civil and Structural Engineering.

**AN ASSESSMENT OF ATM AND SATELLITE DATA FOR ESTIMATING THE GROUNDWATER CONTRIBUTION TO SLOPE STABILITY**

R. S. DRAYTON, M. P. HUGHES, and M. R. TAYLOR *In* ESA, Proceedings of the 1988 International Geoscience and Remote Sensing Symposium (IGARSS) '88 on Remote Sensing: Moving Towards the 21st Century, Volume 3 p 1543-1544 Aug. 1988 Sponsored in part by the Welsh Office, United Kingdom Avail: NTIS HC A99/MF A01; ESA Publications Division, ESTEC, Noordwijk, Netherlands, \$120 US or 250 Dutch guilders

Airborne thematic mapper and LANDSAT Thematic Mapper data were employed to detect seasonal variations in soil moisture which are indicative of ground water conditions. Correlations are made with the ground water parameter used in a model of slope stability, and the value of airborne scanner imagery is discussed in relation to the small-scale, site-specific investigations frequently encountered in civil engineering. It is possible, using LANDSAT TM imagery, to develop parameters which correlate well with those used in the model of slope stability. A field study is required to decide whether spectral features can be interpreted directly to provide a better alternative parameter for ground water conditions. Airborne thematic mapper offers very high spectral and spatial resolution, but for specific sites, and problems where precise location is essential, then the necessary geometric quality cannot be achieved. Second-generation satellite data will continue to be more appropriate until the problem of geometric inaccuracy is overcome. ESA

**N89-18770#** Aston Univ., Birmingham (England). Remote Sensing Unit.

**DIGITAL ELEVATION MODELS AND THEIR APPLICATION TO REMOTE SENSING OF WATER RESOURCES**

J. D. FLACH and T. R. E. CHIDLEY *In* ESA, Proceedings of the 1988 International Geoscience and Remote Sensing Symposium (IGARSS) '88 on Remote Sensing: Moving Towards the 21st Century, Volume 3 p 1545-1546 Aug. 1988 Avail: NTIS HC A99/MF A01; ESA Publications Division, ESTEC, Noordwijk, Netherlands, \$120 US or 250 Dutch guilders

A method for producing digital elevation models (DEM) is described. The system produces a reasonable representation of the topography, and an adequate input for further applications of the DEM. Video digitization provides a low cost method of digitizing topographic maps, and can produce data of sufficient resolution for remote sensing studies. The ideal input to interpolation procedures is the original survey data, contours provide a far from perfect input. This is mainly due to the digitization producing a high concentration of data along the contour line relative to the low concentration (nonexistent) between the contours. This can produce a markedly stepped interpolation surface. If contours are to be used then better results are obtained by extracting points along the contour at a distance equivalent to the distance between the contours. Alternatively the contour map must be examined to find the significant topographic points. ESA

**N89-18775#** Aston Univ., Birmingham (England). Remote Sensing Unit.

**ESTIMATION OF THE AREA OF LAKE KARIBA, ZIMBABWE, USING LANDSAT MSS IMAGERY**

D. J. BOOTH and R. B. OLDFIELD *In* ESA, Proceedings of the 1988 International Geoscience and Remote Sensing Symposium (IGARSS) '88 on Remote Sensing: Moving Towards the 21st Century, Volume 3 p 1565-1567 Aug. 1988 Sponsored in part by the Zambezi River Authority, Zimbabwe Avail: NTIS HC A99/MF A01; ESA Publications Division, ESTEC, Noordwijk, Netherlands, \$120 US or 250 Dutch guilders

The use of LANDSAT MSS imagery to estimate the aerial

extent of lake Kariba, Zimbabwe, at various water levels, for input to hydrological/evaporation models is discussed. The methods used to carry out the project, and problems inherent in applying textbook remote sensing problems to the real world are discussed. The original estimates of lake area, taken at the time of construction are in close agreement with those measured from satellite data. ESA

**N89-18832#** Nairobi Univ. (Kenya).

**SNOW COVER-SUMMER MONSOON RAINFALL OVER PARTS OF SAHEL**

O. S. R. U. BHANUKUMAR *In* ESA, Proceedings of the 1988 International Geoscience and Remote Sensing Symposium (IGARSS) '88 on Remote Sensing: Moving Towards the 21st Century, Volume 3 p 1847-1848 Aug. 1988

Avail: NTIS HC A99/MF A01; ESA Publications Division, ESTEC, Noordwijk, Netherlands, \$120 US or 250 Dutch guilders

Remotely sensed snow cover is compared to summer monsoon rainfall over 15 stations in the Sahel zone of west Africa for 18 yr. There is an inverse relation between Sahelian rainfall and two parameters from the Eurasian snow cover, one being the winter snow cover extent and the other the area of spring snowmelt. Negative correlations to the above relations for each station are in the range of 0.3 to 0.5. The increasing trend of snow cover is consistent with decreasing trend of Sahelian rainfall. A significant power peak around 5 yr is identified in winter snow, spring snowmelt, and monsoon rains. The higher significant negative correlation between the Eurasian winter snow cover and April ridge position reveals the profound interaction of snow on atmosphere. ESA

**N89-18937#** Naval Ocean Research and Development Activity, Bay Saint Louis, MS.

**AIRBORNE NONACOUSTIC BATHYMETRIC SURVEY FLIGHT TEST RESULTS**

S. P. HAIMBACH, K. SMITS, and G. D. HICKMAN *In* ESA, Proceedings of the 1988 International Geoscience and Remote Sensing Symposium (IGARSS) '88 on Remote Sensing: Moving Towards the 21st Century, Volume 2 p 1081-1086 Aug. 1988 Sponsored in part by the Defense Mapping Agency, Washington, DC

Avail: NTIS HC A99/MF A01; ESA Publications Div. ESTEC, Noordwijk, Netherlands, \$120 US or 250 Dutch guilders

Three airborne remote sensor systems to support shallow water hydrographic data collection over a wide range of environmental conditions using nonacoustic methods were developed. The laser sounder and multispectral scanner are active and passive optical sensors, respectively, and together make up the airborne bathymetric survey system. The airborne electromagnetic system uses electromagnetic techniques to obtain hydrographic data. The helicopter borne system operated at 95, 385, and 7200 Hz, in a horizontal coplanar configuration. Concurrent ground truth surveys included acoustic soundings and water conductivity measurements. Results are encouraging, and an operational system is envisioned. ESA

**N89-18984** Air Force Geophysics Lab., Hanscom AFB, MA.

**EHF ATTENUATION THROUGH THE MELTING LAYER**

ARNOLD A. BARNES, JR. *In* Deutscher Wetterdienst, Annals from the German Meteorological Society. No. 25: 10th International Cloud Physics Conference Preprints, Volume 2 p 380-382 1988 Avail: Deutscher Wetterdienst, Frankfurter Strasse 135, D-6050 Offenbach am Main, Fed. Republic of Germany

Signal strengths from the 38 GHz transmitter aboard Lincoln Experimental Satellite (LES-8) clearly demonstrated the attenuation due to the precipitation between the satellite and the ground receiving site. Airborne meteorological data were collected by instrumented aircraft. End products include ice/water content, particle size distributions, temperature, humidity, and aircraft position. An instrument (M-meter) to measure the mass of ice and/or water was also tested for collection of precipitation mass information within the melting layer where both snow and rain coexist. Ten different precipitation events were investigated even

though the amount of rainfall was much below normal for this 69 day period. Satellite signals show attenuation in excess of 15 dB during the showers while light continuous precipitation gives attenuations of 6dB. To study attenuation due to the radome covering the receiving dish being wetted by the rain, it was sprayed on a clear, dry day, and shows a loss of 1 to 2 dB. Tests with the M-meter went better than expected. Speed and altitude corrections are close to predicted, but the sensitivity is greater than expected and is found to be limited by the accuracy of the calculated true air speed. ESA

**N89-19732#** Begeleidingscommissie Remote Sensing, Delft (Netherlands).  
**THE USE OF LANDSAT IMAGERY FOR WATER QUALITY STUDIES IN THE IJSSELMEER AREA (NETHERLANDS) [HET GEBRUIK VAN LANDSAT OPNAMEN VOOR WATERKWALITEITSONDERZOEK IN HET IJSSELMEERGEBIED]**

H. BUITEVELD (Rijkswaterstaat, The Hague, Netherlands ), C. MEULSTEE, and R. JORDANS Dec. 1987 43 p In DUTCH Original contains color illustrations (BCRS-87-18; ETN-89-93872) Avail: NTIS HC A03/MF A01

The procedure for the processing of satellite images to improve water quality aspects, such as sediments, is described. A procedure for airborne multispectral scanner pictures and field observations was extended for LANDSAT thematic mapper pictures. Via multiple linear regression a functional relation between ground observations and remote sensing data was established. This algorithm was applied to satellite pictures resulting in a concentration chart, e.g., of sediment. True color and false color composite pictures were also made. The results show the method to be suitable for the processing of satellite images for inland water applications. The processed images show significant optical differences between two stretches of water. ESA

07

**DATA PROCESSING AND DISTRIBUTION SYSTEMS**

Includes film processing, computer technology, satellite and aircraft hardware, and imagery.

**A89-20764#**  
**SPOT RESULTS OF TOPOGRAPHICAL MAPPING USING SPOT IMAGES OF MALAYSIA**

GUY ROCHON, REJEAN SIMARD, STEVEN L. MACEK, THIERRY TOUTIN, ANDRE LECLERC (Digim, Inc., Montreal, Canada) et al. IN: Asian Conference on Remote Sensing, 8th, Jakarta, Indonesia, Oct. 22-27, 1987, Proceedings. Bogor, Indonesia, EXSA International, 1987, p. B-3-1 to B-3-10. Research supported by the Canadian International Development Agency. refs

**A89-20765#**  
**ACCURACY OF LAND-COVER/USE CLASSIFICATION**

HARUHISA SHIMODA, YOSHIKI MATSUMAE, YUMI KASAI, KIYONARI FUKUE, and TOSHIKUMI SAKATA (Tokai University, Tokyo, Japan) IN: Asian Conference on Remote Sensing, 8th, Jakarta, Indonesia, Oct. 22-27, 1987, Proceedings. Bogor, Indonesia, EXSA International, 1987, p. B-4-1 to B-4-9.

The establishment of the optimal landcover classification algorithm for Landsat TM data is discussed. The influence of spatial and spectral resolutions on land cover classification accuracy and the redundancy of TM data are evaluated. It is found that the increase of spatial resolution does not necessarily provide higher classification accuracies. It is shown that the addition of bands 5 and 7 has not significantly increased landcover classification accuracy. The study of TM data compression suggests that the first four principal components are almost sufficient for landcover classifications. R.B.

**A89-20767#**  
**PRINCIPLE COMPONENT TRANSFORMATION ANALYSIS FOR TENTATIVE LAND USE INTERPRETATION OF LANDSAT MSS OF BOGOR REGION, INDONESIA**

SRI HARDIYANTI PURWADHI and MAWARDI NUR (Indonesian National Institute of Aeronautics and Space, Jakarta, Indonesia) IN: Asian Conference on Remote Sensing, 8th, Jakarta, Indonesia, Oct. 22-27, 1987, Proceedings. Bogor, Indonesia, EXSA International, 1987, p. B-7-1 to B-7-14. refs

**A89-20775#**  
**THE USE OF IMAGE ENHANCEMENT TECHNIQUE FOR PEAT LAND MAPPING USING LANDSAT MASS DATA IN INDONESIA**

HARIYATNO SOEMARMAN (Ministry of Public Works, Remote Sensing Center, Indonesia) IN: Asian Conference on Remote Sensing, 8th, Jakarta, Indonesia, Oct. 22-27, 1987, Proceedings. Bogor, Indonesia, EXSA International, 1987, p. C-8-1 to C-8-10. refs

**A89-20782#**  
**MAPPING OF CONSTRUCTION MATERIAL SITES AROUND BANGALORE CITY USING LANDSAT THEMATIC MAPPER DATA**

A. K. GUPTA and K. GANESHA RAJ (ISRO, Bangalore, India) IN: Asian Conference on Remote Sensing, 8th, Jakarta, Indonesia, Oct. 22-27, 1987, Proceedings. Bogor, Indonesia, EXSA International, 1987, p. D-16-1 to D-16-5.

**A89-20790#**  
**MOS-1 DATA PROCESSING IN TOKAI SPACE CENTER**

YOSHIKI MATSUMAE, TSUKASA HOSOMURA, HARUHISA SHIMODA, TOSHIKUMI SAKATA, and KIYONARI FUKUE (Tokai University, Tokyo, Japan) IN: Asian Conference on Remote Sensing, 8th, Jakarta, Indonesia, Oct. 22-27, 1987, Proceedings. Bogor, Indonesia, EXSA International, 1987, p. F-1-1 to F-1-7.

Data processing facilities at the Tokai (Japan) University Space Information Center are described, focusing on processing techniques for Marine Observation Satellite (MOS-1) data. The features of the MOS-1 receiving system are discussed, including the antenna and control unit, station operation, image and data processing units, archives, and image analysis system. Diagrams of the system and examples of processed imagery are presented. R.B.

**A89-20791#**  
**SPATIAL INFORMATION PROCESSINGS OF TM DATA**

ZI-JUE ZHANG, HARUHISA SHIMODA, KIYONARI FUKUE, YOSHIKI MATSUMAE, and TOSHIKUMI SAKATA (Tokai University, Tokyo, Japan) IN: Asian Conference on Remote Sensing, 8th, Jakarta, Indonesia, Oct. 22-27, 1987, Proceedings. Bogor, Indonesia, EXSA International, 1987, p. F-5-1 to F-5-6.

A spatial information-based approach to the problem of identifying land-cover classes in Landsat TM data is proposed. In the first step of the method, a classification map depicting the spatial distribution of cover components is produced. The frequency distribution of cover components is then extracted and used as the classification feature for spatial information-based classification. A case study is presented using the method for a 6-band Landsat TM image of Hiratsuka City, Japan. The results show that, compared to a point wise classification, the spatial information-based procedure increases classification accuracy by about 7.7 percent. R.B.

**A89-20794#**  
**THE CREATING OF BLUE SYNTHETIC CHANNEL OF MSS LANDSAT IMAGE**

K. MULYADI (Indonesian National Institute of Aeronautics and Space, Jakarta, Indonesia) IN: Asian Conference on Remote Sensing, 8th, Jakarta, Indonesia, Oct. 22-27, 1987, Proceedings. Bogor, Indonesia, EXSA International, 1987, p. F-10-1 to F-10-15.

The blue synthetic channel of MSS Landsat image is observed by using the extrapolation technique from green (500 - 600 nm) and red (600 - 700 nm) channels. It is assumed that the spectral

reflectance of the objects change linearly on blue to red region. The blue synthetic channel data and green and red channel data were used to form a natural color composite image. Author

**A89-20796\*#** National Aeronautics and Space Administration. Goddard Space Flight Center, Greenbelt, MD.

**LOW COST, MICROCOMPUTER-BASED INTERACTIVE ANALYSIS SYSTEM FOR DIRECT-RECEPTION AND ARCHIVED REMOTE SENSING DATA**

CHARLES H. VERMILLION (NASA, Goddard Space Flight Center, Greenbelt, MD) and JAMES C. DODGE (NASA, Washington, DC) IN: Asian Conference on Remote Sensing, 8th, Jakarta, Indonesia, Oct. 22-27, 1987, Proceedings. Bogor, Indonesia, EXSA International, 1987, p. F-13-1 to F-13-5.

A hardware/software system has been developed for use in meteorological field experiments and by developing countries which need low-cost remote sensing data analysis capabilities. The system can directly receive satellite transmissions of the AVHRR, TOVS, Argos, GOES, GMS, and Meteosat systems. Also, the system can process computer tapes from Landsat. Received data are ingested directly into the computer's disk storage, eliminating the need for a wide-band analog tape drive. Data may be interpreted in terms of cloud imagery, cloudtop temperature, sea surface temperature, vegetation index, and temperature/humidity profiles with overlays of geographic boundaries and latitude/longitude grids. The image processing, enhancement functions, and modeling capabilities of the system are discussed. R.B.

**A89-20797#**

**APPLICATION OF THREE DIMENSIONAL IMAGE SYSTEM**

MARCELINA RINNY HENDRAWATI, SRI SARWOASIH (Ministry of Public Works, Remote Sensing Center, Indonesia), and MAMORU ISHIKAWA (Ministry of Agriculture, Forestry and Fisheries, International Cooperation Div., Tokyo, Japan) IN: Asian Conference on Remote Sensing, 8th, Jakarta, Indonesia, Oct. 22-27, 1987, Proceedings. Bogor, Indonesia, EXSA International, 1987, p. F-14-1 to F-14-7. refs

A computer software system for three-dimensional image processing is discussed. The processes for data preparation, elevation data modification, data coordinate transformation, and three-dimensional image creation are described. A case study is presented, using a color composite Landsat image and elevation data taken from existing contour maps to create a three-dimensional image. R.B.

**A89-20798#**

**COMPARISON OF THE ORIENTATION'S ACCURACY FOR SPOT IMAGERY**

OSAMU UCHIDA (Asia Air Survey Co., Information System Div., Atsugi, Japan), SHUNJI MURAI, and SUKIT VISESHSIN (Tokyo, University, Japan) IN: Asian Conference on Remote Sensing, 8th, Jakarta, Indonesia, Oct. 22-27, 1987, Proceedings. Bogor, Indonesia, EXSA International, 1987, p. G-1-1 to G-1-7.

The accuracy of the orientation of SPOT imagery of the area surrounding Mt. Fuji, Japan is investigated. Two orientation methods, single image adjustment and multiple image adjustment, are evaluated. The control point distributions in dense, medium, coarse, and very coarse images are compared. It is found that point-type control is more accurate than feature-type control. R.B.

**A89-20799#**

**AN INTERACTIVE SYSTEM FOR AERIAL PHOTO ORIENTATION OF DIGITAL STEREO IMAGE PAIRS**

Y. KOMETANI (Aero Asahi Corp., Tokyo, Japan), H. SCHEAFER, S. HATTORI, and S. MURAI (Tokyo, University, Japan) IN: Asian Conference on Remote Sensing, 8th, Jakarta, Indonesia, Oct. 22-27, 1987, Proceedings. Bogor, Indonesia, EXSA International, 1987, p. G-2-1 to G-2-8. refs

An interactive system has been developed for measuring pass points and ground control points in digital images with subpixel accuracy. The pass points and ground control points are used to determine relative and absolute orientations. The system uses

iterative least square matching, a type of flexible template matching. An experiment testing the method on actual aerial images is discussed. R.B.

**A89-20800#**

**LOW-COST SECOND ORDER PLANIMETRIC MAPPING TECHNIQUE**

BOBBY S. DIPOKUSUMO (Bandung, Institute of Technology, Indonesia) IN: Asian Conference on Remote Sensing, 8th, Jakarta, Indonesia, Oct. 22-27, 1987, Proceedings. Bogor, Indonesia, EXSA International, 1987, p. G-4-1 to G-4-6.

A technique using low-cost methodology and instrumentation for second order planimetric mapping is described. The technique uses small frame aerial photography. Aspects of the methodology are described, including low-cost mapping techniques and the use of control points obtained by field measurement or planimetric block adjustment. The processes of direct digitation from the aerial photo, digital rectification, edge matching, map sheet preparation, and cartographic enhancement are examined. In addition, the hardware and software used for map processing are considered. R.B.

**A89-20801#**

**ACCURACY OF TERRAIN MEASUREMENT USING SPOT HRV DATA**

RYOSUKE SHIBASAKI (Ministry of Construction, Public Works Research Institute, Japan), SHUNJI MURAI (Tokyo, University, Japan), OSAMU UCHIDA (Okayama University, Japan), and YOSHIKAZU FUKUSHIMA (Ministry of Construction, Geographical Survey Institute, Japan) IN: Asian Conference on Remote Sensing, 8th, Jakarta, Indonesia, Oct. 22-27, 1987, Proceedings. Bogor, Indonesia, EXSA International, 1987, p. G-5-1 to G-5-8.

The accuracy of orientation and terrain measurement using SPOT HRV data is evaluated. The methods for determining exterior orientation and for acquiring a digital terrain model are presented. A case study is presented using three SPOT HRV images of a mountainous area near Mt. Fuji, Japan. It is found that contour lines with 40 to 50 m intervals can be drawn using SPOT HRV data if the coordinates of ground control points are measured on a 1:25,000 scale. R.B.

**A89-20806#**

**RECEIVING AND PROCESSING SYSTEM FOR METEOROLOGICAL SATELLITE (NOAA)**

HIDEKI MUROTA (Nihon University, Tokyo, Japan), MASAYA NAKAYAMA, MASARU KITSUREGAWA, and MIKIO TAKAGI (Tokyo, University, Japan) IN: Asian Conference on Remote Sensing, 8th, Jakarta, Indonesia, Oct. 22-27, 1987, Proceedings. Bogor, Indonesia, EXSA International, 1987, p. H-12-1 to H-12-7. refs

The Cartridge Library System archival system, a secondary storage system that can be operated and accessed directly by the host computer, is described as well as the organization of the data management system for the NOAA images and the quick look image. NOAA data are written in EBCDIC-code. The error rate and the missing line are recorded using binary fixed-point representation. K.K.

**A89-20807#**

**DIGITAL TERRAIN MODEL COMPUTATION USING SPOT DATA**

MICHEL MILLOT, STEPHAN GAVANON, and PHILIPPE REBILLARD (Societe Europeenne de Propulsion, Division de Traitement d'Images, Puteaux, France) IN: Asian Conference on Remote Sensing, 8th, Jakarta, Indonesia, Oct. 22-27, 1987, Proceedings. Bogor, Indonesia, EXSA International, 1987, p. 3-2-1 to 3-2-8. refs

A system which produces a DTM from two stereoscopic SPOT images is discussed. The process of stereoscopic restitution is examined, focusing on the problems of geometric modeling and matching points which correspond to the same terrain feature. Also, the production of epipolar images is considered. Results

from a test of the system using SPOT images of the southern part of France are presented. R.B.

**A89-20811#**  
**A BASIC STUDY OF THE REDUCTION OF THE EXACTNESS OF MESH DATA MAP MADE BY UNITING N-SQUARED MESHES TO ONE MESH**

HIROSHI MORI (Mitsubishi Research Institute, Tokyo, Japan) IN: Asian Conference on Remote Sensing, 8th, Jakarta, Indonesia, Oct. 22-27, 1987, Proceedings. Bogor, Indonesia, EXSA International, 1987, p. P-11-1 to P-11-8.

A method is proposed to estimate the amount by which the exactness of a mesh data map is reduced when n-squared meshes are united into one mesh. Techniques for uniting meshes and the mutual dependence of mesh data on neighbor data are discussed. The method is tested on a 1:50,000 map of a suburb of Sendai City, Japan. It is suggested that the method greatly reduces calculation time. R.B.

**A89-20812#**  
**GEOMETRIC CORRECTION OF SPOT IMAGE**

RYUTARO TATEISHI, FUJIO ANZAI, YUICHIRO KURONUMA, and KIYOSHI TSUCHIYA (Chiba University, Japan) IN: Asian Conference on Remote Sensing, 8th, Jakarta, Indonesia, Oct. 22-27, 1987, Proceedings. Bogor, Indonesia, EXSA International, 1987, p. P-12-1 to P-12-10.

Two types of geometric correction methods for SPOT images are studied. The first method is based on the assumption that coordinate transformation between the image coordinate and map coordinate is defined by polynomials. The optimum degree of the polynomial is studied on the basis of ground control points. In the case of the second method, a computer program for geometric correction without ground control points is developed. K.K.

**A89-20816#**  
**SPOT FOR MAPPING OF ACTUAL LAND INFORMATION**

JOKO SUPRIYANTO (Puslitbang Geoteknologi, Bandung, Indonesia) and ARJEN REIJNEVELD (Euroconsult, Arnhem, Netherlands) IN: Asian Conference on Remote Sensing, 8th, Jakarta, Indonesia, Oct. 22-27, 1987, Proceedings. Bogor, Indonesia, EXSA International, 1987, p. P-21-1 to P-21-6.

SPOT panchromatic digital imagery and aerial photographs are used for land suitability mapping of Irian Jaya. The data processing and map production techniques are discussed. A map is produced with a 10-meter accuracy, or an error of 0.5 mm at a scale of 1:20,000. Land management projects using the map and other field applications of SPOT data are considered. R.B.

**A89-20821#**  
**FEATURE EXTRACTION CONSIDERATIONS IN UTILISING THE OPTICAL POWER SPECTRA FOR TERRAIN CLASSIFICATION**

B. L. DEEKSHATHULU, R. RAMACHANDRAN, K. SRINATH, KIRON K. RAO, and O. P. BAJPAI (National Remote Sensing Agency, Hyderabad, India) IN: Asian Conference on Remote Sensing, 8th, Jakarta, Indonesia, Oct. 22-27, 1987, Proceedings. Bogor, Indonesia, EXSA International, 1987, p. Q-7-1 to Q-7-7. refs

Four feature extraction techniques for terrain classification are applied to optical power spectra of aerial images. The Karhunen-Loeve (Tou and Gonzalez, 1974), Fukunga-Koontz (1970), and Foley-Sammon (1975) transforms and the Hotelling-Trace criterion (1982) are compared. Examples are presented for each of the techniques. It is found that the Karhunen-Loeve transform does not perform as well as the other three techniques. Possible ways to improve feature extraction techniques are suggested. R.B.

**A89-21249**  
**LANDSAT 5 TM IMAGE OF THE MONT SAINT-MICHEL REGION OF FRANCE [IMAGE LANDSAT 5 TM DE LA REGION DU MONT SAINT-MICHEL (FRANCE)]**

R. BARIOU, L. HUBERT, and F. LE HENAFF (Rennes II, Universite, France) Photo Interpretation (ISSN 0031-8523), vol. 27, Jan.-Feb. 1988, p. 25-27, 29, 31, 32. In French, English, and Spanish.

A color composite treatment has been applied to a Landsat 5 TM image (channels 1, 4, and 5) of the Mont Saint-Michel region of France obtained in 1985. The present technique allows the following regional areas to be distinguished: a granite range in the south with mixed woodland and pasture, sandy/muddy regions in the midwest and mideast, the shoreline in the north, and the marine environment. Also distinguished are agricultural types such as carrots, celery, onions, and spinach. R.R.

**A89-22649\*** Massachusetts Inst. of Tech., Cambridge.  
**BAYES CLASSIFICATION OF TERRAIN COVER USING NORMALIZED POLARIMETRIC DATA**

H. A. YUEH, A. A. SWARTZ, J. A. KONG (MIT, Cambridge, MA), R. T. SHIN, and L. M. NOVAK (MIT, Lexington, MA) Journal of Geophysical Research (ISSN 0148-0227), vol. 93, Dec. 10, 1988, p. 15261-15267. Research sponsored by DARPA. refs (Contract DACA39-87-K-0022; NSF ECS-85-04381; NAG5-270; N00014-83-K-0258)

The normalized polarimetric classifier (NPC) which uses only the relative magnitudes and phases of the polarimetric data is proposed for discrimination of terrain elements. The probability density functions (PDFs) of polarimetric data are assumed to have a complex Gaussian distribution, and the marginal PDF of the normalized polarimetric data is derived by adopting the Euclidean norm as the normalization function. The general form of the distance measure for the NPC is also obtained. It is demonstrated that for polarimetric data with an arbitrary PDF, the distance measure of NPC will be independent of the normalization function selected even when the classifier is mistrained. A complex Gaussian distribution is assumed for the polarimetric data consisting of grass and tree regions. The probability of error for the NPC is compared with those of several other single-feature classifiers. The classification error of NPCs is shown to be independent of the normalization function. C.D.

**A89-23645**  
**RADAR IMAGING OF THE SURFACES OF VENUS AND THE EARTH USING SAR DATA [POLUCHENIE RADIOLOKATSIONNYKH IZOBRAZHENII POVERKHNOSTI VENERY I ZEMLI PO DANNYM RADIOLOKATOROV S SINTEZIROVANNOI APERTUROI ANTENNY]**

A. F. BOGOMOLOV, L. V. KUDRIN, M. IU. BERGMAN, and I. I. PRIKHOD'KO (Moskovskii Energeticheskii Institut, Moscow, USSR) Radiotekhnika (ISSN 0033-8486), Nov. 1988, p. 63-65. In Russian. refs

The paper describes a method for generating radar maps with a resolution of 0.5-1 km, utilized in the processing of SAR data on the Venus and earth surfaces acquired during 1983-1985. Experimental results indicate the effectiveness of the proposed data processing methodology in the case of variable indeterminacy in estimating the current distribution of transmission coefficients for SAR spatial channels. B.J.

**A89-25595\*#** National Aeronautics and Space Administration. Ames Research Center, Moffett Field, CA.

**CALIBRATION OF INFRARED SATELLITE IMAGES USING HIGH ALTITUDE AIRCRAFT MEASUREMENTS**

PHILIP D. HAMMER, WARREN J. Y. GORE, and FRANCISCO P. J. VALERO (NASA, Ames Research Center, Moffett Field, CA) AIAA, Aerospace Sciences Meeting, 27th, Reno, NV, Jan. 9-12, 1989. 3 p. refs (AIAA PAPER 89-0817)

The use of infrared radiance measurements made from high altitude aircraft for satellite image validation is discussed. Selected examples are presented to illustrate the techniques and the potentials of such validation studies. Author

**A89-27783**  
**FEX - A KNOWLEDGE-BASED SYSTEM FOR PLANIMETRIC FEATURE EXTRACTION**

JOHN S. ZELEK (MacDonald Dettwiler and Associates, Ltd., Richmond, Canada) IN: Recent advances in sensors, radiometry, and data processing for remote sensing; Proceedings of the Meeting, Orlando, FL, Apr. 6-8, 1988. Bellingham, WA, Society of Photo-Optical Instrumentation Engineers, 1988, p. 292-296. refs

Visual planimetric feature extraction is a very labor-intensive operation; the advantages of automating feature extraction include: time and labor savings, accuracy improvements, and planimetric data consistency. The FEX program combines techniques from image processing, remote sensing, and artificial intelligence for automatic feature extraction. The feature-extraction process coordinates the information and knowledge in a hierarchical data structure. The system simulates the reasoning of a photointerpreter in determining the planimetric features. Present efforts have concentrated on the extraction of roadlike features in SPOT imagery. Author

**A89-27789\*** Vexcell Corp., Boulder, CO.  
**CONCEPTS FOR PROCESSING AND ANALYZING OF  
 MULTIPLE SAR AND LANDSAT IMAGES**

J. THOMAS, R. MULLEN, F. LEBERL, W. KOBER (Vexcel Corp., Boulder, CO), and J. CIMINO (California Institute of Technology, Jet Propulsion Laboratory, Pasadena) IN: Recent advances in sensors, radiometry, and data processing for remote sensing; Proceedings of the Meeting, Orlando, FL, Apr. 6-8, 1988. Bellingham, WA, Society of Photo-Optical Instrumentation Engineers, 1988, p. 332-338. refs

The use and application of multisensor data sets are an absolute necessity for remote sensing to fulfill its promise. Initial efforts at registering dissimilar images have been made, but results are not widely available. This paper describes some initial work to better understand the difficulties of multisensor registration. Accuracies achieved are in excess of a pixel diameter. Author

**A89-27937**  
**THE LUXURIANT IMAGE - AN INTRODUCTION TO REMOTE  
 SENSING DATA PROCESSING**

A. HUBAUX IN: Applications of remote sensing to agrometeorology; Proceedings of the Course, Ispra, Italy, Apr. 6-10, 1987. Dordrecht, Netherlands, Kluwer Academic Publishers, 1989, p. 57-128. refs

An introduction is given to computer-based remote sensing data processing for scientists with little or no computer science background. The nature of remote sensing images, the process of generating digital data, and data visualization are examined. The relationships between digital data and the pictures which can be obtained from them are considered. The role of transfer functions, their relation to channel histograms, the visualization of a single channel image, and the concept of channel space are discussed. Derived systems are reviewed, including intensity-hue-saturation, the tasseled cap, thematic channels, and principal components. The radiometric and geometric corrections needed to obtain workable data are explained. Also, context-free classification procedures are introduced. R.B.

**A89-27938**  
**IMAGE PROCESSING TECHNIQUES - FILTERING,  
 EXOGENOUS DATA, GEOMETRICAL PROCESSING**

J. DEJACE IN: Applications of remote sensing to agrometeorology; Proceedings of the Course, Ispra, Italy, Apr. 6-10, 1987. Dordrecht, Netherlands, Kluwer Academic Publishers, 1989, p. 129-155.

The elementary methods for filtering digital images are described, emphasizing the processes for smoothing and sharpening images. Methods for processing exogenous data are discussed, including relief and soils. The raster and vector formats for storing information for computer use are compared. The digitization of paper documents, geometrical transformation and rasterization, and the digital terrain model are considered. Also, geometrical image processing is examined, including the geometric deformation model, image transformation, and quality control. R.B.

**A89-28036**  
**THE EFFECTS OF VIEWING GEOMETRY ON IMAGE  
 CLASSIFICATION**

GILES M. FOODY (Kingston Polytechnic, Kingston upon Thames, England) International Journal of Remote Sensing (ISSN 0143-1161), vol. 9, Dec. 1988, p. 1909-1915. refs

Thematic classification of remotely-sensed data assumes that class separability is spatial. However, as classifiers discriminate between classes on the basis of their spectral responses, this assumption is invalid since the latter vary spatially with the viewing geometry. Consequently, classification accuracy is spatially variable. Classification accuracy statements can therefore over- and under-estimate inter-class discrimination at different locations within a scene and can therefore be misleading. This is illustrated by a classification of synthetic aperture radar data which had an aggregate accuracy of 75.7 percent but also displayed a variation in accuracy between locations of up to 17.2 percent. Author

**A89-28037**  
**APPLICATION OF THE HAAR TRANSFORM FOR  
 EXTRACTION OF LINEAR AND ANOMALOUS PATTERNS  
 OVER PART OF CAMBAY BASIN, INDIA**

T. J. MAJUMDAR (ISRO, Space Applications Centre, Ahmedabad, India) and B. B. BHATTACHARYA (Indian School of Mines, Dhanbad, India) International Journal of Remote Sensing (ISSN 0143-1161), vol. 9, Dec. 1988, p. 1937-1942. refs

Digital filtering of aerial Multispectral Scanner data using the Haar transform has been attempted for a part of Cambay Basin in India for the extraction of linear and anomalous patterns. In addition, a typical pattern has been generated to assess the capability of filtering the linears. The results show that the major drainage as well as lineament patterns are extracted by digital filtering techniques. Author

**A89-29064**  
**DIGITAL IMAGE PROCESSING IN REMOTE SENSING**

JAN-PETER MULLER, ED. (University College, London, England) London and Philadelphia, PA, Taylor and Francis, 1988, 284 p. For individual items see A89-29065 to A89-29076.

The present work discusses topics in computation for remote sensing images' digital processing, the visualization of topographic data using video animation, the 'Transportable Applications Environment' interactive CADAM development system, a menu-based interface oriented to the display processing of real-time satellite weather images, and the IAX algebraic image-processing language for research. Also discussed are microcomputers and mass-storage devices for image processing, a very low cost microcomputer-based image processor, the capture of image syntax using tesseral addressing and arithmetic, multiple source data-processing in remote sensing, the analysis and simulation of variability and fractals in remote sensing, the processing of IR and visible satellite imagery for oceanographic analysis, and image processing in optical astronomy. O.C.

**A89-29066**  
**VISUALIZATION OF TOPOGRAPHIC DATA USING VIDEO  
 ANIMATION**

JAN-PETER MULLER, TIM DAY, JOHN KOLBUSZ, MIKE DALTON, SAM RICHARDS (University College, London, England) et al. IN: Digital image processing in remote sensing. London and Philadelphia, PA, Taylor and Francis, 1988, p. 21-38. Research supported by SERC and BP Petroleum Development, Ltd. refs

The range of software tools developed to date for the three-dimensional visualization of topographic-features data is presently illustrated by Digital Elevation Models (DEMs) derived from photogrammetric measurements and from digitized contour maps. A number of tools have been developed for the display of perspective views of time sequences of landscapes with a variety of surface-shading models, in order to deepen understanding of the current and potential information content of DEMs. The texture-mapping problem integrates both single-band and multispectral satellite images. Artificial shading models ranging from

simple Lambertian to terrain ray-tracing types are presented.

O.C.

**A89-29073**  
**MULTIPLE SOURCE DATA PROCESSING IN REMOTE SENSING**

P. T. NGUYEN and D. HO (IBM France, S.A., Paris) IN: Digital image processing in remote sensing. London and Philadelphia, PA, Taylor and Francis, 1988, p. 153-176. refs

A series of image processing techniques suitable for the acquisition and integration of data from various multispectral satellite sensor bands has been developed into a geocoded data base for geological and climatological applications; these extract useful information and manipulate it interactively before displaying the results. The amount of effort involved in the acquisition and preprocessing of these heterogeneous data points to the need for standardization of the data format and the interface between different geographical/geophysical information systems. A geoscience expert system will require efforts toward the definition of physical modeling and decision-making processes. O.C.

**A89-29074**  
**EXTREME VARIABILITY, SCALING AND FRACTALS IN REMOTE SENSING - ANALYSIS AND SIMULATION**

S. LOVEJOY (McGill University, Montreal, Canada) and D. SCHERTZER (Etablissement d'Etudes et de Recherches Meteorologiques, Paris, France) IN: Digital image processing in remote sensing. London and Philadelphia, PA, Taylor and Francis, 1988, p. 177-212. refs

The extreme variability or intermittency in remotely-sensed data presently discussed has prompted the development of methods employing stochastic modeling of scales smaller than the remote sensor's resolution. Extreme variability exhibits fluctuations spanning a wide range of scales and a wide range of intensities within a given scale. This large variability of geophysical phenomena leads to statistical properties very different from those usually assumed: they are presently characterized as the 'generalized scale invariance' symmetry principle, in which the small and large scales are related by a magnification, coupled with such geometrical transformations as differential rotation or stratification. O.C.

**A89-30123**  
**IMPROVEMENT OF MULTISPECTRAL COLOR IMAGES BY INTENSIFYING LOCAL CONTRASTS [ULUCHSHENIE MNOGOZONAL'NYKH TSVETNYKH IZOBRAZHENII PUTEM USILENIIA LOKAL'NYKH KONTRASTOV]**

P. A. CHOCHIA (AN SSSR, Institut Problem Peredachi Informatsii, Moscow, USSR) Issledovanie Zemli iz Kosmosa (ISSN 0205-9614), Nov.-Dec. 1988, p. 95-99. In Russian. refs

A method for the transformation of multispectral color images is proposed which enhances local contrasts and clarity. This technique does not degrade the initial mean brightness and the hues of extended features of the image. B.J.

**A89-30239**  
**LANDSCAPE PROCESSING OF SATELLITE IMAGERY FOR A BIOSPHERIC DATA BANK [LANDSHAFTNAIA OBRABOTKA KOSMICHESKIKH IZOBRAZHENII DLIA BIOSFERNOGO BANKA DANNYKH]**

V. V. BUGROVSKII, O. B. BUTUSOV, and V. M. DUBOVSKIKH (Nauchno-Issledovatel'skii Tsentri Tekhnicheskoi Dokumentatsii SSSR, Moscow, USSR) Akademiia Nauk SSSR, Doklady (ISSN 0002-3264), vol. 304, no. 2, 1989, p. 444-447. In Russian.

Data banks using standard forms of natural objects are proposed for the thematic processing of satellite remotely sensed imagery. The use of standards of simplified structure in the data bank leads to a considerable reduction in the image processing time and in the required computing capacity. The satellite imagery is processed according to the following scheme: identification of fragments, identification of boundary points, linking of contours, generalization of contours, and comparison of the generalizations obtained with the standards in the data bank. B.J.

**A89-30256**

**A 10 KM RESOLUTION IMAGE OF THE ENTIRE NIGHT-TIME EARTH BASED ON CLOUD-FREE SATELLITE PHOTOGRAPHS IN THE 400-1100 NM BAND**

WOODRUFF T. SULLIVAN, III (Cambridge University, England) International Journal of Remote Sensing (ISSN 0143-1161), vol. 10, Jan. 1989, p. 1-5. refs

An image of the entire earth at night is assembled for the first time. It consists of a mosaic of photographs, all taken at local midnight in the 400-1100 nm band, made by the Defense Meteorological Satellite program over the period 1974-84. Photographs were selected for freedom from clouds, lack of moonlight, high sensitivity and suitability to illustrate various temporal phenomena. The image primarily reveals activities of humankind such as urban street lighting, rangeland burning, slash-and-burn agriculture, natural gas burn-offs in oil fields, and squidding. Author

**A89-31888**

**NIGHTTIME AND DAYTIME HCMM THERMOGRAPHS OF THE IBERIAN PENINSULA [THERMOGRAPHIES HCMM DE LA PENINSULE IBERIQUE DE NUIT ET DE JOUR]**

S. DAVEAU (Instituto Nacional de Investigacao Cientifica, Lisbon, Portugal) Photo Interpretation (ISSN 0031-8523), vol. 27, Mar.-Apr. 1988, p. 11-13, 15, 17, 19, 20. In French, English, and Portuguese.

Nighttime HCMM thermographs are found to provide good thermal differentiation for the Iberian Peninsula on a regional scale, while daytime thermographs provide good thermal differentiation on a local scale. The night images reveal the differentiation between the cool lands to the north and the warm low regions to the south. It is shown that the daytime heating is mainly controlled by variations in the state of the surface ground layer. Daytime thermal amplitudes do not provide a good measurement of the thermal inertia of the ground surface. R.R.

**A89-31889**

**THERMAL INFRARED AND VISIBLE IMAGES OF THE IBERIAN PENINSULA [LA PENINSULE IBERIQUE DANS L'INFRAROUGE THERMIQUE ET DANS LE VISIBLE]**

S. DAVEAU (Instituto Nacional de Investigacao Cientifica, Lisbon, Portugal) Photo Interpretation (ISSN 0031-8523), vol. 27, Mar.-Apr. 1988, p. 21-23, 25, 27, 29, 30. In French, English, and Portuguese.

The delineation of surface features in the Iberian Peninsula using thermal infrared and visible HCMM images is discussed, along with problems encountered in comparing the two images. The visible image is shown to reveal east-west contrasts, notably differences due to above normal rainfall in the western section of the region. Combined use of the two images results in the identification of such features as forest covering, agricultural areas, and snowy peaks. R.R.

**A89-31949\*** National Aeronautics and Space Administration. Goddard Space Flight Center, Greenbelt, MD.

**LAND IMAGE DATA PROCESSING REQUIREMENTS FOR THE EOS ERA**

STEPHEN W. WHARTON (NASA, Goddard Space Flight Center, Greenbelt, MD) and JEFFREY A. NEWCOMER (ST Systems Corp., Lanham, MD) IEEE Transactions on Geoscience and Remote Sensing (ISSN 0196-2892), vol. 27, March 1989, p. 236-242. refs

Requirements are proposed for a hybrid approach to image analysis that combines the functionality of a general-purpose image processing system with the knowledge representation and manipulation capabilities associated with expert systems to improve the productivity of scientists in extracting information from remotely sensed image data. The overall functional objectives of the proposed system are to: (1) reduce the level of human interaction required on a scene-by-scene basis to perform repetitive image processing tasks; (2) allow the user to experiment with ad hoc rules and procedures for the extraction, description, and identification of the features of interest; and (3) facilitate the



derivation, application, and dissemination of expert knowledge for target recognition whose scope of application is not necessarily limited to the image(s) from which it was derived. I.E.

**A89-32335\*** Jet Propulsion Lab., California Inst. of Tech., Pasadena.

**A SIMPLE SPATIAL FILTERING ROUTINE FOR THE COSMETIC REMOVAL OF SCAN-LINE NOISE FROM LANDSAT TM P-TAPE IMAGERY**

ROBERT E. CRIPPEN (California Institute of Technology, Jet Propulsion Laboratory, Pasadena) Photogrammetric Engineering and Remote Sensing (ISSN 0099-1112), vol. 55, March 1989, p. 327-331. refs

**A89-32337**

**EXTRACTING SPECTRAL CONTRAST IN LANDSAT THEMATIC MAPPER IMAGE DATA USING SELECTIVE PRINCIPAL COMPONENT ANALYSIS**

PAT S. CHAVEZ, JR. (USGS, Flagstaff, AZ) and ANDREW YAW KWARTENG (Texas, University, El Paso) Photogrammetric Engineering and Remote Sensing (ISSN 0099-1112), vol. 55, March 1989, p. 339-348. refs

**N89-15440#** Instituto de Pesquisas Espaciais, Cachoeira Paulista (Brazil).

**STUDY OF GEOMETRIC QUALITY OF THE MSS-LANDSAT IMAGERY**

ANTONIO JOSE F. MACHADOESILVA Aug. 1988 18 p In PORTUGUESE; ENGLISH summary Presented at the 3rd Brazilian Symposium on Remote Sensing, Rio de Janeiro, Brazil, 28-30 Nov. 1984

(INPE-4653-PRE/1360) Avail: NTIS HC A03/MF A01

The present status of LANDSAT MSS imagery processing is discussed. Evaluation is done on images from all satellites of the LANDSAT series, both bulk and precision imagery. Root mean square errors obtained were 120 + or - 20 m for bulk images and 60 + or - 15 m for precision images. The causes of geometric distortion are given, both internal and external, and a simplified correction model is presented. The results of geometric evaluation of LANDSAT imagery are then given. Polynomials, from first to fifth degree, are tested in order to determine the best one for precision image generation. Author

**N89-15442#** European Space Agency, Paris (France). **INVESTIGATION OF INFORMATION CONTENT OF THEMATIC MAPPER AND SPOT MULTIBAND IMAGE DATA, USING SIMULATED IMAGE DATA OF THE FREIBURG REGION (FEDERAL REPUBLIC OF GERMANY)**

WERNER KIRCHHOF, WOLFRUM MAUSER, and HANS-JUERGEN STIBIG (Freiburg Univ., Germany, F.R.) Oct. 1988 139 p Transl. into ENGLISH of Untersuchung des Informationsgehaltes von Landsat-Thematic-Mapper-und SPOT-Multiband-Bilddaten mit Simulierten Multispektralen Bilddaten des Gebietes Freiburg (Oberpfaeffenhofen, Fed. Republic of Germany, DFVLR) Original language document was announced as N86-21972 Original contains color illustrations (ESA-TT-975; DFVLR-FB-85-49; ETN-89-93629) Avail: NTIS HC A07/MF A01; original German version available from DFVLR, VB-PL-DO, Postfach 90 60 58, 5000 Cologne, Fed. Republic of Germany, 52 Deutsche marks

A comparative analysis of information contents was performed using data sets with pixel sizes of 10, 20, 30, 50, and 80 m from LANDSAT TM simulation. The discrimination of objects, structures and texture, depending on pixel size and combination of spectral bands, was investigated by visual interpretation and supervised classification for applications in agriculture and forestry. The new TM bands produce significant improvements in the separation of vegetated and built-up areas as well as in the delineation of the status of growth and humidity in comparison with LANDSAT MSS. The Thematic Mapper is eminently suited for the extraction of thematic information of surface areas of 1 hectare or more. Three to four spectral bands are normally sufficient. The information content of 20 m SPOT multiband data does not differ essentially

from that of comparable TM bands (TM2, TM3, TM4). A substantial complement to the TM information are structure and texture elements of the panchromatic 10 m SPOT band. ESA

**N89-16204#** Lawrence Livermore National Lab., CA. Atmospheric Release Advisory Capability.

**OVERVIEW OF LOW-COST MAP DIGITIZING SYSTEMS**

HOYT WALKER Oct. 1988 47 p Presented at the Improving the Safety Aspects of Nuclear Facilities: Development of A Real-Time Dose Assessment Model, Livermore, CA, 3 Oct. 1988 (Contract W-7405-ENG-48) (DE89-002872; UCRL-99730; CONF-8810243-1) Avail: NTIS HC A03/MF A01

The information that is placed into computer map files may come from many sources. Increasingly, the data is processed directly from surveys and other observations. For example, with relatively minimal processing, LANDSAT data can be input into a raster database as a separate map overlay. However, most data currently requires substantial human interaction to create the necessary map information. While the direct input, or capture, of observational data for cartographic data bases is an area of focused research and development, the majority of data capture processing involves the input of already existing maps and photographs into computer form, i.e., digitizing. The purpose of this document is to provide an overview of the current market for low-cost digitizing systems. No recommendations are made for selection of a particular vendor; however, four packages are highlighted as meeting the minimal requirements for extracting map data to provide base maps for a small emergency response system. Other vendors of similar products that could, with somewhat more difficulty, be adapted to the stated requirements are included. This document is composed of four sections including: (1) a discussion of the basic terminology of digitizing systems; (2) a description of the minimal requirements for a map digitizing system; (3) short discussions of the most appropriate packages based on literature received; (4) copies of portions of the literature sent by the various vendors. This document is intended to function as an introduction into this market area for those who are unfamiliar with the digital mapping field. DOE

**N89-17375#** Pacific Northwest Labs., Richland, WA. **APPLICATIONS OF DIGITAL IMAGE PROCESSING TO ONGOING RESEARCH IN COMPLEX TERRAIN METEOROLOGY**

J. M. HUBBE, C. D. WHITEMAN, H. P. FOOTE, and L. G. MCWETHY Oct. 1988 7 p Presented at the Digital Image Processing and Visual Communications Technologies in Meteorology Conference, Cambridge, MA, 26 Oct. 1987 (Contract DE-AC06-76RL-01830) (DE89-001749; PNL-SA-15073; CONF-8710161-2) Avail: NTIS HC A02/MF A01

Digital elevation models and LANDSAT 5 Thematic Mapper (TM) scenes constitute image resolution data over spatial domains of typical interest in complex terrain meteorology. Techniques in use and under development for applying these data to research problems are presented. Topics include decorrelation of topographic shading under direct beam illumination and investigation of nighttime surface temperature. DOE

**N89-17414#** Instituto de Pesquisas Espaciais, Sao Jose dos Campos (Brazil).

**AUTOMATIC REGISTRATION OF SATELLITE IMAGERY**

GILBERTO CAMARANETO Aug. 1988 5 p In PORTUGUESE; ENGLISH summary Presented at the Latin-American Symposium on Remote Sensing, 4th Brazilian Symposium on Remote Sensing, 6th Penary Meeting, SELPER, Gramado, Brazil, 10-15 Aug. 1986 (INPE-4637-PRE/1349) Avail: NTIS HC A02/MF A01

Registration of satellite imagery is an important need in various application areas in remote sensing. A method is presented for registration which reduces use work to a minimum, the control points being automatically chosen. The method tests in LANDSAT TM imagery with good results. Author



**N89-17922#** Joint Publications Research Service, Arlington, VA.  
**SOME RESULTS OF USE OF SPACE SURVEY MATERIALS IN CARTOGRAPHIC WORK Abstract Only**

YE. A. RESHETOV *In its* JPRS Report: Science and Technology. Science and Technology. USSR: Earth Sciences p 11 8 Sep. 1988 Transl. into ENGLISH from Geodeziya i Kartografiya (Moscow, USSR), no. 4, Apr. 1988 p 42-44  
 Avail: NTIS HC A03/MF A01

There are 4 principal areas in which space photographs and products of space surveys are used, each of which are reviewed: compilation and revision of topographic maps; compilation of topographic bases for various kinds of maps; mapping of natural resources; and specialized interpretation of photographs. Analytical phototriangulation, based on data on orbital motion of artificial earth satellites, was used in establishing a survey base over extensive territories inaccessible for aerial surveys or surface field work. Author

**N89-18705#** Royal Signals and Radar Establishment, Malvern (England).**IMAGE COMPRESSION USING A NEUTRAL NETWORK**

S. P. LUTTRELL *In* ESA, Proceedings of the 1988 International Geoscience and Remote Sensing Symposium (IGARSS) '88 on Remote Sensing: Moving Towards the 21st Century, Volume 3 p 1231-1238 Aug. 1988

Avail: NTIS HC A99/MF A01; ESA Publications Division, ESTEC, Noordwijk, Netherlands, \$120 US or 250 Dutch guilders

An unsupervised neural network was trained on a set of archetype images in order to form an internal representation (or model) of the image features. It is found that a multilayer topographic mapping network has the necessary properties successfully to compress and reconstruct imagery. It is shown how to extend and improve upon existing learning algorithms for this type of network. The network learning dynamics is expressed as a diffusion equation. The application of this technique to synthetic aperture radar images is illustrated. ESA

**N89-18710#** Centre d'Etude Spatiale des Rayonnements, Toulouse (France).**ADAPTIVE SPECKLE FILTERING FOR SAR IMAGES**

A. LOPES and R. TOUZI *In* ESA, Proceedings of the 1988 International Geoscience and Remote Sensing Symposium (IGARSS) '88 on Remote Sensing: Moving Towards the 21st Century, Volume 3 p 1263-1266 Aug. 1988

Avail: NTIS HC A99/MF A01; ESA Publications Division, ESTEC, Noordwijk, Netherlands, \$120 US or 250 Dutch guilders

A generalized adaptive filter is developed which can be adapted to preserve any kind of information characterized by the appropriate index. Filters are tested on a 4 look SAR 580 image. The best known adaptive filters are optimized such that they average well homogeneous areas and preserve edge and textural information (with less noise smoothing) at the same time. However, such filters do not smooth well the noise in textured areas and much work must be done to develop filters which, by taking into account all the properties of the speckle, reduce it as well within homogeneous areas as in the textured ones without loss of information. ESA

**N89-18711#** Ecole Nationale Supérieure des Telecommunications, Brest (France). Groupe Traitement d'Image.**NONLINEAR FILTERING AND EDGE DETECTION IN SPECKLED RADAR IMAGES**

J.-M. BOUCHER and A. HILLION *In* ESA, Proceedings of the 1988 International Geoscience and Remote Sensing Symposium (IGARSS) '88 on Remote Sensing: Moving Towards the 21st Century, Volume 3 p 1267-1268 Aug. 1988

Avail: NTIS HC A99/MF A01; ESA Publications Division, ESTEC, Noordwijk, Netherlands, \$120 US or 250 Dutch guilders

A nonlinear filter reducing the speckle noise on radar images is examined. The filter, which is better than the classical ones according to the mean-square error criterion, depends on a real parameter alpha. For alpha = 0, the filter takes a logarithmic structure; alpha = 1 produces the classical linear filter (Lee filter).

The two methods are compared for a signal taking only two values with a lognormal density of probability for the noise. An adaptive algorithm, involving both filters, can be applied to radar images, showing that edges can be detected by comparing the computed mean square errors of these filters. ESA

**N89-18759#** Naval Research Lab., Washington, DC.**SEGMENTATION OF SAR IMAGES**

J. S. LEE and I. JURKEVICH *In* ESA, Proceedings of the 1988 International Geoscience and Remote Sensing Symposium (IGARSS) '88 on Remote Sensing: Moving Towards the 21st Century, Volume 3 p 1503-1506 Aug. 1988

Avail: NTIS HC A99/MF A01; ESA Publications Division, ESTEC, Noordwijk, Netherlands, \$120 US or 250 Dutch guilders

A SAR image segmentation by the gray level only is discussed. Classification errors of SAR images, the existence of histogram valleys suitable for classification, and a procedure for multilevel thresholdings of SAR images are discussed. Not all images, whether SAR or other types, can be successfully segmented because the image may not contain distinctive classes. Some images may be segmentable visually, but a segmentation algorithm would fail because the image may contain many small objects with gray levels falling between those of large objects or background, or because of the uneven illumination (i.e., lacking radiometric correction). One way to deal with this problem is to divide the image into small blocks and to apply the segmentation algorithm to each block to find local thresholds. The input parameter (ratio of standard deviation to its mean) to the filtering algorithm remains unchanged in the multistage filtering. However, to preserve fine details, this parameter should be gradually reduced until it reaches a lower value, such as 0.13, which corresponds to the value for a 16-look amplitude SAR image. ESA

**N89-18760#** Norwegian Defence Research Establishment, Kjeller.**INTERPRETING SAR IMAGES BY MEANS OF MAP INFORMATION**

E.-A. HERLAND *In* ESA, Proceedings of the 1988 International Geoscience and Remote Sensing Symposium (IGARSS) '88 on Remote Sensing: Moving Towards the 21st Century, Volume 3 p 1507-1510 Aug. 1988

Avail: NTIS HC A99/MF A01; ESA Publications Division, ESTEC, Noordwijk, Netherlands, \$120 US or 250 Dutch guilders

A model for utilization of images from spaceborne synthetic aperture radars over land is being developed. Synthetic SAR images are generated from digital terrain models and knowledge of radar parameters and orbit and attitude information. When sufficient geolocation accuracy is achieved, optical images will also be included. The model is tested on two areas in Norway, one with high relief and one with low relief, by using a nationwide terrain model on grid with 90 m spacing. The position of each point on the ground in the final image is accurately calculated from the imaging geometry. Seasat SAR images are used for comparison, and good consistency between synthetic and actual images is obtained. ESA

**N89-18761#** Deutsche Forschungs- und Versuchsanstalt fuer Luft- und Raumfahrt, Oberpfaffenhofen (West Germany).**INVESTIGATIONS OF SAR BACKSCATTER FOR DIFFERENT TEST AREAS USING TWO GEOCODED SEASAT SAR SCENES**

E. BOENSCH, R. WINTER, and G. SCHREIER (Bonn Univ., Germany, F.R.) *In* ESA, Proceedings of the 1988 International Geoscience and Remote Sensing Symposium (IGARSS) '88 on Remote Sensing: Moving Towards the 21st Century, Volume 3 p 1511-1514 Aug. 1988

Avail: NTIS HC A99/MF A01; ESA Publications Division, ESTEC, Noordwijk, Netherlands, \$120 US or 250 Dutch guilders

An analysis of two precisely geocoded Seasat SAR-scenes is presented. It aims at a visual, that is qualitative, and a quantitative interpretation using statistical parameters of the gray value distribution. The fields of application for the quantitative interpretation are agriculture, forestry, and urban areas. The results in agriculture concern investigations of the influence of different

factors on backscatter: these are row direction, inclination and volume moisture content of sugar beet fields, tillage direction in ploughed fields and fields that are characterized by different soil moisture contents. Investigations in forests comprise the differentiation of backscatter due to different ages in deciduous woods and due to the contrast of deciduous to conifers. In urban areas, a clear correlation of the backscatter to the orientation of streets and houses in relation to the angle of incidence is shown.

ESA

**N89-18763#** GEC-Marconi Electronics Ltd., Chelmsford (England).

**THE VISIBILITY OF LINEAR FEATURES IN SAR IMAGES**

A. HENDRY, S. QUEGAN, and J. WOOD (Royal Signals and Radar Establishment, Malvern, England) *In* ESA, Proceedings of the 1988 International Geoscience and Remote Sensing Symposium (IGARSS) '88 on Remote Sensing: Moving Towards the 21st Century, Volume 3 p 1517-1520 Aug. 1988 Sponsored in part by the Ministry of Defence, London, United Kingdom

Avail: NTIS HC A99/MF A01; ESA Publications Division, ESTEC, Noordwijk, Netherlands, \$120 US or 250 Dutch guilders

A series of SAR images of the same scene from different viewing directions was analyzed. The images were produced by X-band SAR over England. The measurements show clearly how variable the signature of a linear feature is with viewing direction. A road and its boundaries show a far higher response in one out of four orthogonal viewing directions; they are distinguishable in all four directions, but the two broadside signatures are markedly different. A fenced track is also visible in four orthogonal viewing directions; there are differences in the four directions, but nothing as extreme as for the road and its boundaries. A field boundary gives surprising results; it can be seen from two directions which are orthogonal, but not from the other two orthogonal directions. Physical explanations for aspects of the observed behavior can be produced, but the behavior noted for the field boundary is difficult to explain.

ESA

**N89-18764#** GEC-Marconi Electronics Ltd., Chelmsford (England).

**AUTOMATED LINEAR FEATURE DETECTION AND ITS APPLICATION TO CURVE LOCATION IN SYNTHETIC APERTURE RADAR IMAGERY**

A. HENDRY, J. SKINGLEY, and A. J. RYE *In* ESA, Proceedings of the 1988 International Geoscience and Remote Sensing Symposium (IGARSS) '88 on Remote Sensing: Moving Towards the 21st Century, Volume 3 p 1521-1524 Aug. 1988 Sponsored in part by the Royal Signals and Radar Establishment, Malvern, United Kingdom and the Ministry of Defence, London, United Kingdom

Avail: NTIS HC A99/MF A01; ESA Publications Division, ESTEC, Noordwijk, Netherlands, \$120 US or 250 Dutch guilders

The application and performance of the Hough transform to the problem of locating thin lines with arbitrary and variable curvature, in synthetic aperture radar (SAR) imagery is discussed. Performance of the Hough transform technique applied to simple SAR images is established. However, some lines in real images do not obey this simple speckle model. Consequently, there is a need to extend the model to other situations and evaluate performance. These situations are dictated by application needs. The approach to line detection by stages is worth development. Performance of low-level operations imposes constraints on the inferences possible from their output, which is particularly important when constructing rules and selecting appropriate thresholds to link line segments.

ESA

**N89-18776#** Jet Propulsion Lab., California Inst. of Tech., Pasadena.

**MULTIFREQUENCY IMAGING RADAR POLARIMETRY: DEPOLARISATION OF RADAR ECHOES AT THREE WAVELENGTHS**

H. A. ZEBKER and J. J. VANZYL *In* ESA, Proceedings of the 1988 International Geoscience and Remote Sensing Symposium (IGARSS) '88 on Remote Sensing: Moving Towards the 21st

Century, Volume 3 p 1571-1573 Aug. 1988

Avail: NTIS HC A99/MF A01; ESA Publications Division, ESTEC, Noordwijk, Netherlands, \$120 US or 250 Dutch guilders

It is shown that high resolution imaging radar polarimeters can describe depolarization effects in great detail by measuring the complete Stokes matrix for small regions on the Earth's surface, permitting to distinguish between coherent polarization transformation by the surface and diffuse interactions that randomize the polarization state of the received wave. Multiwavelength polarimeter observations of a variety of types of terrain, including images of the coherent and diffuse parts of the received signal are presented. The diffuse image, in particular, is highly indicative of small-scale surface roughness, an effect illustrated by analyzing a set of polarimeter images acquired over lava fields of varying roughness.

ESA

**N89-18777#** Sepimage, Puteaux (France).

**EFFECTS OF SLOPES AND RELIEF TWO-DIMENSIONAL SPATIAL FREQUENCIES ON SPACEBORNE SAR IMAGERY**

C. JUNG, PH. REBILLARD, and D. VIDAL-MADJAR (Centre National d'Etudes des Telecommunications, Issy-les-Moulineaux, France) *In* ESA, Proceedings of the 1988 International Geoscience and Remote Sensing Symposium (IGARSS) '88 on Remote Sensing: Moving Towards the 21st Century, Volume 3 p 1575-1578 Aug. 1988

Avail: NTIS HC A99/MF A01; ESA Publications Division, ESTEC, Noordwijk, Netherlands, \$120 US or 250 Dutch guilders

The influence of local slopes and their orientation, and the mesoscale relief on SAR image interpretation was studied. Local distortions are studied using the SAR point spread function in a plane tangent to the relief in the vicinity of a given point. Mesoscale deformations are studied by computing the radar image of simple reliefs transposed onto spatial sinusoid models.

ESA

**N89-18790#** Canada Centre for Remote Sensing, Yellowknife (Northwest Territories). Dept. of Geography.

**MAPPING SLOPE FAILURE TRACKS WITH DIGITAL THEMATIC MAPPER DATA**

H. EPP and L. BEAVEN (Saskatchewan Univ., Saskatoon.) *In* ESA, Proceedings of the 1988 International Geoscience and Remote Sensing Symposium (IGARSS) '88 on Remote Sensing: Moving Towards the 21st Century, Volume 3 p 1649-1652 Aug. 1988

Avail: NTIS HC A99/MF A01; ESA Publications Division, ESTEC, Noordwijk, Netherlands, \$120 US or 250 Dutch guilders

An attempt to identify and map the distribution of slope failures in the Rennel Sound area of south-western Graham Island in the Queen Charlotte Islands through the use of digital LANDSAT Thematic Mapper (TM) data is discussed. The TM data was geometrically corrected, resampled to 20 m, and visually compared to 1:10,000 scale color infrared photography. Principal component analysis, Martin Taylor enhancement, ratioing, contrast stretching, and edge enhancement techniques were used to better delineate and identify the various occurrences of slope failure forms. Unsupervised and supervised classification algorithms were also used. Field work assessed ground correlation with photographic and classified satellite hard copy products. Approximately 60 percent of all slope failures are discriminated from the TM data.

ESA

**N89-18821#** Scottish Agricultural Statistics Service, Edinburgh.

**NORMAL DISTRIBUTIONAL ASSUMPTIONS IN DISCRIMINATION**

C. A. GLASBEY *In* ESA, Proceedings of the 1988 International Geoscience and Remote Sensing Symposium (IGARSS) '88 on Remote Sensing: Moving Towards the 21st Century, Volume 3 p 1789-1791 Aug. 1988

Avail: NTIS HC A99/MF A01; ESA Publications Division, ESTEC, Noordwijk, Netherlands, \$120 US or 250 Dutch guilders

The appropriateness and importance of normal distributional assumptions are examined for classification of pixels in remotely sensed images. Bands 1 and 3 of SPOT-type data are used. A few pixels on the edges of training sets are found to be outliers

from the corresponding multivariate normal distributions. Pixel values within a field are spatially associated, and correlated relative to other pixels in the same land class, but in other fields. These departures from standard assumptions in discrimination are shown to have large effects on the resultant classification. ESA

**N89-18824#** New South Wales Univ., Kensington (Australia). School of Surveying.

**SPOT MAPPING SOFTWARE FOR WILD AVIOLYT BC2 ANALYTICAL PLOTTER**

J. C. TRINDER, B. E. DONNELLY, and KWOH LEONG KEONG (Ministry of Defence, Singapore.) *In* ESA, Proceedings of the 1988 International Geoscience and Remote Sensing Symposium (IGARSS) '88 on Remote Sensing: Moving Towards the 21st Century, Volume 3 p 1801-1806 Aug. 1988  
Avail: NTIS HC A99/MF A01; ESA Publications Division, ESTEC, Noordwijk, Netherlands, \$120 US or 250 Dutch guilders

Operational software was developed for mapping from SPOT satellite analog images on an analytical plotter. The software is designed to reflect as nearly as possible standard BC2 software procedures. The solution of the scanner geometry is based on a rigorous colinearity formulation with the position and tilts varying according to first or second order polynomials. Satellite ephemeris data are used to provide estimates of the polynomial parameters. Coordinate transformations enable the plotting and computation of coordinates in a local projection system on the analytical plotter in a mapping environment. Precision of computation of object coordinates is of the order of 5 to 10 m in planimetry and height coordinates depending on the precision of ground control points. ESA

**N89-18831#** Genoa Univ. (Italy). Dept. of Biophysical and Electronic Engineering.

**INFORMATION FUSION BY A KNOWLEDGE-BASED SYSTEM FOR SAR IMAGE INTERPRETATION**

S. DELLEPIANE, D. D. GUISTO, S. B. SERPICO, and G. VERNAZZA *In* ESA, Proceedings of the 1988 International Geoscience and Remote Sensing Symposium (IGARSS) '88 on Remote Sensing: Moving Towards the 21st Century, Volume 3 p 1845-1846 Aug. 1988  
Avail: NTIS HC A99/MF A01; ESA Publications Division, ESTEC, Noordwijk, Netherlands, \$120 US or 250 Dutch guilders

A computerized system employing pattern recognition and artificial intelligence techniques for SAR image processing and interpretation is described. Such images are characterized by considerable speckle noise, which gives rise to serious problems in early processing. To overcome this drawback, it is suggested to consider not only intensity images but also texture images (obtained by the fractal approach), since texture is an effective feature for SAR data classification. A combined intensity-texture image segmentation is proposed. The interpretation module is based on production rules and frame networks, as well as on a heterarchical control structure. Results for Seasat SAR are presented. ESA

**N89-18849#** MacDonald, Dettwiler and Associates Ltd., Richmond (British Columbia).

**A HIGH FIDELITY, HIGH THROUGHPUT SYSTEM FOR GEOCODING SAR IMAGERY**

E. C. COLL and R. G. PETTIGREW *In* ESA, Proceedings of the 1988 International Geoscience and Remote Sensing Symposium (IGARSS) '88 on Remote Sensing: Moving Towards the 21st Century, Volume 2 p 687-690 Aug. 1988  
Avail: NTIS HC A99/MF A01; ESA Publications Div. ESTEC, Noordwijk, Netherlands, \$120 US or 250 Dutch guilders

A high-throughput parallel system for geocoding processed SAR imagery that achieves high levels of geometric accuracy using coordinate transformations that incorporate precision spacecraft orbit modeling is presented. Root mean square location accuracy of one-half of the ground range corresponding to one resolution cell (half pixel accuracy) is achieved. In scenes with terrain relief, correction of foreshortening using a digital terrain model is performed as an integral part of the geocoding process. The

geometric and terrain corrections are evaluated in an efficient manner using correction tables. The precision geocoding process; a high throughput architecture for the SAR geocoding system for an operational data processing facility; and an analysis of the geometric accuracy attained by the system are described. ESA

**N89-18894#** Purdue Univ., West Lafayette, IN. Lab. for Applications of Remote Sensing.

**A SPECTRAL FEATURE DESIGN SYSTEM FOR HIGH DIMENSIONAL MULTISPECTRAL DATA**

C. C. T. CHEN and D. A. LANDGREBE *In* ESA, Proceedings of the 1988 International Geoscience and Remote Sensing Symposium (IGARSS) '88 on Remote Sensing: Moving Towards the 21st Century, Volume 2 p 891-894 Aug. 1988  
Avail: NTIS HC A99/MF A01; ESA Publications Div. ESTEC, Noordwijk, Netherlands, \$120 US or 250 Dutch guilders

A spectral feature design system for high dimensional multispectral data is described. Using the ensemble statistics, the optimal features are derived from the weighted K-L transform so that the representation error is minimized. The spectral structure of the optimal features is then extracted from infinite clipping. The resulting infinite clipped optimal features are much simpler than the optimal set from the implementation point of view and they still have classification performance quite near optimal. The received transformed data can be further processed by canonical analysis in which the class statistics of the scene are used and maximal class separability is achieved. Experimental results indicate that the overall probability of correct classification of the proposed system is over 90 percent while providing for a reduced downlink data rate by a factor of 10. ESA

**N89-18896#** European Space Agency. European Space Research and Technology Center, ESTEC, Noordwijk (Netherlands).

**A POSSIBILITY FOR SELECTING SPECTRAL BANDS OF FUTURE LAND APPLICATION SENSORS AT THE EXAMPLE OF AN IMAGING SPECTROMETER**

M. RAST and H. KAUFMANN (Karlsruhe Univ., Germany, F.R.) *In its* Proceedings of the 1988 International Geoscience and Remote Sensing Symposium (IGARSS) '88 on Remote Sensing: Moving Towards the 21st Century, Volume 2 p 901-904 Aug. 1988

Avail: NTIS HC A99/MF A01; ESA Publications Div. ESTEC, Noordwijk, Netherlands, \$120 US or 250 Dutch guilders

Spectral bands for land application optical sensors operating in the visible and/or infrared, applying different observation technologies (e.g., scanning, pushbroom imaging, radiometry, spectrometry) are discussed. As an example, an imaging spectrometer was selected, since this instrument type is widely discussed as a candidate for future Earth observation missions. The approach seems especially attractive, since drawbacks like the vast amount of data produced by an imaging spectrometer are taken into consideration. The approach tries to arrive at an optimized band selection modus taking account of spectral data banks, the philosophy of data handling, and evaluation with regards to various applications. The definition of the observation bands helps in identifying related definition parameters of the discussed sensor. ESA

**N89-18897#** National Aerospace Lab., Amsterdam (Netherlands).

**UPDATING LAND-USE INFORMATION ON TOPOGRAPHIC MAPS USING SATELLITE IMAGERY: COMBINING THE ADVANTAGES OF TWO ACCESSIBLE SOURCES OF GEOGRAPHIC INFORMATION**

F. B. VANDERLAAN and P. G. MEIJER *In* ESA, Proceedings of the 1988 International Geoscience and Remote Sensing Symposium (IGARSS) '88 on Remote Sensing: Moving Towards the 21st Century, Volume 2 p 905-909 Aug. 1988  
Avail: NTIS HC A99/MF A01; ESA Publications Div. ESTEC, Noordwijk, Netherlands, \$120 US or 250 Dutch guilders

The possibilities of using LANDSAT Thematic Mapper images for updating land use information on topographic maps were

examined. Information obtained from satellite images can be kept up to date and a large number of classes can be distinguished. However, the quality of the information still leaves much to be desired, with a reliability of no more than 40 to 90 percent. By using digitized land use information from a topographic map as a source of context information, the reliability is improved considerably. The method permits the identification of a large number of additional classes and provides quantitative insight into the dynamics of landscape change. Verification using 1:18,000 scale aerial photographs and field data shows the results to have a reliability of over 95 percent. It can be expected that wherever topographic maps permit the extraction of land-use information in a similar way, remote sensing information will meet operational accuracy requirements for many fields of application. ESA

**N89-18698#** Hosei Univ., Tokyo (Japan).

**A METHOD FOR THE CLUSTERING OF REMOTELY SENSED MULTISPECTRAL IMAGES BY USING STATISTICAL TEST FOR SPATIAL UNIFORMITY**

H. HANAIZUMI, H. OKUMURA, H. TSUBAKI, and S. FUJIMURA (Tokyo Univ., Japan) /n ESA, Proceedings of the 1988 International Geoscience and Remote Sensing Symposium (IGARSS) '88 on Remote Sensing: Moving Towards the 21st Century, Volume 2 p 911-912 Aug. 1988  
Avail: NTIS HC A99/MF A01; ESA Publications Div. ESTEC, Noordwijk, Netherlands, \$120 US or 250 Dutch guilders

A division and merging clustering method to be used for multispectral images is proposed. The division uses a segmentation technique, in which a multispectral image is divided into spatially uniform areas. The division rule is based on the (spatial) Mahalanobis distance between coefficient vectors of a local regression model fitted to the neighboring areas of the image. As this distance is a chi-square statistic, a statistical test is employed to evaluate the significance of the distance, and the threshold for the test is theoretically derived. The merging uses a clustering technique, in which the divided areas are merged into clusters. The merging rule is based on the (spectral) Mahalanobis distance between mean vectors of the multispectral data in divided areas. As this spectral distance also follows the chi-square statistics, the same statistical test is used. A threshold is determined for the test. The superiority of this method to a pixel-by-pixel method with respect to the accuracy and the processing speed is confirmed quantitatively by numerical simulations. ESA

**N89-18900#** National Remote Sensing Centre, Farnborough (England).

**PATTERN ANALYSIS AND THE ECOLOGICAL INTERPRETATION OF SATELLITE IMAGERY**

G. H. GRIFFITHS and M. G. WOODING (Wooding, M. G., Farnborough, England) /n ESA, Proceedings of the 1988 International Geoscience and Remote Sensing Symposium (IGARSS) '88 on Remote Sensing: Moving Towards the 21st Century, Volume 2 p 917-922 Aug. 1988  
Avail: NTIS HC A99/MF A01; ESA Publications Div. ESTEC, Noordwijk, Netherlands, \$120 US or 250 Dutch guilders

Measures of landscape pattern were developed to assist in defining the ecological characteristics of a sample of lowland and upland areas in the United Kingdom. The results suggest that raster-based image analysis techniques can be used effectively to measure various parameters of landscape pattern from LANDSAT Thematic Mapper imagery. ESA

**N89-18956#** Systems Designers Ltd., Camberley (England).  
**PROGRESS IN AUTOMATIC ANALYSIS OF MULTI-TEMPORAL REMOTELY-SENSED DATA**

D. G. CORR, A. M. TAILOR, A. CROSS, D. C. MASON, M. PETROU, D. C. HOGG, and D. H. LAWRENCE (Sussex Univ., Brighton, England) /n ESA, Proceedings of the 1988 International Geoscience and Remote Sensing Symposium (IGARSS) '88 on Remote Sensing: Moving Towards the 21st Century, Volume 2 p 1175-1178 Aug. 1988 Sponsored in part by the United Kingdom Alvey Man Machine Interface Project

(Contract NERC-F60/96/12)

Avail: NTIS HC A99/MF A01; ESA Publications Div. ESTEC, Noordwijk, Netherlands, \$120 US or 250 Dutch guilders

The increasing volume of remotely sensed data led to a need for efficient automatic, knowledge-based segmentation of remotely sensed images of the land. The system uses the information in time sequences of remotely sensed data together with cartographic map data and domain expertise to build a model of the scene in terms of segments and their possible classes. The accuracies of segmentation and subsequent classification are shown to be superior to traditional automatic techniques. Potential changes in the scene are isolated. ESA

**N89-18957#** Norwegian Computing Center, Oslo (Norway).

**SATELLITE IMAGERY FOR SEMI-AUTOMATIC MAP REVISION**  
R. SOLBERG and M. ROBB /n ESA, Proceedings of the 1988 International Geoscience and Remote Sensing Symposium (IGARSS) '88 on Remote Sensing: Moving Towards the 21st Century, Volume 2 p 1179-1183 Aug. 1988

Avail: NTIS HC A99/MF A01; ESA Publications Div. ESTEC, Noordwijk, Netherlands, \$120 US or 250 Dutch guilders

A prototype system for semi-automatic 1:50,000 topographic map revision from SPOT imagery is presented. Major functions are segmentation of satellite images, image interpretation for identifying map features using information from the satellite images, the result of the segmentation, and the old map; and manipulation of map data before and after image interpretation. ESA

**N89-19733#** Begeleidingscommissie Remote Sensing, Delft (Netherlands).

**LAND USE ANALYSIS USING REMOTE SENSING TECHNIQUES. INVESTIGATION OF THE USEFULNESS OF LANDSAT THEMATIC MAPPER SATELLITE PICTURES FOR OBTAINING AND UP TO DATE PICTURE OF LAND USE IN THE PROVINCE SOUTH HOLLAND Final Report**  
[LANDGEBRUIKSANALYSE MET BEHULP VAN REMOTE SENSING TECHNIKEN. EEN ONDERZOEK NAAR DE BRUIKBAARHEID VAN LANDSAT THEMATIC MAPPER SATELLIETBEELDEN VOOR HET VERKRIJGEN VAN EEN AKTUEEL BEELD VAN HET LANDGEBRUIK IN DE PROVINCE ZUID-HOLLAND]

J. J. CEVAT, F. B. VANDERLAAN (National Aerospace Lab., Amsterdam, Netherlands), and L. F. VERHEIJ Feb. 1988 31 p  
In DUTCH Original contains color illustrations  
(Contract BCRS-PROJ. TO-3.4)

(BCRS-88-01; ETN-89-93873) Avail: NTIS HC A03/MF A01

The usefulness of LANDSAT thematic mapper to update land use maps was investigated in a test area of 300 sq km. Satellite pictures were processed for manual interpretation, for interpretation of the thermal IR image, as well as for automatic classification. Manual interpretation is found to be suitable for a survey on a scale 1:25,000; the result depends strongly on the spatial resolution of the satellite. The thermal IR image does not provide relevant information about the hydrological situation. The classification result varies strongly from class to class and from area to area; a minimum classification error of 10 pct has to be taken into account. ESA

08

## INSTRUMENTATION AND SENSORS

Includes data acquisition and camera systems and remote sensors.

**A89-20795#**

**THE NAVIGATION METHOD FOR NOAA/AVHRR IMAGE**

O. ROSWINTIARTI, M. KARTASMITA, and B. UNTORO (Indonesian National Institute of Aeronautics and Space, Jakarta, Indonesia) IN: Asian Conference on Remote Sensing, 8th, Jakarta,

Indonesia, Oct. 22-27, 1987, Proceedings. Bogor, Indonesia, EXSA International, 1987, p. F-12-1 to F-12-10. refs

A trigonometric approach is proposed for the navigation methods (Brush, 1985, and Cracknel, 1984) for deriving sea surface temperature and vegetation indices from NOAA/AVHRR data. The equator is determined using ground control points. Based on the equator, the locations of points in the image are calculated using trigonometry. A numerical example is presented, using an AVHRR image from channel 2 taken on July 31, 1987 on NOAA-9. R.B.

**A89-21410**

**CARTOGRAPHIC ANALYSIS OF LARGE FORMAT CAMERA PHOTOGRAPHS - COMPARISON WITH SPOT AND THE SPACELAB METRIC CAMERA [EVALUATION CARTOGRAPHIQUE DES PHOTOGRAPHIES DE LA LARGE FORMAT CAMERA - COMPARISON AVEC SPOT ET LA CAMERA METRIQUE SPACELAB]**

MURIEL GAVORET, MICHEL BOSSARD, and PIERRE-YVES LECORDIX (Institut Geographique National, Saint-Mande, France) Societe Francaise de Photogrammetrie et de Teledetection, Bulletin (ISSN 0244-6014), no. 110, 1988, p. 19-50. In French. refs

The results of a photogrammetric, cartographic, and thematic evaluation of photographs of Calgary, Canada obtained by the LFC aboard the Space Shuttle in 1984 are presented. Improvements of the present system over that employed on Spacelab-1 are pointed out. The photogrammetric precision of the LFC photographs is found to be slightly superior to the precision of Spacelab photographs. Also considered is the application of LFC photography to the revision of traditional small and large scale maps. R.R.

**A89-22214**

**DETERMINATION OF CLEAR-SKY PLANETARY ALBEDO [OPREDELNIE PLANETARNOGO AL'BEDO BEZOBLACHNOGO NEBA]**

K. IA. KONDRAT'EV, V. V. KOZODEROV, S. KH. KEEVALLIK, and O. IU. KIARNER (AN SSSR, Institut Ozerovedeniia, Leningrad; AN SSSR, Otdel Vychislitel'noi Matematiki, Moscow, USSR; AN ESSR, Institut Astrofiziki i Fiziki Atmosfery, Tyuravere, Estonian SSR) Issledovanie Zemli iz Kosmosa (ISSN 0205-9614), Sept.-Oct. 1988, p. 44-49. In Russian. refs

This paper describes a method for determining the values of clear-sky planetary albedo from satellite-acquired radiation data. The method is based on the space and time analyses of remote images combined with theoretical estimates which use known climatic albedos of the earth surface. The method is illustrated using Nimbus-7 radiation data to evaluate average monthly clear-sky albedos. It is shown that this method accounts for particular conditions of observations more effectively than do the albedo methods that use climatological data on the earth surface albedos. I.S.

**A89-22225**

**PRINCIPAL RESULTS OF REMOTE-SENSING STUDIES OF SIBERIA'S NATURAL RESOURCES (ON THE OCCASION OF THE 10TH ANNIVERSARY OF THE SCIENTIFIC COORDINATION COUNCIL, 1977-1987) [OSNOVNYE REZULTATY PRAVEDENNYKH ISSLEDOVANIĖ PO PROBLEME 'AEROKOSMICHESKIE ISSLEDOVANIĖ PRIRODNYKH RESURSOV SIBIRI' /K DESIATILETIU NAUCHNO-KOORDINATSIONNOGO SOVETA, 1977-1987 GG./]**

L. K. ZIATKOVA (AN SSSR, Institut Geologii i Geofiziki, Novosibirsk, USSR) Issledovanie Zemli iz Kosmosa (ISSN 0205-9614), Sept.-Oct. 1988, p. 111-115. In Russian. refs

**A89-22622#**

**OPERATIONAL CALIBRATION OF METEOSAT'S INFRARED CHANNEL**

V. GAERTNER (ESA, European Space Operations Centre, Darmstadt, Federal Republic of Germany) ESA Bulletin (ISSN 0376-4265), no. 56, Nov. 1988, p. 53-57.

The calibration of Meteosat's IR channel which is necessary to allow readings of the detector to be converted into physical

radiance and temperature units is described. The overall rms error of Meteosat sea-surface temperature retrievals is only about 1 C. It is noted that the greatest uncertainty in the determination of the calibration coefficient (due to the effect of cloud contamination) results in an overestimation of 2-3 percent in comparison with other independent calibration methods. R.R.

**A89-23464**

**OBSERVATION OF THE DEGREE OF GLACIATION IN MIDDLE-LEVEL STRATIFORM CLOUDS**

GUOSHENG LIU and TAKAO TAKEDA (Nagoya University, Japan) Meteorological Society of Japan, Journal (ISSN 0026-1165), vol. 66, Oct. 1988, p. 645-659. refs

A 19.35-GHz microwave radiometer and an 8.6-mm radar were used simultaneously to observe middle-level stratiform clouds associated with cyclones in spring 1985. The vertically integrated liquid-water and ice contents are estimated. Two types of clouds are defined and the structure and precipitation formation processes in both types of clouds are examined. The degree of glaciation in the clouds, which is defined by the ratio of vertically integrated ice content to the total amount of condensed water, is examined. R.B.

**A89-24022**

**SUMMERTIME STRATOSPHERIC WIND MEASUREMENTS ABOVE THE SOUTH POLE**

G. J. BYRNE, J. R. BENBROOK, E. A. BERING, B. LIAO, and J. R. THEALL (Houston, University, TX) (IAGA, Symposium on Coupling, Energetics, Dynamics and Electrodynamics of Atmospheric Regions, Vancouver, Canada, Aug. 1987) Journal of Atmospheric and Terrestrial Physics (ISSN 0021-9169), vol. 51, Jan. 1989, p. 51-60. refs  
(Contract NSF DPP-84-15203)

The mean wind flow and wave motions in the stratosphere at the South Pole were observed by tracking a high altitude, zero-pressure balloon during the austral summer of 1985-86. The mean flow at altitudes between 25 km and 33 km above the pole was found to be about 3 m/s. Atmospheric motions characteristic of internal gravity waves were observed for about 4.4 h, with vertical and horizontal wavelengths of about 2.5 km and 125 km, respectively. The horizontal and vertical wind velocities due to these waves was about 2-3 m/s and 0.04-0.06 m/s, respectively. The results suggest that wave motions play a dominant role in the transport of stratospheric constituents in regions where the mean winds are light. R.B.

**A89-26178**

**AERIAL AND SPACE REMOTE-SENSING TECHNIQUES FOR GEOGRAPHICAL INVESTIGATIONS [AEROKOSMICHESKIE METODY GEOGRAFICHESKIH ISSLEDOVANIĖ]**

VIKTOR M. SERDIUKOV, GALINA A. PATYCHENKO, and DMITRIĖ A. SINEL'NIKOV Kiev, Izdatel'stvo Vishcha Shkola, 1987, 224 p. In Russian. refs

This work describes various techniques for the remote sensing of the earth surface (photographic, TV, radar, and scanner). Particular attention is given to the geometrical properties of remote-sensing images, image transformations, and the foundations of stereophotogrammetry. Photointerpretation techniques are discussed which can be used in geographical investigations for purposes of earth-resources utilization and environment protection. B.J.

**A89-26398#**

**ALTERNATIVES FOR MAPPING FROM SATELLITES**

G. KONECNY (Hannover, Universitaet, Hanover, Federal Republic of Germany) IN: Commercial opportunities in space; Symposium, Taipei, Republic of China, Apr. 19-24, 1987, Technical Papers. Washington, DC, American Institute of Aeronautics and Astronautics, Inc., 1988, p. 385-398.

The use of remote sensing data for cartography is discussed. The applications of cartography from satellite data and the techniques used to produce maps from satellite data are reviewed. The various data available for cartographic purposes are described

and compared, including Landsat MSS, TM Spacelab, SPOT, and high altitude photography. The prospects for future developments in sensors, platforms, and data reception are examined. R.B.

**A89-26399#**

**JEOS - A LOW-COST APPROACH TO EARTH OBSERVATION**  
PIERRE MOLETTE (Matra Espace, Toulouse, France) IN: Commercial opportunities in space; Symposium, Taipei, Republic of China, Apr. 19-24, 1987, Technical Papers. Washington, DC, American Institute of Aeronautics and Astronautics, Inc., 1988, p. 399-415.

The Janus Earth Observation Satellite (JEOS), which is designed to provide limited coverage with real-time data transmission, is discussed. The Janus platform and the JEOS configuration, electrical architecture, and attitude control are described. The typical JEOS performances for a 700 km altitude are a 30 m spatial resolution, a 120 km swath width, and an off-track capability of 325 km. The components of the JEOS payload are examined, including the optical imaging instrument, the Advanced Ocean Color Monitor, and the payload telemetry. Also, the process of orbit selection and satellite operation are considered. R.B.

**A89-26843\*** Jet Propulsion Lab., California Inst. of Tech., Pasadena.

**UNSUPERVISED CLASSIFICATION OF SCATTERING BEHAVIOR USING RADAR POLARIMETRY DATA**

JAKOB J. VAN ZYL (California Institute of Technology, Jet Propulsion Laboratory, Pasadena) IEEE Transactions on Geoscience and Remote Sensing (ISSN 0196-2892), vol. 27, Jan. 1989, p. 36-45. refs

The use of an imaging radar polarimeter data for unsupervised classification of scattering behavior is described by comparing the polarization properties of each pixel in a image to that of simple classes of scattering such as even number of reflections, odd number of reflections, and diffuse scattering. For example, when this algorithm is applied to data acquired over the San Francisco Bay area in California, it classifies scattering by the ocean as being similar to that predicted by the class of odd number of reflections, scattering by the urban area as being similar to that predicted by the class of even number of reflections, and scattering by the Golden Gate Park as being similar to that predicted by the diffuse scattering class. It also classifies the scattering by a lighthouse in the ocean and boats on the ocean surface as being similar to that predicted by the even number of reflections class, making it easy to identify these objects against the background of the surrounding ocean. The algorithm is also applied to forested areas and shows that scattering from clear-cut areas and agricultural fields is mostly similar to that predicted by the odd number of reflections class, while the scattering from tree-covered areas generally is classified as being a mixture of pixels exhibiting the characteristics of all three classes, although each pixel is identified with only a single class. I.E.

**A89-27753\*** National Aeronautics and Space Administration. Goddard Space Flight Center, Greenbelt, MD.

**OPTICAL SYSTEM DESIGN ALTERNATIVES FOR THE MODERATE-RESOLUTION IMAGING SPECTROMETER-TILT (MODIS-T) FOR THE EARTH OBSERVING SYSTEM (EOS)**

PETER W. MAYMON, STEVEN P. NEECK (NASA, Goddard Space Flight Center, Greenbelt, MD), and JOHN C. MOODY, SR. (Swales and Associates, Inc., Beltsville, MD) IN: Recent advances in sensors, radiometry, and data processing for remote sensing; Proceedings of the Meeting, Orlando, FL, Apr. 6-8, 1988. Bellingham, WA, Society of Photo-Optical Instrumentation Engineers, 1988, p. 10-22. refs

The MODIS consists of two synergistic sensors with a total of 104 spectral bands in the 0.4-14.2-micron range. MODIS-T (Tilt) is one of these sensors. It is a 64-channel imaging spectrometer with a required 10 nm spectral resolution (FWHM) in the 400 to 1040 nm spectral range. The system will have a 1 km IFOV, a wide scan for global coverage in three days, and be capable of being pointed fore and aft of nadir by + or - 50 degrees.

Author

**A89-27779\*** National Aeronautics and Space Administration. Goddard Space Flight Center, Greenbelt, MD.

**PARABOLA DIRECTIONAL FIELD RADIOMETER FOR AIDING IN SPACE SENSOR DATA INTERPRETATIONS**

DONALD W. DEERING (NASA, Goddard Space Flight Center, Greenbelt, MD) IN: Recent advances in sensors, radiometry, and data processing for remote sensing; Proceedings of the Meeting, Orlando, FL, Apr. 6-8, 1988. Bellingham, WA, Society of Photo-Optical Instrumentation Engineers, 1988, p. 249-261. refs

A unique field radiometer, called the Parabola, was developed to accurately measure the multidirectional incoming and outgoing spectral radiances for a variety of earth surface types; these range from rangeland vegetation to ice and snow. It is found that bidirectional reflectance characteristics are not constant for a given type of vegetation. There can be substantial changes in the anisotropic expression with changes in the solar zenith angle and vegetation conditions. K.K.

**A89-27933**

**APPLICATIONS OF REMOTE SENSING TO AGROMETEOROLOGY; PROCEEDINGS OF THE COURSE, ISPRA, ITALY, APR. 6-10, 1987**

F. TOSELLI, ED. (CEC, Joint Research Centre, Ispra, Italy) Course sponsored by CEC. Dordrecht, Netherlands, Kluwer Academic Publishers, 1989, 333 p. For individual items see A89-27934 to A89-27946.

Agrometeorological remote sensing applications are examined, including reviews of the fundamentals of remote sensing, sensors, platforms, and data processing techniques. Other topics include image processing techniques, the fundamentals of imaging radar, radar postprocessing, the extraction of surface temperature from satellite data, and the use of surface temperature in agrometeorology. Also, studying the radiation budget at the ground from satellite data, microwave remote sensing of soil moisture, the vegetation index and vegetation dynamics, and satellite remote sensing of rainfall are discussed. R.B.

**A89-27934**

**FUNDAMENTALS OF REMOTE SENSING**

PH. HARTL (Stuttgart, Universitaet, Federal Republic of Germany) IN: Applications of remote sensing to agrometeorology; Proceedings of the Course, Ispra, Italy, Apr. 6-10, 1987. Dordrecht, Netherlands, Kluwer Academic Publishers, 1989, p. 1-18. refs

This paper defines the purpose and describes the physical background and basic features of remote sensing techniques. It covers the applicable spectral bands of the optical and microwave regions and the basic measurement concepts, which rely on the scattering and/or self-radiating processes of electromagnetic waves and, more generally, on some interaction of electromagnetic energy with matter. Author

**A89-27935**

**SENSORS**

PH. HARTL (Stuttgart, Universitaet, Federal Republic of Germany) IN: Applications of remote sensing to agrometeorology; Proceedings of the Course, Ispra, Italy, Apr. 6-10, 1987. Dordrecht, Netherlands, Kluwer Academic Publishers, 1989, p. 19-34. refs

This paper reviews the various types of sensors applied in optical and microwave remote sensing from satellites, in particular over land. It covers active and passive sensors, imaging and non-imaging sensors, the basic concepts and some types of instruments used. Author

**A89-27936**

**PLATFORMS**

G. FRAYSSE IN: Applications of remote sensing to agrometeorology; Proceedings of the Course, Ispra, Italy, Apr. 6-10, 1987. Dordrecht, Netherlands, Kluwer Academic Publishers, 1989, p. 35-55.

The various types of platforms used in remote sensing are reviewed, including low-, mid-, and high-altitude aircraft, orbiting and geostationary satellites, first generation, present and future satellites. Types, altitudes, period, and inclination of the orbits



together with the characteristics of the various types of sensor embarked, data transmission, reception and preprocessing are examined. Author

A89-27977

**OCEAN OPTICS: INTRODUCTION AND OVERVIEW - 1988**

MARVIN A. BLIZARD (U.S. Navy, Office of Naval Research, Arlington, VA) IN: Ocean optics IX; Proceedings of the Meeting, Orlando, FL, Apr. 4-6, 1988. Bellingham, WA, Society of Photo-Optical Instrumentation Engineers, 1988, p. 2-11. refs

The fundamental optical properties of ocean water and the techniques and instruments used to measure them are discussed, reviewing the results of recent investigations. Consideration is given to the radiometric parameters of the water column; inherent and apparent optical properties; the measurement of the spectral absorption coefficient; the volume scattering function; and the attenuation of downwelling solar or laser light by water molecules, chlorophyll, and other pigments. Diagrams, drawings, and graphs of typical measurement data are provided. T.K.

**A89-27990\*** Biospherical Instruments, Inc., San Diego, CA.  
**MOORABLE SPECTRORADIOMETERS IN THE BIOWATT EXPERIMENT**

C. R. BOOTH (Biospherical Instruments, Inc., San Diego, CA) and R. C. SMITH (California, University, Santa Barbara) IN: Ocean optics IX; Proceedings of the Meeting, Orlando, FL, Apr. 4-6, 1988. Bellingham, WA, Society of Photo-Optical Instrumentation Engineers, 1988, p. 176-188. refs  
 (Contract NAS7-923; NAS7-934; N00014-84-C-0832; NAGW-290)

A new oceanographic instrument, the MER-2020, has been developed for the long term measurement of bio-optical properties. This instrument is a self-contained reflectance spectroradiometer with 40 megabytes of internal data storage and battery power permitting deployments for as long as 6 months. It can serve as the control and recording center for a variety of other sensors including fluorometers, transmissometers, temperature and conductivity probes. Instruments of this type were deployed at depths to 70 meters on a 5000 meter mooring during the BIOWATT experiment between February and November 1987. Measurements of the spectral diffuse attenuation coefficient and of the remote sensed reflectance from the ten month period in 1987 in the Northern Sargasso Sea are presented. In addition, the temperature, pressure, package orientation and sunlight stimulated natural fluorescence of phytoplankton are discussed. This instrument will be a key part of in situ optical calibration for future remote color sensors, and presently permits direct measurement of long term optical variability, important in visibility and communication problems. Author

**A89-27991\*** University of South Florida, Saint Petersburg.  
**SPECTRAL TRANSMISSOMETER AND RADIOMETER - DESIGN AND INITIAL RESULTS**

KENDALL L. CARDER, ROBERT G. STEWARD, THOMAS G. PEACOCK (South Florida, University, Saint Petersburg, FL), PAUL R. PAYNE, and WAYNE PECK (Aztec Computer Engineering, Pinellas Park, FL) IN: Ocean optics IX; Proceedings of the Meeting, Orlando, FL, Apr. 4-6, 1988. Bellingham, WA, Society of Photo-Optical Instrumentation Engineers, 1988, p. 189-195. refs  
 (Contract NAGW-465)

A new solid-state spectral transmissometer and radiometer is described. The radiometer measures upwelling radiance, downwelling irradiance, and beam transmittance from 390 to 750 nm with channel widths of 2.35 nm. The spectrometer consists of a 256 element CCD linear array collecting light dispersed by a reflection grating in a modified Littrow configuration. The spectrometer is time and space-shared among the three signal types. The instrument has been deployed as a free-drifting buoy and in the profiling mode, with data stored internally on a magnetic bubble memory or sent up a conducting cable as desired. Power can be supplied either by a detachable external battery pack or through conducting cable. The instrument has been deployed in the oligotrophic North Pacific Central Gyre and in the eutrophic

Straits of Juan de Fuca, and preliminary results for each region are discussed. Author

A89-27993

**OPTICAL BATHYMETRY FOR THE U.S. NAVY - A FIELD MEASUREMENT PROGRAM**

STEPHEN P. HAIMBACH, HILLARY C. MESICK, H. JERRY BYRNES, and G. DANIEL HICKMAN (U.S. Navy, Naval Ocean Research and Development Activity, Bay Saint Louis, MS) IN: Ocean optics IX; Proceedings of the Meeting, Orlando, FL, Apr. 4-6, 1988. Bellingham, WA, Society of Photo-Optical Instrumentation Engineers, 1988, p. 214-221. Research supported by DMA.

The design and operation of the Airborne Bathymetric Sounder (ABS), a laser sounding instrument developed for U.S. Navy coastal surveys, are described and illustrated with diagrams and graphs. Particular attention is given to the ABS operational scenario, the Nd:YAG laser sounder (employing 1-mJ 5-6-nsec pulses at both 532 nm and 1.054 microns), the multispectral scanner, and the navigation subsystem. Flight tests performed in 1986 demonstrate that the ABS can provide clear-water bathymetric data by day or by night at depths up to 30 m. T.K.

A89-27996

**ANALYSIS OF AIRBORNE LASER HYDROGRAPHY WAVEFORMS**

GARY C. GUENTHER (NOAA, Charting Research and Development Laboratory, Rockville, MD) and HILLARY C. MESICK (U.S. Navy, Mapping, Charting, and Geodesy Div., Bay Saint Louis, MS) IN: Ocean optics IX; Proceedings of the Meeting, Orlando, FL, Apr. 4-6, 1988. Bellingham, WA, Society of Photo-Optical Instrumentation Engineers, 1988, p. 232-241. Research supported by DMA. refs

The U.S. Navy is presently constructing and flight-testing the Airborne Bathymetric Survey System which contains as one of its sensors a lidar system. Automated post-flight waveform processing software has been developed around several sets of heuristic rules to reliably extract accurate depths while exhibiting a low false alarm rate. In 1987, flight tests were conducted in the Key West, Florida area to develop hardware and to provide data for exercising the processing procedures. The performance of the waveform processor, including noise immunity, target discrimination, and limiting cases, is presented. Interesting environmental effects on the surface returns, volume backscatter, and bottom returns are detailed. Work in progress, including comparisons of different pulse location algorithms, is noted. Author

A89-28038

**THE SPECIAL SENSOR MICROWAVE IMAGER - A NEW INSTRUMENT WITH RAINFALL MONITORING POTENTIAL**

ERIC C. BARRETT, CHRISTOPHER KIDD, and JOHN O. BAILEY (Bristol, University, England) International Journal of Remote Sensing (ISSN 0143-1161), vol. 9, Dec. 1988, p. 1943-1950. refs

The new Special Sensor Microwave Imager (SSM/I) is introduced, and its global data acquisition pattern illustrated. Through an image for the morning of July 29, 1987 covering north-western Europe in general, and southern Britain in particular, its rainfall monitoring potential is illustrated and explained. An initial comparison with digital outputs from the FRONTIERS radar system of the U.K. Meteorological Office is presented, revealing very promising spatial correspondences between SSM/I and radar-derived rain areas. Author

A89-28039

**SCENE LOCATIONS AND OVERPASS DATES FOR LANDSAT AND SPOT SENSORS**

JOHN C. PRICE (USDA, Agricultural Research Service, Beltsville, MD) International Journal of Remote Sensing (ISSN 0143-1161), vol. 9, Dec. 1988, p. 1951-1958.

It is frequently necessary to obtain information about scene locations and potential data acquisitions for the high resolution satellite sensors. Formulas and basic data are provided to permit



users to compute locations, dates and times of possible coverage for past and future observations from Landsats 1-5 and SPOT.

Author

**A89-28329**

**ERS-1 ACTIVE MICROWAVE INSTRUMENTATION DESIGN AND PERFORMANCE STATUS**

D. J. Q. CARTER (Marconi Space Systems, Ltd., Portsmouth, England) (IAF, International Astronautical Congress, 38th, Brighton, England, Oct. 10-17, 1987) Acta Astronautica (ISSN 0094-5765), vol. 19, Jan. 1989, p. 27-40. (IAF PAPER 87-136)

The paper describes the European Space Agency's first remote sensing satellite (ERS-1) and the relationship of the active microwave instrumentation (AMI) to the rest of the payload. The requirement method and specification values for performance aspects are laid down for the AMI. The development status of the AMI and present in-orbit performance predictions are presented. The design areas concerning ambiguous energy, AMI antenna interactions, receiver gain setting, and antenna gain variation are discussed.

Author

**A89-29070**

**MICROCOMPUTERS AND MASS STORAGE DEVICES FOR IMAGE PROCESSING**

D. C. FERNS and N. P. PRESS (Nigel Press Associates, Ltd., Edenbridge, England) IN: Digital image processing in remote sensing. London and Philadelphia, PA, Taylor and Francis, 1988, p. 105-121.

Recent advancements in microcomputer-based color-image processing workstations have not yet been taken full advantage of in the field of remote sensing image processing; it is presently estimated that it may be only in the early 1990s that the use of networked microcomputer workstations with optical disk media for archiving and dissemination will be widespread. Optical disk carousels or 'juke boxes' use a mechanical robotic arm that can pick up any disk from a storage rack, typically containing 50-150 disks, and load it into the single disk drive. Comparisons are made of the applicability and comparative advantage of tape drives, floppy disks, and tape cartridges, as well as optical disks.

O.C.

**A89-29372#**

**ANALYSIS OF ATMOSPHERIC EFFECTS IN SPOT HRV IMAGES [ANALYSE DES EFFETS ATMOSPHERIQUES DANS LES IMAGES HRV DE SPOT]**

ALAIN ROYER, NORMAN O'NEILL (Sherbrooke, Universite, Canada), and ANTHONY DAVIS (McGill University, Montreal, Canada) Canadian Journal of Remote Sensing (ISSN 0008-2821), vol. 14, Dec. 1988, p. 80-91. In French. Research supported by the Ministere de l'Education du Quebec. refs (Contract NSERC-A-8643; NSERC-A-1765)

Atmospheric effects on the quality of multispectral SPOT HRV images were investigated by comparing SPOT images with synchronous ground measurements, using water reflectances as the reference standard. The effect of atmospheric scattering on the reflectance of a small target in a heterogeneous area was quantified using a radiative transfer model. It is found that the optical thickness of aerosols can be determined with 20-percent accuracy using the model, and that satellite reflectances corrected for atmospheric effects matched ground measurements with 10-percent accuracy.

R.R.

**A89-29375#**

**COMPARATIVE SPECTRAL ANALYSIS OF HRV AND TM SENSORS [ANALYSE SPECTRALE COMPARATIVE DES CAPTEURS HRV ET TM]**

M. BERNIER, J. CIHLAR (Canada Centre for Remote Sensing, Ottawa), O. DUPONT (Intera Technologies, Ltd., Ottawa, Canada), and S. MOREAU Canadian Journal of Remote Sensing (ISSN 0008-2821), vol. 14, Dec. 1988, p. 118-123. In French. refs

Multispectral data for the Drummondville region of Quebec were obtained in 1986 in order to compare the spectral signatures of various land-types imaged by TM and HRV sensors. The SEPAR

program was used to study the statistical separation of 23 land-use categories. The results show the TM-5 middle-IR band to significantly improve the discrimination of land-use categories. Comparable classification results were obtained using HRV images for west-oriented or close-to-nadir viewing angles.

R.R.

**A89-29433**

**POTENTIAL OF LARGE FORMAT CAMERA PHOTOGRAPHY**

ROOP C. MALHOTRA (NOAA, Charting Research and Development Laboratory, Rockville, MD) Photogrammetric Engineering and Remote Sensing (ISSN 0099-1112), vol. 55, Feb. 1989, p. 183-189. refs

The potential of Large Format Camera (LFC) photography for photogrammetric control extension is studied, based on a series of error propagation analyses in the photogrammetric triangulation of a block of 22 LFC photographs. Several data acquisition and reduction systems are discussed. It is found that the most accurate results are obtained when a system such as GPS is used with ground control in block triangulation. Also, it is suggested that LFC attitude information from the stellar camera array is useful in conjunction with GPS for areas where ground control is not available.

R.B.

**A89-29435**

**USE OF THE VARIABLE GAIN SETTINGS ON SPOT**

PAT S. CHAVEZ, JR. (USGS, Flagstaff, AZ) Photogrammetric Engineering and Remote Sensing (ISSN 0099-1112), vol. 55, Feb. 1989, p. 195-201. refs

The ability of the SPOT imaging system to collect digital image data using one of eight different gain settings is discussed. The proper gain setting selection makes it possible to optimize the brightness or reflectance resolution for any given site. As a test of the variable gain settings, normal/standard and high/maximum gain SPOT images of the island of Hawaii were collected using the HRV 1 and HRV 2 systems simultaneously. Landsat MSS data were used to predict the optimum SPOT gain settings for the site. The results show that the normal/standard gain setting may be too low for use in many areas.

R.B.

**A89-29436**

**BAND-MOMENT ANALYSIS OF IMAGING-SPECTROMETER DATA**

DONALD C. RUNDQUIST and LIPING DI (Nebraska, University, Lincoln) Photogrammetric Engineering and Remote Sensing (ISSN 0099-1112), vol. 55, Feb. 1989, p. 203-208. refs

Modern sensor systems high in spectral resolution, such as the Airborne Imaging Spectrometer (AIS), are challenging from an image-processing standpoint because direct classification of datasets with 100 or more spectral channels is virtually impossible. Thus, it is necessary to conduct pre-classification manipulations and transformations both to reduce the amount of data to be classified and to extract pertinent information from the original dataset. Band-moment analysis is a simple, computationally efficient, and productive alternative to principal-components analysis (PCA), a technique commonly used for data reduction. Results from moment analysis of AIS-1 data for western Nebraska are compared to those derived from PCA. Although additional work is warranted, especially concerning the physical meaning of individual moments, several advantages of moment analysis are documented including computational efficiency, reduction of sensor noise, and an overall image quality which is at least as good as a first-principal-component image.

Author

**A89-30270**

**AN OPTIMUM CALIBRATION PROCEDURE FOR RADIOMETERS**

G. E. PECKHAM (Heriot-Watt University, Edinburgh, Scotland) International Journal of Remote Sensing (ISSN 0143-1161), vol. 10, Jan. 1989, p. 227-236. Research supported by SERC. refs

The filter design problem of the zero calibration of total power radiometers is considered. A calibration filter is discussed which incorporates information from cold target calibration samples in

such a way as to minimize the variance of the corrected signal in the presence of 1/f noise. It is noted that the present method is applicable to modulated Dicke-switch radiometers. R.R.

**A89-30967**  
**THE RELATIVE MERITS OF NARROWBAND CHANNELS FOR ESTIMATING BROADBAND ALBEDOS**

ISTVAN LASZLO (Maryland, University, College Park), HERBERT JACOBOWITZ, and ARNOLD GRUBER (NOAA, Satellite Research Laboratory, Washington, DC) *Journal of Atmospheric and Oceanic Technology* (ISSN 0739-0572), vol. 5, Dec. 1988, p. 757-773. refs

Relative merits of various narrow-band channels for the prediction of broad-band albedo were investigated using the atmospheric radiation model of Wiscombe et al. (1984) to simulate observations of the ocean, vegetative land, cloud, and snow surfaces made with both the current and proposed narrow-band channels aboard the NOAA satellites. Solar zenith angles were varied over the range 0-60 deg. Results indicate that, for all of the surfaces considered, a linear combination of AVHRR channels 1, 2, and 3A, or of channels 1M, 2M, and 3A, would yield a much better approximation of the broad-band albedo than channel 1 alone. I.S.

**A89-31020**  
**SPACEBORNE RECORDING SYSTEMS FOR THE SPACE STATION ERA**

JERRY MUENCH (Odetics, Inc., Space Div., Anaheim, CA) IN: ITC/USA/'88; Proceedings of the International Telemetry Conference, Las Vegas, NV, Oct. 17-20, 1988. Research Triangle Park, NC, Instrument Society of America, 1988, p. 305-316.

A detailed review of spaceborne magnetic tape recorder technology from the late 1970s to the Space Station era is presented. Background information indicates that the oft maligned space tape recorder has continued to demonstrate improving reliability since the marginal performances throughout the 1960s. Specifically, the SPOT recorder is reviewed in technical detail to show its evolution through the LANDSAT 6 and 7 versions, JERS-1, and finally the proposed ultimate version for the Space Station/EOS. Enabling technologies include active tape tracking, magnetic recording head advances, and extensive use of application-specific integrated circuit devices to reduce the EEE piece part count. The suitability of the proposed Space Station/EOS recorder technologies for advanced future applications requiring data rates to 1 Gops and storage capacities to 1 x 10 to the 12th bits is discussed. Author

**A89-31943\*** National Aeronautics and Space Administration. Goddard Space Flight Center, Greenbelt, MD.

**MODIS - ADVANCED FACILITY INSTRUMENT FOR STUDIES OF THE EARTH AS A SYSTEM**

VINCENT V. SALOMONSON, W. L. BARNES, PETER W. MAYMON, HARRY E. MONTGOMERY, and HARVEY OSTROW (NASA, Goddard Space Flight Center, Greenbelt, MD) *IEEE Transactions on Geoscience and Remote Sensing* (ISSN 0196-2892), vol. 27, March 1989, p. 145-153. refs

The moderate resolution imaging spectrometer (MODIS) is discussed as an earth-viewing sensor that is planned as a facility instrument for the Earth Observing System (EOS) scheduled to begin functioning in the mid-1990s. The MODIS is composed of two mutually supporting sensors that cover a swath width sufficient to provide nearly complete two-day global coverage from a polar-orbiting, sun-synchronous, serviceable platform. High signal-to-noise ratios are to be provided, e.g., 500 to 1 or greater with 10-12-bit quantization over the dynamic ranges of the spectral bands. MODIS' lifetime is expected to be about ten years. One of the MODIS sensors is termed MODIS-N, where N signifies nadir-viewing. The companion to MODIS-N is MODIS-T, where T signifies a tiltable field-of-view. The development of the MODIS facility from conceptual design studies (Phase-A) into detailed design studies (Phase-B) is discussed. I.E.

**A89-31946\*** Jet Propulsion Lab., California Inst. of Tech., Pasadena.

**MISR - A MULTIANGLE IMAGING SPECTRORADIOMETER FOR GEOPHYSICAL AND CLIMATOLOGICAL RESEARCH FROM EOS**

DAVID J. DINER, CAROL J. BRUEGGE, JOHN V. MARTONCHIK (California Institute of Technology, Jet Propulsion Laboratory, Pasadena), THOMAS P. ACKERMAN (Pennsylvania State University, University Park), ROGER DAVIES (McGill University, Montreal, Canada) et al. *IEEE Transactions on Geoscience and Remote Sensing* (ISSN 0196-2892), vol. 27, March 1989, p. 200-214. refs

The scientific objectives, instrument concept, and data plan for the multiangle imaging spectroradiometer (MISR), an experiment proposed for the EOS (Earth Observing System) mission, are described. MISR is a pushbroom imaging system designed to obtain continuous imagery of the sunlit Earth at four different view angles (25.8, 45.6, 60.0, and 72.5 deg relative to the vertical at the earth's surface), in both the forward and aftward directions relative to nadir, using eight separate cameras. Observations will be acquired in four spectral bands, centered at 440, 550, 670, and 860 nm. Data analysis algorithms will be applied to MISR imagery to retrieve the optical, geometric, and radiative properties of complex, three-dimensional scenes, such as aerosol-laden atmospheres above a heterogeneously reflecting surface, nonstratified cloud systems, and vegetation canopies. The MISR investigation will address a number of scientific questions concerning the climatic and ecological consequences of many natural and anthropogenic processes, and will furnish aerosol information necessary for atmospheric corrections of surface images. I.E.

**A89-31947\*** National Aeronautics and Space Administration. Wallops Flight Center, Wallops Island, VA.

**OFF-NADIR RADAR ALTIMETRY**

CHESTER L. PARSONS and EDWARD J. WALSH (NASA, Wallops Flight Center, Wallops Island, VA) *IEEE Transactions on Geoscience and Remote Sensing* (ISSN 0196-2892), vol. 27, March 1989, p. 215-224. refs  
 (Contract NASA TASK 161-10-06)

The characteristics of nadir versus off-nadir altimetry are reviewed and contrasted and a potentially serious problem has been pointed out that has been overlooked by earlier investigators, who focused on the nongeophysical error sources in off-nadir altimetry. Spatial gradients of radar cross section on the sea surface, caused by wind or current gradients or the variation of radar cross section with incidence angle, could introduce significant range errors in off-nadir altimeter. This potentially crippling effect can be overcome by leaving the traditional 13-GHz frequency and implementing the multibeam altimeter at 36 GHz. A multibeam altimeter proposed for the EOS (Earth Observing System) is described as well as a multimode airborne radar altimeter being developed to study problems inherent in off-nadir altimetry. I.E.

**A89-32334**  
**ON-LINE ASPECTS OF STEREOPHOTOGAMMETRIC PROCESSING OF SPOT IMAGES**

V. KRATKY (Canada Centre for Mapping, Ottawa) *Photogrammetric Engineering and Remote Sensing* (ISSN 0099-1112), vol. 55, March 1989, p. 311-316. refs

Several aspects must be considered when processing dynamic, time-dependent satellite imagery, such as produced by the SPOT system, in an on-line environment of photogrammetric compilation. The following major problems arise: (1) the computer control of image, stage positioning must cope with dynamic changes in the position and attitude of the imaging sensor and still retain its needed real-time performance, and (2) in the continuous compilation mode, the model heights entered on input must be defined with respect to the curvilinear coordinate system of the ellipsoidal or geoidal surface. These and some other related issues are addressed and solutions presented, based on extensive software simulations, on analysis of numerous experiments, and on practical testing in an analytical plotter. Author

**N89-15459** Wyoming Univ., Laramie.  
**MEASUREMENTS OF SPRINGTIME ANTARCTIC OZONE DEPLETION AND DEVELOPMENT OF A BALLOONBORNE ULTRAVIOLET PHOTOMETER Ph.D. Thesis**  
 JERALD WILLIAM HARDER 1987 244 p  
 Avail: Univ. Microfilms Order No. DA8813304

The research described consists of two parts. The first part is a description of the design of a balloonborne ultraviolet photometer to measure ozone and the results of a flight using this instrument. The second part describes the modifications made on the standard commercially available electrochemical ozonesonde and the results of some experiments performed both in the lab and during stratospheric balloon flights. Using this modified ECC system, 33 successful balloon flights were made at McMurdo Station, Antarctica during the austral spring of 1986 to study the temporal and vertical development of the so-called Antarctic Ozone Hole. The results of these flights are described in detail. The ozonesonde data gave a very clear picture of the development of the Ozone Hole.  
 Dissert. Abstr.

**N89-16202#** Naval Postgraduate School, Monterey, CA.  
**COMPARISON STUDY OF SEASAT SCATTEROMETER AND CONVENTIONAL WIND FIELDS M.S. Thesis**  
 KRISTINE HOLDERIED Sep. 1988 218 p  
 (AD-A200591) Avail: NTIS HC A10/MF A01 CSCL 04B

Better wind field information is needed over the open ocean, especially as a forcing function for ocean circulation models. Microwave scatterometry, as a means of remotely sensing surface wind information, was developed in response to this requirement for a surface wind field with global coverage and improved spatial and temporal resolution; this led to the 1978 deployment of the SEASAT Satellite Scatterometer (SASS). Evaluations of the three months of SEASAT data established the consistency of SASS winds with high quality surface wind data from field experiments over limited areas and time periods. Directional ambiguity of the original SASS vectors has been removed for the entire data set, and the resulting SASS winds from conventional sources. This thesis compares a 1-month (12 Aug. to 9 Sep. 1978) subset of these dealiased winds, in the western North Atlantic, with a conventional, pressure-derived wind field from the 6-hourly surface wind analyses of the Fleet Numerical Oceanographic Center (FNOG). Through an objective mapping procedure, the irregularly spaced SASS winds are regridded to a latitude-longitude grid, facilitating statistical comparisons with the regularly spaced FNOG wind vectors and wind stress curl calculations. The study includes qualitative comparisons to synoptic weather maps, calculations of field statistics and boxed mean differences; and scatter plots of wind speed, direction, and standard deviation. GRA

**N89-16205\*#** National Aeronautics and Space Administration. Goddard Space Flight Center, Greenbelt, MD.  
**MODIS-HIRIS GROUND DATA SYSTEMS COMMONALITY REPORT**  
 D. HAN, H. RAMAPRIYAN, V. SALOMONSON, J. ORMSBY, P. ARDANUY, A. MCKAY, D. HOYT, S. JAFFIN, B. VALLETTE, E. HURLEY (Interferometrics, Inc., Vienna, VA.) et al. Dec. 1988 30 p Prepared in cooperation with JPL, Pasadena, CA and General Sciences Corp., Laurel, MD  
 (Contract NAS5-29373; NAS5-28795)  
 (NASA-TM-100718; REPT-89B00065; NAS 1.15:100718) Avail: NTIS HC A03/MF A01 CSCL 05B

The High Resolution Imaging Spectrometer (HIRIS) and Moderate Resolution Imaging Spectrometer (MODIS) Data Systems Working Group was formed in September 1988 with representatives of the MODIS Data System Study Group and the HIRIS Project Data System Design Group to collaborate in the development of requirements on the EosDIS necessary to meet the science objectives of the two facility instruments. A major objective was to identify and promote commonality between the HIRIS and MODIS data systems, especially from the science users' point of view. A goal was to provide a base set of joint requirements and specifications which could easily be expanded to a Phase-B

representation of the needs of the science users of all EOS instruments. This document describes the points of commonality and difference between the Level-II Requirements, Operations Concepts, and Systems Specifications for the ground data systems for the MODIS and HIRIS instruments at their present state of development. Author

**N89-16886#** National Remote Sensing Agency, Hyderabad (India).

**INDIAN ACTIVITIES IN REMOTE SENSING APPLICATIONS: MICROWAVE REMOTE SENSING**

B. L. DEEKSHATULU *In* DFVLR, Proceedings of the Colloquium about Joint Projects Within the DFVLR/ISRO Cooperation p 39-56 Jun. 1988

Avail: NTIS HC A06/MF A01; DFVLR, VB-PL-DO, Postfach 90 60 58, 5000 Cologne, Fed. Republic of Germany, 34.50 Deutsche marks

Indian and Indo-German programs concerning airborne and spaceborne multispectral scanning and microwave remote sensing are reviewed, including LANDSAT and Meteosat data processing, development of the Rohini satellite, design and development of a six channel chlorophyll scanner, IRS Sun synchronous spaceborne mission for optical remote sensing, SPOT data reception and processing, and microwave signature studies. ESA

**N89-16887#** Deutsche Forschungs- und Versuchsanstalt fuer Luft- und Raumfahrt, Oberpfaffenhofen (West Germany).

**GERMAN SPACEBORNE REMOTE SENSING ACTIVITIES**

H. OETTL *In its* Proceedings of the Colloquium about Joint Projects Within the DFVLR-ISRO Cooperation p 57-67 Jun. 1988

Avail: NTIS HC A06/MF A01; DFVLR, VB-PL-DO, Postfach 90 60 58, 5000 Cologne, Fed. Republic of Germany, 34.50 Deutsche marks

Metric camera, which is a modified version of a classical airborne camera for spaceborne use, a modular optoelectronic multispectral scanner implemented with charge coupled device (CCD) technology and already flown twice in shuttle missions, and a LIDAR system to study the backscattering properties of low and high atmosphere aerosols are discussed. ESA

**N89-17931#** South Carolina Univ., Columbia. Dept. of Geography.

**THE DERIVATION AND VERIFICATION OF SURFACE REFLECTANCES USING AIRBORNE MSS DATA AND A RADIATIVE TRANSFER MODEL**

ELIJAH W. RAMSEY, III and JOHN R. JENSEN 1988 17 p Presented at the Fall Technical Meeting of the American Society of Photogrammetry and Remote Sensing, Virginia Beach, VA, 11 Sep. 1988

(Contract DE-AC09-76SR-00001)  
 (DE89-004881; DP-MS-88-153; CONF-8809220-2) Avail: NTIS HC A03/MF A01

Surface reflectance images were derived from airborne MSS data using a radiative transfer model to eliminate atmospheric effects and to derive downwelling irradiances. Input radiative transfer model parameters and Brightness Value (BV) to radiance conversion gain and bias factors were generated for each band using an optimization procedure to minimize the difference between modelled and image BV. Subsequently, reflectance images were derived at five wavelengths from the blue to red bands using the optimized parameters as inputs into the radiative transfer model. Modelled surface reflectance images were evaluated for accuracy by statistical comparison to measured reflectances, and for improved contrast by subjective comparison to the original images. Daedalus DS-1260 MSS bands 3, 4 and 5 modelled reflectances explained 25, 75 and 72 percent of the measured reflectance variances, respectively; while bands 2 and 7 correlation were not significant (p less than .05). Finally, the generated reflectance images showed dramatic improvement in contrast, revealing textures that were not apparent in the original images. DOE

**N89-17981\*#** Wisconsin Univ., Madison. Space Science and Engineering Center.

**PROGRESS OF RESEARCH TO IDENTIFY ROTATING THUNDERSTORMS USING SATELLITE IMAGERY Final Report**  
CHARLES E. ANDERSON 1 Dec. 1988 5 p  
(Contract NAS8-36547)  
(NASA-CR-183555; NAS 1.26:183555) Avail: NTIS HC A02/MF A01 CSCL 04B

The possibility of detecting potentially tornadic thunderstorm cells from geosynchronous satellite imagery is determined. During the life of the contract, we examined eight tornado outbreak cases which had a total of 124 individual thunderstorm cells, 37 of which were tornadic. These 37 cells produced a total of 119 tornadoes. The outflow characteristics of all the cells were measured. Through the use of a 2-D flow field model, we were able to simulate the downstream development of an anvil cloud plume which was emitted by the storm updraft at or near the tropopause. We used two parameters to characterize the anvil plume behavior: its speed of downstream propagation (U max) and the clockwise deviation of the centerline of the anvil plume from the storm relative ambient wind at the anvil plume outflow level (MDA). U max was the maximum U-component of the anvil wind parameter required to successfully maintain an envelope of translating particles at the tip of the expanding anvil cloud. MDA was the measured deviation angle acquired from McIDAS, between the storm relative ambient wind direction and the storm relative anvil plume outflow direction; the latter being manipulated by controlling a tangential wind component to force the envelope of particles to maintain their position of surrounding the expanding outflow cloud. Author

**N89-18704#** European Space Agency, Paris (France).  
**THE 1988 INTERNATIONAL GEOSCIENCE AND REMOTE SENSING SYMPOSIUM (IGARSS 1988) ON REMOTE SENSING: MOVING TOWARDS THE 21ST CENTURY, VOLUME 3**

T. D. GUYENNE, ed. and J. J. HUNT, ed. Aug. 1988 641 p  
Symposium held in Edinburgh, United Kingdom, 12-16 Sep. 1988; sponsored by the Remote Sensing Society, the Geoscience and Remote Sensing Society, IEEE and IURS  
(ESA-SP-284-VOL-3; IEEE-88CH2497-6-VOL-3; ISSN-0379-6566; LC-87-83254; ETN-89-93244) Avail: NTIS HC A99/MF A01; ESA Publications Div., ESTEC, Noordwijk, Netherlands, \$120 US or 250 Dutch guilders

Speckle and noise effects in radar imagery; microwave remote sensing for agriculture; SAR oceanography; forestry; ocean color; winter marginal ice zone remote sensing; legal and commercial aspects of remote sensing; ground segments; image analysis and ship detection were some of the topics discussed at the symposium. Others included hydrology; radar land and atmosphere studies; backscatter measures of the sea surface; geophysics; sea ice; below ground sensing; the Earth Observing System; image processing; and infrared sounding of the atmosphere.

ESA

**N89-18751#** National Remote Sensing Centre, Farnborough (England).

**OPERATIONAL REMOTE SENSING IN THE UNITED KINGDOM: PROBLEMS OF IMAGE ACQUISITION**

C. A. LEGG *In* ESA, Proceedings of the 1988 International Geoscience and Remote Sensing Symposium (IGARSS) '88 on Remote Sensing: Moving Towards the 21st Century, Volume 3 p 1457-1461 Aug. 1988  
Avail: NTIS HC A99/MF A01; ESA Publications Division, ESTEC, Noordwijk, Netherlands, \$120 US or 250 Dutch guilders

A study of historical acquisition of cloud-free LANDSAT MSS imagery of Britain, based on quicklook prints, indicates that operational remote sensing applications requiring imagery within specific time intervals each year are impractical in the British climate. Numerous other applications with less stringent image acquisition requirements are shown to be practical with current sensor systems. The need for improvement in contextual classification procedures to make maximum use of available data is emphasized, and it is suggested that operational remote sensing

has a more urgent requirement for additional co-orbiting satellites of LANDSAT and SPOT spatial and spectral resolution than for new single satellites carrying more advanced sensors. ESA

**N89-18753#** Canada Centre for Remote Sensing, Ottawa (Ontario). Data Acquisition Div.  
**SATELLITE DATA ACQUISITION PLANNING AT THE CANADA CENTER FOR REMOTE SENSING**

T. LUKOWSKI *In* ESA, Proceedings of the 1988 International Geoscience and Remote Sensing Symposium (IGARSS) '88 on Remote Sensing: Moving Towards the 21st Century, Volume 3 p 1471-1474 Aug. 1988

Avail: NTIS HC A99/MF A01; ESA Publications Division, ESTEC, Noordwijk, Netherlands, \$120 US or 250 Dutch guilders

The Canada Centre for Remote Sensing (CCRS) receives satellite data at its ground stations in Prince Albert, Saskatchewan and Gatineau, Quebec. The Satellite Systems and Operations Section of CCRS is responsible for the operation of the ground stations and for ensuring that satellite imagery is provided to those users requesting data. To facilitate the handling of user requests for satellite data acquisition and to aid in optimal utilization of the available receiving equipment, a software system was developed. This program can accommodate current and future satellites and ground stations operated by CCRS for the reception of satellite imagery of North America. ESA

**N89-18754#** MacDonald, Dettwiler and Associates Ltd., Richmond (British Columbia).

**THE CENTRAL USER SERVICES SYSTEM FOR ERS-1**

P. WIDMER, M. FEA, and S. DELIA (European Space Agency, ESRIN, Frascati, Italy) *In* ESA, Proceedings of the 1988 International Geoscience and Remote Sensing Symposium (IGARSS) '88 on Remote Sensing: Moving Towards the 21st Century, Volume 3 p 1475-1479 Aug. 1988

Avail: NTIS HC A99/MF A01; ESA Publications Division, ESTEC, Noordwijk, Netherlands, \$120 US or 250 Dutch guilders

The Central User Services (CUS) system is part of the Earthnet ERS-1 Central Facility (EECF), which is the central node of the ERS-1 ground segment. The CUS assembles a variety of functions dedicated to providing a friendly interface between the ERS-1 system and its users. It includes an efficient, centralized set of functions catering to the user's needs. It is capable of translating those needs into system operation plans and has the functionality to implement and propagate those plans. The system includes an on-line worldwide ERS-1 data and products catalog; on-line acceptance of user requests for ERS-1 products; facilities for payload operation planning; and planning, control, and monitoring of ERS-1 ground stations. ESA

**N89-18755#** Earth Observation Sciences Ltd., Guildford (England). Surrey Technology Center.

**THE ALGORITHM DEVELOPMENT FACILITY: ITS ROLE IN THE DEVELOPMENT AND OPERATION OF A SATELLITE DATA CENTRE**

M. D. ELKINGTON, R. J. PROUD, and D. CLEDEN *In* ESA, Proceedings of the 1988 International Geoscience and Remote Sensing Symposium (IGARSS) '88 on Remote Sensing: Moving Towards the 21st Century, Volume 3 p 1481-1484 Aug. 1988  
Avail: NTIS HC A99/MF A01; ESA Publications Division, ESTEC, Noordwijk, Netherlands, \$120 US or 250 Dutch guilders

The development of the Earth Observation Data Center (EODC), and the interface between the scientific and commercial communities is discussed. The scientific community is largely responsible for the definition and development of product generation algorithms, while commercial organizations are implement the varied facilities that comprise a complete satellite data center. The algorithm Development Facility (ADF) aims to provide technical support to both the scientific and technological elements of the Data Center and perhaps more importantly, act as an interface between them. The ADF is described in terms of the overall design and concept of the facility; its role during the development of the EODC; its future role during the operational

phase of the EODC; and how it might be seen as a model for future satellite data centers. ESA

**N89-18757#** Jet Propulsion Lab., California Inst. of Tech., Pasadena.

**PLANS FOR THE DEVELOPMENT OF EOS SAR SYSTEMS USING THE ALASKA SAR FACILITY**

F. D. CARSEY and W. WEEKS (Alaska Univ., Fairbanks.) *In* ESA, Proceedings of the 1988 International Geoscience and Remote Sensing Symposium (IGARSS) '88 on Remote Sensing: Moving Towards the 21st Century, Volume 3 p 1491-1494 Aug. 1988

Avail: NTIS HC A99/MF A01; ESA Publications Division, ESTEC, Noordwijk, Netherlands, \$120 US or 250 Dutch guilders

The Alaska SAR Facility (ASF) program for the acquisition and processing of data from the ESA ERS-1, the NASDA ERS-1, and Radarsat and to carry out a program of science investigations using the data is introduced. Agreements for data acquisition and analysis are in place except for the agreement between NASA and Radarsat which is in negotiation. The ASF baseline system, consisting of the Receiving Ground System, the SAR Processor System and the Archive and Operations System, passed critical design review and is fully in implementation phase. Augments to the baseline system for systems to perform geophysical processing and for processing of J-ERS-1 optical data are in the design and implementation phase. The ASF provides a very effective vehicle with which to prepare for the Earth Observing System (EOS) in that it will aid the development of systems and technologies for handling the data volumes produced by the systems of the next decades, and it will also supply some of the data types that will be produced by EOS. ESA

**N89-18813#** Vexcell Corp., Boulder, CO.

**REQUIREMENTS FOR AN EOS-ORIENTED WORKSTATION**

W. KOBER, J. THOMAS, D. MEYER, F. LEBERL, and J. CIMINO (Jet Propulsion Lab., California Inst. of Tech., Pasadena.) *In* ESA, Proceedings of the 1988 International Geoscience and Remote Sensing Symposium (IGARSS) '88 on Remote Sensing: Moving Towards the 21st Century, Volume 3 p 1741-1747 Aug. 1988

Avail: NTIS HC A99/MF A01; ESA Publications Division, ESTEC, Noordwijk, Netherlands, \$120 US or 250 Dutch guilders

The determination of functional and performance requirements of a workstation specifically directed toward scientific users of the proposed NASA Earth Observing System information system is discussed. Image processing, user interface; data product visualization; and text processing are considered. ESA

**N89-18826#** Imperial Coll. of Science and Technology, London (England). Center for Remote Sensing.

**ARTEFACTS IN AIS-I IMAGERY**

C. CLARK, Y. C. ROBERTSON, and M. E. BARNETT *In* ESA, Proceedings of the 1988 International Geoscience and Remote Sensing Symposium (IGARSS) '88 on Remote Sensing: Moving Towards the 21st Century, Volume 3 p 1813-1814 Aug. 1988

Avail: NTIS HC A99/MF A01; ESA Publications Division, ESTEC, Noordwijk, Netherlands, \$120 US or 250 Dutch guilders

Horizontal striping in Airborne Image Spectrometer (AIS) imagery was investigated. The cause is identified as vibration of the detector array. Spatial and temporal statistics of this detector vibration are inferred from an AIS-I data set. Standard destriping algorithms can improve the appearance of the image data but do not restore its spectral resolution. ESA

**N89-18828#** Tokyo Univ. (Japan). Inst. of Industrial Science.

**AN ATMOSPHERIC CORRECTION METHOD FOR AVHRR INFRARED DATA USING HIRS/2 DATA**

Y. MINOWA, W. D. SUN, and M. TAKAGI *In* ESA, Proceedings of the 1988 International Geoscience and Remote Sensing Symposium (IGARSS) '88 on Remote Sensing: Moving Towards the 21st Century, Volume 3 p 1825-1826 Aug. 1988

Avail: NTIS HC A99/MF A01; ESA Publications Division, ESTEC, Noordwijk, Netherlands, \$120 US or 250 Dutch guilders

An atmospheric correction method for NOAA AVHRR infrared data using HIRS/2 data is proposed and the results of experiments are given. Experiments show that the average error is -0.026 C, standard deviation is 1.279 C and correlation is 0.972 for all points; and average error is -0.283 C, standard deviation is 0.449 C, correlation is 0.997 for selected points. For the research of the distribution of sea surface temperature (SST) and the monitoring of the ocean current, it is necessary to keep the average error less than 0.5 C, so this method satisfies it. The main remaining problems are the cloud removing method, skin and bulk SST estimation, and use of the water vapor channels for the atmospheric correction. ESA

**N89-18836#** European Space Agency, Paris (France).

**PROCEEDINGS OF THE 1988 INTERNATIONAL GEOSCIENCE AND REMOTE SENSING SYMPOSIUM (IGARSS) '88 ON REMOTE SENSING: MOVING TOWARDS THE 21ST CENTURY, VOLUME 2**

T. D. GUYENNE, ed. and J. J. HUNT, ed. Aug. 1988 606 p Symposium held in Edinburgh, United Kingdom, 12-16 Sep. 1988; sponsored by the Remote Sensing Society, the Geoscience and Remote Sensing Society, the Institute of Electrical and Electronics Engineers and the International Union of Radio Sciences (ESA-SP-284-VOL-2; IEEE-88CH2497-6-VOL-2; ISSN-0379-6566; LC-87-83254; ETN-89-93243) Avail: NTIS HC A99/MF A01; ESA Publications Div. ESTEC, Noordwijk, Netherlands, \$120 US or 250 Dutch guilders

Radar altimetry; microwave interaction with soils and vegetation, including trees; synthetic aperture radar processing, geocoding, and calibration; geology; HF radar measurement of winds, waves, and currents; sea ice; land sensing; ERS-1; pattern recognition and feature extraction; millimeter wave atmospheric sounding; radar altimetry; microwave backscatter and forests; marine and oceanographic remote sensing; the Winter Marginal Ice Zone Experiment; the ESA Earth observation program; and expert systems were discussed. ESA

**N89-18842#** Mullard Space Science Lab., Dorking (England).

**SATELLITE RADAR ALTIMETRY OVER ARID REGIONS**

M. A. J. GUZKOWSKA, C. G. RAPLEY, W. CUDLIP, and I. M. MASON *In* ESA, Proceedings of the 1988 International Geoscience and Remote Sensing Symposium (IGARSS) '88 on Remote Sensing: Moving Towards the 21st Century, Volume 2 p 659-662 Aug. 1988

Avail: NTIS HC A99/MF A01; ESA Publications Div. ESTEC, Noordwijk, Netherlands, \$120 US or 250 Dutch guilders

The response of the Seasat radar altimeter to a variety of arid surfaces in the Taklimakan Shamo in China was investigated. Comparisons with maps based on air photography and LANDSAT imagery demonstrate that the radar altimeter detects differences in surface morphology and provides topographic information complementary to the image data. ESA

**N89-18850#** GEC-Marconi Electronics Ltd., Chelmsford (England).

**NEW ARCHITECTURE FOR A REAL-TIME SAR PROCESSOR**

B. ARAMBEPOLA *In* ESA, Proceedings of the 1988 International Geoscience and Remote Sensing Symposium (IGARSS) '88 on Remote Sensing: Moving Towards the 21st Century, Volume 2 p 691-694 Aug. 1988

Avail: NTIS HC A99/MF A01; ESA Publications Div. ESTEC, Noordwijk, Netherlands, \$120 US or 250 Dutch guilders

A processor architecture for real-time SAR azimuth processing is presented. It consists of a linear or circular array of identical processing modules. Hardware design is simplified by having a regular array of modules with nearest neighbor connectivity. Architecture is expandable to meet a variety of swath width, resolution, and throughput requirements. There is no explicit corner-turning. Input and output are in range line order. Memory requirements are minimized. ESA

**N89-18851\*#** Jet Propulsion Lab., California Inst. of Tech., Pasadena.

**THE ALASKA SAR PROCESSOR**

R. E. CARANDE and B. CHARNY *In* ESA, Proceedings of the 1988 International Geoscience and Remote Sensing Symposium (IGARSS) '88 on Remote Sensing: Moving Towards the 21st Century, Volume 2 p 695-698 Aug. 1988  
 Avail: NTIS HC A99/MF A01; ESA Publications Div. ESTEC, Noordwijk, Netherlands, \$120 US or 250 Dutch guilders C SCL 171

The Alaska SAR processor was designed to process over 200 100 km x 100 km (Seasat like) frames per day from the raw SAR data, at a ground resolution of 30 m x 30 m from ERS-1, J-ERS-1, and Radarsat. The near real time processor is a set of custom hardware modules operating in a pipelined architecture, controlled by a general purpose computer. Input to the processor is provided from a high density digital cassette recording of the raw data stream as received by the ground station. A two pass processing is performed. During the first pass clutter-lock and auto-focus measurements are made. The second pass uses the results to accomplish final image formation which is recorded on a high density digital cassette. The processing algorithm uses fast correlation techniques for range and azimuth compression. Radiometric compensation, interpolation and deskewing is also performed by the processor. The standard product of the ASP is a high resolution four-look image, with a low resolution (100 to 200 m) many look image provided simultaneously. ESA

**N89-18853#** Marconi Space Systems Ltd., Portsmouth (England).

**IMPACT OF PHASE AND AMPLITUDE ERRORS ON THE ERS-1 ACTIVE MICROWAVE INSTRUMENTATION PERFORMANCE**

B. E. RICHARDS, G. A. WHITEHURST, and M. A. BROWN (GEC-Marconi Electronics Ltd., Chelmsford, England) *In* ESA, Proceedings of the 1988 International Geoscience and Remote Sensing Symposium (IGARSS) '88 on Remote Sensing: Moving Towards the 21st Century, Volume 2 p 703-705 Aug. 1988  
 Avail: NTIS HC A99/MF A01; ESA Publications Div. ESTEC, Noordwijk, Netherlands, \$120 US or 250 Dutch guilders

The effects of amplitude and phase errors were analyzed to show the effect on ERS-1 SAR and wind scatterometer (SCATT) performance. For the SAR, the errors affect the impulse response function, and engineering model test results produce performance compliant with all parameter requirements, except for the azimuth peak sidelobe ratio. For the SCATT, the effects on the radiometric stability and radiometric resolution were determined. Uncorrected, the HPA phase error effects can seriously degrade the stability performance. The effect on the radiometric resolution is only significant when the signal-to-noise ratio is low, otherwise the effect is negligible. ESA

**N89-18854#** Canada Centre for Remote Sensing, Ottawa (Ontario).

**TOWARDS A CALIBRATION OF THE CCRS AIRBORNE SARS**

A. L. GRAY, R. K. HAWKINS, C. E. LIVINGSTONE, J. CAMPBELL, E. ATTEMA, and J. C. MORIN (Groupement pour le Developpement de la Teledetection Aerospatiale, Toulouse, France) *In* ESA, Proceedings of the 1988 International Geoscience and Remote Sensing Symposium (IGARSS) '88 on Remote Sensing: Moving Towards the 21st Century, Volume 2 p 707-709 Aug. 1988  
 Avail: NTIS HC A99/MF A01; ESA Publications Div. ESTEC, Noordwijk, Netherlands, \$120 US or 250 Dutch guilders

A method whereby SAR system noise can be subtracted from image data to create an output linearly related to terrain backscatter is described. This is illustrated by the generation of a relative backscatter plot along one of the test lines used for the ESA Agriscatt campaign and flown by the CCRS C-SAR. Data from an array of 26 corner reflectors deployed at the Dutch Agriscatt site are also analyzed to check system response and to investigate methodology whereby known reflectors can be used to calibrate the CCRS SAR's. Results show that the CCRS SAR system

dynamic range and linearity are sufficient to proceed with system calibration using external point targets. ESA

**N89-18855#** Environmental Research Inst. of Michigan, Ann Arbor. Radar Science Lab.

**RADIOMETRIC CALIBRATION OF AIRBORNE SAR DATA**

E. S. KASISCHKE, D. R. SHEEN, and G. F. FOWLER (Michigan Univ., Ann Arbor.) *In* ESA, Proceedings of the 1988 International Geoscience and Remote Sensing Symposium (IGARSS) '88 on Remote Sensing: Moving Towards the 21st Century, Volume 2 p 711-714 Aug. 1988

Avail: NTIS HC A99/MF A01; ESA Publications Div. ESTEC, Noordwijk, Netherlands, \$120 US or 250 Dutch guilders

A model to estimate a relative error bound associated with radiometric calibration of the scattering coefficient derived from SAR data was developed. This error bound is based upon a statistical coefficient of variation error model. This error model was exercised to determine the expected error bounds for a multichannel, airborne SAR system. The expected error bounds were compared to the actual rms errors obtained during the initial calibration of this system, which shows that the actual errors are on the order of 0.7 dB and lower than the model predicted errors. ESA

**N89-18856#** Centre National d'Etudes Spatiales, Toulouse (France). Image Processing Div.

**PREPROCESSING OF THE VARAN SYNTHETIC APERTURE AIRBORNE RADAR**

D. MASSONNET *In* ESA, Proceedings of the 1988 International Geoscience and Remote Sensing Symposium (IGARSS) '88 on Remote Sensing: Moving Towards the 21st Century, Volume 2 p 715-720 Aug. 1988

Avail: NTIS HC A99/MF A01; ESA Publications Div. ESTEC, Noordwijk, Netherlands, \$120 US or 250 Dutch guilders

Preprocessing of VARAN airborne X-band SAR is described. The preprocessing achieves a standard resolution of 1.8 V/pulse repetition frequency, whatever accelerations are encountered. The speed V has to be understood as a pseudo-V. For example, if the instantaneous point of rotation of the plane is within the image, pseudo-V over this point is zero and will be negative for farther points. This does not prevent processing (correlation is replaced by convolution) but the achieved resolution is not very homogenous. The accuracy of VARAN S geometric processing is better than 100 m within an image. This is to be compared with the drift of the inertial navigation system (at most 2 nautical mph) taking into account that an image is made in an average 2 min. If the main cause of geometric unaccuracies is drift, the use of Global Positioning System will improve the geometry. ESA

**N89-18877#** Kanazawa Inst. of Tech. (Japan).

**SIGNATURE VARIATIONS DUE TO ATMOSPHERIC AND TOPOGRAPHIC EFFECTS ON SATELLITE MSS DATA OVER RUGGED TERRAIN**

T. KUSAKA, Y. KAWATA, H. EGAWA, and S. UENO *In* ESA, Proceedings of the 1988 International Geoscience and Remote Sensing Symposium (IGARSS) '88 on Remote Sensing: Moving Towards the 21st Century, Volume 2 p 825-828 Aug. 1988

Avail: NTIS HC A99/MF A01; ESA Publications Div. ESTEC, Noordwijk, Netherlands, \$120 US or 250 Dutch guilders

A model for the radiance applicable to remote sensing of mountainous terrain is described. The model includes the radiation arising from adjacent terrain outside the instantaneous field of view of the sensor. The atmosphere is treated as an optically thin, horizontally uniform slab layer bounded by a nonhomogeneous Lambertian surface. The results from the radiance equation show that the sky irradiance component on the target due to multiple reflections by adjacent terrain is of no significance. It is also shown that the path radiance reflected by the background is important in poorly illuminated regions. ESA



**N89-18884#** European Space Agency. European Space Research and Technology Center, ESTEC, Noordwijk (Netherlands).

**ERS-1 OPERATION CAPABILITIES**

J. LOUET *In its* Proceedings of the 1988 International Geoscience and Remote Sensing Symposium (IGARSS) '88 on Remote Sensing: Moving Towards the 21st Century, Volume 2 p 855-858 Aug. 1988

Avail: NTIS HC A99/MF A01; ESA Publications Div. ESTEC, Noordwijk, Netherlands, \$120 US or 250 Dutch guilders

Operation capabilities of the satellite in orbit, and the satellite operation scheme being prepared for using ERS-1 in a preoperational manner are described. Status of satellite design: available energy, instrument power demand, and operation constraints is summarized. Mission analysis results, using data obtained from the satellite engineering model, are presented to demonstrate the satellite capability to fulfil the global oceanic and ice mission in parallel with the SAR imaging regional mission.

ESA

**N89-18885#** European Space Agency. European Space Research and Technology Center, ESTEC, Noordwijk (Netherlands).

**ENGINEERING CALIBRATION OF THE ERS-1 ACTIVE MICROWAVE INSTRUMENTATION IN ORBIT**

E. ATTEMA *In its* Proceedings of the 1988 International Geoscience and Remote Sensing Symposium (IGARSS) '88 on Remote Sensing: Moving Towards the 21st Century, Volume 2 p 859-862 Aug. 1988

Avail: NTIS HC A99/MF A01; ESA Publications Div. ESTEC, Noordwijk, Netherlands, \$120 US or 250 Dutch guilders

The ESA baseline plan for radiometrical calibration of the output of the synthetic aperture radar and the scatterometer that constitute a sensor known as Active Microwave Instrument (AMI) onboard the ERS-1 satellite, is outlined. On the basis of a nonlinear, time-variant system model for the AMI, a composite strategy is described consisting a prelaunch instrument characterization and postlaunch instrument monitoring, using internal stimuli, as well as external reference targets.

ESA

**N89-18886#** Marconi Space Systems Ltd., Portsmouth (England).

**THE PRE-LAUNCH PERFORMANCE VERIFICATION OF THE ERS-1 ACTIVE MICROWAVE INSTRUMENTATION**

R. STUNT and D. J. Q. CARTER *In* ESA, Proceedings of the 1988 International Geoscience and Remote Sensing Symposium (IGARSS) '88 on Remote Sensing: Moving Towards the 21st Century, Volume 2 p 863-864 Aug. 1988

Avail: NTIS HC A99/MF A01; ESA Publications Div. ESTEC, Noordwijk, Netherlands, \$120 US or 250 Dutch guilders

The test philosophy, methods, and equipment employed for the prelaunch verification of the ERS-1 scatterometer/SAR instruments are described.

ESA

**N89-18887#** Marconi Space Systems Ltd., Portsmouth (England).

**A SOFTWARE PACKAGE FOR PERFORMANCE EVALUATION OF THE ERS-1 AMI**

S. J. AUSTIN and D. J. Q. CARTER *In* ESA, Proceedings of the 1988 International Geoscience and Remote Sensing Symposium (IGARSS) '88 on Remote Sensing: Moving Towards the 21st Century, Volume 2 p 865-866 Aug. 1988

Avail: NTIS HC A99/MF A01; ESA Publications Div. ESTEC, Noordwijk, Netherlands, \$120 US or 250 Dutch guilders

A software package consisting of performance modeling software and performance modeling data base and control software was developed for ERS-1. It provides a facility which can be maintained through all the stages of the Active Microwave Instrument on-ground verification process. Performance predictions of engineering parameters can be made from technical parameters with the minimum amount of user knowledge and time, with clear and concise outputs designed to ensure easy inspection of results.

ESA

**N89-18888#** Marconi Space Systems Ltd., Portsmouth (England).

**ERS-1 ACTIVE MICROWAVE INSTRUMENTATION ENGINEERING MODEL PERFORMANCE**

D. J. Q. CARTER and S. HARTLEY *In* ESA, Proceedings of the 1988 International Geoscience and Remote Sensing Symposium (IGARSS) '88 on Remote Sensing: Moving Towards the 21st Century, Volume 2 p 867-870 Aug. 1988

Avail: NTIS HC A99/MF A01; ESA Publications Div. ESTEC, Noordwijk, Netherlands, \$120 US or 250 Dutch guilders

The ERS-1 Active Microwave Instrumentation (AMI) requirements and verification; significant distortions, including calibration pulse stability, digitization errors, and phase and amplitude errors; and performance are described. The AMI consists of a scatterometer and a SAR, whose engineering and technical parameters are presented.

ESA

**N89-18889#** Marconi Space Systems Ltd., Portsmouth (England).

**STABILITY CONSIDERATIONS FOR THE ERS-1 WIND SCATTEROMETER RADIOMETRIC PERFORMANCE**

D. J. Q. CARTER *In* ESA, Proceedings of the 1988 International Geoscience and Remote Sensing Symposium (IGARSS) '88 on Remote Sensing: Moving Towards the 21st Century, Volume 2 p 871-872 Aug. 1988

Avail: NTIS HC A99/MF A01; ESA Publications Div. ESTEC, Noordwijk, Netherlands, \$120 US or 250 Dutch guilders

Radiometric stability of the ERS-1 wind scatterometer is discussed. Instability sources and compensation techniques are summarized. The temperature and time characteristics of the identified contributors to instability are extremely complex and so a set of simplifying assumptions was determined in order to define the method by which all the contributions are combined. Where variations have the same prime origin they are linearly added; those that are driven primarily by independent factors are combined by the method of root sum of squares. Of the parameters that influence scatterometer stability, three vary with swath position: antenna gain variation, elevation pattern maximum gain slope, and pointing error induced frequency offsets.

ESA

**N89-18890#** Marconi Space Systems Ltd., Portsmouth (England).

**ERS-1 AMI ANTENNAS: THE DESIGN AND DEVELOPMENT EXPERIENCE**

W. E. HARDY *In* ESA, Proceedings of the 1988 International Geoscience and Remote Sensing Symposium (IGARSS) '88 on Remote Sensing: Moving Towards the 21st Century, Volume 2 p 873-876 Aug. 1988

Avail: NTIS HC A99/MF A01; ESA Publications Div. ESTEC, Noordwijk, Netherlands, \$120 US or 250 Dutch guilders

The evolution of ERS-1 antenna specifications from overall instrument and mission constraints is outlined. Design solution development, technological, and verification aspects are reviewed. The antennas are of slotted waveguide array type, with aluminum waveguides for the wind scatterometer, and carbon fiber for the SAR antenna.

ESA

**N89-18891#** European Space Agency. European Space Research and Technology Center, ESTEC, Noordwijk (Netherlands).

**ERS-1 ALTIMETER HEIGHT CALIBRATION**

C. R. FRANCIS and B. DUESMANN *In its* Proceedings of the 1988 International Geoscience and Remote Sensing Symposium (IGARSS) '88 on Remote Sensing: Moving Towards the 21st Century, Volume 2 p 877-880 Aug. 1988

Avail: NTIS HC A99/MF A01; ESA Publications Div. ESTEC, Noordwijk, Netherlands, \$120 US or 250 Dutch guilders

The height calibration of the ERS-1 altimeter using an overpass of an instrumented reference point at a coastal site is described. This overpass will be tracked by a network of lasers and by the PRARE system, which allows high precision in the satellite position in the local reference frame of these tracking systems. Water surface and environmental measurements will be made at the



reference point, which is a research tower in the northern Adriatic Sea. The error budget for this approach was analyzed, including geometrical, instrumental and media effects, and shows that an uncertainty of 5 cm will remain in the determination of the altimeter bias. ESA

**N89-18892#** European Space Agency. European Space Research and Technology Center, ESTEC, Noordwijk (Netherlands).

**QUALITY CONTROL OF FAST DELIVERY PROCESSORS AND PRODUCTS**

J. P. GUIGNARD *In its* Proceedings of the 1988 International Geoscience and Remote Sensing Symposium (IGARSS) '88 on Remote Sensing: Moving Towards the 21st Century, Volume 2 p 881-884 Aug. 1988

Avail: NTIS HC A99/MF A01; ESA Publications Div. ESTEC, Noordwijk, Netherlands, \$120 US or 250 Dutch guilders

Performance of the ERS-1 SAR fast delivery processor is described. The quality control of the scatterometer processor is outlined. The fast delivery processor processes images in 27 min in an operational environment, while maintaining high image quality. ESA

**N89-18893#** GEC-Marconi Electronics Ltd., Chelmsford (England).

**A SAR DATA QUALITY ASSESSMENT SCHEME FOR THE ERS-1 MISSION**

L. M. J. BROWN, D. J. SMITH, and M. DOHERTY (European Space Agency. ESRIN, Frascati, Italy) *In* ESA, Proceedings of the 1988 International Geoscience and Remote Sensing Symposium (IGARSS) '88 on Remote Sensing: Moving Towards the 21st Century, Volume 2 p 887-888 Aug. 1988 (Contract ESA-6635/86-HGE-1)

Avail: NTIS HC A99/MF A01; ESA Publications Div. ESTEC, Noordwijk, Netherlands, \$120 US or 250 Dutch guilders

An end-to-end synthetic aperture radar (SAR) data quality assessment scheme which forms the basis for a detailed system design for the Earthnet ERS-1 Central Facility and is a useful guideline for those Processing and Archiving Facilities which will generate and distribute ERS-1 SAR imagery is outlined. The scheme operates by performing routine measurements of a comprehensive set of SAR performance parameters, characterizing the properties of the raw data, complex image data, and final image products generated during the mission. The measured parameter values are checked routinely against specified performance criteria, thus allowing routine verification of the data quality and enabling any degradations in instrument performance to be detected and, where possible, rectified. ESA

**N89-18905\*#** National Aeronautics and Space Administration. Goddard Space Flight Center, Greenbelt, MD.

**RETRIEVAL OF WATER VAPOR PROFILES FROM MICROWAVE RADIOMETRIC MEASUREMENTS AT 183 AND 92 GHZ**

J. R. WANG, T. T. WILHEIT, L. A. CHANG, and B. M. KRUPP (Science Applications Research, Lanham, MD.) *In* ESA, Proceedings of the 1988 International Geoscience and Remote Sensing Symposium (IGARSS) '88 on Remote Sensing: Moving Towards the 21st Century, Volume 2 p 945-948 Aug. 1988

Avail: NTIS HC A99/MF A01; ESA Publications Div. ESTEC, Noordwijk, Netherlands, \$120 US or 250 Dutch guilders CSCL 04A

Microwave radiometric measurements made from an aircraft altitude of 20 km at 183.3 + or - 2, 183.3 + or - 5, and 183.3 + or - GHz, and at 92 GHz were used to retrieve the atmospheric water vapor profiles. Retrieval techniques shown to function properly in cloudfree conditions, were improved and extended to profile water vapor under moderate cloud cover conditions. The retrieved water vapor profiles compare favorably with those of rawinsonde observations at times nearly concurrent with the radiometric measurements. ESA

**N89-18906#** Chalmers Univ. of Technology, Goeteborg (Sweden).

**ATMOSPHERIC ATTENUATION AS DERIVED FROM MICROWAVE RADIOMETRY AT 52.8 GHZ**

J. ASKNE and E. WINBURG *In* ESA, Proceedings of the 1988 International Geoscience and Remote Sensing Symposium (IGARSS) '88 on Remote Sensing: Moving Towards the 21st Century, Volume 2 p 949-950 Aug. 1988 Sponsored in part by the Swedish Board for Space Activities, Solna  
Avail: NTIS HC A99/MF A01; ESA Publications Div. ESTEC, Noordwijk, Netherlands, \$120 US or 250 Dutch guilders

A microwave radiometer at 52.8 to 58.8 GHz was used to observe atmospheric brightness temperature together with simultaneous radiosonde observations. The measurements can be used to provide constraints on models of atmospheric attenuation especially the model dependence of the precipitable water vapor. A difference between models and observations is found. This difference can indicate another frequency dependence of the continuum term than that assumed. However other possible effects exist as well. It is important to do further observations by microwave radiometry at several frequencies to resolve the obtained difference. ESA

**N89-18908#** Jet Propulsion Lab., California Inst. of Tech., Pasadena.

**ATMOSPHERIC PROFILING OF WATER VAPOUR WITH A 20.5-23.5 GHZ AUTOCORRELATION RADIOMETER**

C. S. RUFF and C. T. SWIFT (Massachusetts Univ., Amherst.) *In* ESA, Proceedings of the 1988 International Geoscience and Remote Sensing Symposium (IGARSS) '88 on Remote Sensing: Moving Towards the 21st Century, Volume 2 p 957-960 Aug. 1988

Avail: NTIS HC A99/MF A01; ESA Publications Div. ESTEC, Noordwijk, Netherlands, \$120 US or 250 Dutch guilders

A tropospheric water vapor profiling system is presented. The hardware consists of an upward looking radiometer (CORRAD) deployed at ground level. The CORRAD measures the autocorrelation of the downwelling thermal emission from the atmosphere over a passband of 20.5 to 23.5 GHz out to a maximum time delay of 6.1 ns. This produces 100 MHz resolution imaging of the complete emission spectrum about the 22.235 GHz water vapor resonance line. The 31 equivalent frequency channels produced by Fourier transformation of the data provide additional constraints on the inversion process required to estimate the water vapor profile, as compared to standard 2 to 5 frequency channel profiling systems. The CORRAD hardware is described, and radiometer and radiosonde profiles are compared. ESA

**N89-18911#** Rome Univ. (Italy). INFOCOM Dept.

**TRACKING ALGORITHMS IN RADAR ALTIMETRY**

T. BUCCIARELLI, S. CACOPARDI, G. PICARDI, R. SEU, G. LEVRINI, and R. PERFETTI (Fondazione Ugo Bordoni, Rome, Italy) *In* ESA, Proceedings of the 1988 International Geoscience and Remote Sensing Symposium (IGARSS) '88 on Remote Sensing: Moving Towards the 21st Century, Volume 2 p 973-976 Aug. 1988

Avail: NTIS HC A99/MF A01; ESA Publications Div. ESTEC, Noordwijk, Netherlands, \$120 US or 250 Dutch guilders

In order to extend radar altimeter operations over surfaces different from ocean, tracking algorithms able to maintain range tracking in environments such as sea ice, land, and the transitions between them were studied. Range discriminators suitable for robust range tracking are analyzed and compared from the point of view of linearity, sensitivity, and processing load. The term robust is intended in the sense of good performance in lock maintenance for the typical echo waveforms in the described scenarios. A tradeoff seems to be necessary between a wide linear dynamic range, for locking, and the complexity of the algorithm from the point of view of processing load. Noise power mean level must be removed before applying the algorithm to obtain satisfactory results with all kinds of discriminators analyzed. A digital chirp generator is likely to be used to control resolution while changing the received waveform. ESA

**N89-18913#** University Coll., London (England). Dept. of Electronic and Electrical Engineering.

**A SYNTHETIC APERTURE ALTIMETER**

B. PURSEYED and H. D. GRIFFITHS *In* ESA, Proceedings of the 1988 International Geoscience and Remote Sensing Symposium (IGARSS) '88 on Remote Sensing: Moving Towards the 21st Century, Volume 2 p 981-982 Aug. 1988 (Contract ESA-7088/87-NL-JG(SC); NATO-0209/87)

Avail: NTIS HC A99/MF A01; ESA Publications Div. ESTEC, Noordwijk, Netherlands, \$120 US or 250 Dutch guilders

The application of synthetic aperture processing to provide high spatial resolution from radar altimeters was studied. The requirements are reviewed, and signal processing is considered. Ideas for an aircraft-borne system to demonstrate the concept and provide design information for future instruments are presented. ESA

**N89-18914#** University Coll., London (England). Dept. of Electronic Engineering.

**A NEW APPROACH TO TOPOGRAPHIC ALTIMETRY**

D. J. WINGHAM and C. G. RAPLEY (Mullard Space Science Lab., Dorking, England) *In* ESA, Proceedings of the 1988 International Geoscience and Remote Sensing Symposium (IGARSS) '88 on Remote Sensing: Moving Towards the 21st Century, Volume 2 p 985-988 Aug. 1988

Avail: NTIS HC A99/MF A01; ESA Publications Div. ESTEC, Noordwijk, Netherlands, \$120 US or 250 Dutch guilders

A technique for surveying the Earth's topographic elevation from satellites with a pulse-limited altimeter was investigated. The technique is based on a data processing scheme that permits the formation of synthetic resolution from power detected radar echoes from incoherent targets. The method is examined theoretically and it is shown that the technique is practicable for the surface geometries examined. Limitations imposed by the nature of normal incidence backscatter are discussed and key areas needing further work are identified. ESA

**N89-18921\*#** Jet Propulsion Lab., California Inst. of Tech., Pasadena.

**OVERVIEW OF THE SHUTTLE IMAGING RADAR (SIR-C)**

D. EVANS and C. ELACHI *In* ESA, Proceedings of the 1988 International Geoscience and Remote Sensing Symposium (IGARSS) '88 on Remote Sensing: Moving Towards the 21st Century, Volume 2 p 1015-1017 Aug. 1988 (Contract NAS7-100)

Avail: NTIS HC A99/MF A01; ESA Publications Div. ESTEC, Noordwijk, Netherlands, \$120 US or 250 Dutch guilders CSCL 171

The Shuttle Imaging Radar-C (SIR-C) experiment will provide increased capability over Seasat and the two previous Shuttle Imaging Radars by acquiring digital images simultaneously at two microwave frequencies (L- and C-band) with multiple signal polarizations (HH, VV, HV, VH). The SIR-C is a dual bandwidth system so that investigators can choose a high or low resolution mode (20 and 10 MHz, respectively). An X-band SAR with VV polarization will be flown with SIR-C, resulting in a three-frequency capability. The SIR-C prototype data will be acquired using an airborne imaging radar to test designs that will be implemented on SIR-C, to develop the overall calibration strategy for SIR-C, and to develop data analysis tools for SIR-C data. ESA

**N89-18923#** Dornier-Werke G.m.b.H., Friedrichshafen (Germany, F.R.).

**X-SAR: A NEW SPACEBORNE SYNTHETIC APERTURE RADAR**

E. H. VELTEN *In* ESA, Proceedings of the 1988 International Geoscience and Remote Sensing Symposium (IGARSS) '88 on Remote Sensing: Moving Towards the 21st Century, Volume 2 p 1021-1024 Aug. 1988

Avail: NTIS HC A99/MF A01; ESA Publications Div. ESTEC, Noordwijk, Netherlands, \$120 US or 250 Dutch guilders

The X-synthetic aperture radar (SAR) instrument design is described, including mechanical and electrical layout, operation

modes, and interfaces to Shuttle and SIR-C, as well as major design parameters of the subsystems. The configuration of the ground segment is illustrated. The X-SAR design is determined by the selection of the resonant slotted waveguide CRFP antenna working at a center frequency of 9.6 GHz and the high power amplifier using a 3 kW traveling wave tube. The radio frequency electronics comprises the frequency and chirp generation, up- and down-conversion, and filtering. The digital instrument control and data handling electronics provides high speed A/D conversion with selectable bandwidth, buffering, and conversion to serial format for onboard storage on tape or direct transmission to ground. The X-SAR includes an onboard calibration system with two different loops. ESA

**N89-18924#** Deutsche Forschungs- und Versuchsanstalt fuer Luft- und Raumfahrt, Wesseling (Germany, F.R.). Inst. for Radiofrequency Technology.

**E-SAR: THE EXPERIMENTAL AIRBORNE L/C-BAND SAR SYSTEM OF DFVLR**

R. HORN *In* ESA, Proceedings of the 1988 International Geoscience and Remote Sensing Symposium (IGARSS) '88 on Remote Sensing: Moving Towards the 21st Century, Volume 2 p 1025-1026 Aug. 1988

Avail: NTIS HC A99/MF A01; ESA Publications Div. ESTEC, Noordwijk, Netherlands, \$120 US or 250 Dutch guilders

The E-SAR system was developed to study the SAR method and its problems, such as motion error correction and overall system calibration. The sensor is designed to operate on board DO 228 aircraft in either L- or C-band. The system features stripline active array antennas, built in test equipment for system calibration, real time motion error correction, and quicklook data processing. ESA

**N89-18925#** Spar Aerospace Ltd., Ste-Anne-de-Bellevue (Quebec).

**TAKING A BROADER VIEW: RADARSAT ADDS SCANSAR TO ITS OPERATIONS**

A. P. LUSCOMBE *In* ESA, Proceedings of the 1988 International Geoscience and Remote Sensing Symposium (IGARSS) '88 on Remote Sensing: Moving Towards the 21st Century, Volume 2 p 1027-1032 Aug. 1988 Sponsored in part by the Canadian government

Avail: NTIS HC A99/MF A01; ESA Publications Div. ESTEC, Noordwijk, Netherlands, \$120 US or 250 Dutch guilders

ScanSAR operations were added to Radarsat SAR capabilities to enable very wide swaths to be imaged. The principle of ScanSAR is outlined and the criteria used in defining the operations are explained. The major implications of ScanSAR for the SAR system, in the instrument on-board the satellite and in the processor on the ground, are identified. The definition of 2 standard forms of ScanSAR operation, providing coverage respectively of swaths of over 300 and 500 km, is described. These swath widths compare with the maximum of 150 km previously available with Radarsat using conventional SAR imaging. The ScanSAR operations are not restricted to these two standard forms, however; the SAR can also image with a variety of other combinations of beams on command from the ground. ESA

**N89-18926#** GEC-Marconi Electronics Ltd., Chelmsford (England).

**ADVANCED SAR CONCEPTS**

M. A. BROWN and F. G. SAWYER (Marconi Space Systems Ltd., Portsmouth, England) *In* ESA, Proceedings of the 1988 International Geoscience and Remote Sensing Symposium (IGARSS) '88 on Remote Sensing: Moving Towards the 21st Century, Volume 2 p 1035-1036 Aug. 1988 Sponsored in part by ESA

Avail: NTIS HC A99/MF A01; ESA Publications Div. ESTEC, Noordwijk, Netherlands, \$120 US or 250 Dutch guilders

A flexible SAR design capable of reconfiguration into different operating modes, offering both wide swath coverage (500 km, 15 to 50 deg incidence), and high resolution (10m spatial) coverage is considered. System concepts capable of achieving the various

modes of operation are discussed, compared, and contrasted with regard to their salient features. An overall system selection is presented with the major SAR design features necessary being identified. It is important to be able to switch the beams both in ScanSAR mode and between ScanSAR and high resolution, narrow swath modes. However, the tradeoff between antenna area and transmitter power is only possible with a distributed amplifier design, which allows the power to be controlled, and adjusted to satisfy the design requirements. The ability to change the transmitted signal bandwidth allows a continuous tradeoff between spatial resolution and data bandwidth necessary for any required swath width. Flexibility is achieved using a digital chirp generator with, if required, variable bandwidth correlator. The design is estimated to weigh less than 600 kg and consume less than 2 kW of dc power, i.e., compatible with the ESA polar platform. ESA

**N89-18928#** Technical Univ. of Denmark, Lyngby. Inst. of Electromagnetics.

**THE TECHNICAL UNIVERSITY OF DENMARK (TUD) C-BAND SAR**

N. SKOU, S. N. MADSEN, and E. L. CHRISTENSEN *In* ESA, Proceedings of the 1988 International Geoscience and Remote Sensing Symposium (IGARSS) '88 on Remote Sensing: Moving Towards the 21st Century, Volume 2 p 1039-1040 Aug. 1988  
 Avail: NTIS HC A99/MF A01; ESA Publications Div. ESTEC, Noordwijk, Netherlands, \$120 US or 250 Dutch guilders

A C-band high resolution airborne SAR is described. The radar uses digital pulse generation with a bandwidth beyond 100 MHz. This ensures large flexibility and a possibility to use predistorted codes to account for a nonperfect transfer function of the modulator and the up-converter. Pulse compression is also performed digitally. The radar data is preprocessed and dumped to a high density digital tape recorder, for processing on off-line computers. A real-time processor and a display facility to be carried with the radar in the aircraft is planned. The calibration fidelity of the radar was stressed. The analog parts of the radar are temperature stabilized, and several calibration loops are incorporated in the system. ESA

**N89-18952#** European Space Agency. European Space Research and Technology Center, ESTEC, Noordwijk (Netherlands).

**MISSION ASPECTS OF A FUTURE EUROPEAN POLAR ORBIT EARTH OBSERVATION FACILITY**

M. RAST and M. MOREL *In its* Proceedings of the 1988 International Geoscience and Remote Sensing Symposium (IGARSS) '88 on Remote Sensing: Moving Towards the 21st Century, Volume 2 p 1151-1155 Aug. 1988  
 Avail: NTIS HC A99/MF A01; ESA Publications Div. ESTEC, Noordwijk, Netherlands, \$120 US or 250 Dutch guilders

The ESA Earth Observation Facility possible payload and mission configurations for a polar orbiting platform to be launched in the late nineties are discussed. Possible mission scenarios and the related application objectives are outlined. The main objectives for these configurations are the continuation of operational meteorological data acquisition and the exploitation of new remote sensing techniques. User requirements and the data service are considered. ESA

**N89-18954#** Selenia Spazio S.p.A., Rome (Italy).  
**THE ADVANCED TERRAIN TRACKING ALTIMETER INSTRUMENT**

G. LEVRINI *In* ESA, Proceedings of the 1988 International Geoscience and Remote Sensing Symposium (IGARSS) '88 on Remote Sensing: Moving Towards the 21st Century, Volume 2 p 1163-1166 Aug. 1988  
 Avail: NTIS HC A99/MF A01; ESA Publications Div. ESTEC, Noordwijk, Netherlands, \$120 US or 250 Dutch guilders

The Advanced Terrain Tracking Altimeter instrument for ESA's Earth Observation Preparatory Program is described. It is designed as a multimode adaptive instrument able to ensure full coverage of the Earth's surface, including land regions. Over oceans it is characterized by an accuracy better than 5 cm, including the

correction of errors due to the ionosphere and to the troposphere. Both these corrections are performed by the instruments itself, without the need of any additional data from external sources. This marks a difference with a past approach (with respect to ERS-1, for instance) and enables to optimize the quality of the auxiliary data for altimeter measurement purposes. The adaptivity of the resolution over the different surfaces is ensured by a digital chirp generator. ESA

**N89-18958#** University Coll., London (England). Dept. of Photogrammetry and Surveying.

**REAL-TIME STEREO MATCHING SPOT USING TRANSPUTER ARRAYS**

J.-P. MULLER, G. P. OTTO, T. K. W. CHAU, K. A. COLLINS, N. DALTON, T. DAY, I. J. DOWMAN, M. J. JACKSON (Laser-Scan Labs. Ltd., Cambridge, England), M. A. ONEILL, V. PARAMANANDA et al. *In* ESA, Proceedings of the 1988 International Geoscience and Remote Sensing Symposium (IGARSS) '88 on Remote Sensing: Moving Towards the 21st Century, Volume 2 p 1185-1186 Aug. 1988 Prepared in cooperation with Royal Signals and Radar Establishment, Malvern, United Kingdom  
 Avail: NTIS HC A99/MF A01; ESA Publications Div. ESTEC, Noordwijk, Netherlands, \$120 US or 250 Dutch guilders

An accurate (rms less than 10 m) automated stereo matching system for SPOT image data was developed. It permits digital elevation models to be derived at very high sampling density (over 50 m) directly from level 1A data without geocoding or resampling. Results illustrating the accuracy, reliability, and sampling density of the stereo matcher are shown using statistical and dynamic visualization techniques. A 22 (T414) transputer array was used to test architecture issues of real-time performance. Timings on transputer arrays and distributed Sun-3 workstations are shown. The complete system is being implemented on a 32 (T800-4MB) PARSYS supercomputer. ESA

**N89-18960#** Edinburgh Univ. (Scotland). Dept. of Meteorology.  
**TEXTURAL AND SPECTRAL FEATURES AS AN AID TO CLOUD CLASSIFICATION**

ZHIQIANG GU and C. DUNCAN *In* ESA, Proceedings of the 1988 International Geoscience and Remote Sensing Symposium (IGARSS) '88 on Remote Sensing: Moving Towards the 21st Century, Volume 2 p 1193-1194 Aug. 1988  
 Avail: NTIS HC A99/MF A01; ESA Publications Div. ESTEC, Noordwijk, Netherlands, \$120 US or 250 Dutch guilders

Textural features are studied to determine their discriminating power across a number of cloud classes including those previously found difficult to separate. Although several features in the spatial frequency domain are tested they are found to be less useful than those in the spatial domain with only one exception. ESA

**N89-18964#** Purdue Univ., West Lafayette, IN. Lab. for Applications of Remote Sensing.

**SIMULATION OF OPTICAL REMOTE SENSING SYSTEMS FOR EARTH RESOURCE ANALYSIS**

J. P. KERESKES and D. A. LANDGREBE *In* ESA, Proceedings of the 1988 International Geoscience and Remote Sensing Symposium (IGARSS) '88 on Remote Sensing: Moving Towards the 21st Century, Volume 2 p 1211-1214 Aug. 1988 (Contract NSF ECS-85-07405)

Avail: NTIS HC A99/MF A01; ESA Publications Div. ESTEC, Noordwijk, Netherlands, \$120 US or 250 Dutch guilders

A model for the simulation of remote sensing systems is presented. The system is seen to be divided into three parts: the scene, the sensor, and the processing algorithms. Models for these component systems are presented. Results of the simulation for various scene and sensor configurations are included. ESA

**N89-19039** Nagoya Univ. (Japan). Water Research Inst.  
**STRUCTURE OF LAYER CLOUDS AS OBSERVED SIMULTANEOUSLY BY A MICROWAVE RADIOMETER AND AN 8.6 MM-RADAR**

GUOSHENG LIU and TAKAO TAKEDA *In* Deutscher Wetterdienst,

Annals from the German Meteorological Society. No. 25: 10th International Cloud Physics Conference Preprints, Volume 2 p 541-543 1988

Avail: Deutscher Wetterdienst, Frankfurter Strasse 135, D-6050 Offenbach am Main, Fed. Republic of Germany

Middle-level layer clouds associated with subtropical cyclones near Japan were observed in spring simultaneously by a microwave radiometer and an 8.6 mm radar. Observational results are analyzed, especially glaciation degree, which is defined by the ratio of ice-water amount to the sum of liquid-water and ice-water amounts. Results show that a middle-level cloud can not efficiently produce solid precipitation even though it forms by a strong updraft, unless an upper-level cloud supplies sufficient amount of ice particles to it. ESA

**N89-19079** Colorado State Univ., Fort Collins. Dept. of Atmospheric Science.

**COMPARISONS OF SATELLITE DATA SURFACE-BASED REMOTE SENSING MEASUREMENTS IN UTAH WINTER OROGRAPHIC STORMS**

DAVID C. ROGERS, KENNETH SASSEN, and GREGORY C. DODD (Utah Univ., Salt Lake City.) *In* Deutscher Wetterdienst, Annals from the German Meteorological Society. No. 25: 10th International Cloud Physics Conference Preprints, Volume 2 p 659-661 1988 Sponsored in cooperation with the Utah Div. of Water Resources and NOAA

Avail: Deutscher Wetterdienst, Frankfurter Strasse 135, D-6050 Offenbach am Main, Fed. Republic of Germany

Remote sensing data obtained during a winter storm episode are presented. Structure, composition, and evolution of cloud features as observed by different techniques are compared. Differences in estimates of cloud top temperature are consistent with plausible physical causes, such as cirrus clouds contaminating GOES CTT measurements. The particular advantage of satellite data is the potential to examine orographic cloud top characteristics over large mountainous regions which do not have the benefit of surface-based instrumentation. Additional case study research is needed to clarify the interpretation of these kinds of data and improve their diagnostic capability. The results confirm that, in orographic storms, the radiometric liquid water depends strongly on local terrain and on active ice precipitation processes. Small scale maxima were identified in the liquid water field. ESA

**N89-19475#** Massachusetts Univ., Amherst.  
**NORMALIZED RADAR CROSS SECTION OF NATURAL SURFACES AT MILLIMETER WAVELENGTHS Final Report, 22 - 23 Sep. 1985**

ROBERT E. MCINTOSH Nov. 1988 11 p  
(Contract DAAG29-85-K-0227)  
(AD-A202252; ARO-22851.1-GS) Avail: NTIS HC A03/MF A01 CSCL 171

The scattering of millimeter waves by foliated and snow-covered surfaces is of interest to designers of future radar and communication systems. It is also of interest to the remote sensing community, which is interested in the high-frequency behavior of radar signatures of natural surfaces. The University of Massachusetts Microwave Remote Sensing Laboratory developed a unique high-powered 215 GHz radar system. It used this system to measure the Normalized Radar Cross Section (NRCS) of trees and snow packs. Results of these studies are described in this report. GRA

**N89-19483#** University Coll., London (England). Dept. of Electronic and Electrical Engineering.

**A STUDY OF ADVANCED RADAR ALTIMETER TECHNIQUES Final Report**

H. D. GRIFFITHS and B. PURSEYED Paris, France ESA  
Jan. 1988 166 p  
(Contract ESA-7088/87-NL-JG(SC))  
(ESA-CR(P)-2699; ETN-89-93940) Avail: NTIS HC A08/MF A01

The use of synthetic aperture processing to provide a narrow antenna beamwidth and hence high spatial resolution, and the use of multiple off-nadir beams to provide swath coverage rather

than just a single nadir-pointing altimeter beam were studied. It is demonstrated that synthetic aperture processing is compatible with the full-deramp pulse compression method conventionally employed on altimeters. Calculations indicate that a considerable amount of processing power is required for the aperture synthesis operation, and that this would be better carried out off-line on the ground. Transmit power requirements are modest, and likely to be compatible with the use of solid-state transmitters. An aircraft-borne proof-of-concept instrument which could be built and flown at a very low cost is proposed. A computer simulation to model the altimeter returns and extract the elevation and surface roughness information was developed. It is shown that surface elevation can be recovered to a similar precision to that achieved by the Seasat altimeter, but that proper recovery of significant waveheight from off-nadir beams needs an impractically-large antenna system. ESA

**N89-19717** National Center for Atmospheric Research, Boulder, CO.

**APPLICATIONS OF THE NCAR ELECTRA DOPPLER RADAR FOR THE STUDY OF PHYSICAL PARAMETERS OF CLOUDS**  
CRAIG WALTHER, CHARLES FRUSH, and PETER HILDEBRAND *In* Deutscher Wetterdienst, Annals from the German Meteorological Society, No. 25: 10th International Cloud Physics Conference Preprints, Volume 1 p 335-337 1988

Avail: Deutscher Wetterdienst, Frankfurter Strasse 135, D-6050 Offenbach am Main, Fed. Republic of Germany

An airborne Doppler X-band radar to be mounted in the tail of a Lockheed Electra (ELDORA) is presented. The ELDORA is designed with a primary emphasis on the study of storm and mesoscale weather phenomena. However, the radar will also be very useful for the study of cloud physical parameters. Because the aircraft can be positioned close to the area of interest, reasonably fine scale data can be taken in a very short length of time. Since these types of measurements are not available, there is much to be learned even with the moderately coarse resolution of the ELDORA. The use of a larger, vertically pointing antenna will further enhance the ability of the ELDORA to measure these properties. Once this effort is completed, the information obtained will greatly enhance the cloud physics community's ability to determine what specific properties of airborne radar are necessary to measure their phenomena of interest. ESA

**N89-19729\*#** National Aeronautics and Space Administration. Goddard Space Flight Center, Greenbelt, MD.

**MODIS INFORMATION, DATA AND CONTROL SYSTEM (MIDACS) OPERATIONS CONCEPTS**

D. HAN, V. SALOMONSON, J. ORMSBY, P. ARDANUY, A. MCKAY, D. HOYT, S. JAFFIN, B. VALLETTE, B. SHARTS, D. FOLTA (General Sciences Corp., Laurel, MD.) et al. Dec. 1988 84 p Prepared in cooperation with Interferometrics, Inc., Vienna, VA (Contract NAS5-29373; NAS5-28795) (NASA-TM-100720; REPT-89B00065; NAS 1.15:100720) Avail: NTIS HC A05/MF A01 CSCL 05B

The MODIS Information, Data, and Control System (MIDACS) Operations Concepts Document provides a basis for the mutual understanding between the users and the designers of the MIDACS, including the requirements, operating environment, external interfaces, and development plan. In defining the concepts and scope of the system, how the MIDACS will operate as an element of the Earth Observing System (EOS) within the EosDIS environment is described. This version follows an earlier release of a preliminary draft version. The individual operations concepts for planning and scheduling, control and monitoring, data acquisition and processing, calibration and validation, data archive and distribution, and user access do not yet fully represent the requirements of the data system needed to achieve the scientific objectives of the MODIS instruments and science teams. The teams are not yet formed; however, it is possible to develop the operations concepts based on the present concept of EosDIS, the level 1 and level 2 Functional Requirements Documents, and through interviews and meetings with key members of the scientific

community. The operations concepts were exercised through the application of representative scenarios. Author

**N89-19868\*#** Carnegie-Mellon Univ., Pittsburgh, PA. The Robotics Inst.

**SENSOR FUSION OF RANGE AND REFLECTANCE DATA FOR OUTDOOR SCENE ANALYSIS**

IN SO KWEON, MARTIAL HEBVERT, and TAKEO KANADE /*n* NASA. Lyndon B. Johnson Space Center, 2nd Annual Workshop on Space Operations Automation and Robotics (SOAR 1988) p 373-382 Nov. 1988

(Contract NAGW-1175; DACA76-85-C-0003; NSF DCR-86-04199; ARPA ORDER 5351)

Avail: NTIS HC A22/MF A01 CSCL 20F

In recognizing objects in an outdoor scene, range and reflectance (or color) data provide complementary information. Results of experiments in recognizing outdoor scenes containing roads, trees, and cars are presented. The recognition program uses range and reflectance data obtained by a scanning laser range finder, as well as color data from a color TV camera. After segmentation of each image into primitive regions, models of objects are matched using various properties. Author

## 09

## GENERAL

Includes economic analysis.

**A89-20751**

**ASIAN CONFERENCE ON REMOTE SENSING, 8TH, JAKARTA, INDONESIA, OCT. 22-27, 1987, PROCEEDINGS**

Conference sponsored by the Asian Association on Remote Sensing. Bogor, Indonesia, EXSA International, 1987, 990 p. For individual items see A89-20752 to A89-20826.

Papers concerning remote sensing activities in Asia are presented, including reports of activities in Australia, Bangladesh, China, India, Japan, Korea, Thailand, Vietnam, and Indonesia. Technical issues related to the use of remote sensing in agriculture, forestry, land use management, cartography, water resources, geology, and oceanography, and problems related to data processing and special airborne remote sensing applications are examined. Other topics include cooperative studies between Asian countries, applications of SIR-B, Meteosat, NOAA-AVHRR, Landsat TM and MSS, SPOT, aerial photography, and radar imagery, urban monitoring, planimetric mapping, stereo image matching, the use of geographic information systems, crop yield estimation, and technical reports from companies involved in commercial remote sensing. R.B.

**A89-21397**

**COMMERCIAL REMOTE SENSING SATELLITES GENERATE DEBATE, FOREIGN COMPETITION**

CHRISTOPHER P. FOTOS Aviation Week and Space Technology (ISSN 0005-2175), vol. 129, Dec. 19, 1988, p. 48-51, 55.

Commercial remote sensing programs are discussed, focusing on Landsat and SPOT. The dependence of commercial remote sensing industries on government participation, the market for private customers, and the development of new products are examined. The introduction of Soyuzkarta into the remote sensing market, electrooptical and digital technology versus film-return technology, and the use of remote sensing imagery by news organizations are considered. R.B.

**A89-31560**

**THE DEVELOPMENT OF REMOTE SENSING IN CHINA**

CHANGCHUI HE (National Remote Sensing Centre, Beijing, People's Republic of China) Space Policy (ISSN 0265-9646), vol. 5, Feb. 1989, p. 65-74. refs

Remote sensing activities in China are reviewed. The Chinese

organizations involved in remote sensing activities are listed. The major remote sensing programs in China are discussed, including land resource inventories, agricultural studies, urban planning and environmental studies, geology and mineral resources exploration, forest inventories, grassland surveys, and natural disaster monitoring. Developments in remote sensing technology are examined, including sensors, image processing technology, a Landsat receiving station, and remote sensing satellites. Also, plans for future development programs are considered. R.B.

**N89-18748#** Aberdeen Univ. (Scotland). Faculty of Law.

**THE UN DECLARATION OF LEGAL PRINCIPALS ON REMOTE SENSING, 1986**

F. LYALL /*n* ESA, Proceedings of the 1988 International Geoscience and Remote Sensing Symposium (IGARSS) '88 on Remote Sensing: Moving Towards the 21st Century, Volume 3 p 1445-1447 Aug. 1988

Avail: NTIS HC A99/MF A01; ESA Publications Division, ESTEC, Noordwijk, Netherlands, \$120 US or 250 Dutch guilders

Principles on remote sensing were adopted by the United Nations. They are Principles and not Law, not enforceable but indicators of good practice. However, the principles are very weak. Attempts by the sensed nations to insist on rights to prohibit sensing or to preferential access to raw or processed data failed. Assistance will be provided on terms to be agreed. The sensing nations are not fettered by the Principles. ESA

**N89-18750#** Environmental Remote Sensing Applications Centre, Livingston (Scotland).

**THE GEOSPACE PHILOSOPHY: A NEW PRACTICAL APPROACH IN REMOTE SENSING AND PLANNING FOR LOCAL AUTHORITIES**

G. C. STOVE and R. G. L. STIRRAT (Northern Planners Ltd., Edinburgh, Scotland) /*n* ESA, Proceedings of the 1988 International Geoscience and Remote Sensing Symposium (IGARSS) '88 on Remote Sensing: Moving Towards the 21st Century, Volume 3 p 1453-1456 Aug. 1988

Avail: NTIS HC A99/MF A01; ESA Publications Division, ESTEC, Noordwijk, Netherlands, \$120 US or 250 Dutch guilders

An approach to developing local authorities in Europe as a major potential user of remote sensing data and services is discussed. The aim of the Geospace market research proposal, by involving 10 representative U.K. Local Authorities, is to test their interest and responsiveness to a year's close practical involvement with in-house equipment, local data, and regular training. The proposal to the European Space Agency is that it is only by the free provision of such assistance that the gulf between municipal public sector users and industry will be bridged. The U.K. experience and information transfer will be of European relevance and also assist ESA's commercialization effort. ESA

**N89-18752#** Aston Univ., Birmingham (England). Remote Sensing Unit.

**EFFECTS OF COMMERCIALISATION ON INTERNATIONAL REMOTE SENSING ACTIVITIES**

L. M. OCONNOR and W. G. COLLINS /*n* ESA, Proceedings of the 1988 International Geoscience and Remote Sensing Symposium (IGARSS) '88 on Remote Sensing: Moving Towards the 21st Century, Volume 3 p 1463-1467 Aug. 1988

Avail: NTIS HC A99/MF A01; ESA Publications Division, ESTEC, Noordwijk, Netherlands, \$120 US or 250 Dutch guilders

Significant changes since the adoption of the U.S. Remote Sensing Commercialization Act of 1984 to remote sensing commercial policies are discussed. These changes developed with the transferral of the LANDSAT system to the EOSAT Corporation, and with the launch of SPOT 1 in February 1986. It is believed that services improved as a result of commercialization. However, data prices increased and the use of data is now controlled by various copyright regulations. The changes are analyzed from a global perspective and from the viewpoint of developing countries. An international body similar to the International Telecommunication Union is suggested. ESA

**N89-18816\*#** National Aeronautics and Space Administration.  
Goddard Space Flight Center, Greenbelt, MD.

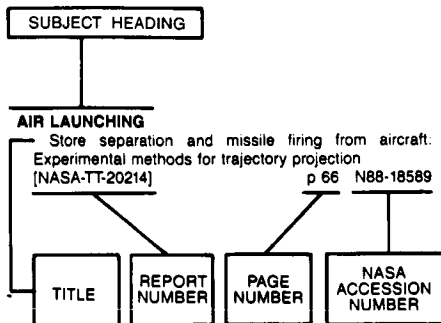
**NASA'S EARTH OBSERVING SYSTEM (EOS): AN  
OPPORTUNITY FOR MANKIND**

M. L. IMHOFF and M. J. DONOHOE *In* ESA, Proceedings of  
the 1988 International Geoscience and Remote Sensing  
Symposium (IGARSS) '88 on Remote Sensing: Moving Towards  
the 21st Century, Volume 3 p 1761-1767 Aug. 1988

Avail: NTIS HC A99/MF A01; ESA Publications Division, ESTEC,  
Noordwijk, Netherlands, \$120 US or 250 Dutch guilders CSCL  
05B

The Earth Observing System (EOS) is a suite of instruments  
joined by a common data information system and will carry out  
multidisciplinary Earth science studies using a variety of remote  
sensing techniques. The mission is planned for the 1990's and  
will focus on the Earth as a system requiring measurements in  
the areas of hydrology, geology, forestry, meteorology,  
oceanography, and agriculture. Two platforms are envisioned on  
the U.S. side each carrying a payload of between 3500 and 4000  
kgs. The European Space Agency and Japan are integrating plans  
for their own programs with EOS and will provide a third and  
fourth platform. The results of the EOS program will be applied to  
biogeochemistry and climate studies, and to environment  
management. ESA

### Typical Subject Index Listing



The subject heading is a key to the subject content of the document. The title is used to provide a description of the subject matter. When the title is insufficiently descriptive of document content, a title extension is added, separated from the title by three hyphens. The (NASA or AIAA) accession number and the page number are included in each entry to assist the user in locating the abstract in the abstract section. If applicable, a report number is also included as an aid in identifying the document. Under any one subject heading, the accession numbers are arranged in sequence with the AIAA accession numbers appearing first.

## A

### ACCURACY

Accuracy assessment, using stratified plurality sampling, of portions of a LANDSAT classification of the Arctic National Wildlife Refuge Coastal Plain [NASA-TM-101042] p 8 N89-17339

### ADAPTIVE FILTERS

Adaptive speckle filtering for SAR images p 58 N89-18710

### ADJUSTING

The geometry of geodetic inverse linear mapping and nonlinear adjustment [ETN-89-93900] p 20 N89-19736

### ADVANCED VERY HIGH RESOLUTION RADIOMETER

Comparative study of vegetation index and false colour composite image of NOAA-AVHRR data for bio-mass studies p 1 A89-20752

The retrieval of sea surface temperature from NOAA-AVHRR satellite data - Comparison between Singh's and McClain's methods p 28 A89-20787

The navigation method for NOAA-AVHRR image p 61 A89-20795

New technology for displaying of NOAA AVHRR thermal band image p 29 A89-20810

Edge detection applied to satellite imagery of the oceans p 33 A89-26844

Comparison of NOAA-AVHRR-2 sea surface temperatures with surface measurements in coastal waters p 36 A89-30259

### AERIAL PHOTOGRAPHY

The use of aerial photographs in Quaternary-volcanic terrains mapping p 20 A89-20784

An interactive system for aerial photo orientation of digital stereo image pairs p 53 A89-20799

Low-cost second order planimetric mapping technique p 53 A89-20800

The application of remote sensing for forest inventory p 2 A89-20809

Correlation of Landsat TM and aeromagnetic data along the Eastern Margin of the Cuddapah Basin, South India p 21 A89-20817

A tomographic approach to lineament identification on aerial and space images p 22 A89-22223  
Principal results of remote-sensing studies of Siberia's natural resources (On the occasion of the 10th anniversary of the Scientific Coordination Council, 1977-1987) p 62 A89-22225

Erosional furrows formed during the lateral blast at Mount St. Helens, May 18, 1980 p 22 A89-22632

Agrometeorological aspects of the utilization of remote-sensing data p 3 A89-23663

Calibration of infrared satellite images using high altitude aircraft measurements [AIAA PAPER 89-0817] p 54 A89-25595

Aerial and space remote-sensing techniques for geographical investigations --- Russian book p 62 A89-26178

Using a top-down and bottom-up strategy to analyze high resolution aerial photographs of urban areas p 18 A89-27630

Interactive image feature compilation for geographic information systems p 18 A89-27785

Airborne MSS for land cover classification p 5 A89-28131

Area measurement of agricultural fields from satellite images p 5 A89-29374

Features of the geological structure of the polar Urals and the distribution of certain minerals, as evaluated on the basis of the interpretation of aerial and space photographs p 23 A89-30119

Visual and computer classifications of remotely-sensed images - A case study of grasslands in Cambridgeshire p 7 A89-30269

A comparison of images from a pushbroom scanner with normal color aerial photographs for detecting scattered recent conifer mortality p 7 A89-32336

Annular and block-folded structures on space and aerial photographs p 25 N89-17915

Mapping of phytoplankton fluorescence with the Fluorescence Line Imager (FLI) imaging spectrometer p 39 N89-18737

Interpreting the geology of Glen Coe using LANDSAT MSS data and aerial photographs p 26 N89-18860

### AEROMAGNETISM

Correlation of Landsat TM and aeromagnetic data along the Eastern Margin of the Cuddapah Basin, South India p 21 A89-20817

Integrated study of Landsat, aeromagnetic and Bouguer gravity anomaly data for geological appraisal - A case study from Tamil Nadu, India p 21 A89-20823

Integration of geological, geophysical and remotely sensed data for the Solway Basin, England p 26 N89-18794

### AEROSOLS

Long-range transport of giant mineral aerosol particles p 17 A89-21931

Determination of atmospheric turbidity from remotely-sensed data - A case study p 34 A89-28034

Analysis of atmospheric effects in SPOT HRV images p 65 A89-29372

### AFRICA

Monitoring of agro-forestry production systems in the Sudano-Sahelian zone of West Africa p 11 N89-18825

Snow cover-summer monsoon rainfall over parts of Sahel p 51 N89-18832

### AGRICULTURE

The use of SPOT imagery in Medan agriculture area for monitoring features changes p 1 A89-20755

Remote sensing applications for agricultural landuse survey in Indonesia - Isimu case study p 2 A89-20763

Determination of relative crop areas from spectrometric data p 22 A89-22218

Area measurement of agricultural fields from satellite images p 5 A89-29374

X-band scatterometry in agriculture p 9 N89-18715

### AGROMETEOROLOGY

Applications of remote sensing to agrometeorology; Proceedings of the Course, Ispra, Italy, Apr. 6-10, 1987 p 63 A89-27933

Use of surface temperature in agrometeorology p 4 A89-27942

Satellite remote sensing of rainfall p 49 A89-27946

### AIR LAND INTERACTIONS

Dependence of snow melting and surface-atmosphere interactions on the forest structure p 3 A89-21740

### AIR POLLUTION

A model for the propagation of industrial atmospheric pollution registered on multispectral earth images p 17 A89-22213

### AIR WATER INTERACTIONS

Circulation in the East Asian seas from satellite and ship data p 29 A89-20803

Inertial wind path and sea surface temperature patterns near the Gulf of Tehuantepec and Gulf of Papagayo p 30 A89-22592

Satellite determination of the carbon dioxide exchange coefficient at the ocean-atmosphere interface - A first step p 31 A89-22598

Simulated effects of barometric pressure and ozone content upon the estimate of marine phytoplankton from space p 33 A89-26443

Determination of atmospheric turbidity from remotely-sensed data - A case study p 34 A89-28034

Evaluation of satellite-tracked surface drifting buoys for simulating the movement of spilled oil in the marine environment. Volume 1: Executive summary [PB88-226048] p 37 N89-17357

Evaluation of satellite-tracked surface drifting buoys for simulating the movement of spilled oil in the marine environment, volume 2 [PB88-226055] p 37 N89-17358

### AIRBORNE EQUIPMENT

The extraction of sea fishery potential area from Airborne Ocean Color Radiometer data p 28 A89-20786

Application of airborne scanners in remote sensing of sea p 29 A89-20789

Airborne gravity as a supporting tool for hydrocarbon exploration in Indonesia p 21 A89-20829

Intercomparison of synthetic- and real-aperture radar observations of Arctic sea ice during winter MIZEX '87 p 40 N89-18744

Microcomputer-based radiometer data acquisition and processing system for large-area mapping of soil moisture content in the top one meter layer p 11 N89-18774

Artefacts in AIS-I imagery --- Airborne Image Spectrometer (AIS) p 69 N89-18826

Experiments in Bulgaria for determination of soil moisture in the top one-meter layer using microwave radiometry and a priori information p 11 N89-18843

Towards a calibration of the CCRS airborne SARS --- Canada Center for Remote Sensing (CCRS) p 70 N89-18854

Radiometric calibration of airborne SAR data p 70 N89-18855

Preprocessing of the VARAN synthetic aperture airborne radar p 70 N89-18856

E-SAR: The experimental airborne L/C-band SAR system of DFVLR p 73 N89-18924

The Technical University of Denmark (TUD) C-band SAR p 74 N89-18928

Investigations of sea ice using coincident Geosat altimetry and synthetic aperture radar during MIZEX-87 p 46 N89-18945

EHF attenuation through the melting layer p 51 N89-18984

Applications of the NCAR Electra Doppler radar for the study of physical parameters of clouds p 75 N89-19717

### AIRBORNE LASERS

Laser airborne sensing field experiments using the 'Chaika' assembly --- for probing water bodies p 35 A89-29728

Effects of round trip laser emission propagation through a turbulent surface for laser airborne oceanic sensing p 35 A89-29729

### ALBEDO

The relative merits of narrowband channels for estimating broadband albedos p 66 A89-30967

### ALGORITHMS

Application of a flux algorithm to a field-satellite campaign over vegetated area p 6 A89-29411

SUBJECT



- Segmentation of Synthetic Aperture Radar (SAR) images of ocean surface by the texture energy transform method  
[AD-A199536] p 37 N89-15309
- An algorithm for analysis of plate motions in Crust Dynamics Project (CDP) networks  
[B8821606] p 19 N89-17371
- The algorithm development facility: its role in the development and operation of a satellite data centre  
p 68 N89-18755
- An advanced terrain tracking altimeter  
p 45 N89-18910
- Tracking algorithms in radar altimetry  
p 72 N89-18911
- AMAZON REGION (SOUTH AMERICA)**
- Comparison of satellite total ozone measurements with the distribution of tropospheric ozone obtained by an airborne UV-DIAL system over the Amazon Basin  
p 17 A89-21892
- AMPLIFICATION**
- Use of the variable gain settings on SPOT  
p 65 A89-29435
- ANALOG TO DIGITAL CONVERTERS**
- Overview of low-cost map digitizing systems  
[DE89-002872] p 57 N89-16204
- ANDES MOUNTAINS (SOUTH AMERICA)**
- Tectonics of the central Andes  
[NASA-CR-184683] p 28 N89-18973
- ANIMATION**
- Visualization of topographic data using video animation  
p 55 A89-29066
- ANNUAL VARIATIONS**
- Variability of the diffuse attenuation coefficient in waters off the US East Coast  
p 39 N89-18738
- ANTARCTIC REGIONS**
- Measurements of springtime Antarctic ozone depletion and development of a balloonborne ultraviolet photometer  
p 67 N89-15459
- Antarctic Ocean polynyas  
[NASA-CR-184805] p 47 N89-19102
- ANTENNA DESIGN**
- ERS-1 AMI antennas: The design and development experience --- Active Microwave Instrumentation (AMI)  
p 71 N89-18890
- ANTENNA RADIATION PATTERNS**
- A study of advanced radar altimeter techniques --- satellite altimetry  
[ESA-CR(P)-2699] p 75 N89-19483
- ARCHITECTURE (COMPUTERS)**
- New architecture for a real-time SAR processor  
p 69 N89-18850
- The Alaska SAR processor  
p 70 N89-18851
- AREA**
- Estimation of the area of Lake Kariba, Zimbabwe, using LANDSAT MSS imagery  
p 51 N89-18775
- ARID LANDS**
- Extension of a drought monitoring and vegetation classification methodology to the western Sahel  
p 4 A89-28127
- Monitoring of agro-forestry production systems in the Sudano-Sahelian zone of West Africa  
p 11 N89-18825
- Snow cover-summer monsoon rainfall over parts of Sahel  
p 51 N89-18832
- Satellite radar altimetry over arid regions  
p 69 N89-18842
- Soil influences on vegetation reflectance of a semi-arid shrubland  
p 13 N89-18880
- ARTIFICIAL INTELLIGENCE**
- Using a top-down and bottom-up strategy to analyze high resolution aerial photographs of urban areas  
p 18 A89-27630
- ASIA**
- Asian Conference on Remote Sensing, 8th, Jakarta, Indonesia, Oct. 22-27, 1987, Proceedings  
p 76 A89-20751
- ATLANTIC OCEAN**
- Satellite sea surface temperature at the North Atlantic Polar Front related to high-resolution towed conductivity-temperature-depth data  
p 31 A89-22594
- A tide-generated internal waveform in the western approaches to the Strait of Gibraltar  
p 31 A89-22597
- Comparison study of SEASAT scatterometer and conventional wind fields  
[AD-A200591] p 67 N89-16202
- Coastal ocean margins program  
[DE89-005837] p 47 N89-18972
- ATMOSPHERIC ATTENUATION**
- Atmospheric attenuation as derived from microwave radiometry at 52.8 GHz  
p 72 N89-18906
- EHF attenuation through the melting layer  
p 51 N89-18984
- ATMOSPHERIC CIRCULATION**
- Summertime stratospheric wind measurements above the South Pole  
p 62 A89-24022

**ATMOSPHERIC COMPOSITION**

- Comparison of satellite total ozone measurements with the distribution of tropospheric ozone obtained by an airborne UV-DIAL system over the Amazon Basin  
p 17 A89-21892
- Applications of the NCAR Electra Doppler radar for the study of physical parameters of clouds  
p 75 N89-19717

**ATMOSPHERIC CORRECTION**

- An atmospheric correction method for AVHRR infrared data using HIRS/2 data  
p 69 N89-18828
- Image-based atmospheric correction of multitemporal Thematic Mapping data for agricultural land cover classification  
p 14 N89-18895

**ATMOSPHERIC DIFFUSION**

- Long-range transport of giant mineral aerosol particles  
p 17 A89-21931
- Dispersion parameters over forested terrain  
p 3 A89-22728

**ATMOSPHERIC EFFECTS**

- Analysis of atmospheric effects in SPOT HRV images  
p 65 A89-29372
- The influence of water vapor on the detection of ocean mesoscale fronts and eddies by the Geosat altimeter  
p 44 N89-18839
- Signature variations due to atmospheric and topographic effects on satellite MSS data over rugged terrain  
p 70 N89-18877

**ATMOSPHERIC MODELS**

- Hindcasts and data assimilation studies with the WAM model during the Seasat period --- wave model  
p 32 A89-26442
- Studies of the dependence of the microwave radar cross section on ocean surface variables during the FASINEX experiment  
p 41 N89-18782
- An atmospheric correction method for AVHRR infrared data using HIRS/2 data  
p 69 N89-18828
- The directional reflectance of heather canopies: Towards a descriptive model  
p 13 N89-18878
- Atmospheric attenuation as derived from microwave radiometry at 52.8 GHz  
p 72 N89-18906

**ATMOSPHERIC MOISTURE**

- VHF radar remote sensing of vertical profile of liquid water content and rainfall rate over Taiwan during the time period of Typhoon Wayne  
p 48 A89-20771
- Retrieval of water vapor profiles from microwave radiometric measurements at 183 and 92 GHz  
p 72 N89-18905
- Atmospheric profiling of water vapour with a 20.5-23.5 GHz autocorrelation radiometer  
p 72 N89-18908
- EHF attenuation through the melting layer  
p 51 N89-18984

**ATMOSPHERIC PRESSURE**

- Simulated effects of barometric pressure and ozone content upon the estimate of marine phytoplankton from space  
p 33 A89-26443

**ATMOSPHERIC RADIATION**

- A method for processing and results of microwave radiometer studies of the earth from the Intercosmos 20 and 21 satellites  
p 36 A89-30122

**ATMOSPHERIC SOUNDING**

- Laser sounding of the troposphere and the underlying surface --- Russian book  
p 17 A89-22066
- Optical methods of satellite hydrophysics. Investigation of the environment from manned orbital stations --- Russian book  
p 32 A89-26181
- Retrieval of water vapor profiles from microwave radiometric measurements at 183 and 92 GHz  
p 72 N89-18905

**ATMOSPHERIC TEMPERATURE**

- Satellite derived earth surface temperatures: A crop assessment tool  
p 8 N89-17930

**ATTENUATION COEFFICIENTS**

- Modeling vegetation as a set of scatterers  
p 7 A89-32110
- Optical properties of sea water bodies: Measurements with an underwater radiometer and a high-resolution spectroradiometer  
p 39 N89-18734
- Variability of the diffuse attenuation coefficient in waters off the US East Coast  
p 39 N89-18738

**AUTOCORRELATION**

- Speckle correlation in SAR images of dynamic discrete scatterers  
p 37 N89-18707
- Auto and cross correlation analysis of environment, system and target parameters for iceberg detection using airborne radar  
p 45 N89-18874
- Atmospheric profiling of water vapour with a 20.5-23.5 GHz autocorrelation radiometer  
p 72 N89-18908

**AUTOMATIC CONTROL**

- Automatic registration of satellite imagery  
[INPE-4637-PRE/1349] p 57 N89-17414

**B****BACKSCATTERING**

- Fine resolution signatures of coniferous and deciduous trees at C band  
p 6 A89-30266
- Theoretical study of the sensitivity of the microwave backscattering coefficient to the soil surface parameters  
p 6 A89-30267
- Comparison of measured C-band scattering coefficients with model predictions as a function of leaf area index and Biomass  
p 8 N89-18712
- Leaf backscattering measurements and modelling at 94 GHz  
p 8 N89-18713
- A measurement of microwave backscattering coefficients of rice plants  
p 8 N89-18714
- X-band scatterometry in agriculture  
p 9 N89-18715
- Distribution of specular points on the ocean surface:  
Bistatic scattering  
p 38 N89-18721
- Specular scattering with effective reflection coefficient  
p 39 N89-18723
- Association of radar backscattering with biophysical characteristics of Australian forests  
p 10 N89-18731
- Investigations of SAR backscatter for different test areas using two geocoded Seasat SAR scenes  
p 58 N89-18761
- Simulation of SAR imaging of ship wakes  
p 41 N89-18765
- Observations of the effect of geometric properties of agricultural soils on radar backscatter, from C-SAR images  
p 11 N89-18781
- Analysis of ocean backscatter data obtained by the University of Kansas during TOWARD 84/85  
p 42 N89-18787
- Comparison between microwave emissivity and backscattering coefficient of agricultural fields  
p 12 N89-18844
- The leaf-shape effect on electromagnetic scattering from vegetated media  
p 12 N89-18846
- Measurements of microwave backscatter from conifers  
p 12 N89-18848
- Backscatter behavior of low-salinity sea ice at C and X-band  
p 44 N89-18869
- Evaluation of VARAN-S SAR data from the BEPERS study project --- sea ice  
p 45 N89-18875
- Radar backscatter characteristics of trees at 215 GHz  
p 14 N89-18917
- Radar backscatter of sea ice during winter  
p 46 N89-18943
- BALLOON-BORNE INSTRUMENTS**
- Measurements of springtime Antarctic ozone depletion and development of a balloonborne ultraviolet photometer  
p 67 N89-15459
- BANDPASS FILTERS**
- An optimum calibration procedure for radiometers  
p 65 A89-30270
- BARLEY**
- Problems in the estimation of barley yields by remote sensing  
p 13 N89-18861
- BARREN LAND**
- Remote sensing of evaporite mineral zonation in salt flats (salars)  
p 23 A89-30271
- BATHYMETERS**
- Optical bathymetry for the U.S. Navy - A field measurement program  
p 64 A89-27993
- Bathymetry using Thematic Mapper imagery  
p 34 A89-27995
- Analysis of airborne laser hydrography waveforms  
p 64 A89-27996
- Airborne nonacoustic bathymetric survey flight test results  
p 51 N89-18937
- BATHYTHERMOGRAPHS**
- Geosat crossover analysis in the tropical Pacific. II - Verification analysis of altimetric sea level maps with expendable bathythermograph and island sea level data  
p 32 A89-26438
- BAYS (TOPOGRAPHIC FEATURES)**
- Bayes classification of terrain cover using normalized polarimetric data  
p 54 A89-22649
- BEARING (DIRECTION)**
- Directional wave data recorded in the southern North Sea  
[IOS-258] p 47 N89-19793
- BIDIRECTIONAL REFLECTANCE**
- Parabola directional field radiometer for aiding in space sensor data interpretations  
p 63 A89-27779
- BIOMASS**
- Comparative study of vegetation index and false colour composite image of NOAA-AVHRR data for bio-mass studies  
p 1 A89-20752
- Comparison of measured C-band scattering coefficients with model predictions as a function of leaf area index and Biomass  
p 8 N89-18712
- Monitoring of agro-forestry production systems in the Sudano-Sahelian zone of West Africa  
p 11 N89-18825

- Estimating absorbed radiation and phytomass from multispectral reflectance of corn and soybeans  
p 13 N89-18876
- BIOSPHERE**  
Landscape processing of satellite imagery for a biospheric data bank p 56 A89-30239
- BISTATIC REFLECTIVITY**  
Distribution of specular points on the ocean surface: Bistatic scattering p 38 N89-18721
- BLACK SEA**  
An experiment to invert Seasat altimetry for the Mediterranean and Black Sea mean surfaces p 36 A89-30900
- BOUQUER LAW**  
Integrated study of Landsat, aeromagnetic and Bouguer gravity anomaly data for geological appraisal - A case study from Tamil Nadu, India p 21 A89-20823
- BRIGHTNESS TEMPERATURE**  
Procedures for the determination of geophysical parameters from spaceborne microwave polarimeter measurements p 30 A89-22224  
Shipborne passive microwave sea ice experiment in the East Greenland Sea: May-July 1987 p 42 N89-18799
- BRILLOUIN EFFECT**  
Remote sensing of ocean physical properties - A comparison of Raman and Brillouin techniques p 34 A89-28003
- BROADBAND**  
The relative merits of narrowband channels for estimating broadband albedos p 66 A89-30967
- BUOYS**  
Evaluation of satellite-tracked surface drifting buoys for simulating the movement of spilled oil in the marine environment. Volume 1: Executive summary [PB88-226048] p 37 N89-17357  
Evaluation of satellite-tracked surface drifting buoys for simulating the movement of spilled oil in the marine environment, volume 2 [PB88-226055] p 37 N89-17358
- C**
- C BAND**  
Fine resolution signatures of coniferous and deciduous trees at C band p 6 A89-30266  
Comparison of measured C-band scattering coefficients with model predictions as a function of leaf area index and Biomass p 8 N89-18712  
Assessment of clearcut mapping accuracy with C-band SAR p 9 N89-18725  
Backscatter behavior of low-salinity sea ice at C and X-band p 44 N89-18869  
E-SAR: The experimental airborne L/C-band SAR system of DFVLR p 73 N89-18924  
The Technical University of Denmark (TUD) C-band SAR p 74 N89-18928
- CALIBRATING**  
An optimum calibration procedure for radiometers p 65 A89-30270  
The derivation and verification of surface reflectances using airborne MSS data and a radiative transfer model [DE89-004881] p 67 N89-17931  
Association of radar backscattering with biophysical characteristics of Australian forests p 10 N89-18731  
Towards a calibration of the CCRS airborne SARS --- Canada Center for Remote Sensing (CCRS) p 70 N89-18854  
Radiometric calibration of airborne SAR data p 70 N89-18855  
Vegetation sampling for studies using remotely sensed data p 13 N89-18883  
Engineering calibration of the ERS-1 active microwave instrumentation in orbit p 71 N89-18885  
ERS-1 altimeter height calibration p 71 N89-18891  
MODIS information, data and control system (MIDACS) operations concepts [NASA-TM-100720] p 75 N89-19729
- CALIFORNIA**  
Geodetic measurement of deformation in California [NASA-CR-184604] p 19 N89-15476  
Comparison of GPS surveys with historical triangulation surveys in the southern California borderland [NASA-CR-183405] p 24 N89-16199  
Local geoid determination using the global positioning system [AD-A202220] p 20 N89-19731
- CAMERAS**  
Potential of Large Format Camera photography p 65 A89-29433  
German spaceborne remote sensing activities p 67 N89-16887
- CANADA**  
Satellite data acquisition planning at the Canada Center for Remote Sensing p 68 N89-18753
- Integration of digital satellite and geophysical data, Heath Steele Mines, New Brunswick, Canada p 25 N89-18792
- CANOPIES (VEGETATION)**  
A comparison of models for deriving dry deposition fluxes of O<sub>3</sub> and SO<sub>2</sub> to a forest canopy p 3 A89-20923  
Brightness of a laser-beam halo in vegetation cover p 3 A89-22221  
Remote sensing of canopy chemistry and nitrogen cycling in temperate forest ecosystems p 3 A89-23431  
Effects of solar angle on reflectance from wetland vegetation p 5 A89-29409  
Complementarity of middle-infrared with visible and near-infrared reflectance for monitoring wheat canopies p 5 A89-29410  
Tersail - A numerical model for combined analysis of vegetation canopy bidirectional reflectance and thermal emissions p 6 A89-29415  
Bidirectional canopy reflectance and its relationship to vegetation characteristics p 6 A89-30264  
The directional reflectance of heather canopies: Towards a descriptive model p 13 N89-18878  
Soil influences on vegetation reflectance of a semi-arid shrubland p 13 N89-18880  
Radar polarimetric observations of a tree canopy p 15 N89-18920  
Geological applications of thermal infrared characteristics of vegetation p 27 N89-18932  
Alternative approaches to the classification of upland semi-natural vegetation --- remote sensing p 16 N89-18961
- CARBON CYCLE**  
Distribution and variations of oceanic carbon dioxide in the western North Pacific, eastern Indian, and Southern Ocean south of Australia p 29 A89-20925
- CARBON DIOXIDE**  
Satellite determination of the carbon dioxide exchange coefficient at the ocean-atmosphere interface - A first step p 31 A89-22598  
Satellite detection of transient enhanced primary production in the western Mediterranean Sea p 31 A89-23438
- CARBON DIOXIDE CONCENTRATION**  
Distribution and variations of oceanic carbon dioxide in the western North Pacific, eastern Indian, and Southern Ocean south of Australia p 29 A89-20925
- CARBONATES**  
A quantitative geomorphology study of main carbonate massifs of central and southern Apennines (Italy) based on a digital elevations archive p 25 N89-18791
- CENTRAL AMERICA**  
Upwelling off the Gulfs of Panama and Papagayo in the tropical Pacific during March 1985 p 30 A89-22591  
Inertial wind path and sea surface temperature patterns near the Gulf of Tehuantepec and Gulf of Papagayo p 30 A89-22592
- CHANGE DETECTION**  
The use of SPOT imagery in Medan agriculture area for monitoring features changes p 1 A89-20755  
Study on changes of mangrove forest in Thailand by using Landsat imagery p 3 A89-20822  
Accuracy assessment of Landsat-based visual change detection methods applied to the rural-urban fringe p 18 A89-29437  
LANDSAT TM study of afforestation in northern Scotland and its impact on breeding bird populations p 10 N89-18732  
Preprocessing and analysis of airborne visible near and shortwave infrared data for the detection of alteration in weathered vegetated terrain p 12 N89-18862  
Change detection in AGRISAR images p 15 N89-18949
- CHANNELS (DATA TRANSMISSION)**  
The relative merits of narrowband channels for estimating broadband albedos p 66 A89-30967
- CHAPARRAL**  
Trace gas emissions from chaparral and boreal forest fires p 7 A89-32432
- CHECKOUT**  
The pre-launch performance verification of the ERS-1 active microwave instrumentation p 71 N89-18886  
A software package for performance evaluation of the ERS-1 AMI --- Active Microwave Instrument (AMI) p 71 N89-18887
- CHEMICAL COMPOSITION**  
Observed effects of soil organic matter content on the microwave intensity of soils p 12 N89-18845
- CHINA**  
Quick reporting state of fishery and sea on the East China Sea and the Yellow Sea with NOAA p 39 N89-18741
- CHINESE SPACE PROGRAM**  
The development of remote sensing in China p 76 A89-31560
- CHLOROPHYLLS**  
Laser airborne sensing field experiments using the 'Chaika' assembly --- for probing water bodies p 35 A89-29728  
Correlation of reflectance and chlorophyll fluorescence signatures of healthy and damaged forest trees p 9 N89-18726  
Correlation of radar reflectivity and chlorophyll fluorescence of forest trees p 9 N89-18727  
Quantitative remote detection of suspended sediment content and chlorophyll concentration of water in different depths p 50 N89-18733  
Data processing for the determination of pigments and suspended solids from Thematic Mapper data p 50 N89-18736  
A mathematical model of reflectance and transmittance of plant leaves as a function of chlorophyll pigment content p 13 N89-18879
- CITIES**  
Contribution of second-generation Landsat TM and SPOT HRV satellites to urban analysis (Rennes, France) p 17 A89-21250  
Analysis and interpretation of SPOT images of urban and agricultural/forest sections of the Sherbrooke region p 5 A89-29373  
Accuracy assessment of Landsat-based visual change detection methods applied to the rural-urban fringe p 18 A89-29437  
Integration of SPOT data in an urban data bank - Locating work sites p 18 A89-31891
- CLASSIFICATIONS**  
On classification of forests of some portions of central India using satellite imagery p 2 A89-20761  
Accuracy of land-cover/use classification p 52 A89-20765  
Land use suitability classification using remote sensing data and geographic information for volcanic regions p 16 A89-20766  
Normal distributional assumptions in discrimination --- image processing p 59 N89-18821  
The use of SPOT-1 imagery for forest classification in Flanders (Belgium) p 14 N89-18899  
Textural and spectral features as an aid to cloud classification p 74 N89-18960  
Alternative approaches to the classification of upland semi-natural vegetation --- remote sensing p 16 N89-18961
- CLIMATE**  
Tectonics of the central Andes [NASA-CR-184683] p 28 N89-18973
- CLIMATE CHANGE**  
Satellite detection of transient enhanced primary production in the western Mediterranean Sea p 31 A89-23438
- CLIMATOLOGY**  
MISR - A multiangle imaging spectroradiometer for geophysical and climatological research from EOS p 86 A89-31946
- CLOUD COVER**  
Satellite remote sensing of cloud distribution and amount of rainfall over the Tibet Plateau area of China p 48 A89-20770  
Operational remote sensing in the United Kingdom: Problems of image acquisition p 68 N89-18751
- CLOUD GLACIATION**  
Observation of the degree of glaciation in middle-level stratiform clouds p 62 A89-23464  
Structure of layer clouds as observed simultaneously by a microwave radiometer and an 8.6 mm-radar p 74 N89-19039
- CLOUD PHYSICS**  
Structure of layer clouds as observed simultaneously by a microwave radiometer and an 8.6 mm-radar p 74 N89-19039  
Applications of the NCAR Electra Doppler radar for the study of physical parameters of clouds p 75 N89-19717
- CLOUDS (METEOROLOGY)**  
Textural and spectral features as an aid to cloud classification p 74 N89-18960
- CLUSTER ANALYSIS**  
A quantitative geomorphology study of main carbonate massifs of central and southern Apennines (Italy) based on a digital elevations archive p 25 N89-18791  
A method for the clustering of remotely sensed multispectral images by using statistical test for spatial uniformity p 61 N89-18898  
Estimating the extent of irrigated cropland in a large catchment using LANDSAT MSS data p 14 N89-18902
- CLUTTER**  
Can better environmental inputs improve sea clutter estimation? A numerical experiment p 36 A89-30258  
A comparison of clutter texture properties in optical and SAR images p 8 N89-18708

## COASTAL CURRENTS

- Ocean wave directional spectra and wave-current interaction in the Agulhas from the Shuttle Imaging Radar-B synthetic aperture radar p 30 A89-22585
- COASTAL ECOLOGY**  
Coastal ocean margins program [DE89-005937] p 47 N89-18972
- COASTAL PLAINS**  
Coastal ocean margins program [DE89-005937] p 47 N89-18972
- COASTAL WATER**  
Upwelling off the Gulfs of Panama and Papagayo in the tropical Pacific during March 1985 p 30 A89-22591  
Inertial wind path and sea surface temperature patterns near the Gulf of Tehuantepec and Gulf of Papagayo p 30 A89-22592  
The relationship between suspended sediment concentration and remotely sensed spectral radiance - A review p 48 A89-24649  
Optical bathymetry for the U.S. Navy - A field measurement program p 64 A89-27993  
Bathymetry using Thematic Mapper imagery p 34 A89-27995  
Comparison of NOAA/AVHRR-2 sea surface temperatures with surface measurements in coastal waters p 36 A89-30259  
Remote sensing of macrophytic algae of the Molene Archipelago in France - Terrain radiometry and application to SPOT satellite data p 36 A89-30260  
Monitoring offshore water quality from space p 39 N89-18739
- COASTAL ZONE COLOR SCANNER**  
Satellite detection of transient enhanced primary production in the western Mediterranean Sea p 31 A89-23438  
Variability of the diffuse attenuation coefficient in waters off the US East Coast p 39 N89-18738  
Monitoring offshore water quality from space p 39 N89-18739  
The structure and variability of a filament in the northwest African upwelling area as observed from AVHRR and CXCS images p 46 N89-18939
- COASTS**  
Coastline monitoring in Madura Strait, Indonesia on 1972-1985 p 29 A89-20804  
Technology transfer for development of coastal zone resources: Caribbean experts examine critical issues p 40 N89-18749
- CODING**  
A high fidelity, high throughput system for geocoding SAR imagery p 60 N89-18849
- COLD FRONTS**  
Satellite sea surface temperature at the North Atlantic Polar Front related to high-resolution towed conductivity-temperature-depth data p 31 A89-22594
- COLOR INFRARED PHOTOGRAPHY**  
The studies for the computer classification and the investigation of grasslands in Tibet using Space-Lab color infrared image p 1 A89-20754
- COLOR PHOTOGRAPHY**  
Improvement of multispectral color images by intensifying local contrasts p 56 A89-30123
- COMBUSTION PRODUCTS**  
Trace gas emissions from chaparral and boreal forest fires p 7 A89-32432
- COMMERCIAL SPACECRAFT**  
Commercial remote sensing satellites generate debate, foreign competition p 76 A89-21397
- COMMONALITY**  
MODIS-HIRIS ground data systems commonality report [NASA-TM-100718] p 67 N89-16205
- COMPUTER AIDED MAPPING**  
Interactive image feature compilation for geographic information systems p 18 A89-27785  
Overview of low-cost map digitizing systems [DE89-002872] p 57 N89-18204  
SPOT mapping software for Wild Aviolet BC2 analytical plotter p 60 N89-18824  
Satellite imagery for semi-automatic map revision p 61 N89-18957
- COMPUTER AIDED TOMOGRAPHY**  
A tomographic approach to lineament identification on aerial and space images p 22 A89-22223
- COMPUTER GRAPHICS**  
Interactive image feature compilation for geographic information systems p 18 A89-27785  
Overview of low-cost map digitizing systems [DE89-002872] p 57 N89-18204  
Automatic registration of satellite imagery [INPE-4637-PRE/1349] p 57 N89-17414  
Real-time processing of digital image data in support of the Canadian sea ice analysis and prediction program p 43 N89-18803

## COMPUTER NETWORKS

- Image compression using a neural network p 58 N89-18705
- Real-time stereo matching SPOT using transputer arrays p 74 N89-18958
- COMPUTER PROGRAMMING**  
An algorithm for analysis of plate motions in Crust Dynamics Project (CDP) networks [B8821606] p 19 N89-17371
- COMPUTER PROGRAMS**  
Application of three dimensional image system p 53 A89-20797  
Satellite data acquisition planning at the Canada Center for Remote Sensing p 68 N89-18753
- COMPUTER SYSTEMS DESIGN**  
Real-time processing of digital image data in support of the Canadian sea ice analysis and prediction program p 43 N89-18803  
Sea-ice software: ICEMAN p 43 N89-18805  
Requirements for an EOS-oriented workstation --- Earth Observing System (EOS) p 69 N89-18813
- COMPUTER SYSTEMS PERFORMANCE**  
Results of software simulation of a real-time SAR processor capable of providing ocean wave spectra p 38 N89-18720
- COMPUTER SYSTEMS PROGRAMS**  
An ERDAS module for routine processing of AVHRR data p 43 N89-18817  
A software package for performance evaluation of the ERS-1 AMI --- Active Microwave Instrument (AMI) p 71 N89-18887
- COMPUTER TECHNIQUES**  
Drainage pattern analysis with the aid of Landsat MSS data of the Citarium river basin, West Java, Indonesia p 48 A89-20778
- COMPUTER VISION**  
Using a top-down and bottom-up strategy to analyze high resolution aerial photographs of urban areas p 18 A89-27630  
Knowledge related aspects of lineation and lineament extraction [INPE-4709-PRE/1391] p 24 N89-15446  
Using different sources of information in automated linear feature extraction from remote sensing data [INPE-4708-PRE/1390] p 24 N89-15447  
Sensor fusion of range and reflectance data for outdoor scene analysis p 76 N89-18868
- COMPUTERIZED SIMULATION**  
A simulation of the global ocean circulation with resolved eddies p 30 A89-22593  
A simulation for spaceborne SAR imagery of a distributed, moving scene p 33 A89-26846  
Results of software simulation of a real-time SAR processor capable of providing ocean wave spectra p 38 N89-18720  
Computer simulation of multipath sea echo near grazing incidence p 38 N89-18722  
Simulation of SAR imaging of ship wakes p 41 N89-18765  
Digital elevation models and their application to remote sensing of water resources p 51 N89-18770
- CONCENTRATION (COMPOSITION)**  
Quantitative remote detection of suspended sediment content and chlorophyll concentration of water in different depths p 50 N89-18733
- CONFERENCES**  
Asian Conference on Remote Sensing, 8th, Jakarta, Indonesia, Oct. 22-27, 1987, Proceedings p 76 A89-20751  
Applications of remote sensing to agrometeorology: Proceedings of the Course, Ispra, Italy, Apr. 6-10, 1987 p 63 A89-27933  
Ocean optics IX; Proceedings of the Meeting, Orlando, FL, Apr. 4-6, 1988 [SPIE-925] p 33 A89-27976  
The 1988 International Geoscience and Remote Sensing Symposium (IGARSS 1988) on Remote Sensing: Moving Towards the 21st Century, volume 3 [ESA-SP-284-VOL-3] p 68 N89-18704  
Proceedings of the 1988 International Geoscience and Remote Sensing Symposium (IGARSS) '88 on Remote Sensing: Moving Towards the 21st Century, Volume 2 [ESA-SP-284-VOL-2] p 69 N89-18836
- CONFORMAL MAPPING**  
The geometry of geodetic inverse linear mapping and nonlinear adjustment [ETN-89-93900] p 20 N89-19736
- CONIFERS**  
A comparison of images from a pushbroom scanner with normal color aerial photographs for detecting scattered recent conifer mortality p 7 A89-32336  
Spectral response characteristics of a metal-stressed coniferous forest as measured by the Fluorescence Line Imager (FLI) airborne imaging spectrometer p 9 N89-18724

Measurements of microwave backscatter from conifers p 12 N89-18848

## CONSTRUCTION MATERIALS

- Mapping of construction material sites around Bangalore City using Landsat Thematic Mapper data p 52 A89-20782

## CONTINENTAL SHELVES

Major crustal lineaments on Seasat SAR and their off-shore extensions in the UK p 26 N89-18861

## COORDINATES

Reference coordinate systems: An update. Supplement 11 [NASA-CR-184764] p 19 N89-16207

## COPYRIGHTS

Effects of commercialisation on international remote sensing activities p 76 N89-18752

## CORN

Estimating absorbed radiation and phytomass from multispectral reflectance of corn and soybeans p 13 N89-18876

## CROP GROWTH

Relationship of spectral data and grain yield variation in rice (*Oryza sativa* L.) ADT 31 p 2 A89-20762  
Problems in the estimation of barley yields by remote sensing p 13 N89-18881

## CROP IDENTIFICATION

Aerial remote sensing technique in the identification and acreage estimation of various plantations - A case study in Gorakhpur district, Uttar Pradesh, India p 2 A89-20819  
Development of principal component analysis applied to multitemporal Landsat TM data p 4 A89-28035  
Crops radar responses analysis based on AGRISAR '86 data p 15 N89-18947  
Extraction of agricultural plant parameters from multitemporal Thematic Mapper (TM) and X-SAR data p 15 N89-18948  
Change detection in AGRISAR images p 15 N89-18949

## CROP INVENTORIES

Digital image analysis of Landsat MSS data in an estate crop inventory of the Island of Bali p 1 A89-20756  
The feasibility study of oil palm area estimation in the southern part of Thailand using Landsat data p 2 A89-20760  
Relationship of spectral data and grain yield variation in rice (*Oryza sativa* L.) ADT 31 p 2 A89-20762  
Determination of relative crop areas from spectrometric data p 22 A89-22218  
Water turbidity and perpendicular vegetation indices for paddy rice flood damage analyses p 6 A89-29412  
Satellite derived earth surface temperatures: A crop assessment tool p 8 N89-17930  
Correlations between agricultural plant parameters and multitemporal radar scatterometer data: First results from the European AGRISAR 87 campaign p 16 N89-18951

## CROP VIGOR

Aerospace imagery and data for modelling erosion, sediment yield and crop yield prediction using GIS, applied to the Upper Komering catchment, Sumatra p 2 A89-20802  
Assessing extent of damage caused by flooding and drought in dominantly rice cropland area using Landsat data p 2 A89-20814

## CROPS

Radar signature measurements during the AGRISAR campaigns p 15 N89-18950

## CROSS CORRELATION

Auto and cross correlation analysis of environment, system and target parameters for iceberg detection using airborne radar p 45 N89-18874

## CURVES (GEOMETRY)

Automated linear feature detection and its application to curve location in synthetic aperture radar imagery p 59 N89-18764

## CYCLONES

Observation of the degree of glaciation in middle-level stratiform clouds p 62 A89-23464  
Physical retrieval of rainfall rates over the ocean by multispectral microwave radiometry - Application to tropical cyclones p 37 A89-32434

## D

## DAMAGE ASSESSMENT

Correlation of reflectance and chlorophyll fluorescence signatures of healthy and damaged forest trees p 9 N89-18726  
Possibilities of the satellite imagery to locate the forest decline areas in the Voages Massif (France) p 10 N89-18729  
Assessment of land/soil degradation in northern Burkina Faso p 13 N89-18882

## E

## DATA ACQUISITION

- Operational remote sensing in the United Kingdom:  
Problems of image acquisition p 68 N89-18751  
Satellite data acquisition planning at the Canada Center  
for Remote Sensing p 68 N89-18753  
MODIS information, data and control system (MIDACS)  
operations concepts  
[NASA-TM-100720] p 75 N89-19729

## DATA BASES

- Landscape processing of satellite imagery for a  
biospheric data bank p 56 A89-30239  
The algorithm development facility: Its role in the  
development and operation of a satellite data centre  
p 68 N89-18755

## DATA COMPRESSION

- Image compression using a neural network  
p 58 N89-18705

## DATA INTEGRATION

- Prioritization of watershed with regard to silt yield  
potential through data integration technique  
p 48 A89-20818  
Integration of SPOT data in an urban data bank - Locating  
work sites p 18 A89-31891

## DATA MANAGEMENT

- Plans for the development of EOS SAR systems using  
the Alaska SAR facility --- Earth Observing System  
(EOS) p 69 N89-18757

## DATA PROCESSING

- Soil and vegetation mapping by using SPOT image  
p 1 A89-20758  
MOS-1 data processing in Tokai Space Center  
p 52 A89-20790  
Spatial information processings of TM data  
p 52 A89-20791  
The luxuriant image - An introduction to remote sensing  
data processing p 55 A89-27937  
Mapping and inventory of forest fires from digital  
processing of TM data p 5 A89-28129  
Visual and digital classification of Landsat TM data for  
soil, physiography and land use mapping in Axios alluvial  
plain, Thessaloniki, Greece p 5 A89-28130  
Image compression using a neural network  
p 58 N89-18705  
Post-processing airborne SAR data for multitemporal  
land-cover studies p 12 N89-18857  
MODIS information, data and control system (MIDACS)  
operations concepts  
[NASA-TM-100720] p 75 N89-19729

## DATA PROCESSING EQUIPMENT

- The Alaska SAR processor p 70 N89-18851

## DATA RECORDERS

- Receiving and processing system for meteorological  
satellite (NOAA) p 53 A89-20806

## DATA REDUCTION

- Using different sources of information in automated  
linear feature extraction from remote sensing data  
[INPC-4708-PRE/1390] p 24 N89-15447

## DATA RETRIEVAL

- Receiving and processing system for meteorological  
satellite (NOAA) p 53 A89-20806

## DATA SAMPLING

- Optimal sampling for remote sensing: Estimating the  
regional mean p 11 N89-18822  
Vegetation sampling for studies using remotely sensed  
data p 13 N89-18883

## DATA SIMULATION

- Simulation of radiometric ocean images recorded from  
high-altitude platforms p 33 A89-27980  
Extreme variability, scaling and fractals in remote  
sensing - Analysis and simulation p 56 A89-29074

## DATA STORAGE

- Microcomputers and mass storage devices for image  
processing p 65 A89-29070

## DEFECTS

- Artefacts in AIS-1 imagery --- Airborne Image  
Spectrometer (AIS) p 69 N89-18826

## DEFOCUSING

- Estimation of the SAR system transfer through processor  
defocus p 37 N89-18706

## DEFORESTATION

- Airborne multispectral remote sensing of forest decline  
in West Germany p 1 A89-20757  
Possibilities of the satellite imagery to locate the forest  
decline areas in the Vosges Massif (France)  
p 10 N89-18729

## DEFORMATION

- Displacement calculations from geodetic data and the  
testing of geophysical deformation models  
p 19 A89-22639  
Geodetic measurement of deformation in California  
[NASA-CR-184604] p 19 N89-15476

## DEGRADATION

- Assessment of land/soil degradation in northern Burkina  
Faso p 13 N89-18882

## DELINEATION

- Delineation of salt-affected soils through digital analysis  
of Landsat MSS data p 6 A89-30262

## DESERTIFICATION

- Assessment of land/soil degradation in northern Burkina  
Faso p 13 N89-18882

## DESERTS

- Large-scale, low-amplitude bedforms (chevrons) in the  
Selima sand sheet, Egypt p 23 A89-31755  
The effect of soil moisture on reflectance characteristics  
of salt crusts p 16 N89-18966

## DEVELOPING NATIONS

- Technology transfer for development of coastal zone  
resources: Caribbean experts examine critical issues  
p 40 N89-18749

## DELECTRIC PROPERTIES

- Active and passive remote sensing of ice  
[AD-A201915] p 47 N89-19792

## DELECTRICS

- Passive microwave remote sensing system for soil  
moisture - Some supporting research p 49 A89-31848

## DIGITAL DATA

- Digital image analysis of Landsat MSS data in an estate  
crop inventory of the island of Bali p 1 A89-20756  
An interactive system for aerial photo orientation of  
digital stereo image pairs p 53 A89-20799  
Multiple source data processing in remote sensing  
p 58 A89-29073  
Overview of low-cost map digitizing systems  
[DE89-002872] p 57 N89-16204  
Mapping slope failure tracks with digital Thematic  
Mapper data p 59 N89-18790

## DIGITAL FILTERS

- Image processing techniques - Filtering, exogenous  
data, geometrical processing p 55 A89-27938  
Application of the Haar transform for extraction of linear  
and anomalous patterns over part of Cambay Basin,  
India p 55 A89-28037

## DIGITAL SIMULATION

- Visualization of topographic data using video  
animation p 55 A89-29066

## DIGITAL SYSTEMS

- Overview of low-cost map digitizing systems  
[DE89-002872] p 57 N89-16204

## DIGITAL TECHNIQUES

- Usefulness of remote sensing in uranium exploration  
programme in parts of Karnataka state, India  
p 21 A89-20828

- A procedure for land area classification using Landsat  
TM digital imagery p 17 A89-24651

- Digital image processing in remote sensing --- Book  
p 55 A89-29064

- Digital processing of a lineament grid with the aim of  
analyzing regional tectonic structures of the western  
Himalayas in India p 23 A89-30116

## DISASTERS

- Some aspects of space applications for disaster  
management - The use of space technology for disaster  
warning and for determining the effects of natural  
disasters  
[IAF PAPER 86-426] p 18 A89-24849

## DISPLACEMENT

- Displacement calculations from geodetic data and the  
testing of geophysical deformation models  
p 19 A89-22639

## DISPLAY DEVICES

- New technology for displaying of NOAA AVHRR thermal  
band image p 29 A89-20810

## DOPPLER EFFECT

- The effect of internal waves on the Doppler spectrum  
of microwaves scattered from the ocean surface  
p 41 N89-18783

## DOPPLER RADAR

- Applications of the NCAR Electra Doppler radar for the  
study of physical parameters of clouds  
p 75 N89-19717

## DRAINAGE PATTERNS

- Drainage pattern analysis with the aid of Landsat MSS  
data of the Citarium river basin, West Java, Indonesia  
p 48 A89-20778

## DROUGHT

- Assessing extent of damage caused by flooding and  
drought in dominantly rice cropland area using Landsat  
data p 2 A89-20814

- Extension of a drought monitoring and vegetation  
classification methodology to the western Sahel  
p 4 A89-28127

## DUNES

- Large-scale, low-amplitude bedforms (chevrons) in the  
Selima sand sheet, Egypt p 23 A89-31755

## DUST

- Long-range transport of giant mineral aerosol particles  
p 17 A89-21931

## EARLY WARNING SYSTEMS

- Some aspects of space applications for disaster  
management - The use of space technology for disaster  
warning and for determining the effects of natural  
disasters  
[IAF PAPER 86-426] p 18 A89-24849

## EARTH ALBEDO

- Determination of clear-sky planetary albedo  
p 62 A89-22214  
Modeling vegetation as a set of scatterers  
p 7 A89-32110

## EARTH ATMOSPHERE

- Applications of the NCAR Electra Doppler radar for the  
study of physical parameters of clouds  
p 75 N89-19717

## EARTH CORE

- Research in geodesy and geophysics based upon radio  
interferometric observations of extragalactic radio  
sources  
[AD-A200958] p 25 N89-17933

## EARTH CRUST

- A surface-wave study of the Pacific Ocean basin  
p 29 A89-21798  
Neotectonic zoning of Belorussia on the basis of space  
data p 21 A89-22215  
The crustal field p 22 A89-22677  
The solid oceanic crust (The Lithos project) --- Russian  
book p 36 A89-32108  
Tectonics of the central Andes  
[NASA-CR-184683] p 28 N89-18973

## EARTH MANTLE

- A surface-wave study of the Pacific Ocean basin  
p 29 A89-21798  
The solid oceanic crust (The Lithos project) --- Russian  
book p 36 A89-32108  
Principal problems in upgrading quality and efficiency  
of geological survey work p 24 N89-17910  
Research in geodesy and geophysics based upon radio  
interferometric observations of extragalactic radio  
sources  
[AD-A200958] p 25 N89-17933

## EARTH MOVEMENTS

- The application of remote sensing to geomorphological  
mapping and mass movement study in the vicinity of Provo,  
Utah p 23 N89-15439

## EARTH OBSERVATIONS (FROM SPACE)

- Effectiveness of soil mapping on the basis of space  
photographic data p 3 A89-22249  
Optical methods of satellite hydrophysics. Investigation  
of the environment from manned orbital stations --- Russian  
book p 32 A89-26181  
JEOS - A low-cost approach to earth observation  
p 63 A89-26399

- The characterization of sources of illumination in a  
Ponderosa Pine (*Pinus ponderosa*) forest community using  
the portable instantaneous display and analysis  
spectrometer p 4 A89-27781  
Fundamentals of remote sensing p 63 A89-27934  
Large-scale, low-amplitude bedforms (chevrons) in the  
Selima sand sheet, Egypt p 23 A89-31755

- The 1988 International Geoscience and Remote Sensing  
Symposium (IGARSS 1988) on Remote Sensing: Moving  
Towards the 21st Century, Volume 3  
[ESA-SP-284-VOL-3] p 68 N89-18704  
Requirements for an EOS-oriented workstation --- Earth  
Observing System (EOS) p 69 N89-18813  
NASA's Earth Observing System (EOS): An opportunity  
for mankind p 77 N89-18816

- Proceedings of the 1988 International Geoscience and  
Remote Sensing Symposium (IGARSS '88 on Remote  
Sensing: Moving Towards the 21st Century, Volume 2  
[ESA-SP-284-VOL-2] p 69 N89-18836  
Signature variations due to atmospheric and topographic  
effects on satellite MSS data over rugged terrain  
p 70 N89-18877

- A possibility for selecting spectral bands of future land  
application sensors at the example of an imaging  
spectrometer p 60 N89-18896  
X-SAR: A new spaceborne synthetic aperture radar  
p 73 N89-18923

## EARTH OBSERVING SYSTEM (EOS)

- Optical system design alternatives for the  
Moderate-Resolution Imaging Spectrometer-Tilt  
(MODIS-T) for the Earth Observing System (EOS)  
p 63 A89-27753  
MODIS - Advanced facility instrument for studies of the  
earth as a system --- Moderate Resolution Imaging  
Spectrometer p 66 A89-31943  
MISR - A multiangle imaging spectroradiometer for  
geophysical and climatological research from EOS  
p 66 A89-31946

- Passive microwave remote sensing system for soil  
moisture - Some supporting research p 49 A89-31948

- Land image data processing requirements for the EOS era p 56 A89-31949  
Plans for the development of EOS SAR systems using the Alaska SAR facility --- Earth Observing System (EOS) p 69 N89-18757
- EARTH RESOURCES**  
Principal results of remote-sensing studies of Siberia's natural resources (On the occasion of the 10th anniversary of the Scientific Coordination Council, 1977-1987) p 62 A89-22225  
Principal problems in upgrading quality and efficiency of geological survey work p 24 N89-17910  
Simulation of optical remote sensing systems for earth resource analysis p 74 N89-18964
- EARTH SURFACE**  
Displacement calculations from geodetic data and the testing of geophysical deformation models p 19 A89-22639  
Radar imaging of the surfaces of Venus and the earth using SAR data p 54 A89-23645  
Aerial and space remote-sensing techniques for geographical investigations --- Russian book p 62 A89-26178  
A 10 km resolution image of the entire night-time earth based on cloud-free satellite photographs in the 400-1100 nm band p 58 A89-30256  
Theoretical study of the sensitivity of the microwave backscattering coefficient to the soil surface parameters p 6 A89-30267  
The application of remote sensing to geomorphological mapping and mass movement study in the vicinity of Provo, Utah p 23 N89-15439
- ECOLOGY**  
Pattern analysis and the ecological interpretation of satellite imagery p 61 N89-18900
- ECOSYSTEMS**  
Study on changes of mangrove forest in Thailand by using Landsat imagery p 3 A89-20822  
Characterizing forest ecosystem dynamics through modelling and remote sensing observations p 10 N89-18728  
LANDSAT TM study of afforestation in northern Scotland and its impact on breeding bird populations p 10 N89-18732
- EL NINO**  
Circulation in the East Asian seas from satellite and ship data p 29 A89-20803
- ELASTIC DEFORMATION**  
Research in geodesy and geophysics based upon radio interferometric observations of extragalactic radio sources [AD-A200958] p 25 N89-17933
- ELASTIC PLATES**  
Research in geodesy and geophysics based upon radio interferometric observations of extragalactic radio sources [AD-A200958] p 25 N89-17933
- ELECTROMAGNETIC NOISE**  
A comparison of clutter texture properties in optical and SAR images p 8 N89-18708
- ELECTROMAGNETIC RADIATION**  
Normalized radar cross section of natural surfaces at millimeter wavelengths [AD-A202252] p 75 N89-19475
- ELECTROMAGNETIC SCATTERING**  
Modeling vegetation as a set of scatterers p 7 A89-32110
- EMERGENCIES**  
Some aspects of space applications for disaster management - The use of space technology for disaster warning and for determining the effects of natural disasters [IAF PAPER 86-426] p 18 A89-24849
- EMISSIVITY**  
Comparison between microwave emissivity and backscattering coefficient of agricultural fields p 12 N89-18844  
Observed effects of soil organic matter content on the microwave intensity of soils p 12 N89-18845
- EMITTANCE**  
An evaluation of surface emittance and temperature data derived from Thermal Infrared Multispectral Scanner (TIMS) for lithological mapping in weathered vegetated terrain: N. Queensland, Australia p 27 N89-18934
- ENERGY METHODS**  
Segmentation of Synthetic Aperture Radar (SAR) images of ocean surface by the texture energy transform method [AD-A199536] p 37 N89-15309
- ENVIRONMENT EFFECTS**  
LANDSAT TM study of afforestation in northern Scotland and its impact on breeding bird populations p 10 N89-18732
- ENVIRONMENT MODELS**  
A comparison of models for deriving dry deposition fluxes of O<sub>3</sub> and SO<sub>2</sub> to a forest canopy p 3 A89-20923
- ENVIRONMENTAL MONITORING**  
Airborne multispectral remote sensing of forest decline in West Germany p 1 A89-20757  
The relationship between suspended sediment concentration and remotely sensed spectral radiance - A review p 48 A89-24649  
Effectiveness of satellite remote sensing on monitoring of marine environment [IAF PAPER 88-153] p 32 A89-24875  
Definition and design of an operational environment-monitoring system p 18 A89-27788  
Monitoring surface mineral workings using TM and SPOT p 26 N89-18796
- EQUATIONS OF MOTION**  
A method to forecast open pack ice speed of motion using remotely-sensed data p 42 N89-18801
- ERROR ANALYSIS**  
Errors of the gravitational field determined by the satellite p 19 A89-24442
- ERS-1 (ESA SATELLITE)**  
ERS-1 active microwave instrumentation design and performance status [IAF PAPER 87-136] p 65 A89-28329  
The central user services system for ERS-1 p 68 N89-18754  
Impact of phase and amplitude errors on the ERS-1 active microwave instrumentation performance p 70 N89-18853  
ERS-1 operation capabilities p 71 N89-18884  
Engineering calibration of the ERS-1 active microwave instrumentation in orbit p 71 N89-18885  
The pre-launch performance verification of the ERS-1 active microwave instrumentation p 71 N89-18886  
A software package for performance evaluation of the ERS-1 AMI --- Active Microwave Instrument (AMI) p 71 N89-18887  
ERS-1 active microwave instrumentation engineering model performance p 71 N89-18888  
Stability considerations for the ERS-1 wind scatterometer radiometric performance p 71 N89-18889  
ERS-1 AMI antennas: The design and development experience --- Active Microwave Instrumentation (AMI) p 71 N89-18890  
ERS-1 altimeter height calibration p 71 N89-18891  
Quality control of fast delivery processors and products --- ERS-1 p 72 N89-18892  
A SAR data quality assessment scheme for the ERS-1 mission p 72 N89-18893
- EUROPEAN SPACE PROGRAMS**  
German spaceborne remote sensing activities p 67 N89-18887  
NASA's Earth Observing System (EOS): An opportunity for mankind p 77 N89-18816  
Mission aspects of a future European polar orbit earth observation facility p 74 N89-18952
- EUTROPHICATION**  
Radiation models of mesotrophic and eutrophic bodies of water p 36 A89-30120
- EVAPORATION**  
The effect of soil moisture on reflectance characteristics of salt crusts p 16 N89-18966
- EVAPOTRANSPIRATION**  
An estimation of areal evapotranspiration using Landsat and elevation data p 48 A89-20776
- EXPERIMENT DESIGN**  
Remote sensing in a marginal ice zone: A brief overview p 46 N89-18941
- EXPERT SYSTEMS**  
Land image data processing requirements for the EOS era p 56 A89-31949  
Information fusion by a knowledge-based system for SAR image interpretation p 60 N89-18831  
Progress in automatic analysis of multi-temporal remotely-sensed data p 61 N89-18956
- EXTINCTION**  
The extinction properties of forest components p 14 N89-18918
- EXTREMELY HIGH FREQUENCIES**  
Retrieval of water vapor profiles from microwave radiometric measurements at 183 and 92 GHz p 72 N89-18905  
Atmospheric attenuation as derived from microwave radiometry at 52.8 GHz p 72 N89-18906  
EHF attenuation through the melting layer p 51 N89-18984
- F**
- FARM CROPS**  
Determination of relative crop areas from spectrometric data p 22 A89-22218  
Agrometeorological aspects of the utilization of remote-sensing data p 3 A89-23663
- Modeling vegetation as a set of scatterers p 7 A89-32110
- FARMLANDS**  
Comparison between microwave emissivity and backscattering coefficient of agricultural fields p 12 N89-18844  
Estimating the extent of irrigated cropland in a large catchment using LANDSAT MSS data p 14 N89-18902
- FEASIBILITY ANALYSIS**  
The feasibility study of oil palm area estimation in the southern part of Thailand using Landsat data p 2 A89-20760
- FEATURE IDENTIFICATION AND LOCATION EXPER**  
Using different sources of information in automated linear feature extraction from remote sensing data [INPE-4708-PRE/1390] p 24 N89-15447
- FISHERIES**  
The extraction of sea fishery potential area from Airborne Ocean Color Radiometer data p 28 A89-20786  
The preliminary study on correlation between satellite information and bottom trawling ground in the East China Sea and the Yellow Sea p 29 A89-20805  
A multi-sensor remote sensing approach for measuring primary production from space [NASA-CR-184662] p 37 N89-15444  
Quick reporting state of fishery and sea on the East China Sea and the Yellow Sea with NOAA p 39 N89-18741
- FLIGHT CHARACTERISTICS**  
Features of the calculation of the main characteristics of an oceanographic radar altimeter p 32 A89-23646
- FLIGHT TESTS**  
Airborne nonacoustic bathymetric survey flight test results p 51 N89-18937
- FLOOD DAMAGE**  
Water turbidity and perpendicular vegetation indices for paddy rice flood damage analyses p 6 A89-29412
- FLOOD PREDICTIONS**  
Flooded and inundation dangerous area prediction and its visualisation - A case study on the Pemali-Comal River Basin, Central Java, Indonesia p 48 A89-20774  
Hydrological aspects of combined effects of storm surges and heavy rainfall on river flow [WMO-704] p 49 N89-17340
- FLOODS**  
Monitoring inundation area of Aliran Sungai Bengawan Solo Jawa Timur with Landsat images p 48 A89-20768  
Assessing extent of damage caused by flooding and drought in dominantly rice cropland area using Landsat data p 2 A89-20814  
Hydrological aspects of combined effects of storm surges and heavy rainfall on river flow [WMO-704] p 49 N89-17340
- FLUID BOUNDARIES**  
Loop Current boundary variations --- in eastern Gulf of Mexico p 31 A89-22596
- FLUID MECHANICS**  
Erosional furrows formed during the lateral blast at Mount St. Helens, May 18, 1980 p 22 A89-22632
- FLUORESCENCE**  
Correlation of reflectance and chlorophyll fluorescence signatures of healthy and damaged forest trees p 9 N89-18726  
Correlation of radar reflectivity and chlorophyll fluorescence of forest trees p 9 N89-18727  
Mapping of phytoplankton fluorescence with the Fluorescence Line Imager (FLI) imaging spectrometer p 39 N89-18737
- FORECASTING**  
A comparison of original aircraft MSS and generated surface water reflectance images as predictors of lake water quality indicators [DE89-004882] p 50 N89-17932  
A method to forecast open pack ice speed of motion using remotely-sensed data p 42 N89-18801  
Toward the automated use of remote sensing data in operational ice forecasting p 43 N89-18804
- FOREST FIRE DETECTION**  
Mapping and inventory of forest fires from digital processing of TM data p 5 A89-28129
- FOREST FIRES**  
Trace gas emissions from chaparral and boreal forest fires p 7 A89-32432
- FOREST MANAGEMENT**  
Monitoring of agro-forestry production systems in the Sudano-Sahelian zone of West Africa p 11 N89-18825  
The use of SPOT-1 imagery for forest classification in Flanders (Belgium) p 14 N89-18899  
Application of radar polarimetry to forestry p 15 N89-18919

## FORESTS

- Comparative study of vegetation index and false colour composite image of NOAA-AVHRR data for bio-mass studies p 1 A89-20752
- Spectral reflectance properties of a leaf of some mangrove species in Okinawa p 1 A89-20753
- Airborne multispectral remote sensing of forest decline in West Germany p 1 A89-20757
- Forest observation by satellite p 1 A89-20759
- On classification of forests of some portions of central India using satellite imageries p 2 A89-20761
- Study on changes of mangrove forest in Thailand by using Landsat imagery p 3 A89-20822
- A comparison of models for deriving dry deposition fluxes of O<sub>3</sub> and SO<sub>2</sub> to a forest canopy p 3 A89-20923
- Dependence of snow melting and surface-atmosphere interactions on the forest structure p 3 A89-21740
- Dispersion parameters over forested terrain p 3 A89-22728
- Remote sensing of canopy chemistry and nitrogen cycling in temperate forest ecosystems p 3 A89-23431
- The characterization of sources of illumination in a Ponderosa Pine (*Pinus ponderosa*) forest community using the portable instantaneous display and analysis spectrometer p 4 A89-27781
- Analysis and interpretation of SPOT images of urban and agricultural/forest sections of the Sherbrooke region p 5 A89-29373
- Unsupervised training area selection in forests using a nonparametric distance measure and spatial information p 6 A89-30265
- The classification of loamy ground in the Outre-Forêt region of Alsace in France using Landsat 5 TM images p 7 A89-31890
- Determining the age of cut forest areas in Quebec, Canada using the Landsat-5 TM p 7 A89-31893
- Extraction of small-scale spatial information from SLAR raw data of forests through an analysis of speckle p 8 A89-18709
- Assessment of clearcut mapping accuracy with C-band SAR p 9 A89-18725
- Characterizing forest ecosystem dynamics through modelling and remote sensing observations p 10 A89-18728
- Possibilities of the satellite imagery to locate the forest decline areas in the Vosges Massif (France) p 10 A89-18729
- Texture analysis of forest regeneration sites in high-resolution SAR imagery p 10 A89-18730
- Association of radar backscattering with biophysical characteristics of Australian forests p 10 A89-18731
- LANDSAT TM study of afforestation in northern Scotland and its impact on breeding bird populations p 10 A89-18732
- Radar signature measurements during the AGRISCATT campaigns p 15 A89-18950

## FORWARD SCATTERING

- The extinction properties of forest components p 14 A89-18918

## FRACTALS

- Fractal features of sea surface manifested in microwave remote sensing signatures p 32 A89-24872
- Extreme variability, scaling and fractals in remote sensing - Analysis and simulation p 56 A89-29074
- Fractal properties of the sea surface manifested in microwave remote sensing signatures p 41 A89-18784

## FRESH WATER

- Data processing for the determination of pigments and suspended solids from Thematic Mapper data p 50 A89-18736

## G

## GAS EXCHANGE

- Satellite determination of the carbon dioxide exchange coefficient at the ocean-atmosphere interface - A first step p 31 A89-22598

## GEOCHEMISTRY

- Application of Landsat imagery and surficial geochemistry to the discovery of tungsten skarn deposits associated with buried plutons, Yukon and Northwest Territories, Canada p 23 A89-28126

## GEOCHRONOLOGY

- The use of aerial photographs in Quaternary-volcanic terrains mapping p 20 A89-20784

## GEODESY

- Reports on cartography and geodesy, series 1, number 100 [ISSN-0469-4236] p 20 A89-17935
- The geometry of geodetic inverse linear mapping and nonlinear adjustment [ETN-89-93900] p 20 A89-19736

## GEODETTIC COORDINATES

- The geometry of geodetic inverse linear mapping and nonlinear adjustment [ETN-89-93900] p 20 A89-19736

## GEODETTIC SATELLITES

- An algorithm for analysis of plate motions in Crust Dynamics Project (CDP) networks [B8821606] p 19 A89-17371

## GEODETTIC SURVEYS

- Displacement calculations from geodetic data and the testing of geophysical deformation models p 19 A89-22639
- Geodetic measurement of deformation in California [NASA-CR-184604] p 19 A89-15476
- Comparison of GPS surveys with historical triangulation surveys in the southern California borderland [NASA-CR-183405] p 24 A89-16199
- Reference coordinate systems: An update. Supplement 11 [NASA-CR-184764] p 19 A89-16207
- Research, investigations and technical developments. National mapping program, 1985-1986 [USGS-OPEN-FILE-REPT-87-315] p 24 A89-16208

## GEOGRAPHIC INFORMATION SYSTEMS

- The role of remote sensing in geographic information systems using computer p 17 A89-20792
- Aerospace imagery and data for modelling erosion, sediment yield and crop yield prediction using GIS, applied to the Upper Komering catchment, Sumatra p 2 A89-20802
- Interactive image feature compilation for geographic information systems p 18 A89-27785
- Landscape processing of satellite imagery for a biosphere data bank p 56 A89-30239
- Updating land-use information on topographic maps using satellite imagery: Combining the advantages of two accessible sources of geographic information p 60 A89-18897

## GEOIDS

- Detection of ocean bottom relief by local geoid p 35 A89-29731
- Local geoid determination using the global positioning system [AD-A202220] p 20 A89-19731

## GEOLOGICAL FAULTS

- Fault classification for the geological support of the tunnel construction project for the Caucasus mountain-pass railroad, using space images p 22 A89-22216
- Annular and block-folded structures on space and aerial photographs p 25 A89-17915
- Enhancement of glacial fractures by analysis of Thematic Mapper data: Glen Roy, Scotland p 26 A89-18859

## GEOLOGICAL SURVEYS

- Neotectonic zoning of Belorussia on the basis of space data p 21 A89-22215
- Features of the geological structure of the polar Urals and the distribution of certain minerals, as evaluated on the basis of the interpretation of aerial and space photographs p 23 A89-30119
- Knowledge related aspects of lineation and lineament extraction [INPE-4709-PRE/1391] p 24 A89-15446
- Research, investigations and technical developments. National mapping program, 1985-1986 [USGS-OPEN-FILE-REPT-87-315] p 24 A89-16208
- Principal problems in upgrading quality and efficiency of geological survey work p 24 A89-17910
- Annular and block-folded structures on space and aerial photographs p 25 A89-17915
- Integration of digital satellite and geophysical data, Heath Steele Mines, New Brunswick, Canada p 25 A89-18792
- Image processing methods for the presentation of multiple geological datasets from the English Lake District p 25 A89-18793
- Integration of geological, geophysical and remotely sensed data for the Solway Basin, England p 26 A89-18794
- Enhancement of glacial fractures by analysis of Thematic Mapper data: Glen Roy, Scotland p 26 A89-18859
- Interpreting the geology of Glen Coe using LANDSAT MSS data and aerial photographs p 26 A89-18860
- Applications of LANDSAT Thematic Mapper imagery to the study of subtle variations in lithology p 27 A89-18863
- Results of tectonic and spectral investigations in the coast range of northern Chile using special processed Thematic Mapper (TM) data p 27 A89-18929
- Investigations of the Cerro Colorado pluton, northern Chile, using enhanced LANDSAT Thematic Mapper images p 27 A89-18930
- Automatic mineral map generation procedure from imaging spectrometer data p 27 A89-18931
- Geological applications of thermal infrared characteristics of vegetation p 27 A89-18932

- Improvements in the forward and inverse principal component transformations for geological mapping in a semi-arid terrain p 27 A89-18933
- An evaluation of surface emittance and temperature data derived from Thermal Infrared Multispectral Scanner (TIMS) for lithological mapping in weathered vegetated terrain: N. Queensland, Australia p 27 A89-18934
- Geological remote sensing of Palaeogene rocks in the Wind River Basin, Wyoming, USA p 28 A89-18935

## GEOLOGY

- The geology of the area surrounding Lake Kerinci, Indonesia as interpreted through SIR-B imageries p 20 A89-20781
- Tectonics of the central Andes [NASA-CR-184683] p 28 A89-18973

## GEOMAGNETISM

- The crustal field p 22 A89-22877

## GEOMETRIC ACCURACY

- A high fidelity, high throughput system for geocoding SAR imagery p 60 A89-18849

## GEOMETRIC RECTIFICATION (IMAGERY)

- Geometric correction of SPOT image p 54 A89-20812
- Image processing techniques - Filtering, exogenous data, geometrical processing p 55 A89-27938

## GEOMETRICAL OPTICS

- The effects of viewing geometry on image classification p 55 A89-28036
- Observations of the effect of geometric properties of agricultural soils on radar backscatter, from C-SAR images p 11 A89-18781

## GEOMETRY

- Study of geometric quality of the MSS-LANDSAT imagery [INPE-4653-PRE/1360] p 57 A89-15440

## GEOMORPHOLOGY

- Coastline monitoring in Madura Strait, Indonesia on 1972-1985 p 29 A89-20804
- Identification of geological features from their surface textural properties using OPS measurements --- Optical Power Spectra p 21 A89-20820
- Visual and digital classification of Landsat TM data for soil, physiography and land use mapping in Axios alluvial plain, Thessaloniki, Greece p 5 A89-28130
- Ring structures of buried platform areas and the evaluation of their tectonic activity on the basis of geomorphological data p 23 A89-30118
- Geological mapping and analysis of fracturing in the south part of the Central Anti-Atlas in Morocco using a Landsat MSS image p 23 A89-31887
- The solid oceanic crust (The Lithos project) --- Russian book p 36 A89-32108
- The application of remote sensing to geomorphological mapping and mass movement study in the vicinity of Provo, Utah p 23 A89-15439
- A quantitative geomorphology study of main carbonate massifs of central and southern Apennines (Italy) based on a digital elevations archive p 25 A89-18791
- Tectonics of the central Andes [NASA-CR-184683] p 28 A89-18973

## GEOPHYSICS

- MISR - A multiangle imaging spectroradiometer for geophysical and climatological research from EOS p 66 A89-31946
- Research in geodesy and geophysics based upon radio interferometric observations of extragalactic radio sources [AD-A200958] p 25 A89-17933
- Integration of geological, geophysical and remotely sensed data for the Solway Basin, England p 26 A89-18794

## GEOPOTENTIAL

- Errors of the gravitational field determined by the satellite p 19 A89-24442

## GEOSAT SATELLITES

- The Geosat orbit adjust p 19 A89-22316
- Frontal signals east of Iceland from the Geosat altimeter p 33 A89-26643
- Dynamic topography as measured by the Geosat altimeter in regions of small surface height signatures p 43 A89-18837
- The influence of water vapor on the detection of ocean mesoscale fronts and eddies by the Geosat altimeter p 44 A89-18839
- The Navy Geosat radar altimeter satellite mission p 45 A89-18909
- Investigations of sea ice using coincident Geosat altimetry and synthetic aperture radar during MIZEX-87 p 46 A89-18945
- Estimation of sea-ice type and concentration by linear unmixing of Geosat altimeter waveforms p 47 A89-18946

## GEOTECHNICAL ENGINEERING

- Applications of image scanning and processing in rock shear surface study p 20 A89-20779



## GEOTEMPERATURE

Application of a flux algorithm to a field-satellite campaign over vegetated area p 6 A89-29411

## GLACIOLOGY

Technological limitations to satellite glaciology p 36 A89-30257  
Enhancement of glacial fractures by analysis of Thematic Mapper data: Glen Roy, Scotland p 26 N89-18659

## GLOBAL POSITIONING SYSTEM

Comparison of GPS surveys with historical triangulation surveys in the southern California borderland [NASA-CR-183405] p 24 N89-16199  
Local geoid determination using the global positioning system [AD-A202220] p 20 N89-19731

## GOLD

Radar imagery as a tool for mineral exploration - A case study of gold mineralization in East Kalimantan p 20 A89-20780

## GONIOMETERS

Goniometric observations of light scattered from soils and leaves p 4 A89-24873

## GOVERNMENT/INDUSTRY RELATIONS

The Geospace philosophy: A new practical approach in remote sensing and planning for local authorities p 76 N89-18750

## GOVERNMENTS

Research, investigations and technical developments. National mapping program, 1985-1986 [USGS-OPEN-FILE-REPT-87-315] p 24 N89-16208

## GRASSLANDS

The studies for the computer classification and the investigation of grasslands in Tibet using Space-Lab color infrared image p 1 A89-20754  
Visual and computer classifications of remotely-sensed images - A case study of grasslands in Cambridgeshire p 7 A89-30269  
Multitemporal study of differently farmed permanent grazing lands in the Lorraine region of France using SPOT-1 data p 7 A89-31894  
Mapping of natural vegetation in north-east Zimbabwe by means of LANDSAT Thematic Mapper data p 14 N89-18901

## GRAVELS

Monitoring surface mineral workings using TM and SPOT p 26 N89-18796

## GRAVIMETRY

Airborne gravity as a supporting tool for hydrocarbon exploration in Indonesia p 21 A89-20829  
Local geoid determination using the global positioning system [AD-A202220] p 20 N89-19731

## GRAVITATION

Integration of geological, geophysical and remotely sensed data for the Solway Basin, England p 26 N89-18794

## GRAVITATIONAL FIELDS

Integrated study of Landsat, aeromagnetic and Bouguer gravity anomaly data for geological appraisal - A case study from Tamil Nadu, India p 21 A89-20823  
Errors of the gravitational field determined by the satellite p 19 A89-24442

## GRAVITY WAVES

Wavenumber spectra of short gravity waves p 35 A89-30019  
SAR imaging of ocean waves in the marginal ice zone p 40 N89-18747

## GRAY SCALE

Segmentation of SAR images p 58 N89-18759

## GRID GENERATION (MATHEMATICS)

A basic study of the reduction of the exactness of mesh data map made by uniting n-squared meshes to one mesh p 54 A89-20811

## GROUND STATIONS

MODIS-HIRIS ground data systems commonality report [NASA-TM-100718] p 67 N89-16205  
Plans for the development of EOS SAR systems using the Alaska SAR facility --- Earth Observing System (EOS) p 69 N89-18757

## GROUND SUPPORT EQUIPMENT

Receiving and processing system for meteorological satellite (NOAA) p 53 A89-20806

## GROUND SUPPORT SYSTEMS

MOS-1 data processing in Tokai Space Center p 52 A89-20790  
Low cost, microcomputer-based interactive analysis system for direct-reception and archived remote sensing data p 53 A89-20796  
The central user services system for ERS-1 p 68 N89-18754

## GROUND TRUTH

Vegetation sampling for studies using remotely sensed data p 13 N89-18883

Correlations between agricultural plant parameters and multitemporal radar scatterometer data: First results from the European AGRISCATT 87 campaign p 16 N89-18951

## GROUND WATER

Reconnaissance groundwater appraisal of Bohol Island, Philippines, by satellite data analysis p 48 A89-20772  
Identification of surface-groundwater interaction zones in the Bogor volcanic fan p 48 A89-20777  
Extracting spectral contrast in Landsat Thematic Mapper image data using selective principal component analysis p 57 A89-32337  
Improvements in ground water recharge estimation using satellite remote sensing p 50 N89-18768  
An assessment of ATM and satellite data for estimating the groundwater contribution to slope stability --- Airborne Thematic Mapper (ATM) p 51 N89-18769  
The effect of soil moisture on reflectance characteristics of salt crusts p 16 N89-18966

## GULF OF MEXICO

Loop Current boundary variations --- in eastern Gulf of Mexico p 31 A89-22596

## H

## HALOS

Brightness of a laser-beam halo in vegetation cover p 3 A89-22221

## HEAT CAPACITY MAPPING MISSION

Nighttime and daytime HCMM thermographs of the Iberian Peninsula p 56 A89-31888

## HEIGHT

ERS-1 altimeter height calibration p 71 N89-18891

## HIGH FREQUENCIES

Normalized radar cross section of natural surfaces at millimeter wavelengths [AD-A202252] p 75 N89-19475

## HIGH RESOLUTION

MODIS-HIRIS ground data systems commonality report [NASA-TM-100718] p 67 N89-16205

## HYDROCARBONS

Application of remote sensing for hydrocarbon exploration on Timor Island, Indonesia p 21 A89-20825

## HYDROGEOLOGY

Reconnaissance groundwater appraisal of Bohol Island, Philippines, by satellite data analysis p 48 A89-20772  
The source of marine magnetic anomalies [MPL-U-42/87] p 31 A89-22876

## HYDROGRAPHY

Analysis of airborne laser hydrography waveforms p 64 A89-27996  
Airborne nonacoustic bathymetric survey flight test results p 51 N89-18937

## HYDROLOGY

Identification of surface-groundwater interaction zones in the Bogor volcanic fan p 48 A89-20777  
Radiation models of mesotrophic and eutrophic bodies of water p 36 A89-30120  
An assessment of ATM and satellite data for estimating the groundwater contribution to slope stability --- Airborne Thematic Mapper (ATM) p 51 N89-18769

## HYDROLOGY MODELS

Estimation of the water exchange and contamination zones of basins from satellite imagery p 49 A89-30252

Improvements in ground water recharge estimation using satellite remote sensing p 50 N89-18768

## HYDROMETEOROLOGY

Satellite remote sensing of rainfall p 49 A89-27946

## HYDROPHONES

The source of marine magnetic anomalies [MPL-U-42/87] p 31 A89-22876

## I

## ICE

Variations of the infrared emission of snow and ice cover p 49 A89-30121

## ICE ENVIRONMENTS

Antarctic Ocean polynyas [NASA-CR-184805] p 47 N89-19102

## ICE FLOES

Physical properties of snow and ice in the winter marginal ice zone of Fram Strait p 46 N89-18944

## ICE FORMATION

Use of SAR imagery and other remotely-sensed data in deriving ice information during a severe ice event on the Grand Banks (Newfoundland) p 40 N89-18746  
Antarctic Ocean polynyas [NASA-CR-184805] p 47 N89-19102

## ICE MAPPING

Step frequency radar experiments on the Antarctic Sea ice p 34 A89-28365

## ICE REPORTING

Intercomparison of synthetic- and real-aperture radar observations of Arctic sea ice during winter MIZEX '87 p 40 N89-18744

SAR imagery of the Grand Banks (Newfoundland) pack ice pack and its relationship to surface features p 40 N89-18745

Observations of ice types in satellite altimeter data p 44 N89-18841

Measuring lead area changes in sea ice imagery --- satellite imagery p 44 N89-18871

Ice ridge observations by means of SAR p 45 N89-18872

Evaluation of VARAN-S SAR data from the BEPERS study project --- sea ice p 45 N89-18875

Remote sensing in a marginal ice zone: A brief overview p 46 N89-18941

Geophysical information on the winter marginal ice zone obtained from SAR p 46 N89-18942

Investigations of sea ice using coincident Geosat altimetry and synthetic aperture radar during MIZEX-87 p 46 N89-18945

Estimation of sea-ice type and concentration by linear unmixing of Geosat altimeter waveforms p 47 N89-18946

Active and passive remote sensing of ice [AD-A201915] p 47 N89-19792

## ICEBERGS

Auto and cross correlation analysis of environment, system and target parameters for iceberg detection using airborne radar p 45 N89-18874

## IGNEOUS ROCKS

The use of aerial photographs in Quaternary-volcanic terrains mapping p 20 A89-20784

Investigations of the Cerro Colorado pluton, northern Chile, using enhanced LANDSAT Thematic Mapper images p 27 N89-18930

## IMAGE ANALYSIS

Digital image analysis of Landsat MSS data in an estate crop inventory of the Island of Bali p 1 A89-20756

The geology of the area surrounding Lake Kerinci, Indonesia as interpreted through SIR-B imageries p 20 A89-20781

Landsat 5 TM image of the Mont Saint-Michel region of France p 54 A89-21249

Contribution of second-generation Landsat TM and SPOT HRV satellites to urban analysis (Rennes, France) p 17 A89-21250

The procedure for and the results of the geological interpretation of photographic images of the Bukhtarma lineament zone p 22 A89-22217

Agrometeorological aspects of the utilization of remote-sensing data p 3 A89-23683

Unsupervised classification of scattering behavior using radar polarimetry data p 63 A89-26843

Using a top-down and bottom-up strategy to analyze high resolution aerial photographs of urban areas p 18 A89-27630

Concepts for processing and analyzing of multiple SAR and Landsat images p 55 A89-27789

Integrated NDVI images for Niger 1986-1987 --- Normalized Difference Vegetation Index p 4 A89-28128

Landscape processing of satellite imagery for a biospheric data bank p 56 A89-30239

Delineation of salt-affected soils through digital analysis of Landsat MSS data p 6 A89-30262

Unsupervised training area selection in forests using a nonparametric distance measure and spatial information p 6 A89-30265

Visual and computer classifications of remotely-sensed images - A case study of grasslands in Cambridgeshire p 7 A89-30269

Knowledge related aspects of lineation and lineament extraction [INPE-4709-PRE/1391] p 24 N89-15446

Extraction of small-scale spatial information from SLAR raw data of forests through an analysis of speckle p 8 N89-18709

Nonlinear filtering and edge detection in speckled radar images p 58 N89-18711

Statistical evaluation of the intensity distribution of sea surface radar images p 38 N89-18717

Sea bottom topography with X-band SLAR: Evaluation of existing models p 38 N89-18718

Texture analysis of forest regeneration sites in high-resolution SAR imagery p 10 N89-18730

Interpreting SAR images by means of map information p 58 N89-18760

Effects of slopes and relief two-dimensional spatial frequencies on spaceborne SAR imagery p 59 N89-18777



- Observations of the effect of geometric properties of agricultural soils on radar backscatter, from C-SAR images p 11 N89-18781
- Mapping slope failure tracks with digital Thematic Mapper data p 59 N89-18790
- Preprocessing and analysis of airborne visible near and shortwave infrared data for the detection of alteration in weathered vegetated terrain p 12 N89-18862
- A method for the clustering of remotely sensed multispectral images by using statistical test for spatial uniformity p 61 N89-18898
- Improvements in the forward and inverse principal component transformations for geological mapping in a semi-arid terrain p 27 N89-18933
- An evaluation of surface emittance and temperature data derived from Thermal Infrared Multispectral Scanner (TIMS) for lithological mapping in weathered vegetated terrain: N. Queensland, Australia p 27 N89-18934
- Progress in automatic analysis of multi-temporal remotely-sensed data p 61 N89-18956
- The use of LANDSAT imagery for water quality studies in the IJsselmeer area (Netherlands) [BCRS-87-18] p 52 N89-19732
- IMAGE CONTRAST**
- Extracting spectral contrast in Landsat Thematic Mapper image data using selective principal component analysis p 57 A89-32337
- IMAGE ENHANCEMENT**
- The use of image enhancement technique for peat land mapping using Landsat mass data in Indonesia p 52 A89-20775
- Improvement of multispectral color images by intensifying local contrasts p 56 A89-30123
- Investigations of the Cerro Colorado pluton, northern Chile, using enhanced LANDSAT Thematic Mapper images p 27 N89-18930
- IMAGE PROCESSING**
- Principle component transformation analysis for tentative land use interpretation of Landsat MSS of Bogor region, Indonesia p 52 A89-20767
- Applications of image scanning and processing in rock shear surface study p 20 A89-20779
- Suspended solid classification of the Jakarta Bay p 28 A89-20785
- Spatial information processings of TM data p 52 A89-20791
- The navigation method for NOAA-AVHRR image p 61 A89-20795
- Low cost, microcomputer-based interactive analysis system for direct-reception and archived remote sensing data p 53 A89-20796
- Application of three dimensional image system p 53 A89-20797
- Comparison of the orientation's accuracy for SPOT imagery p 53 A89-20798
- A basic study of the reduction of the exactness of mesh data map made by uniting n-squared meshes to one mesh p 54 A89-20811
- Identification of geological features from their surface textural properties using OPS measurements --- Optical Power Spectra p 21 A89-20820
- Usefulness of remote sensing in uranium exploration programme in parts of Karnataka state, India p 21 A89-20828
- A procedure for land area classification using Landsat TM digital imagery p 17 A89-24651
- Alternatives for mapping from satellites p 62 A89-26398
- Edge detection applied to satellite imagery of the oceans p 33 A89-26844
- Interactive image feature compilation for geographic information systems p 18 A89-27785
- Concepts for processing and analyzing of multiple SAR and Landsat images p 55 A89-27789
- The luxuriant image - An introduction to remote sensing data processing p 55 A89-27937
- Image processing techniques - Filtering, exogenous data, geometrical processing p 55 A89-27938
- The effects of viewing geometry on image classification p 55 A89-28036
- Extension of a drought monitoring and vegetation classification methodology to the western Sahel p 4 A89-28127
- Integrated NDVI images for Niger 1966-1987 --- Normalized Difference Vegetation Index p 4 A89-28128
- Mapping and inventory of forest fires from digital processing of TM data p 5 A89-28129
- Visual and digital classification of Landsat TM data for soil, physiography and land use mapping in Axios alluvial plain, Thessaloniki, Greece p 5 A89-28130
- Digital image processing in remote sensing --- Book p 55 A89-29064
- Microcomputers and mass storage devices for image processing p 65 A89-29070
- Multiple source data processing in remote sensing p 56 A89-29073
- Processing satellite infrared and visible imagery for oceanographic analyses p 34 A89-29075
- Comparative spectral analysis of HRV and TM sensors p 65 A89-29375
- Band-moment analysis of imaging-spectrometer data p 65 A89-29436
- Remote sensing of macrophytic algae of the Molene Archipelago in France - Terrain radiometry and application to SPOT satellite data p 36 A89-30260
- Land image data processing requirements for the EOS era p 56 A89-31949
- On-line aspects of stereophotogrammetric processing of SPOT images p 66 A89-32334
- A simple spatial filtering routine for the cosmetic removal of scan-line noise from Landsat TM P-tape imagery p 57 A89-32335
- A comparison of images from a pushbroom scanner with normal color aerial photographs for detecting scattered recent conifer mortality p 7 A89-32336
- Study of geometric quality of the MSS-LANDSAT imagery [INPE-4653-PRE/1380] p 57 N89-15440
- Investigation of information content of Thematic Mapper and SPOT multiband image data, using simulated image data of the Freiburg region (Federal Republic of Germany) [ESA-TT-975] p 57 N89-15442
- Applications of digital image processing to ongoing research in complex terrain meteorology [DE89-001749] p 57 N89-17375
- Automatic registration of satellite imagery [INPE-4637-PRE/1349] p 57 N89-17414
- Image compression using a neural network p 58 N89-18705
- Data processing for the determination of pigments and suspended solids from Thematic Mapper data p 50 N89-18736
- Segmentation of SAR images p 58 N89-18759
- A quantitative geomorphology study of main carbonate massifs of central and southern Apennines (Italy) based on a digital elevations archive p 25 N89-18791
- Image processing methods for the presentation of multiple geological datasets from the English Lake District p 25 N89-18793
- Real-time processing of digital image data in support of the Canadian sea ice analysis and prediction program p 43 N89-18803
- Sea-ice software: ICEMAN p 43 N89-18805
- Requirements for an EOS-oriented workstation --- Earth Observing System (EOS) p 69 N89-18813
- An ERDAS module for routine processing of AVHRR data p 43 N89-18817
- Geological lineament detection using the Hough transform p 26 N89-18818
- Normal distributional assumptions in discrimination --- image processing p 59 N89-18821
- Optimal sampling for remote sensing: Estimating the regional mean p 11 N89-18822
- Artefacts in AIS-I imagery --- Airborne Image Spectrometer (AIS) p 69 N89-18826
- Information fusion by a knowledge-based system for SAR image interpretation p 60 N89-18831
- A high fidelity, high throughput system for geocoding SAR imagery p 60 N89-18849
- The Alaska SAR processor p 70 N89-18851
- Post-processing airborne SAR data for multitemporal land-cover studies p 12 N89-18857
- Image-based atmospheric correction of multitemporal Thematic Mapping data for agricultural land cover classification p 14 N89-18895
- Results of tectonic and spectral investigations in the coast range of northern Chile using special processed Thematic Mapper (TM) data p 27 N89-18929
- The use of LANDSAT imagery for water quality studies in the IJsselmeer area (Netherlands) [BCRS-87-18] p 52 N89-19732
- IMAGE RESOLUTION**
- Comparison of the orientation's accuracy for SPOT imagery p 53 A89-20798
- The effects of viewing geometry on image classification p 55 A89-28036
- IMAGING RADAR**
- Multifrequency imaging radar polarimetry: Depolarisation of radar echoes at three wavelengths p 59 N89-18776
- IMAGING SPECTROMETERS**
- Optical system design alternatives for the Moderate-Resolution Imaging Spectrometer-Tilt (MODIS-T) for the Earth Observing System (EOS) p 63 A89-27753
- Band-moment analysis of imaging-spectrometer data p 65 A89-29436
- MODIS - Advanced facility instrument for studies of the earth as a system --- Moderate Resolution Imaging Spectrometer p 66 A89-31943
- MISR - A multiangle imaging spectroradiometer for geophysical and climatological research from EOS p 66 A89-31946
- MODIS-HIRIS ground data systems commonality report [NASA-TM-100718] p 67 N89-16205
- Mapping of phytoplankton fluorescence with the Fluorescence Line Imager (FLI) imaging spectrometer p 39 N89-18737
- INDIA**
- Wasteland identification in India using satellite remote sensing p 18 A89-30263
- INDIAN SPACE PROGRAM**
- Indian activities in remote sensing applications: Microwave remote sensing p 67 N89-16886
- INDIAN SPACECRAFT**
- Indian activities in remote sensing applications: Microwave remote sensing p 67 N89-16886
- INDONESIA**
- Remote sensing applications for agricultural landuse survey in Indonesia - Isimu case study p 2 A89-20763
- Flooded and inundation dangerous area prediction and its visualisation - A case study on the Pemali-Comal River Basin, Central Java, Indonesia p 48 A89-20774
- INDUSTRIAL AREAS**
- A model for the propagation of industrial atmospheric pollution registered on multispectral earth images p 17 A89-22213
- INERTIAL REFERENCE SYSTEMS**
- Reference coordinate systems: An update. Supplement 11 [NASA-CR-184784] p 19 N89-16207
- INFORMATION MANAGEMENT**
- The role of remote sensing in geographic information systems using computer p 17 A89-20792
- INFORMATION RETRIEVAL**
- Investigation of information content of Thematic Mapper and SPOT multiband image data, using simulated image data of the Freiburg region (Federal Republic of Germany) [ESA-TT-975] p 57 N89-15442
- INFORMATION SYSTEMS**
- MOS-1 data processing in Tokai Space Center p 52 A89-20790
- The algorithm development facility: Its role in the development and operation of a satellite data centre p 68 N89-18755
- INFRARED IMAGERY**
- Relative dating of Hawaiian lava flows using multispectral thermal infrared images - A new tool for geologic mapping of young volcanic terranes p 22 A89-22847
- Calibration of infrared satellite images using high altitude aircraft measurements [AIAA PAPER 89-0817] p 54 A89-25595
- Use of surface temperature in agrometeorology p 4 A89-27942
- Buoyant surface jet analysis of the Yukon River p 49 A89-28033
- Processing satellite infrared and visible imagery for oceanographic analyses p 34 A89-29075
- Thermal infrared and visible images of the Iberian Peninsula p 56 A89-31889
- The preliminary study of current shifting state by the use of infrared images of NOAA-9 p 39 N89-18742
- An atmospheric correction method for AVHRR infrared data using HIRS/2 data p 69 N89-18828
- Automatic mineral map generation procedure from imaging spectrometer data p 27 N89-18931
- An evaluation of surface emittance and temperature data derived from Thermal Infrared Multispectral Scanner (TIMS) for lithological mapping in weathered vegetated terrain: N. Queensland, Australia p 27 N89-18934
- INFRARED RADIATION**
- Variations of the infrared emission of snow and ice cover p 49 A89-30121
- INFRARED REFLECTION**
- Complementarity of middle-infrared with visible and near-infrared reflectance for monitoring wheat canopies p 5 A89-29410
- INFRARED SCANNERS**
- Operational calibration of Meteosat's infrared channel p 62 A89-22622
- An assessment of ATM and satellite data for estimating the groundwater contribution to slope stability --- Airborne Thematic Mapper (ATM) p 51 N89-18769
- Improvements in the forward and inverse principal component transformations for geological mapping in a semi-arid terrain p 27 N89-18933
- An evaluation of surface emittance and temperature data derived from Thermal Infrared Multispectral Scanner (TIMS) for lithological mapping in weathered vegetated terrain: N. Queensland, Australia p 27 N89-18934

## INFRARED SPECTROMETERS

## INFRARED SPECTROMETERS

- A possibility for selecting spectral bands of future land application sensors at the example of an imaging spectrometer p 60 N89-18896  
Automatic mineral map generation procedure from imaging spectrometer data p 27 N89-18931

## INFRARED SPECTROSCOPY

- Spectral response characteristics of a metal-stressed coniferous forest as measured by the Fluorescence Line Imager (FLI) airborne imaging spectrometer p 9 N89-18724

## INLAND WATERS

- Variations of the infrared emission of snow and ice cover p 49 A89-30121

## INSTRUMENT ERRORS

- Impact of phase and amplitude errors on the ERS-1 active microwave instrumentation performance p 70 N89-18853

## INTERFEROMETRY

- Research in geodesy and geophysics based upon radio interferometric observations of extragalactic radio sources [AD-A200958] p 25 N89-17933

## INTERNAL WAVES

- Remote sensing of surface manifestations of short-period internal waves in the ocean p 35 A89-30114  
The effect of internal waves on the Doppler spectrum of microwaves scattered from the ocean surface p 41 N89-18783

## INTERNATIONAL COOPERATION

- The development of remote sensing in China p 76 A89-31560

## INVERSIONS

- The geometry of geodetic inverse linear mapping and nonlinear adjustment [ETN-89-93900] p 20 N89-18736

## IRRIGATION

- Estimating the extent of irrigated cropland in a large catchment using LANDSAT MSS data p 14 N89-18902

## J

## JAPANESE SPACE PROGRAM

- NASA's Earth Observing System (EOS): An opportunity for mankind p 77 N89-18816

## JAPANESE SPACECRAFT

- MOS-1 data processing in Tokai Space Center p 52 A89-20790

## K

## KNOWLEDGE BASES (ARTIFICIAL INTELLIGENCE)

- FEX - A knowledge-based system for planimetric feature extraction p 54 A89-27783  
Knowledge related aspects of lineation and lineament extraction [INPE-4709-PRE/1391] p 24 N89-15446

## KNOWLEDGE REPRESENTATION

- Land image data processing requirements for the EOS era p 58 A89-31949

## KRIGING

- Optimal sampling for remote sensing: Estimating the regional mean p 11 N89-18822

## L

## LAKES

- The geology of the area surrounding Lake Kerinci, Indonesia as interpreted through SIR-B imageries p 20 A89-20781

- Estimation of the water exchange and contamination zones of basins from satellite imagery p 49 A89-30252

- A comparison of original aircraft MSS and generated surface water reflectance images as predictors of lake water quality indicators [DE89-004882] p 50 N89-17932

- Estimation of the area of Lake Kariba, Zimbabwe, using LANDSAT MSS imagery p 51 N89-18775  
The effect of soil moisture on reflectance characteristics of salt crusts p 16 N89-18966

## LAND

- Land image data processing requirements for the EOS era p 56 A89-31949

- Remote sensing of land processes: Sponsored programs of study by the National Aeronautics and Space Administration p 19 N89-18833

## LAND ICE

- Technological limitations to satellite glaciology p 36 A89-30257

## LAND MANAGEMENT

- Aerospace imagery and data for modelling erosion, sediment yield and crop yield prediction using GIS, applied to the Upper Komering catchment, Sumatra p 2 A89-20802

- Land use and land cover applications of Landsat MSS data p 17 A89-20813

- Study of the monitoring of land cover/use using remote sensing data by personal computer in southern part of Bandung area, West Java p 2 A89-20815

- Prioritization of watershed with regard to silt yield potential through data integration technique p 48 A89-20818

## LAND USE

- Remote sensing applications for agricultural land use survey in Indonesia - Isimu case study p 2 A89-20763

- Accuracy of land-cover/use classification p 52 A89-20765

- Land use suitability classification using remote sensing data and geographic information for volcanic regions p 16 A89-20766

- Principle component transformation analysis for tentative land use interpretation of Landsat MSS of Bogor region, Indonesia p 52 A89-20767

- Applications of SPOT HRV data for land use and soil mapping in Rayong basin p 2 A89-20769

- A basic study of the reduction of the exactness of mesh data map made by uniting n-squared meshes to one mesh p 54 A89-20811

- Land use and land cover applications of Landsat MSS data p 17 A89-20813

- Study of the monitoring of land cover/use using remote sensing data by personal computer in southern part of Bandung area, West Java p 2 A89-20815

- SPOT for mapping of actual land information p 54 A89-20816

- SPOT image interpretation for information on human settlement growth p 17 A89-20824

- A procedure for land area classification using Landsat TM digital imagery p 17 A89-24651

- Visual and digital classification of Landsat TM data for soil, physiography and land use mapping in Axios alluvial plain, Thessaloniki, Greece p 5 A89-28130

- Multispectral classification of land use at the rural-urban fringe using spot data p 18 A89-29371

- Comparative spectral analysis of HRV and TM sensors p 65 A89-29375

- Investigation of water content from airborne MSS data p 49 A89-30261

- Delineation of salt-affected soils through digital analysis of Landsat MSS data p 6 A89-30262

- Wasteland identification in India using satellite remote sensing p 18 A89-30263

- Post-processing airborne SAR data for multitemporal land-cover studies p 12 N89-18857

- Updating land-use information on topographic maps using satellite imagery: Combining the advantages of two accessible sources of geographic information p 60 N89-18897

- Land use analysis using remote sensing techniques. Investigation of the usefulness of LANDSAT Thematic Mapper satellite pictures for obtaining and up to date picture of land use in the province South Holland [BCRS-88-01] p 61 N89-19733

- Land use analysis using remote sensing techniques. Investigation of the usefulness of LANDSAT Thematic Mapper satellite pictures for obtaining and up to date picture of land use in the province South Holland [BCRS-88-01] p 61 N89-19733

## LANDSAT SATELLITES

- Digital image analysis of Landsat MSS data in an estate crop inventory of the Island of Bali p 1 A89-20756

- The feasibility study of oil palm area estimation in the southern part of Thailand using Landsat data p 2 A89-20760

- Principle component transformation analysis for tentative land use interpretation of Landsat MSS of Bogor region, Indonesia p 52 A89-20767

- Monitoring inundation area of Aliran Sungai Bengawan Solo Jawa Timur with Landsat images p 48 A89-20768

- Soil surface moisture estimation - A case study area on North Banten, West Java, Indonesia p 2 A89-20773

- Flooded and inundation dangerous area prediction and its visualisation - A case study on the Pemali-Cornal River Basin, Central Java, Indonesia p 48 A89-20774

- The use of image enhancement technique for peat land mapping using Landsat mass data in Indonesia p 52 A89-20775

- An estimation of areal evapotranspiration using Landsat and elevation data p 48 A89-20776

- Drainage pattern analysis with the aid of Landsat MSS data of the Citarium river basin, West Java, Indonesia p 48 A89-20778

- Mapping of construction material sites around Bangalore City using Landsat Thematic Mapper data p 52 A89-20782

- The creating of blue synthetic channel of MSS Landsat image p 52 A89-20794

- On geology of some districts in Central India using Landsat imageries p 21 A89-20808

- The applications of Landsat imagery to soil erosion study in Northern Thailand p 3 A89-20826

- Usefulness of remote sensing in uranium exploration programme in parts of Karnataka state, India p 21 A89-20828

- Scene locations and overpass dates for Landsat and SPOT sensors p 64 A89-28039

- Mapping in the Oman ophiolite using enhanced Landsat Thematic Mapper images p 23 A89-29301

- Multispectral classification of land use at the rural-urban fringe using spot data p 18 A89-29371

- Area measurement of agricultural fields from satellite images p 5 A89-29374

- Study of geometric quality of the MSS-LANDSAT imagery [INPE-4653-PRE/1360] p 57 N89-15440

- Investigation of information content of Thematic Mapper and SPOT multiband image data, using simulated image data of the Freiburg region (Federal Republic of Germany) p 57 N89-15442

- Accuracy assessment, using stratified plurality sampling, of portions of a LANDSAT classification of the Arctic National Wildlife Refuge Coastal Plain [NASA-TM-101042] p 8 N89-17339

- Integration of digital satellite and geophysical data, Heath Steele Mines, New Brunswick, Canada p 25 N89-18792

- An ERDAS module for routine processing of AVHRR data p 43 N89-18817

- Interpreting the geology of Glen Coe using LANDSAT MSS data and aerial photographs p 26 N89-18860

- The use of coregistered LANDSAT MSS, TM and SIR-A imagery for lithological mapping p 28 N89-18936

- Land use analysis using remote sensing techniques. Investigation of the usefulness of LANDSAT Thematic Mapper satellite pictures for obtaining and up to date picture of land use in the province South Holland [BCRS-88-01] p 61 N89-19733

- Land use analysis using remote sensing techniques. Investigation of the usefulness of LANDSAT Thematic Mapper satellite pictures for obtaining and up to date picture of land use in the province South Holland [BCRS-88-01] p 61 N89-19733

- Land use analysis using remote sensing techniques. Investigation of the usefulness of LANDSAT Thematic Mapper satellite pictures for obtaining and up to date picture of land use in the province South Holland [BCRS-88-01] p 61 N89-19733

- Land use analysis using remote sensing techniques. Investigation of the usefulness of LANDSAT Thematic Mapper satellite pictures for obtaining and up to date picture of land use in the province South Holland [BCRS-88-01] p 61 N89-19733

- Land use analysis using remote sensing techniques. Investigation of the usefulness of LANDSAT Thematic Mapper satellite pictures for obtaining and up to date picture of land use in the province South Holland [BCRS-88-01] p 61 N89-19733

- Land use analysis using remote sensing techniques. Investigation of the usefulness of LANDSAT Thematic Mapper satellite pictures for obtaining and up to date picture of land use in the province South Holland [BCRS-88-01] p 61 N89-19733

- Land use analysis using remote sensing techniques. Investigation of the usefulness of LANDSAT Thematic Mapper satellite pictures for obtaining and up to date picture of land use in the province South Holland [BCRS-88-01] p 61 N89-19733

- Land use analysis using remote sensing techniques. Investigation of the usefulness of LANDSAT Thematic Mapper satellite pictures for obtaining and up to date picture of land use in the province South Holland [BCRS-88-01] p 61 N89-19733

- Land use analysis using remote sensing techniques. Investigation of the usefulness of LANDSAT Thematic Mapper satellite pictures for obtaining and up to date picture of land use in the province South Holland [BCRS-88-01] p 61 N89-19733

- Land use analysis using remote sensing techniques. Investigation of the usefulness of LANDSAT Thematic Mapper satellite pictures for obtaining and up to date picture of land use in the province South Holland [BCRS-88-01] p 61 N89-19733

- Land use analysis using remote sensing techniques. Investigation of the usefulness of LANDSAT Thematic Mapper satellite pictures for obtaining and up to date picture of land use in the province South Holland [BCRS-88-01] p 61 N89-19733

- Land use analysis using remote sensing techniques. Investigation of the usefulness of LANDSAT Thematic Mapper satellite pictures for obtaining and up to date picture of land use in the province South Holland [BCRS-88-01] p 61 N89-19733

- Land use analysis using remote sensing techniques. Investigation of the usefulness of LANDSAT Thematic Mapper satellite pictures for obtaining and up to date picture of land use in the province South Holland [BCRS-88-01] p 61 N89-19733

- Land use analysis using remote sensing techniques. Investigation of the usefulness of LANDSAT Thematic Mapper satellite pictures for obtaining and up to date picture of land use in the province South Holland [BCRS-88-01] p 61 N89-19733

- Land use analysis using remote sensing techniques. Investigation of the usefulness of LANDSAT Thematic Mapper satellite pictures for obtaining and up to date picture of land use in the province South Holland [BCRS-88-01] p 61 N89-19733

- Land use analysis using remote sensing techniques. Investigation of the usefulness of LANDSAT Thematic Mapper satellite pictures for obtaining and up to date picture of land use in the province South Holland [BCRS-88-01] p 61 N89-19733

- Land use analysis using remote sensing techniques. Investigation of the usefulness of LANDSAT Thematic Mapper satellite pictures for obtaining and up to date picture of land use in the province South Holland [BCRS-88-01] p 61 N89-19733

- Land use analysis using remote sensing techniques. Investigation of the usefulness of LANDSAT Thematic Mapper satellite pictures for obtaining and up to date picture of land use in the province South Holland [BCRS-88-01] p 61 N89-19733

- Land use analysis using remote sensing techniques. Investigation of the usefulness of LANDSAT Thematic Mapper satellite pictures for obtaining and up to date picture of land use in the province South Holland [BCRS-88-01] p 61 N89-19733

- Land use analysis using remote sensing techniques. Investigation of the usefulness of LANDSAT Thematic Mapper satellite pictures for obtaining and up to date picture of land use in the province South Holland [BCRS-88-01] p 61 N89-19733

- Land use analysis using remote sensing techniques. Investigation of the usefulness of LANDSAT Thematic Mapper satellite pictures for obtaining and up to date picture of land use in the province South Holland [BCRS-88-01] p 61 N89-19733

- Land use analysis using remote sensing techniques. Investigation of the usefulness of LANDSAT Thematic Mapper satellite pictures for obtaining and up to date picture of land use in the province South Holland [BCRS-88-01] p 61 N89-19733

- Land use analysis using remote sensing techniques. Investigation of the usefulness of LANDSAT Thematic Mapper satellite pictures for obtaining and up to date picture of land use in the province South Holland [BCRS-88-01] p 61 N89-19733

- Land use analysis using remote sensing techniques. Investigation of the usefulness of LANDSAT Thematic Mapper satellite pictures for obtaining and up to date picture of land use in the province South Holland [BCRS-88-01] p 61 N89-19733

- Land use analysis using remote sensing techniques. Investigation of the usefulness of LANDSAT Thematic Mapper satellite pictures for obtaining and up to date picture of land use in the province South Holland [BCRS-88-01] p 61 N89-19733

- Land use analysis using remote sensing techniques. Investigation of the usefulness of LANDSAT Thematic Mapper satellite pictures for obtaining and up to date picture of land use in the province South Holland [BCRS-88-01] p 61 N89-19733

- Land use analysis using remote sensing techniques. Investigation of the usefulness of LANDSAT Thematic Mapper satellite pictures for obtaining and up to date picture of land use in the province South Holland [BCRS-88-01] p 61 N89-19733

- Land use analysis using remote sensing techniques. Investigation of the usefulness of LANDSAT Thematic Mapper satellite pictures for obtaining and up to date picture of land use in the province South Holland [BCRS-88-01] p 61 N89-19733

- Land use analysis using remote sensing techniques. Investigation of the usefulness of LANDSAT Thematic Mapper satellite pictures for obtaining and up to date picture of land use in the province South Holland [BCRS-88-01] p 61 N89-19733

- Land use analysis using remote sensing techniques. Investigation of the usefulness of LANDSAT Thematic Mapper satellite pictures for obtaining and up to date picture of land use in the province South Holland [BCRS-88-01] p 61 N89-19733

- Land use analysis using remote sensing techniques. Investigation of the usefulness of LANDSAT Thematic Mapper satellite pictures for obtaining and up to date picture of land use in the province South Holland [BCRS-88-01] p 61 N89-19733

- Land use analysis using remote sensing techniques. Investigation of the usefulness of LANDSAT Thematic Mapper satellite pictures for obtaining and up to date picture of land use in the province South Holland [BCRS-88-01] p 61 N89-19733

- Land use analysis using remote sensing techniques. Investigation of the usefulness of LANDSAT Thematic Mapper satellite pictures for obtaining and up to date picture of land use in the province South Holland [BCRS-88-01] p 61 N89-19733

- Land use analysis using remote sensing techniques. Investigation of the usefulness of LANDSAT Thematic Mapper satellite pictures for obtaining and up to date picture of land use in the province South Holland [BCRS-88-01] p 61 N89-19733

- LIGHT SCATTERING**  
Goniometric observations of light scattered from soils and leaves p 4 A89-24873
- LIGNIN**  
Remote sensing of canopy chemistry and nitrogen cycling in temperate forest ecosystems p 3 A89-23431
- LINEAR POLARIZATION**  
Multitemporal and dual polarization of agricultural crops by X-band SAR images p 9 N89-18716
- LINEAR PREDICTION**  
Comparison of Shuttle Imaging Radar-B ocean wave image spectra with linear model predictions based on aircraft measurements p 30 A89-22584
- LINEAR SYSTEMS**  
Using different sources of information in automated linear feature extraction from remote sensing data [INPE-4708-PRE/1390] p 24 N89-15447
- LINES (GEOMETRY)**  
The visibility of linear features in SAR images p 59 N89-18783
- LITHOLOGY**  
Mapping in the Oman ophiolite using enhanced Landsat Thematic Mapper images p 23 A89-29301  
Applications of LANDSAT Thematic Mapper imagery to the study of subtle variations in lithology p 27 N89-18863  
An evaluation of surface emittance and temperature data derived from Thermal Infrared Multispectral Scanner (TIMS) for lithological mapping in weathered vegetated terrain: N. Queensland, Australia p 27 N89-18934  
The use of coregistered LANDSAT MSS, TM and SIR-A imagery for lithological mapping p 28 N89-18936
- LITHOSPHERE**  
A new view of the mid-ocean ridge from the behaviour of ridge-axis discontinuities p 31 A89-23433
- LITTORAL DRIFT**  
Evaluation of satellite-tracked surface drifting buoys for simulating the movement of spilled oil in the marine environment. Volume 1: Executive summary [PB88-226048] p 37 N89-17357  
Evaluation of satellite-tracked surface drifting buoys for simulating the movement of spilled oil in the marine environment, volume 2 [PB88-226055] p 37 N89-17358
- LOW COST**  
Low-cost second order planimetric mapping technique p 53 A89-20800  
JEOS - A low-cost approach to earth observation p 63 A89-26399  
Overview of low-cost map digitizing systems [DE89-002872] p 57 N89-16204
- M**
- MAGMA**  
Erosional furrows formed during the lateral blast at Mount St. Helens, May 18, 1980 p 22 A89-22632
- MAGNETIC ANOMALIES**  
The source of marine magnetic anomalies [MPL-U-42/87] p 31 A89-22876  
The crustal field p 22 A89-22877
- MAGNETIC RECORDING**  
Spaceborne recording systems for the Space Station era p 66 A89-31020
- MAN ENVIRONMENT INTERACTIONS**  
A model for the propagation of industrial atmospheric pollution registered on multispectral earth images p 17 A89-22213
- MAPPING**  
Research, investigations and technical developments. National mapping program, 1985-1986 [USGS-OPEN-FILE-REPT-87-315] p 24 N89-16208  
Reports on cartography and geodesy, series 1, number 100 [ISSN-0469-4236] p 20 N89-17935
- MAPS**  
Interpreting SAR images by means of map information p 58 N89-18760
- MARINE BIOLOGY**  
Satellite detection of transient enhanced primary production in the western Mediterranean Sea p 31 A89-23438
- MARINE ENVIRONMENTS**  
The source of marine magnetic anomalies [MPL-U-42/87] p 31 A89-22876  
Effectiveness of satellite remote sensing on monitoring of marine environment [IAF PAPER 88-153] p 32 A89-24875  
A multi-sensor remote sensing approach for measuring primary production from space [NASA-CR-184662] p 37 N89-15444  
Coastal ocean margins program [DE89-005937] p 47 N89-18972
- MARINE METEOROLOGY**  
Physical retrieval of rainfall rates over the ocean by multispectral microwave radiometry - Application to tropical cyclones p 37 A89-32434
- MASSIFS**  
A quantitative geomorphology study of main carbonate massifs of central and southern Apennines (Italy) based on a digital elevations archive p 25 N89-18791
- MATHEMATICAL MODELS**  
Leaf backscattering measurements and modelling at 94 GHz p 8 N89-18713  
Sea bottom topography with X-band SLAR: Evaluation of existing models p 38 N89-18718  
Modelling the SIR-B image response to partially coherent seas p 38 N89-18719  
Characterizing forest ecosystem dynamics through modelling and remote sensing observations p 10 N89-18728  
The effect of internal waves on the Doppler spectrum of microwaves scattered from the ocean surface p 41 N89-18783  
Important changes in microwave scattering properties of young snow-covered sea ice as indicated from dielectric modelling p 44 N89-18870  
The directional reflectance of heather canopies: Towards a descriptive model p 13 N89-18878  
A mathematical model of reflectance and transmittance of plant leaves as a function of chlorophyll pigment content p 13 N89-18879  
Study of the use of radar X-band data of bare soil in a radar scattering model [BCRS-88-04] p 16 N89-19735
- MAXIMUM LIKELIHOOD ESTIMATES**  
Normal distributional assumptions in discrimination - image processing p 59 N89-18821
- MEDITERRANEAN SEA**  
A tide-generated internal waveform in the western approaches to the Strait of Gibraltar p 31 A89-22597  
Satellite detection of transient enhanced primary production in the western Mediterranean Sea p 31 A89-23438  
An experiment to invert Seasat altimetry for the Mediterranean and Black Sea mean surfaces p 36 A89-30900
- MELTING**  
Dependence of snow melting and surface-atmosphere interactions on the forest structure p 3 A89-21740  
EHF attenuation through the melting layer p 51 N89-18984
- MESOSCALE PHENOMENA**  
Edge detection applied to satellite imagery of the oceans p 33 A89-26844  
The influence of water vapor on the detection of ocean mesoscale fronts and eddies by the Geosat altimeter p 44 N89-18839
- METEOROLOGICAL CHARTS**  
Comparison study of SEASAT scatterometer and conventional wind fields [AD-A200591] p 67 N89-16202
- METEOROLOGICAL RADAR**  
Applications of the NCAR Electra Doppler radar for the study of physical parameters of clouds p 75 N89-19717
- METEOROLOGICAL SATELLITES**  
Low cost, microcomputer-based interactive analysis system for direct-reception and archived remote sensing data p 53 A89-20796  
Mission aspects of a future European polar orbit earth observation facility p 74 N89-18952
- METEOROLOGY**  
Applications of remote sensing to agrometeorology; Proceedings of the Course, Ispra, Italy, Apr. 6-10, 1987 p 63 A89-27933  
Applications of digital image processing to ongoing research in complex terrain meteorology [DE89-001749] p 57 N89-17375
- METEOSAT SATELLITE**  
Operational calibration of Meteosat's infrared channel p 62 A89-22622
- MICROCOMPUTERS**  
Low cost, microcomputer-based interactive analysis system for direct-reception and archived remote sensing data p 53 A89-20796  
Microcomputers and mass storage devices for image processing p 65 A89-29070
- MICROMETEOROLOGY**  
Dispersion parameters over forested terrain p 3 A89-22728
- MICROWAVE ANTENNAS**  
ERS-1 active microwave instrumentation design and performance status [IAF PAPER 87-136] p 65 A89-28329
- MICROWAVE IMAGERY**  
The Special Sensor Microwave Imager - A new instrument with rainfall monitoring potential p 64 A89-28038
- Detection of periodic characteristics of rice field vegetation by microwave backscatter measurement p 5 A89-28364
- MICROWAVE PHOTOGRAPHY**  
Indian activities in remote sensing applications: Microwave remote sensing p 67 N89-16886
- MICROWAVE RADIOMETERS**  
Procedures for the determination of geophysical parameters from spaceborne microwave polarimeter measurements p 30 A89-22224  
Observation of the degree of glaciation in middle-level stratiform clouds p 62 A89-23464  
A method for processing and results of microwave radiometer studies of the earth from the Intercosmos 20 and 21 satellites p 36 A89-30122  
An optimum calibration procedure for radiometers p 65 A89-30270  
Physical retrieval of rainfall rates over the ocean by multispectral microwave radiometry - Application to tropical cyclones p 37 A89-32434  
Microwave X-band radiometric characterization of Brazilian soils by measurement of the complex permittivity p 11 N89-18773  
Microcomputer-based radiometer data acquisition and processing system for large-area mapping of soil moisture content in the top one meter layer p 11 N89-18774  
Estimating sea ice concentration from satellite passive microwave data and a physical model p 42 N89-18797  
Shipborne passive microwave sea ice experiment in the East Greenland Sea: May-July 1987 p 42 N89-18799  
An ERDAS module for routine processing of AVHRR data p 43 N89-18817  
Experiments in Bulgaria for determination of soil moisture in the top one-meter layer using microwave radiometry and a priori information p 11 N89-18843  
Retrieval of water vapor profiles from microwave radiometric measurements at 183 and 92 GHz p 72 N89-18905  
Atmospheric attenuation as derived from microwave radiometry at 52.8 GHz p 72 N89-18906  
Atmospheric profiling of water vapour with a 20.5-23.5 GHz autocorrelation radiometer p 72 N89-18908  
The structure and variability of a filament in the northwest African upwelling area as observed from AVHRR and CXCS images p 46 N89-18939  
Antarctic Ocean polynyas [NASA-CR-184805] p 47 N89-19102
- MICROWAVE SCATTERING**  
Theoretical study of the sensitivity of the microwave backscattering coefficient to the soil surface parameters p 6 A89-30267  
Leaf backscattering measurements and modelling at 94 GHz p 8 N89-18713  
A measurement of microwave backscattering coefficients of rice plants p 8 N89-18714  
X-band scatterometry in agriculture p 9 N89-18715  
The effect of internal waves on the Doppler spectrum of microwaves scattered from the ocean surface p 41 N89-18783  
Fractal properties of the sea surface manifested in microwave remote sensing signatures p 41 N89-18784  
Measurements of microwave backscatter from conifers p 12 N89-18848  
Backscatter behavior of low-salinity sea ice at C and X-band p 44 N89-18869  
Important changes in microwave scattering properties of young snow-covered sea ice as indicated from dielectric modelling p 44 N89-18870
- MICROWAVE SENSORS**  
The Special Sensor Microwave Imager - A new instrument with rainfall monitoring potential p 64 A89-28038  
Passive microwave remote sensing system for soil moisture - Some supporting research p 49 A89-31948
- MICROWAVE SIGNATURES**  
Fractal features of sea surface manifested in microwave remote sensing signatures p 32 A89-24872
- MICROWAVE SOUNDING**  
Effective permittivity of vegetation in the microwave range p 3 A89-21612  
Microwave remote sensing of soil moisture p 4 A89-27944  
Polarization of microwave emission of a water surface in a wide range of angles of sight p 34 A89-28290
- MICROWAVES**  
Preliminary observations of polar sea ice with the Special Sensor Microwave Imager p 42 N89-18800  
Overview of the Shuttle Imaging Radar (SIR-C) p 73 N89-18921
- MILLIMETER WAVES**  
Leaf backscattering measurements and modelling at 94 GHz p 8 N89-18713  
Radar backscatter characteristics of trees at 215 GHz p 14 N89-18917

- A study of passive microwave remote sensing p 45 N89-18938
- Normalized radar cross section of natural surfaces at millimeter wavelengths [AD-A202252] p 75 N89-19475
- MINERAL DEPOSITS**
- Radar imagery as a tool for mineral exploration - A case study of gold mineralization in East Kalimantan p 20 A89-20780
- STAR-1 high resolution synthetic aperture radar imagery for precious metal exploration p 21 A89-20827
- Application of Landsat imagery and surficial geochemistry to the discovery of tungsten skarn deposits associated with buried plutons, Yukon and Northwest Territories, Canada p 23 A89-28126
- Extracting spectral contrast in Landsat Thematic Mapper image data using selective principal component analysis p 57 A89-32337
- MINERAL EXPLORATION**
- Radar imagery as a tool for mineral exploration - A case study of gold mineralization in East Kalimantan p 20 A89-20780
- STAR-1 high resolution synthetic aperture radar imagery for precious metal exploration p 21 A89-20827
- Usefulness of remote sensing in uranium exploration programme in parts of Karnataka state, India p 21 A89-20828
- Application of Landsat imagery and surficial geochemistry to the discovery of tungsten skarn deposits associated with buried plutons, Yukon and Northwest Territories, Canada p 23 A89-28126
- Features of the geological structure of the polar Urals and the distribution of certain minerals, as evaluated on the basis of the interpretation of aerial and space photographs p 23 A89-30119
- Integration of digital satellite and geophysical data, Heath Steele Mines, New Brunswick, Canada p 25 N89-18792
- MINERALOGY**
- Remote sensing of evaporite mineral zonation in salt flats (salars) p 23 A89-30271
- MINERALS**
- Automatic mineral map generation procedure from imaging spectrometer data p 27 N89-18931
- MINES (EXCAVATIONS)**
- Integration of digital satellite and geophysical data, Heath Steele Mines, New Brunswick, Canada p 25 N89-18792
- Monitoring surface mineral workings using TM and SPOT p 26 N89-18796
- MISSION PLANNING**
- MODIS information, data and control system (MIDACS) operations concepts [NASA-TM-100720] p 75 N89-19729
- MONSOONS**
- Snow cover-summer monsoon rainfall over parts of Sahel p 51 N89-18832
- MOORING**
- Moorable spectroradiometers in the BIOWATT experiment p 64 A89-27990
- MULTIPATH TRANSMISSION**
- Computer simulation of multipath sea echo near grazing incidence p 38 N89-18722
- MULTISENSOR APPLICATIONS**
- Concepts for processing and analyzing of multiple SAR and Landsat images p 55 A89-27789
- MULTISPECTRAL BAND SCANNERS**
- Digital image analysis of Landsat MSS data in an estate crop inventory of the Island of Bali p 1 A89-20756
- Airborne multispectral remote sensing of forest decline in West Germany p 1 A89-20757
- Soil and vegetation mapping by using SPOT image p 1 A89-20758
- Drainage pattern analysis with the aid of Landsat MSS data of the Citarium river basin, West Java, Indonesia p 48 A89-20778
- The creating of blue synthetic channel of MSS Landsat image p 52 A89-20794
- Application of Landsat MSS and TM data to geological resource exploration p 22 A89-26397
- Simulation of radiometric ocean images recorded from high-altitude platforms p 33 A89-27980
- Application of the Haar transform for extraction of linear and anomalous patterns over part of Cambay Basin, India p 55 A89-28037
- Airborne MSS for land cover classification p 5 A89-28131
- Multispectral classification of land use at the rural-urban fringe using spot data p 18 A89-29371
- Analysis and interpretation of SPOT images of urban and agricultural/forest sections of the Sherbrooke region p 5 A89-29373
- Band-moment analysis of imaging-spectrometer data p 65 A89-29436
- Investigation of water content from airborne MSS data p 49 A89-30261

- Delineation of salt-affected soils through digital analysis of Landsat MSS data p 6 A89-30262
- Geological mapping and analysis of fracturing in the south part of the Central Anti-Atlas in Morocco using a Landsat MSS image p 23 A89-31887
- German spaceborne remote sensing activities p 67 N89-16887
- Accuracy assessment, using stratified plurality sampling, of portions of a LANDSAT classification of the Arctic National Wildlife Refuge Coastal Plain [NASA-TM-101042] p 8 N89-17339
- The derivation and verification of surface reflectances using airborne MSS data and a radiative transfer model [DE89-004881] p 67 N89-17931
- A comparison of original aircraft MSS and generated surface water reflectance images as predictors of lake water quality indicators [DE89-004882] p 50 N89-17932
- Interpreting the geology of Glen Coe using LANDSAT MSS data and aerial photographs p 26 N89-18860
- Preprocessing and analysis of airborne visible near and shortwave infrared data for the detection of alteration in weathered vegetated terrain p 12 N89-18862
- Signature variations due to atmospheric and topographic effects on satellite MSS data over rugged terrain p 70 N89-18877
- An evaluation of surface emittance and temperature data derived from Thermal Infrared Multi-spectral Scanner (TIMS) for lithological mapping in weathered vegetated terrain: N. Queensland, Australia p 27 N89-18934
- The use of coregistered LANDSAT MSS, TM and SIR-A imagery for lithological mapping p 28 N89-18936
- MULTISPECTRAL PHOTOGRAPHY**
- Improvement of multispectral color images by intensifying local contrasts p 56 A89-30123
- A spectral feature design system for high dimensional multispectral data p 60 N89-18894
- A method for the clustering of remotely sensed multispectral images by using statistical test for spatial uniformity p 61 N89-18896

## N

- NARROWBAND**
- The relative merits of narrowband channels for estimating broadband albedos p 66 A89-30967
- NASA PROGRAMS**
- Remote sensing of land processes: Sponsored programs of study by the National Aeronautics and Space Administration p 19 N89-18833
- NASA SPACE PROGRAMS**
- NASA's Earth Observing System (EOS): An opportunity for mankind p 77 N89-18816
- NEAR INFRARED RADIATION**
- Complementarity of middle-infrared with visible and near-infrared reflectance for monitoring wheat canopies p 5 A89-29410
- NEARSHORE WATER**
- A preliminary study on nearshore water in China with NOAA satellite images p 40 N89-18743
- NEURAL NETS**
- Image compression using a neural network p 58 N89-18705
- NIGHT**
- A 10 km resolution image of the entire night-time earth based on cloud-free satellite photographs in the 400-1100 nm band p 56 A89-30256
- Applications of digital image processing to ongoing research in complex terrain meteorology [DE89-001749] p 57 N89-17375
- NIMBUS 7 SATELLITE**
- Antarctic Ocean polynyas [NASA-CR-184805] p 47 N89-19102
- NITROGEN**
- Remote sensing of canopy chemistry and nitrogen cycling in temperate forest ecosystems p 3 A89-23431
- NOAA SATELLITES**
- Comparative study of vegetation index and false colour composite image of NOAA-AVHRR data for bio-mass studies p 1 A89-20752
- Receiving and processing system for meteorological satellite (NOAA) p 53 A89-20806
- Comparison of NOAA-AVHRR-2 sea surface temperatures with surface measurements in coastal waters p 36 A89-30259
- The relative merits of narrowband channels for estimating broadband albedos p 66 A89-30967
- Quick reporting state of fishery and sea on the East China Sea and the Yellow Sea with NOAA p 39 N89-18741
- The preliminary study of current shifting state by the use of infrared images of NOAA-9 p 39 N89-18742
- A preliminary study on nearshore water in China with NOAA satellite images p 40 N89-18743
- NOISE REDUCTION**
- A simple spatial filtering routine for the cosmetic removal of scan-line noise from Landsat TM P-tape imagery p 57 A89-32335
- NONLINEAR FILTERS**
- Nonlinear filtering and edge detection in speckled radar images p 58 N89-18711
- NONPARAMETRIC STATISTICS**
- A method for the clustering of remotely sensed multispectral images by using statistical test for spatial uniformity p 61 N89-18898
- NORTH SEA**
- Validation of a synthetic aperture radar ocean wave imaging theory by the Shuttle Imaging Radar-B experiment over the North Sea p 30 A89-22586
- Directional wave data recorded in the southern North Sea [IOS-258] p 47 N89-19793
- OCEAN BOTTOM**
- The preliminary study on correlation between satellite information and bottom trawling ground in the East China Sea and the Yellow Sea p 29 A89-20805
- The source of marine magnetic anomalies [MPL-U-42/87] p 31 A89-22876
- A new view of the mid-ocean ridge from the behaviour of ridge-axis discontinuities p 31 A89-23433
- Detection of ocean bottom relief by local geoid p 35 A89-29731
- The solid oceanic crust (The Lithos project) --- Russian book p 36 A89-32108
- Sea bottom topography with X-band SLAR: Evaluation of existing models p 38 N89-18718
- Dynamic topography as measured by the Geosat altimeter in regions of small surface height signatures p 43 N89-18837
- Major crustal lineaments on Seasat SAR and their off-shore extensions in the UK p 26 N89-18861
- OCEAN COLOR SCANNER**
- The extraction of sea fishery potential area from Airborne Ocean Color Radiometer data p 28 A89-20786
- Antarctic Ocean polynyas [NASA-CR-184805] p 47 N89-19102
- OCEAN CURRENTS**
- Circulation in the East Asian seas from satellite and ship data p 29 A89-20803
- Distribution and variations of oceanic carbon dioxide in the western North Pacific, eastern Indian, and Southern Ocean south of Australia p 29 A89-20925
- Ocean wave directional spectra and wave-current interaction in the Agulhas from the Shuttle Imaging Radar-B synthetic aperture radar p 30 A89-22585
- A simulation of the global ocean circulation with resolved eddies p 30 A89-22593
- Loop Current boundary variations --- in eastern Gulf of Mexico p 31 A89-22596
- Edge detection applied to satellite imagery of the oceans p 33 A89-26844
- The impact of satellite altimetry data on numerical simulations of general midlatitude oceanic circulation p 34 A89-28305
- Evaluation of satellite-tracked surface drifting buoys for simulating the movement of spilled oil in the marine environment. Volume 1: Executive summary [PB88-226048] p 37 N89-17357
- Evaluation of satellite-tracked surface drifting buoys for simulating the movement of spilled oil in the marine environment, volume 2 [PB88-226055] p 37 N89-17358
- The preliminary study of current shifting state by the use of infrared images of NOAA-9 p 39 N89-18742
- A preliminary study on nearshore water in China with NOAA satellite images p 40 N89-18743
- Remote studies of the ocean surface by a tower-based multifrequency microwave radar p 41 N89-18785
- Study on directional spectrum characteristics of marine radar images of ocean waves p 41 N89-18786
- Assimilation of altimeter data into numerical ocean models p 43 N89-18838
- The influence of water vapor on the detection of ocean mesoscale fronts and eddies by the Geosat altimeter p 44 N89-18839
- Coastal ocean margins program [DE89-005937] p 47 N89-18972
- OCEAN DATA ACQUISITIONS SYSTEMS**
- Distribution and variations of oceanic carbon dioxide in the western North Pacific, eastern Indian, and Southern Ocean south of Australia p 29 A89-20925
- The preliminary study of current shifting state by the use of infrared images of NOAA-9 p 39 N89-18742
- Assimilation of altimeter data into numerical ocean models p 43 N89-18838

- Radiometric problems in the use of the Thematic Mapper for marine research p 46 N89-18940
- Directional wave data recorded in the southern North Sea [IOS-258] p 47 N89-19793
- OCEAN DYNAMICS**
- Circulation in the East Asian seas from satellite and ship data p 29 A89-20803
- Distribution and variations of oceanic carbon dioxide in the western North Pacific, eastern Indian, and Southern Ocean south of Australia p 29 A89-20925
- A simulation of the global ocean circulation with resolved eddies p 30 A89-22593
- The impact of satellite altimetry data on numerical simulations of general midlatitude oceanic circulation p 34 A89-28305
- Dynamic topography as measured by the Geosat altimeter in regions of small surface height signatures p 43 N89-18837
- OCEAN MODELS**
- A simulation of the global ocean circulation with resolved eddies p 30 A89-22593
- Computer simulation of multipath sea echo near grazing incidence p 38 N89-18722
- Simulation of SAR imaging of ship wakes p 41 N89-18785
- Studies of the dependence of the microwave radar cross section on ocean surface variables during the FASINEX experiment p 41 N89-18782
- Toward the automated use of remote sensing data in operational ice forecasting p 43 N89-18804
- Assimilation of altimeter data into numerical ocean models p 43 N89-18838
- OCEAN SURFACE**
- Suspended solid classification of the Jakarta Bay p 28 A89-20785
- The extraction of sea fishery potential area from Airborne Ocean Color Radiometer data p 28 A89-20786
- Application of airborne scanners in remote sensing of sea p 29 A89-20789
- Determination of the spectrum of energy-containing surface waves from a sun-glitter image p 29 A89-22210
- Ocean wave spectra derived from Shuttle Imaging Radar-B imagery and surface measurements p 30 A89-22583
- Comparison of Shuttle Imaging Radar-B ocean wave image spectra with linear model predictions based on aircraft measurements p 30 A89-22584
- Validation of a synthetic aperture radar ocean wave imaging theory by the Shuttle Imaging Radar-B experiment over the North Sea p 30 A89-22586
- Satellite determination of the carbon dioxide exchange coefficient at the ocean-atmosphere interface - A first step p 31 A89-22598
- Motion characteristics of sea waves p 32 A89-23590
- Features of the calculation of the main characteristics of an oceanographic radar altimeter p 32 A89-23646
- Fractal features of sea surface manifested in microwave remote sensing signatures p 32 A89-24872
- Hindcasts and data assimilation studies with the WAM model during the Seasat period --- wave model p 32 A89-26442
- Frontal signals east of Iceland from the Geosat altimeter p 33 A89-26643
- A simulation for spaceborne SAR imagery of a distributed, moving scene p 33 A89-26846
- Simulation of radiometric ocean images recorded from high-altitude platforms p 33 A89-27980
- Polarization of microwave emission of a water surface in a wide range of angles of sight p 34 A89-28290
- Processing satellite infrared and visible imagery for oceanographic analyses p 34 A89-29075
- Oceanic remote sensing p 35 A89-29726
- Effects of round trip laser emission propagation through a turbulent surface for laser airborne oceanic sensing p 35 A89-29729
- Detection of ocean bottom relief by local geoid p 35 A89-29731
- Surface wave interaction - Theory and capability of oceanic remote sensing p 35 A89-29732
- Wavenumber spectra of short gravity waves p 35 A89-30019
- Remote sensing of surface manifestations of short-period internal waves in the ocean p 35 A89-30114
- Radiation models of mesotrophic and eutrophic bodies of water p 36 A89-30120
- Can better environmental inputs improve sea clutter estimation? A numerical experiment p 36 A89-30258
- An experiment to invert Seasat altimetry for the Mediterranean and Black Sea mean surfaces p 36 A89-30900
- Segmentation of Synthetic Aperture Radar (SAR) images of ocean surface by the texture energy transform method [AD-A199536] p 37 N89-15309
- Speckle correlation in SAR images of dynamic discrete scatterers p 37 N89-18707
- Statistical evaluation of the intensity distribution of sea surface radar images p 38 N89-18717
- Modelling the SIR-B image response to partially coherent seas p 38 N89-18719
- Distribution of specular points on the ocean surface: Bistatic scattering p 38 N89-18721
- Computer simulation of multipath sea echo near grazing incidence p 38 N89-18722
- Specular scattering with effective reflection coefficient p 39 N89-18723
- Studies of the dependence of the microwave radar cross section on ocean surface variables during the FASINEX experiment p 41 N89-18782
- The effect of internal waves on the Doppler spectrum of microwaves scattered from the ocean surface p 41 N89-18783
- Fractal properties of the sea surface manifested in microwave remote sensing signatures p 41 N89-18784
- Remote studies of the ocean surface by a tower-based multifrequency microwave radar p 41 N89-18785
- Analysis of ocean backscatter data obtained by the University of Kansas during TOWARD 84/85 p 42 N89-18787
- A study of the effect of rain on Seasat radar altimeter data p 44 N89-18840
- The Navy Geosat radar altimeter satellite mission p 45 N89-18909
- An advanced terrain tracking altimeter p 45 N89-18910
- A study of passive microwave remote sensing p 45 N89-18938
- OCEANOGRAPHIC PARAMETERS**
- Seasat - Results of the mission p 29 A89-22000
- Optical methods of satellite hydrophysics. Investigation of the environment from manned orbital stations --- Russian book p 32 A89-26181
- Processing satellite infrared and visible imagery for oceanographic analyses p 34 A89-29075
- A multi-sensor remote sensing approach for measuring primary production from space [NASA-CR-184662] p 37 N89-15444
- The influence of water vapor on the detection of ocean mesoscale fronts and eddies by the Geosat altimeter p 44 N89-18839
- OCEANOGRAPHY**
- Ocean optics IX; Proceedings of the Meeting, Orlando, FL, Apr. 4-6, 1988 [SPIE-925] p 33 A89-27976
- Ocean optics: Introduction and overview - 1988 p 64 A89-27977
- Moorable spectroradiometers in the BIOWATT experiment p 64 A89-27990
- Spectral transmissometer and radiometer - Design and initial results --- of free drifting experiment in Pacific Ocean p 64 A89-27991
- Remote sensing of ocean physical properties - A comparison of Raman and Brillouin techniques p 34 A89-28003
- Oceanic remote sensing p 35 A89-29726
- Dynamic topography as measured by the Geosat altimeter in regions of small surface height signatures p 43 N89-18837
- OCEANS**
- Edge detection applied to satellite imagery of the oceans p 33 A89-26844
- OFFSHORE ENERGY SOURCES**
- Airborne gravity as a supporting tool for hydrocarbon exploration in Indonesia p 21 A89-20829
- OIL EXPLORATION**
- Application of remote sensing for hydrocarbon exploration on Timor Island, Indonesia p 21 A89-20825
- Airborne gravity as a supporting tool for hydrocarbon exploration in Indonesia p 21 A89-20829
- Application of Landsat MSS and TM data to geological resource exploration p 22 A89-26397
- OIL POLLUTION**
- Application of airborne scanners in remote sensing of sea p 29 A89-20789
- A study of passive microwave remote sensing p 45 N89-18938
- OIL SLICKS**
- Evaluation of satellite-tracked surface drifting buoys for simulating the movement of spilled oil in the marine environment. Volume 1: Executive summary [PB88-226048] p 37 N89-17357
- Evaluation of satellite-tracked surface drifting buoys for simulating the movement of spilled oil in the marine environment, volume 2 [PB88-226055] p 37 N89-17358
- ON-LINE SYSTEMS**
- On-line aspects of stereophotogrammetric processing of SPOT images p 66 A89-32334
- The central user services system for ERS-1 p 68 N89-18754
- ONBOARD DATA PROCESSING**
- Results of software simulation of a real-time SAR processor capable of providing ocean wave spectra p 38 N89-18720
- Microcomputer-based radiometer data acquisition and processing system for large-area mapping of soil moisture content in the top one meter layer p 11 N89-18774
- OPTICAL EQUIPMENT**
- MODIS - Advanced facility instrument for studies of the earth as a system --- Moderate Resolution Imaging Spectrometer p 66 A89-31943
- OPTICAL MEASURING INSTRUMENTS**
- Ocean optics: Introduction and overview - 1988 p 64 A89-27977
- Moorable spectroradiometers in the BIOWATT experiment p 64 A89-27990
- Spectral transmissometer and radiometer - Design and initial results --- of free drifting experiment in Pacific Ocean p 64 A89-27991
- Optical bathymetry for the U.S. Navy - A field measurement program p 64 A89-27993
- OPTICAL PROPERTIES**
- Ocean optics: Introduction and overview - 1988 p 64 A89-27977
- OPTICAL RADAR**
- Analysis of airborne laser hydrography waveforms p 64 A89-27998
- Remote sensing of ocean physical properties - A comparison of Raman and Brillouin techniques p 34 A89-28003
- German spaceborne remote sensing activities p 67 N89-16887
- OPTICAL THICKNESS**
- Determination of atmospheric turbidity from remotely-sensed data - A case study p 34 A89-28034
- OPTICS**
- Ocean optics IX; Proceedings of the Meeting, Orlando, FL, Apr. 4-6, 1988 [SPIE-925] p 33 A89-27976
- ORBITAL ELEMENTS**
- The Geosat orbit adjust p 19 A89-22316
- ORBITAL POSITION ESTIMATION**
- The navigation method for NOAA/AVHRR image p 61 A89-20785
- ORGANIC CHEMISTRY**
- Observed effects of soil organic matter content on the microwave intensity of soils p 12 N89-18845
- OZONE**
- A comparison of models for deriving dry deposition fluxes of O3 and SO2 to a forest canopy p 3 A89-20923
- OZONE DEPLETION**
- Measurements of springtime Antarctic ozone depletion and development of a balloonborne ultraviolet photometer p 67 N89-15459
- OZONOMETRY**
- Comparison of satellite total ozone measurements with the distribution of tropospheric ozone obtained by an airborne UV-DIAL system over the Amazon Basin p 17 A89-21892
- Simulated effects of barometric pressure and ozone content upon the estimate of marine phytoplankton from space p 33 A89-26443
- Measurements of springtime Antarctic ozone depletion and development of a balloonborne ultraviolet photometer p 67 N89-15459

P

## PACIFIC OCEAN

- The preliminary study on correlation between satellite information and bottom trawling ground in the East China Sea and the Yellow Sea p 29 A89-20805
- A surface-wave study of the Pacific Ocean basin p 29 A89-21798
- Upwelling off the Gulfs of Panama and Papagayo in the tropical Pacific during March 1985 p 30 A89-22591
- Inertial wind path and sea surface temperature patterns near the Gulf of Tehuantepec and Gulf of Papagayo p 30 A89-22592
- Geosat crossover analysis in the tropical Pacific. II - Verification analysis of altimetric sea level maps with expendable bathythermograph and island sea level data p 32 A89-26438
- Coastal ocean margins program [DE89-005937] p 47 N89-18972

**PARALLEL PROCESSING (COMPUTERS)**

- A high fidelity, high throughput system for geocoding SAR imagery p 60 N89-18849
- PARAMETER IDENTIFICATION**  
Auto and cross correlation analysis of environment, system and target parameters for iceberg detection using airborne radar p 45 N89-18874
- PATTERN RECOGNITION**  
Comparison of the orientation's accuracy for SPOT imagery p 53 A89-20798  
Identification of geological features from their surface textural properties using OPS measurements --- Optical Power Spectra p 21 A89-20820  
Feature extraction considerations in utilising the optical power spectra for terrain classification p 54 A89-20821  
FEX - A knowledge-based system for planimetric feature extraction p 54 A89-27783  
Application of the Haar transform for extraction of linear and anomalous patterns over part of Cambay Basin, India p 55 A89-28037  
Integration of SPOT data in an urban data bank - Locating work sites p 18 A89-31891  
Knowledge related aspects of lineation and lineament extraction [INPE-4708-PRE/1391] p 24 N89-15446  
Using different sources of information in automated linear feature extraction from remote sensing data [INPE-4708-PRE/1390] p 24 N89-15447  
The visibility of linear features in SAR images p 59 N89-18763  
Automated linear feature detection and its application to curve location in synthetic aperture radar imagery p 59 N89-18764  
Automatic ship and ship wake detection in spaceborne SAR images from coastal regions p 41 N89-18766  
A spectral feature design system for high dimensional multispectral data p 60 N89-18894  
Pattern analysis and the ecological interpretation of satellite imagery p 61 N89-18900  
Satellite imagery for semi-automatic map revision p 61 N89-18957  
Sensor fusion of range and reflectance data for outdoor scene analysis p 76 N89-19868
- PATTERN REGISTRATION**  
Sensor fusion of range and reflectance data for outdoor scene analysis p 76 N89-19868
- PEAT**  
The use of image enhancement technique for peat land mapping using Landsat mass data in Indonesia p 52 A89-20775
- PERMITTIVITY**  
Effective permittivity of vegetation in the microwave range p 3 A89-21612  
Microwave X-band radiometric characterization of Brazilian soils by measurement of the complex permittivity p 11 N89-18773  
Important changes in microwave scattering properties of young snow-covered sea ice as indicated from dielectric modelling p 44 N89-18870
- PERSONAL COMPUTERS**  
Study of the monitoring of land cover/use using remote sensing data by personal computer in southern part of Bandung area, West Java p 2 A89-20815
- PHASE ERROR**  
Impact of phase and amplitude errors on the ERS-1 active microwave instrumentation performance p 70 N89-18853
- PHILIPPINES**  
Reconnaissance groundwater appraisal of Bohol Island, Philippines, by satellite data analysis p 48 A89-20772
- PHOTO GEOLOGY**  
On geology of some districts in Central India using Landsat imageries p 21 A89-20808  
Neotectonic zoning of Belorussia on the basis of space data p 21 A89-22215  
Fault classification for the geological support of the tunnel construction project for the Caucasus mountain-pass railroad, using space images p 22 A89-22216  
The procedure for and the results of the geological interpretation of photographic images of the Bukhtarma lineament zone p 22 A89-22217  
A tomographic approach to lineament identification on aerial and space images p 22 A89-22223  
Mapping in the Oman ophiolite using enhanced Landsat Thematic Mapper images p 23 A89-29301  
Digital processing of a lineament grid with the aim of analyzing regional tectonic structures of the western Himalayas in India p 23 A89-30116  
Ring structures of buried platform areas and the evaluation of their tectonic activity on the basis of geomorphological data p 23 A89-30118

- Features of the geological structure of the polar Urals and the distribution of certain minerals, as evaluated on the basis of the interpretation of aerial and space photographs p 23 A89-30119  
Some results of use of space survey materials in cartographic work p 58 N89-17922  
Automatic mineral map generation procedure from imaging spectrometer data p 27 N89-18931
- PHOTOGRAMMETRY**  
An interactive system for aerial photo orientation of digital stereo image pairs p 53 A89-20799  
Low-cost second order planimetric mapping technique p 53 A89-20800  
SPOT for mapping of actual land information p 54 A89-20816  
Aerial remote sensing technique in the identification and acreage estimation of various plantations - A case study in Gorakhpur district, Uttar Pradesh, India p 2 A89-20819  
Potential of Large Format Camera photography p 65 A89-29433  
On-line aspects of stereophotogrammetric processing of SPOT images p 66 A89-32334
- PHOTOGRAPHY**  
Potential of Large Format Camera photography p 65 A89-29433  
A comparison of clutter texture properties in optical and SAR images p 8 N89-18708
- PHOTOINTERPRETATION**  
On geology of some districts in Central India using Landsat imageries p 21 A89-20808  
Cartographic analysis of Large Format Camera photographs - Comparison with SPOT and the Spacelab metric camera p 62 A89-21410  
The procedure for and the results of the geological interpretation of photographic images of the Bukhtarma lineament zone p 22 A89-22217  
FEX - A knowledge-based system for planimetric feature extraction p 54 A89-27783  
Combining oblique SPOT-1 images for the analysis of certain soil properties p 7 A89-31892  
Determining the age of cut forest areas in Quebec, Canada using the Landsat-5 TM p 7 A89-31893  
Some results of use of space survey materials in cartographic work p 58 N89-17922  
Satellite imagery for semi-automatic map revision p 61 N89-18957
- PHOTOMAPPING**  
First results of topographical mapping using SPOT images of Malaysia p 52 A89-20764  
Low-cost second order planimetric mapping technique p 53 A89-20800  
Accuracy of terrain measurement using SPOT HRV data --- high resolution video p 53 A89-20801  
Cartographic analysis of Large Format Camera photographs - Comparison with SPOT and the Spacelab metric camera p 62 A89-21410  
Alternatives for mapping from satellites p 62 A89-26398  
Geological mapping and analysis of fracturing in the south part of the Central Anti-Atlas in Morocco using a Landsat MSS image p 23 A89-31887  
The application of remote sensing to geomorphological mapping and mass movement study in the vicinity of Provo, Utah p 23 N89-15439  
Some results of use of space survey materials in cartographic work p 58 N89-17922  
Automatic mineral map generation procedure from imaging spectrometer data p 27 N89-18931
- PHOTOMAPS**  
SPOT for mapping of actual land information p 54 A89-20816
- PHYTOPLANKTON**  
Simulated effects of barometric pressure and ozone content upon the estimate of marine phytoplankton from space p 33 A89-26443  
Simulation of radiometric ocean images recorded from high-altitude platforms p 33 A89-27980  
Moorable spectroradiometers in the BIOWATT experiment p 64 A89-27990
- PIPELINING (COMPUTERS)**  
The Alaska SAR processor p 70 N89-18851
- PLANKTON**  
Laser airborne sensing field experiments using the 'Chaika' assembly --- for probing water bodies p 35 A89-29728  
Mapping of phytoplankton fluorescence with the Fluorescence Line Imager (FLI) imaging spectrometer p 39 N89-18737
- PLANT STRESS**  
Assessing extent of damage caused by flooding and drought in dominantly rice cropland area using Landsat data p 2 A89-20814

- Spectral response characteristics of a metal-stressed coniferous forest as measured by the Fluorescence Line Imager (FLI) airborne imaging spectrometer p 9 N89-18724  
Possibilities of the satellite imagery to locate the forest decline areas in the Vosges Massif (France) p 10 N89-18729  
Geological applications of thermal infrared characteristics of vegetation p 27 N89-18932
- PLANTS (BOTANY)**  
A mathematical model of reflectance and transmittance of plant leaves as a function of chlorophyll pigment content p 13 N89-18879  
Extraction of agricultural plant parameters from multitemporal Thematic Mapper (TM) and X-SAR data p 15 N89-18948  
Correlations between agricultural plant parameters and multitemporal radar scatterometer data: First results from the European AGRISCAIT 87 campaign p 16 N89-18951
- PLATES (TECTONICS)**  
A new view of the mid-ocean ridge from the behaviour of ridge-axis discontinuities p 31 A89-23433  
An algorithm for analysis of plate motions in Crust Dynamics Project (CDP) networks [88821606] p 19 N89-17371
- PLATFORMS**  
Platforms --- for remote sensors p 63 A89-27936
- PLOTTERS**  
SPOT mapping software for Wild Aviolyt BC2 analytical plotter p 60 N89-18824
- POISSON DENSITY FUNCTIONS**  
Modelling the SIR-B image response to partially coherent seas p 38 N89-18719
- POLAR METEOROLOGY**  
Summertime stratospheric wind measurements above the South Pole p 62 A89-24022
- POLAR ORBITS**  
MODIS - Advanced facility instrument for studies of the earth as a system --- Moderate Resolution Imaging Spectrometer p 66 A89-31843  
Mission aspects of a future European polar orbit earth observation facility p 74 N89-18952
- POLAR REGIONS**  
Satellite sea surface temperature at the North Atlantic Polar Front related to high-resolution towed conductivity-temperature-depth data p 31 A89-22594
- POLARIMETERS**  
Unsupervised classification of scattering behavior using radar polarimetry data p 63 A89-26843  
Polarization of microwave emission of a water surface in a wide range of angles of sight p 34 A89-28290
- POLARIMETRY**  
Bayes classification of terrain cover using normalized polarimetric data p 54 A89-22649  
Multifrequency imaging radar polarimetry: Depolarisation of radar echoes at three wavelengths p 59 N89-18776  
Application of radar polarimetry to forestry p 15 N89-18919  
Radar polarimetric observations of a tree canopy p 15 N89-18920
- POLARIZATION (WAVES)**  
Application of radar polarimetry to forestry p 15 N89-18919
- POLARIZATION CHARACTERISTICS**  
Procedures for the determination of geophysical parameters from spaceborne microwave polarimeter measurements p 30 A89-22224
- POLLUTION MONITORING**  
A comparison of models for deriving dry deposition fluxes of O<sub>3</sub> and SO<sub>2</sub> to a forest canopy p 3 A89-20923  
Ocean wave spectra derived from Shuttle Imaging Radar-B imagery and surface measurements p 30 A89-22583  
UV laser fluorosensor for remote sensing p 35 A89-29763
- POLLUTION TRANSPORT**  
A model for the propagation of industrial atmospheric pollution registered on multispectral earth images p 17 A89-22213
- PORTABLE EQUIPMENT**  
Parabola directional field radiometer for aiding in space sensor data interpretations p 63 A89-27779
- POSITION (LOCATION)**  
The navigation method for NOAA/AVHRR image p 61 A89-20795
- POSITION ERRORS**  
Geometric correction of SPOT image p 54 A89-20812
- POSTMISSION ANALYSIS (SPACECRAFT)**  
Seasat - Results of the mission p 29 A89-22000
- POWER SPECTRA**  
Identification of geological features from their surface textural properties using OPS measurements --- Optical Power Spectra p 21 A89-20820



- Feature extraction considerations in utilising the optical power spectra for terrain classification p 54 A89-20821
- PRECIPITATION PARTICLE MEASUREMENT**  
EHF attenuation through the melting layer p 51 N89-18984
- PREDICTION ANALYSIS TECHNIQUES**  
An assessment of ATM and satellite data for estimating the groundwater contribution to slope stability --- Airborne Thematic Mapper (ATM) p 51 N89-18769  
Problems in the estimation of barley yields by remote sensing p 13 N89-18881
- PREDICTIONS**  
A comparison of original aircraft MSS and generated surface water reflectance images as predictors of lake water quality indicators [DE89-004882] p 50 N89-17932
- PRELAUNCH TESTS**  
The pre-launch performance verification of the ERS-1 active microwave instrumentation p 71 N89-18886
- PREPROCESSING**  
Preprocessing of the VARAN synthetic aperture airborne radar p 70 N89-18856  
Preprocessing and analysis of airborne visible near and shortwave infrared data for the detection of alteration in weathered vegetated terrain p 12 N89-18862
- PRINCIPAL COMPONENTS ANALYSIS**  
Principle component transformation analysis for tentative land use interpretation of Landsat MSS of Bogor region, Indonesia p 52 A89-20767  
Development of principal component analysis applied to multitemporal Landsat TM data p 4 A89-28035  
Combining oblique SPOT-1 images for the analysis of certain soil properties p 7 A89-31892  
Extracting spectral contrast in Landsat Thematic Mapper image data using selective principal component analysis p 57 A89-32337  
Improvements in the forward and inverse principal component transformations for geological mapping in a semi-arid terrain p 27 N89-18933
- PROBABILITY DISTRIBUTION FUNCTIONS**  
Statistical evaluation of the intensity distribution of sea surface radar images p 38 N89-18717  
Normal distributional assumptions in discrimination --- image processing p 59 N89-18821
- PROGRAM VERIFICATION (COMPUTERS)**  
MODIS information, data and control system (MIDACS) operations concepts [NASA-TM-100720] p 75 N89-19729
- PROJECT MANAGEMENT**  
ERS-1 operation capabilities p 71 N89-18884
- PROVING**  
The derivation and verification of surface reflectances using airborne MSS data and a radiative transfer model [DE89-004881] p 67 N89-17931
- PULSE AMPLITUDE**  
Impact of phase and amplitude errors on the ERS-1 active microwave instrumentation performance p 70 N89-18853
- PUSHBROOM SENSOR MODES**  
A comparison of images from a pushbroom scanner with normal color aerial photographs for detecting scattered recent conifer mortality p 7 A89-32336
- Q**
- QUALITY**  
Study of geometric quality of the MSS-LANDSAT imagery [INPE-4653-PRE/1360] p 57 N89-15440
- QUALITY CONTROL**  
Quality control of fast delivery processors and products --- ERS-1 p 72 N89-18892  
A SAR data quality assessment scheme for the ERS-1 mission p 72 N89-18893
- R**
- RADAR ATTENUATION**  
Fine resolution signatures of coniferous and deciduous trees at C band p 6 A89-30266
- RADAR CROSS SECTIONS**  
Fractal features of sea surface manifested in microwave remote sensing signatures p 32 A89-24872  
Off-nadir radar altimetry p 66 A89-31947  
Studies of the dependence of the microwave radar cross section on ocean surface variables during the FASINEX experiment p 41 N89-18782  
Normalized radar cross section of natural surfaces at millimeter wavelengths [AD-A202252] p 75 N89-19475
- RADAR DATA**  
VHF radar remote sensing of vertical profile of liquid water content and rainfall rate over Taiwan during the time period of Typhoon Wayne p 48 A89-20771  
The Alaska SAR processor p 70 N89-18851  
Radiometric calibration of airborne SAR data p 70 N89-18855  
Preprocessing of the VARAN synthetic aperture airborne radar p 70 N89-18856  
Post-processing airborne SAR data for multitemporal land-cover studies p 12 N89-18857  
A SAR data quality assessment scheme for the ERS-1 mission p 72 N89-18893
- RADAR ECHOES**  
Observation of the degree of glaciation in middle-level stratiform clouds p 62 A89-23464  
Features of the calculation of the main characteristics of an oceanographic radar altimeter p 32 A89-23646  
Can better environmental inputs improve sea clutter estimation? A numerical experiment p 36 A89-30258  
Computer simulation of multipath sea echo near grazing incidence p 38 N89-18722  
Multifrequency imaging radar polarimetry: Depolarisation of radar echoes at three wavelengths p 59 N89-18776  
A new approach to topographic altimetry p 73 N89-18914
- RADAR GEOLOGY**  
Major crustal lineaments on Seasat SAR and their off-shore extensions in the UK p 26 N89-18861
- RADAR IMAGERY**  
Radar imagery as a tool for mineral exploration - A case study of gold mineralization in East Kalimantan p 20 A89-20780  
The geology of the area surrounding Lake Kerinci, Indonesia as interpreted through SIR-B imagery p 20 A89-20781  
STAR-1 high resolution synthetic aperture radar imagery for precious metal exploration p 21 A89-20827  
Ocean wave spectra derived from Shuttle Imaging Radar-B imagery and surface measurements p 30 A89-22583  
Comparison of Shuttle Imaging Radar-B ocean wave image spectra with linear model predictions based on aircraft measurements p 30 A89-22584  
Ocean wave directional spectra and wave-current interaction in the Agulhas from the Shuttle Imaging Radar-B synthetic aperture radar p 30 A89-22585  
Motion characteristics of sea waves p 32 A89-23590  
Radar imaging of the surfaces of Venus and the earth using SAR data p 54 A89-23645  
Aerial and space remote-sensing techniques for geographical investigations --- Russian book p 62 A89-26178  
Unsupervised classification of scattering behavior using radar polarimetry data p 63 A89-26843  
Step frequency radar experiments on the Antarctic Sea ice p 34 A89-28365  
Segmentation of Synthetic Aperture Radar (SAR) images of ocean surface by the texture energy transform method [AD-A199536] p 37 N89-15309  
The 1988 International Geoscience and Remote Sensing Symposium (IGARSS 1988) on Remote Sensing: Moving Towards the 21st Century, volume 3 [ESA-SP-284-VOL-3] p 68 N89-18704  
A comparison of clutter texture properties in optical and SAR images p 8 N89-18708  
Extraction of small-scale spatial information from SLAR raw data of forests through an analysis of speckle p 8 N89-18709  
Adaptive speckle filtering for SAR images p 58 N89-18710  
Nonlinear filtering and edge detection in speckled radar images p 58 N89-18711  
Multitemporal and dual polarization of agricultural crops by X-band SAR images p 9 N89-18716  
Statistical evaluation of the intensity distribution of sea surface radar images p 38 N89-18717  
Modelling the SIR-B image response to partially coherent seas p 38 N89-18719  
Assessment of clearcut mapping accuracy with C-band SAR p 9 N89-18725  
Texture analysis of forest regeneration sites in high-resolution SAR imagery p 10 N89-18730  
SAR imagery of the Grand Banks (Newfoundland) pack ice pack and its relationship to surface features p 40 N89-18745  
Use of SAR imagery and other remotely-sensed data in deriving ice information during a severe ice event on the Grand Banks (Newfoundland) p 40 N89-18746  
SAR imaging of ocean waves in the marginal ice zone p 40 N89-18747
- Plans for the development of EOS SAR systems using the Alaska SAR facility --- Earth Observing System (EOS) p 69 N89-18757  
Segmentation of SAR images p 58 N89-18759  
Interpreting SAR images by means of map information p 58 N89-18760  
The visibility of linear features in SAR images p 59 N89-18763  
Automated linear feature detection and its application to curve location in synthetic aperture radar imagery p 59 N89-18764  
Simulation of SAR imaging of ship wakes p 41 N89-18765  
Automatic ship and ship wake detection in spaceborne SAR images from coastal regions p 41 N89-18766  
Effects of slopes and relief two-dimensional spatial frequencies on spaceborne SAR imagery p 59 N89-18777  
Study on directional spectrum characteristics of marine radar images of ocean waves p 41 N89-18786  
Information fusion by a knowledge-based system for SAR image interpretation p 60 N89-18831  
A high fidelity, high throughput system for geocoding SAR imagery p 60 N89-18849  
Measuring lead area changes in sea ice imagery --- satellite imagery p 44 N89-18871  
Crops radar responses analysis based on AGRISAR '86 data p 15 N89-18947  
Extraction of agricultural plant parameters from multitemporal Thematic Mapper (TM) and X-SAR data p 15 N89-18948  
Change detection in AGRISAR images p 15 N89-18949  
Correlations between agricultural plant parameters and multitemporal radar scatterometer data: First results from the European AGRISCATT 87 campaign p 16 N89-18951  
Active and passive remote sensing of ice [AD-A201915] p 47 N89-19792
- RADAR MAPS**  
Unsupervised classification of scattering behavior using radar polarimetry data p 63 A89-26843  
Sea bottom topography with X-band SLAR: Evaluation of existing models p 38 N89-18718  
Assessment of clearcut mapping accuracy with C-band SAR p 9 N89-18725
- RADAR MEASUREMENT**  
Remote studies of the ocean surface by a tower-based multifrequency microwave radar p 41 N89-18785  
Study on directional spectrum characteristics of marine radar images of ocean waves p 41 N89-18786  
Step frequency radar experiments on the Antarctic Sea ice p 43 N89-18802  
Application of radar polarimetry to forestry p 15 N89-18919  
Radar polarimetric observations of a tree canopy p 15 N89-18920  
Radar signature measurements during the AGRISCATT campaigns p 15 N89-18950
- RADAR SCANNING**  
Advanced SAR concepts p 73 N89-18926
- RADAR SCATTERING**  
Unsupervised classification of scattering behavior using radar polarimetry data p 63 A89-26843  
Fine resolution signatures of coniferous and deciduous trees at C band p 6 A89-30266  
Theoretical study of the sensitivity of the microwave backscattering coefficient to the soil surface parameters p 6 A89-30267  
Speckle correlation in SAR images of dynamic discrete scatterers p 37 N89-18707  
A measurement of microwave backscattering coefficients of rice plants p 8 N89-18714  
Association of radar backscattering with biophysical characteristics of Australian forests p 10 N89-18731  
Investigations of SAR backscatter for different test areas using two geocoded Seasat SAR scenes p 58 N89-18761  
A simulation test for soil moisture sensing p 10 N89-18772  
Observations of the effect of geometric properties of agricultural soils on radar backscatter, from C-SAR images p 11 N89-18781  
Analysis of ocean backscatter data obtained by the University of Kansas during TOWARD 84/85 p 42 N89-18787  
Important changes in microwave scattering properties of young snow-covered sea ice as indicated from dielectric modelling p 44 N89-18870  
Radar backscatter characteristics of trees at 215 GHz p 14 N89-18917  
Taking a broader view: Radarsat adds ScanSAR to its operations p 73 N89-18925  
Radar backscatter of sea ice during winter p 46 N89-18943



## RADAR SIGNATURES

- Correlations between agricultural plant parameters and multitemporal radar scatterometer data: First results from the European AGRISCATT 87 campaign p 16 N89-18951
- Normalized radar cross section of natural surfaces at millimeter wavelengths [AD-A202252] p 75 N89-19475
- Study of the use of radar X-band data of bare soil in a radar scattering model [BCRS-88-04] p 16 N89-19735
- Active and passive remote sensing of ice [AD-A201915] p 47 N89-19792
- RADAR SIGNATURES**
- Fine resolution signatures of coniferous and deciduous trees at C band p 6 A89-30266
- Correlation of radar reflectivity and chlorophyll fluorescence of forest trees p 9 N89-18727
- Fractal properties of the sea surface manifested in microwave remote sensing signatures p 41 N89-18784
- Dynamic topography as measured by the Geosat altimeter in regions of small surface height signatures p 43 N89-18837
- Radar signature measurements during the AGRISCATT campaigns p 15 N89-18950
- Normalized radar cross section of natural surfaces at millimeter wavelengths [AD-A202252] p 75 N89-19475
- RADAR TRACKING**
- Remote studies of the ocean surface by a tower-based multifrequency microwave radar p 41 N89-18785
- Auto and cross correlation analysis of environment, system and target parameters for iceberg detection using airborne radar p 45 N89-18874
- Tracking algorithms in radar altimetry p 72 N89-18911
- The advanced terrain tracking altimeter instrument p 74 N89-18954
- RADARSAT**
- Taking a broader view: Radarsat adds ScanSAR to its operations p 73 N89-18925
- RADIANCE**
- Calibration of infrared satellite images using high altitude aircraft measurements [AIAA PAPER 89-0617] p 54 A89-25505
- Optical properties of sea water bodies: Measurements with an underwater radiometer and a high-resolution spectroradiometer p 39 N89-18734
- RADIATION ABSORPTION**
- Estimating absorbed radiation and phytomass from multispectral reflectance of corn and soybeans p 13 N89-18876
- RADIATION MEASUREMENT**
- A method for processing and results of microwave radiometer studies of the earth from the Intercosmos 20 and 21 satellites p 36 A89-30122
- RADIATIVE TRANSFER**
- The derivation and verification of surface reflectances using airborne MSS data and a radiative transfer model [DE89-004881] p 67 N89-17931
- RADIO ALTIMETERS**
- Features of the calculation of the main characteristics of an oceanographic radar altimeter p 32 A89-23646
- A synthetic aperture altimeter p 73 N89-18913
- A study of advanced radar altimeter techniques --- satellite altimetry [ESA-CR(P)-2699] p 75 N89-19483
- RADIO GALAXIES**
- Research in geodesy and geophysics based upon radio interferometric observations of extragalactic radio sources [AD-A200958] p 25 N89-17933
- RADIOMETERS**
- Parabola directional field radiometer for aiding in space sensor data interpretations p 63 A89-27779
- Research in geodesy and geophysics based upon radio interferometric observations of extragalactic radio sources [AD-A200958] p 25 N89-17933
- Radiometric problems in the use of the Thematic Mapper for marine research p 46 N89-18940
- RADIOMETRIC CORRECTION**
- Radiometric calibration of airborne SAR data p 70 N89-18855
- RADIOMETRIC RESOLUTION**
- Simulation of radiometric ocean images recorded from high-altitude platforms p 33 A89-27980
- Stability considerations for the ERS-1 wind scatterometer radiometric performance p 71 N89-18889
- RADIOSONDES**
- Satellite derived earth surface temperatures: A crop assessment tool p 8 N89-17930

## RAIN

- Satellite remote sensing of cloud distribution and amount of rainfall over the Tibet Plateau area of China p 48 A89-20770
- VHF radar remote sensing of vertical profile of liquid water content and rainfall rate over Taiwan during the time period of Typhoon Wayne p 48 A89-20771
- Satellite remote sensing of rainfall p 49 A89-27946
- The Special Sensor Microwave Imager - A new instrument with rainfall monitoring potential p 64 A89-28038
- Physical retrieval of rainfall rates over the ocean by multispectral microwave radiometry - Application to tropical cyclones p 37 A89-32434
- Hydrological aspects of combined effects of storm surges and heavy rainfall on river flow [WMO-704] p 49 N89-17340
- Snow cover-summer monsoon rainfall over parts of Sahel p 51 N89-18832
- A study of the effect of rain on Seasat radar altimeter data p 44 N89-18840
- EHF attenuation through the melting layer p 51 N89-18964

## RAMAN SPECTRA

- Remote sensing of ocean physical properties - A comparison of Raman and Brillouin techniques p 34 A89-28003
- Oceanic remote sensing p 35 A89-29726
- The capabilities of nonlinear Raman spectroscopy for remote diagnostics of water bodies p 35 A89-29730

## RANGELANDS

- Integrated NDVI images for Niger 1986-1987 --- Normalized Difference Vegetation Index p 4 A89-28128

## RAY TRACING

- Goniometric observations of light scattered from soils and leaves p 4 A89-24873

## REAL TIME OPERATION

- Real-time processing of digital image data in support of the Canadian sea ice analysis and prediction program p 43 N89-18803

## New architecture for a real-time SAR processor

- p 69 N89-18850
- Real-time stereo matching SPOT using transputer arrays p 74 N89-18958
- MODIS information, data and control system (MIDACS) operations concepts [NASA-TM-100720] p 75 N89-19729

## REFLECTANCE

- A comparison of original aircraft MSS and generated surface water reflectance images as predictors of lake water quality indicators [DE89-004882] p 50 N89-17932
- The directional reflectance of heather canopies: Towards a descriptive model p 13 N89-18878

## REFLECTORS

- Preliminary observations of polar sea ice with the Special Sensor Microwave Imager p 42 N89-18800

## REGIONAL PLANNING

- The Geospace philosophy: A new practical approach in remote sensing and planning for local authorities p 76 N89-18750

## REMOTE SENSING

- Asian Conference on Remote Sensing, 8th, Jakarta, Indonesia, Oct. 22-27, 1987, Proceedings p 76 A89-20751
- Spectral reflectance properties of a leaf of some mangrove species in Okinawa p 1 A89-20753
- The studies for the computer classification and the investigation of grasslands in Tibet using Space-Lab color infrared image p 1 A89-20754
- Airborne multispectral remote sensing of forest decline in West Germany p 1 A89-20757
- Forest observation by satellite p 1 A89-20759
- The feasibility study of oil palm area estimation in the southern part of Thailand using Landsat data p 2 A89-20760
- On classification of forests of some portions of central India using satellite imagery p 2 A89-20761
- Relationship of spectral data and grain yield variation in rice (*Oryza sativa* L.) ADT 31 p 2 A89-20762
- Remote sensing applications for agricultural landuse survey in Indonesia - Isimu case study p 2 A89-20763
- Accuracy of land-cover/use classification p 52 A89-20765
- Land use suitability classification using remote sensing data and geographic information for volcanic regions p 16 A89-20766
- Monitoring inundation area of Aliran Sungai Bengawan Solo Jawa Timur with Landsat images p 48 A89-20768
- Satellite remote sensing of cloud distribution and amount of rainfall over the Tibet Plateau area of China p 48 A89-20770

- VHF radar remote sensing of vertical profile of liquid water content and rainfall rate over Taiwan during the time period of Typhoon Wayne p 48 A89-20771
- Reconnaissance groundwater appraisal of Bohol Island, Philippines, by satellite data analysis p 48 A89-20772
- Soil surface moisture estimation - A case study area on North Banten, West Java, Indonesia p 2 A89-20773

- An estimation of areal evapotranspiration using Landsat and elevation data p 48 A89-20776
- Identification of surface-groundwater interaction zones in the Bogor volcanic fan p 48 A89-20777
- Drainage pattern analysis with the aid of Landsat MSS data of the Citarium river basin, West Java, Indonesia p 48 A89-20778
- Radar imagery as a tool for mineral exploration - A case study of gold mineralization in East Kalimantan p 20 A89-20780
- The geology of the area surrounding Lake Kerinci, Indonesia as interpreted through SIR-B imagery p 20 A89-20781
- Mapping of construction material sites around Bangalore City using Landsat Thematic Mapper data p 52 A89-20782
- Volcanic eruption monitoring using satellite platform p 20 A89-20783
- Suspended solid classification of the Jakarta Bay p 28 A89-20785
- The extraction of sea fishery potential area from Airborne Ocean Color Radiometer data p 28 A89-20786
- Water quality estimation from Landsat data with spectral and sea truth data base system p 28 A89-20788
- Application of airborne scanners in remote sensing of sea p 29 A89-20789
- The role of remote sensing in geographic information systems using computer p 17 A89-20792
- The creating of blue synthetic channel of MSS Landsat image p 52 A89-20794
- Low cost, microcomputer-based interactive analysis system for direct-reception and archived remote sensing data p 53 A89-20796
- Application of three dimensional image system p 53 A89-20797
- Coastline monitoring in Madura Strait, Indonesia on 1972-1985 p 29 A89-20804
- The application of remote sensing for forest inventory p 2 A89-20809
- New technology for displaying of NOAA AVHRR thermal band image p 29 A89-20810
- A basic study of the reduction of the exactness of mesh data map made by uniting n-squared meshes to one mesh p 54 A89-20811
- Land use and land cover applications of Landsat MSS data p 17 A89-20813
- Study of the monitoring of land cover/use using remote sensing data by personal computer in southern part of Bandung area, West Java p 2 A89-20815
- Correlation of Landsat TM and aeromagnetic data along the Eastern Margin of the Cuddapah Basin, South India p 21 A89-20817
- Prioritization of watershed with regard to silt yield potential through data integration technique p 48 A89-20818
- Aerial remote sensing technique in the identification and acreage estimation of various plantations - A case study in Gorakhpur district, Uttar Pradesh, India p 2 A89-20819
- Feature extraction considerations in utilising the optical power spectra for terrain classification p 54 A89-20821
- SPOT image interpretation for information on human settlement growth p 17 A89-20824
- Application of remote sensing for hydrocarbon exploration on Timor Island, Indonesia p 21 A89-20825
- The applications of Landsat imagery to soil erosion study in Northern Thailand p 3 A89-20826
- Usefulness of remote sensing in uranium exploration programme in parts of Karnataka state, India p 21 A89-20828
- Airborne gravity as a supporting tool for hydrocarbon exploration in Indonesia p 21 A89-20829
- Landsat 5 TM image of the Mont Saint-Michel region of France p 54 A89-21249
- Commercial remote sensing satellites generate debate, foreign competition p 76 A89-21397
- Effective permittivity of vegetation in the microwave range p 3 A89-21612
- Dependence of snow melting and surface-atmosphere interactions on the forest structure p 3 A89-21740
- Laser sounding of the troposphere and the underlying surface --- Russian book p 17 A89-22066
- A model for the propagation of industrial atmospheric pollution registered on multispectral earth images p 17 A89-22213

- Determination of clear-sky planetary albedo p 62 A89-22214
- Determination of relative crop areas from spectrometric data p 22 A89-22218
- Brightness of a laser-beam halo in vegetation cover p 3 A89-22221
- Principal results of remote-sensing studies of Siberia's natural resources (On the occasion of the 10th anniversary of the Scientific Coordination Council, 1977-1987) p 62 A89-22225
- Remote sensing of canopy chemistry and nitrogen cycling in temperate forest ecosystems p 3 A89-23431
- Agrometeorological aspects of the utilization of remote-sensing data p 3 A89-23663
- The relationship between suspended sediment concentration and remotely sensed spectral radiance - A review p 48 A89-24649
- Fractal features of sea surface manifested in microwave remote sensing signatures p 32 A89-24872
- Goniometric observations of light scattered from soils and leaves p 4 A89-24873
- Effectiveness of satellite remote sensing on monitoring of marine environment [IAF PAPER 88-153] p 32 A89-24875
- Aerial and space remote-sensing techniques for geographical investigations --- Russian book p 62 A89-26178
- Application of Landsat MSS and TM data to geological resource exploration p 22 A89-26397
- Alternatives for mapping from satellites p 62 A89-26398
- Hindcasts and data assimilation studies with the WAM model during the Seasat period --- wave model p 32 A89-26442
- Simulated effects of barometric pressure and ozone content upon the estimate of marine phytoplankton from space p 33 A89-26443
- The characterization of sources of illumination in a Ponderosa Pine (*Pinus ponderosa*) forest community using the portable instantaneous display and analysis spectrometer p 4 A89-27781
- Applications of remote sensing to agrometeorology; Proceedings of the Course, Ispra, Italy, Apr. 6-10, 1987 p 63 A89-27933
- Fundamentals of remote sensing p 63 A89-27934
- Platforms --- for remote sensors p 63 A89-27936
- The luxuriant image - An introduction to remote sensing data processing p 55 A89-27937
- Microwave remote sensing of soil moisture p 4 A89-27944
- The vegetation index and the study of vegetation dynamics p 4 A89-27945
- Satellite remote sensing of rainfall p 49 A89-27946
- Ocean optics IX; Proceedings of the Meeting, Orlando, FL, Apr. 4-6, 1988 [SPIE-925] p 33 A89-27976
- Remote sensing of ocean physical properties - A comparison of Raman and Brillouin techniques p 34 A89-28003
- Buoyant surface jet analysis of the Yukon River p 49 A89-28033
- Determination of atmospheric turbidity from remotely-sensed data - A case study p 34 A89-28034
- Development of principal component analysis applied to multitemporal Landsat TM data p 4 A89-28035
- Application of the Haar transform for extraction of linear and anomalous patterns over part of Cambay Basin, India p 55 A89-28037
- Polarization of microwave emission of a water surface in a wide range of angles of sight p 34 A89-28290
- ERS-1 active microwave instrumentation design and performance status [IAF PAPER 87-136] p 65 A89-28329
- Detection of periodic characteristics of rice field vegetation by microwave backscatter measurement p 5 A89-28364
- Step frequency radar experiments on the Antarctic Sea ice p 34 A89-28365
- Digital image processing in remote sensing --- Book p 55 A89-29064
- Visualization of topographic data using video animation p 55 A89-29066
- Multiple source data processing in remote sensing p 56 A89-29073
- Extreme variability, scaling and fractals in remote sensing - Analysis and simulation p 56 A89-29074
- Analysis and interpretation of SPOT images of urban and agricultural/forest sections of the Sherbrooke region p 5 A89-29373
- Effects of solar angle on reflectance from wetland vegetation p 5 A89-29409
- Complementarity of middle-infrared with visible and near-infrared reflectance for monitoring wheat canopies p 5 A89-29410
- Application of a flux algorithm to a field-satellite campaign over vegetated area p 6 A89-29411
- Tersail - A numerical model for combined analysis of vegetation canopy bidirectional reflectance and thermal emissions p 6 A89-29415
- Band-moment analysis of imaging-spectrometer data p 65 A89-29436
- Accuracy assessment of Landsat-based visual change detection methods applied to the rural-urban fringe p 18 A89-29437
- Oceanic remote sensing p 35 A89-29726
- Laser airborne sensing field experiments using the 'Chaika' assembly --- for probing water bodies p 35 A89-29728
- Effects of round trip laser emission propagation through a turbulent surface for laser airborne oceanic sensing p 35 A89-29729
- The capabilities of nonlinear Raman spectroscopy for remote diagnostics of water bodies p 35 A89-29730
- Detection of ocean bottom relief by local geoid p 35 A89-29731
- Surface wave interaction - Theory and capability of oceanic remote sensing p 35 A89-29732
- UV laser fluorosensor for remote sensing p 35 A89-29763
- Wavenumber spectra of short gravity waves p 35 A89-30019
- Remote sensing of surface manifestations of short-period internal waves in the ocean p 35 A89-30114
- Radiation models of mesotrophic and eutrophic bodies of water p 36 A89-30120
- Variations of the infrared emission of snow and ice cover p 49 A89-30121
- Improvement of multispectral color images by intensifying local contrasts p 56 A89-30123
- Technological limitations to satellite glaciology p 36 A89-30257
- Comparison of NOAA-AVHRR-2 sea surface temperatures with surface measurements in coastal waters p 36 A89-30259
- Investigation of water content from airborne MSS data p 49 A89-30261
- Wasteland identification in India using satellite remote sensing p 18 A89-30263
- Bidirectional canopy reflectance and its relationship to vegetation characteristics p 6 A89-30264
- Analysis and representation of vegetation continua from Landsat Thematic Mapper data for lowland heaths p 7 A89-30268
- Visual and computer classifications of remotely-sensed images - A case study of grasslands in Cambridgeshire p 7 A89-30269
- Remote sensing of evaporite mineral zonation in salt flats (salars) p 23 A89-30271
- The development of remote sensing in China p 76 A89-31560
- Large-scale, low-amplitude bedforms (chevrons) in the Selima sand sheet, Egypt p 23 A89-31755
- Off-nadir radar altimetry p 66 A89-31947
- Passive microwave remote sensing system for soil moisture - Some supporting research p 49 A89-31948
- Land image data processing requirements for the EOS era p 56 A89-31949
- Modeling vegetation as a set of scatterers p 7 A89-32110
- A comparison of images from a pushbroom scanner with normal color aerial photographs for detecting scattered recent conifer mortality p 7 A89-32336
- Monitoring water quality and river plume transport in Green Bay, Lake Michigan with SPOT-1 imagery p 49 A89-32338
- Trace gas emissions from chaparral and boreal forest fires p 7 A89-32432
- The application of remote sensing to geomorphological mapping and mass movement study in the vicinity of Provo, Utah p 23 A89-15439
- A multi-sensor remote sensing approach for measuring primary production from space [NASA-CR-184662] p 37 A89-15444
- Using different sources of information in automated linear feature extraction from remote sensing data [INPE-4708-PRE/1390] p 24 A89-15447
- MODIS-HIRIS ground data systems commonality report [NASA-TM-100718] p 67 A89-16205
- Indian activities in remote sensing applications: Microwave remote sensing p 67 A89-16886
- Accuracy assessment, using stratified plurality sampling, of portions of a LANDSAT classification of the Arctic National Wildlife Refuge Coastal Plain [NASA-TM-101042] p 8 A89-17339
- The 1988 International Geoscience and Remote Sensing Symposium (IGARSS 1988) on Remote Sensing: Moving Towards the 21st Century, volume 3 [ESA-SP-284-VOL-3] p 68 A89-18704
- Nonlinear filtering and edge detection in speckled radar images p 58 A89-18711
- Characterizing forest ecosystem dynamics through modelling and remote sensing observations p 10 A89-18728
- The impact of multiviewing reflectance data on the estimation of suspended sediment concentration p 50 A89-18735
- Monitoring offshore water quality from space p 39 A89-18739
- Monitoring of suspended sediments in Jatiluhur Reservoir using satellite images p 50 A89-18740
- The UN declaration of legal principals on remote sensing, 1986 p 76 A89-18748
- Technology transfer for development of coastal zone resources: Caribbean experts examine critical issues p 40 A89-18749
- The Geospace philosophy: A new practical approach in remote sensing and planning for local authorities p 76 A89-18750
- Operational remote sensing in the United Kingdom: Problems of image acquisition p 68 A89-18751
- Effects of commercialisation on international remote sensing activities p 76 A89-18752
- The algorithm development facility: its role in the development and operation of a satellite data centre p 68 A89-18755
- Improvements in ground water recharge estimation using satellite remote sensing p 50 A89-18768
- Digital elevation models and their application to remote sensing of water resources p 51 A89-18770
- A simulation test for soil moisture sensing p 10 A89-18772
- Integration of geological, geophysical and remotely sensed data for the Solway Basin, England p 26 A89-18794
- A method to forecast open pack ice speed of motion using remotely-sensed data p 42 A89-18801
- Toward the automated use of remote sensing data in operational ice forecasting p 43 A89-18804
- Optimal sampling for remote sensing: Estimating the regional mean p 11 A89-18822
- Remote sensing of land processes: Sponsored programs of study by the National Aeronautics and Space Administration p 19 A89-18833
- Proceedings of the 1988 International Geoscience and Remote Sensing Symposium (IGARSS '88 on Remote Sensing: Moving Towards the 21st Century, Volume 2 [ESA-SP-284-VOL-2] p 69 A89-18836
- Experiments in Bulgaria for determination of soil moisture in the top one-meter layer using microwave radiometry and a priori information p 11 A89-18843
- Problems in the estimation of barley yields by remote sensing p 13 A89-18881
- Vegetation sampling for studies using remotely sensed data p 13 A89-18883
- A method for the clustering of remotely sensed multispectral images by using statistical test for spatial uniformity p 61 A89-18898
- Geological remote sensing of Palaeogene rocks in the Wind River Basin, Wyoming, USA p 28 A89-18935
- Airborne nonacoustic bathymetric survey flight test results p 51 A89-18937
- A study of passive microwave remote sensing p 45 A89-18938
- Remote sensing in a marginal ice zone: A brief overview p 46 A89-18941
- Mission aspects of a future European polar orbit earth observation facility p 74 A89-18952
- Progress in automatic analysis of multi-temporal remotely-sensed data p 61 A89-18956
- Alternative approaches to the classification of upland semi-natural vegetation --- remote sensing p 16 A89-18961
- Simulation of optical remote sensing systems for earth resource analysis p 74 A89-18964
- Comparisons of satellite data surface-based remote sensing measurements in Utah winter orographic storms p 75 A89-19079
- Land use analysis using remote sensing techniques. Investigation of the usefulness of LANDSAT Thematic Mapper satellite pictures for obtaining and up to date picture of land use in the province South Holland [BCRS-88-01] p 61 A89-19733
- Salinity mapping based on SPOT images of the Punjab, Pakistan [BCRS-88-03] p 16 A89-19734
- Active and passive remote sensing of ice [AD-A201915] p 47 A89-19792
- REMOTE SENSORS**
- Parabola directional field radiometer for aiding in space sensor data interpretations p 63 A89-27779
- Sensors p 63 A89-27935
- Normalized radar cross section of natural surfaces at millimeter wavelengths [AD-A202252] p 75 A89-19475

## RESERVOIRS

## RESERVOIRS

- Monitoring of suspended sediments in Jatiluhur Reservoir using satellite images p 50 N89-18740

## RESOURCES MANAGEMENT

- Technology transfer for development of coastal zone resources: Caribbean experts examine critical issues p 40 N89-18749

## RICE

- Relationship of spectral data and grain yield variation in rice (*Oryza sativa* L.) ADT 31 p 2 A89-20762  
 Detection of periodic characteristics of rice field vegetation by microwave backscatter measurement p 5 A89-28364  
 Water turbidity and perpendicular vegetation indices for paddy rice flood damage analyses p 6 A89-29412  
 A measurement of microwave backscattering coefficients of rice plants p 8 N89-18714  
 Multitemporal and dual polarization of agricultural crops by X-band SAR images p 9 N89-18716

## RIDGES

- A new view of the mid-ocean ridge from the behaviour of ridge-axis discontinuities p 31 A89-23433

## RING STRUCTURES

- Ring structures of buried platform areas and the evaluation of their tectonic activity on the basis of geomorphological data p 23 A89-30118

## RIVER BASINS

- Annular and block-folded structures on space and aerial photographs p 25 N89-17915  
 Geological remote sensing of Palaeogene rocks in the Wind River Basin, Wyoming, USA p 28 N89-18935

## RIVERS

- Buoyant surface jet analysis of the Yukon River p 49 A89-28033  
 Hydrological aspects of combined effects of storm surges and heavy rainfall on river flow [WMO-704] p 49 N89-17340

## ROBOTICS

- Sensor fusion of range and reflectance data for outdoor scene analysis p 76 N89-19868

## ROCK MECHANICS

- Applications of image scanning and processing in rock shear surface study p 20 A89-20779

## ROSS ICE SHELF

- Antarctic Ocean polynyas [NASA-CR-184805] p 47 N89-19102

## RURAL AREAS

- Accuracy assessment of Landsat-based visual change detection methods applied to the rural-urban fringe p 18 A89-29437

## RURAL LAND USE

- Aerial remote sensing technique in the identification and acreage estimation of various plantations - A case study in Gorakhpur district, Uttar Pradesh, India p 2 A89-20819  
 Image-based atmospheric correction of multitemporal Thematic Mapping data for agricultural land cover classification p 14 N89-18895

## S

## SALINITY

- Delineation of salt-affected soils through digital analysis of Landsat MSS data p 6 A89-30262  
 Salinity mapping based on SPOT images of the Punjab, Pakistan [BCRS-88-03] p 16 N89-19734

## SAMPLING

- Accuracy assessment, using stratified plurality sampling, of portions of a LANDSAT classification of the Arctic National Wildlife Refuge Coastal Plain [NASA-TM-101042] p 8 N89-17339

## SANDS

- Monitoring surface mineral workings using TM and SPOT p 26 N89-18796

## SATELLITE ALTIMETRY

- Geosat crossover analysis in the tropical Pacific. II - Verification analysis of altimetric sea level maps with expendable bathythermograph and island sea level data p 32 A89-26438  
 Frontal signals east of Iceland from the Geosat altimeter p 33 A89-26643  
 The impact of satellite altimetry data on numerical simulations of general midlatitude oceanic circulation p 34 A89-28305  
 An experiment to invert Seasat altimetry for the Mediterranean and Black Sea mean surfaces p 36 A89-30900  
 Off-nadir radar altimetry p 66 A89-31947  
 Proceedings of the 1988 International Geoscience and Remote Sensing Symposium (IGARSS '88 on Remote Sensing: Moving Towards the 21st Century, Volume 2 [ESA-SP-284-VOL-2] p 69 N89-18836

- Dynamic topography as measured by the Geosat altimeter in regions of small surface height signatures p 43 N89-18837

- Assimilation of altimeter data into numerical ocean models p 43 N89-18838

- The influence of water vapor on the detection of ocean mesoscale fronts and eddies by the Geosat altimeter p 44 N89-18839

- A study of the effect of rain on Seasat radar altimeter data p 44 N89-18840

- Observations of ice types in satellite altimeter data p 44 N89-18841

- Satellite radar altimetry over arid regions p 69 N89-18842

- ERS-1 altimeter height calibration p 71 N89-18891

- The Navy Geosat radar altimeter satellite mission p 45 N89-18909

- An advanced terrain tracking altimeter p 45 N89-18910

- Tracking algorithms in radar altimetry p 72 N89-18911

- A new approach to topographic altimetry p 73 N89-18914

- Investigations of sea ice using coincident Geosat altimetry and synthetic aperture radar during MIZEX-87 p 46 N89-18945

- The advanced terrain tracking altimeter instrument p 74 N89-18954

## SATELLITE DESIGN

- ERS-1 operation capabilities p 71 N89-18884

## SATELLITE IMAGERY

- Asian Conference on Remote Sensing, 8th, Jakarta, Indonesia, Oct. 22-27, 1987, Proceedings p 78 A89-20751

- Comparative study of vegetation index and false colour composite image of NOAA-AVHRR data for bio-mass studies p 1 A89-20752

- The studies for the computer classification and the investigation of grasslands in Tibet using Space-Lab color infrared image p 1 A89-20754

- The use of SPOT imagery in Medan agriculture area for monitoring features changes p 1 A89-20755

- Digital image analysis of Landsat MSS data in an estate crop inventory of the Island of Bali p 1 A89-20756

- Soil and vegetation mapping by using SPOT image p 1 A89-20758

- Forest observation by satellite p 1 A89-20759

- The feasibility study of oil palm area estimation in the southern part of Thailand using Landsat data p 2 A89-20760

- On classification of forests of some portions of central India using satellite imagery p 2 A89-20761

- First results of topographical mapping using SPOT images of Malaysia p 52 A89-20764

- Accuracy of land-cover/use classification p 52 A89-20765

- Principle component transformation analysis for tentative land use interpretation of Landsat MSS of Bogor region, Indonesia p 52 A89-20767

- Monitoring inundation area of Aliran Sungai Bengawan Solo Jawa Timur with Landsat images p 48 A89-20768

- Applications of SPOT HRV data for land use and soil mapping in Rayong basin p 2 A89-20769

- Satellite remote sensing of cloud distribution and amount of rainfall over the Tibet Plateau area of China p 48 A89-20770

- VHF radar remote sensing of vertical profile of liquid water content and rainfall rate over Taiwan during the time period of Typhoon Wayne p 48 A89-20771

- Reconnaissance groundwater appraisal of Bohol Island, Philippines, by satellite data analysis p 48 A89-20772

- Soil surface moisture estimation - A case study area on North Banten, West Java, Indonesia p 2 A89-20773

- Flooded and inundation dangerous area prediction and its visualisation - A case study on the Pemali-Comal River Basin, Central Java, Indonesia p 48 A89-20774

- The use of image enhancement technique for peat land mapping using Landsat mass data in Indonesia p 52 A89-20775

- Mapping of construction material sites around Bangalore City using Landsat Thematic Mapper data p 52 A89-20782

- Volcanic eruption monitoring using satellite platform p 20 A89-20783

- The creating of blue synthetic channel of MSS Landsat image p 52 A89-20794

- The navigation method for NOAA-AVHRR image p 61 A89-20795

- Low cost, microcomputer-based interactive analysis system for direct-reception and archived remote sensing data p 53 A89-20796

- Application of three dimensional image system p 53 A89-20797

- Comparison of the orientation's accuracy for SPOT imagery p 53 A89-20798

- Accuracy of terrain measurement using SPOT HRV data --- high resolution video p 53 A89-20801

- Aerospace imagery and data for modelling erosion, sediment yield and crop yield prediction using GIS, applied to the Upper Komering catchment, Sumatra p 2 A89-20802

- Coastline monitoring in Madura Strait, Indonesia on 1972-1985 p 29 A89-20804

- The preliminary study on correlation between satellite information and bottom trawling ground in the East China Sea and the Yellow Sea p 29 A89-20805

- Digital Terrain Model computation using SPOT data p 53 A89-20807

- On geology of some districts in Central India using Landsat imagery p 21 A89-20808

- New technology for displaying of NOAA AVHRR thermal band image p 29 A89-20810

- Geometric correction of SPOT image p 54 A89-20812

- Land use and land cover applications of Landsat MSS data p 17 A89-20813

- Assessing extent of damage caused by flooding and drought in dominantly rice cropland area using Landsat data p 2 A89-20814

- Correlation of Landsat TM and aeromagnetic data along the Eastern Margin of the Cuddapah Basin, South India p 21 A89-20817

- Identification of geological features from their surface textural properties using OPS measurements --- Optical Power Spectra p 21 A89-20820

- Study on changes of mangrove forest in Thailand by using Landsat imagery p 3 A89-20822

- Integrated study of Landsat, aeromagnetic and Bouguer gravity anomaly data for geological appraisal - A case study from Tamil Nadu, India p 21 A89-20823

- Application of remote sensing for hydrocarbon exploration on Timor Island, Indonesia p 21 A89-20825

- The applications of Landsat imagery to soil erosion study in Northern Thailand p 3 A89-20826

- Landsat 5 TM image of the Mont Saint-Michel region of France p 54 A89-21249

- Contribution of second-generation Landsat TM and SPOT HRV satellites to urban analysis (Rennes, France) p 17 A89-21250

- Neotectonic zoning of Belorussia on the basis of space data p 21 A89-22215

- A tomographic approach to lineament identification on aerial and space images p 22 A89-22223

- Operational calibration of Meteosat's infrared channel p 62 A89-22622

- A procedure for land area classification using Landsat TM digital imagery p 17 A89-24651

- Calibration of infrared satellite images using high altitude aircraft measurements [AIAA PAPER 89-0817] p 54 A89-25595

- Alternatives for mapping from satellites p 62 A89-26398

- Edge detection applied to satellite imagery of the oceans p 33 A89-26844

- Parabola directional field radiometer for aiding in space sensor data interpretations p 63 A89-27779

- Definition and design of an operational environment-monitoring system p 18 A89-27788

- Concepts for processing and analyzing of multiple SAR and Landsat images p 55 A89-27789

- Bathymetry using Thematic Mapper imagery p 34 A89-27995

- Buoyant surface jet analysis of the Yukon River p 49 A89-28033

- The Special Sensor Microwave Imager - A new instrument with rainfall monitoring potential p 64 A89-28038

- Scene locations and overpass dates for Landsat and SPOT sensors p 64 A89-28039

- Application of Landsat imagery and surficial geochemistry to the discovery of tungsten skarn deposits associated with buried plutons, Yukon and Northwest Territories, Canada p 23 A89-28126

- Extension of a drought monitoring and vegetation classification methodology to the western Sahel p 4 A89-28127

- Integrated NDVI images for Niger 1986-1987 --- Normalized Difference Vegetation Index p 4 A89-28128

- Mapping and inventory of forest fires from digital processing of TM data p 5 A89-28129

- Visual and digital classification of Landsat TM data for soil, physiography and land use mapping in Axios alluvial plain, Thessaloniki, Greece p 5 A89-28130

- Visualization of topographic data using video animation p 55 A89-29066

- Microcomputers and mass storage devices for image processing p 65 A89-29070

- Multiple source data processing in remote sensing p 56 A89-29073
- Processing satellite infrared and visible imagery for oceanographic analyses p 34 A89-29075
- Mapping in the Oman ophiolite using enhanced Landsat Thematic Mapper images p 23 A89-29301
- Multispectral classification of land use at the rural-urban fringe using spot data p 18 A89-29371
- Analysis of atmospheric effects in SPOT HRV images p 65 A89-29372
- Analysis and interpretation of SPOT images of urban and agricultural/forest sections of the Sherbrooke region p 5 A89-29373
- Area measurement of agricultural fields from satellite images p 5 A89-29374
- Comparative spectral analysis of HRV and TM sensors p 65 A89-29375
- Water turbidity and perpendicular vegetation indices for paddy rice flood damage analyses p 6 A89-29412
- Use of the variable gain settings on SPOT p 65 A89-29435
- Accuracy assessment of Landsat-based visual change detection methods applied to the rural-urban fringe p 18 A89-29437
- Landscape processing of satellite imagery for a biospheric data bank p 56 A89-30239
- A 10 km resolution image of the entire night-time earth based on cloud-free satellite photographs in the 400-1100 nm band p 56 A89-30256
- Remote sensing of macrophytic algae of the Molene Archipelago in France - Terrain radiometry and application to SPOT satellite data p 36 A89-30260
- Delineation of salt-affected soils through digital analysis of Landsat MSS data p 6 A89-30262
- Wasteland identification in India using satellite remote sensing p 18 A89-30263
- Unsupervised training area selection in forests using a nonparametric distance measure and spatial information p 6 A89-30265
- Analysis and representation of vegetation continua from Landsat Thematic Mapper data for lowland heaths p 7 A89-30268
- Visual and computer classifications of remotely-sensed images - A case study of grasslands in Cambridgeshire p 7 A89-30269
- Large-scale, low-amplitude bedforms (chevrons) in the Selima sand sheet, Egypt p 23 A89-31755
- Geological mapping and analysis of fracturing in the south part of the Central Anti-Atlas in Morocco using a Landsat MSS image p 23 A89-31887
- Nighttime and daytime HCMM thermographs of the Iberian Peninsula p 56 A89-31888
- Thermal infrared and visible images of the Iberian Peninsula p 56 A89-31889
- Integration of SPOT data in an urban data bank - Locating work sites p 18 A89-31891
- Combining oblique SPOT-1 images for the analysis of certain soil properties p 7 A89-31892
- Multitemporal study of differently farmed permanent grazing lands in the Lorraine region of France using SPOT-1 data p 7 A89-31894
- On-line aspects of stereophotogrammetric processing of SPOT images p 66 A89-32334
- A simple spatial filtering routine for the cosmetic removal of scan-line noise from Landsat TM P-type imagery p 57 A89-32335
- Monitoring water quality and river plume transport in Green Bay, Lake Michigan with SPOT-1 imagery p 49 A89-32338
- Study of geometric quality of the MSS-LANDSAT imagery [INPE-4653-PRE/1360] p 57 N89-15440
- Investigation of information content of Thematic Mapper and SPOT multiband image data, using simulated image data of the Freiburg region (Federal Republic of Germany) [ESA-TT-975] p 57 N89-15442
- Automatic registration of satellite imagery [INPE-4637-PRE/1349] p 57 N89-17414
- Progress of research to identify rotating thunderstorms using satellite imagery [NASA-CR-183555] p 68 N89-17981
- The 1988 International Geoscience and Remote Sensing Symposium (IGARSS 1988) on Remote Sensing: Moving Towards the 21st Century, volume 3 [ESA-SP-284-VOL-3] p 68 N89-18704
- Statistical evaluation of the intensity distribution of sea surface radar images p 38 N89-18717
- Possibilities of the satellite imagery to locate the forest decline areas in the Vosges Massif (France) p 10 N89-18729
- Variability of the diffuse attenuation coefficient in waters off the US East Coast p 39 N89-18738
- Monitoring of suspended sediments in Jatiluhur Reservoir using satellite images p 50 N89-18740
- The preliminary study of current shifting state by the use of infrared images of NOAA-9 p 39 N89-18742
- Operational remote sensing in the United Kingdom: Problems of image acquisition p 68 N89-18751
- Effects of commercialisation on international remote sensing activities p 76 N89-18752
- Satellite data acquisition planning at the Canada Center for Remote Sensing p 68 N89-18753
- Plans for the development of EOS SAR systems using the Alaska SAR facility --- Earth Observing System (EOS) p 69 N89-18757
- Investigations of SAR backscatter for different test areas using two geocoded Seasat SAR scenes p 58 N89-18761
- Estimation of the area of Lake Kariba, Zimbabwe, using LANDSAT MSS imagery p 51 N89-18775
- Integration of digital satellite and geophysical data, Heath Steele Mines, New Brunswick, Canada p 25 N89-18792
- Image processing methods for the presentation of multiple geological datasets from the English Lake District p 25 N89-18793
- Monitoring surface mineral workings using TM and SPOT p 26 N89-18796
- Preliminary observations of polar sea ice with the Special Sensor Microwave Imager p 42 N89-18800
- A method to forecast open pack ice speed of motion using remotely-sensed data p 42 N89-18801
- An ERDAS module for routine processing of AVHRR data p 43 N89-18817
- Geological lineament detection using the Hough transform p 26 N89-18818
- SPOT mapping software for Wild Aviolet BC2 analytical plotter p 60 N89-18824
- Monitoring of agro-forestry production systems in the Sudano-Sahelian zone of West Africa p 11 N89-18825
- An atmospheric correction method for AVHRR infrared data using HIRS/2 data p 69 N89-18828
- Proceedings of the 1988 International Geoscience and Remote Sensing Symposium (IGARSS) '88 on Remote Sensing: Moving Towards the 21st Century, Volume 2 [ESA-SP-284-VOL-2] p 69 N89-18836
- The Alaska SAR processor p 70 N89-18851
- Measuring lead area changes in sea ice imagery --- satellite imagery p 44 N89-18871
- Problems in the estimation of barley yields by remote sensing p 13 N89-18881
- Assessment of land/soil degradation in northern Burkina Faso p 13 N89-18882
- Quality control of fast delivery processors and products --- ERS-1 p 72 N89-18892
- A possibility for selecting spectral bands of future land application sensors at the example of an imaging spectrometer p 60 N89-18896
- Updating land-use information on topographic maps using satellite imagery: Combining the advantages of two accessible sources of geographic information p 60 N89-18897
- The use of SPOT-1 imagery for forest classification in Flanders (Belgium) p 14 N89-18899
- Pattern analysis and the ecological interpretation of satellite imagery p 61 N89-18900
- Mapping of natural vegetation in north-east Zimbabwe by means of LANDSAT Thematic Mapper data p 14 N89-18901
- Estimating the extent of irrigated cropland in a large catchment using LANDSAT MSS data p 14 N89-18902
- Results of tectonic and spectral investigations in the coast range of northern Chile using special processed Thematic Mapper (TM) data p 27 N89-18929
- The use of coregistered LANDSAT MSS, TM and SIR-A imagery for lithological mapping p 28 N89-18936
- The structure and variability of a filament in the northwest African upwelling area as observed from AVHRR and CXCS images p 46 N89-18939
- Estimation of sea-ice type and concentration by linear unmixing of Geosat altimeter waveforms p 47 N89-18946
- Satellite imagery for semi-automatic map revision p 61 N89-18957
- Real-time stereo matching SPOT using transputer arrays p 74 N89-18958
- Alternative approaches to the classification of upland semi-natural vegetation --- remote sensing p 16 N89-18961
- The effect of soil moisture on reflectance characteristics of salt crusts p 16 N89-18966
- The use of LANDSAT imagery for water quality studies in the IJsselmeer area (Netherlands) [BCRS-87-18] p 52 N89-19732
- Land use analysis using remote sensing techniques. Investigation of the usefulness of LANDSAT Thematic Mapper satellite pictures for obtaining and up to date picture of land use in the province South Holland [BCRS-88-01] p 61 N89-19733
- Salinity mapping based on SPOT images of the Punjab, Pakistan [BCRS-88-03] p 16 N89-19734
- SATELLITE OBSERVATION**
- The retrieval of sea surface temperature from NOAA/AVHRR satellite data - Comparison between Singh's and McClain's methods p 28 A89-20787
- Commercial remote sensing satellites generate debate, foreign competition p 76 A89-21397
- Seasat - Results of the mission p 29 A89-22000
- Satellite sea surface temperature at the North Atlantic Polar Front related to high-resolution towed conductivity-temperature-depth data p 31 A89-22594
- Satellite determination of the carbon dioxide exchange coefficient at the ocean-atmosphere interface - A first step p 31 A89-22598
- Satellite detection of transient enhanced primary production in the western Mediterranean Sea p 31 A89-23438
- Errors of the gravitational field determined by the satellite p 19 A89-24442
- Some aspects of space applications for disaster management - The use of space technology for disaster warning and for determining the effects of natural disasters [IAF PAPER 86-426] p 18 A89-24849
- JEOS - A low-cost approach to earth observation p 63 A89-26399
- The impact of satellite altimetry data on numerical simulations of general midlatitude oceanic circulation p 34 A89-28305
- Application of a flux algorithm to a field-satellite campaign over vegetated area p 6 A89-29411
- Radiation models of mesotrophic and eutrophic bodies of water p 36 A89-30120
- Technological limitations to satellite glaciology p 36 A89-30257
- The development of remote sensing in China p 76 A89-31560
- Evaluation of satellite-tracked surface drifting buoys for simulating the movement of spilled oil in the marine environment. Volume 1: Executive summary [PB88-226048] p 37 N89-17357
- Evaluation of satellite-tracked surface drifting buoys for simulating the movement of spilled oil in the marine environment, volume 2 [PB88-226055] p 37 N89-17358
- Some results of use of space survey materials in cartographic work p 58 N89-17922
- Characterizing forest ecosystem dynamics through modelling and remote sensing observations p 10 N89-18728
- Monitoring offshore water quality from space p 39 N89-18739
- Quick reporting state of fishery and sea on the East China Sea and the Yellow Sea with NOAA p 39 N89-18741
- The algorithm development facility: Its role in the development and operation of a satellite data centre p 68 N89-18755
- Improvements in ground water recharge estimation using satellite remote sensing p 50 N89-18768
- Estimating sea ice concentration from satellite passive microwave data and a physical model p 42 N89-18797
- Mission aspects of a future European polar orbit earth observation facility p 74 N89-18952
- The advanced terrain tracking altimeter instrument p 74 N89-18954
- Comparisons of satellite data surface-based remote sensing measurements in Utah winter orographic storms p 75 N89-19079
- SATELLITE ORBITS**
- The Geosat orbit adjust p 19 A89-22316
- SATELLITE ORIENTATION**
- Accuracy of terrain measurement using SPOT HRV data --- high resolution video p 53 A89-20801
- SATELLITE SOUNDING**
- Comparison of satellite total ozone measurements with the distribution of tropospheric ozone obtained by an airborne UV-DIAL system over the Amazon Basin p 17 A89-21892
- Determination of clear-sky planetary albedo p 62 A89-22214
- Procedures for the determination of geophysical parameters from spaceborne microwave polarimeter measurements p 30 A89-22224
- Effectiveness of satellite remote sensing on monitoring of marine environment [IAF PAPER 88-153] p 32 A89-24875

Extraction of surface temperature from satellite data p 33 A89-27941  
 Satellite remote sensing of rainfall p 49 A89-27946  
 A method for processing and results of microwave radiometer studies of the earth from the Intercosmos 20 and 21 satellites p 36 A89-30122  
 Satellite derived earth surface temperatures: A crop assessment tool p 8 N89-17930

**SATELLITE TRANSMISSION**

MOS-1 data processing in Tokai Space Center p 52 A89-20790

**SATELLITE-BORNE INSTRUMENTS**

Optical system design alternatives for the Moderate-Resolution Imaging Spectrometer-Tilt (MODIS-T) for the Earth Observing System (EOS) p 63 A89-27753  
 Sensors p 63 A89-27935

ERS-1 active microwave instrumentation design and performance status [IAF PAPER 87-136] p 65 A89-28329

Analysis of atmospheric effects in SPOT HRV images p 65 A89-29372

Spaceborne recording systems for the Space Station era p 66 A89-31020

Physical retrieval of rainfall rates over the ocean by multispectral microwave radiometry - Application to tropical cyclones p 37 A89-32434

Engineering calibration of the ERS-1 active microwave instrumentation in orbit p 71 N89-18885

The pre-launch performance verification of the ERS-1 active microwave instrumentation p 71 N89-18886

A software package for performance evaluation of the ERS-1 AMI --- Active Microwave Instrument (AMI) p 71 N89-18887

ERS-1 active microwave instrumentation engineering model performance p 71 N89-18888

Stability considerations for the ERS-1 wind scatterometer radiometric performance p 71 N89-18889

An advanced terrain tracking altimeter p 45 N89-18910

**SATELLITE-BORNE PHOTOGRAPHY**

Fault classification for the geological support of the tunnel construction project for the Caucasus mountain-pass railroad, using space images p 22 A89-22216

The procedure for and the results of the geological interpretation of photographic images of the Bukhtarma lineament zone p 22 A89-22217

Principal results of remote-sensing studies of Siberia's natural resources (On the occasion of the 10th anniversary of the Scientific Coordination Council, 1977-1987) p 62 A89-22225

Agrometeorological aspects of the utilization of remote-sensing data p 3 A89-23663

Aerial and space remote-sensing techniques for geographical investigations --- Russian book p 62 A89-26178

Optical methods of satellite hydrophysics. Investigation of the environment from manned orbital stations --- Russian book p 32 A89-26181

Digital processing of a lineament grid with the aim of analyzing regional tectonic structures of the western Himalayas in India p 23 A89-30116

Ring structures of buried platform areas and the evaluation of their tectonic activity on the basis of geomorphological data p 23 A89-30118

Features of the geological structure of the polar Urals and the distribution of certain minerals, as evaluated on the basis of the interpretation of aerial and space photographs p 23 A89-30119

Estimation of the water exchange and contamination zones of basins from satellite imagery p 49 A89-30252

A 10 km resolution image of the entire night-time earth based on cloud-free satellite photographs in the 400-1100 nm band p 56 A89-30256

German spaceborne remote sensing activities p 67 N89-16887

**SATELLITE-BORNE RADAR**

Wavenumber spectra of short gravity waves p 35 A89-30019

Theoretical study of the sensitivity of the microwave backscattering coefficient to the soil surface parameters p 6 A89-30267

Off-nadir radar altimetry p 66 A89-31947

**SCATTERING COEFFICIENTS**

Comparison of measured C-band scattering coefficients with model predictions as a function of leaf area index and Biomass p 8 N89-18712

A measurement of microwave backscattering coefficients of rice plants p 8 N89-18714

Specular scattering with effective reflection coefficient p 39 N89-18723

Evaluation of VARAN-S SAR data from the BEPERS study project --- sea ice p 45 N89-18875

**SCATTEROMETERS**

Comparison study of SEASAT scatterometer and conventional wind fields [AD-A200591] p 67 N89-16202

X-band scatterometry in agriculture p 9 N89-18715

Intercomparison of synthetic- and real-aperture radar observations of Arctic sea ice during winter MIZEX '87 p 40 N89-18744

Impact of phase and amplitude errors on the ERS-1 active microwave instrumentation performance p 70 N89-18853

Engineering calibration of the ERS-1 active microwave instrumentation in orbit p 71 N89-18885

The pre-launch performance verification of the ERS-1 active microwave instrumentation p 71 N89-18886

Stability considerations for the ERS-1 wind scatterometer radiometric performance p 71 N89-18889

Correlations between agricultural plant parameters and multitemporal radar scatterometer data: First results from the European AGRISCATT 87 campaign p 16 N89-18951

**SCENE ANALYSIS**

Identification of geological features from their surface textural properties using OPS measurements --- Optical Power Spectra p 21 A89-20820

A simulation for spaceborne SAR imagery of a distributed, moving scene p 33 A89-26846

Using a top-down and bottom-up strategy to analyze high resolution aerial photographs of urban areas p 18 A89-27630

The effects of viewing geometry on image classification p 55 A89-28036

Scene locations and overpass dates for Landsat and SPOT sensors p 64 A89-28039

Thermal infrared and visible images of the Iberian Peninsula p 56 A89-31889

A spectral feature design system for high dimensional multispectral data p 60 N89-18894

Sensor fusion of range and reflectance data for outdoor scene analysis p 76 N89-19888

**SCINTILLATION**

Determination of the spectrum of energy-containing surface waves from a sun-glitter image p 29 A89-22210

**SCOTLAND**

Enhancement of glacial fractures by analysis of Thematic Mapper data: Glen Roy, Scotland p 26 N89-18859

Interpreting the geology of Glen Coe using LANDSAT MSS data and aerial photographs p 26 N89-18860

Geological applications of thermal infrared characteristics of vegetation p 27 N89-18932

**SEA ICE**

Application of airborne scanners in remote sensing of sea ice p 29 A89-20789

Step frequency radar experiments on the Antarctic Sea ice p 34 A89-28365

Technological limitations to satellite glaciology p 36 A89-30257

Intercomparison of synthetic- and real-aperture radar observations of Arctic sea ice during winter MIZEX '87 p 40 N89-18744

SAR imagery of the Grand Banks (Newfoundland) pack ice pack and its relationship to surface features p 40 N89-18745

Use of SAR imagery and other remotely-sensed data in deriving ice information during a severe ice event on the Grand Banks (Newfoundland) p 40 N89-18746

SAR imaging of ocean waves in the marginal ice zone p 40 N89-18747

Estimating sea ice concentration from satellite passive microwave data and a physical model p 42 N89-18797

Shipborne passive microwave sea ice experiment in the East Greenland Sea: May-July 1987 p 42 N89-18799

Preliminary observations of polar sea ice with the Special Sensor Microwave Imager p 42 N89-18800

A method to forecast open pack ice speed of motion using remotely-sensed data p 42 N89-18801

Step frequency radar experiments on the Antarctic Sea ice p 43 N89-18802

Real-time processing of digital image data in support of the Canadian sea ice analysis and prediction program p 43 N89-18803

Toward the automated use of remote sensing data in operational ice forecasting p 43 N89-18804

Sea-ice software: ICEMAN p 43 N89-18805

Observations of ice types in satellite altimeter data p 44 N89-18841

Backscatter behavior of low-salinity sea ice at C and X-band p 44 N89-18869

Ice ridge observations by means of SAR p 45 N89-18872

Evaluation of VARAN-S SAR data from the BEPERS study project --- sea ice p 45 N89-18875

Geophysical information on the winter marginal ice zone obtained from SAR p 46 N89-18942

Radar backscatter of sea ice during winter p 46 N89-18943

Investigations of sea ice using coincident Geosat altimetry and synthetic aperture radar during MIZEX-87 p 46 N89-18945

Estimation of sea-ice type and concentration by linear unmixing of Geosat altimeter waveforms p 47 N89-18946

Antarctic Ocean polynyas [NASA-CR-184805] p 47 N89-19102

**SEA LEVEL**

Geosat crossover analysis in the tropical Pacific. II - Verification analysis of altimetric sea level maps with expendable bathythermograph and island sea level data p 32 A89-26438

**SEA STATES**

Motion characteristics of sea waves p 32 A89-23590

Quick reporting state of fishery and sea on the East China Sea and the Yellow Sea with NOAA p 39 N89-18741

The preliminary study of current shifting state by the use of infrared images of NOAA-9 p 39 N89-18742

**SEA SURFACE TEMPERATURE**

The retrieval of sea surface temperature from NOAA/AVHRR satellite data - Comparison between Singh's and McClain's methods p 28 A89-20787

Circulation in the East Asian seas from satellite and ship data p 29 A89-20803

New technology for displaying of NOAA AVHRR thermal band image p 29 A89-20810

Upwelling off the Gulfs of Panama and Papagayo in the tropical Pacific during March 1985 p 30 A89-22591

Inertial wind path and sea surface temperature patterns near the Gulf of Tehuantepec and Gulf of Papagayo p 30 A89-22592

Satellite sea surface temperature at the North Atlantic Polar Front related to high-resolution towed conductivity-temperature-depth data p 31 A89-22594

Frontal signals east of Iceland from the Geosat altimeter p 33 A89-26643

The capabilities of nonlinear Raman spectroscopy for remote diagnostics of water bodies p 35 A89-29730

Comparison of NOAA/AVHRR-2 sea surface temperatures with surface measurements in coastal waters p 36 A89-30259

A preliminary study on nearshore water in China with NOAA satellite images p 40 N89-18743

An ERDAS module for routine processing of AVHRR data p 43 N89-18817

**SEA TRUTH**

Water quality estimation from Landsat data with spectral and sea truth data base system p 28 A89-20788

**SEA WATER**

The capabilities of nonlinear Raman spectroscopy for remote diagnostics of water bodies p 35 A89-29730

Optical properties of sea water bodies: Measurements with an underwater radiometer and a high-resolution spectroradiometer p 39 N89-18734

**SEASAT SATELLITES**

Seasat - Results of the mission p 29 A89-22000

Hindcasts and data assimilation studies with the WAM model during the Seasat period --- wave model p 32 A89-26442

Comparison study of SEASAT scatterometer and conventional wind fields [AD-A200591] p 67 N89-16202

A study of the effect of rain on Seasat radar altimeter data p 44 N89-18940

Major crustal lineaments on Seasat SAR and their off-shore extensions in the UK p 26 N89-18861

**SEAWEEDES**

Remote sensing of macrophytic algae of the Molene Archipelago in France - Terrain radiometry and application to SPOT satellite data p 36 A89-30260

**SEDIMENT TRANSPORT**

Identification of surface-groundwater interaction zones in the Bogor volcanic fan p 48 A89-20777

Prioritization of watershed with regard to silt yield potential through data integration technique p 48 A89-20818

Large-scale, low-amplitude bedforms (chevrons) in the Selima sand sheet, Egypt p 23 A89-31755

**SEDIMENTS**

Long-range transport of giant mineral aerosol particles p 17 A89-21931

The relationship between suspended sediment concentration and remotely sensed spectral radiance - A review p 48 A89-24649

- The classification of loamy ground in the Outre-Foret region of Alsace in France using Landsat 5 TM images p 7 A89-31890
- Quantitative remote detection of suspended sediment content and chlorophyll concentration of water in different depths p 50 N89-18733
- The impact of multiviewing reflectance data on the estimation of suspended sediment concentration p 50 N89-18735
- Data processing for the determination of pigments and suspended solids from Thematic Mapper data p 50 N89-18736
- Monitoring of suspended sediments in Jatiluhur Reservoir using satellite images p 50 N89-18740
- SEGMENTS**  
Segmentation of SAR images p 58 N89-18759
- SEISMIC WAVES**  
A surface-wave study of the Pacific Ocean basin p 29 A89-21798
- Wigner distribution analysis of surface waves p 42 N89-18789
- SHAPES**  
The leaf-shape effect on electromagnetic scattering from vegetated media p 12 N89-18846
- SHIPS**  
Simulation of SAR imaging of ship wakes p 41 N89-18765
- Automatic ship and ship wake detection in spaceborne SAR images from coastal regions p 41 N89-18766
- SHUTTLE IMAGING RADAR**  
The geology of the area surrounding Lake Kerinci, Indonesia as interpreted through SIR-B images p 20 A89-20781
- Ocean wave spectra derived from Shuttle Imaging Radar-B imagery and surface measurements p 30 A89-22583
- Comparison of Shuttle Imaging Radar-B ocean wave image spectra with linear model predictions based on aircraft measurements p 30 A89-22584
- Ocean wave directional spectra and wave-current interaction in the Agulhas from the Shuttle Imaging Radar-B synthetic aperture radar p 30 A89-22585
- Validation of a synthetic aperture radar ocean wave imaging theory by the Shuttle Imaging Radar-B experiment over the North Sea p 30 A89-22586
- Modelling the SIR-B image response to partially coherent seas p 38 N89-18719
- Results of software simulation of a real-time SAR processor capable of providing ocean wave spectra p 38 N89-18720
- Overview of the Shuttle Imaging Radar (SIR-C) p 73 N89-18921
- The use of coregistered LANDSAT MSS, TM and SIR-A imagery for lithological mapping p 28 N89-18936
- SIBERIA**  
Principal results of remote-sensing studies of Siberia's natural resources (On the occasion of the 10th anniversary of the Scientific Coordination Council, 1977-1987) p 62 A89-22225
- SIDE-LOOKING RADAR**  
Extraction of small-scale spatial information from SLAR raw data of forests through an analysis of speckle p 8 N89-18709
- Sea bottom topography with X-band SLAR: Evaluation of existing models p 38 N89-18718
- Auto and cross correlation analysis of environment, system and target parameters for iceberg detection using airborne radar p 45 N89-18874
- Study of the use of radar X-band data of bare soil in a radar scattering model [BCRS-88-04] p 16 N89-19735
- SIGNAL DETECTION**  
EHF attenuation through the melting layer p 51 N89-18984
- SIGNAL PROCESSING**  
Wigner distribution analysis of surface waves p 42 N89-18789
- New architecture for a real-time SAR processor p 69 N89-18850
- A new approach to topographic altimetry p 73 N89-18914
- A study of advanced radar altimeter techniques --- satellite altimetry [ESA-CR(P)-2699] p 75 N89-19483
- SIGNAL TO NOISE RATIOS**  
MODIS - Advanced facility instrument for studies of the earth as a system --- Moderate Resolution Imaging Spectrometer p 66 A89-31943
- SILICON DIOXIDE**  
Long-range transport of giant mineral aerosol particles p 17 A89-21931
- SIMULATION**  
A simulation test for soil moisture sensing p 10 N89-18772
- Simulation of optical remote sensing systems for earth resource analysis p 74 N89-18964
- SITE SELECTION**  
Investigation of water content from airborne MSS data p 49 A89-30261
- SKY RADIATION**  
Signature variations due to atmospheric and topographic effects on satellite MSS data over rugged terrain p 70 N89-18877
- SLOPES**  
Mapping slope failure tracks with digital Thematic Mapper data p 59 N89-18790
- SMOKE**  
Trace gas emissions from chaparral and boreal forest fires p 7 A89-32432
- SNOW**  
Dependence of snow melting and surface-atmosphere interactions on the forest structure p 3 A89-21740
- Physical properties of snow and ice in the winter marginal ice zone of Fram Strait p 46 N89-18944
- EHF attenuation through the melting layer p 51 N89-18984
- SNOW COVER**  
Variations of the infrared emission of snow and ice cover p 49 A89-30121
- Snow cover-summer monsoon rainfall over parts of Sahel p 51 N89-18832
- Normalized radar cross section of natural surfaces at millimeter wavelengths [AD-A202252] p 75 N89-19475
- SNOWSTORMS**  
Comparisons of satellite data surface-based remote sensing measurements in Utah winter orographic storms p 75 N89-19079
- SOFTWARE ENGINEERING**  
The algorithm development facility: Its role in the development and operation of a satellite data centre p 68 N89-18755
- SOIL EROSION**  
The applications of Landsat imagery to soil erosion study in Northern Thailand p 3 A89-20826
- SOIL MAPPING**  
Soil and vegetation mapping by using SPOT image p 1 A89-20758
- Applications of SPOT HRV data for land use and soil mapping in Rayong basin p 2 A89-20769
- Effectiveness of soil mapping on the basis of space photographic data p 3 A89-22249
- Goniometric observations of light scattered from soils and leaves p 4 A89-24873
- Visual and digital classification of Landsat TM data for soil, physiography and land use mapping in Axios alluvial plain, Thessaloniki, Greece p 5 A89-28130
- Combining oblique SPOT-1 images for the analysis of certain soil properties p 7 A89-31892
- Salinity mapping based on SPOT images of the Punjab, Pakistan [BCRS-88-03] p 16 N89-19734
- Study of the use of radar X-band data of bare soil in a radar scattering model [BCRS-88-04] p 16 N89-19735
- SOIL MOISTURE**  
Soil surface moisture estimation - A case study area on North Banten, West Java, Indonesia p 2 A89-20773
- Microwave remote sensing of soil moisture p 4 A89-27944
- Investigation of water content from airborne MSS data p 49 A89-30261
- Theoretical study of the sensitivity of the microwave backscattering coefficient to the soil surface parameters p 6 A89-30267
- Passive microwave remote sensing system for soil moisture - Some supporting research p 49 A89-31948
- A simulation test for soil moisture sensing p 10 N89-18772
- Microcomputer-based radiometer data acquisition and processing system for large-area mapping of soil moisture content in the top one meter layer p 11 N89-18774
- Experiments in Bulgaria for determination of soil moisture in the top one-meter layer using microwave radiometry and a priori information p 11 N89-18843
- Observed effects of soil organic matter content on the microwave intensity of soils p 12 N89-18845
- The effect of soil moisture on reflectance characteristics of salt crusts p 16 N89-18966
- SOIL SCIENCE**  
X-band scatterometry in agriculture p 9 N89-18715
- Microwave X-band radiometric characterization of Brazilian soils by measurement of the complex permittivity p 11 N89-18773
- Observed effects of soil organic matter content on the microwave intensity of soils p 12 N89-18845
- SOILS**  
Soil influences on vegetation reflectance of a semi-arid shrubland p 13 N89-18880
- Assessment of land/soil degradation in northern Burkina Faso p 13 N89-18882
- SOLID SUSPENSIONS**  
Suspended solid classification of the Jakarta Bay p 28 A89-20785
- SOYBEANS**  
Estimating absorbed radiation and phytomass from multispectral reflectance of corn and soybeans p 13 N89-18876
- SPACE BASED RADAR**  
A simulation for spaceborne SAR imagery of a distributed, moving scene p 33 A89-28846
- Off-nadir radar altimetry p 66 A89-31947
- Advanced SAR concepts p 73 N89-18926
- SPACE COMMERCIALIZATION**  
Commercial remote sensing satellites generate debate, foreign competition p 76 A89-21397
- The Geospace philosophy: A new practical approach in remote sensing and planning for local authorities p 76 N89-18750
- Effects of commercialisation on international remote sensing activities p 76 N89-18752
- SPACE LAW**  
The UN declaration of legal principals on remote sensing, 1986 p 76 N89-18748
- SPACE MISSIONS**  
Spaceborne recording systems for the Space Station era p 66 A89-31020
- SPACE SHUTTLE PAYLOADS**  
X-SAR: A new spaceborne synthetic aperture radar p 73 N89-18923
- SPACE STATION PAYLOADS**  
Spaceborne recording systems for the Space Station era p 66 A89-31020
- SPACEBORNE PHOTOGRAPHY**  
Cartographic analysis of Large Format Camera photographs - Comparison with SPOT and the Spacelab metric camera p 62 A89-21410
- Effectiveness of soil mapping on the basis of space photographic data p 3 A89-22249
- Annular and block-folded structures on space and aerial photographs p 25 N89-17915
- Some results of use of space survey materials in cartographic work p 58 N89-17922
- SPACECRAFT COMMUNICATION**  
EHF attenuation through the melting layer p 51 N89-18984
- SPACECRAFT MODELS**  
ERS-1 active microwave instrumentation engineering model performance p 71 N89-18888
- SPACECRAFT PERFORMANCE**  
ERS-1 active microwave instrumentation engineering model performance p 71 N89-18888
- SPACELAB**  
The studies for the computer classification and the investigation of grasslands in Tibet using Space-Lab color infrared image p 1 A89-20754
- SPACELAB PAYLOADS**  
Cartographic analysis of Large Format Camera photographs - Comparison with SPOT and the Spacelab metric camera p 62 A89-21410
- SPATIAL DISTRIBUTION**  
Segmentation of Synthetic Aperture Radar (SAR) images of ocean surface by the texture energy transform method [AD-A199536] p 37 N89-15309
- Estimating sea ice concentration from satellite passive microwave data and a physical model p 42 N89-18797
- Estimation of sea-ice type and concentration by linear unmixing of Geosat altimeter waveforms p 47 N89-18946
- SPATIAL FILTERING**  
A simple spatial filtering routine for the cosmetic removal of scan-line noise from Landsat TM P-tape imagery p 57 A89-32335
- SPATIAL RESOLUTION**  
Spatial information processings of TM data p 52 A89-20791
- Comparison study of SEASAT scatterometer and conventional wind fields [AD-A200591] p 67 N89-16202
- Extraction of small-scale spatial information from SLAR raw data of forests through an analysis of speckle p 8 N89-18709
- A synthetic aperture altimeter p 73 N89-18913
- A study of advanced radar altimeter techniques --- satellite altimetry [ESA-CR(P)-2699] p 75 N89-19483
- SPECKLE PATTERNS**  
Estimation of the SAR system transfer through processor defocus p 37 N89-18706
- Speckle correlation in SAR images of dynamic discrete scatterers p 37 N89-18707
- Extraction of small-scale spatial information from SLAR raw data of forests through an analysis of speckle p 8 N89-18709



- Adaptive speckle filtering for SAR images  
p 58 N89-18710
- Nonlinear filtering and edge detection in speckled radar images  
p 58 N89-18711
- SPECTRAL METHODS**
- Water quality estimation from Landsat data with spectral and sea truth data base system  
p 28 A89-20788
- SPECTRAL RECONNAISSANCE**
- The application of remote sensing to geomorphological mapping and mass movement study in the vicinity of Provo, Utah  
p 23 N89-15439
- A spectral feature design system for high dimensional multispectral data  
p 60 N89-18894
- SPECTRAL REFLECTANCE**
- Spectral reflectance properties of a leaf of some mangrove species in Okinawa  
p 1 A89-20753
- The characterization of sources of illumination in a Ponderosa Pine (*Pinus ponderosa*) forest community using the portable instantaneous display and analysis spectrometer  
p 4 A89-27781
- Effects of solar angle on reflectance from wetland vegetation  
p 5 A89-29409
- Complementarity of middle-infrared with visible and near-infrared reflectance for monitoring wheat canopies  
p 5 A89-29410
- Tersail - A numerical model for combined analysis of vegetation canopy bidirectional reflectance and thermal emissions  
p 6 A89-29415
- Bidirectional canopy reflectance and its relationship to vegetation characteristics  
p 6 A89-30264
- Spectral response characteristics of a metal-stressed coniferous forest as measured by the Fluorescence Line Imager (FLI) airborne imaging spectrometer  
p 9 N89-18724
- Correlation of reflectance and chlorophyll fluorescence signatures of healthy and damaged forest trees  
p 9 N89-18726
- Correlation of radar reflectivity and chlorophyll fluorescence of forest trees  
p 9 N89-18727
- Quantitative remote detection of suspended sediment content and chlorophyll concentration of water in different depths  
p 50 N89-18733
- The impact of multiviewing reflectance data on the estimation of suspended sediment concentration  
p 50 N89-18735
- Estimating absorbed radiation and phytomass from multispectral reflectance of corn and soybeans  
p 13 N89-18876
- A mathematical model of reflectance and transmittance of plant leaves as a function of chlorophyll pigment content  
p 13 N89-18879
- Soil influences on vegetation reflectance of a semi-arid shrubland  
p 13 N89-18880
- The effect of soil moisture on reflectance characteristics of salt crusts  
p 16 N89-18966
- Sensor fusion of range and reflectance data for outdoor scene analysis  
p 78 N89-19868
- SPECTRAL RESOLUTION**
- MODIS - Advanced facility instrument for studies of the earth as a system --- Moderate Resolution Imaging Spectrometer  
p 66 A89-31943
- SPECTRAL SIGNATURES**
- Correlation of reflectance and chlorophyll fluorescence signatures of healthy and damaged forest trees  
p 9 N89-18726
- Signature variations due to atmospheric and topographic effects on satellite MSS data over rugged terrain  
p 70 N89-18877
- Textural and spectral features as an aid to cloud classification  
p 74 N89-18960
- SPECTROMETERS**
- Artefacts in AIS-I imagery --- Airborne Image Spectrometer (AIS)  
p 69 N89-18826
- SPECTRORADIOMETERS**
- Moorable spectroradiometers in the BIOWATT experiment  
p 64 A89-27990
- Spectral transmissometer and radiometer - Design and initial results --- of free drifting experiment in Pacific Ocean  
p 64 A89-27991
- MISR - A multiangle imaging spectroradiometer for geophysical and climatological research from EOS  
p 66 A89-31946
- Optical properties of sea water bodies: Measurements with an underwater radiometer and a high-resolution spectroradiometer  
p 39 N89-18734
- SPECTRUM ANALYSIS**
- Determination of the spectrum of energy-containing surface waves from a sun-glitter image  
p 29 A89-22210
- Comparative spectral analysis of HRV and TM sensors  
p 65 A89-29375
- Study on directional spectrum characteristics of marine radar images of ocean waves  
p 41 N89-18786
- SPECULAR REFLECTION**
- Distribution of specular points on the ocean surface: Bistatic scattering  
p 38 N89-18721
- Specular scattering with effective reflection coefficient  
p 39 N89-18723
- SPHERICAL COORDINATES**
- Reference coordinate systems: An update. Supplement 11  
[NASA-CR-184764]  
p 19 N89-16207
- SPOT (FRENCH SATELLITE)**
- The use of SPOT imagery in Medan agriculture area for monitoring features changes  
p 1 A89-20755
- Soil and vegetation mapping by using SPOT image  
p 1 A89-20758
- First results of topographical mapping using SPOT images of Malaysia  
p 52 A89-20764
- Applications of SPOT HRV data for land use and soil mapping in Rayong basin  
p 2 A89-20769
- Comparison of the orientation's accuracy for SPOT imagery  
p 53 A89-20798
- Accuracy of terrain measurement using SPOT HRV data --- high resolution video  
p 53 A89-20801
- Digital Terrain Model computation using SPOT data  
p 53 A89-20807
- Geometric correction of SPOT image  
p 54 A89-20812
- SPOT for mapping of actual land information  
p 54 A89-20816
- SPOT image interpretation for information on human settlement growth  
p 17 A89-20824
- Contribution of second-generation Landsat TM and SPOT HRV satellites to urban analysis (Rennes, France)  
p 17 A89-21250
- Cartographic analysis of Large Format Camera photographs - Comparison with SPOT and the Spacelab metric camera  
p 62 A89-21410
- Scene locations and overpass dates for Landsat and SPOT sensors  
p 64 A89-28039
- Multispectral classification of land use at the rural-urban fringe using spot data  
p 18 A89-29371
- Analysis of atmospheric effects in SPOT HRV images  
p 65 A89-29372
- Analysis and interpretation of SPOT images of urban and agricultural/forest sections of the Sherbrooke region  
p 5 A89-29373
- Area measurement of agricultural fields from satellite images  
p 5 A89-29374
- Comparative spectral analysis of HRV and TM sensors  
p 65 A89-29375
- Use of the variable gain settings on SPOT  
p 65 A89-29435
- Remote sensing of macrophytic algae of the Molene Archipelago in France - Terrain radiometry and application to SPOT satellite data  
p 36 A89-30260
- Integration of SPOT data in an urban data bank - Locating work sites  
p 18 A89-31891
- Combining oblique SPOT-1 images for the analysis of certain soil properties  
p 7 A89-31892
- Multitemporal study of differently farmed permanent grazing lands in the Lorraine region of France using SPOT-1 data  
p 7 A89-31894
- On-line aspects of stereophotogrammetric processing of SPOT images  
p 66 A89-32334
- Monitoring water quality and river plume transport in Green Bay, Lake Michigan with SPOT-1 imagery  
p 49 A89-32338
- Investigation of information content of Thematic Mapper and SPOT multiband image data, using simulated image data of the Freiburg region (Federal Republic of Germany)  
[ESA-TT-975]  
p 57 N89-15442
- SPOT mapping software for Wild Avioflyt BC2 analytical plotter  
p 60 N89-18824
- The use of SPOT-1 imagery for forest classification in Flanders (Belgium)  
p 14 N89-18899
- Satellite imagery for semi-automatic map revision  
p 61 N89-18957
- Real-time stereo matching SPOT using transputer arrays  
p 74 N89-18958
- Salinity mapping based on SPOT images of the Punjab, Pakistan  
[BCRS-88-03]  
p 16 N89-19734
- STANDARDS**
- Reference coordinate systems: An update. Supplement 11  
[NASA-CR-184764]  
p 19 N89-16207
- STEREOPHOTOGRAPHY**
- An interactive system for aerial photo orientation of digital stereo image pairs  
p 53 A89-20799
- On-line aspects of stereophotogrammetric processing of SPOT images  
p 66 A89-32334
- STOCHASTIC PROCESSES**
- Modelling the SIR-B image response to partially coherent seas  
p 38 N89-18719
- STRAITS**
- A tide-generated internal waveform in the western approaches to the Strait of Gibraltar  
p 31 A89-22597
- Physical properties of snow and ice in the winter marginal ice zone of Fram Strait  
p 46 N89-18944
- STRATOSPHERE**
- Summertime stratospheric wind measurements above the South Pole  
p 62 A89-24022
- STRATUS CLOUDS**
- Observation of the degree of glaciation in middle-level stratiform clouds  
p 62 A89-23464
- Structure of layer clouds as observed simultaneously by a microwave radiometer and an 8.6 mm-radar  
p 74 N89-19039
- STRIATION**
- Artefacts in AIS-I imagery --- Airborne Image Spectrometer (AIS)  
p 69 N89-18826
- STRUCTURAL ANALYSIS**
- Integration of geological, geophysical and remotely sensed data for the Solway Basin, England  
p 26 N89-18794
- STRUCTURAL BASINS**
- A surface-wave study of the Pacific Ocean basin  
p 29 A89-21798
- Application of the Haar transform for extraction of linear and anomalous patterns over part of Cambay Basin, India  
p 55 A89-28037
- STRUCTURAL PROPERTIES (GEOLOGY)**
- Correlation of Landsat TM and aeromagnetic data along the Eastern Margin of the Cuddapah Basin, South India  
p 21 A89-20817
- The procedure for and the results of the geological interpretation of photographic images of the Bukhtarma lineament zone  
p 22 A89-22217
- A tomographic approach to lineament identification on aerial and space images  
p 22 A89-22223
- Digital processing of a lineament grid with the aim of analyzing regional tectonic structures of the western Himalayas in India  
p 23 A89-30116
- Ring structures of buried platform areas and the evaluation of their tectonic activity on the basis of geomorphological data  
p 23 A89-30118
- Features of the geological structure of the polar Urals and the distribution of certain minerals, as evaluated on the basis of the interpretation of aerial and space photographs  
p 23 A89-30119
- Annular and block-folded structures on space and aerial photographs  
p 25 N89-17915
- Geological lineament detection using the Hough transform  
p 26 N89-18818
- Major crustal lineaments on Seasat SAR and their off-shore extensions in the UK  
p 26 N89-18861
- STRUCTURES**
- Knowledge related aspects of lineation and lineament extraction  
[INPE-4709-PRE/1391]  
p 24 N89-15446
- SULFUR DIOXIDES**
- A comparison of models for deriving dry deposition fluxes of O<sub>3</sub> and SO<sub>2</sub> to a forest canopy  
p 3 A89-20923
- SUPERHIGH FREQUENCIES**
- X-band scatterometry in agriculture  
p 9 N89-18715
- Multitemporal and dual polarization of agricultural crops by X-band SAR images  
p 9 N89-18716
- Comparison between microwave emissivity and backscattering coefficient of agricultural fields  
p 12 N89-18844
- Backscatter behavior of low-salinity sea ice at C and X-band  
p 44 N89-18869
- Atmospheric profiling of water vapour with a 20.5-23.5 GHz autocorrelation radiometer  
p 72 N89-18908
- X-SAR: A new spaceborne synthetic aperture radar  
p 73 N89-18923
- Applications of the NCAR Electra Doppler radar for the study of physical parameters of clouds  
p 75 N89-19717
- Study of the use of radar X-band data of bare soil in a radar scattering model  
[BCRS-88-04]  
p 16 N89-19735
- SURFACE ENERGY**
- Segmentation of Synthetic Aperture Radar (SAR) images of ocean surface by the texture energy transform method  
[AD-A199536]  
p 37 N89-15309
- SURFACE ROUGHNESS EFFECTS**
- Dependence of snow melting and surface-atmosphere interactions on the forest structure  
p 3 A89-21740
- Distribution of specular points on the ocean surface: Bistatic scattering  
p 38 N89-18721
- Signature variations due to atmospheric and topographic effects on satellite MSS data over rugged terrain  
p 70 N89-18877
- SURFACE TEMPERATURE**
- Extraction of surface temperature from satellite data  
p 33 A89-27941
- Use of surface temperature in agrometeorology  
p 4 A89-27942
- Application of a flux algorithm to a field-satellite campaign over vegetated area  
p 6 A89-29411
- Variations of the infrared emission of snow and ice cover  
p 49 A89-30121



## T

- Applications of digital image processing to ongoing research in complex terrain meteorology [DE89-001749] p 57 N89-17375
- Satellite derived earth surface temperatures: A crop assessment tool p 8 N89-17930
- SURFACE WATER**
- Buoyant surface jet analysis of the Yukon River p 49 A89-28033
- SURFACE WAVES**
- A surface-wave study of the Pacific Ocean basin p 29 A89-21798
- Determination of the spectrum of energy-containing surface waves from a sun-glitter image p 29 A89-22210
- Laser airborne sensing field experiments using the 'Chaika' assembly --- for probing water bodies p 35 A89-29728
- Surface wave interaction - Theory and capability of oceanic remote sensing p 35 A89-29732
- Wigner distribution analysis of surface waves p 42 N89-18789
- SURGES**
- Hydrological aspects of combined effects of storm surges and heavy rainfall on river flow [WMO-704] p 49 N89-17340
- SUSPENDING (MIXING)**
- Quantitative remote detection of suspended sediment content and chlorophyll concentration of water in different depths p 50 N89-18733
- The impact of multiviewing reflectance data on the estimation of suspended sediment concentration p 50 N89-18735
- Monitoring of suspended sediments in Jatiluhur Reservoir using satellite images p 50 N89-18740
- SUSPENSIONS**
- The relationship between suspended sediment concentration and remotely sensed spectral radiance - A review p 48 A89-24649
- SWATH WIDTH**
- Advanced SAR concepts p 73 N89-18926
- A study of advanced radar altimeter techniques --- satellite altimetry [ESA-CR(P)-2699] p 75 N89-19483
- SYNOPTIC METEOROLOGY**
- Comparison study of SEASAT scatterometer and conventional wind fields [AD-A200591] p 67 N89-16202
- SYNTHETIC APERTURE RADAR**
- STAR-1 high resolution synthetic aperture radar imagery for precious metal exploration p 21 A89-20827
- Validation of a synthetic aperture radar ocean wave imaging theory by the Shuttle Imaging Radar-B experiment over the North Sea p 30 A89-22586
- Radar imaging of the surfaces of Venus and the earth using SAR data p 54 A89-23645
- A simulation for spaceborne SAR imagery of a distributed, moving scene p 33 A89-26846
- Concepts for processing and analyzing of multiple SAR and Landsat images p 55 A89-27789
- Detection of ocean bottom relief by local geoid p 35 A89-29731
- Estimation of the SAR system transfer through processor defocus p 37 N89-18706
- Adaptive speckle filtering for SAR images p 58 N89-18710
- Multitemporal and dual polarization of agricultural crops by X-band SAR images p 9 N89-18716
- Assessment of clearcut mapping accuracy with C-band SAR p 9 N89-18725
- Texture analysis of forest regeneration sites in high-resolution SAR imagery p 10 N89-18730
- Intercomparison of synthetic- and real-aperture radar observations of Arctic sea ice during winter MIZEX '87 p 40 N89-18744
- SAR imagery of the Grand Banks (Newfoundland) pack ice pack and its relationship to surface features p 40 N89-18745
- Use of SAR imagery and other remotely-sensed data in deriving ice information during a severe ice event on the Grand Banks (Newfoundland) p 40 N89-18746
- SAR imaging of ocean waves in the marginal ice zone p 40 N89-18747
- Plans for the development of EOS SAR systems using the Alaska SAR facility --- Earth Observing System (EOS) p 69 N89-18757
- Segmentation of SAR images p 58 N89-18759
- Interpreting SAR images by means of map information p 58 N89-18760
- Investigations of SAR backscatter for different test areas using two geocoded Seasat SAR scenes p 58 N89-18761
- The visibility of linear features in SAR images p 59 N89-18763
- Automated linear feature detection and its application to curve location in synthetic aperture radar imagery p 59 N89-18764
- Simulation of SAR imaging of ship wakes p 41 N89-18765
- Automatic ship and ship wake detection in spaceborne SAR images from coastal regions p 41 N89-18766
- Effects of slopes and relief two-dimensional spatial frequencies on spaceborne SAR imagery p 59 N89-18777
- Observations of the effect of geometric properties of agricultural soils on radar backscatter, from C-SAR images p 11 N89-18781
- Information fusion by a knowledge-based system for SAR image interpretation p 60 N89-18831
- Proceedings of the 1988 International Geoscience and Remote Sensing Symposium (IGARSS) '88 on Remote Sensing: Moving Towards the 21st Century, Volume 2 [ESA-SP-284-VOL-2] p 69 N89-18836
- A high fidelity, high throughput system for geocoding SAR imagery p 60 N89-18849
- New architecture for a real-time SAR processor p 69 N89-18850
- The Alaska SAR processor p 70 N89-18851
- Impact of phase and amplitude errors on the ERS-1 active microwave instrumentation performance p 70 N89-18853
- Towards a calibration of the CCRS airborne SARs --- Canada Center for Remote Sensing (CCRS) p 70 N89-18854
- Radiometric calibration of airborne SAR data p 70 N89-18855
- Preprocessing of the VARAN synthetic aperture airborne radar p 70 N89-18856
- Post-processing airborne SAR data for multitemporal land-cover studies p 12 N89-18857
- Major crustal lineaments on Seasat SAR and their off-shore extensions in the UK p 26 N89-18861
- Ice ridge observations by means of SAR p 45 N89-18872
- Evaluation of VARAN-S SAR data from the BEPERS study project --- sea ice p 45 N89-18875
- Engineering calibration of the ERS-1 active microwave instrumentation in orbit p 71 N89-18885
- The pre-launch performance verification of the ERS-1 active microwave instrumentation p 71 N89-18886
- A SAR data quality assessment scheme for the ERS-1 mission p 72 N89-18893
- A synthetic aperture altimeter p 73 N89-18913
- X-SAR: A new spaceborne synthetic aperture radar p 73 N89-18923
- E-SAR: The experimental airborne L/C-band SAR system of DFVLR p 73 N89-18924
- Taking a broader view: Radarsat adds ScansAR to its operations p 73 N89-18925
- Advanced SAR concepts p 73 N89-18926
- The Technical University of Denmark (TUD) C-band SAR p 74 N89-18928
- Geophysical information on the winter marginal ice zone obtained from SAR p 46 N89-18942
- Investigations of sea ice using coincident Geosat altimetry and synthetic aperture radar during MIZEX-87 p 46 N89-18945
- Crops radar responses analysis based on AGRISAR '86 data p 15 N89-18947
- Extraction of agricultural plant parameters from multitemporal Thematic Mapper (TM) and X-SAR data p 15 N89-18948
- Change detection in AGRISAR images p 15 N89-18949
- SYNTHETIC APERTURES**
- A study of advanced radar altimeter techniques --- satellite altimetry [ESA-CR(P)-2699] p 75 N89-19483
- SYSTEMS ENGINEERING**
- Optical system design alternatives for the Moderate-Resolution Imaging Spectrometer-Tilt (MODIS-T) for the Earth Observing System (EOS) p 63 A89-27753
- Definition and design of an operational environment-monitoring system p 18 A89-27788
- Overview of the Shuttle Imaging Radar (SIR-C) p 73 N89-18921
- SYSTEMS INTEGRATION**
- Sensor fusion of range and reflectance data for outdoor scene analysis p 76 N89-18968
- SYSTEMS SIMULATION**
- Simulation of optical remote sensing systems for earth resource analysis p 74 N89-18964
- SYSTEMS STABILITY**
- Stability considerations for the ERS-1 wind scatterometer radiometric performance p 71 N89-18889
- TARGET ACQUISITION**
- Automatic ship and ship wake detection in spaceborne SAR images from coastal regions p 41 N89-18766
- TECHNOLOGY ASSESSMENT**
- Applications of digital image processing to ongoing research in complex terrain meteorology [DE89-001749] p 57 N89-17375
- Comparisons of satellite data surface-based remote sensing measurements in Utah winter orographic storms p 75 N89-19079
- TECHNOLOGY TRANSFER**
- Technology transfer for development of coastal zone resources: Caribbean experts examine critical issues p 40 N89-18749
- TECTONICS**
- Neotectonic zoning of Belorussia on the basis of space data p 21 A89-22215
- Digital processing of a lineament grid with the aim of analyzing regional tectonic structures of the western Himalayas in India p 23 A89-30116
- Ring structures of buried platform areas and the evaluation of their tectonic activity on the basis of geomorphological data p 23 A89-30118
- Results of tectonic and spectral investigations in the coast range of northern Chile using special processed Thematic Mapper (TM) data p 27 N89-18929
- Tectonics of the central Andes [NASA-CR-184683] p 28 N89-18973
- TEMPERATURE DISTRIBUTION**
- A preliminary study on nearshore water in China with NOAA satellite images p 40 N89-18743
- TEMPERATURE MEASUREMENT**
- Extraction of surface temperature from satellite data p 33 A89-27941
- TEMPORAL DISTRIBUTION**
- Development of principal component analysis applied to multitemporal Landsat TM data p 4 A89-28035
- Multitemporal study of differently farmed permanent grazing lands in the Lorraine region of France using SPOT-1 data p 7 A89-31894
- TERRAIN**
- Applications of digital image processing to ongoing research in complex terrain meteorology [DE89-001749] p 57 N89-17375
- Digital elevation models and their application to remote sensing of water resources p 51 N89-18770
- Effects of slopes and relief two-dimensional spatial frequencies on spaceborne SAR imagery p 59 N89-18777
- Preprocessing and analysis of airborne visible near and shortwave infrared data for the detection of alteration in weathered vegetated terrain p 12 N89-18862
- Signature variations due to atmospheric and topographic effects on satellite MSS data over rugged terrain p 70 N89-18877
- Pattern analysis and the ecological interpretation of satellite imagery p 61 N89-18900
- An advanced terrain tracking altimeter p 45 N89-18910
- The advanced terrain tracking altimeter instrument p 74 N89-18954
- TERRAIN ANALYSIS**
- Digital Terrain Model computation using SPOT data p 53 A89-20807
- Feature extraction considerations in utilising the optical power spectra for terrain classification p 54 A89-20821
- Bayes classification of terrain cover using normalized polarimetric data p 54 A89-22649
- Parabola directional field radiometer for aiding in space sensor data interpretations p 63 A89-27779
- Applications of digital image processing to ongoing research in complex terrain meteorology [DE89-001749] p 57 N89-17375
- Reports on cartography and geodesy, series 1, number 100 [ISSN-0469-4236] p 20 N89-17935
- Mapping slope failure tracks with digital Thematic Mapper data p 59 N89-18790
- TERRESTRIAL RADIATION**
- Determination of clear-sky planetary albedo p 62 A89-22214
- A method for processing and results of microwave radiometer studies of the earth from the IntercoSMOS 20 and 21 satellites p 36 A89-30122
- TEXTURES**
- Segmentation of Synthetic Aperture Radar (SAR) images of ocean surface by the texture energy transform method [AD-A199536] p 37 N89-15309
- A comparison of clutter texture properties in optical and SAR images p 8 N89-18708
- Texture analysis of forest regeneration sites in high-resolution SAR imagery p 10 N89-18730

- Textural and spectral features as an aid to cloud classification p 74 N89-18960
- THAILAND**  
The feasibility study of oil palm area estimation in the southern part of Thailand using Landsat data p 2 A89-20760
- THEMATIC MAPPERS (LANDSAT)**  
Mapping of construction material sites around Bangalore City using Landsat Thematic Mapper data p 52 A89-20782  
Spatial information processings of TM data p 52 A89-20791  
Correlation of Landsat TM and aeromagnetic data along the Eastern Margin of the Cuddapah Basin, South India p 21 A89-20817  
Landsat 5 TM image of the Mont Saint-Michel region of France p 54 A89-21249  
Contribution of second-generation Landsat TM and SPOT HRV satellites to urban analysis (Rennes, France) p 17 A89-21250  
A procedure for land area classification using Landsat TM digital imagery p 17 A89-24651  
Application of Landsat MSS and TM data to geological resource exploration p 22 A89-26397  
Bathymetry using Thematic Mapper imagery p 34 A89-27995  
Development of principal component analysis applied to multitemporal Landsat TM data p 4 A89-28035  
Mapping and inventory of forest fires from digital processing of TM data p 5 A89-28129  
Area measurement of agricultural fields from satellite images p 5 A89-29374  
Comparative spectral analysis of HRV and TM sensors p 65 A89-29375  
Wasteland identification in India using satellite remote sensing p 18 A89-30263  
Analysis and representation of vegetation continua from Landsat Thematic Mapper data for lowland heaths p 7 A89-30268  
Visual and computer classifications of remotely-sensed images - A case study of grasslands in Cambridgeshire p 7 A89-30269  
Remote sensing of evaporite mineral zonation in salt flats (salars) p 23 A89-30271  
The classification of loamy ground in the Outre-Forêt region of Alsace in France using Landsat 5 TM images p 7 A89-31890  
Determining the age of cut forest areas in Quebec, Canada using the Landsat-5 TM p 7 A89-31893  
A simple spatial filtering routine for the cosmetic removal of scan-line noise from Landsat TM P-tape imagery p 57 A89-32335  
Extracting spectral contrast in Landsat Thematic Mapper image data using selective principal component analysis p 57 A89-32337  
LANDSAT TM study of afforestation in northern Scotland and its impact on breeding bird populations p 10 N89-18732  
Data processing for the determination of pigments and suspended solids from Thematic Mapper data p 50 N89-18736  
An assessment of ATM and satellite data for estimating the groundwater contribution to slope stability --- Airborne Thematic Mapper (ATM) p 51 N89-18769  
Mapping slope failure tracks with digital Thematic Mapper data p 59 N89-18790  
Enhancement of glacial fractures by analysis of Thematic Mapper data: Glen Roy, Scotland p 26 N89-18859  
Applications of LANDSAT Thematic Mapper imagery to the study of subtle variations in lithology p 27 N89-18863  
Image-based atmospheric correction of multitemporal Thematic Mapping data for agricultural land cover classification p 14 N89-18895  
Mapping of natural vegetation in north-east Zimbabwe by means of LANDSAT Thematic Mapper data p 14 N89-18901  
Investigations of the Cerro Colorado pluton, northern Chile, using enhanced LANDSAT Thematic Mapper images p 27 N89-18930  
The use of coregistered LANDSAT MSS, TM and SIR-A imagery for lithological mapping p 28 N89-18936  
Radiometric problems in the use of the Thematic Mapper for marine research p 46 N89-18940  
Extraction of agricultural plant parameters from multitemporal Thematic Mapper (TM) and X-SAR data p 15 N89-18948  
Land use analysis using remote sensing techniques. Investigation of the usefulness of LANDSAT Thematic Mapper satellite pictures for obtaining and up to date picture of land use in the province South Holland [BCRS-88-01] p 61 N89-19733
- THEMATIC MAPPING**  
Applications of SPOT HRV data for land use and soil mapping in Rayong basin p 2 A89-20769
- The use of image enhancement technique for peat land mapping using Landsat mass data in Indonesia p 52 A89-20775  
Digital Terrain Model computation using SPOT data p 53 A89-20807  
Alternatives for mapping from satellites p 62 A89-26398  
The effects of viewing geometry on image classification p 55 A89-28036  
Mapping in the Oman ophiolite using enhanced Landsat Thematic Mapper images p 23 A89-29301  
Multispectral classification of land use at the rural-urban fringe using spot data p 18 A89-29371  
Unsupervised training area selection in forests using a nonparametric distance measure and spatial information p 6 A89-30265  
Determining the age of cut forest areas in Quebec, Canada using the Landsat-5 TM p 7 A89-31893  
Investigation of information content of Thematic Mapper and SPOT multiband image data, using simulated image data of the Freiburg region (Federal Republic of Germany) [ESA-TT-975] p 57 N89-15442  
Applications of digital image processing to ongoing research in complex terrain meteorology [DEAR-001749] p 57 N89-17375  
Principal problems in upgrading quality and efficiency of geological survey work p 24 N89-17910  
Mapping of phytoplankton fluorescence with the Fluorescence Line Imager (FLI) imaging spectrometer p 39 N89-18737  
Microcomputer-based radiometer data acquisition and processing system for large-area mapping of soil moisture content in the top one meter layer p 11 N89-18774  
Updating land-use information on topographic maps using satellite imagery: Combining the advantages of two accessible sources of geographic information p 60 N89-18897  
Mapping of natural vegetation in north-east Zimbabwe by means of LANDSAT Thematic Mapper data p 14 N89-18901  
Improvements in the forward and inverse principal component transformations for geological mapping in a semi-arid terrain p 27 N89-18933  
The use of coregistered LANDSAT MSS, TM and SIR-A imagery for lithological mapping p 28 N89-18936  
Tectonics of the central Andes [NASA-CR-184683] p 28 N89-18973  
Land use analysis using remote sensing techniques. Investigation of the usefulness of LANDSAT Thematic Mapper satellite pictures for obtaining and up to date picture of land use in the province South Holland [BCRS-88-01] p 61 N89-19733
- THERMAL EMISSION**  
Tersail - A numerical model for combined analysis of vegetation canopy bidirectional reflectance and thermal emissions p 6 A89-29415
- THERMAL MAPPING**  
Relative dating of Hawaiian lava flows using multispectral thermal infrared images - A new tool for geologic mapping of young volcanic terranes p 22 A89-22647  
Use of surface temperature in agrometeorology p 4 A89-27942
- THERMOGRAPHY**  
Nighttime and daytime HCMM thermographs of the Iberian Peninsula p 56 A89-31888
- THREE DIMENSIONAL MODELS**  
Application of three dimensional image system p 53 A89-20797  
Digital Terrain Model computation using SPOT data p 53 A89-20807
- THUNDERSTORMS**  
Progress of research to identify rotating thunderstorms using satellite imagery [NASA-CR-183555] p 68 N89-17981
- TIBET**  
Satellite remote sensing of cloud distribution and amount of rainfall over the Tibet Plateau area of China p 48 A89-20770
- TIDES**  
A tide-generated internal waveform in the western approaches to the Strait of Gibraltar p 31 A89-22597
- TIMBER IDENTIFICATION**  
The characterization of sources of illumination in a Ponderosa Pine (*Pinus ponderosa*) forest community using the portable instantaneous display and analysis spectrometer p 4 A89-27781
- TIMBER INVENTORY**  
The application of remote sensing for forest inventory p 2 A89-20809  
Determining the age of cut forest areas in Quebec, Canada using the Landsat-5 TM p 7 A89-31893  
Correlation of reflectance and chlorophyll fluorescence signatures of healthy and damaged forest trees p 9 N89-18726
- TIMBER VIGOR**  
A comparison of images from a pushbroom scanner with normal color aerial photographs for detecting scattered recent conifer mortality p 7 A89-32336
- TOPOGRAPHY**  
First results of topographical mapping using SPOT images of Malaysia p 52 A89-20764  
FEX - A knowledge-based system for planimetric feature extraction p 54 A89-27783  
Visualization of topographic data using video animation p 55 A89-29066  
Sea bottom topography with X-band SLAR: Evaluation of existing models p 38 N89-18718  
Dynamic topography as measured by the Geosat altimeter in regions of small surface height signatures p 43 N89-18837  
Satellite radar altimetry over arid regions p 69 N89-18842  
Pattern analysis and the ecological interpretation of satellite imagery p 61 N89-18900  
A new approach to topographic altimetry p 73 N89-18914
- TORNADOES**  
Progress of research to identify rotating thunderstorms using satellite imagery [NASA-CR-183555] p 68 N89-17981
- TRANSFER FUNCTIONS**  
Estimation of the SAR system transfer through processor defocus p 37 N89-18706
- TRANSFORMATIONS (MATHEMATICS)**  
Application of the Haar transform for extraction of linear and anomalous patterns over part of Cambay Basin, India p 55 A89-28037
- TRANSMITTANCE**  
Spectral transmissometer and radiometer - Design and initial results --- of free drifting experiment in Pacific Ocean p 64 A89-27991  
A mathematical model of reflectance and transmittance of plant leaves as a function of chlorophyll pigment content p 13 N89-18879
- TREES**  
Correlation of reflectance and chlorophyll fluorescence signatures of healthy and damaged forest trees p 9 N89-18726  
Correlation of radar reflectivity and chlorophyll fluorescence of forest trees p 9 N89-18727
- TREES (PLANTS)**  
Fine resolution signatures of coniferous and deciduous trees at C band p 6 A89-30266  
The use of SPOT-1 imagery for forest classification in Flanders (Belgium) p 14 N89-18899  
Radar backscatter characteristics of trees at 215 GHz p 14 N89-18917  
The extinction properties of forest components p 14 N89-18918  
Radar polarimetric observations of a tree canopy p 15 N89-18920
- TRIANGULATION**  
Potential of Large Format Camera photography p 3 A89-29433  
Comparison of GPS surveys with historical triangulation surveys in the southern California borderland [NASA-CR-183405] p 24 N89-16199
- TROPICAL METEOROLOGY**  
Dispersion parameters over forested terrain p 3 A89-22728  
Geosat crossover analysis in the tropical Pacific. II - Verification analysis of altimetric sea level maps with expendable bathythermograph and island sea level data p 32 A89-26438  
Physical retrieval of rainfall rates over the ocean by multispectral microwave radiometry - Application to tropical cyclones p 37 A89-32434
- TROPICAL REGIONS**  
Upwelling off the Gulfs of Panama and Papagayo in the tropical Pacific during March 1985 p 30 A89-22591
- TROPOSPHERE**  
Comparison of satellite total ozone measurements with the distribution of tropospheric ozone obtained by an airborne UV-DIAL system over the Amazon Basin p 17 A89-21892  
Laser sounding of the troposphere and the underlying surface --- Russian book p 17 A89-22066
- TUNGSTEN**  
Application of Landsat imagery and surficial geochemistry to the discovery of tungsten skarn deposits associated with buried plutons, Yukon and Northwest Territories, Canada p 23 A89-28126
- TUNNELS**  
Fault classification for the geological support of the tunnel construction project for the Caucasus mountain-pass railroad, using space images p 22 A89-22216

**TURBIDITY**

- Determination of atmospheric turbidity from remotely-sensed data - A case study p 34 A89-28034  
Water turbidity and perpendicular vegetation indices for paddy rice flood damage analyses p 6 A89-29412

**TYPHOONS**

- VHF radar remote sensing of vertical profile of liquid water content and rainfall rate over Taiwan during the time period of Typhoon Wayne p 48 A89-20771

**U****U.S.S.R. SPACE PROGRAM**

- Principal results of remote-sensing studies of Siberia's natural resources (On the occasion of the 10th anniversary of the Scientific Coordination Council, 1977-1987) p 62 A89-22225

**ULTRAHIGH FREQUENCIES**

- Step frequency radar experiments on the Antarctic Sea ice p 43 N89-18802  
E-SAR: The experimental airborne L/C-band SAR system of DFVLR p 73 N89-18924

**UNDERWATER OPTICS**

- Optical bathymetry for the U.S. Navy - A field measurement program p 64 A89-27993  
Optical properties of sea water bodies: Measurements with an underwater radiometer and a high-resolution spectroradiometer p 39 N89-18734  
Variability of the diffuse attenuation coefficient in waters off the US East Coast p 39 N89-18738

**UNITED KINGDOM**

- Operational remote sensing in the United Kingdom: Problems of image acquisition p 68 N89-18751  
Major crustal lineaments on Seasat SAR and their off-shore extensions in the UK p 26 N89-18861

**UNITED NATIONS**

- The UN declaration of legal principals on remote sensing, 1986 p 76 N89-18748

**UNITED STATES**

- Research, investigations and technical developments. National mapping program, 1985-1986 [USGS-OPEN-FILE-REPT-87-315] p 24 N89-16208

**UPWELLING WATER**

- Upwelling off the Gulfs of Panama and Papagayo in the tropical Pacific during March 1985 p 30 A89-22591  
The structure and variability of a filament in the northwest African upwelling area as observed from AVHRR and CXCS images p 46 N89-18939

**URANIUM**

- Usefulness of remote sensing in uranium exploration programme in parts of Karnataka state, India p 21 A89-20828

**URBAN PLANNING**

- SPOT image interpretation for information on human settlement growth p 17 A89-20824

**USER REQUIREMENTS**

- Satellite data acquisition planning at the Canada Center for Remote Sensing p 68 N89-18753  
The central user services system for ERS-1 p 68 N89-18754

**V****VALLEYS**

- Interpreting the geology of Glen Coe using LANDSAT MSS data and aerial photographs p 26 N89-18860

**VEGETATION**

- Soil and vegetation mapping by using SPOT image p 1 A89-20758  
Effective permittivity of vegetation in the microwave range p 3 A89-21612  
Application of a flux algorithm to a field-satellite campaign over vegetated area p 6 A89-29411  
Analysis and representation of vegetation continua from Landsat Thematic Mapper data for lowland heaths p 7 A89-30268  
Modeling vegetation as a set of scatterers p 7 A89-32110  
The leaf-shape effect on electromagnetic scattering from vegetated media p 12 N89-18846  
Preprocessing and analysis of airborne visible near and shortwave infrared data for the detection of alteration in weathered vegetated terrain p 12 N89-18862  
Vegetation sampling for studies using remotely sensed data p 13 N89-18883  
Mapping of natural vegetation in north-east Zimbabwe by means of LANDSAT Thematic Mapper data p 14 N89-18901

**VEGETATION GROWTH**

- Mapping and inventory of forest fires from digital processing of TM data p 5 A89-28129

- Detection of periodic characteristics of rice field vegetation by microwave backscatter measurement p 5 A89-28364

- Texture analysis of forest regeneration sites in high-resolution SAR imagery p 10 N89-18730

**VEGETATIVE INDEX**

- Comparative study of vegetation index and false colour composite image of NOAA-AVHRR data for bio-mass studies p 1 A89-20752  
The vegetation index and the study of vegetation dynamics p 4 A89-27945  
Extension of a drought monitoring and vegetation classification methodology to the western Sahel p 4 A89-28127  
Integrated NDVI images for Niger 1986-1987 --- Normalized Difference Vegetation Index p 4 A89-28128

- Airborne MSS for land cover classification p 5 A89-28131

- Water turbidity and perpendicular vegetation indices for paddy rice flood damage analyses p 6 A89-29412  
Satellite derived earth surface temperatures: A crop assessment tool p 8 N89-17930  
Possibilities of the satellite imagery to locate the forest decline areas in the Vosges Massif (France) p 10 N89-18729

- An ERDAS module for routine processing of AVHRR data p 43 N89-18817

**VELOCITY DISTRIBUTION**

- Comparison study of SEASAT scatterometer and conventional wind fields [AD-A200591] p 67 N89-16202

**VELOCITY MEASUREMENT**

- A method to forecast open pack ice speed of motion using remotely-sensed data p 42 N89-18801

**VENUS SURFACE**

- Radar imaging of the surfaces of Venus and the earth using SAR data p 54 A89-23645

**VERTICAL DISTRIBUTION**

- Atmospheric profiling of water vapour with a 20.5-23.5 GHz autocorrelation radiometer p 72 N89-18908

**VERY LONG BASE INTERFEROMETRY**

- Geodetic measurement of deformation in California [NASA-CR-184604] p 19 N89-15476

**VIDEO EQUIPMENT**

- Visualization of topographic data using video animation p 55 A89-29066

**VIEW EFFECTS**

- The visibility of linear features in SAR images p 59 N89-18763

**VISIBLE SPECTRUM**

- Radiation models of mesotrophic and eutrophic bodies of water p 36 A89-30120

**VISUAL PERCEPTION**

- Reports on cartography and geodesy, series 1, number 100 [ISSN-0469-4236] p 20 N89-17935

**VOLCANOES**

- Land use suitability classification using remote sensing data and geographic information for volcanic regions p 16 A89-20766  
Identification of surface-groundwater interaction zones in the Bogor volcanic fan p 48 A89-20777  
Volcanic eruption monitoring using satellite platform p 20 A89-20783  
Erosional furrows formed during the lateral blast at Mount St. Helens, May 18, 1980 p 22 A89-22632  
Relative dating of Hawaiian lava flows using multispectral thermal infrared images - A new tool for geologic mapping of young volcanic terranes p 22 A89-22647

**VOLCANOLOGY**

- Volcanic eruption monitoring using satellite platform p 20 A89-20783  
The use of aerial photographs in Quaternary-volcanic terrains mapping p 20 A89-20784

**VORTICES**

- A simulation of the global ocean circulation with resolved eddies p 30 A89-22593

**W****WAKES**

- Simulation of SAR imaging of ship wakes p 41 N89-18765  
Automatic ship and ship wake detection in spaceborne SAR images from coastal regions p 41 N89-18766

**WASTE WATER**

- Estimation of the water exchange and contamination zones of basins from satellite imagery p 49 A89-30252

**WATER CIRCULATION**

- Estimation of the water exchange and contamination zones of basins from satellite imagery p 49 A89-30252

**WATER COLOR**

- The extraction of sea fishery potential area from Airborne Ocean Color Radiometer data p 28 A89-20786  
Variability of the diffuse attenuation coefficient in waters off the US East Coast p 39 N89-18738

**WATER DEPTH**

- Optical bathymetry for the U.S. Navy - A field measurement program p 64 A89-27993

**WATER FLOW**

- Buoyant surface jet analysis of the Yukon River p 49 A89-28033

**WATER MANAGEMENT**

- Passive microwave remote sensing system for soil moisture - Some supporting research p 49 A89-31948  
Estimating the extent of irrigated cropland in a large catchment using LANDSAT MSS data p 14 N89-18902

- Salinity mapping based on SPOT images of the Punjab, Pakistan [BCRS-88-03] p 16 N89-19734

**WATER POLLUTION**

- Estimation of the water exchange and contamination zones of basins from satellite imagery p 49 A89-30252

- Coastal ocean margins program [DE89-005937] p 47 N89-18972

**WATER QUALITY**

- Suspended solid classification of the Jakarta Bay p 28 A89-20785

- Water quality estimation from Landsat data with spectral and sea truth data base system p 28 A89-20788

- Monitoring water quality and river plume transport in Green Bay, Lake Michigan with SPOT-1 imagery p 49 A89-32338

- A comparison of original aircraft MSS and generated surface water reflectance images as predictors of lake water quality indicators [DE89-004882] p 50 N89-17932

- Quantitative remote detection of suspended sediment content and chlorophyll concentration of water in different depths p 50 N89-18733

- Monitoring offshore water quality from space p 39 N89-18739

- Monitoring of suspended sediments in Jatiluhur Reservoir using satellite images p 50 N89-18740

- Radiometric problems in the use of the Thematic Mapper for marine research p 46 N89-18940

- The use of LANDSAT imagery for water quality studies in the IJsselmeer area (Netherlands) [BCRS-87-18] p 52 N89-19732

- Water quality indicators [DE89-004882] p 50 N89-17932

- Quantitative remote detection of suspended sediment content and chlorophyll concentration of water in different depths p 50 N89-18733

- Monitoring offshore water quality from space p 39 N89-18739

- Monitoring of suspended sediments in Jatiluhur Reservoir using satellite images p 50 N89-18740

- Radiometric problems in the use of the Thematic Mapper for marine research p 46 N89-18940

- The use of LANDSAT imagery for water quality studies in the IJsselmeer area (Netherlands) [BCRS-87-18] p 52 N89-19732

- Water quality indicators [DE89-004882] p 50 N89-17932

- Quantitative remote detection of suspended sediment content and chlorophyll concentration of water in different depths p 50 N89-18733

- Monitoring offshore water quality from space p 39 N89-18739

- Monitoring of suspended sediments in Jatiluhur Reservoir using satellite images p 50 N89-18740

- Radiometric problems in the use of the Thematic Mapper for marine research p 46 N89-18940

- The use of LANDSAT imagery for water quality studies in the IJsselmeer area (Netherlands) [BCRS-87-18] p 52 N89-19732

- Water quality indicators [DE89-004882] p 50 N89-17932

- Quantitative remote detection of suspended sediment content and chlorophyll concentration of water in different depths p 50 N89-18733

- Monitoring offshore water quality from space p 39 N89-18739

- Monitoring of suspended sediments in Jatiluhur Reservoir using satellite images p 50 N89-18740

- Radiometric problems in the use of the Thematic Mapper for marine research p 46 N89-18940

- The use of LANDSAT imagery for water quality studies in the IJsselmeer area (Netherlands) [BCRS-87-18] p 52 N89-19732

- Water quality indicators [DE89-004882] p 50 N89-17932

- Quantitative remote detection of suspended sediment content and chlorophyll concentration of water in different depths p 50 N89-18733

- Monitoring offshore water quality from space p 39 N89-18739

- Monitoring of suspended sediments in Jatiluhur Reservoir using satellite images p 50 N89-18740

- Radiometric problems in the use of the Thematic Mapper for marine research p 46 N89-18940

- The use of LANDSAT imagery for water quality studies in the IJsselmeer area (Netherlands) [BCRS-87-18] p 52 N89-19732

- Remote sensing of surface manifestations of short-period internal waves in the ocean p 35 A89-30114
- SAR imaging of ocean waves in the marginal ice zone p 40 N89-18747
- Remote studies of the ocean surface by a tower-based multifrequency microwave radar p 41 N89-18785
- Directional wave data recorded in the southern North Sea [IOS-258] p 47 N89-19793

**WATERFOWL**

- LANDSAT TM study of afforestation in northern Scotland and its impact on breeding bird populations p 10 N89-18732

**WATERSHEDS**

- An estimation of areal evapotranspiration using Landsat and elevation data p 48 A89-20776
- Aerospace imagery and data for modelling erosion, sediment yield and crop yield prediction using GIS, applied to the Upper Komering catchment, Sumatra p 2 A89-20802
- Prioritization of watershed with regard to silt yield potential through data integration technique p 48 A89-20818
- Estimating the extent of irrigated cropland in a large catchment using LANDSAT MSS data p 14 N89-18902

**WAVE FUNCTIONS**

- Fractal features of sea surface manifested in microwave remote sensing signatures p 32 A89-24872

**WAVE INTERACTION**

- Ocean wave directional spectra and wave-current interaction in the Agulhas from the Shuttle Imaging Radar-B synthetic aperture radar p 30 A89-22585
- Surface wave interaction - Theory and capability of oceanic remote sensing p 35 A89-29732

**WAVE PROPAGATION**

- Directional wave data recorded in the southern North Sea [IOS-258] p 47 N89-19793

**WAVEFORMS**

- Analysis of airborne laser hydrography waveforms p 64 A89-27996

**WAVEGUIDE ANTENNAS**

- ERS-1 AMI antennas: The design and development experience --- Active Microwave Instrumentation (AMI) p 71 N89-18890

**WEATHER FORECASTING**

- Progress of research to identify rotating thunderstorms using satellite imagery [NASA-CR-183555] p 68 N89-17981

**WEATHER STATIONS**

- Comparisons of satellite data surface-based remote sensing measurements in Utah winter orographic storms p 75 N89-19079

**WEATHERING**

- Preprocessing and analysis of airborne visible near and shortwave infrared data for the detection of alteration in weathered vegetated terrain p 12 N89-18862
- Applications of LANDSAT Thematic Mapper imagery to the study of subtle variations in lithology p 27 N89-18863

**WETLANDS**

- Effects of solar angle on reflectance from wetland vegetation p 5 A89-29409
- LANDSAT TM study of afforestation in northern Scotland and its impact on breeding bird populations p 10 N89-18732

**WHEAT**

- Complementarity of middle-infrared with visible and near-infrared reflectance for monitoring wheat canopies p 5 A89-29410

**WIGNER COEFFICIENT**

- Wigner distribution analysis of surface waves p 42 N89-18789

**WIND EFFECTS**

- Inertial wind path and sea surface temperature patterns near the Gulf of Tehuantepec and Gulf of Papagayo p 30 A89-22592
- Hindcasts and data assimilation studies with the WAM model during the Seasat period --- wave model p 32 A89-26442

**WIND MEASUREMENT**

- Summertime stratospheric wind measurements above the South Pole p 62 A89-24022

**WIND VELOCITY**

- Comparison study of SEASAT scatterometer and conventional wind fields [AD-A200591] p 67 N89-18202
- Specular scattering with effective reflection coefficient p 39 N89-18723

**WINTER**

- Radar backscatter of sea ice during winter p 46 N89-18943
- Physical properties of snow and ice in the winter marginal ice zone of Fram Strait p 46 N89-18944

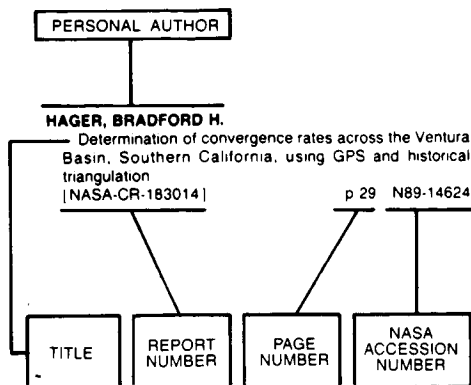
**WORKSTATIONS**

- Sea-ice software: ICEMAN p 43 N89-18805
- Requirements for an EOS-oriented workstation --- Earth Observing System (EOS) p 69 N89-18813

**WYOMING**

- Geological remote sensing of Palaeogene rocks in the Wind River Basin, Wyoming, USA p 28 N89-18935

## Typical Personal Author Index Listing



Listings in this index are arranged alphabetically by personal author. The title of the document provides the user with a brief description of the subject matter. The report number helps to indicate the type of document listed (e.g., NASA report, translation, NASA contractor report). The page and accession numbers are located beneath and to the right of the title. Under any one author's name the accession numbers are arranged in sequence with the AIAA accession numbers appearing first.

### A

- AARHOLT, E.**  
Remote studies of the ocean surface by a tower-based multifrequency microwave radar p 41 N89-18785
- ABBOTT, ELSA A.**  
Relative dating of Hawaiian lava flows using multispectral thermal infrared images - A new tool for geologic mapping of young volcanic terranes p 22 A89-22647
- ABDELHAMID, G. A. A.**  
Interpreting the geology of Glen Coe using LANDSAT MSS data and aerial photographs p 26 N89-18860
- ABDULLAYEV, A. Z.**  
Annular and block-folded structures on space and aerial photographs p 25 N89-17915
- ABER, JOHN D.**  
Remote sensing of canopy chemistry and nitrogen cycling in temperate forest ecosystems p 3 A89-23431
- ABRAMS, M. J.**  
Mapping in the Oman ophiolite using enhanced Landsat Thematic Mapper images p 23 A89-29301
- ABRAMS, MICHAEL J.**  
Relative dating of Hawaiian lava flows using multispectral thermal infrared images - A new tool for geologic mapping of young volcanic terranes p 22 A89-22647
- ABROSKIN, A. G.**  
Laser airborne sensing field experiments using the 'Chaika' assembly p 35 A89-29728
- ACHAR, K. K.**  
Usefulness of remote sensing in uranium exploration programme in parts of Karnataka state, India p 21 A89-20828
- ACKERMAN, THOMAS P.**  
MISR - A multiangle imaging spectroradiometer for geophysical and climatological research from EOS p 66 A89-31846
- AGNEW, DUNCAN C.**  
Comparison of GPS surveys with historical triangulation surveys in the southern California borderland [NASA-CR-183405] p 24 N89-16199
- AHERN, F. J.**  
A comparison of images from a pushbroom scanner with normal color aerial photographs for detecting scattered recent conifer mortality p 7 A89-32336
- Assessment of clearcut mapping accuracy with C-band SAR** p 9 N89-18725
- AHMED, Z.**  
Association of radar backscattering with biophysical characteristics of Australian forests p 10 N89-18731
- AHOLA, P. J.**  
Backscatter behavior of low-salinity sea ice at C and X-band p 44 N89-18869
- AKAMATSU, YUKIO**  
Land use suitability classification using remote sensing data and geographic information for volcanic regions p 16 A89-20766
- AKIYAMA, T.**  
Water turbidity and perpendicular vegetation indices for paddy rice flood damage analyses p 6 A89-29412
- AKTAR, M.**  
Wigner distribution analysis of surface waves p 42 N89-18789
- AKVILONOVA, A. B.**  
A method for processing and results of microwave radiometer studies of the earth from the Intercosmos 20 and 21 satellites p 36 A89-30122
- AL-DAGHASTANI, NABIL SUBHI**  
The application of remote sensing to geomorphological mapping and mass movement study in the vicinity of Provo, Utah p 23 N89-15439
- ALEKSEEV, A. S.**  
A tomographic approach to lineament identification on aerial and space images p 22 A89-22223
- ALPERS, WERNER**  
Validation of a synthetic aperture radar ocean wave imaging theory by the Shuttle Imaging Radar-B experiment over the North Sea p 30 A89-22586
- AMARAKUL, VICHARN**  
The feasibility study of oil palm area estimation in the southern part of Thailand using Landsat data p 2 A89-20760
- AMBROSIA, VINCENT G.**  
Trace gas emissions from chaparral and boreal forest fires p 7 A89-32432
- AMNUAY, CHALIT**  
The feasibility study of oil palm area estimation in the southern part of Thailand using Landsat data p 2 A89-20760
- AMRIN, SUDARNO**  
Airborne gravity as a supporting tool for hydrocarbon exploration in Indonesia p 21 A89-20829
- AMSBURY, DAVID L.**  
Extension of a drought monitoring and vegetation classification methodology to the western Sahel p 4 A89-28127
- ANDERSEN, P.**  
Mapping of natural vegetation in north-east Zimbabwe by means of LANDSAT Thematic Mapper data p 14 N89-18901
- ANDERSON, CHARLES E.**  
Progress of research to identify rotating thunderstorms using satellite imagery [NASA-CR-183555] p 68 N89-17981
- ANDRE, JEAN-MICHEL**  
Simulated effects of barometric pressure and ozone content upon the estimate of marine phytoplankton from space p 33 A89-26443
- ANDREWARTHA, R.**  
An advanced terrain tracking altimeter p 45 N89-18910
- ANWAR, MARWADI**  
Airborne gravity as a supporting tool for hydrocarbon exploration in Indonesia p 21 A89-20829
- ANZAI, FUJIO**  
Geometric correction of SPOT image p 54 A89-20812
- ARAI, IKUO**  
A procedure for land area classification using Landsat TM digital imagery p 17 A89-24651
- ARAMBEPOLA, B.**  
New architecture for a real-time SAR processor p 69 N89-18850
- ARDANUY, P.**  
MODIS-HIRIS ground data systems commonality report [NASA-TM-100718] p 67 N89-16205

- MODIS information, data and control system (MIDACS) operations concepts [NASA-TM-100720]** p 75 N89-19729
- ARGUS, S. D.**  
SAR imagery of the Grand Banks (Newfoundland) pack ice pack and its relationship to surface features p 40 N89-18745  
Use of SAR imagery and other remotely-sensed data in deriving ice information during a severe ice event on the Grand Banks (Newfoundland) p 40 N89-18746
- ARNONE, ROBERT A.**  
A tide-generated internal waveform in the western approaches to the Strait of Gibraltar p 31 A89-22597  
Satellite detection of transient enhanced primary production in the western Mediterranean Sea p 31 A89-23438
- ARONOFF, S.**  
Application of Landsat imagery and surficial geochemistry to the discovery of tungsten skarn deposits associated with buried plutons, Yukon and Northwest Territories, Canada p 23 A89-28126
- ASKNE, J.**  
Ice ridge observations by means of SAR p 45 N89-18872  
Atmospheric attenuation as derived from microwave radiometry at 52.8 GHz p 72 N89-18906
- ASRAR, G.**  
Remote sensing of land processes: Sponsored programs of study by the National Aeronautics and Space Administration p 19 N89-18833
- ATANASSOV, V.**  
Study on directional spectrum characteristics of marine radar images of ocean waves p 41 N89-18786
- ATKINSON, P. M.**  
Optimal sampling for remote sensing: Estimating the regional mean p 11 N89-18922
- ATTEMA, E.**  
Towards a calibration of the CCRS airborne SARS p 70 N89-18654  
Engineering calibration of the ERS-1 active microwave instrumentation in orbit p 71 N89-18885  
Radar signature measurements during the AGRISCATT campaigns p 15 N89-18950
- AUSTIN, S. J.**  
A software package for performance evaluation of the ERS-1 AMI p 71 N89-18887
- AUTRET, M.**  
Theoretical study of the sensitivity of the microwave backscattering coefficient to the soil surface parameters p 6 A89-30267

### B

- BABA, SHIGEYUKI**  
Spectral reflectance properties of a leaf of some mangrove species in Okinawa p 1 A89-20753
- BADHWAR, G. D.**  
Comparison of measured C-band scattering coefficients with model predictions as a function of leaf area index and Biomass p 8 N89-18712
- BAHARUDDIN, A.**  
The use of aerial photographs in Quaternary-volcanic terrains mapping p 20 A89-20784
- BAILEY, JOHN O.**  
The Special Sensor Microwave Imager - A new instrument with rainfall monitoring potential p 64 A89-28038
- BAJPAI, O. P.**  
Feature extraction considerations in utilising the optical power spectra for terrain classification p 54 A89-20821
- BAKLANOVA, O. A.**  
The procedure for and the results of the geological interpretation of photographic images of the Bukhtarna lineament zone p 22 A89-22217
- BALDOCCHI, DENNIS D.**  
A comparison of models for deriving dry deposition fluxes of O<sub>3</sub> and SO<sub>2</sub> to a forest canopy p 3 A89-20923

- BALTUCK, M.**  
Remote sensing of land processes: Sponsored programs of study by the National Aeronautics and Space Administration p 19 N89-18833
- BANNER, M. L.**  
Wavenumber spectra of short gravity waves p 35 A89-30019
- BANNINGER, C.**  
Spectral response characteristics of a metal-stressed coniferous forest as measured by the Fluorescence Line Imager (FLI) airborne imaging spectrometer p 9 N89-18724
- BARET, F.**  
Complementarity of middle-infrared with visible and near-infrared reflectance for monitoring wheat canopies p 5 A89-29410
- BARIOU, R.**  
Landsat 5 TM image of the Mont Saint-Michel region of France p 54 A89-21249  
Contribution of second-generation Landsat TM and SPOT HRV satellites to urban analysis (Rennes, France) p 17 A89-21250
- BARNES, ARNOLD A., JR.**  
EHF attenuation through the melting layer p 51 N89-18984
- BARNES, W. L.**  
MODIS - Advanced facility instrument for studies of the earth as a system p 66 A89-31943
- BARNETT, M. E.**  
Artefacts in AIS-I imagery p 69 N89-18826
- BARRETT, ERIC C.**  
Satellite remote sensing of rainfall p 49 A89-27946  
The Special Sensor Microwave Imager - A new instrument with rainfall monitoring potential p 64 A89-28038
- BASKAKOV, A. I.**  
Features of the calculation of the main characteristics of an oceanographic radar altimeter p 32 A89-23646
- BATE, E.**  
Reconnaissance groundwater appraisal of Bohol Island, Philippines, by satellite data analysis p 48 A89-20772
- BAYRAMOV, A. A.**  
Annular and block-folded structures on space and aerial photographs p 25 N89-17915
- BDEOLIVEIRA, PEDRO PAULO**  
Knowledge related aspects of lineation and lineament extraction [INPE-4709-PRE/1391] p 24 N89-15446  
Using different sources of information in automated linear feature extraction from remote sensing data [INPE-4708-PRE/1390] p 24 N89-15447
- BEAUDOIN, A.**  
Observations of the effect of geometric properties of agricultural soils on radar backscatter, from C-SAR images p 11 N89-18781
- BEAVEN, L.**  
Mapping slope failure tracks with digital Thematic Mapper data p 59 N89-18790
- BEDELL, R. L.**  
Major crustal lineaments on Seasat SAR and their off-shore extensions in the UK p 26 N89-18861
- BEQUE, A.**  
Complementarity of middle-infrared with visible and near-infrared reflectance for monitoring wheat canopies p 5 A89-29410
- BELSHER, T.**  
Remote sensing of macrophytic algae of the Molene Archipelago in France - Terrain radiometry and application to SPOT satellite data p 36 A89-30260
- BEN MOUSSA, H.**  
Remote sensing of macrophytic algae of the Molene Archipelago in France - Terrain radiometry and application to SPOT satellite data p 38 A89-30260
- BENBROOK, J. R.**  
Summertime stratospheric wind measurements above the South Pole p 62 A89-24022
- BENOIT, M.**  
Multitemporal study of differently farmed permanent grazing lands in the Lorraine region of France using SPOT-1 data p 7 A89-31894
- BERA, R. N.**  
Identification of geological features from their surface textural properties using OPS measurements p 21 A89-20820
- BERCHA, F. G.**  
Auto and cross correlation analysis of environment, system and target parameters for iceberg detection using airborne radar p 45 N89-18874
- BERGMAN, M. IU.**  
Radar imaging of the surfaces of Venus and the earth using SAR data p 54 A89-23645
- BERING, E. A.**  
Summertime stratospheric wind measurements above the South Pole p 62 A89-24022

- BERNARD, R.**  
Theoretical study of the sensitivity of the microwave backscattering coefficient to the soil surface parameters p 6 A89-30267
- BERNIER, M.**  
Comparative spectral analysis of HRV and TM sensors p 65 A89-29375
- BERRY, P. J.**  
Assimilation of altimeter data into numerical ocean models p 43 N89-18838
- BETZER, P. R.**  
Long-range transport of giant mineral aerosol particles p 17 A89-21931
- BGATOV, A. P.**  
Fault classification for the geological support of the tunnel construction project for the Caucasus mountain-pass railroad, using space images p 22 A89-22216
- BHANUKUMAR, O. S. R. U.**  
Snow cover-summer monsoon rainfall over parts of Sahel p 51 N89-18832
- BHATTACHARYA, B. B.**  
Application of the Haar transform for extraction of linear and anomalous patterns over part of Cambay Basin, India p 55 A89-28037
- BLACK, S.**  
Change detection in AGRISAR images p 15 N89-18949
- BLANCHARD, A. J.**  
The leaf-shape effect on electromagnetic scattering from vegetated media p 12 N89-18846  
The extinction properties of forest components p 14 N89-18918
- BLIZARD, MARVIN A.**  
Ocean optics IX; Proceedings of the Meeting, Orlando, FL, Apr. 4-6, 1988 [SPIE-925] p 33 A89-27976  
Ocean optics: Introduction and overview - 1988 p 64 A89-27977
- BLOOM, ARTHUR L.**  
Tectonics of the central Andes [NASA-CR-184683] p 28 N89-18973
- BOENSCH, E.**  
Investigations of SAR backscatter for different test areas using two geocoded Seasat SAR scenes p 58 N89-18761
- BOGOMOLOV, A. F.**  
Radar imaging of the surfaces of Venus and the earth using SAR data p 54 A89-23645
- BOL'SHAKOV, A. N.**  
Determination of the spectrum of energy-containing surface waves from a sun-glitter image p 29 A89-22210
- BONN, F.**  
Analysis and interpretation of SPOT images of urban and agricultural/forest sections of the Sherbrooke region p 5 A89-29373
- BOOTH, C. R.**  
Moorable spectroradiometers in the BIOWATT experiment p 64 A89-27990
- BOOTH, D. J.**  
Estimation of the area of Lake Kariba, Zimbabwe, using LANDSAT MSS imagery p 51 N89-18775
- BORDONSKII, G. S.**  
Variations of the infrared emission of snow and ice cover p 49 A89-30121
- BOREL, C. C.**  
Leaf backscattering measurements and modelling at 94 GHz p 8 N89-18713  
Radar backscatter characteristics of trees at 215 GHz p 14 N89-18917
- BORRY, F.**  
The use of SPOT-1 imagery for forest classification in Flanders (Belgium) p 14 N89-18899
- BORSTAD, G. A.**  
Mapping of phytoplankton fluorescence with the Fluorescence Line Imager (FLI) imaging spectrometer p 39 N89-18737
- BOSSARD, MICHEL**  
Cartographic analysis of Large Format Camera photographs - Comparison with SPOT and the Spacelab metric camera p 62 A89-21410
- BOUCHER, J.-M.**  
Nonlinear filtering and edge detection in speckled radar images p 58 N89-18711
- BOZO, P.**  
Agrometeorological aspects of the utilization of remote-sensing data p 3 A89-23663
- BOZSOKI, I.**  
X-band scatterometry in agriculture p 9 N89-18715
- BRADFORD, J.**  
An advanced terrain tracking altimeter p 45 N89-18910
- BRASSE, THOMAS W.**  
Goniometric observations of light scattered from soils and leaves p 4 A89-24873
- BRASS, JAMES A.**  
Trace gas emissions from chaparral and boreal forest fires p 7 A89-32432
- BREDDOW, J.**  
Fine resolution signatures of coniferous and deciduous trees at C band p 6 A89-30266
- BROCHU, R.**  
Analysis and interpretation of SPOT images of urban and agricultural/forest sections of the Sherbrooke region p 5 A89-29373
- BROWELL, EDWARD V.**  
Comparison of satellite total ozone measurements with the distribution of tropospheric ozone obtained by an airborne UV-DIAL system over the Amazon Basin p 17 A89-21892
- BROWN, B.**  
Estimating the extent of irrigated cropland in a large catchment using LANDSAT MSS data p 14 N89-18902
- BROWN, L. M. J.**  
A SAR data quality assessment scheme for the ERS-1 mission p 72 N89-18893
- BROWN, M. A.**  
Impact of phase and amplitude errors on the ERS-1 active microwave instrumentation performance p 70 N89-18853  
Advanced SAR concepts p 73 N89-18926
- BRUEGGE, CAROL J.**  
MISR - A multiangle imaging spectroradiometer for geophysical and climatological research from EOS p 66 A89-31946
- BRUENING, CLAUS**  
Validation of a synthetic aperture radar ocean wave imaging theory by the Shuttle Imaging Radar-B experiment over the North Sea p 30 A89-22586
- BUCCIARELLI, T.**  
Tracking algorithms in radar altimetry p 72 N89-18911
- BUGROVSKII, V. V.**  
Landscape processing of satellite imagery for a biospheric data bank p 56 A89-30239
- BUITEVELD, H.**  
The use of LANDSAT imagery for water quality studies in the IJsselmeer area (Netherlands) [BCRS-87-18] p 52 N89-19732
- BULAYEVSKIY, D. S.**  
Principal problems in upgrading quality and efficiency of geological survey work p 24 N89-17910
- BUNKIN, A. F.**  
Laser airborne sensing field experiments using the 'Chaika' assembly p 35 A89-29728  
The capabilities of nonlinear Raman spectroscopy for remote diagnostics of water bodies p 35 A89-29730
- BUNKIN, F. V.**  
Oceanic remote sensing p 35 A89-29726
- BURDIUGOV, V. M.**  
Determination of the spectrum of energy-containing surface waves from a sun-glitter image p 29 A89-22210
- BURGE, R. E.**  
Speckle correlation in SAR images of dynamic discrete scatterers p 37 N89-18707  
Computer simulation of multipath sea echo near grazing incidence p 38 N89-18722
- BUSCHMANN, C.**  
Correlation of reflectance and chlorophyll fluorescence signatures of healthy and damaged forest trees p 9 N89-18726
- BUTUSOV, O. B.**  
Landscape processing of satellite imagery for a biospheric data bank p 56 A89-30239
- BYRNE, G. J.**  
Summertime stratospheric wind measurements above the South Pole p 62 A89-24022
- BYRNES, H. JERRY**  
Optical bathymetry for the U.S. Navy - A field measurement program p 64 A89-27993

## C

- CACOPARDI, S.**  
Tracking algorithms in radar altimetry p 72 N89-18911
- CALMAN, J.**  
Frontal signals east of Iceland from the Geosat altimeter p 33 A89-26643
- CAMARANETO, GILBERTO**  
Automatic registration of satellite imagery [INPE-4637-PRE/1349] p 57 N89-17414
- CAMPBELL, J.**  
Towards a calibration of the CCRS airborne SARS p 70 N89-18854
- CAMTEZ, N.**  
Wigner distribution analysis of surface waves p 42 N89-18789

- CARANDE, R. E.**  
The Alaska SAR processor p 70 N89-18851
- CARD, DON H.**  
Accuracy assessment, using stratified plurality sampling, of portions of a LANDSAT classification of the Arctic National Wildlife Refuge Coastal Plain [NASA-TM-101042] p 8 N89-17339
- CARDER, K. L.**  
Long-range transport of giant mineral aerosol particles p 17 A89-21831
- CARDER, KENDALL L.**  
Spectral transmissometer and radiometer - Design and initial results p 64 A89-27991
- CARSEY, F. D.**  
SAR imagery of the Grand Banks (Newfoundland) pack ice pack and its relationship to surface features p 40 N89-18745  
Use of SAR imagery and other remotely-sensed data in deriving ice information during a severe ice event on the Grand Banks (Newfoundland) p 40 N89-18746  
Plans for the development of EOS SAR systems using the Alaska SAR facility p 69 N89-18757
- CARSON, L.**  
Real-time processing of digital image data in support of the Canadian sea ice analysis and prediction program p 43 N89-18803
- CARTER, D. J. Q.**  
ERS-1 active microwave instrumentation design and performance status [IAF PAPER 87-136] p 65 A89-28329  
The pre-launch performance verification of the ERS-1 active microwave instrumentation p 71 N89-18886  
A software package for performance evaluation of the ERS-1 AMI p 71 N89-18887  
ERS-1 active microwave instrumentation engineering model performance p 71 N89-18888  
Stability considerations for the ERS-1 wind scatterometer radiometric performance p 71 N89-18889
- CARTER, N. J.**  
Improvements in ground water recharge estimation using satellite remote sensing p 50 N89-18768
- CAVALIERI, D. J.**  
Preliminary observations of polar sea ice with the Special Sensor Microwave Imager p 42 N89-18800
- CERVILLE, B.**  
Geological mapping and analysis of fracturing in the south part of the Central Anti-Atlas in Morocco using a Landsat MSS image p 23 A89-31887
- CEVAT, J. J.**  
Land use analysis using remote sensing techniques. Investigation of the usefulness of LANDSAT Thematic Mapper satellite pictures for obtaining and up to date picture of land use in the province South Holland [BCRS-88-01] p 61 N89-19733
- CHANG, L. A.**  
Retrieval of water vapor profiles from microwave radiometric measurements at 183 and 92 GHz p 72 N89-18905
- CHANG, RUEY-GANG**  
Errors of the gravitational field determined by the satellite p 19 A89-24442
- CHAO, CHUNG-HUEI**  
A surface-wave study of the Pacific Ocean basin p 29 A89-21798
- CHAPMAN, J. E.**  
Remote sensing of evaporite mineral zonation in salt flats (salars) p 23 A89-30271
- CHARBONNEAU, L.**  
Analysis and interpretation of SPOT images of urban and agricultural/forest sections of the Sherbrooke region p 5 A89-29373
- CHARNY, B.**  
The Alaska SAR processor p 70 N89-18851
- CHARUPPAT, THONGCHAI**  
Study on changes of mangrove forest in Thailand by using Landsat imagery p 3 A89-20822
- CHASE, J. R.**  
Estimation of sea-ice type and concentration by linear unmixing of Geosat altimeter waveforms p 47 N89-18946
- CHAU, T. K. W.**  
Real-time stereo matching SPOT using transputer arrays p 74 N89-18958
- CHAVEZ, PAT S., JR.**  
Use of the variable gain settings on SPOT p 65 A89-29435  
Extracting spectral contrast in Landsat Thematic Mapper image data using selective principal component analysis p 57 A89-32337
- CHEN, A. J.**  
VHF radar remote sensing of vertical profile of liquid water content and rainfall rate over Taiwan during the time period of Typhoon Wayne p 48 A89-20771
- CHEM, C. C. T.**  
A spectral feature design system for high dimensional multispectral data p 60 N89-18894
- CHEN, CHUN-SUNG**  
Errors of the gravitational field determined by the satellite p 19 A89-24442
- CHEN, JIAN**  
Quantitative remote detection of suspended sediment content and chlorophyll concentration of water in different depths p 50 N89-18733
- CHERVIN, ROBERT M.**  
A simulation of the global ocean circulation with resolved eddies p 30 A89-22593
- CHEUNG, TAK KEE**  
Can better environmental inputs improve sea clutter estimation? A numerical experiment p 36 A89-30258
- CHIDLEY, T. R. E.**  
Digital elevation models and their application to remote sensing of water resources p 51 N89-18770
- CHIKOV, B. M.**  
The procedure for and the results of the geological interpretation of photographic images of the Bukhtarma lineament zone p 22 A89-22217
- CHOCIA, P. A.**  
Improvement of multispectral color images by intensifying local contrasts p 56 A89-30123
- CHOROWICZ, J.**  
Geological mapping and analysis of fracturing in the south part of the Central Anti-Atlas in Morocco using a Landsat MSS image p 23 A89-31887
- CHRISTENSEN, E. L.**  
The Technical University of Denmark (TUD) C-band SAR p 74 N89-18928
- CHUKHLANTSEV, A. A.**  
Effective permittivity of vegetation in the microwave range p 3 A89-21612  
Modeling vegetation as a set of scatterers p 7 A89-32110
- CHUVIECO, EMILIO**  
Mapping and inventory of forest fires from digital processing of TM data p 5 A89-28129
- CIHLAR, J.**  
Comparative spectral analysis of HRV and TM sensors p 65 A89-29375
- CIHLAR, JOSEF**  
Area measurement of agricultural fields from satellite images p 5 A89-29374
- CIMINO, J.**  
Concepts for processing and analyzing of multiple SAR and Landsat images p 55 A89-27789  
Requirements for an EOS-oriented workstation p 69 N89-18813
- CLARK, C.**  
Artefacts in AIS-1 imagery p 69 N89-18826
- CLARK, R. KENT**  
Bathymetry using Thematic Mapper imagery p 34 A89-27995
- CLARKE, ALLAN J.**  
Inertial wind path and sea surface temperature patterns near the Gulf of Tehuantepec and Gulf of Papagayo p 30 A89-22592
- CLAYSON, C. H.**  
Directional wave data recorded in the southern North Sea [IOS-258] p 47 N89-19793
- CLEDEN, D.**  
The algorithm development facility: Its role in the development and operation of a satellite data centre p 68 N89-18755
- COFER, WESLEY R., III**  
Trace gas emissions from chaparral and boreal forest fires p 7 A89-32432
- COLL, E. C.**  
A high fidelity, high throughput system for geocoding SAR imagery p 60 N89-18849
- COLLINS, K. A.**  
Real-time stereo matching SPOT using transputer arrays p 74 N89-18958
- COLLINS, W. G.**  
Effects of commercialisation on international remote sensing activities p 76 N89-18752  
Monitoring of agro-forestry production systems in the Sudano-Sahelian zone of West Africa p 11 N89-18825
- COMISO, JOSEPH C.**  
Antarctic Ocean polynias [NASA-CR-184805] p 47 N89-19102
- CONGALTON, RUSSEL G.**  
Mapping and inventory of forest fires from digital processing of TM data p 5 A89-28129
- CORR, D. G.**  
Progress in automatic analysis of multi-temporal remotely-sensed data p 61 N89-18956
- COUR, PH.**  
Possibilities of the satellite imagery to locate the forest decline areas in the Vosges Massif (France) p 10 N89-18729
- COWARD, SAMUEL N.**  
Tersail - A numerical model for combined analysis of vegetation canopy bidirectional reflectance and thermal emissions p 6 A89-29415
- CRACKNELL, A. P.**  
Geological applications of thermal infrared characteristics of vegetation p 27 N89-18932
- CRIPPEN, ROBERT E.**  
A simple spatial filtering routine for the cosmetic removal of scan-line noise from Landsat TM P-tape imagery p 57 A89-32335
- CROSIAR, CHRISTY LYNN**  
Satellite derived earth surface temperatures: A crop assessment tool p 8 N89-17930
- CROSS, A.**  
Geological lineament detection using the Hough transform p 26 N89-18818  
Progress in automatic analysis of multi-temporal remotely-sensed data p 61 N89-18956
- CUDLIP, W.**  
Satellite radar altimetry over arid regions p 69 N89-18842  
An advanced terrain tracking altimeter p 45 N89-18910
- CUNNINGHAM, CYNTHIA L.**  
Research, investigations and technical developments. National mapping program, 1985-1986 [USGS-OPEN-FILE-REPT-87-315] p 24 N89-16208
- CURRAN, P. J.**  
The relationship between suspended sediment concentration and remotely sensed spectral radiance - A review p 48 A89-24649
- CURRAN, PAUL J.**  
Airborne MSS for land cover classification p 5 A89-28131
- CURTISS, BRIAN**  
The characterization of sources of illumination in a Ponderosa Pine (*Pinus ponderosa*) forest community using the portable instantaneous display and analysis spectrometer p 4 A89-27781

## D

- DALTON, MIKE**  
Visualization of topographic data using video animation p 55 A89-29066
- DALTON, N.**  
Real-time stereo matching SPOT using transputer arrays p 74 N89-18958
- DANSON, M.**  
Change detection in AGRISAR images p 15 N89-18949
- DAUGHTRY, C. S. T.**  
Estimating absorbed radiation and phytomass from multispectral reflectance of corn and soybeans p 13 N89-18876
- DAVEAU, S.**  
Nighttime and daytime HCMM thermographs of the Iberian Peninsula p 56 A89-31888  
Thermal infrared and visible images of the Iberian Peninsula p 56 A89-31889
- DAVENPORT, C. A.**  
Enhancement of glacial fractures by analysis of Thematic Mapper data: Glen Roy, Scotland p 26 N89-18859
- DAVIES, ROGER**  
MISR - A multiangle imaging spectroradiometer for geophysical and climatological research from EOS p 66 A89-31946
- DAVIS, ANTHONY**  
Analysis of atmospheric effects in SPOT HRV images p 65 A89-28372
- DAY, T.**  
Real-time stereo matching SPOT using transputer arrays p 74 N89-18958
- DAY, TIM**  
Visualization of topographic data using video animation p 55 A89-29066
- DE VAUBERNIER, E.**  
Multitemporal study of differently farmed permanent grazing lands in the Lorraine region of France using SPOT-1 data p 7 A89-31894
- DEEKSHATULU, B. L.**  
Identification of geological features from their surface textural properties using OPS measurements p 21 A89-20820  
Feature extraction considerations in utilising the optical power spectra for terrain classification p 54 A89-20821
- DEEKSHATULU, B. L.**  
Indian activities in remote sensing applications: Microwave remote sensing p 67 N89-16886



- DEERING, DONALD W.**  
Parabola directional field radiometer for aiding in space sensor data interpretations p 63 A89-27779
- DEGROOF, H.**  
Post-processing airborne SAR data for multitemporal land-cover studies p 12 N89-18857
- DEJACE, J.**  
Image processing techniques - Filtering, exogenous data, geometrical processing p 55 A89-27938
- DELEZIR, J.**  
Combining oblique SPOT-1 images for the analysis of certain soil properties p 7 A89-31892
- DELIA, S.**  
The central user services system for ERS-1 p 68 N89-18754
- DELINOM, R.**  
Radar imagery as a tool for mineral exploration - A case study of gold mineralization in East Kalimantan p 20 A89-20780
- DELLEPIANE, S.**  
Information fusion by a knowledge-based system for SAR image interpretation p 60 N89-18831
- DELOOR, G. P.**  
Sea bottom topography with X-band SLAR: Evaluation of existing models p 38 N89-18718
- DEMENTEV, V. N.**  
The procedure for and the results of the geological interpretation of photographic images of the Bukhtarma lineament zone p 22 A89-22217
- DENBO, D. W.**  
Frontal signals east of Iceland from the Geosat altimeter p 33 A89-26643
- DEPALMA, IRENE P.**  
Satellite detection of transient enhanced primary production in the western Mediterranean Sea p 31 A89-23438
- DEROOVER, B.**  
The use of SPOT-1 imagery for forest classification in Flanders (Belgium) p 14 N89-18899
- DEWULF, R.**  
The use of SPOT-1 imagery for forest classification in Flanders (Belgium) p 14 N89-18899
- DI, LIPING**  
Band-moment analysis of imaging-spectrometer data p 65 A89-29436
- DIMYATI, MUH.**  
The role of remote sensing in geographic information systems using computer p 17 A89-20792  
Study of the monitoring of land cover/use using remote sensing data by personal computer in southern part of Bandung area, West Java p 2 A89-20815
- DINER, DAVID J.**  
MISR - A multiangle imaging spectroradiometer for geophysical and climatological research from EOS p 66 A89-31946
- DIPOKUSUMO, BOBBY S.**  
Low-cost second order planimetric mapping technique p 53 A89-20800
- DOBSON, E. B.**  
Frontal signals east of Iceland from the Geosat altimeter p 33 A89-26643  
Dynamic topography as measured by the Geosat altimeter in regions of small surface height signatures p 43 N89-18837
- DOBSON, M. C.**  
Radar polarimetric observations of a tree canopy p 15 N89-18920
- DODD, GREGORY C.**  
Comparisons of satellite data surface-based remote sensing measurements in Utah winter orographic storms p 75 N89-19079
- DODGE, JAMES C.**  
Satellite remote sensing of cloud distribution and amount of rainfall over the Tibet Plateau area of China p 48 A89-20770  
Low cost, microcomputer-based interactive analysis system for direct-reception and archived remote sensing data p 53 A89-20796
- DOHERTY, M.**  
A SAR data quality assessment scheme for the ERS-1 mission p 72 N89-18893
- DONNELLY, B. E.**  
SPOT mapping software for Wild Aviolyt BC2 analytical plotter p 60 N89-18824
- DONOHUE, M. J.**  
NASA's Earth Observing System (EOS): An opportunity for mankind p 77 N89-18816
- DORSON, DONALD**  
Evaluation of satellite-tracked surface drifting buoys for simulating the movement of spilled oil in the marine environment. Volume 1: Executive summary [PB88-226048] p 37 N89-17357  
Evaluation of satellite-tracked surface drifting buoys for simulating the movement of spilled oil in the marine environment, volume 2 [PB88-226055] p 37 N89-17358
- DOWMAN, I. J.**  
Real-time stereo matching SPOT using transputer arrays p 74 N89-18958
- DRAKE, N.**  
Alternative approaches to the classification of upland semi-natural vegetation p 16 N89-18961
- DRANNIK, A. S.**  
Principal problems in upgrading quality and efficiency of geological survey work p 24 N89-17910
- DRAYTON, R. S.**  
Improvements in ground water recharge estimation using satellite remote sensing p 50 N89-18768  
An assessment of ATM and satellite data for estimating the groundwater contribution to slope stability p 51 N89-18769
- DRIEMAN, J. A.**  
Assessment of clearcut mapping accuracy with C-band SAR p 9 N89-18725
- DRINKWATER, M. R.**  
Important changes in microwave scattering properties of young snow-covered sea ice as indicated from dielectric modelling p 44 N89-18870
- DRURY, S. A.**  
Integration of geological, geophysical and remotely sensed data for the Solway Basin, England p 26 N89-18794
- DU, LI-JEN**  
Segmentation of Synthetic Aperture Radar (SAR) images of ocean surface by the texture energy transform method [AD-A199536] p 37 N89-15309
- DUBOIS, J. M. M.**  
Determining the age of cut forest areas in Quebec, Canada using the Landsat-5 TM p 7 A89-31893
- DUBOVSKIKH, V. M.**  
Landscape processing of satellite imagery for a biospheric data bank p 56 A89-30239
- DUCE, R. A.**  
Long-range transport of giant mineral aerosol particles p 17 A89-21931
- DUESMANN, B.**  
ERS-1 altimeter height calibration p 71 N89-18891
- DUNCAN, C.**  
Textural and spectral features as an aid to cloud classification p 74 N89-18960
- DUPONT, O.**  
Comparative spectral analysis of HRV and TM sensors p 65 A89-29375
- DURDEN, S. L.**  
Application of radar polarimetry to forestry p 15 N89-18919
- DURRANT, R.**  
An advanced terrain tracking altimeter p 45 N89-18910
- DVORAK, T. Z.**  
A model for the propagation of industrial atmospheric pollution registered on multispectral earth images p 17 A89-22213
- DWIVEDI, R. S.**  
Delineation of salt-affected soils through digital analysis of Landsat MSS data p 6 A89-30262

## E

- EDWARDS, G.**  
Texture analysis of forest regeneration sites in high-resolution SAR imagery p 10 N89-18730
- EGAWA, H.**  
Signature variations due to atmospheric and topographic effects on satellite MSS data over rugged terrain p 70 N89-18877
- EGOROV, S. T.**  
Procedures for the determination of geophysical parameters from spaceborne microwave polarimeter measurements p 30 A89-22224
- EISEN, M. F.**  
A new view of the mid-ocean ridge from the behaviour of ridge-axis discontinuities p 31 A89-23433
- EIUMNOH, APISIT**  
Applications of SPOT HRV data for land use and soil mapping in Rayong basin p 2 A89-20769
- ELACHI, C.**  
Overview of the Shuttle Imaging Radar (SIR-C) p 73 N89-18921
- ELDHUSET, K.**  
Automatic ship and ship wake detection in spaceborne SAR images from coastal regions p 41 N89-18766
- ELGY, J.**  
The use of coregistered LANDSAT MSS, TM and SIR-A imagery for lithological mapping p 28 N89-18936
- ELKINGTON, M. D.**  
The algorithm development facility: Its role in the development and operation of a satellite data centre p 68 N89-18755
- ELTOFT, T.**  
Remote studies of the ocean surface by a tower-based multifrequency microwave radar p 41 N89-18785
- EMERY, WILLIAM J.**  
A simulation for spaceborne SAR imagery of a distributed, moving scene p 33 A89-26846
- EMRAN, A.**  
Geological mapping and analysis of fracturing in the south part of the Central Anti-Atlas in Morocco using a Landsat MSS image p 23 A89-31887
- EPP, H.**  
Mapping slope failure tracks with digital Thematic Mapper data p 59 N89-18790
- ERDMANN, J. C.**  
Simulation of radiometric ocean images recorded from high-altitude platforms p 33 A89-27980
- ERGINTAV, S.**  
Wigner distribution analysis of surface waves p 42 N89-18789
- ERIKSEN, S.**  
Simulation of SAR imaging of ship wakes p 41 N89-18765
- ETCHETO, J.**  
Satellite determination of the carbon dioxide exchange coefficient at the ocean-atmosphere interface - A first step p 31 A89-22598
- EVANS, D.**  
Overview of the Shuttle Imaging Radar (SIR-C) p 73 N89-18921
- EWING, J. A.**  
Directional wave data recorded in the southern North Sea [IOS-258] p 47 N89-19793

## F

- FARKYA, V. K.**  
On classification of forests of some portions of central India using satellite imageries p 2 A89-20761
- FAY, TEMPLE H.**  
Bathymetry using Thematic Mapper imagery p 34 A89-27995
- FEA, M.**  
The central user services system for ERS-1 p 68 N89-18754
- FEIVESON, A. H.**  
Comparison of measured C-band scattering coefficients with model predictions as a function of leaf area index and Biomass p 8 N89-18712
- FELDMAN, U.**  
A method to forecast open pack ice speed of motion using remotely-sensed data p 42 N89-18801
- FERNS, D. C.**  
Microcomputers and mass storage devices for image processing p 65 A89-29070
- FERRAZZOLI, P.**  
Comparison between microwave emissivity and backscattering coefficient of agricultural fields p 12 N89-18844
- FERRER, A.**  
Reconnaissance groundwater appraisal of Bohol Island, Philippines, by satellite data analysis p 48 A89-20772
- FETTERER, F.**  
Investigations of sea ice using coincident Geosat altimetry and synthetic aperture radar during MIZEX-87 p 46 N89-18945
- FIELDING, ERIC J.**  
Tectonics of the central Andes [NASA-CR-184683] p 28 N89-18973
- FILATOV, N. N.**  
Estimation of the water exchange and contamination zones of basins from satellite imagery p 49 A89-30252
- FILY, M.**  
Measuring lead area changes in sea ice imagery p 44 N89-18871
- FISCHER, J.**  
Satellite sea surface temperature at the North Atlantic Polar Front related to high-resolution towed conductivity-temperature-depth data p 31 A89-22594
- FISHMAN, JACK**  
Comparison of satellite total ozone measurements with the distribution of tropospheric ozone obtained by an airborne UV-DIAL system over the Amazon Basin p 17 A89-21892
- FIUMARA, A.**  
Crops radar responses analysis based on AGRISAR '86 data p 15 N89-18947
- FLACH, J. D.**  
Digital elevation models and their application to remote sensing of water resources p 51 N89-18770
- FOLTA, D.**  
MODIS information, data and control system (MIDACS) operations concepts [NASA-TM-100720] p 75 N89-19729

- FOLVING, S.**  
Assessment of land/soil degradation in northern Burkina Faso p 13 N89-18882
- FOODY, G. M.**  
Analysis and representation of vegetation continua from Landsat Thematic Mapper data for lowland heaths p 7 A89-30268
- FOODY, GILES M.**  
The effects of viewing geometry on image classification p 55 A89-28036
- FOOTE, H. P.**  
Applications of digital image processing to ongoing research in complex terrain meteorology [DC89-001749] p 57 N89-17375
- FORREST, M. D.**  
Image processing methods for the presentation of multiple geological datasets from the English Lake District p 25 N89-18793
- FOTOS, CHRISTOPHER P.**  
Commercial remote sensing satellites generate debate, foreign competition p 76 A89-21397
- FWLER, G. F.**  
Radiometric calibration of airborne SAR data p 70 N89-18855
- FOX, ANDREW N.**  
Tectonics of the central Andes [NASA-CR-184683] p 28 N89-18973
- FOX, P. J.**  
A new view of the mid-ocean ridge from the behaviour of ridge-axis discontinuities p 31 A89-23433
- FRANCIS, C. R.**  
ERS-1 altimeter height calibration p 71 N89-18891
- FRANCIS, P. W.**  
Remote sensing of evaporite mineral zonation in salt flats (salars) p 23 A89-30271
- FRAYBERGER, A. A.**  
Principal problems in upgrading quality and efficiency of geological survey work p 24 N89-17910
- FRAYSSE, G.**  
Platforms p 63 A89-27936
- FRUSH, CHARLES**  
Applications of the NCAR Electra Doppler radar for the study of physical parameters of clouds p 75 N89-19717
- FUGONO, NOBUYOSHI**  
Ocean wave spectra derived from Shuttle Imaging Radar-B imagery and surface measurements p 30 A89-22583
- FUJIMURA, S.**  
A mathematical model of reflectance and transmittance of plant leaves as a function of chlorophyll pigment content p 13 N89-18879  
A method for the clustering of remotely sensed multispectral images by using statistical test for spatial uniformity p 61 N89-18898
- FUKUE, KIYONARI**  
Accuracy of land-cover/use classification p 52 A89-20765  
MOS-1 data processing in Tokai Space Center p 52 A89-20790  
Spatial information processings of TM data p 52 A89-20791
- FUKUSHIMA, YOSHIKAZU**  
Accuracy of terrain measurement using SPOT HRV data p 53 A89-20801
- FULLER, R. M.**  
Visual and computer classifications of remotely-sensed images - A case study of grasslands in Cambridgeshire p 7 A89-30269
- FUNG, A. K.**  
The leaf-shape effect on electromagnetic scattering from vegetated media p 12 N89-18846  
The extinction properties of forest components p 14 N89-18918
- G**
- GABELL, A. R.**  
An evaluation of surface emittance and temperature data derived from Thermal Infrared Multispectral Scanner (TIMS) for lithological mapping in weathered vegetated terrain: N. Queensland, Australia p 27 N89-18934
- GAERTNER, V.**  
Operational calibration of Meteosat's infrared channel p 62 A89-22622
- GALUMIAN, A. S.**  
The capabilities of nonlinear Raman spectroscopy for remote diagnostics of water bodies p 35 A89-29730
- GANTINI, TUTI**  
Monitoring inundation area of Aliran Sungai Bengawan Solo Jawa Timur with Landsat images p 48 A89-20768
- GARELLO, R.**  
Statistical evaluation of the intensity distribution of sea surface radar images p 38 N89-18717
- GARRITY, C.**  
Shipborne passive microwave sea ice experiment in the East Greenland Sea: May-July 1987 p 42 N89-18799
- GARSDIE, J. R.**  
A comparison of clutter texture properties in optical and SAR images p 8 N89-18708
- GAUTAM, N. C.**  
Wasteland identification in India using satellite remote sensing p 18 A89-30263
- GAUTIER, CATHERINE**  
A multi-sensor remote sensing approach for measuring primary production from space [NASA-CR-184662] p 37 N89-15444
- GAVANON, STEPHAN**  
Digital Terrain Model computation using SPOT data p 53 A89-20807
- GAVORET, MURIEL**  
Cartographic analysis of Large Format Camera photographs - Comparison with SPOT and the Spacelab metric camera p 62 A89-21410
- GAYLE, D.**  
Technology transfer for development of coastal zone resources: Caribbean experts examine critical issues p 40 N89-18749
- GERSHENZON, V. E.**  
Remote sensing of surface manifestations of short-period internal waves in the ocean p 35 A89-30114
- GIANNINI, J. A.**  
Variability of the diffuse attenuation coefficient in waters off the US East Coast p 39 N89-18738
- GILLESPIE, ALAN R.**  
Relative dating of Hawaiian lava flows using multispectral thermal infrared images - A new tool for geologic mapping of young volcanic terranes p 22 A89-22647
- GIRARD, C. M.**  
Multitemporal study of differently farmed permanent grazing lands in the Lorraine region of France using SPOT-1 data p 7 A89-31894
- GITEL'SON, A. A.**  
Radiation models of mesotrophic and eutrophic bodies of water p 36 A89-30120
- GLASBEY, C. A.**  
Normal distributional assumptions in discrimination p 59 N89-18821
- GLAZMAN, R. E.**  
Fractal properties of the sea surface manifested in microwave remote sensing signatures p 41 N89-18784
- GLAZMAN, ROMAN E.**  
Fractal features of sea surface manifested in microwave remote sensing signatures p 32 A89-24872
- GLIBIN, IU. V.**  
Motion characteristics of sea waves p 32 A89-23590
- GOEL, NARENDRA S.**  
Bidirectional canopy reflectance and its relationship to vegetation characteristics p 6 A89-30264
- GOODFELLOW, W. D.**  
Application of Landsat imagery and surficial geochemistry to the discovery of tungsten skarn deposits associated with buried plutons, Yukon and Northwest Territories, Canada p 23 A89-28126
- GOOSSENS, R.**  
The use of SPOT-1 imagery for forest classification in Flanders (Belgium) p 14 N89-18899
- GORBENKO, V. P.**  
The procedure for and the results of the geological interpretation of photographic images of the Bukhtarma lineament zone p 22 A89-22217
- GORDON, ARNOLD L.**  
Antarctic Ocean polynyas [NASA-CR-184805] p 47 N89-19102
- GORE, WARREN J. Y.**  
Calibration of infrared satellite images using high altitude aircraft measurements [AIAA PAPER 89-0817] p 54 A89-25595
- GORVUNOV, A. L.**  
Laser airborne sensing field experiments using the 'Chaika' assembly p 35 A89-29728
- GOSINK, J. P.**  
Buoyant surface jet analysis of the Yukon River p 49 A89-28033
- GOW, A. J.**  
Physical properties of snow and ice in the winter marginal ice zone of Fram Strait p 46 N89-18944
- GOWER, J. F. R.**  
Mapping of phytoplankton fluorescence with the Fluorescence Line Imager (FLI) imaging spectrometer p 39 N89-18737
- GRANT, DAVID F.**  
STAR-1 high resolution synthetic aperture radar imagery for precious metal exploration p 21 A89-20827
- GRASSL, HARTMUT**  
Extraction of surface temperature from satellite data p 33 A89-27941
- GRAY, A. L.**  
Towards a calibration of the CCRS airborne SARS p 70 N89-18854
- GRAZIANI, MARY E.**  
Research, investigations and technical developments. National mapping program, 1985-1986 [USGS-OPEN-FILE-REPT-87-315] p 24 N89-16208
- GREEN, A. A.**  
An evaluation of surface emittance and temperature data derived from Thermal Infrared Multispectral Scanner (TIMS) for lithological mapping in weathered vegetated terrain: N. Queensland, Australia p 27 N89-18934
- GREICHGAEUER, T.**  
Correlations between agricultural plant parameters and multitemporal radar scatterometer data: First results from the European AGRISCATT 87 campaign p 16 N89-18951
- GRIFFITHS, G. H.**  
Pattern analysis and the ecological interpretation of satellite imagery p 61 N89-18900
- GRIFFITHS, H. D.**  
An advanced terrain tracking altimeter p 45 N89-18910  
A synthetic aperture altimeter p 73 N89-18913  
A study of advanced radar altimeter techniques [ESA-CR(P)-2699] p 75 N89-19483
- GRISHIN, GENNADI A.**  
Optical methods of satellite hydrophysics. Investigation of the environment from manned orbital stations p 32 A89-26181
- GRODSKII, S. A.**  
Determination of the spectrum of energy-containing surface waves from a sun-glitter image p 29 A89-22210
- GROSS, M. F.**  
Effects of solar angle on reflectance from wetland vegetation p 5 A89-29409
- GRUBER, ARNOLD**  
The relative merits of narrowband channels for estimating broadband albedos p 66 A89-30967
- GRUNWALD, B.**  
Data processing for the determination of pigments and suspended solids from Thematic Mapper data p 50 N89-18736
- GU, ZHIQIANG**  
Textural and spectral features as an aid to cloud classification p 74 N89-18960
- GUAN, ZHE-QUN**  
The studies for the computer classification and the investigation of grasslands in Tibet using Space-Lab color infrared image p 1 A89-20754
- GUBBELS, TIMOTHY L.**  
Tectonics of the central Andes [NASA-CR-184683] p 28 N89-18973
- GUBIN, V. N.**  
Neotectonic zoning of Belorussia on the basis of space data p 21 A89-22215
- GUENTHER, GARY C.**  
Analysis of airborne laser hydrography waveforms p 64 A89-27996
- GUIGNARD, J. P.**  
Quality control of fast delivery processors and products p 72 N89-18892
- GUISTO, D. D.**  
Information fusion by a knowledge-based system for SAR image interpretation p 60 N89-18831
- GULARSO, SRI KUSNO**  
Soil and vegetation mapping by using SPOT image p 1 A89-20758
- GUPTA, A. K.**  
Mapping of construction material sites around Bangalore City using Landsat Thematic Mapper data p 52 A89-20782
- GUPTA, P. C.**  
Aerial remote sensing technique in the identification and acreage estimation of various plantations - A case study in Gorakhpur district, Uttar Pradesh, India p 2 A89-20819
- GUY, M.**  
Combining oblique SPOT-1 images for the analysis of certain soil properties p 7 A89-31892
- GUYENNE, T. D.**  
The 1988 International Geoscience and Remote Sensing Symposium (IGARSS 1988) on Remote Sensing: Moving Towards the 21st Century, volume 3 [ESA-SP-284-VOL-3] p 68 N89-18704  
Proceedings of the 1988 International Geoscience and Remote Sensing Symposium (IGARSS) '88 on Remote Sensing: Moving Towards the 21st Century, Volume 2 [ESA-SP-284-VOL-2] p 69 N89-18836
- GUYMER, T. H.**  
A study of the effect of rain on Seasat radar altimeter data p 44 N89-18840

## GUYOT, G.

Complementarity of middle-infrared with visible and near-infrared reflectance for monitoring wheat canopies p 5 A89-29410

## GUZKOWSKA, M. A. J.

Satellite radar altimetry over arid regions p 69 N89-18842  
An advanced terrain tracking altimeter p 45 N89-18910

## GWYN, Q. H. J.

Observations of the effect of geometric properties of agricultural soils on radar backscatter, from C-SAR images p 11 N89-18781

## H

## HAAPANEN, J. A. E.

Backscatter behavior of low-salinity sea ice at C and X-band p 44 N89-18869

## HADJAR, NASRIL

Forest observation by satellite p 1 A89-20759

## HAGER, BRADFORD H.

Comparison of GPS surveys with historical triangulation surveys in the southern California borderland [NASA-CR-183405] p 24 N89-16199

## HAIMBACH, S. P.

Airborne nonacoustic bathymetric survey flight test results p 51 N89-18937

## HAIMBACH, STEPHEN P.

Optical bathymetry for the U.S. Navy - A field measurement program p 64 A89-27993

## HAITZ, M.

Correlation of radar reflectivity and chlorophyll fluorescence of forest trees p 9 N89-18727

## HALL, F. G.

Characterizing forest ecosystem dynamics through modelling and remote sensing observations p 10 N89-18728

## HALLIKAINEN, M. T.

Backscatter behavior of low-salinity sea ice at C and X-band p 44 N89-18869

## HAMMER, PHILIP D.

Calibration of infrared satellite images using high altitude aircraft measurements [AIAA PAPER 89-0817] p 54 A89-25595

## HAMRAN, S. E.

Remote studies of the ocean surface by a tower-based multifrequency microwave radar p 41 N89-18785

## HAN, D.

MODIS-HIRIS ground data systems commonality report [NASA-TM-100718] p 67 N89-16205  
MODIS information, data and control system (MIDACS) operations concepts [NASA-TM-100720] p 75 N89-18929

## HAN, SHIXING

The preliminary study on correlation between satellite information and bottom trawling ground in the East China Sea and the Yellow Sea p 29 A89-20805

## HANAIZUMI, H.

A method for the clustering of remotely sensed multispectral images by using statistical test for spatial uniformity p 61 N89-18898

## HAPIP, A. S.

The retrieval of sea surface temperature from NOAA/AVHRR satellite data - Comparison between Singh's and McClain's methods p 28 A89-20787

## HARDER, JERALD WILLIAM

Measurements of springtime Antarctic ozone depletion and development of a balloonborne ultraviolet photometer p 67 N89-15459

## HARDING, A. E.

Image processing methods for the presentation of multiple geological datasets from the English Lake District p 25 N89-18793  
Monitoring surface mineral workings using TM and SPOT p 26 N89-18796

## HARDISKY, M. A.

Effects of solar angle on reflectance from wetland vegetation p 5 A89-29409

## HARDJOPRAWIRO, S.

The geology of the area surrounding Lake Kerinci, Indonesia as interpreted through SIR-B imageries p 20 A89-20781

## HARDJOSUWARNO, JOKO SETIYONO

Drainage pattern analysis with the aid of Landsat MSS data of the Citarium river basin, West Java, Indonesia p 48 A89-20778

## HARDY, W. E.

ERS-1 AMI antennas: The design and development experience p 71 N89-18890

## HARRINGTON, JOHN A., JR.

Integrated NDVI images for Niger 1986-1987 p 4 A89-28128

## HARRISON, C. G. A.

The crustal field p 22 A89-22877

## HARRISON, CHRISTOPHER G. A.

The source of marine magnetic anomalies [MPL-U-42/87] p 31 A89-22876

## HARTL, PH.

Fundamentals of remote sensing p 63 A89-27934  
Sensors p 63 A89-27935

## HARTLEY, S.

ERS-1 active microwave instrumentation engineering model performance p 71 N89-18888

## HARTONO, U.

The use of aerial photographs in Quaternary-volcanic terrains mapping p 20 A89-20784

## HATTORI, S.

An interactive system for aerial photo orientation of digital stereo image pairs p 53 A89-20799

## HAUCK, M.

Results of tectonic and spectral investigations in the coast range of northern Chile using special processed Thematic Mapper (TM) data p 27 N89-18929

## HAWKINS, J.

Investigations of sea ice using coincident Geosat altimetry and synthetic aperture radar during MIZEX-87 p 46 N89-18945

## HAWKINS, R. K.

Towards a calibration of the CCRS airborne SARS p 70 N89-18854

## HAYMON, R. M.

A new view of the mid-ocean ridge from the behaviour of ridge-axis discontinuities p 31 A89-23433

## HAYNES, C. VANCE, JR.

Large-scale, low-amplitude bedforms (chevrons) in the Selima sand sheet, Egypt p 23 A89-31755

## HE, CHANGCHUI

The development of remote sensing in China p 76 A89-31560

## HEBVERT, MARTIAL

Sensor fusion of range and reflectance data for outdoor scene analysis p 76 N89-19868

## HEHANUSSA, P. E.

Identification of surface-groundwater interaction zones in the Bogor volcanic fan p 48 A89-20777

## HEHUWAT, F.

Application of remote sensing for hydrocarbon exploration on Timor Island, Indonesia p 21 A89-20825

## HENDERSON, D.

Real-time processing of digital image data in support of the Canadian sea ice analysis and prediction program p 43 N89-18803

## HENDRAWATI, MARCELINA RINNY

Application of three dimensional image system p 53 A89-20797

## HENDRY, A.

The visibility of linear features in SAR images p 59 N89-18763

Automated linear feature detection and its application to curve location in synthetic aperture radar imagery p 59 N89-18764

## HERLAND, E.-A.

Interpreting SAR images by means of map information p 58 N89-18760

## HERRING, T. A.

Research in geodesy and geophysics based upon radio interferometric observations of extragalactic radio sources [AD-A200858] p 25 N89-17933

## HESANY, V.

Analysis of ocean backscatter data obtained by the University of Kansas during TOWARD 84/85 p 42 N89-18787

## HICKMAN, G. D.

Airborne nonacoustic bathymetric survey flight test results p 51 N89-18937

## HICKMAN, G. DANIEL

Optical bathymetry for the U.S. Navy - A field measurement program p 64 A89-27993

## HILDEBRAND, PETER

Applications of the NCAR Electra Doppler radar for the study of physical parameters of clouds p 75 N89-19717

## HILL, GREG J. E.

Land use and land cover applications of Landsat MSS data p 17 A89-20813

## HILL, J.

Image-based atmospheric correction of multitemporal Thematic Mapping data for agricultural land cover classification p 14 N89-18895

## HILLER, K.

Results of tectonic and spectral investigations in the coast range of northern Chile using special processed Thematic Mapper (TM) data p 27 N89-18929

## HILLION, A.

Nonlinear filtering and edge detection in speckled radar images p 58 N89-18711

Statistical evaluation of the intensity distribution of sea surface radar images p 38 N89-18717

## HIROSAWA, H.

Measurements of microwave backscatter from conifers p 12 N89-18848

## HIROSE, T.

Toward the automated use of remote sensing data in operational ice forecasting p 43 N89-18804

## HO, D.

Multiple source data processing in remote sensing p 56 A89-29073

## HOEKMAN, D. H.

Extraction of small-scale spatial information from SLAR raw data of forests through an analysis of speckle p 8 N89-18709

## HOGG, D. C.

Progress in automatic analysis of multi-temporal remotely-sensed data p 61 N89-18956

## HOLDER, GLENN H.

Multispectral classification of land use at the rural-urban fringe using spot data p 18 A89-29371

## HOLDER, KRISTINE

Comparison study of SEASAT scatterometer and conventional wind fields [AD-A200591] p 67 N89-16202

## HOLLAND, J. Z.

Dispersion parameters over forested terrain p 3 A89-22728

## HOLLAND, WILLIAM R.

The impact of satellite altimetry data on numerical simulations of general midlatitude oceanic circulation p 34 A89-28305

## HOLLINGSWORTH, ANTHONY

Hindcasts and data assimilation studies with the WAM model during the Seasat period p 32 A89-26442

## HOLTZMAN, J. C.

Analysis of ocean backscatter data obtained by the University of Kansas during TOWARD 84/85 p 42 N89-18787

## HOLYER, R. J.

Estimation of sea-ice type and concentration by linear unmixing of Geosat altimeter waveforms p 47 N89-18946

## HOLYER, RONALD J.

Edge detection applied to satellite imagery of the oceans p 33 A89-26844

## HOOK, S. J.

Preprocessing and analysis of airborne visible near and shortwave infrared data for the detection of alteration in weathered vegetated terrain p 12 N89-18862  
An evaluation of surface emittance and temperature data derived from Thermal Infrared Multispectral Scanner (TIMS) for lithological mapping in weathered vegetated terrain: N. Queensland, Australia p 27 N89-18934

## HOPE, ALLEN S.

Tersail - A numerical model for combined analysis of vegetation canopy bidirectional reflectance and thermal emissions p 6 A89-29415

## HORINO, MASAKATSU

Land use suitability classification using remote sensing data and geographic information for volcanic regions p 16 A89-20766

## HORN, R.

E-SAR: The experimental airborne L/C-band SAR system of DFVLR p 73 N89-18924

## HOSHI, TAKASHI

Spectral reflectance properties of a leaf of some mangrove species in Okinawa p 1 A89-20753  
An estimation of areal evapotranspiration using Landsat and elevation data p 48 A89-20776

## HOSOMURA, TSUKASA

MOS-1 data processing in Tokai Space Center p 52 A89-20790  
New technology for displaying of NOAA AVHRR thermal band image p 29 A89-20810

## HOURY, S.

An experiment to invert Seasat altimetry for the Mediterranean and Black Sea mean surfaces p 36 A89-30900

## HOWARTH, PHILIP J.

Multispectral classification of land use at the rural-urban fringe using spot data p 18 A89-29371

## HOYT, D.

MODIS-HIRIS ground data systems commonality report [NASA-TM-100718] p 67 N89-16205  
MODIS information, data and control system (MIDACS) operations concepts [NASA-TM-100720] p 75 N89-18929

## HUA, FU LE

The preliminary study of current shifting state by the use of infrared images of NOAA-9 p 39 N89-18742

## HUANG, SCOTT L.

Applications of image scanning and processing in rock shear surface study p 20 A89-20779

- HUBAUX, A.**  
The luxuriant image - An introduction to remote sensing data processing p 55 A89-27937
- HUBBE, J. M.**  
Applications of digital image processing to ongoing research in complex terrain meteorology [DE89-001749] p 57 N89-17375
- HUBERT, L.**  
Landsat 5 TM image of the Mont Saint-Michel region of France p 54 A89-21249  
Contribution of second-generation Landsat TM and SPOT HRV satellites to urban analysis (Rennes, France) p 17 A89-21250
- HUGHES, M. P.**  
An assessment of ATM and satellite data for estimating the groundwater contribution to slope stability p 51 N89-18769
- HUNG, R. J.**  
Satellite remote sensing of cloud distribution and amount of rainfall over the Tibet Plateau area of China p 48 A89-20770  
VHF radar remote sensing of vertical profile of liquid water content and rainfall rate over Taiwan during the time period of Typhoon Wayne p 48 A89-20771
- HUNT, G. A.**  
Improvements in the forward and inverse principal component transformations for geological mapping in a semi-arid terrain p 27 N89-18933
- HUNT, J. J.**  
The 1988 International Geoscience and Remote Sensing Symposium (IGARSS 1988) on Remote Sensing: Moving Towards the 21st Century, volume 3 [ESA-SP-284-VOL-3] p 68 N89-18704  
Proceedings of the 1988 International Geoscience and Remote Sensing Symposium (IGARSS) '88 on Remote Sensing: Moving Towards the 21st Century, Volume 2 [ESA-SP-284-VOL-2] p 69 N89-18836
- HURLEY, E.**  
MODIS-HIRIS ground data systems commonality report [NASA-TM-100718] p 67 N89-16205
- HURLEY, P. C. F.**  
Monitoring offshore water quality from space p 39 N89-18739
- HYYPPIA, J. M.**  
Backscatter behavior of low-salinity sea ice at C and X-band p 44 N89-18869
- I**
- IGUCHI, TOSHIO**  
Ocean wave spectra derived from Shuttle Imaging Radar-B imagery and surface measurements p 30 A89-22583
- IMHOFF, M. L.**  
NASA's Earth Observing System (EOS): An opportunity for mankind p 77 N89-18816
- INOMATA, HIDEYUKI**  
Ocean wave spectra derived from Shuttle Imaging Radar-B imagery and surface measurements p 30 A89-22583
- INOUE, HISAYUKI**  
Distribution and variations of oceanic carbon dioxide in the western North Pacific, eastern Indian, and Southern Ocean south of Australia p 29 A89-20925
- IRONS, JAMES R.**  
Goniometric observations of light scattered from soils and leaves p 4 A89-24873
- IRVINE, D. E.**  
Ocean wave directional spectra and wave-current interaction in the Agulhas from the Shuttle Imaging Radar-B synthetic aperture radar p 30 A89-22585
- ISACKS, BRYAN L.**  
Tectonics of the central Andes [NASA-CR-184683] p 28 N89-18973
- ISHIKAWA, MAMORU**  
Application of three dimensional image system p 53 A89-20797
- ISMANGUN**  
Aerospace imagery and data for modelling erosion, sediment yield and crop yield prediction using GIS, applied to the Upper Komering catchment, Sumatra p 2 A89-20802
- ITTEN, K. I.**  
Dependence of snow melting and surface-atmosphere interactions on the forest structure p 3 A89-21740
- J**
- JACKSON, M. J.**  
Real-time stereo matching SPOT using transputer arrays p 74 N89-18958
- JACKSON, T. J.**  
Observed effects of soil organic matter content on the microwave intensity of soils p 12 N89-18845
- JACKSON, THOMAS J.**  
Passive microwave remote sensing system for soil moisture - Some supporting research p 49 A89-31948
- JACOBOWITZ, HERBERT**  
The relative merits of narrowband channels for estimating broadband albedos p 66 A89-30967
- JACOBS, STANLEY S.**  
Antarctic Ocean polynyas [NASA-CR-184805] p 47 N89-19102
- JAFFIN, S.**  
MODIS-HIRIS ground data systems commonality report [NASA-TM-100718] p 67 N89-16205  
MODIS information, data and control system (MIDACS) operations concepts [NASA-TM-100720] p 75 N89-19729
- JANSEN, PETER A. E. M.**  
Hindcasts and data assimilation studies with the WAM model during the Seasat period p 32 A89-26442
- JANTO, SUWI**  
Radar imagery as a tool for mineral exploration - A case study of gold mineralization in East Kalimantan p 20 A89-20780
- JAYARAMAN, M.**  
Relationship of spectral data and grain yield variation in rice (*Oryza sativa* L.) ADT 31 p 2 A89-20782
- JAYKO, KATHERINE**  
Evaluation of satellite-tracked surface drifting buoys for simulating the movement of spilled oil in the marine environment. Volume 1: Executive summary [PB88-226048] p 37 N89-17357  
Evaluation of satellite-tracked surface drifting buoys for simulating the movement of spilled oil in the marine environment, volume 2 [PB88-226055] p 37 N89-17358
- JEAMCHARETON, MONTOL**  
The feasibility study of oil palm area estimation in the southern part of Thailand using Landsat data p 2 A89-20760
- JEFFERIES, WILLIAM C.**  
STAR-1 high resolution synthetic aperture radar imagery for precious metal exploration p 21 A89-20827
- JENSEN, JOHN R.**  
The derivation and verification of surface reflectances using airborne MSS data and a radiative transfer model [DE89-004881] p 67 N89-17931  
A comparison of original aircraft MSS and generated surface water reflectance images as predictors of lake water quality indicators [DE89-004882] p 50 N89-17932
- JI, JIANKANG**  
A simulation test for soil moisture sensing p 10 N89-18772
- JOHANNESSEN, O. M.**  
Geophysical information on the winter marginal ice zone obtained from SAR p 46 N89-18942
- JOHANNESSEN, O.**  
SAR imaging of ocean waves in the marginal ice zone p 40 N89-18747
- JOHANSEN, OISTEIN**  
Evaluation of satellite-tracked surface drifting buoys for simulating the movement of spilled oil in the marine environment. Volume 1: Executive summary [PB88-226048] p 37 N89-17357  
Evaluation of satellite-tracked surface drifting buoys for simulating the movement of spilled oil in the marine environment, volume 2 [PB88-226055] p 37 N89-17358
- JOHANSSON, R.**  
Ice ridge observations by means of SAR p 45 N89-18872
- JOHNSON, D.**  
Evaluation of VARAN-S SAR data from the BEPERS study project p 45 N89-18875
- JOHNSON, D. L.**  
Investigations of sea ice using coincident Geosat altimetry and synthetic aperture radar during MIZEX-87 p 46 N89-18945
- JOHNSON, D. L.**  
VHF radar remote sensing of vertical profile of liquid water content and rainfall rate over Taiwan during the time period of Typhoon Wayne p 48 A89-20771
- JONES, A.**  
Alternative approaches to the classification of upland semi-natural vegetation p 16 N89-18961
- JONES, IAN S. F.**  
Wavenumber spectra of short gravity waves p 35 A89-30019
- JORDAN, S.**  
Analysis of ocean backscatter data obtained by the University of Kansas during TOWARD 84/85 p 42 N89-18787
- JORDANS, R.**  
The use of LANDSAT imagery for water quality studies in the IJsselmeer area (Netherlands) [BCRS-87-18] p 52 N89-19732
- JUNG, C.**  
Effects of slopes and relief two-dimensional spatial frequencies on spaceborne SAR imagery p 59 N89-18777
- JURKEVICH, I.**  
Segmentation of SAR images p 58 N89-18759
- K**
- K'NCHEVA, R. KH.**  
Determination of relative crop areas from spectrometric data p 22 A89-22218
- KAHNEN, D. H.**  
Correlation of radar reflectivity and chlorophyll fluorescence of forest trees p 9 N89-18727
- KAHLE, ANNE B.**  
Relative dating of Hawaiian lava flows using multispectral thermal infrared images - A new tool for geologic mapping of young volcanic terranes p 22 A89-22647
- KAK, S. N.**  
Usefulness of remote sensing in uranium exploration programme in parts of Karnataka state, India p 21 A89-20828
- KANADE, TAKEO**  
Sensor fusion of range and reflectance data for outdoor scene analysis p 76 N89-19868
- KARABANOV, A. K.**  
Neotectonic zoning of Belorussia on the basis of space data p 21 A89-22215
- KARAM, M. A.**  
The leaf-shape effect on electromagnetic scattering from vegetated media p 12 N89-18846  
The extinction properties of forest components p 14 N89-18918
- KARNCHANASUTHAM, SUPAN**  
The feasibility study of oil palm area estimation in the southern part of Thailand using Landsat data p 2 A89-20760
- KARTASASMITA, M.**  
The retrieval of sea surface temperature from NOAA/AVHRR satellite data - Comparison between Singh's and McClain's methods p 28 A89-20787  
The navigation method for NOAA/AVHRR image p 61 A89-20795
- KASAI, YUMI**  
Accuracy of land-cover/use classification p 52 A89-20765
- KASISCHKE, E. S.**  
Radiometric calibration of airborne SAR data p 70 N89-18855
- KATAMSI, IBNU**  
Coastline monitoring in Madura Strait, Indonesia on 1972-1985 p 29 A89-20804
- KATTI, V. J.**  
Usefulness of remote sensing in uranium exploration programme in parts of Karnataka state, India p 21 A89-20828
- KAUFMANN, H.**  
A possibility for selecting spectral bands of future land application sensors at the example of an imaging spectrometer p 60 N89-18896
- KAWATA, Y.**  
Signature variations due to atmospheric and topographic effects on satellite MSS data over rugged terrain p 70 N89-18877
- KAZANTSEV, I. G.**  
A tomographic approach to lineament identification on aerial and space images p 22 A89-22223
- KEEVALLIK, S. KH.**  
Determination of clear-sky planetary albedo p 62 A89-22214
- KELLY, GAIL D.**  
Land use and land cover applications of Landsat MSS data p 17 A89-20813
- KENYON, N.**  
Major crustal lineaments on Seasat SAR and their off-shore extensions in the UK p 26 N89-18861
- KEONG, KWONG LEONG**  
SPOT mapping software for Wild Aviolyt BC2 analytical plotter p 60 N89-18824
- KEREKES, J. P.**  
Simulation of optical remote sensing systems for earth resource analysis p 74 N89-18964
- KERPELMAN, CHARLES**  
Some aspects of space applications for disaster management - The use of space technology for disaster warning and for determining the effects of natural disasters [IAF PAPER 86-426] p 18 A89-24849

- KERTOPERMONO, ARIS PONIMAN**  
Remote sensing applications for agricultural landuse survey in Indonesia - Isimu case study p 2 A89-20763
- KESTNER, JOANN M.**  
Goniometric observations of light scattered from soils and leaves p 4 A89-24873
- KHACHATRIAN, ZHIUL'VERN B.**  
Polarization of microwave emission of a water surface in a wide range of angles of sight p 34 A89-28290
- KIARNER, O. IJ.**  
Determination of clear-sky planetary albedo p 62 A89-22214
- KIDD, CHRISTOPHER**  
The Special Sensor Microwave Imager - A new instrument with rainfall monitoring potential p 64 A89-28038
- KIEFFER, SUSAN WERNER**  
Erosional furrows formed during the lateral blast at Mount St. Helens, May 18, 1980 p 22 A89-22632
- KIENKO, IURII P.**  
Optical methods of satellite hydrophysics. Investigation of the environment from manned orbital stations p 32 A89-26181
- KILGUS, C. C.**  
The Navy Geosat radar altimeter satellite mission p 45 N89-18909
- KIRCHHOF, WERNER**  
Investigation of information content of Thematic Mapper and SPOT multiband image data, using simulated image data of the Freiburg region (Federal Republic of Germany) [ESA-TT-975] p 57 N89-15442
- KITSUREGAWA, MASARU**  
Receiving and processing system for meteorological satellite (NOAA) p 53 A89-20806
- KLEMAS, V.**  
Effects of solar angle on reflectance from wetland vegetation p 5 A89-29409
- KLESHCHENKO, A. D.**  
Agrometeorological aspects of the utilization of remote-sensing data p 3 A89-23663
- KNEPPECK, I. D.**  
A comparison of images from a pushbroom scanner with normal color aerial photographs for detecting scattered recent conifer mortality p 7 A89-32336
- KOBAYASHI, O.**  
Measurements of microwave backscatter from conifers p 12 N89-18848
- KOBER, W.**  
Concepts for processing and analyzing of multiple SAR and Landsat images p 55 A89-27789  
Requirements for an EOS-oriented workstation p 69 N89-18813
- KOGER, DAVID G.**  
Application of Landsat MSS and TM data to geological resource exploration p 22 A89-26397
- KOLBUSZ, JOHN**  
Visualization of topographic data using video animation p 55 A89-29066
- KOMETANI, Y.**  
An interactive system for aerial photo orientation of digital stereo image pairs p 53 A89-20799
- KONDRAT'EV, K. IA.**  
Determination of clear-sky planetary albedo p 62 A89-22214  
Estimation of the water exchange and contamination zones of basins from satellite imagery p 49 A89-30252
- KONECNY, G.**  
Alternatives for mapping from satellites p 62 A89-26398
- KONG, J. A.**  
Bayes classification of terrain cover using normalized polarimetric data p 54 A89-22649
- KONG, JIN AU**  
Active and passive remote sensing of ice [AD-A201915] p 47 N89-19792
- KOSASIH, SHYARIF**  
Aerospace imagery and data for modelling erosion, sediment yield and crop yield prediction using GIS, applied to the Upper Komering catchment, Sumatra p 2 A89-20802
- KOSTOV, K. G.**  
Microcomputer-based radiometer data acquisition and processing system for large-area mapping of soil moisture content in the top one meter layer p 11 N89-18774  
Experiments in Bulgaria for determination of soil moisture in the top one-meter layer using microwave radiometry and a priori information p 11 N89-18843
- KOVAL', ALEKSANDR D.**  
Optical methods of satellite hydrophysics. Investigation of the environment from manned orbital stations p 32 A89-26181
- KOZODEROV, V. V.**  
Determination of clear-sky planetary albedo p 62 A89-22214
- KOZU, TOSHIAKI**  
Detection of periodic characteristics of rice field vegetation by microwave backscatter measurement p 5 A89-28364
- KRATKY, V.**  
On-line aspects of stereophotogrammetric processing of SPOT images p 66 A89-32334
- KRISHITALKA, L.**  
Geological remote sensing of Palaeogene rocks in the Wind River Basin, Wyoming, USA p 28 N89-18935
- KROTKOVA, O. T.**  
Ring structures of buried platform areas and the evaluation of their tectonic activity on the basis of geomorphological data p 23 A89-30118
- KRUPP, B. M.**  
Retrieval of water vapor profiles from microwave radiometric measurements at 183 and 92 GHz p 72 N89-18905
- KRYLOV, S. D.**  
Variations of the infrared emission of snow and ice cover p 49 A89-30121
- KRYLOVA, M. S.**  
A method for processing and results of microwave radiometer studies of the earth from the Intercosmos 20 and 21 satellites p 36 A89-30122
- KUDRIAVTSEV, V. N.**  
Determination of the spectrum of energy-containing surface waves from a sun-glitter image p 29 A89-22210
- KUDRIN, L. V.**  
Radar imaging of the surfaces of Venus and the earth using SAR data p 54 A89-23645
- KUKLA, G.**  
Dependence of snow melting and surface-atmosphere interactions on the forest structure p 3 A89-21740
- KULESHOV, L. N.**  
Effectiveness of soil mapping on the basis of space photographic data p 3 A89-22249
- KUMAR, R.**  
Specular scattering with effective reflection coefficient p 39 N89-18723
- KURONUMA, YUICHIRO**  
Geometric correction of SPOT image p 54 A89-20812
- KUROSU, TAKASHI**  
Detection of periodic characteristics of rice field vegetation by microwave backscatter measurement p 5 A89-28364  
A measurement of microwave backscattering coefficients of rice plants p 8 N89-18714
- KUSAKA, T.**  
Signature variations due to atmospheric and topographic effects on satellite MSS data over rugged terrain p 70 N89-18877
- KUTUZA, B. G.**  
A method for processing and results of microwave radiometer studies of the earth from the Intercosmos 20 and 21 satellites p 36 A89-30122
- KUUSK, A. E.**  
Brightness of a laser-beam halo in vegetation cover p 3 A89-22221
- KUZNETSOV, E. V.**  
Features of the geological structure of the polar Urals and the distribution of certain minerals, as evaluated on the basis of the interpretation of aerial and space photographs p 23 A89-30119
- KWARTENG, ANDREW YAW**  
Extracting spectral contrast in Landsat Thematic Mapper image data using selective principal component analysis p 57 A89-32337
- KWEON, IN SO**  
Sensor fusion of range and reflectance data for outdoor scene analysis p 76 N89-19868
- L**
- LA VIOLETTE, PAUL E.**  
A tide-generated internal waveform in the western approaches to the Strait of Gibraltar p 31 A89-22597  
Processing satellite infrared and visible imagery for oceanographic analyses p 34 A89-29075
- LANDAUER, GERD**  
Airborne multispectral remote sensing of forest decline in West Germany p 1 A89-20757
- LANDGREBE, D. A.**  
A spectral feature design system for high dimensional multispectral data p 60 N89-18894  
Simulation of optical remote sensing systems for earth resource analysis p 74 N89-18964
- LANDRY, R.**  
Texture analysis of forest regeneration sites in high-resolution SAR imagery p 10 N89-18730
- LASZLO, ISTVAN**  
The relative merits of narrowband channels for estimating broadband albedos p 66 A89-30967
- LATHROP, RICHARD G., JR.**  
Monitoring water quality and river plume transport in Green Bay, Lake Michigan with SPOT-1 imagery p 49 A89-32338
- LAUR, H.**  
Multitemporal and dual polarization of agricultural crops by X-band SAR images p 9 N89-18716
- LAWNER, R.**  
Analysis of ocean backscatter data obtained by the University of Kansas during TOWARD 84/85 p 42 N89-18787
- LAWRENCE, D. H.**  
Progress in automatic analysis of multi-temporal remotely-sensed data p 61 N89-18956
- LAXON, S.**  
Investigations of sea ice using coincident Geosat altimetry and synthetic aperture radar during MIZEX-87 p 46 N89-18945
- LE HENAFF, F.**  
Landsat 5 TM image of the Mont Saint-Michel region of France p 54 A89-21249  
Contribution of second-generation Landsat TM and SPOT HRV satellites to urban analysis (Rennes, France) p 17 A89-21250
- LEAVITT, E. D.**  
Geophysical information on the winter marginal ice zone obtained from SAR p 46 N89-18942
- LEBERL, F.**  
Concepts for processing and analyzing of multiple SAR and Landsat images p 55 A89-27789  
Requirements for an EOS-oriented workstation p 69 N89-18813
- LECLERC, ANDRE**  
First results of topographical mapping using SPOT images of Malaysia p 52 A89-20764
- LECORDIX, PIERRE-YVES**  
Cartographic analysis of Large Format Camera photographs - Comparison with SPOT and the Spacelab metric camera p 62 A89-21410
- LEE, J. S.**  
Segmentation of SAR images p 58 N89-18759
- LEE, M.**  
Automatic mineral map generation procedure from imaging spectrometer data p 27 N89-18931
- LEE, MEEMONG**  
Sea-ice software: ICEMAN p 43 N89-18805
- LEGECKIS, RICHARD**  
Upwelling off the Gulfs of Panama and Papagayo in the tropical Pacific during March 1985 p 30 A89-22591
- LEGG, C. A.**  
Operational remote sensing in the United Kingdom: Problems of image acquisition p 68 N89-18751
- LEIDECKER, HENNING W.**  
Goniometric observations of light scattered from soils and leaves p 4 A89-24873
- LENCO, M.**  
Possibilities of the satellite imagery to locate the forest decline areas in the Vosges Massif (France) p 10 N89-18729
- LEONARD, DONALD A.**  
Remote sensing of ocean physical properties - A comparison of Raman and Brillouin techniques p 34 A89-28003
- LESTAK, SH.**  
Agrometeorological aspects of the utilization of remote-sensing data p 3 A89-23663
- LETOAN, T.**  
Multitemporal and dual polarization of agricultural crops by X-band SAR images p 9 N89-18716  
Observations of the effect of geometric properties of agricultural soils on radar backscatter, from C-SAR images p 11 N89-18781
- LEVINE, JOEL S.**  
Trace gas emissions from chaparral and boreal forest fires p 7 A89-32432
- LEVKOV, E. A.**  
Neotectonic zoning of Belorussia on the basis of space data p 21 A89-22215
- LEVRINI, G.**  
Tracking algorithms in radar altimetry p 72 N89-18911  
The advanced terrain tracking altimeter instrument p 74 N89-18954
- LI, FUK**  
Studies of the dependence of the microwave radar cross section on ocean surface variables during the FASINEX experiment p 41 N89-18782
- LIKHOV, G. A.**  
Surface wave interaction - Theory and capability of oceanic remote sensing p 35 A89-29732
- LIAO, B.**  
Summertime stratospheric wind measurements above the South Pole p 62 A89-24022

- LICHTENTHALER, H. K.**  
Correlation of reflectance and chlorophyll fluorescence signatures of healthy and damaged forest trees p 9 N89-18726  
Correlation of radar reflectivity and chlorophyll fluorescence of forest trees p 9 N89-18727
- LILLESAND, THOMAS M.**  
Monitoring water quality and river plume transport in Green Bay, Lake Michigan with SPOT-1 imagery p 49 A89-32338
- LIN, C. H.**  
VHF radar remote sensing of vertical profile of liquid water content and rainfall rate over Taiwan during the time period of Typhoon Wayne p 48 A89-20771
- LIONELLO, PIERO**  
Hindcasts and data assimilation studies with the WAM model during the Seasat period p 32 A89-26442
- LIU, GUOSHENG**  
Observation of the degree of glaciation in middle-level stratiform clouds p 62 A89-23464  
Structure of layer clouds as observed simultaneously by a microwave radiometer and an 8.6 mm-radar p 74 N89-19039
- LIVINGSTONE, C. E.**  
Towards a calibration of the CCRS airborne SARS p 70 N89-18854
- LODIN, M.**  
Integration of digital satellite and geophysical data, Heath Steele Mines, New Brunswick, Canada p 25 N89-18792
- LOHRENTZ, STEVEN E.**  
Satellite detection of transient enhanced primary production in the western Mediterranean Sea p 31 A89-23438
- LOPES, A.**  
Adaptive speckle filtering for SAR images p 58 N89-18710
- LOUET, J.**  
ERS-1 operation capabilities p 71 N89-18884
- LOURENS, U.**  
Estimating the extent of irrigated cropland in a large catchment using LANDSAT MSS data p 14 N89-18902
- LOVEJOY, S.**  
Extreme variability, scaling and fractals in remote sensing - Analysis and simulation p 56 A89-29074
- LOWRY, RAYMOND T.**  
STAR-1 high resolution synthetic aperture radar imagery for precious metal exploration p 21 A89-20827
- LU, JIAJU**  
Development of principal component analysis applied to multitemporal Landsat TM data p 4 A89-28035
- LUKOWSKI, T.**  
Satellite data acquisition planning at the Canada Center for Remote Sensing p 68 N89-18753
- LUSCOMBE, A. P.**  
Taking a broader view: Radarsat adds ScansAR to its operations p 73 N89-18925
- LUTHER, C. A.**  
Remote sensing in a marginal ice zone: A brief overview p 46 N89-18941
- LUTTRELL, S. P.**  
Image compression using a neural network p 58 N89-18705
- LUZI, G.**  
Comparison between microwave emissivity and backscattering coefficient of agricultural fields p 12 N89-18844
- LYALL, F.**  
The UN declaration of legal principals on remote sensing, 1986 p 76 N89-18748
- LYBERIS, N.**  
Geological mapping and analysis of fracturing in the south part of the Central Anti-Atlas in Morocco using a Landsat MSS image p 23 A89-31887
- LYDEN, J.**  
SAR imaging of ocean waves in the marginal ice zone p 40 N89-18747
- LYZENGA, DAVID R.**  
Comparison of Shuttle Imaging Radar-B ocean wave image spectra with linear model predictions based on aircraft measurements p 30 A89-22584
- M**
- MA, WEI-MING**  
Local geoid determination using the global positioning system [AD-A202220] p 20 N89-19731
- MACDONALD, KEN C.**  
A new view of the mid-ocean ridge from the behaviour of ridge-axis discontinuities p 31 A89-23433
- MACEK, STEVEN L.**  
First results of topographical mapping using SPOT images of Malaysia p 52 A89-20764
- MACHADOESILVA, ANTONIO JOSE F.**  
Study of geometric quality of the MSS-LANDSAT imagery [INPE-4653-PRE/1360] p 57 N89-15440
- MADSEN, S. N.**  
The Technical University of Denmark (TUD) C-band SAR p 74 N89-18928
- MAE, S.**  
Step frequency radar experiments on the Antarctic Sea ice p 43 N89-18802
- MAE, SHINJI**  
Step frequency radar experiments on the Antarctic Sea ice p 34 A89-28365
- MAJUMDAR, T. J.**  
Application of the Haar transform for extraction of linear and anomalous patterns over part of Cambay Basin, India p 55 A89-28037
- MALHOTRA, ROOP C.**  
Potential of Large Format Camera photography p 65 A89-29433
- MALINGREAU, J. P.**  
The vegetation index and the study of vegetation dynamics p 4 A89-27945
- MANAVALAN, P.**  
Prioritization of watershed with regard to silt yield potential through data integration technique p 48 A89-20818
- MANIKIAM, B.**  
Comparative study of vegetation index and false colour composite image of NOAA-AVHRR data for bio-mass studies p 1 A89-20752  
Prioritization of watershed with regard to silt yield potential through data integration technique p 48 A89-20818
- MANNING, C. R.**  
Comparison of NOAA-AVHRR-2 sea surface temperatures with surface measurements in coastal waters p 36 A89-30259
- MAO, PEIFEN**  
Application of airborne scanners in remote sensing of sea p 29 A89-20789
- MARACCI, G.**  
Determination of atmospheric turbidity from remotely-sensed data - A case study p 34 A89-28034  
Optical properties of sea water bodies: Measurements with an underwater radiometer and a high-resolution spectroradiometer p 39 N89-18734
- MARCIALEAODEMORAESNOVO, EVLYN**  
The impact of multiviewing reflectance data on the estimation of suspended sediment concentration p 50 N89-18735
- MARDIO, P.**  
The retrieval of sea surface temperature from NOAA-AVHRR satellite data - Comparison between Singh's and McClain's methods p 28 A89-20787
- MARTIN, LARRY R. G.**  
Multispectral classification of land use at the rural-urban fringe using spot data p 18 A89-29371  
Accuracy assessment of Landsat-based visual change detection methods applied to the rural-urban fringe p 18 A89-29437
- MARTIN, SHEILA E.**  
Research, investigations and technical developments. National mapping program, 1985-1986 [USGS-OPEN-FILE-REPT-87-315] p 24 N89-16208
- MARTONCHIK, JOHN V.**  
MISR - A multiangle imaging spectroradiometer for geophysical and climatological research from EOS p 66 A89-31946
- MASLOV, I. A.**  
Detection of ocean bottom relief by local geoid p 35 A89-29731
- MASON, D. C.**  
Progress in automatic analysis of multi-temporal remotely-sensed data p 61 N89-18956
- MASON, I. M.**  
Satellite radar altimetry over arid regions p 69 N89-18842
- MASSONNET, D.**  
Preprocessing of the VARAN synthetic aperture airborne radar p 70 N89-18856
- MASTRA, RIADIKA**  
The use of SPOT imagery in Medan agriculture area for monitoring features changes p 1 A89-20755
- MASUKO, HARUNOBU**  
Ocean wave spectra derived from Shuttle Imaging Radar-B imagery and surface measurements p 30 A89-22583
- MATEJEK, S.**  
Determining the age of cut forest areas in Quebec, Canada using the Landsat-5 TM p 7 A89-31893
- MATSUMAE, YOSHIKI**  
Accuracy of land-cover/use classification p 52 A89-20765  
MOS-1 data processing in Tokai Space Center p 52 A89-20790
- Spatial information processings of TM data p 52 A89-20791
- MATSUO, YOSHIO**  
The role of remote sensing in geographic information systems using computer p 17 A89-20792
- MATSUSHITA, KEISHIN**  
Water quality estimation from Landsat data with spectral and sea truth data base system p 28 A89-20788
- MATSUZAKA, Y.**  
Measurements of microwave backscatter from conifers p 12 N89-18848
- MATTHEWS, M. V.**  
Displacement calculations from geodetic data and the testing of geophysical deformation models p 19 A89-22639
- MAUREL, P.**  
Complementarity of middle-infrared with visible and near-infrared reflectance for monitoring wheat canopies p 5 A89-29410
- MAUSER, W.**  
Data processing for the determination of pigments and suspended solids from Thematic Mapper data p 50 N89-18736  
Extraction of agricultural plant parameters from multitemporal Thematic Mapper (TM) and X-SAR data p 15 N89-18948  
Correlations between agricultural plant parameters and multitemporal radar scatterometer data: First results from the European AGRISCATT 87 campaign p 16 N89-18951
- MAUSER, WOLFRUM**  
Investigation of information content of Thematic Mapper and SPOT multiband image data, using simulated image data of the Freiburg region (Federal Republic of Germany) [ESA-TT-975] p 57 N89-15442
- MAXWELL, TED A.**  
Large-scale, low-amplitude bedforms (chevrons) in the Selima sand sheet, Egypt p 23 A89-31755
- MAYMON, PETER W.**  
Optical system design alternatives for the Moderate-Resolution Imaging Spectrometer-Tilt (MODIS-T) for the Earth Observing System (EOS) p 63 A89-27753  
MODIS - Advanced facility instrument for studies of the earth as a system p 66 A89-31943
- MAZZEGA, P.**  
An experiment to invert Seasat altimetry for the Mediterranean and Black Sea mean surfaces p 36 A89-30900
- MCINTOSH, R. E.**  
Leaf backscattering measurements and modelling at 94 GHz p 8 N89-18713  
Radar backscatter characteristics of trees at 215 GHz p 14 N89-18917
- MCINTOSH, ROBERT E.**  
Normalized radar cross section of natural surfaces at millimeter wavelengths [AD-A202252] p 75 N89-19475
- MCKAY, A.**  
MODIS-HIRIS ground data systems commonality report [NASA-TM-100718] p 67 N89-16205  
MODIS information, data and control system (MIDACS) operations concepts [NASA-TM-100720] p 75 N89-19729
- MCNUTT, L.**  
Toward the automated use of remote sensing data in operational ice forecasting p 43 N89-18804
- MCRUER, W. H.**  
Auto and cross correlation analysis of environment, system and target parameters for iceberg detection using airborne radar p 45 N89-18874
- MCWETHY, L. G.**  
Applications of digital image processing to ongoing research in complex terrain meteorology [DE89-001749] p 57 N89-17375
- MEIJER, P. G.**  
Updating land-use information on topographic maps using satellite imagery: Combining the advantages of two accessible sources of geographic information p 60 N89-18897
- MEIJERINK, A. M.**  
Aerospace imagery and data for modelling erosion, sediment yield and crop yield prediction using GIS, applied to the Upper Komering catchment, Sumatra p 2 A89-20802
- MELILLO, JERRY M.**  
Remote sensing of canopy chemistry and nitrogen cycling in temperate forest ecosystems p 3 A89-23431
- MERLIVAT, L.**  
Satellite determination of the carbon dioxide exchange coefficient at the ocean-atmosphere interface - A first step p 31 A89-22598

- MERRILL, J. T.**  
Long-range transport of giant mineral aerosol particles  
p 17 A89-21931
- MESICK, HILLARY C.**  
Optical bathymetry for the U.S. Navy - A field measurement program p 64 A89-27993  
Analysis of airborne laser hydrography waveforms p 64 A89-27996
- MEULSTEE, C.**  
The use of LANDSAT imagery for water quality studies in the IJsselmeer area (Netherlands) [BCRS-87-18] p 52 N89-19732
- MEYER, D.**  
Requirements for an EOS-oriented workstation p 69 N89-18813
- MEYERS, TILDEN P.**  
A comparison of models for deriving dry deposition fluxes of O<sub>3</sub> and SO<sub>2</sub> to a forest canopy p 3 A89-20923
- MICHALEW, M. A.**  
Distribution of specular points on the ocean surface: Bilateral scattering p 38 N89-18721  
Microcomputer-based radiometer data acquisition and processing system for large-area mapping of soil moisture content in the top one meter layer p 11 N89-18774  
Experiments in Bulgaria for determination of soil moisture in the top one-meter layer using microwave radiometry and a priori information p 11 N89-18843
- MIHALY, S.**  
X-band scatterometry in agriculture p 9 N89-18715
- MILLOT, MICHEL**  
Digital Terrain Model computation using SPOT data p 53 A89-20807
- MILTON, E. J.**  
The directional reflectance of heather canopies: Towards a descriptive model p 13 N89-18878
- MINENO, H.**  
Step frequency radar experiments on the Antarctic Sea ice p 43 N89-18802
- MINENO, HITOSHI**  
Step frequency radar experiments on the Antarctic Sea ice p 34 N89-28365
- MINOWA, Y.**  
An atmospheric correction method for AVHRR infrared data using HIRS/2 data p 69 N89-18828
- MIRKAMILOV, D. M.**  
Laser airborne sensing field experiments using the 'Chaika' assembly p 35 A89-29728
- MIROSHNICHENKO, S. I.**  
Motion characteristics of sea waves p 32 A89-23590
- MIRZABEKOV, KH. S.**  
Annular and block-folded structures on space and aerial photographs p 25 N89-17915
- MISHEV, D. N.**  
Determination of relative crop areas from spectrometric data p 22 A89-22218
- MISRA, D. K.**  
Digital processing of a lineament grid with the aim of analyzing regional tectonic structures of the western Himalayas in India p 23 A89-30116
- MKRTCHJAN, F. A.**  
Microcomputer-based radiometer data acquisition and processing system for large-area mapping of soil moisture content in the top one meter layer p 11 N89-18774  
Experiments in Bulgaria for determination of soil moisture in the top one-meter layer using microwave radiometry and a priori information p 11 N89-18843
- MLADENOV, L.**  
Study on directional spectrum characteristics of marine radar images of ocean waves p 41 N89-18786
- MOHLER, ROBERT R. J.**  
Extension of a drought monitoring and vegetation classification methodology to the western Sahel p 4 A89-28127
- MOLETTE, PIERRE**  
JEOS - A low-cost approach to earth observation p 63 A89-26399
- MOLL, J. R.**  
Monitoring of suspended sediments in Jatiluhur Reservoir using satellite images p 50 N89-18740
- MONALDO, F.**  
Results of software simulation of a real-time SAR processor capable of providing ocean wave spectra p 38 N89-18720  
The influence of water vapor on the detection of ocean mesoscale fronts and eddies by the Geosat altimeter p 44 N89-18839
- MONALDO, FRANK M.**  
Comparison of Shuttle Imaging Radar-B ocean wave image spectra with linear model predictions based on aircraft measurements p 30 A89-22584
- MONTGOMERY, HARRY E.**  
MODIS - Advanced facility instrument for studies of the earth as a system p 66 A89-31943
- MOODY, JOHN C., SR.**  
Optical system design alternatives for the Moderate-Resolution Imaging Spectrometer-Tilt (MODIS-T) for the Earth Observing System (EOS) p 63 A89-27753
- MOORE, R. K.**  
Fine resolution signatures of coniferous and deciduous trees at C band p 6 A89-30266  
Analysis of ocean backscatter data obtained by the University of Kansas during TOWARD 84/85 p 42 N89-18787
- MORALEV, V. M.**  
Digital processing of a lineament grid with the aim of analyzing regional tectonic structures of the western Himalayas in India p 23 A89-30116
- MOREAU, S.**  
Comparative spectral analysis of HRV and TM sensors p 65 A89-29375
- MOREL, ANDRE**  
Simulated effects of barometric pressure and ozone content upon the estimate of marine phytoplankton from space p 33 A89-26443
- MOREL, M.**  
Mission aspects of a future European polar orbit earth observation facility p 74 N89-18952
- MORGAN, KEN M.**  
Application of Landsat MSS and TM data to geological resource exploration p 22 A89-26397
- MORI, HIROSHI**  
A basic study of the reduction of the exactness of mesh data map made by uniting n-squared meshes to one mesh p 54 A89-20811
- MORIN, J. C.**  
Towards a calibration of the CCRS airborne SARS p 70 N89-18854
- MORRIS-JONES, DONALD R.**  
Application of Landsat MSS and TM data to geological resource exploration p 22 A89-26397
- MORTON, J. A.**  
The use of coregistered LANDSAT MSS, TM and SIR-A imagery for lithological mapping p 28 N89-18936
- MOTOMURA, KAZUMA**  
A procedure for land area classification using Landsat TM digital imagery p 17 A89-24651
- MUELLER, IVAN I.**  
Reference coordinate systems: An update. Supplement 11 [NASA-CR-184764] p 19 N89-16207
- MUENCH, JERRY**  
Spaceborne recording systems for the Space Station era p 66 A89-31020
- MULHADJONO**  
Application of remote sensing for hydrocarbon exploration on Timor Island, Indonesia p 21 A89-20825
- MULLANE, T.**  
Toward the automated use of remote sensing data in operational ice forecasting p 43 N89-18804
- MULLEN, R.**  
Concepts for processing and analyzing of multiple SAR and Landsat images p 55 A89-27789
- MULLER, J.-P.**  
Real-time stereo matching SPOT using transputer arrays p 74 N89-18958
- MULLER, JAN-PETER**  
Digital image processing in remote sensing p 55 A89-29064  
Visualization of topographic data using video animation p 55 A89-29066
- MULYADI, K.**  
The creating of blue synthetic channel of MSS Landsat image p 52 A89-20794
- MUNASRI**  
Identification of surface-groundwater interaction zones in the Bogor volcanic fan p 48 A89-20777
- MUNDAY, T. J.**  
Preprocessing and analysis of airborne visible near and shortwave infrared data for the detection of alteration in weathered vegetated terrain p 12 N89-18862  
An evaluation of surface emittance and temperature data derived from Thermal Infrared Multispectral Scanner (TIMS) for lithological mapping in weathered vegetated terrain: N. Queensland, Australia p 27 N89-18934
- MURAI, S.**  
An interactive system for aerial photo orientation of digital stereo image pairs p 53 A89-20799
- MURAI, SHUNJI**  
The use of SPOT imagery in Medan agriculture area for monitoring features changes p 1 A89-20755  
Comparison of the orientation's accuracy for SPOT imagery p 53 A89-20798  
Accuracy of terrain measurement using SPOT HRV data p 53 A89-20801
- MURDJATI, NANIIEK SITI**  
Soil surface moisture estimation - A case study area on North Banten, West Java, Indonesia p 2 A89-20773
- MUROTA, HIDEKI**  
Receiving and processing system for meteorological satellite (NOAA) p 53 A89-20806
- MURPHY, R. E.**  
Remote sensing of land processes: Sponsored programs of study by the National Aeronautics and Space Administration p 19 N89-18833

## N

- NAKAJIMA, MINORU**  
Water quality estimation from Landsat data with spectral and sea truth data base system p 28 A89-20788
- NAKANO, RYOSHI**  
New technology for displaying of NOAA AVHRR thermal band image p 29 A89-20810
- NAKAYAMA, MASAYA**  
Receiving and processing system for meteorological satellite (NOAA) p 53 A89-20806
- NANCE, C. E.**  
The extinction properties of forest components p 14 N89-18918
- NAQVI, SYED GUL MOHAMMED**  
A procedure for land area classification using Landsat TM digital imagery p 17 A89-24651
- NARAYAN, L. R. A.**  
Wasteland identification in India using satellite remote sensing p 18 A89-30263
- NARAYANAN, R. M.**  
Radar backscatter characteristics of trees at 215 GHz p 14 N89-18917
- NEDELTCHEV, N. M.**  
Microcomputer-based radiometer data acquisition and processing system for large-area mapping of soil moisture content in the top one meter layer p 11 N89-18774  
Experiments in Bulgaria for determination of soil moisture in the top one-meter layer using microwave radiometry and a priori information p 11 N89-18843
- NEECK, STEVEN P.**  
Optical system design alternatives for the Moderate-Resolution Imaging Spectrometer-Tilt (MODIS-T) for the Earth Observing System (EOS) p 63 A89-27753
- NELEPO, BORIS A.**  
Optical methods of satellite hydrophysics. Investigation of the environment from manned orbital stations p 32 A89-26181
- NEWCOMER, JEFFREY A.**  
Land image data processing requirements for the EOS era p 56 A89-31949
- NGUYEN, P. T.**  
Multiple source data processing in remote sensing p 56 A89-29073
- NICHOL, J. E.**  
Monitoring of agro-forestry production systems in the Sudano-Sahelian zone of West Africa p 11 N89-18825
- NIKOLAOS, SILLEOS**  
Visual and digital classification of Landsat TM data for soil, physiography and land use mapping in Axios alluvial plain, Thessaloniki, Greece p 5 A89-28130
- NISHIO, F.**  
Step frequency radar experiments on the Antarctic Sea ice p 43 N89-18802
- NISHIO, FUMIHIKO**  
Step frequency radar experiments on the Antarctic Sea ice p 34 A89-28365
- NOVAK, L. M.**  
Bayes classification of terrain cover using normalized polarimetric data p 54 A89-22649
- NOVO, E. M. M.**  
The relationship between suspended sediment concentration and remotely sensed spectral radiance - A review p 48 A89-24649
- NUGROHO, SRI UTAMINGSIH**  
The extraction of sea fishery potential area from Airborne Ocean Color Radiometer data p 28 A89-20786
- NUR, MAWARDI**  
Principle component transformation analysis for tentative land use interpretation of Landsat MSS of Bogor region, Indonesia p 52 A89-20767
- NYKJAER, C.**  
The structure and variability of a filament in the northwest African upwelling area as observed from AVHRR and CXCS images p 46 N89-18939



## O

- O'NEILL, NORMAN**  
Analysis of atmospheric effects in SPOT HRV images  
p 65 A89-29372
- OCHIAI, HIROAKI**  
Effectiveness of satellite remote sensing on monitoring of marine environment  
[IAF PAPER 88-153] p 32 A89-24875
- CONNOR, L. M.**  
Effects of commercialisation on international remote sensing activities p 76 N89-18752
- OETTL, H.**  
German spaceborne remote sensing activities  
p 67 N89-16887
- OJEDELE, BABAFEMI**  
Airborne MSS for land cover classification  
p 5 A89-28131
- OKAMOTO, HARUTO**  
Water quality estimation from Landsat data with spectral and sea truth data base system p 28 A89-20788
- OKAMOTO, K.**  
Step frequency radar experiments on the Antarctic Sea ice p 43 N89-18802
- OKAMOTO, KEN'ICHI**  
Step frequency radar experiments on the Antarctic Sea ice p 34 A89-28365
- OKUMURA, H.**  
A method for the clustering of remotely sensed multispectral images by using statistical test for spatial uniformity p 61 N89-18898
- OLDFIELD, R. B.**  
Estimation of the area of Lake Kariba, Zimbabwe, using LANDSAT MSS imagery p 51 N89-18775  
The use of coregistered LANDSAT MSS, TM and SIR-A imagery for lithological mapping p 28 N89-18936
- OLIVER, C. J.**  
A comparison of clutter texture properties in optical and SAR images p 8 N89-18708
- OLIVER, M.**  
Visual and computer classifications of remotely-sensed images - A case study of grasslands in Cambridgeshire p 7 A89-30269
- OLSON, WILLIAM S.**  
Physical retrieval of rainfall rates over the ocean by multispectral microwave radiometry - Application to tropical cyclones p 37 A89-32434
- ONEILL, M. A.**  
Real-time stereo matching SPOT using transputer arrays p 74 N89-18958
- ONEILL, P. E.**  
Observed effects of soil organic matter content on the microwave intensity of soils p 12 N89-18845
- ONORATI, G.**  
A quantitative geomorphology study of main carbonate massifs of central and southern Apennines (Italy) based on a digital elevations archive p 25 N89-18791
- ONSTOTT, R. G.**  
Intercomparison of synthetic- and real-aperture radar observations of Arctic sea ice during winter MIZEX '87 p 40 N89-18744  
Radar backscatter of sea ice during winter p 46 N89-18943
- OOMS, M.**  
Optical properties of sea water bodies: Measurements with an underwater radiometer and a high-resolution spectroradiometer p 39 N89-18734
- ORMSBY, J.**  
MODIS-HIRIS ground data systems commonality report [NASA-TM-100718] p 67 N89-16205  
MODIS information, data and control system (MIDACS) operations concepts [NASA-TM-100720] p 75 N89-19729
- OSHIMA, TAICHI**  
Water quality estimation from Landsat data with spectral and sea truth data base system p 28 A89-20788
- OSMAN, S.**  
Fine resolution signatures of coniferous and deciduous trees at C band p 6 A89-30266
- OSTROW, HARVEY**  
MODIS - Advanced facility instrument for studies of the earth as a system p 66 A89-31943
- OTTERMAN, J.**  
Dependence of snow melting and surface-atmosphere interactions on the forest structure p 3 A89-21740
- OTTO, G. P.**  
Real-time stereo matching SPOT using transputer arrays p 74 N89-18958
- OUCHI, K.**  
Speckle correlation in SAR images of dynamic discrete scatterers p 37 N89-18707  
Computer simulation of multipath sea echo near grazing incidence p 38 N89-18722

## OUVERASIMONI, PAULO

- Knowledge related aspects of lineation and lineament extraction [INPE-4709-PRE/1391] p 24 N89-15446  
Using different sources of information in automated linear feature extraction from remote sensing data [INPE-4708-PRE/1390] p 24 N89-15447

## P

- PALANIVELU, R.**  
Relationship of spectral data and grain yield variation in rice (*Oryza sativa* L.) ADT 31 p 2 A89-20762
- PALME, U. W.**  
Microwave X-band radiometric characterization of Brazilian soils by measurement of the complex permittivity p 11 N89-18773
- PALOSCIA, S.**  
Comparison between microwave emissivity and backscattering coefficient of agricultural fields p 12 N89-18844
- PAMPALONI, P.**  
Comparison between microwave emissivity and backscattering coefficient of agricultural fields p 12 N89-18844
- PARAMANANDA, V.**  
Real-time stereo matching SPOT using transputer arrays p 74 N89-18958
- PARSELL, R. J.**  
Visual and computer classifications of remotely-sensed images - A case study of grasslands in Cambridgeshire p 7 A89-30269
- PARSONS, CHESTER L.**  
Off-nadir radar altimetry p 66 A89-31947
- PATYCHENKO, GALINA A.**  
Aerial and space remote-sensing techniques for geographical investigations p 62 A89-26178
- PAYNE, PAUL R.**  
Spectral transmissometer and radiometer - Design and initial results p 64 A89-27991
- PAZAN, STEPHEN E.**  
Geosat crossover analysis in the tropical Pacific. II - Verification analysis of altimetric sea level maps with expendable bathythermograph and island sea level data p 32 A89-26438
- PEACOCK, THOMAS G.**  
Spectral transmissometer and radiometer - Design and initial results p 64 A89-27991
- PEARCE, A. F.**  
Comparison of NOAA/AVHRR-2 sea surface temperatures with surface measurements in coastal waters p 36 A89-30259
- PECK, WAYNE**  
Spectral transmissometer and radiometer - Design and initial results p 64 A89-27991
- PECKHAM, G. E.**  
An optimum calibration procedure for radiometers p 65 A89-30270
- PECKINPAUGH, SARAH H.**  
Edge detection applied to satellite imagery of the oceans p 33 A89-26844
- PEDRON, C.**  
Integration of SPOT data in an urban data bank - Locating work sites p 18 A89-31891
- PEEBLES, R.**  
Reconnaissance groundwater appraisal of Bohol Island, Philippines, by satellite data analysis p 48 A89-20772
- PEIVE, A. A.**  
The solid oceanic crust (The Lithos project) p 36 A89-32108
- PERFETTI, R.**  
Tracking algorithms in radar altimetry p 72 N89-18911
- PEROVICH, D. K.**  
Physical properties of snow and ice in the winter marginal ice zone of Fram Strait p 46 N89-18944
- PERRAM, L. J.**  
A new view of the mid-ocean ridge from the behaviour of ridge-axis discontinuities p 31 A89-23433
- PERRAS, S.**  
Analysis and interpretation of SPOT images of urban and agricultural/forest sections of the Sherbrooke region p 5 A89-29373
- PERUMAL, N. V. A. S.**  
Usefulness of remote sensing in uranium exploration programme in parts of Karnataka state, India p 21 A89-20828
- PETERS, H. C.**  
Sea bottom topography with X-band SLAR: Evaluation of existing models p 38 N89-18718
- PETERSON, DAVID L.**  
Remote sensing of canopy chemistry and nitrogen cycling in temperate forest ecosystems p 3 A89-23431
- PETROU, M.**  
Progress in automatic analysis of multi-temporal remotely-sensed data p 61 N89-18956
- PETTIGREW, R. G.**  
A high fidelity, high throughput system for geocoding SAR imagery p 60 N89-18849
- PETZOLD, DONALD E.**  
Tersail - A numerical model for combined analysis of vegetation canopy bidirectional reflectance and thermal emissions p 6 A89-29415
- PHILLIPS, DWAYNE**  
Using a top-down and bottom-up strategy to analyze high resolution aerial photographs of urban areas p 18 A89-27630
- PIATKIN, V. P.**  
A tomographic approach to lineament identification on aerial and space images p 22 A89-22223
- PICARDI, G.**  
Tracking algorithms in radar altimetry p 72 N89-18911
- PIERDICCIA, N.**  
Crops radar responses analysis based on AGRISAR '86 data p 15 N89-18947
- PINKER, R. T.**  
Dispersion parameters over forested terrain p 3 A89-22728
- PITTS, D. E.**  
Comparison of measured C-band scattering coefficients with model predictions as a function of leaf area index and Biomass p 8 N89-18712
- PIYAPONGSE, PONGPIT**  
The applications of Landsat imagery to soil erosion study in Northern Thailand p 3 A89-20826
- PLIUSHCHEV, V. A.**  
Procedures for the determination of geophysical parameters from spaceborne microwave polarimeter measurements p 30 A89-22224
- PODAIRE, A.**  
Complementarity of middle-infrared with visible and near-infrared reflectance for monitoring wheat canopies p 5 A89-29410
- POLIAKOV, S. V.**  
Variations of the infrared emission of snow and ice cover p 49 A89-30121
- POLLE, VICTOR F. L.**  
SPOT image interpretation for information on human settlement growth p 17 A89-20824
- PONTUAL, A.**  
Mapping in the Oman ophiolite using enhanced Landsat Thematic Mapper images p 23 A89-29301  
Remote sensing of evaporite mineral zonation in salt flats (salars) p 23 A89-30271  
Applications of LANDSAT Thematic Mapper imagery to the study of subtle variations in lithology p 27 N89-18863  
Investigations of the Cerro Colorado pluton, northern Chile, using enhanced LANDSAT Thematic Mapper images p 27 N89-18930
- POSCOLIERI, M.**  
A quantitative geomorphology study of main carbonate massifs of central and southern Apennines (Italy) based on a digital elevations archive p 25 N89-18791
- POUWELS, H.**  
Sea bottom topography with X-band SLAR: Evaluation of existing models p 38 N89-18718
- POWELL, R. J.**  
An advanced terrain tracking altimeter p 45 N89-18910
- PRATA, A. J.**  
Comparison of NOAA/AVHRR-2 sea surface temperatures with surface measurements in coastal waters p 36 A89-30259
- PRESS, N. P.**  
Microcomputers and mass storage devices for image processing p 65 A89-29070
- PRICE, JOHN C.**  
Scene locations and overpass dates for Landsat and SPOT sensors p 64 A89-28039
- PRIES, RICHARD A.**  
Interactive image feature compilation for geographic information systems p 18 A89-27785
- PRIKHOD'KO, I. I.**  
Radar imaging of the surfaces of Venus and the earth using SAR data p 54 A89-23645
- PROUD, R. J.**  
The algorithm development facility: Its role in the development and operation of a satellite data centre p 68 N89-18755
- PURSEYED, B.**  
A synthetic aperture altimeter p 73 N89-18913  
A study of advanced radar altimeter techniques [ESA-CR(P)-2699] p 75 N89-19483
- PURWADHI, SRI HARDIYANTI**  
Principle component transformation analysis for tentative land use interpretation of Landsat MSS of Bogor region, Indonesia p 52 A89-20767

## PUSHCHAROVSKII, I. U. M.

- The solid oceanic crust (The Lithos project)  
p 36 A89-32108

## Q

## QUEGAN, S.

- The visibility of linear features in SAR images  
p 59 N89-18763  
Change detection in AGRISAR images  
p 15 N89-18949

## R

## RAJ, K. GANESHA

- Mapping of construction material sites around Bangalore  
City using Landsat Thematic Mapper data  
p 52 A89-20782

## RAJA, M.

- Relationship of spectral data and grain yield variation  
in rice (*Oryza sativa* L.) ADT 31  
p 2 A89-20762

## RAMACHANDRAN, R.

- Identification of geological features from their surface  
textural properties using OPS measurements  
p 21 A89-20820  
Feature extraction considerations in utilising the optical  
power spectra for terrain classification  
p 54 A89-20821

## RAMACHANDRAN, T. V.

- Integrated study of Landsat, aeromagnetic and Bouguer  
gravity anomaly data for geological appraisal - A case study  
from Tamil Nadu, India  
p 21 A89-20823

## RAMAPRIYAN, H.

- MODIS-HIRIS ground data systems commonality  
report  
[NASA-TM-100718]  
p 67 N89-16205

## RAMSAY, B.

- Real-time processing of digital image data in support  
of the Canadian sea ice analysis and prediction program  
p 43 N89-18803

## RAMSEY, ELIJAH W., III

- The derivation and verification of surface reflectances  
using airborne MSS data and a radiative transfer model  
[DE89-004881]  
p 67 N89-17931  
A comparison of original aircraft MSS and generated  
surface water reflectance images as predictors of lake  
water quality indicators  
[DE89-004882]  
p 50 N89-17932

## RANEY, R. K.

- Estimation of the SAR system transfer through processor  
defocus  
p 37 N89-18706

## RANEY, R. KEITH

- A simulation for spaceborne SAR imagery of a  
distributed, moving scene  
p 33 A89-26846

## RANGSIKANBHUM, THANOMSRI

- The feasibility study of oil palm area estimation in the  
southern part of Thailand using Landsat data  
p 2 A89-20760

## RANSON, K. J.

- Characterizing forest ecosystem dynamics through  
modelling and remote sensing observations  
p 10 N89-18728

## RAO, D. P.

- Wasteland identification in India using satellite remote  
sensing  
p 18 A89-30263

## RAO, KIRON K.

- Identification of geological features from their surface  
textural properties using OPS measurements  
p 21 A89-20820  
Feature extraction considerations in utilising the optical  
power spectra for terrain classification  
p 54 A89-20821

## RAPLEY, C. G.

- Satellite radar altimetry over arid regions  
p 69 N89-18842  
An advanced terrain tracking altimeter  
p 45 N89-18910  
A new approach to topographic altimetry  
p 73 N89-18914

## RAST, M.

- A possibility for selecting spectral bands of future land  
application sensors at the example of an imaging  
spectrometer  
p 60 N89-18896  
Mission aspects of a future European polar orbit earth  
observation facility  
p 74 N89-18952

## RAVINDRAN, K. V.

- Correlation of Landsat TM and aeromagnetic data along  
the Eastern Margin of the Cuddapah Basin, South India  
p 21 A89-20817

## REBILLARD, PH.

- Effects of slopes and relief two-dimensional spatial  
frequencies on spaceborne SAR imagery  
p 59 N89-18777

## REBILLARD, PHILIPPE

- Digital Terrain Model computation using SPOT data  
p 53 A89-20807

## REDLINE, A. D.

- Geological remote sensing of Palaeogene rocks in the  
Wind River Basin, Wyoming, USA  
p 28 N89-18935

## REED, MARK

- Evaluation of satellite-tracked surface drifting buoys for  
simulating the movement of spilled oil in the marine  
environment. Volume 1: Executive summary  
[PB88-226048]  
p 37 N89-17357  
Evaluation of satellite-tracked surface drifting buoys for  
simulating the movement of spilled oil in the marine  
environment, volume 2  
[PB88-226055]  
p 37 N89-17358

## REES, W. G.

- Technological limitations to satellite glaciology  
p 36 A89-30257

## REIJNEVELD, ARJEN

- SPOT for mapping of actual land information  
p 54 A89-20816

## REISTAD, MAGNAR

- Hindcasts and data assimilation studies with the WAM  
model during the Seasat period  
p 32 A89-26442

## RESHETOV, YE. A.

- Some results of use of space survey materials in  
cartographic work  
p 58 N89-17922

## REUTOV, E. A.

- Microcomputer-based radiometer data acquisition and  
processing system for large-area mapping of soil moisture  
content in the top one meter layer  
p 11 N89-18774  
Experiments in Bulgaria for determination of soil moisture  
in the top one-meter layer using microwave radiometry  
and a priori information  
p 11 N89-18843

## REYNOLDS, NIKKI E.

- Bidirectional canopy reflectance and its relationship to  
vegetation characteristics  
p 6 A89-30264

## RIABOVA, L. D.

- Variations of the infrared emission of snow and ice  
cover  
p 49 A89-30121

## RICHARDS, B. E.

- Impact of phase and amplitude errors on the ERS-1  
active microwave instrumentation performance  
p 70 N89-18853

## RICHARDS, J. A.

- Association of radar backscattering with biophysical  
characteristics of Australian forests  
p 10 N89-18731

## RICHARDS, SAM

- Visualization of topographic data using video  
animation  
p 55 A89-29066

## RICOTTILLI, M.

- Crops radar responses analysis based on AGRISAR '86  
data  
p 15 N89-18947

## RIDLEY, J.

- An advanced terrain tracking altimeter  
p 45 N89-18910

## RIEG, A.

- Extraction of agricultural plant parameters from  
multitemporal Thematic Mapper (TM) and X-SAR data  
p 15 N89-18948

## RIGGAN, PHILIP J.

- Trace gas emissions from chaparral and boreal forest  
fires  
p 7 A89-32432

## RIKIMARU, ATSUSHI

- Water quality estimation from Landsat data with spectral  
and sea truth data base system  
p 28 A89-20788

## RINDERLE, U.

- Correlation of radar reflectivity and chlorophyll  
fluorescence of forest trees  
p 9 N89-18727

## RINGROSE, P. S.

- Enhancement of glacial fractures by analysis of Thematic  
Mapper data: Glen Roy, Scotland  
p 26 N89-18859

## ROBB, M.

- Satellite imagery for semi-automatic map revision  
p 61 N89-18957

## ROBERTSON, Y. C.

- Artefacts in AIS-I imagery  
p 69 N89-18826

## ROBINSON, A. R.

- Frontal signals east of Iceland from the Geosat  
altimeter  
p 33 A89-26643

## ROCHON, GUY

- First results of topographical mapping using SPOT  
images of Malaysia  
p 52 A89-20764

## RODRIGUES, VALTER

- Knowledge related aspects of lineation and lineament  
extraction  
[INPE-4709-PRE/1391]  
p 24 N89-15446

- Using different sources of information in automated  
linear feature extraction from remote sensing data  
[INPE-4708-PRE/1390]  
p 24 N89-15447

## ROETERS, P. B.

- The effect of soil moisture on reflectance characteristics  
of salt crusts  
p 16 N89-18966

## ROGERS, DAVID C.

- Comparisons of satellite data surface-based remote  
sensing measurements in Utah winter orographic storms  
p 75 N89-19079

## ROLLIN, E. M.

- The directional reflectance of heather canopies:  
Towards a descriptive model  
p 13 N89-18878

## ROMBE, Y. L.

- The application of remote sensing for forest inventory  
p 2 A89-20809

## ROSWINTIARTI, O.

- The navigation method for NOAA/AVHRR image  
p 61 A89-20795

## ROTHERY, D. A.

- Mapping in the Oman ophiolite using enhanced Landsat  
Thematic Mapper images  
p 23 A89-29301  
Remote sensing of evaporite mineral zonation in salt  
flats (salars)  
p 23 A89-30271

## ROTHROCK, D. A.

- Estimating sea ice concentration from satellite passive  
microwave data and a physical model  
p 42 N89-18797

- Measuring lead area changes in sea ice imagery  
p 44 N89-18871

## ROTTIER, P.

- SAR imaging of ocean waves in the marginal ice zone  
p 40 N89-18747

## ROYER, ALAIN

- Analysis of atmospheric effects in SPOT HRV images  
p 65 A89-29372

## RUFF, C. S.

- Atmospheric profiling of water vapour with a 20.5-23.5  
GHz autocorrelation radiometer  
p 72 N89-18908

## RUNDQUIST, DONALD C.

- Band-moment analysis of imaging-spectrometer data  
p 65 A89-29436

## RUSSELL, G.

- Problems in the estimation of barley yields by remote  
sensing  
p 13 N89-18881

## RUZEK, M. J.

- Remote sensing of land processes: Sponsored  
programs of study by the National Aeronautics and Space  
Administration  
p 19 N89-18833

## RYE, A. J.

- Automated linear feature detection and its application  
to curve location in synthetic aperture radar imagery  
p 59 N89-18764

## S

## SAID, MD AZLIN MD

- Improvements in ground water recharge estimation using  
satellite remote sensing  
p 50 N89-18768

## SAINT CLAIR, J. M.

- Simulation of radiometric ocean images recorded from  
high-altitude platforms  
p 33 A89-27980

## SAKATA, TOSHIBUMI

- Accuracy of land-cover/use classification  
p 52 A89-20765

- MOS-1 data processing in Tokai Space Center  
p 52 A89-20790

- Spatial information processings of TM data  
p 52 A89-20791

## SALOMONSON, V.

- MODIS-HIRIS ground data systems commonality  
report  
[NASA-TM-100718]  
p 67 N89-16205

- MODIS information, data and control system (MIDACS)  
operations concepts  
[NASA-TM-100720]  
p 75 N89-19729

## SALOMONSON, VINCENT V.

- MODIS - Advanced facility instrument for studies of the  
earth as a system  
p 66 A89-31943

## SARAF, A. K.

- Geological applications of thermal infrared  
characteristics of vegetation  
p 27 N89-18932

## SARASWAT, A. C.

- Usefulness of remote sensing in uranium exploration  
programme in parts of Karnataka state, India  
p 21 A89-20828

## SARKAR, A.

- Specular scattering with effective reflection coefficient  
p 39 N89-18723

## SARWOASIH, SRI

- Flooded and inundation dangerous area prediction and  
its visualisation - A case study on the Pemali-Comal River  
Basin, Central Java, Indonesia  
p 48 A89-20774

- Application of three dimensional image system  
p 53 A89-20797

## SASSEN, KENNETH

- Comparisons of satellite data surface-based remote  
sensing measurements in Utah winter orographic storms  
p 75 N89-19079

- SASUTJI, ADI**  
Suspended solid classification of the Jakarta Bay  
p 28 A89-20785
- SATO, KAZUHIRO**  
Spectral reflectance properties of a leaf of some mangrove species in Okinawa  
p 1 A89-20753
- SAUBER, JEANNE MARIE**  
Geodetic measurement of deformation in California [NASA-CR-184604]  
p 19 N89-15476
- SAVORSKII, V. P.**  
A method for processing and results of microwave radiometer studies of the earth from the Intercosmos 20 and 21 satellites  
p 36 A89-30122
- SAWYER, F. G.**  
Advanced SAR concepts  
p 73 N89-18926
- SAXENA, V. N.**  
UV laser fluorosensor for remote sensing  
p 35 A89-29763
- SCHEAFER, H.**  
An interactive system for aerial photo orientation of digital stereo image pairs  
p 53 A89-20799
- SCHERTZER, D.**  
Extreme variability, scaling and fractals in remote sensing - Analysis and simulation  
p 56 A89-29074
- SCHIAVON, G.**  
Comparison between microwave emissivity and backscattering coefficient of agricultural fields  
p 12 N89-18844
- SCHLITTENHARDT, P.**  
The structure and variability of a filament in the northwest African upwelling area as observed from AVHRR and CXCS images  
p 46 N89-18939
- SCHMUGGE, THOMAS**  
Microwave remote sensing of soil moisture  
p 4 A89-27944
- SCHMUGGE, THOMAS J.**  
Passive microwave remote sensing system for soil moisture - Some supporting research  
p 49 A89-31948
- SCHNEIDER, K.**  
Data processing for the determination of pigments and suspended solids from Thematic Mapper data  
p 50 N89-18736
- SCHOWENGERDT, ROBERT A.**  
Interactive image feature compilation for geographic information systems  
p 18 A89-27785
- SCHREIER, G.**  
Investigations of SAR backscatter for different test areas using two geocoded Seasat SAR scenes  
p 58 N89-18761
- SCHUCHMANN, R. A.**  
Intercomparison of synthetic- and real-aperture radar observations of Arctic sea ice during winter MIZEX '87  
p 40 N89-18744
- SCOON, A.**  
Major crustal lineaments on Seasat SAR and their off-shore extensions in the UK  
p 26 N89-18861
- SEBACHER, DANIEL I.**  
Trace gas emissions from chaparral and boreal forest fires  
p 7 A89-32432
- SEED, A.**  
Estimating the extent of irrigated cropland in a large catchment using LANDSAT MSS data  
p 14 N89-18902
- SEGALL, P.**  
Displacement calculations from geodetic data and the testing of geophysical deformation models  
p 19 A89-22639
- SEGUIN, BERNARD**  
Use of surface temperature in agrometeorology  
p 4 A89-27942
- SEMTNER, ALBERT J., JR.**  
A simulation of the global ocean circulation with resolved eddies  
p 30 A89-22593
- SENECHAL, J. M.**  
Statistical evaluation of the intensity distribution of sea surface radar images  
p 38 N89-18717
- SERDIUKOV, VIKTOR M.**  
Aerial and space remote-sensing techniques for geographical investigations  
p 62 A89-26178
- SERPICO, S. B.**  
Information fusion by a knowledge-based system for SAR image interpretation  
p 60 N89-18831
- SETOJIMA, MASAHIRO**  
Land use suitability classification using remote sensing data and geographic information for volcanic regions  
p 16 A89-20766
- SETTLE, J.**  
Alternative approaches to the classification of upland semi-natural vegetation  
p 16 N89-18961
- SEU, R.**  
Tracking algorithms in radar altimetry  
p 72 N89-18911
- SHA, XINGWEI**  
Quick reporting state of fishery and sea on the East China Sea and the Yellow Sea with NOAA  
p 39 N89-18741
- A preliminary study on nearshore water in China with NOAA satellite images  
p 40 N89-18743
- SHAPIRO, BRUCE**  
The Geosat orbit adjust  
p 19 A89-22316
- SHARTS, B.**  
MODIS information, data and control system (MIDACS) operations concepts [NASA-TM-100720]  
p 75 N89-19729
- SHAW, V. L.**  
Auto and cross correlation analysis of environment, system and target parameters for iceberg detection using airborne radar  
p 45 N89-18874
- SHEEN, D. R.**  
Radiometric calibration of airborne SAR data  
p 70 N89-18855
- SHEN, G. X.**  
The leaf-shape effect on electromagnetic scattering from vegetated media  
p 12 N89-18846
- SHEN, JIANHUA**  
The preliminary study on correlation between satellite information and bottom trawling ground in the East China Sea and the Yellow Sea  
p 29 A89-20805
- SHEN, MINGMING**  
Application of airborne scanners in remote sensing of sea  
p 29 A89-20789
- SHEREMET, O. G.**  
Digital processing of a lineament grid with the aim of analyzing regional tectonic structures of the western Himalayas in India  
p 23 A89-30116
- SHI, Z.**  
Correlation of radar reflectivity and chlorophyll fluorescence of forest trees  
p 9 N89-18727
- SHIBASAKI, RYOSUKE**  
Accuracy of terrain measurement using SPOT HRV data  
p 53 A89-20801
- SHIBAYAMA, M.**  
Water turbidity and perpendicular vegetation indices for paddy rice flood damage analyses  
p 6 A89-29412
- SHIMODA, HARUHISA**  
Accuracy of land-cover/use classification  
p 52 A89-20765
- MOS-1 data processing in Tokai Space Center  
p 52 A89-20790
- Spatial information processings of TM data  
p 52 A89-20791
- SHIN, R. T.**  
Bayes classification of terrain cover using normalized polarimetric data  
p 54 A89-22649
- SHU, NING**  
The studies for the computer classification and the investigation of grasslands in Tibet using Space-Lab color infrared image  
p 1 A89-20754
- SHU, SHOURONG**  
Quantitative remote detection of suspended sediment content and chlorophyll concentration of water in different depths  
p 50 N89-18733
- SHUCHMAN, R. A.**  
SAR imaging of ocean waves in the marginal ice zone  
p 40 N89-18747
- Geophysical information on the winter marginal ice zone obtained from SAR  
p 46 N89-18942
- Radar backscatter of sea ice during winter  
p 46 N89-18943
- SHUGAN, I. V.**  
Surface wave interaction - Theory and capability of oceanic remote sensing  
p 35 A89-29732
- SHUTKO, A. M.**  
Microcomputer-based radiometer data acquisition and processing system for large-area mapping of soil moisture content in the top one meter layer  
p 11 N89-18774
- Experiments in Bulgaria for determination of soil moisture in the top one-meter layer using microwave radiometry and a priori information  
p 11 N89-18843
- SIDARTO**  
The geology of the area surrounding Lake Kerinci, Indonesia as interpreted through SIR-B imageries  
p 20 A89-20781
- SIMARD, REJEAN**  
First results of topographical mapping using SPOT images of Malaysia  
p 52 A89-20764
- SIMBOLON, B.**  
Airborne gravity as a supporting tool for hydrocarbon exploration in Indonesia  
p 21 A89-20829
- SINEL'NIKOV, DMITRII A.**  
Aerial and space remote-sensing techniques for geographical investigations  
p 62 A89-26178
- SINGH, A. N.**  
Assessing extent of damage caused by flooding and drought in dominantly rice cropland area using Landsat data  
p 2 A89-20814
- Delineation of salt-affected soils through digital analysis of Landsat MSS data  
p 6 A89-30262
- SIRIPONG, ABSORNUSUDA**  
Circulation in the East Asian seas from satellite and ship data  
p 29 A89-20803
- SKIDMORE, A. K.**  
Unsupervised training area selection in forests using a nonparametric distance measure and spatial information  
p 6 A89-30265
- SKINGLEY, J.**  
Automated linear feature detection and its application to curve location in synthetic aperture radar imagery  
p 59 N89-18764
- SKOELV, A.**  
Simulation of SAR imaging of ship wakes  
p 41 N89-18765
- SKOU, N.**  
The Technical University of Denmark (TUD) C-band SAR  
p 74 N89-18928
- SLOBODIANIN, V. P.**  
Effects of round trip laser emission propagation through a turbulent surface for laser airborne oceanic sensing  
p 35 A89-29729
- SMIRNOV, M. T.**  
A method for processing and results of microwave radiometer studies of the earth from the Intercosmos 20 and 21 satellites  
p 36 A89-30122
- SMITH, D. J.**  
A SAR data quality assessment scheme for the ERS-1 mission  
p 72 N89-18893
- SMITH, J. A.**  
Characterizing forest ecosystem dynamics through modelling and remote sensing observations  
p 10 N89-18728
- SMITH, J. M.**  
LANDSAT TM study of afforestation in northern Scotland and its impact on breeding bird populations  
p 10 N89-18732
- SMITH, JAMES A.**  
Goniometric observations of light scattered from soils and leaves  
p 4 A89-24873
- SMITH, R. C.**  
Moorable spectroradiometers in the BIOWATT experiment  
p 64 A89-27990
- SMITS, K.**  
Airborne nonacoustic bathymetric survey flight test results  
p 51 N89-18937
- SOEMARMAN, HARIYATNO**  
The use of image enhancement technique for peat land mapping using Landsat mass data in Indonesia  
p 52 A89-20775
- SOERMANMAN, HARIYATNO**  
Soil surface moisture estimation - A case study area on North Banten, West Java, Indonesia  
p 2 A89-20773
- SOLBERG, R.**  
Satellite imagery for semi-automatic map revision  
p 61 N89-18957
- SOLIMINI, D.**  
Comparison between microwave emissivity and backscattering coefficient of agricultural fields  
p 12 N89-18844
- SOLOVITSKIY, V. N.**  
Principal problems in upgrading quality and efficiency of geological survey work  
p 24 N89-17910
- SPASOV, A. Y.**  
Microcomputer-based radiometer data acquisition and processing system for large-area mapping of soil moisture content in the top one meter layer  
p 11 N89-18774
- Experiments in Bulgaria for determination of soil moisture in the top one-meter layer using microwave radiometry and a priori information  
p 11 N89-18843
- SPAULDING, MALCOLM**  
Evaluation of satellite-tracked surface drifting buoys for simulating the movement of spilled oil in the marine environment. Volume 1: Executive summary [PB88-226048]  
p 37 N89-17357
- Evaluation of satellite-tracked surface drifting buoys for simulating the movement of spilled oil in the marine environment, volume 2 [PB88-226055]  
p 37 N89-17358
- SPECK, ROBERT C.**  
Applications of image scanning and processing in rock shear surface study  
p 20 A89-20779
- SPECTER, C.**  
Technology transfer for development of coastal zone resources: Caribbean experts examine critical issues  
p 40 N89-18749
- SQUIRE, V. A.**  
Technological limitations to satellite glaciology  
p 36 A89-30257
- SRINATH, K.**  
Identification of geological features from their surface textural properties using OPS measurements  
p 21 A89-20820
- Feature extraction considerations in utilising the optical power spectra for terrain classification  
p 54 A89-20821
- SROKOSZ, M. A.**  
A study of the effect of rain on Seasat radar altimeter data  
p 44 N89-18840

## STAENZ, K.

- STAENZ, K.**  
Dependence of snow melting and surface-atmosphere interactions on the forest structure p 3 A89-21740
- STEWART, ROBERT G.**  
Spectral transmissometer and radiometer - Design and initial results p 64 A89-27991
- STEWART, ROBERT H.**  
Seasat - Results of the mission p 29 A89-22000
- STIBIG, HANS-JUERGEN**  
Investigation of information content of Thematic Mapper and SPOT multiband image data, using simulated image data of the Freiburg region (Federal Republic of Germany) [ESA-TT-975] p 57 N89-15442
- STRIRAT, R. G. L.**  
The Geospace philosophy: A new practical approach in remote sensing and planning for local authorities p 76 N89-18750
- STOCKS, BRIAN J.**  
Trace gas emissions from chaparral and boreal forest fires p 7 A89-32432
- STOLP, J.**  
Study of the use of radar X-band data of bare soil in a radar scattering model [BCRS-88-04] p 16 N89-19735
- STOVE, G. C.**  
The Geospace philosophy: A new practical approach in remote sensing and planning for local authorities p 76 N89-18750
- STRELTSOV, V. N.**  
Effects of round trip laser emission propagation through a turbulent surface for laser airborne oceanic sensing p 35 A89-29729
- STRONG, LAURENCE L.**  
Accuracy assessment, using stratified plurality sampling, of portions of a LANDSAT classification of the Arctic National Wildlife Refuge Coastal Plain [NASA-TM-101042] p 8 N89-17339
- STUCKY, R. K.**  
Geological remote sensing of Palaeogene rocks in the Wind River Basin, Wyoming, USA p 28 N89-18935
- STUNT, R.**  
The pre-launch performance verification of the ERS-1 active microwave instrumentation p 71 N89-18886
- STURM, B.**  
Image-based atmospheric correction of multitemporal Thematic Mapping data for agricultural land cover classification p 14 N89-18895
- STURTEVANT, BRADFORD**  
Erosional furrows formed during the lateral blast at Mount St. Helens, May 18, 1980 p 22 A89-22632
- SUARDHY, ATK**  
Application of remote sensing for hydrocarbon exploration on Timor Island, Indonesia p 21 A89-20825
- SUBADIYASA, I. L.**  
Digital image analysis of Landsat MSS data in an estate crop inventory of the Island of Bali p 1 A89-20756
- SUDRADJAT, ADJAT**  
Volcanic eruption monitoring using satellite platform p 20 A89-20783
- SUGIMURA, TOSHIRO**  
Comparative study of vegetation index and false colour composite image of NOAA-AVHRR data for bio-mass studies p 1 A89-20752
- SUGIMURA, YUKIO**  
Distribution and variations of oceanic carbon dioxide in the western North Pacific, eastern Indian, and Southern Ocean south of Australia p 29 A89-20925
- SUITZ, TAKESHI**  
Detection of periodic characteristics of rice field vegetation by microwave backscatter measurement p 5 A89-28364  
A measurement of microwave backscattering coefficients of rice plants p 8 N89-18714
- SULLIVAN, WOODRUFF T., III**  
A 10 km resolution image of the entire night-time earth based on cloud-free satellite photographs in the 400-1100 nm band p 56 A89-30256
- SUN, W. D.**  
An atmospheric correction method for AVHRR infrared data using HIRS/2 data p 69 N89-18828
- SUPRIYANTO, JOKO**  
SPOT for mapping of actual land information p 54 A89-20816
- SURSKII, K. O.**  
The capabilities of nonlinear Raman spectroscopy for remote diagnostics of water bodies p 35 A89-29730
- SUTHERLAND, L. L.**  
Intercomparison of synthetic- and real-aperture radar observations of Arctic sea ice during winter MIZEX '87 p 40 N89-18744  
Geophysical information on the winter marginal ice zone obtained from SAR p 46 N89-18942

## SUZUKI, TSUTOMU

- A procedure for land area classification using Landsat TM digital imagery p 17 A89-24651

## SUZUKI, YOSHIRO

- Investigation of water content from airborne MSS data p 49 A89-30261

## SWARTZ, A. A.

- Bayes classification of terrain cover using normalized polarimetric data p 54 A89-22649

## SWEENEY, HAROLD E.

- Remote sensing of ocean physical properties - A comparison of Raman and Brillouin techniques p 34 A89-28003

## SWIFT, C. T.

- Atmospheric profiling of water vapour with a 20.5-23.5 GHz autocorrelation radiometer p 72 N89-18908

## SYLAGGI, F.

- Radiation models of mesotrophic and eutrophic bodies of water p 36 A89-30120

## T

## TACONET, O.

- Application of a flux algorithm to a field-satellite campaign over vegetated area p 6 A89-29411

## TAI, CHANG-KOU

- Geosat crossover analysis in the tropical Pacific. II - Verification analysis of altimetric sea level maps with expendable bathythermograph and island sea level data p 32 A89-26438

## TAILOR, A. M.

- Progress in automatic analysis of multi-temporal remotely-sensed data p 61 N89-18956

## TAKAGI, M.

- An atmospheric correction method for AVHRR infrared data using HIRS/2 data p 69 N89-18828

## TAKAGI, MIKIO

- Receiving and processing system for meteorological satellite (NOAA) p 53 A89-20806

## TAKAHASHI, H.

- Measurements of microwave backscatter from conifers p 12 N89-18848

## TAKEDA, TAKAO

- Observation of the degree of glaciation in middle-level stratiform clouds p 62 A89-23464  
Structure of layer clouds as observed simultaneously by a microwave radiometer and an 8.6 mm-radar p 74 N89-19039

## TAMAIN, G.

- Geological mapping and analysis of fracturing in the south part of the Central Anti-Atlas in Morocco using a Landsat MSS image p 23 A89-31887

## TANABE, M.

- Measurements of microwave backscatter from conifers p 12 N89-18848

## TARES, T. I.

- Backscatter behavior of low-salinity sea ice at C and X-band p 44 N89-18869

## TASSAN, S.

- Radiometric problems in the use of the Thematic Mapper for marine research p 46 N89-18940

## TATEISHI, RYUTARO

- Geometric correction of SPOT image p 54 A89-20812

## TAYLOR, M. R.

- An assessment of ATM and satellite data for estimating the groundwater contribution to slope stability p 51 N89-18769

## TENG, TA-LIANG

- A surface-wave study of the Pacific Ocean basin p 29 A89-21798

## TEUNISSEN, PETER J. G.

- The geometry of geodetic inverse linear mapping and nonlinear adjustment [ETN-89-93900] p 20 N89-19736

## THEALL, J. R.

- Summertime stratospheric wind measurements above the South Pole p 62 A89-24022

## THOMAS, D. R.

- Estimating sea ice concentration from satellite passive microwave data and a physical model p 42 N89-18797

## THOMAS, J.

- Concepts for processing and analyzing of multiple SAR and Landsat images p 55 A89-27789  
Requirements for an EOS-oriented workstation p 69 N89-18813

## THOMPSON, D. R.

- The effect of internal waves on the Doppler spectrum of microwaves scattered from the ocean surface p 41 N89-18783

## THOMPSON, K. P. B.

- Texture analysis of forest regeneration sites in high-resolution SAR imagery p 10 N89-18730

## TILLEY, D. G.

- Ocean wave directional spectra and wave-current interaction in the Agulhas from the Shuttle Imaging Radar-B synthetic aperture radar p 30 A89-22585

- Modelling the SIR-B image response to partially coherent seas p 38 N89-18719

## TILLEY, DAVID G.

- Validation of a synthetic aperture radar ocean wave imaging theory by the Shuttle Imaging Radar-B experiment over the North Sea p 30 A89-22586

## TINDALE, N. W.

- Long-range transport of giant mineral aerosol particles p 17 A89-21931

## TOIKKA, M. V. O.

- Backscatter behavior of low-salinity sea ice at C and X-band p 44 N89-18869

## TOPLISS, B. J.

- Monitoring offshore water quality from space p 39 N89-18739

## TORRANCE, J. G.

- Integration of digital satellite and geophysical data, Heath Steele Mines, New Brunswick, Canada p 25 N89-18792

## TOSELLI, F.

- Applications of remote sensing to agrometeorology; Proceedings of the Course, Ispra, Italy, Apr. 6-10, 1987 p 63 A89-27933

## TOUTIN, THIERRY

- First results of topographical mapping using SPOT images of Malaysia p 52 A89-20764

## TOUZI, R.

- Adaptive speckle filtering for SAR images p 58 N89-18710

## TRAVAGLIA, C.

- Reconnaissance groundwater appraisal of Bohol Island, Philippines, by satellite data analysis p 48 A89-20772

## TRINDER, J. C.

- Wavenumber spectra of short gravity waves p 35 A89-30019

- SPOT mapping software for Wild Aviolet BC2 analytical plotter p 60 N89-18824

## TSAO, Y. D.

- VHF radar remote sensing of vertical profile of liquid water content and rainfall rate over Taiwan during the time period of Typhoon Wayne p 48 A89-20771

## TSUBAKI, H.

- A method for the clustering of remotely sensed multispectral images by using statistical test for spatial uniformity p 61 N89-18898

## TSUCHIYA, KIYOSHI

- Geometric correction of SPOT image p 54 A89-20812

## TSUKAGOSHI, Y.

- Measurements of microwave backscatter from conifers p 12 N89-18848

## TUCKER, COMPTON J.

- Integrated NDVI images for Niger 1986-1987 p 4 A89-28128

## TUCKER, W. B., III

- Physical properties of snow and ice in the winter marginal ice zone of Fram Strait p 46 N89-18944

## TURNER, CHRIS

- Evaluation of satellite-tracked surface drifting buoys for simulating the movement of spilled oil in the marine environment. Volume 1: Executive summary [PB88-226048] p 37 N89-17357

- Evaluation of satellite-tracked surface drifting buoys for simulating the movement of spilled oil in the marine environment, volume 2 [PB88-226055] p 37 N89-17358

## U

## UCHIDA, OSAMU

- Comparison of the orientation's accuracy for SPOT imagery p 53 A89-20798

- Accuracy of terrain measurement using SPOT HRV data p 53 A89-20801

## UCHIDA, SATOSHI

- An estimation of areal evapotranspiration using Landsat and elevation data p 48 A89-20776

## UCHIDA, YASUHIRO

- Land use suitability classification using remote sensing data and geographic information for volcanic regions p 16 A89-20766

## UENO, S.

- Signature variations due to atmospheric and topographic effects on satellite MSS data over rugged terrain p 70 N89-18877

## ULABY, F. T.

- Radar polarimetric observations of a tree canopy p 15 N89-18920

## ULANDER, L.

- Observations of ice types in satellite altimeter data p 44 N89-18841

- UMEHARA, TOSHIHIKO**  
Detection of periodic characteristics of rice field vegetation by microwave backscatter measurement p 5 A89-28364  
A measurement of microwave backscattering coefficients of rice plants p 8 N89-18714
- UNTORO, B.**  
The retrieval of sea surface temperature from NOAA/AVHRR satellite data - Comparison between Singh's and McClain's methods p 28 A89-20787  
The navigation method for NOAA/AVHRR image p 61 A89-20795
- URATSUKA, S.**  
Step frequency radar experiments on the Antarctic Sea ice p 43 N89-18802
- URATSUKA, SEIHO**  
Step frequency radar experiments on the Antarctic Sea ice p 34 A89-28365
- USTIN, SUSAN L.**  
The characterization of sources of illumination in a Ponderosa Pine (*Pinus ponderosa*) forest community using the portable instantaneous display and analysis spectrometer p 4 A89-27781
- V**
- VACHON, P. W.**  
Estimation of the SAR system transfer through processor defocus p 37 N89-18706
- VACHON, PARIS W.**  
A simulation for spaceborne SAR imagery of a distributed, moving scene p 33 A89-26846
- VADASZ, V.**  
Agrometeorological aspects of the utilization of remote-sensing data p 3 A89-23663
- VALENZUELA, C. R.**  
Aerospace imagery and data for modelling erosion, sediment yield and crop yield prediction using GIS, applied to the Upper Komering catchment, Sumatra p 2 A89-20802
- VALERO, FRANCISCO P. J.**  
Calibration of infrared satellite images using high altitude aircraft measurements [AIAA PAPER 89-0817] p 54 A89-25595
- VALLETTE, B.**  
MODIS-HIRIS ground data systems commonality report [NASA-TM-100718] p 67 N89-16205  
MODIS information, data and control system (MIDACS) operations concepts [NASA-TM-100720] p 75 N89-19729
- VAN INGEN SCHENAU, H. A.**  
Definition and design of an operational environment-monitoring system p 18 A89-27788
- VAN ZYL, JAKOB J.**  
Unsupervised classification of scattering behavior using radar polarimetry data p 63 A89-26843
- VANCAMP, L.**  
An ERDAS module for routine processing of AVHRR data p 43 N89-18817  
The structure and variability of a filament in the northwest African upwelling area as observed from AVHRR and CXCS images p 46 N89-18939
- VANDERLAAN, F. B.**  
Updating land-use information on topographic maps using satellite imagery: Combining the advantages of two accessible sources of geographic information p 60 N89-18897  
Land use analysis using remote sensing techniques. Investigation of the usefulness of LANDSAT Thematic Mapper satellite pictures for obtaining and up to date picture of land use in the province South Holland [BCRS-88-01] p 61 N89-19733
- VANGEIN, R.**  
An algorithm for analysis of plate motions in Crust Dynamics Project (CDP) networks [B8821606] p 19 N89-17371
- VANZYL, J. J.**  
Multifrequency imaging radar polarimetry: Depolarisation of radar echoes at three wavelengths p 59 N89-18776  
Application of radar polarimetry to forestry p 15 N89-18919
- VARKYA, V. K.**  
On geology of some districts in Central India using Landsat imageries p 21 A89-20808
- VAUGHAN, R. A.**  
Interpreting the geology of Glen Coe using LANDSAT MSS data and aerial photographs p 26 N89-18860
- VELIKANOV, V. A.**  
Principal problems in upgrading quality and efficiency of geological survey work p 24 N89-17910
- VELTEN, E. H.**  
X-SAR: A new spaceborne synthetic aperture radar p 73 N89-18923
- VENEMA, J. C.**  
Definition and design of an operational environment-monitoring system p 18 A89-27788
- VERHEIJ, L. F.**  
Land use analysis using remote sensing techniques. Investigation of the usefulness of LANDSAT Thematic Mapper satellite pictures for obtaining and up to date picture of land use in the province South Holland [BCRS-88-01] p 61 N89-19733
- VERMILLION, CHARLES H.**  
Low cost, microcomputer-based interactive analysis system for direct-reception and archived remote sensing data p 53 A89-20796
- VERNAZZA, G.**  
Information fusion by a knowledge-based system for SAR image interpretation p 60 N89-18831
- VERRON, JACQUES**  
The impact of satellite altimetry data on numerical simulations of general midlatitude oceanic circulation p 34 A89-28305
- VICHEV, B. I.**  
Microcomputer-based radiometer data acquisition and processing system for large-area mapping of soil moisture content in the top one meter layer p 11 N89-18774  
Experiments in Bulgaria for determination of soil moisture in the top one-meter layer using microwave radiometry and a priori information p 11 N89-18843
- VIDAL-MADJAR, D.**  
Application of a flux algorithm to a field-satellite campaign over vegetated area p 6 A89-29411  
Theoretical study of the sensitivity of the microwave backscattering coefficient to the soil surface parameters p 6 A89-30267  
Effects of slopes and relief two-dimensional spatial frequencies on spaceborne SAR imagery p 59 N89-18777
- VIEHOFF, T.**  
Satellite sea surface temperature at the North Atlantic Polar Front related to high-resolution towed conductivity-temperature-depth data p 31 A89-22594
- VIOLLIER, M.**  
Remote sensing of macrophytic algae of the Molene Archipelago in France - Terrain radiometry and application to SPOT satellite data p 36 A89-30260
- VIRCHENKO, O. V.**  
Agrometeorological aspects of the utilization of remote-sensing data p 3 A89-23663
- VISESHSIN, SUKIT**  
Comparison of the orientation's accuracy for SPOT imagery p 53 A89-20798
- VISSERS, M. A. P.**  
Study of the use of radar X-band data of bare soil in a radar scattering model [BCRS-88-04] p 16 N89-19735
- VLASOV, A. A.**  
Procedures for the determination of geophysical parameters from spaceborne microwave polarimeter measurements p 30 A89-22224
- VLASOV, D. V.**  
Laser airborne sensing field experiments using the 'Chaika' assembly p 35 A89-29728  
Effects of round trip laser emission propagation through a turbulent surface for laser airborne oceanic sensing p 35 A89-29729  
The capabilities of nonlinear Raman spectroscopy for remote diagnostics of water bodies p 35 A89-29730
- VOGELZANG, J.**  
Sea bottom topography with X-band SLAR: Evaluation of existing models p 38 N89-18718
- VOGT, T.**  
The classification of loamy ground in the Outre-Foret region of Alsace in France using Landsat 5 TM images p 7 A89-31890
- VOLIAK, K. I.**  
Oceanic remote sensing p 35 A89-29726  
Surface wave interaction - Theory and capability of oceanic remote sensing p 35 A89-29732
- VOLODIN, D. F.**  
Principal problems in upgrading quality and efficiency of geological survey work p 24 N89-17910
- VUKOVICH, FRED M.**  
Loop Current boundary variations p 31 A89-22596
- W**
- WACKERMAN, C. C.**  
Intercomparison of synthetic- and real-aperture radar observations of Arctic sea ice during winter MIZEX '87 p 40 N89-18744
- WADGE, G.**  
Geological lineament detection using the Hough transform p 26 N89-18818
- WADHAMS, P.**  
SAR imaging of ocean waves in the marginal ice zone p 40 N89-18747
- WAHL, T.**  
Simulation of SAR imaging of ship wakes p 41 N89-18765
- WALKER, A. S. D.**  
Integration of geological, geophysical and remotely sensed data for the Solway Basin, England p 26 N89-18794
- WALKER, CHARLES L.**  
Bathymetry using Thematic Mapper imagery p 34 A89-27995
- WALKER, HOYT**  
Overview of low-cost map digitizing systems [DE89-002872] p 57 N89-16204
- WALKER, RICHARD E.**  
Relative dating of Hawaiian lava flows using multispectral thermal infrared images - A new tool for geologic mapping of young volcanic terranes p 22 A89-22647
- WALSH, EDWARD J.**  
Off-nadir radar altimetry p 66 A89-31947
- WALSTAD, L. J.**  
Frontal signals east of Iceland from the Geosat altimeter p 33 A89-26643
- WALTHER, CRAIG**  
Applications of the NCAR Electra Doppler radar for the study of physical parameters of clouds p 75 N89-19717
- WANG, J. R.**  
Retrieval of water vapor profiles from microwave radiometric measurements at 183 and 92 GHz p 72 N89-18905
- WEBB, FRANK H.**  
Comparison of GPS surveys with historical triangulation surveys in the southern California borderland [NASA-CR-183405] p 24 N89-16199
- WEEKS, W.**  
Plans for the development of EOS SAR systems using the Alaska SAR facility p 69 N89-18757
- WEISSMAN, D. A.**  
Studies of the dependence of the microwave radar cross section on ocean surface variables during the FASINEX experiment p 41 N89-18782
- WENSINK, G. J.**  
Sea bottom topography with X-band SLAR: Evaluation of existing models p 38 N89-18718
- WESSMAN, CAROL A.**  
Remote sensing of canopy chemistry and nitrogen cycling in temperate forest ecosystems p 3 A89-23431
- WEST, J. C.**  
Analysis of ocean backscatter data obtained by the University of Kansas during TOWARD 84/85 p 42 N89-18787
- WHARTON, STEPHEN W.**  
Land image data processing requirements for the EOS era p 56 A89-31949
- WHITE, WARREN B.**  
Geosat crossover analysis in the tropical Pacific. II - Verification analysis of altimetric sea level maps with expendable bathythermograph and island sea level data p 32 A89-26438
- WHITEHOUSE, LAURIE**  
STAR-1 high resolution synthetic aperture radar imagery for precious metal exploration p 21 A89-20827
- WHITEHURST, G. A.**  
Impact of phase and amplitude errors on the ERS-1 active microwave instrumentation performance p 70 N89-18853
- WHITEMAN, C. D.**  
Applications of digital image processing to ongoing research in complex terrain meteorology [DE89-001749] p 57 N89-17375
- WHITT, M. W.**  
Radar polarimetric observations of a tree canopy p 15 N89-18920
- WICKLAND, D. E.**  
Remote sensing of land processes: Sponsored programs of study by the National Aeronautics and Space Administration p 19 N89-18833
- WIDMER, P.**  
The central user services system for ERS-1 p 68 N89-18754
- WIEGAND, C.**  
Water turbidity and perpendicular vegetation indices for paddy rice flood damage analyses p 6 A89-29412
- WIESBECK, W.**  
Correlation of radar reflectivity and chlorophyll fluorescence of forest trees p 9 N89-18727  
A study of passive microwave remote sensing p 45 N89-18938
- WIESENBURG, DENIS A.**  
Satellite detection of transient enhanced primary production in the western Mediterranean Sea p 31 A89-23438

## WILHEIT, T. T.

## WILHEIT, T. T.

Retrieval of water vapor profiles from microwave radiometric measurements at 183 and 92 GHz p 72 N89-18905

## WILLIAMSON, H. D.

Soil influences on vegetation reflectance of a semi-arid shrubland p 13 N89-18880  
Vegetation sampling for studies using remotely sensed data p 13 N89-18883

## WINBURG, E.

Atmospheric attenuation as derived from microwave radiometry at 52.8 GHz p 72 N89-18906

## WINGHAM, D. J.

An advanced terrain tracking altimeter p 45 N89-18910  
A new approach to topographic altimetry p 73 N89-18914

## WINSTEAD, EDWARD L.

Trace gas emissions from chaparral and boreal forest fires p 7 A89-32432

## WINTER, R.

Investigations of SAR backscatter for different test areas using two geocoded Seasat SAR scenes p 58 N89-18761

## WIRADISAstra, U. S.

Digital image analysis of Landsat MSS data in an estate crop inventory of the Island of Bali p 1 A89-20756

## WIRJOSEDIRDJO, SRI JATNO

Soil and vegetation mapping by using SPOT image p 1 A89-20758

## WISNUWARDHANI, WIEKE

Soil and vegetation mapping by using SPOT image p 1 A89-20758

## WOOD, J.

The visibility of linear features in SAR images p 59 N89-18763

## WOOD, T. F.

Analysis and representation of vegetation continua from Landsat Thematic Mapper data for lowland heaths p 7 A89-30268

## WOODING, M. G.

Pattern analysis and the ecological interpretation of satellite imagery p 61 N89-18900

## WYATT, B.

Alternative approaches to the classification of upland semi-natural vegetation p 16 N89-18961

## WYATT, G.

Visual and computer classifications of remotely-sensed images - A case study of grasslands in Cambridgeshire p 7 A89-30269

## WYLIE, BRUCE K.

Integrated NDVI images for Niger 1986-1987 p 4 A89-28128

## X

## XU, BAIDE

Quick reporting state of fishery and sea on the East China Sea and the Yellow Sea with NOAA p 39 N89-18741

A preliminary study on nearshore water in China with NOAA satellite images p 40 N89-18743

## XUE, YONGQI

Application of airborne scanners in remote sensing of sea p 29 A89-20789

## Y

## YAMADA, N.

A mathematical model of reflectance and transmittance of plant leaves as a function of chlorophyll pigment content p 13 N89-18879

## YAMAGATA, Y.

Water turbidity and perpendicular vegetation indices for paddy rice flood damage analyses p 6 A89-29412

## YAMAJI, EIJI

Study of the monitoring of land cover/use using remote sensing data by personal computer in southern part of Bandung area, West Java p 2 A89-20815

## YANASSE, C.

Change detection in AGRISAR images p 15 N89-18949

## YORDANOV, O. I.

Distribution of specular points on the ocean surface: Bistatic scattering p 38 N89-18721

## YUEH, H. A.

Bayes classification of terrain cover using normalized polarimetric data p 54 A89-22649

## YUMADIATI, SRI

Coastline monitoring in Madura Strait, Indonesia on 1972-1985 p 29 A89-20804

## Z

## ZABELIN, V. A.

The procedure for and the results of the geological interpretation of photographic images of the Bukhtarma lineament zone p 22 A89-22217

## ZAGO, C.

SAR imaging of ocean waves in the marginal ice zone p 40 N89-18747

## ZAGORODNIKOV, A. A.

Motion characteristics of sea waves p 32 A89-23590

## ZAITSEV, L. V.

Estimation of the water exchange and contamination zones of basins from satellite imagery p 49 A89-30252

## ZAMBRESKY, LIANA F.

Validation of a synthetic aperture radar ocean wave imaging theory by the Shuttle Imaging Radar-B experiment over the North Sea p 30 A89-22586

## ZEBKER, H. A.

Multifrequency imaging radar polarimetry: Depolarisation of radar echoes at three wavelengths p 59 N89-18776  
Application of radar polarimetry to forestry p 15 N89-18919

## ZELEK, JOHN S.

FEX - A knowledge-based system for planimetric feature extraction p 54 A89-27783

## ZHANG, ZI-JUE

Spatial information processings of TM data p 52 A89-20791

## ZHIFU, SHI

A study of passive microwave remote sensing p 45 N89-18938

## ZHILKO, E. O.

Motion characteristics of sea waves p 32 A89-23590

## ZIATKOVA, L. K.

Principal results of remote-sensing studies of Siberia's natural resources (On the occasion of the 10th anniversary of the Scientific Coordination Council, 1977-1987) p 62 A89-22225

## ZIBORDI, G.

Determination of atmospheric turbidity from remotely-sensed data - A case study p 34 A89-28034

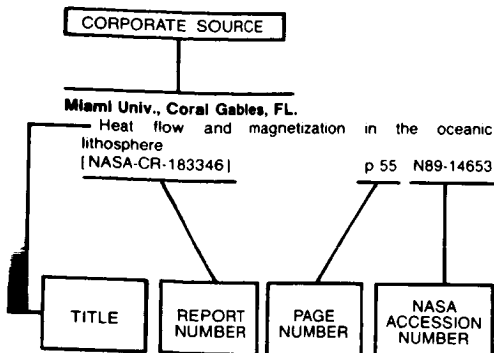
## ZOUGH, R.

Fine resolution signatures of coniferous and deciduous trees at C band p 6 A89-30266

## ZUEV, V. E.

Laser sounding of the troposphere and the underlying surface p 17 A89-22066

## Typical Corporate Source Index Listing



Listings in this index are arranged alphabetically by corporate source. The title of the document is used to provide a brief description of the subject matter. The page number and the accession number are included in each entry to assist the user in locating the abstract in the abstract section. If applicable, a report number is also included as an aid in identifying the document.

## A

- Aberdeen Univ. (Scotland).**  
The UN declaration of legal principals on remote sensing, 1986 p 76 N89-18748
- Academy of Sciences (USSR), Moscow.**  
Microcomputer-based radiometer data acquisition and processing system for large-area mapping of soil moisture content in the top one meter layer p 11 N89-18774  
Experiments in Bulgaria for determination of soil moisture in the top one-meter layer using microwave radiometry and a priori information p 11 N89-18843
- Air Force Geophysics Lab., Hanscom AFB, MA.**  
EHF attenuation through the melting layer p 51 N89-18984
- Alabama Univ., Huntsville.**  
Satellite remote sensing of cloud distribution and amount of rainfall over the Tibet Plateau area of China p 48 A89-20770  
VHF radar remote sensing of vertical profile of liquid water content and rainfall rate over Taiwan during the time period of Typhoon Wayne p 48 A89-20771
- Alaska Univ., Fairbanks.**  
Buoyant surface jet analysis of the Yukon River p 49 A89-28033
- Applied Science Associates, Inc., Narragansett, RI.**  
Evaluation of satellite-tracked surface drifting buoys for simulating the movement of spilled oil in the marine environment. Volume 1: Executive summary [PB88-226048] p 37 N89-17357  
Evaluation of satellite-tracked surface drifting buoys for simulating the movement of spilled oil in the marine environment, volume 2 [PB88-226055] p 37 N89-17358
- Army Cold Regions Research and Engineering Lab., Hanover, NH.**  
Physical properties of snow and ice in the winter marginal ice zone of Fram Strait p 46 N89-18944
- Aston Univ., Birmingham (England).**  
Effects of commercialisation on international remote sensing activities p 76 N89-18752

- Digital elevation models and their application to remote sensing of water resources p 51 N89-18770  
Estimation of the area of Lake Kariba, Zimbabwe, using LANDSAT MSS imagery p 51 N89-18775  
Monitoring of agro-forestry production systems in the Sudano-Sahelian zone of West Africa p 11 N89-18825  
The use of coregistered LANDSAT MSS, TM and SIR-A imagery for lithological mapping p 28 N89-18936
- Aztec Computer Engineering, Pinellas Park, FL.**  
Spectral transmissometer and radiometer - Design and initial results p 64 A89-27991

## B

- Bar-Ilan Univ., Ramat-Gan (Israel).**  
A method to forecast open pack ice speed of motion using remotely-sensed data p 42 N89-18801
- Bedford Inst. of Oceanography, Dartmouth (Nova Scotia).**  
Monitoring offshore water quality from space p 39 N89-18739
- Begeleidingscommissie Remote Sensing, Delft (Netherlands).**  
The use of LANDSAT imagery for water quality studies in the IJsselmeer area (Netherlands) [BCRS-87-18] p 52 N89-19732  
Land use analysis using remote sensing techniques. Investigation of the usefulness of LANDSAT Thematic Mapper satellite pictures for obtaining and up to date picture of land use in the province South Holland [BCRS-88-01] p 61 N89-19733  
Salinity mapping based on SPOT images of the Punjab, Pakistan [BCRS-88-03] p 16 N89-19734  
Study of the use of radar X-band data of bare soil in a radar scattering model [BCRS-88-04] p 16 N89-19735
- Bercha (F. G.) and Associates Ltd., Calgary (Alberta).**  
Auto and cross correlation analysis of environment, system and target parameters for iceberg detection using airborne radar p 45 N89-18874
- Biospherical Instruments, Inc., San Diego, CA.**  
Moorable spectroradiometers in the BIOWATT experiment p 64 A89-27990
- British Aerospace Public Ltd. Co., Bristol (England).**  
An advanced terrain tracking altimeter p 45 N89-18910
- Budapest Science Univ. (Hungary).**  
X-band scatterometry in agriculture p 9 N89-18715
- Bulgarian Academy of Sciences, Sofia.**  
Distribution of specular points on the ocean surface: Bistatic scattering p 38 N89-18721  
Study on directional spectrum characteristics of marine radar images of ocean waves p 41 N89-18786

## C

- California Inst. of Tech., Pasadena.**  
Comparison of GPS surveys with historical triangulation surveys in the southern California borderland [NASA-CR-183405] p 24 N89-16199
- California Univ., Davis.**  
The characterization of sources of illumination in a Ponderosa Pine (Pinus ponderosa) forest community using the portable instantaneous display and analysis spectrometer p 4 A89-27781
- California Univ., La Jolla.**  
Seasat - Results of the mission p 29 A89-22000  
Geosat crossover analysis in the tropical Pacific. II - Verification analysis of altimetric sea level maps with expendable bathythermograph and island sea level data p 32 A89-26438
- California Univ., Santa Barbara.**  
Moorable spectroradiometers in the BIOWATT experiment p 64 A89-27990
- Canada Centre for Remote Sensing, Ottawa (Ontario).**  
Estimation of the SAR system transfer through processor defocus p 37 N89-18706  
Assessment of clearcut mapping accuracy with C-band SAR p 9 N89-18725
- SAR imagery of the Grand Banks (Newfoundland) pack ice pack and its relationship to surface features p 40 N89-18745  
Satellite data acquisition planning at the Canada Center for Remote Sensing p 68 N89-18753  
Toward the automated use of remote sensing data in operational ice forecasting p 43 N89-18804  
Towards a calibration of the CCRS airborne SARS p 70 N89-18854
- Canada Centre for Remote Sensing, Yellowknife (Northwest Territories).**  
Mapping slope failure tracks with digital Thematic Mapper data p 59 N89-18790
- Canadian Forestry Service, Ottawa (Ontario).**  
Trace gas emissions from chaparral and boreal forest fires p 7 N89-32432
- Carnegie-Mellon Univ., Pittsburgh, PA.**  
Sensor fusion of range and reflectance data for outdoor scene analysis p 76 N89-19868
- Carnegie Museum of Natural History, Pittsburgh, PA.**  
Geological remote sensing of Palaeogene rocks in the Wind River Basin, Wyoming, USA p 28 N89-18935
- Centre d'Etude Spatiale des Rayonnements, Toulouse (France).**  
Adaptive speckle filtering for SAR images p 58 N89-18710  
Multitemporal and dual polarization of agricultural crops by X-band SAR images p 9 N89-18716
- Centre National d'Etudes Spatiales, Toulouse (France).**  
Preprocessing of the VARAN synthetic aperture airborne radar p 70 N89-18856
- Centre National de Recherche Scientifique, Saint Martin d'Heres (France).**  
Measuring lead area changes in sea ice imagery p 44 N89-18871
- Chalmers Univ. of Technology, Goeteborg (Sweden).**  
Observations of ice types in satellite altimeter data p 44 N89-18841  
Ice ridge observations by means of SAR p 45 N89-18872  
Evaluation of VARAN-S SAR data from the BEPERS study project p 45 N89-18875  
Atmospheric attenuation as derived from microwave radiometry at 52.8 GHz p 72 N89-18906
- China Research Inst. of Radiowave Propagation, Xinxiang.**  
A simulation test for soil moisture sensing p 10 N89-18772
- Colorado State Univ., Fort Collins.**  
Comparisons of satellite data surface-based remote sensing measurements in Utah winter orographic storms p 75 N89-19079
- Colorado Univ., Boulder.**  
The characterization of sources of illumination in a Ponderosa Pine (Pinus ponderosa) forest community using the portable instantaneous display and analysis spectrometer p 4 A89-27781
- Consiglio Nazionale delle Ricerche, Frascati (Italy).**  
A quantitative geomorphology study of main carbonate massifs of central and southern Apennines (Italy) based on a digital elevations archive p 25 N89-18791
- Copenhagen Univ. (Denmark).**  
An ERDAS module for routine processing of AVHRR data p 43 N89-18817  
The structure and variability of a filament in the northwest African upwelling area as observed from AVHRR and CXCS images p 46 N89-18939
- Cornell Univ., Ithaca, NY.**  
Tectonics of the central Andes [NASA-CR-184683] p 28 N89-18973

## D

- Dames and Moore International, Twickenham (England).**  
Enhancement of glacial fractures by analysis of Thematic Mapper data: Glen Roy, Scotland p 26 N89-18859
- Delaware Univ., Newark.**  
Comparison of Shuttle Imaging Radar-B ocean wave image spectra with linear model predictions based on aircraft measurements p 30 A89-22584



## Delft Hydraulics Lab.

- Effects of solar angle on reflectance from wetland vegetation p 5 A89-29409
- Delft Hydraulics Lab. (Netherlands).**  
Monitoring of suspended sediments in Jatiluhur Reservoir using satellite images p 50 N89-18740
- Department of Agriculture, Beltsville, MD.**  
Estimating absorbed radiation and phytomass from multispectral reflectance of corn and soybeans p 13 N89-18876
- Department of Agriculture, Riverside, CA.**  
Trace gas emissions from chaparral and boreal forest fires p 7 A89-32432
- Department of Energy, Washington, DC.**  
Coastal ocean margins program [DE89-005937] p 47 N89-18972
- Deutsche Forschungs- und Versuchsanstalt fuer Luft- und Raumfahrt, Oberpfaffenhofen (West Germany).**  
German spaceborne remote sensing activities p 67 N89-16887
- Investigations of SAR backscatter for different test areas using two geocoded Seasat SAR scenes p 58 N89-18781
- Results of tectonic and spectral investigations in the coast range of northern Chile using special processed Thematic Mapper (TM) data p 27 N89-18929
- Deutsche Forschungs- und Versuchsanstalt fuer Luft- und Raumfahrt, Wesseling (Germany, F.R.).**  
E-SAR: The experimental airborne L/C-band SAR system of DFVLR p 73 N89-18924
- Dornier-Werke G.m.b.H., Friedrichshafen (Germany, F.R.).**  
X-SAR: A new spaceborne synthetic aperture radar p 73 N89-18923
- Dundee Univ. (Scotland).**  
Interpreting the geology of Glen Coe using LANDSAT MSS data and aerial photographs p 26 N89-18860
- Geological applications of thermal infrared characteristics of vegetation p 27 N89-18932
- Durham Univ. (England).**  
Preprocessing and analysis of airborne visible near and shortwave infrared data for the detection of alteration in weathered vegetated terrain p 12 N89-18862
- An evaluation of surface emittance and temperature data derived from Thermal Infrared Multispectral Scanner (TIMS) for lithological mapping in weathered vegetated terrain: N. Queensland, Australia p 27 N89-18934
- E**
- Earth Observation Sciences Ltd., Guildford (England).**  
The algorithm development facility: its role in the development and operation of a satellite data centre p 68 N89-18755
- Ecole Nationale Supérieure des Telecommunications, Brest (France).**  
Nonlinear filtering and edge detection in speckled radar images p 58 N89-18711
- Statistical evaluation of the intensity distribution of sea surface radar images p 38 N89-18717
- Edinburgh Univ. (Scotland).**  
Problems in the estimation of barley yields by remote sensing p 13 N89-18881
- Textural and spectral features as an aid to cloud classification p 74 N89-18960
- Environmental Remote Sensing Applications Centre, Livingston (Scotland).**  
The Geospace philosophy: A new practical approach in remote sensing and planning for local authorities p 76 N89-18750
- Environmental Research Inst. of Michigan, Ann Arbor.**  
Intercomparison of synthetic- and real-aperture radar observations of Arctic sea ice during winter MIZEX '87 p 40 N89-18744
- SAR imaging of ocean waves in the marginal ice zone p 40 N89-18747
- Radiometric calibration of airborne SAR data p 70 N89-18855
- Geophysical information on the winter marginal ice zone obtained from SAR p 46 N89-18942
- Radar backscatter of sea ice during winter p 46 N89-18943
- Ericsson Radar Electronics A.B., Moindal (Sweden).**  
An advanced terrain tracking altimeter p 45 N89-18910
- EUROCONSULT B.V., Arnhem (Netherlands).**  
Salinity mapping based on SPOT images of the Punjab, Pakistan [BCRS-88-03] p 16 N89-19734
- European Space Agency, Paris (France).**  
Investigation of information content of Thematic Mapper and SPOT multiband image data, using simulated image data of the Freiburg region (Federal Republic of Germany) [ESA-TT-975] p 57 N89-15442

- The 1988 International Geoscience and Remote Sensing Symposium (IGARSS 1988) on Remote Sensing: Moving Towards the 21st Century, volume 3 [ESA-SP-284-VOL-3] p 68 N89-18704
- Proceedings of the 1988 International Geoscience and Remote Sensing Symposium (IGARSS) '88 on Remote Sensing: Moving Towards the 21st Century, Volume 2 [ESA-SP-284-VOL-2] p 69 N89-18836
- European Space Agency. European Space Research and Technology Center, ESTEC, Noordwijk (Netherlands).**  
ERS-1 operation capabilities p 71 N89-18884
- Engineering calibration of the ERS-1 active microwave instrumentation in orbit p 71 N89-18885
- ERS-1 altimeter height calibration p 71 N89-18891
- Quality control of fast delivery processors and products p 72 N89-18892
- A possibility for selecting spectral bands of future land application sensors at the example of an imaging spectrometer p 60 N89-18896
- Radar signature measurements during the AGRISCATT campaigns p 15 N89-18950
- Mission aspects of a future European polar orbit earth observation facility p 74 N89-18952
- F**
- Florida International Univ., Miami.**  
Technology transfer for development of coastal zone resources: Caribbean experts examine critical issues p 40 N89-18749
- Freiburg Univ. (Germany, F.R.).**  
Data processing for the determination of pigments and suspended solids from Thematic Mapper data p 50 N89-18736
- Extraction of agricultural plant parameters from multitemporal Thematic Mapper (TM) and X-SAR data p 15 N89-18948
- Correlations between agricultural plant parameters and multitemporal radar scatterometer data: First results from the European AGRISCATT 87 campaign p 16 N89-18951

## F

- GEC-Marconi Electronics Ltd., Chelmsford (England).**  
The visibility of linear features in SAR images p 59 N89-18763
- Automated linear feature detection and its application to curve location in synthetic aperture radar imagery p 59 N89-18764
- New architecture for a real-time SAR processor p 69 N89-18850
- A SAR data quality assessment scheme for the ERS-1 mission p 72 N89-18893
- Advanced SAR concepts p 73 N89-18926
- General Sciences Corp., Laurel, MD.**  
MODIS-HIRIS ground data systems commonality report [NASA-TM-100718] p 67 N89-16205
- Genoa Univ. (Italy).**  
Information fusion by a knowledge-based system for SAR image interpretation p 60 N89-18831
- Geological Survey, Reston, VA.**  
Research, investigations and technical developments. National mapping program, 1985-1986 [USGS-OPEN-FILE-REPT-87-315] p 24 N89-16208
- Ghent Univ. (Belgium).**  
The use of SPOT-1 imagery for forest classification in Flanders (Belgium) p 14 N89-18899

## G

- Harvard Coll. Observatory, Cambridge, MA.**  
Research in geodesy and geophysics based upon radio interferometric observations of extragalactic radio sources [AD-A200958] p 25 N89-17933
- Helisinki Univ. of Technology, Espoo (Finland).**  
Backscatter behavior of low-salinity sea ice at C and X-band p 44 N89-18869
- Hosel Univ., Tokyo (Japan).**  
A method for the clustering of remotely sensed multispectral images by using statistical test for spatial uniformity p 61 N89-18898
- Hydrological Research Inst., Pretoria (South Africa).**  
Estimating the extent of irrigated cropland in a large catchment using LANDSAT MSS data p 14 N89-18902

## H

- Ice Centre Environment Canada, Ottawa (Ontario).**  
Real-time processing of digital image data in support of the Canadian sea ice analysis and prediction program p 43 N89-18833
- Imperial Coll. of Science and Technology, London (England).**  
Artefacts in AIS-1 imagery p 69 N89-18826
- Assimilation of altimeter data into numerical ocean models p 43 N89-18838
- Indian Space Research Organization, Ahmedabad.**  
Specular scattering with effective reflection coefficient p 39 N89-18723
- Institut fuer Angewandte Geodesie, Frankfurt am Main (Germany, F.R.).**  
Reports on cartography and geodesy, series 1, number 100 [ISSN-0469-4236] p 20 N89-17935
- Institut für Image Processing Computer Mapping, Graz (Austria).**  
Spectral response characteristics of a metal-stressed coniferous forest as measured by the Fluorescence Line Imager (FLI) airborne imaging spectrometer p 9 N89-18724
- Institute of Karst Geology, Gulin (China).**  
Quantitative remote detection of suspended sediment content and chlorophyll concentration of water in different depths p 50 N89-18733
- Institute of Ocean Sciences, Sidney (British Columbia).**  
Mapping of phytoplankton fluorescence with the Fluorescence Line Imager (FLI) imaging spectrometer p 39 N89-18737
- Institute of Oceanographic Sciences, Wormley (England).**  
Directional wave data recorded in the southern North Sea [IOS-258] p 47 N89-19793
- Instituto de Pesquisas Espaciais, Cachoeira Paulista (Brazil).**  
Study of geometric quality of the MSS-LANDSAT imagery [INPE-4653-PRE/1360] p 57 N89-15440
- Instituto de Pesquisas Espaciais, Rio de Janeiro (Brazil).**  
Microwave X-band radiometric characterization of Brazilian soils by measurement of the complex permittivity p 11 N89-18773
- Instituto de Pesquisas Espaciais, Sao Jose dos Campos (Brazil).**  
Knowledge related aspects of lineation and lineament extraction [INPE-4709-PRE/1391] p 24 N89-15446
- Using different sources of information in automated linear feature extraction from remote sensing data [INPE-4708-PRE/1390] p 24 N89-15447
- Automatic registration of satellite imagery [INPE-4637-PRE/1349] p 57 N89-17414
- The impact of multiviewing reflectance data on the estimation of suspended sediment concentration p 50 N89-18735
- Instituut voor Cultuurtechniek en Waterhuishouding, Wageningen (Netherlands).**  
The effect of soil moisture on reflectance characteristics of salt crusts p 16 N89-18966
- Interferometrics, Inc., Vienna, VA.**  
MODIS information, data and control system (MIDACS) operations concepts [NASA-TM-100720] p 75 N89-19729
- J**
- Jet Propulsion Lab., California Inst. of Tech., Pasadena.**  
Seasat - Results of the mission p 29 A89-22000
- Relative dating of Hawaiian lava flows using multispectral thermal infrared images - A new tool for geologic mapping of young volcanic terranes p 22 A89-22647
- Fractal features of sea surface manifested in microwave remote sensing signatures p 32 A89-24872
- Unsupervised classification of scattering behavior using radar polarimetry data p 63 A89-26843
- Concepts for processing and analyzing of multiple SAR and Landsat images p 55 A89-27789
- Mapping in the Oman ophiolite using enhanced Landsat Thematic Mapper images p 23 A89-29301
- MISR - A multiangle imaging spectroradiometer for geophysical and climatological research from EOS p 66 A89-31946
- A simple spatial filtering routine for the cosmetic removal of scan-line noise from Landsat TM P-tape imagery p 57 A89-32335
- MODIS-HIRIS ground data systems commonality report [NASA-TM-100718] p 67 N89-16205

## J

- Use of SAR imagery and other remotely-sensed data in deriving ice information during a severe ice event on the Grand Banks (Newfoundland) p 40 N89-18746
- Plans for the development of EOS SAR systems using the Alaska SAR facility p 69 N89-18757
- Multifrequency imaging radar polarimetry: Depolarisation of radar echoes at three wavelengths p 59 N89-18776
- Studies of the dependence of the microwave radar cross section on ocean surface variables during the FASINEX experiment p 41 N89-18782
- Fractal properties of the sea surface manifested in microwave remote sensing signatures p 41 N89-18784
- Sea-ice software: ICEMAN p 43 N89-18805
- The Alaska SAR processor p 70 N89-18851
- Important changes in microwave scattering properties of young snow-covered sea ice as indicated from dielectric modelling p 44 N89-18870
- Atmospheric profiling of water vapour with a 20.5-23.5 GHz autocorrelation radiometer p 72 N89-18908
- Application of radar polarimetry to forestry p 15 N89-18919
- Overview of the Shuttle Imaging Radar (SIR-C) p 73 N89-18921
- Automatic mineral map generation procedure from imaging spectrometer data p 27 N89-18931
- Johns Hopkins Univ., Laurel, MD.**
- Comparison of Shuttle Imaging Radar-B ocean wave image spectra with linear model predictions based on aircraft measurements p 30 A89-22584
- Ocean wave directional spectra and wave-current interaction in the Agulhas from the Shuttle Imaging Radar-B synthetic aperture radar p 30 A89-22585
- Modelling the SIR-B image response to partially coherent seas p 38 N89-18719
- Results of software simulation of a real-time SAR processor capable of providing ocean wave spectra p 38 N89-18720
- Variability of the diffuse attenuation coefficient in waters off the US East Coast p 39 N89-18738
- The effect of internal waves on the Doppler spectrum of microwaves scattered from the ocean surface p 41 N89-18783
- Dynamic topography as measured by the Geosat altimeter in regions of small surface height signatures p 43 N89-18837
- The influence of water vapor on the detection of ocean mesoscale fronts and eddies by the Geosat altimeter p 44 N89-18839
- The Navy Geosat radar altimeter satellite mission p 45 N89-18909
- Joint Publications Research Service, Arlington, VA.**
- Principal problems in upgrading quality and efficiency of geological survey work p 24 N89-17910
- Annular and block-folded structures on space and aerial photographs p 25 N89-17915
- Some results of use of space survey materials in cartographic work p 58 N89-17922
- Joint Research Centre of the European Communities, Ispra (Italy).**
- Optical properties of sea water bodies: Measurements with an underwater radiometer and a high-resolution spectroradiometer p 39 N89-18734
- Post-processing airborne SAR data for multitemporal land-cover studies p 12 N89-18857
- Image-based atmospheric correction of multitemporal Thematic Mapping data for agricultural land cover classification p 14 N89-18895
- Radiometric problems in the use of the Thematic Mapper for marine research p 46 N89-18940
- K**
- Kanagawa Univ. (Japan).**
- Measurements of microwave backscatter from conifers p 12 N89-18848
- Kanazawa Inst. of Tech. (Japan).**
- Signature variations due to atmospheric and topographic effects on satellite MSS data over rugged terrain p 70 N89-18877
- Kansas Univ., Lawrence.**
- Analysis of ocean backscatter data obtained by the University of Kansas during TOWARD 84/85 p 42 N89-18787
- Kansas Univ. Center for Research, Inc., Lawrence.**
- Fine resolution signatures of coniferous and deciduous trees at C band p 6 A89-30266
- Karlsruhe Univ. (Germany, F.R.).**
- Correlation of reflectance and chlorophyll fluorescence signatures of healthy and damaged forest trees p 9 N89-18726
- Correlation of radar reflectivity and chlorophyll fluorescence of forest trees p 9 N89-18727

- A study of passive microwave remote sensing p 45 N89-18938
- Kings Coll., London (England).**
- Speckle correlation in SAR images of dynamic discrete scatterers p 37 N89-18707
- Computer simulation of multipath sea echo near grazing incidence p 38 N89-18722

## L

- Lamont-Doherty Geological Observatory, Palisades, NY.**
- Dependence of snow melting and surface-atmosphere interactions on the forest structure p 3 A89-21740
- Antarctic Ocean polynya [NASA-CR-184805] p 47 N89-19102
- Laval Univ. (Quebec).**
- Texture analysis of forest regeneration sites in high-resolution SAR imagery p 10 N89-18730
- Lawrence Livermore National Lab., CA.**
- Overview of low-cost map digitizing systems [DE89-002872] p 57 N89-16204
- Lockheed Engineering and Sciences Co., Houston, TX.**
- Extension of a drought monitoring and vegetation classification methodology to the western Sahel p 4 A89-28127
- Lunar and Planetary Inst., Houston, TX.**
- Remote sensing of evaporite mineral zonation in salt flats (salars) p 23 A89-30271

## M

- MacDonald, Dettwiler and Associates Ltd., Richmond (British Columbia).**
- The central user services system for ERS-1 p 68 N89-18754
- A high fidelity, high throughput system for geocoding SAR imagery p 60 N89-18849
- Marconi Space Systems Ltd., Portsmouth (England).**
- Impact of phase and amplitude errors on the ERS-1 active microwave instrumentation performance p 70 N89-18853
- The pre-launch performance verification of the ERS-1 active microwave instrumentation p 71 N89-18886
- A software package for performance evaluation of the ERS-1 AMI p 71 N89-18887
- ERS-1 active microwave instrumentation engineering model performance p 71 N89-18888
- Stability considerations for the ERS-1 wind scatterometer radiometric performance p 71 N89-18889
- ERS-1 AMI antennas: The design and development experience p 71 N89-18890
- Maryland Univ., College Park.**
- Tersail - A numerical model for combined analysis of vegetation canopy bidirectional reflectance and thermal emissions p 6 A89-29415
- Massachusetts Inst. of Tech., Cambridge.**
- Bayes classification of terrain cover using normalized polarimetric data p 54 A89-22649
- Geodetic measurement of deformation in California [NASA-CR-184604] p 19 N89-15476
- Active and passive remote sensing of ice [AD-A201915] p 47 N89-19792
- Massachusetts Inst. of Tech., Lexington.**
- Bayes classification of terrain cover using normalized polarimetric data p 54 A89-22649
- Massachusetts Univ., Amherst.**
- Leaf backscattering measurements and modelling at 94 GHz p 8 N89-18713
- Radar backscatter characteristics of trees at 215 GHz p 14 N89-18917
- Normalized radar cross section of natural surfaces at millimeter wavelengths [AD-A202252] p 75 N89-19475
- McGill Univ., Montreal (Quebec).**
- MISR - A multiangle imaging spectroradiometer for geophysical and climatological research from EOS p 66 A89-31946
- Miami Univ., FL.**
- The source of marine magnetic anomalies [MPL-U-42/87] p 31 A89-22876
- Michigan Univ., Ann Arbor.**
- Radar polarimetric observations of a tree canopy p 15 N89-18920
- Ministere de l'Environnement et du Cadre de Vie, Neuilly (France).**
- Possibilities of the satellite imagery to locate the forest decline areas in the Vosges Massif (France) p 10 N89-18729
- Ministry of Posts and Telecommunications, Tokyo (Japan).**
- A measurement of microwave backscattering coefficients of rice plants p 8 N89-18714

## NASA. Lyndon B. Johnson Space Center

- Step frequency radar experiments on the Antarctic Sea ice p 43 N89-18802
- Missouri Univ., Columbia.**
- Satellite derived earth surface temperatures: A crop assessment tool p 8 N89-17930
- Mullard Space Science Lab., Dorking (England).**
- Satellite radar altimetry over arid regions p 69 N89-18842
- N**
- Nagoya Univ. (Japan).**
- Structure of layer clouds as observed simultaneously by a microwave radiometer and an 8.6 mm-radar p 74 N89-19039
- Nairobi Univ. (Kenya).**
- Snow cover-summer monsoon rainfall over parts of Sahel p 51 N89-18832
- National Aeronautics and Space Administration, Washington, DC.**
- Satellite remote sensing of cloud distribution and amount of rainfall over the Tibet Plateau area of China p 48 A89-20770
- Low cost, microcomputer-based interactive analysis system for direct-reception and archived remote sensing data p 53 A89-20796
- Remote sensing of land processes: Sponsored programs of study by the National Aeronautics and Space Administration p 19 N89-18833
- National Aeronautics and Space Administration, Ames Research Center, Moffett Field, CA.**
- Remote sensing of canopy chemistry and nitrogen cycling in temperate forest ecosystems p 3 A89-23431
- Calibration of infrared satellite images using high altitude aircraft measurements [AIAA PAPER 89-0817] p 54 A89-25595
- Monitoring water quality and river plume transport in Green Bay, Lake Michigan with SPOT-1 imagery p 49 A89-32338
- Trace gas emissions from chaparral and boreal forest fires p 7 A89-32432
- Accuracy assessment, using stratified plurality sampling, of portions of a LANDSAT classification of the Arctic National Wildlife Refuge Coastal Plain [NASA-TM-101042] p 8 N89-17339
- National Aeronautics and Space Administration, Goddard Space Flight Center, Greenbelt, MD.**
- Low cost, microcomputer-based interactive analysis system for direct-reception and archived remote sensing data p 53 A89-20796
- Dependence of snow melting and surface-atmosphere interactions on the forest structure p 3 A89-21740
- Goniometric observations of light scattered from soils and leaves p 4 A89-24873
- Optical system design alternatives for the Moderate-Resolution Imaging Spectrometer-Tilt (MODIS-T) for the Earth Observing System (EOS) p 63 A89-27753
- Parabola directional field radiometer for aiding in space sensor data interpretations p 63 A89-27779
- Integrated NDVI images for Niger 1986-1987 p 4 A89-28128
- MODIS - Advanced facility instrument for studies of the earth as a system p 66 A89-31943
- Land image data processing requirements for the EOS era p 56 A89-31949
- MODIS-HIRIS ground data systems commonality report [NASA-TM-100718] p 67 N89-16205
- Characterizing forest ecosystem dynamics through modelling and remote sensing observations p 10 N89-18728
- Preliminary observations of polar sea ice with the Special Sensor Microwave Imager p 42 N89-18800
- NASA's Earth Observing System (EOS): An opportunity for mankind p 77 N89-18816
- Observed effects of soil organic matter content on the microwave intensity of soils p 12 N89-18845
- Retrieval of water vapor profiles from microwave radiometric measurements at 183 and 92 GHz p 72 N89-18905
- MODIS information, data and control system (MIDACS) operations concepts [NASA-TM-100720] p 75 N89-19729
- National Aeronautics and Space Administration, John C. Stennis Space Center, Bay Saint Louis, MS.**
- Satellite detection of transient enhanced primary production in the western Mediterranean Sea p 31 A89-23438
- National Aeronautics and Space Administration, Lyndon B. Johnson Space Center, Houston, TX.**
- Extension of a drought monitoring and vegetation classification methodology to the western Sahel p 4 A89-28127

- Comparison of measured C-band scattering coefficients with model predictions as a function of leaf area index and Biomass p 8 N89-18712
- National Aeronautics and Space Administration, Langley Research Center, Hampton, VA.**
- Comparison of satellite total ozone measurements with the distribution of tropospheric ozone obtained by an airborne UV-DIAL system over the Amazon Basin p 17 A89-21892
- Trace gas emissions from chaparral and boreal forest fires p 7 A89-32432
- National Aeronautics and Space Administration, Marshall Space Flight Center, Huntsville, AL.**
- VHF radar remote sensing of vertical profile of liquid water content and rainfall rate over Taiwan during the time period of Typhoon Wayne p 48 A89-20771
- National Aeronautics and Space Administration, Wallops Flight Center, Wallops Island, VA.**
- Off-nadir radar altimetry p 68 A89-31947
- National Aerospace Lab., Amsterdam (Netherlands).**
- Updating land-use information on topographic maps using satellite imagery: Combining the advantages of two accessible sources of geographic information p 60 N89-18897
- National Center for Atmospheric Research, Boulder, CO.**
- Applications of the NCAR Electra Doppler radar for the study of physical parameters of clouds p 75 N89-19717
- National Central Univ., Chung-Li (Taiwan).**
- VHF radar remote sensing of vertical profile of liquid water content and rainfall rate over Taiwan during the time period of Typhoon Wayne p 48 A89-20771
- National Electric Reliability Council, Bangor (Wales).**
- Alternative approaches to the classification of upland semi-natural vegetation p 16 N89-18961
- National Remote Sensing Agency, Hyderabad (India).**
- Indian activities in remote sensing applications: Microwave remote sensing p 67 N89-18886
- National Remote Sensing Centre, Farnborough (England).**
- LANDSAT TM study of afforestation in northern Scotland and its impact on breeding bird populations p 10 N89-18732
- Operational remote sensing in the United Kingdom: Problems of image acquisition p 68 N89-18751
- Image processing methods for the presentation of multiple geological datasets from the English Lake District p 25 N89-18793
- Monitoring surface mineral workings using TM and SPOT p 26 N89-18796
- Pattern analysis and the ecological interpretation of satellite imagery p 61 N89-18900
- Naval Ocean Research and Development Activity, Bay Saint Louis, MS.**
- Satellite detection of transient enhanced primary production in the western Mediterranean Sea p 31 A89-23438
- Airborne nonacoustic bathymetric survey flight test results p 51 N89-18937
- Investigations of sea ice using coincident Geosat altimetry and synthetic aperture radar during MIZEX-87 p 46 N89-18945
- Naval Postgraduate School, Monterey, CA.**
- Comparison study of SEASAT scatterometer and conventional wind fields [AD-A200591] p 67 N89-16202
- Local geoid determination using the global positioning system [AD-A202220] p 20 N89-19731
- Naval Research Lab., Washington, DC.**
- Segmentation of Synthetic Aperture Radar (SAR) images of ocean surface by the texture energy transform method [AD-A199536] p 37 N89-15309
- Segmentation of SAR images p 58 N89-18759
- New Brunswick Univ., Fredericton.**
- Integration of digital satellite and geophysical data, Heath Steele Mines, New Brunswick, Canada p 25 N89-18792
- New Mexico State Univ., Las Cruces.**
- Integrated NDVI images for Niger 1986-1987 p 4 A89-28128
- New South Wales Univ., Campbell (Australia).**
- Association of radar backscattering with biophysical characteristics of Australian forests p 10 N89-18731
- New South Wales Univ., Kensington (Australia).**
- SPOT mapping software for Wild Aviolyt BC2 analytical plotter p 60 N89-18824
- Soil influences on vegetation reflectance of a semi-arid shrubland p 13 N89-18880
- Vegetation sampling for studies using remotely sensed data p 13 N89-18883
- New York State Univ., Binghamton.**
- Bidirectional canopy reflectance and its relationship to vegetation characteristics p 6 A89-30264

- Norwegian Computing Center, Oslo (Norway).**
- Satellite imagery for semi-automatic map revision p 61 N89-18957
- Norwegian Defence Research Establishment, Kjeller.**
- Interpreting SAR images by means of map information p 58 N89-18760
- Simulation of SAR imaging of ship wakes p 41 N89-18765
- Automatic ship and ship wake detection in spaceborne SAR images from coastal regions p 41 N89-18766

## O

- Office of Naval Research, Arlington, VA.**
- Remote sensing in a marginal ice zone: A brief overview p 46 N89-18941
- Ohio State Univ., Columbus.**
- Reference coordinate systems: An update. Supplement 11 [NASA-CR-184764] p 19 N89-16207
- Open Univ., Milton (England).**
- Mapping in the Oman ophiolite using enhanced Landsat Thematic Mapper images p 23 A89-29301
- Remote sensing of evaporite mineral zonation in salt flats (salars) p 23 A89-30271
- Integration of geological, geophysical and remotely sensed data for the Solway Basin, England p 26 N89-18794
- Applications of LANDSAT Thematic Mapper imagery to the study of subtle variations in lithology p 27 N89-18863
- Investigations of the Cerro Colorado pluton, northern Chile, using enhanced LANDSAT Thematic Mapper images p 27 N89-18930
- Improvements in the forward and inverse principal component transformations for geological mapping in a semi-arid terrain p 27 N89-18933

## P

- Pacific Northwest Labs., Richland, WA.**
- Applications of digital image processing to ongoing research in complex terrain meteorology [DE89-001749] p 57 N89-17375
- Pennsylvania State Univ., University Park.**
- MISR - A multiangle imaging spectroradiometer for geophysical and climatological research from EOS p 66 A89-31946
- Purdue Univ., West Lafayette, IN.**
- The application of remote sensing to geomorphological mapping and mass movement study in the vicinity of Provo, Utah p 23 N89-15439
- A spectral feature design system for high dimensional multispectral data p 60 N89-18894
- Simulation of optical remote sensing systems for earth resource analysis p 74 N89-18964
- Pusat Penelitian Dan Pengembangan, Pengairan (Indonesia).**
- Monitoring of suspended sediments in Jatiluhur Reservoir using satellite images p 50 N89-18740

## R

- Reading Univ. (England).**
- Geological lineament detection using the Hough transform p 26 N89-18818
- Rijkswaterstaat, The Hague (Netherlands).**
- Sea bottom topography with X-band SLAR: Evaluation of existing models p 38 N89-18718
- Rome Univ. (Italy).**
- Tracking algorithms in radar altimetry p 72 N89-18911
- Roskilde Univ. (Denmark).**
- Assessment of land/soil degradation in northern Burkina Faso p 13 N89-18882
- Mapping of natural vegetation in north-east Zimbabwe by means of LANDSAT Thematic Mapper data p 14 N89-18901
- Rothamsted Experimental Station, Harpenden (England).**
- Optimal sampling for remote sensing: Estimating the regional mean p 11 N89-18822
- Royal Aerospace Establishment, Farnborough (England).**
- A study of the effect of rain on Seasat radar altimeter data p 44 N89-18840
- Royal Signals and Radar Establishment, Malvern (England).**
- Image compression using a neural network p 58 N89-18705
- A comparison of clutter texture properties in optical and SAR images p 8 N89-18708
- Real-time stereo matching SPOT using transputer arrays p 74 N89-18958

## S

- Saint John's Coll., Annapolis, MD.**
- Ocean wave directional spectra and wave-current interaction in the Agulhas from the Shuttle Imaging Radar-B synthetic aperture radar p 30 A89-22585
- San Diego State Univ., CA.**
- Tersail - A numerical model for combined analysis of vegetation canopy bidirectional reflectance and thermal emissions p 6 A89-29415
- Scottish Agricultural Statistics Service, Edinburgh.**
- Normal distributional assumptions in discrimination p 59 N89-18821
- Scranton Univ., PA.**
- Effects of solar angle on reflectance from wetland vegetation p 5 A89-29409
- Scripps Institution of Oceanography, San Diego, CA.**
- A multi-sensor remote sensing approach for measuring primary production from space [NASA-CR-184662] p 37 N89-15444
- Selenia Spazio S.p.A., Rome (Italy).**
- The advanced terrain tracking altimeter instrument p 74 N89-18954
- Sepimage, Puteaux (France).**
- Effects of slopes and relief two-dimensional spatial frequencies on spaceborne SAR imagery p 59 N89-18777
- Sheffield Univ. (England).**
- Optimal sampling for remote sensing: Estimating the regional mean p 11 N89-18822
- Change detection in AGRISAR images p 15 N89-18949
- Sherbrooke Univ. (Quebec).**
- Observations of the effect of geometric properties of agricultural soils on radar backscatter, from C-SAR images p 11 N89-18781
- South Carolina Univ., Columbia.**
- The derivation and verification of surface reflectances using airborne MSS data and a radiative transfer model [DE89-004881] p 67 N89-17931
- A comparison of original aircraft MSS and generated surface water reflectance images as predictors of lake water quality indicators [DE89-004882] p 50 N89-17932
- Southampton Univ. (England).**
- The directional reflectance of heather canopies: Towards a descriptive model p 13 N89-18878
- Spar Aerospace Ltd., Ste-Anne-de-Bellevue (Quebec).**
- Taking a broader view: Radarsat adds ScanSAR to its operations p 73 N89-18925
- ST Systems Corp., Lanham, MD.**
- Land image data processing requirements for the EOS era p 56 A89-31949
- ST Systems Corp., Hampton, VA.**
- Trace gas emissions from chaparral and boreal forest fires p 7 A89-32432
- State Oceanic Administration, Zhejiang (China).**
- Quick reporting state of fishery and sea on the East China Sea and the Yellow Sea with NOAA p 39 N89-18741
- The preliminary study of current shifting state by the use of infrared images of NOAA-9 p 39 N89-18742
- A preliminary study on nearshore water in China with NOAA satellite images p 40 N89-18743
- Sverdrup Technology, Inc., Middleburg Heights, OH.**
- Estimation of sea-ice type and concentration by linear unmixing of Geosat altimeter waveforms p 47 N89-18946
- Swales and Associates, Beltsville, MD.**
- Optical system design alternatives for the Moderate-Resolution Imaging Spectrometer-Tilt (MODIS-T) for the Earth Observing System (EOS) p 63 A89-27753
- Systems Designers Ltd., Camberley (England).**
- Progress in automatic analysis of multi-temporal remotely-sensed data p 61 N89-18956

## T

- Technical Univ. of Denmark, Lyngby.**
- The Technical University of Denmark (TUD) C-band SAR p 74 N89-18928
- Technische Hogeschool, Delft (Netherlands).**
- Monitoring of suspended sediments in Jatiluhur Reservoir using satellite images p 50 N89-18740
- Technische Univ., Delft (Netherlands).**
- An algorithm for analysis of plate motions in Crust Dynamics Project (CDP) networks [B8821606] p 19 N89-17371
- The geometry of geodetic inverse linear mapping and nonlinear adjustment [ETN-89-93900] p 20 N89-19736
- Tel-Aviv Univ. (Israel).**
- Dependence of snow melting and surface-atmosphere interactions on the forest structure p 3 A89-21740

**Telespazio, S.p.A., Rome (Italy).**

Crops radar responses analysis based on AGRISAR '86 data p 15 N89-18947

**Terra Investigations and Imaging Ltd., Surrey (England).**

Major crustal lineaments on Seasat SAR and their off-shore extensions in the UK p 26 N89-18861

**Texas Univ., Arlington.**

The leaf-shape effect on electromagnetic scattering from vegetated media p 12 N89-18846

The extinction properties of forest components p 14 N89-18918

**TGS Technology, Inc., Moffett Field, CA.**

Monitoring water quality and river plume transport in Green Bay, Lake Michigan with SPOT-1 imagery p 49 A89-32338

**Tokyo Univ. (Japan).**

An atmospheric correction method for AVHRR infrared data using HIRS/2 data p 69 N89-18828

A mathematical model of reflectance and transmittance of plant leaves as a function of chlorophyll pigment content p 13 N89-18879

**Tor Vergata Univ., Rome (Italy).**

Comparison between microwave emissivity and backscattering coefficient of agricultural fields p 12 N89-18844

**Tromsø Univ. (Norway).**

Remote studies of the ocean surface by a tower-based multifrequency microwave radar p 41 N89-18785

**Tubitak, Kocaeli (Turkey).**

Wigner distribution analysis of surface waves p 42 N89-18789

**U****University Coll., Cardiff (Wales).**

Improvements in ground water recharge estimation using satellite remote sensing p 50 N89-18768

An assessment of ATM and satellite data for estimating the groundwater contribution to slope stability p 51 N89-18769

**University Coll., London (England).**

A synthetic aperture altimeter p 73 N89-18913

A new approach to topographic altimetry p 73 N89-18914

Real-time stereo matching SPOT using transputer arrays p 74 N89-18958

A study of advanced radar altimeter techniques [ESA-CR(P)-2699] p 75 N89-19483

**University of South Florida, Saint Petersburg.**

Spectral transmissometer and radiometer - Design and initial results p 64 A89-27991

**V****Vexcel Corp., Boulder, CO.**

Concepts for processing and analyzing of multiple SAR and Landsat images p 55 A89-27789

Requirements for an EOS-oriented workstation p 69 N89-18813

**W****Wageningen Agricultural Univ. (Netherlands).**

Extraction of small-scale spatial information from SLAR raw data of forests through an analysis of speckle p 8 N89-18709

**Washington Univ., Seattle.**

Estimating sea ice concentration from satellite passive microwave data and a physical model p 42 N89-18797

**Wisconsin Univ., Madison.**

Remote sensing of canopy chemistry and nitrogen cycling in temperate forest ecosystems p 3 A89-23431

Monitoring water quality and river plume transport in Green Bay, Lake Michigan with SPOT-1 imagery p 49 A89-32338

Progress of research to identify rotating thunderstorms using satellite imagery [NASA-CR-183555] p 68 N89-17981

**Woods Hole Oceanographic Institution, MA.**

Remote sensing of canopy chemistry and nitrogen cycling in temperate forest ecosystems p 3 A89-23431

**World Meteorological Organization, Geneva**

(Switzerland). Hydrological aspects of combined effects of storm surges and heavy rainfall on river flow [WMO-704] p 49 N89-17340

**Wyoming Univ., Laramie.**

Measurements of springtime Antarctic ozone depletion and development of a balloonborne ultraviolet photometer p 67 N89-15459

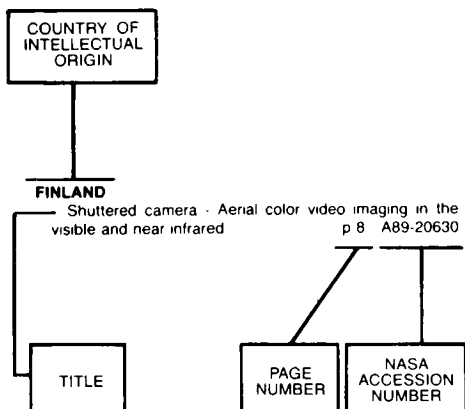
**Y****York Univ., Downsview (Ontario).**

Shipborne passive microwave sea ice experiment in the East Greenland Sea: May-July 1987 p 42 N89-18799

**Z****Zurich Univ. (Switzerland).**

Dependence of snow melting and surface-atmosphere interactions on the forest structure p 3 A89-21740

## Typical Foreign Technology Index Listing



Listings in this index are arranged alphabetically by country of intellectual origin. The title of the document is used to provide a brief description of the subject matter. The page number and the accession number are included in each entry to assist the user in locating the citation in the abstract section. If applicable, a report number is also included as an aid in identifying the document.

### A

#### AUSTRALIA

- Land use and land cover applications of Landsat MSS data p 17 A89-20813
- Wavenumber spectra of short gravity waves p 35 A89-30019
- Comparison of NOAA/AVHRR-2 sea surface temperatures with surface measurements in coastal waters p 36 A89-30259
- Unsupervised training area selection in forests using a nonparametric distance measure and spatial information p 6 A89-30265
- Association of radar backscattering with biophysical characteristics of Australian forests p 10 N89-18731
- Mapping of phytoplankton fluorescence with the Fluorescence Line Imager (FLI) imaging spectrometer p 39 N89-18737
- SPOT mapping software for Wild Aviolyt BC2 analytical plotter p 60 N89-18824
- Soil influences on vegetation reflectance of a semi-arid shrubland p 13 N89-18880
- Vegetation sampling for studies using remotely sensed data p 13 N89-18883

#### AUSTRIA

- Spectral response characteristics of a metal-stressed coniferous forest as measured by the Fluorescence Line Imager (FLI) airborne imaging spectrometer p 9 N89-18724

### B

#### BELGIUM

- The use of SPOT-1 imagery for forest classification in Flanders (Belgium) p 14 N89-18899

#### BRAZIL

- Study of geometric quality of the MSS-LANDSAT imagery [INPE-4653-PRE/1360] p 57 N89-15440

- Knowledge related aspects of lineation and lineament extraction [INPE-4709-PRE/1391] p 24 N89-15446
- Using different sources of information in automated linear feature extraction from remote sensing data [INPE-4708-PRE/1390] p 24 N89-15447
- Automatic registration of satellite imagery [INPE-4637-PRE/1349] p 57 N89-17414
- The impact of multiviewing reflectance data on the estimation of suspended sediment concentration p 50 N89-18735
- Microwave X-band radiometric characterization of Brazilian soils by measurement of the complex permittivity p 11 N89-18773

#### BULGARIA

- Determination of relative crop areas from spectrometric data p 22 A89-22218
- Distribution of specular points on the ocean surface: Bistatic scattering p 38 N89-18721
- Study on directional spectrum characteristics of marine radar images of ocean waves p 41 N89-18786

### C

#### CANADA

- First results of topographical mapping using SPOT images of Malaysia p 52 A89-20764
- STAR-1 high resolution synthetic aperture radar imagery for precious metal exploration p 21 A89-20827
- A simulation for spaceborne SAR imagery of a distributed, moving scene p 33 A89-26846
- FEX - A knowledge-based system for planimetric feature extraction p 54 A89-27783
- Application of Landsat imagery and surficial geochemistry to the discovery of tungsten skarn deposits associated with buried plutons, Yukon and Northwest Territories, Canada p 23 A89-28126
- Extreme variability, scaling and fractals in remote sensing - Analysis and simulation p 56 A89-29074
- Multispectral classification of land use at the rural-urban fringe using spot data p 18 A89-29371
- Analysis of atmospheric effects in SPOT HRV images p 65 A89-29372
- Analysis and interpretation of SPOT images of urban and agricultural/forest sections of the Sherbrooke region p 5 A89-29373
- Area measurement of agricultural fields from satellite images p 5 A89-29374
- Comparative spectral analysis of HRV and TM sensors p 65 A89-29375
- Accuracy assessment of Landsat-based visual change detection methods applied to the rural-urban fringe p 18 A89-29437
- Determining the age of cut forest areas in Quebec, Canada using the Landsat-5 TM p 7 A89-31893
- On-line aspects of stereophotogrammetric processing of SPOT images p 66 A89-32334
- A comparison of images from a pushbroom scanner with normal color aerial photographs for detecting scattered recent conifer mortality p 7 A89-32336
- Estimation of the SAR system transfer through processor defocus p 37 N89-18706
- Assessment of clearcut mapping accuracy with C-band SAR p 9 N89-18725
- Texture analysis of forest regeneration sites in high-resolution SAR imagery p 10 N89-18730
- Monitoring offshore water quality from space p 39 N89-18739
- Satellite data acquisition planning at the Canada Center for Remote Sensing p 68 N89-18753
- The central user services system for ERS-1 p 68 N89-18754
- Observations of the effect of geometric properties of agricultural soils on radar backscatter, from C-SAR images p 11 N89-18781
- Mapping slope failure tracks with digital Thematic Mapper data p 59 N89-18790
- Integration of digital satellite and geophysical data, Heath Steele Mines, New Brunswick, Canada p 25 N89-18792

- Shipborne passive microwave sea ice experiment in the East Greenland Sea: May-July 1987 p 42 N89-18799
- Real-time processing of digital image data in support of the Canadian sea ice analysis and prediction program p 43 N89-18803
- Toward the automated use of remote sensing data in operational ice forecasting p 43 N89-18804
- A high fidelity, high throughput system for geocoding SAR imagery p 60 N89-18849
- Towards a calibration of the CCRS airborne SARS p 70 N89-18854
- Auto and cross correlation analysis of environment, system and target parameters for iceberg detection using airborne radar p 45 N89-18874
- Taking a broader view: Radarsat adds ScanSAR to its operations p 73 N89-18925

#### CHINA, PEOPLE'S REPUBLIC OF

- The studies for the computer classification and the investigation of grasslands in Tibet using Space-Lab color infrared image p 1 A89-20754
- Application of airborne scanners in remote sensing of sea p 29 A89-20789
- The preliminary study on correlation between satellite information and bottom trawling ground in the East China Sea and the Yellow Sea p 29 A89-20805
- The development of remote sensing in China p 76 A89-31560
- Quantitative remote detection of suspended sediment content and chlorophyll concentration of water in different depths p 50 N89-18733
- Quick reporting state of fishery and sea on the East China Sea and the Yellow Sea with NOAA p 39 N89-18741
- The preliminary study of current shifting state by the use of infrared images of NOAA-9 p 39 N89-18742
- A preliminary study on nearshore water in China with NOAA satellite images p 40 N89-18743
- A simulation test for soil moisture sensing p 10 N89-18772

### D

#### DENMARK

- An ERDAS module for routine processing of AVHRR data p 43 N89-18817
- Assessment of land/soil degradation in northern Burkina Faso p 13 N89-18882
- Mapping of natural vegetation in north-east Zimbabwe by means of LANDSAT Thematic Mapper data p 14 N89-18901
- The Technical University of Denmark (TUD) C-band SAR p 74 N89-18928
- The structure and variability of a filament in the northwest African upwelling area as observed from AVHRR and CXCS images p 46 N89-18939

### E

#### ESTONIA

- Brightness of a laser-beam halo in vegetation cover p 3 A89-22221

### F

#### FINLAND

- Backscatter behavior of low-salinity sea ice at C and X-band p 44 N89-18869

#### FRANCE

- Digital Terrain Model computation using SPOT data p 53 A89-20807
- Landsat 5 TM image of the Mont Saint-Michel region of France p 54 A89-21249
- Contribution of second-generation Landsat TM and SPOT HRV satellites to urban analysis (Rennes, France) p 17 A89-21250
- Cartographic analysis of Large Format Camera photographs - Comparison with SPOT and the Spacelab metric camera p 62 A89-21410

Satellite determination of the carbon dioxide exchange coefficient at the ocean-atmosphere interface - A first step p 31 A89-22598

JEOS - A low-cost approach to earth observation p 63 A89-26399

Simulated effects of barometric pressure and ozone content upon the estimate of marine phytoplankton from space p 33 A89-26443

Use of surface temperature in agrometeorology p 4 A89-27942

Multiple source data processing in remote sensing p 56 A89-29073

Complementarity of middle-infrared with visible and near-infrared reflectance for monitoring wheat canopies p 5 A89-29410

Application of a flux algorithm to a field-satellite campaign over vegetated area p 6 A89-29411

Remote sensing of macrophytic algae of the Molene Archipelago in France - Terrain radiometry and application to SPOT satellite data p 36 A89-30260

Theoretical study of the sensitivity of the microwave backscattering coefficient to the soil surface parameters p 6 A89-30267

An experiment to invert Seasat altimetry for the Mediterranean and Black Sea mean surfaces p 36 A89-30900

Geological mapping and analysis of fracturing in the south part of the Central Anti-Atlas in Morocco using a Landsat MSS image p 23 A89-31887

The classification of loamy ground in the Outre-Forêt region of Alsace in France using Landsat 5 TM images p 7 A89-31890

Integration of SPOT data in an urban data bank - Locating work sites p 18 A89-31891

Combining oblique SPOT-1 images for the analysis of certain soil properties p 7 A89-31892

Multitemporal study of differently farmed permanent grazing lands in the Lorraine region of France using SPOT-1 data p 7 A89-31894

The 1988 International Geoscience and Remote Sensing Symposium (IGARSS 1988) on Remote Sensing: Moving Towards the 21st Century, volume 3

[ESA-SP-284-VOL-3] p 68 N89-18704

Adaptive speckle filtering for SAR images p 58 N89-18710

Nonlinear filtering and edge detection in speckled radar images p 58 N89-18711

Multitemporal and dual polarization of agricultural crops by X-band SAR images p 9 N89-18716

Statistical evaluation of the intensity distribution of sea surface radar images p 38 N89-18717

Possibilities of the satellite imagery to locate the forest decline areas in the Vosges Massif (France) p 10 N89-18729

Effects of slopes and relief two-dimensional spatial frequencies on spaceborne SAR imagery p 59 N89-18777

Proceedings of the 1988 International Geoscience and Remote Sensing Symposium (IGARSS) '88 on Remote Sensing: Moving Towards the 21st Century, Volume 2 [ESA-SP-284-VOL-2] p 69 N89-18836

Preprocessing of the VARAN synthetic aperture airborne radar p 70 N89-18856

## G

### GERMANY, FEDERAL REPUBLIC OF

Airborne multispectral remote sensing of forest decline in West Germany p 1 A89-20757

Satellite sea surface temperature at the North Atlantic Polar Front related to high-resolution towed conductivity-temperature-depth data p 31 A89-22594

Alternatives for mapping from satellites p 62 A89-26398

Fundamentals of remote sensing p 63 A89-27934

Sensors p 63 A89-27935

Extraction of surface temperature from satellite data p 33 A89-27941

Investigation of information content of Thematic Mapper and SPOT multiband image data, using simulated image data of the Freiburg region (Federal Republic of Germany)

[ESA-TT-975] p 57 N89-15442

German spaceborne remote sensing activities p 67 N89-16887

Reports on cartography and geodesy, series 1, number 100

[ISSN-0469-4236] p 20 N89-17935

Correlation of reflectance and chlorophyll fluorescence signatures of healthy and damaged forest trees p 9 N89-18726

Correlation of radar reflectivity and chlorophyll fluorescence of forest trees p 9 N89-18727

Data processing for the determination of pigments and suspended solids from Thematic Mapper data p 50 N89-18736

Investigations of SAR backscatter for different test areas using two geocoded Seasat SAR scenes p 58 N89-18761

X-SAR: A new spaceborne synthetic aperture radar p 73 N89-18923

E-SAR: The experimental airborne L/C-band SAR system of DFVLR p 73 N89-18924

Results of tectonic and spectral investigations in the coast range of northern Chile using special processed Thematic Mapper (TM) data p 27 N89-18929

A study of passive microwave remote sensing p 45 N89-18938

Extraction of agricultural plant parameters from multitemporal Thematic Mapper (TM) and X-SAR data p 15 N89-18948

Correlations between agricultural plant parameters and multitemporal radar scatterometer data: First results from the European AGRISCATT 87 campaign p 16 N89-18951

### GREECE

Visual and digital classification of Landsat TM data for soil, physiography and land use mapping in Axios alluvial plain, Thessaloniki, Greece p 5 A89-28130

## H

### HUNGARY

X-band scatterometry in agriculture p 9 N89-18715

## I

### INDIA

Comparative study of vegetation index and false colour composite image of NOAA-AVHRR data for bio-mass studies p 1 A89-20752

On classification of forests of some portions of central India using satellite imageries p 2 A89-20761

Relationship of spectral data and grain yield variation in rice (*Oryza sativa* L.) ADT 31 p 2 A89-20762

Mapping of construction material sites around Bangalore City using Landsat Thematic Mapper data p 52 A89-20782

On geology of some districts in Central India using Landsat imageries p 21 A89-20808

Assessing extent of damage caused by flooding and drought in dominantly rice cropland area using Landsat data p 2 A89-20814

Correlation of Landsat TM and aeromagnetic data along the Eastern Margin of the Cuddappah Basin, South India p 21 A89-20817

Prioritization of watershed with regard to silt yield potential through data integration technique p 48 A89-20818

Aerial remote sensing technique in the identification and acreage estimation of various plantations - A case study in Gorakhpur district, Uttar Pradesh, India p 2 A89-20819

Identification of geological features from their surface textural properties using OPS measurements p 21 A89-20820

Feature extraction considerations in utilising the optical power spectra for terrain classification p 54 A89-20821

Integrated study of Landsat, aeromagnetic and Bouguer gravity anomaly data for geological appraisal - A case study from Tamil Nadu, India p 21 A89-20823

Usefulness of remote sensing in uranium exploration programme in parts of Karnataka state, India p 21 A89-20828

Application of the Haar transform for extraction of linear and anomalous patterns over part of Cambay Basin, India p 55 A89-28037

UV laser fluorosensor for remote sensing p 35 A89-29763

Digital processing of a lineament grid with the aim of analyzing regional tectonic structures of the western Himalayas in India p 23 A89-30116

Delineation of salt-affected soils through digital analysis of Landsat MSS data p 6 A89-30262

Wasteland identification in India using satellite remote sensing p 18 A89-30263

Indian activities in remote sensing applications: Microwave remote sensing p 67 N89-16886

Specular scattering with effective reflection coefficient p 39 N89-18723

### INDONESIA

Asian Conference on Remote Sensing, 8th, Jakarta, Indonesia, Oct. 22-27, 1987, Proceedings p 76 A89-20751

Digital image analysis of Landsat MSS data in an estate crop inventory of the Island of Bali p 1 A89-20756

Soil and vegetation mapping by using SPOT image p 1 A89-20758

Forest observation by satellite p 1 A89-20759

Remote sensing applications for agricultural land use survey in Indonesia - Isimu case study p 2 A89-20763

Principle component transformation analysis for tentative land use interpretation of Landsat MSS of Bogor region, Indonesia p 52 A89-20767

Monitoring inundation area of Aliran Sungai Bengawan Solo Jawa Timur with Landsat images p 48 A89-20768

Soil surface moisture estimation - A case study area on North Banten, West Java, Indonesia p 2 A89-20773

Flooded and inundation dangerous area prediction and its visualisation - A case study on the Pemali-Comal River Basin, Central Java, Indonesia p 48 A89-20774

The use of image enhancement technique for peat land mapping using Landsat mass data in Indonesia p 52 A89-20775

Identification of surface-groundwater interaction zones in the Bogor volcanic fan p 48 A89-20777

Drainage pattern analysis with the aid of Landsat MSS data of the Citarium river basin, West Java, Indonesia p 48 A89-20778

Radar imagery as a tool for mineral exploration - A case study of gold mineralization in East Kalimantan p 20 A89-20780

The geology of the area surrounding Lake Kerinci, Indonesia as interpreted through SIR-B imageries p 20 A89-20781

Volcanic eruption monitoring using satellite platform p 20 A89-20783

The use of aerial photographs in Quaternary-volcanic terrains mapping p 20 A89-20784

Suspended solid classification of the Jakarta Bay p 28 A89-20785

The extraction of sea fishery potential area from Airborne Ocean Color Radiometer data p 28 A89-20786

The retrieval of sea surface temperature from NOAA-AVHRR satellite data - Comparison between Singh's and McClain's methods p 28 A89-20787

The role of remote sensing in geographic information systems using computer p 17 A89-20792

The creating of blue synthetic channel of MSS Landsat image p 52 A89-20794

The navigation method for NOAA-AVHRR image p 61 A89-20795

Application of three dimensional image system p 53 A89-20797

Low-cost second order planimetric mapping technique p 53 A89-20800

Aerospace imagery and data for modelling erosion, sediment yield and crop yield prediction using GIS, applied to the Upper Komering catchment, Sumatra p 2 A89-20802

Coastline monitoring in Madura Strait, Indonesia on 1972-1985 p 29 A89-20804

The application of remote sensing for forest inventory p 2 A89-20809

Study of the monitoring of land cover/use using remote sensing data by personal computer in southern part of Bandung area, West Java p 2 A89-20815

SPOT for mapping of actual land information p 54 A89-20816

Application of remote sensing for hydrocarbon exploration on Timor Island, Indonesia p 21 A89-20825

Airborne gravity as a supporting tool for hydrocarbon exploration in Indonesia p 21 A89-20829

### INTERNATIONAL ORGANIZATION

Reconnaissance groundwater appraisal of Bohol Island, Philippines, by satellite data analysis p 48 A89-20772

Validation of a synthetic aperture radar ocean wave imaging theory by the Shuttle Imaging Radar-B experiment over the North Sea p 30 A89-22586

Operational calibration of Meteosat's infrared channel p 62 A89-22622

Some aspects of space applications for disaster management - The use of space technology for disaster warning and for determining the effects of natural disasters [IAF PAPER 86-426] p 18 A89-24849

Hindcasts and data assimilation studies with the WAM model during the Seasat period p 32 A89-26442

Applications of remote sensing to agrometeorology; Proceedings of the Course, Ispra, Italy, Apr. 6-10, 1987 p 63 A89-27933

The vegetation index and the study of vegetation dynamics p 4 A89-27945

### ISRAEL

A method to forecast open pack ice speed of motion using remotely-sensed data p 42 N89-18801

### ITALY

Determination of atmospheric turbidity from remotely-sensed data - A case study p 34 A89-28034

Optical properties of sea water bodies: Measurements with an underwater radiometer and a high-resolution spectroradiometer p 39 N89-18734  
 A quantitative geomorphology study of main carbonate massifs of central and southern Apennines (Italy) based on a digital elevations archive p 25 N89-18791  
 Information fusion by a knowledge-based system for SAR image interpretation p 60 N89-18831  
 Comparison between microwave emissivity and backscattering coefficient of agricultural fields p 12 N89-18844

Post-processing airborne SAR data for multitemporal land-cover studies p 12 N89-18857  
 Image-based atmospheric correction of multitemporal Thematic Mapping data for agricultural land cover classification p 14 N89-18895  
 Tracking algorithms in radar altimetry p 72 N89-18911  
 Radiometric problems in the use of the Thematic Mapper for marine research p 46 N89-18940  
 Crops radar responses analysis based on AGRISAR '86 data p 15 N89-18947  
 The advanced terrain tracking altimeter instrument p 74 N89-18954

## J

## JAPAN

Spectral reflectance properties of a leaf of some mangrove species in Okinawa p 1 A89-20753  
 The use of SPOT imagery in Medan agriculture area for monitoring features changes p 1 A89-20755  
 Accuracy of land-cover/use classification p 52 A89-20765  
 Land use suitability classification using remote sensing data and geographic information for volcanic regions p 16 A89-20766  
 An estimation of areal evapotranspiration using Landsat and elevation data p 48 A89-20776  
 Water quality estimation from Landsat data with spectral and sea truth data base system p 28 A89-20788  
 MOS-1 data processing in Tokai Space Center p 52 A89-20790  
 Spatial information processings of TM data p 52 A89-20791  
 Comparison of the orientation's accuracy for SPOT imagery p 53 A89-20798  
 An interactive system for aerial photo orientation of digital stereo image pairs p 53 A89-20799  
 Accuracy of terrain measurement using SPOT HRV data p 53 A89-20801  
 Receiving and processing system for meteorological satellite (NOAA) p 53 A89-20806  
 New technology for displaying of NOAA AVHRR thermal band image p 29 A89-20810  
 A basic study of the reduction of the exactness of mesh data map made by uniting n-squared meshes to one mesh p 54 A89-20811  
 Geometric correction of SPOT image p 54 A89-20812

Distribution and variations of oceanic carbon dioxide in the western North Pacific, eastern Indian, and Southern Ocean south of Australia p 29 A89-20925  
 Ocean wave spectra derived from Shuttle Imaging Radar-B imagery and surface measurements p 30 A89-22583  
 Observation of the degree of glaciation in middle-level stratiform clouds p 62 A89-23464  
 A procedure for land area classification using Landsat TM digital imagery p 17 A89-24651  
 Effectiveness of satellite remote sensing on monitoring of marine environment [IAF PAPER 88-153] p 32 A89-24875  
 Detection of periodic characteristics of rice field vegetation by microwave backscatter measurement p 5 A89-28364  
 Step frequency radar experiments on the Antarctic Sea ice p 34 A89-28365  
 Water turbidity and perpendicular vegetation indices for paddy rice flood damage analyses p 6 A89-29412  
 Investigation of water content from airborne MSS data p 49 A89-30261  
 A measurement of microwave backscattering coefficients of rice plants p 8 N89-18714  
 Step frequency radar experiments on the Antarctic Sea ice p 43 N89-18802  
 An atmospheric correction method for AVHRR infrared data using HIRS/2 data p 69 N89-18828  
 Measurements of microwave backscatter from conifers p 12 N89-18848  
 Signature variations due to atmospheric and topographic effects on satellite MSS data over rugged terrain p 70 N89-18877

A mathematical model of reflectance and transmittance of plant leaves as a function of chlorophyll pigment content p 13 N89-18879  
 A method for the clustering of remotely sensed multispectral images by using statistical test for spatial uniformity p 61 N89-18898  
 Structure of layer clouds as observed simultaneously by a microwave radiometer and an 8.6 mm-radar p 74 N89-19039

## K

## KENYA

Snow cover-summer monsoon rainfall over parts of Sahel p 51 N89-18832

## N

## NETHERLANDS

SPOT image interpretation for information on human settlement growth p 17 A89-20824  
 Definition and design of an operational environment-monitoring system p 18 A89-27788  
 Platforms p 63 A89-27936  
 The luxuriant image - An introduction to remote sensing data processing p 55 A89-27937  
 Image processing techniques - Filtering, exogenous data, geometrical processing p 55 A89-27938  
 An algorithm for analysis of plate motions in Crust Dynamics Project (CDP) networks [B8821606] p 19 N89-17371  
 Extraction of small-scale spatial information from SLAR raw data of forests through an analysis of speckle p 8 N89-18709  
 Sea bottom topography with X-band SLAR: Evaluation of existing models p 38 N89-18718  
 Monitoring of suspended sediments in Jatiluhur Reservoir using satellite images p 50 N89-18740  
 ERS-1 operation capabilities p 71 N89-18884  
 Engineering calibration of the ERS-1 active microwave instrumentation in orbit p 71 N89-18885  
 ERS-1 altimeter height calibration p 71 N89-18891  
 Quality control of fast delivery processors and products p 72 N89-18892  
 A possibility for selecting spectral bands of future land application sensors at the example of an imaging spectrometer p 60 N89-18896  
 Updating land-use information on topographic maps using satellite imagery: Combining the advantages of two accessible sources of geographic information p 60 N89-18897  
 Radar signature measurements during the AGRISCATT campaigns p 15 N89-18950  
 Mission aspects of a future European polar orbit earth observation facility p 74 N89-18952  
 The effect of soil moisture on reflectance characteristics of salt crusts p 16 N89-18966  
 The use of LANDSAT imagery for water quality studies in the IJsselmeer area (Netherlands) [BCRS-87-18] p 52 N89-19732  
 Land use analysis using remote sensing techniques. Investigation of the usefulness of LANDSAT Thematic Mapper satellite pictures for obtaining and up to date picture of land use in the province South Holland [BCRS-88-01] p 61 N89-19733  
 Salinity mapping based on SPOT images of the Punjab, Pakistan [BCRS-88-03] p 16 N89-19734  
 Study of the use of radar X-band data of bare soil in a radar scattering model [BCRS-88-04] p 16 N89-19735  
 The geometry of geodetic inverse linear mapping and nonlinear adjustment [ETN-89-93900] p 20 N89-19736

## NORWAY

Interpreting SAR images by means of map information p 58 N89-18760  
 Simulation of SAR imaging of ship wakes p 41 N89-18765  
 Automatic ship and ship wake detection in spaceborne SAR images from coastal regions p 41 N89-18766  
 Remote studies of the ocean surface by a tower-based multifrequency microwave radar p 41 N89-18785  
 Satellite imagery for semi-automatic map revision p 61 N89-18957

## P

## POLAND

A model for the propagation of industrial atmospheric pollution registered on multispectral earth images p 17 A89-22213

## PORTUGAL

Nighttime and daytime HCMM thermographs of the Iberian Peninsula p 56 A89-31888  
 Thermal infrared and visible images of the Iberian Peninsula p 56 A89-31889

## S

## SOUTH AFRICA, REPUBLIC OF

Estimating the extent of irrigated cropland in a large catchment using LANDSAT MSS data p 14 N89-18902

## SPAIN

Mapping and inventory of forest fires from digital processing of TM data p 5 A89-28129

## SWEDEN

Development of principal component analysis applied to multitemporal Landsat TM data p 4 A89-28035  
 Observations of ice types in satellite altimeter data p 44 N89-18841  
 Ice ridge observations by means of SAR p 45 N89-18872  
 Evaluation of VARAN-S SAR data from the BEPERS study project p 45 N89-18875  
 Atmospheric attenuation as derived from microwave radiometry at 52.8 GHz p 72 N89-18906

## SWITZERLAND

Hydrological aspects of combined effects of storm surges and heavy rainfall on river flow [WMO-704] p 49 N89-17340

## T

## TAIWAN

Errors of the gravitational field determined by the satellite p 19 A89-24442

## THAILAND

The feasibility study of oil palm area estimation in the southern part of Thailand using Landsat data p 2 A89-20760  
 Applications of SPOT HRV data for land use and soil mapping in Rayong basin p 2 A89-20769  
 Circulation in the East Asian seas from satellite and ship data p 29 A89-20803  
 Study on changes of mangrove forest in Thailand by using Landsat imagery p 3 A89-20822  
 The applications of Landsat imagery to soil erosion study in Northern Thailand p 3 A89-20826

## TURKEY

Wigner distribution analysis of surface waves p 42 N89-18789

## U

## U.S.S.R.

Effective permittivity of vegetation in the microwave range p 3 A89-21612  
 Laser sounding of the troposphere and the underlying surface p 17 A89-22066  
 Determination of the spectrum of energy-containing surface waves from a sun-glitter image p 29 A89-22210  
 Determination of clear-sky planetary albedo p 62 A89-22214  
 Neotectonic zoning of Belorussia on the basis of space data p 21 A89-22215  
 Fault classification for the geological support of the tunnel construction project for the Caucasus mountain-pass railroad, using space images p 22 A89-22216  
 The procedure for and the results of the geological interpretation of photographic images of the Bukhtarma lineament zone p 22 A89-22217  
 A tomographic approach to lineament identification on aerial and space images p 22 A89-22223  
 Procedures for the determination of geophysical parameters from spaceborne microwave polarimeter measurements p 30 A89-22224  
 Principal results of remote-sensing studies of Siberia's natural resources (On the occasion of the 10th anniversary of the Scientific Coordination Council, 1977-1987) p 62 A89-22225  
 Effectiveness of soil mapping on the basis of space photographic data p 3 A89-22249  
 Motion characteristics of sea waves p 32 A89-23590  
 Radar imaging of the surfaces of Venus and the earth using SAR data p 54 A89-23645  
 Features of the calculation of the main characteristics of an oceanographic radar altimeter p 32 A89-23646  
 Agrometeorological aspects of the utilization of remote-sensing data p 3 A89-23663  
 Aerial and space remote-sensing techniques for geographical investigations p 62 A89-26178



Optical methods of satellite hydrophysics. Investigation of the environment from manned orbital stations p 32 A89-26181

Polarization of microwave emission of a water surface in a wide range of angles of sight p 34 A89-28290

Oceanic remote sensing p 35 A89-29726

Laser airborne sensing field experiments using the 'Chaika' assembly p 35 A89-29728

Effects of round trip laser emission propagation through a turbulent surface for laser airborne oceanic sensing p 35 A89-29729

The capabilities of nonlinear Raman spectroscopy for remote diagnostics of water bodies p 35 A89-29730

Detection of ocean bottom relief by local geoid p 35 A89-29731

Surface wave interaction - Theory and capability of oceanic remote sensing p 35 A89-29732

Remote sensing of surface manifestations of short-period internal waves in the ocean p 35 A89-30114

Ring structures of buried platform areas and the evaluation of their tectonic activity on the basis of geomorphological data p 23 A89-30118

Features of the geological structure of the polar Urals and the distribution of certain minerals, as evaluated on the basis of the interpretation of aerial and space photographs p 23 A89-30119

Radiation models of mesotrophic and eutrophic bodies of water p 36 A89-30120

Variations of the infrared emission of snow and ice cover p 49 A89-30121

A method for processing and results of microwave radiometer studies of the earth from the Intercosmos 20 and 21 satellites p 36 A89-30122

Improvement of multispectral color images by intensifying local contrasts p 56 A89-30123

Landscape processing of satellite imagery for a biospheric data bank p 56 A89-30239

Estimation of the water exchange and contamination zones of basins from satellite imagery p 49 A89-30252

The solid oceanic crust (The Lithos project) p 36 A89-32108

Modeling vegetation as a set of scatterers p 7 A89-32110

Principal problems in upgrading quality and efficiency of geological survey work p 24 N89-17910

Annular and block-folded structures on space and aerial photographs p 25 N89-17915

Some results of use of space survey materials in cartographic work p 58 N89-17922

Microcomputer-based radiometer data acquisition and processing system for large-area mapping of soil moisture content in the top one meter layer p 11 N89-18774

Experiments in Bulgaria for determination of soil moisture in the top one-meter layer using microwave radiometry and a priori information p 11 N89-18843

**UNITED KINGDOM**

The crustal field p 22 A89-22877

The relationship between suspended sediment concentration and remotely sensed spectral radiance - A review p 48 A89-24649

Satellite remote sensing of rainfall p 49 A89-27946

The effects of viewing geometry on image classification p 55 A89-28036

The Special Sensor Microwave Imager - A new instrument with rainfall monitoring potential p 64 A89-28038

Airborne MSS for land cover classification p 5 A89-28131

ERS-1 active microwave instrumentation design and performance status [IAF PAPER 87-136] p 65 A89-28329

Digital image processing in remote sensing p 55 A89-29064

Visualization of topographic data using video animation p 55 A89-29066

Microcomputers and mass storage devices for image processing p 65 A89-29070

A 10 km resolution image of the entire night-time earth based on cloud-free satellite photographs in the 400-1100 nm band p 56 A89-30256

Technological limitations to satellite glaciology p 36 A89-30257

Analysis and representation of vegetation continua from Landsat Thematic Mapper data for lowland heaths p 7 A89-30268

Visual and computer classifications of remotely-sensed images - A case study of grasslands in Cambridgeshire p 7 A89-30269

An optimum calibration procedure for radiometers p 65 A89-30270

Remote sensing of evaporite mineral zonation in salt flats (salars) p 23 A89-30271

Image compression using a neural network p 58 N89-18705

Speckle correlation in SAR images of dynamic discrete scatterers p 37 N89-18707

A comparison of clutter texture properties in optical and SAR images p 8 N89-18708

Computer simulation of multipath sea echo near grazing incidence p 38 N89-18722

LANDSAT TM study of afforestation in northern Scotland and its impact on breeding bird populations p 10 N89-18732

The UN declaration of legal principals on remote sensing, 1986 p 76 N89-18748

The Geospace philosophy: A new practical approach in remote sensing and planning for local authorities p 76 N89-18750

Operational remote sensing in the United Kingdom: Problems of image acquisition p 68 N89-18751

Effects of commercialisation on international remote sensing activities p 76 N89-18752

The algorithm development facility: Its role in the development and operation of a satellite data centre p 68 N89-18755

The visibility of linear features in SAR images p 59 N89-18763

Automated linear feature detection and its application to curve location in synthetic aperture radar imagery p 59 N89-18764

Improvements in ground water recharge estimation using satellite remote sensing p 50 N89-18768

An assessment of ATM and satellite data for estimating the groundwater contribution to slope stability p 51 N89-18769

Digital elevation models and their application to remote sensing of water resources p 51 N89-18770

Estimation of the area of Lake Kariba, Zimbabwe, using LANDSAT MSS imagery p 51 N89-18775

Image processing methods for the presentation of multiple geological datasets from the English Lake District p 25 N89-18793

Integration of geological, geophysical and remotely sensed data for the Solway Basin, England p 26 N89-18794

Monitoring surface mineral workings using TM and SPOT p 26 N89-18796

Geological lineament detection using the Hough transform p 26 N89-18818

Normal distributional assumptions in discrimination p 59 N89-18821

Optimal sampling for remote sensing: Estimating the regional mean p 11 N89-18822

Monitoring of agro-forestry production systems in the Sudano-Sahelian zone of West Africa p 11 N89-18825

Artefacts in AIS-I imagery p 69 N89-18826

Assimilation of altimeter data into numerical ocean models p 43 N89-18838

A study of the effect of rain on Seasat radar altimeter data p 44 N89-18840

Satellite radar altimetry over arid regions p 69 N89-18842

New architecture for a real-time SAR processor p 69 N89-18850

Impact of phase and amplitude errors on the ERS-1 active microwave instrumentation performance p 70 N89-18853

Enhancement of glacial fractures by analysis of Thematic Mapper data: Glen Roy, Scotland p 26 N89-18859

Interpreting the geology of Glen Coe using LANDSAT MSS data and aerial photographs p 26 N89-18860

Major crustal lineaments on Seasat SAR and their off-shore extensions in the UK p 26 N89-18861

Preprocessing and analysis of airborne visible near and shortwave infrared data for the detection of alteration in weathered vegetated terrain p 12 N89-18862

Applications of LANDSAT Thematic Mapper imagery to the study of subtle variations in lithology p 27 N89-18863

The directional reflectance of heather canopies: Towards a descriptive model p 13 N89-18878

Problems in the estimation of barley yields by remote sensing p 13 N89-18881

The pre-launch performance verification of the ERS-1 active microwave instrumentation p 71 N89-18886

A software package for performance evaluation of the ERS-1 AMI p 71 N89-18887

ERS-1 active microwave instrumentation engineering model performance p 71 N89-18888

Stability considerations for the ERS-1 wind scatterometer radiometric performance p 71 N89-18889

ERS-1 AMI antennas: The design and development experience p 71 N89-18890

A SAR data quality assessment scheme for the ERS-1 mission p 72 N89-18893

Pattern analysis and the ecological interpretation of satellite imagery p 61 N89-18900

An advanced terrain tracking altimeter p 45 N89-18910

A synthetic aperture altimeter p 73 N89-18913

A new approach to topographic altimetry p 73 N89-18914

Advanced SAR concepts p 73 N89-18926

Investigations of the Cerro Colorado pluton, northern Chile, using enhanced LANDSAT Thematic Mapper images p 27 N89-18930

Geological applications of thermal infrared characteristics of vegetation p 27 N89-18932

Improvements in the forward and inverse principal component transformations for geological mapping in a semi-arid terrain p 27 N89-18933

An evaluation of surface emittance and temperature data derived from Thermal Infrared Multispectral Scanner (TIMS) for lithological mapping in weathered vegetated terrain: N. Queensland, Australia p 27 N89-18934

The use of coregistered LANDSAT MSS, TM and SIR-A imagery for lithological mapping p 28 N89-18936

Change detection in AGRISAR images p 15 N89-18949

Progress in automatic analysis of multi-temporal remotely-sensed data p 61 N89-18956

Real-time stereo matching SPOT using transputer arrays p 74 N89-18958

Textural and spectral features as an aid to cloud classification p 74 N89-18960

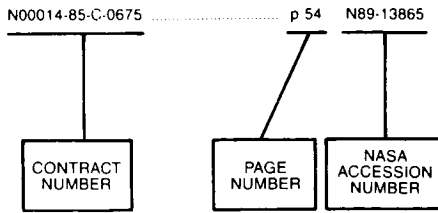
Alternative approaches to the classification of upland semi-natural vegetation p 16 N89-18961

A study of advanced radar altimeter techniques [ESA-CR(P)-2699] p 75 N89-19483

Directional wave data recorded in the southern North Sea [IOS-258] p 47 N89-19793

# CONTRACT NUMBER INDEX

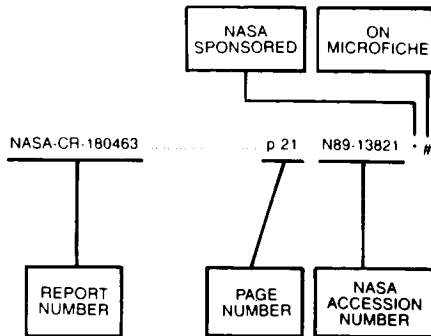
## Typical Contract Number Index Listing



Listings in this index are arranged alphanumerically by contract number. Under each contract number, the accession numbers denoting documents that have been produced as a result of research done under the contract are arranged in ascending order with the AIAA accession numbers appearing first. The accession number denotes the number by which the citation is identified in the abstract section. Preceding the accession number is the page number on which the citation may be found.

N00014-85-C-0675	p 54	N89-13865		
			CONTRACT NUMBER	
			PAGE NUMBER	
			NASA ACCESSION NUMBER	
AID-AFR-0242-C-003017-00	p 4	A89-28128		
ARPA ORDER 5351	p 76	N89-19868		
BCRS-PROJ. AO-2.1	p 16	N89-19735		
BCRS-PROJ. CO-1.6	p 16	N89-19734		
BCRS-PROJ. TO-3.4	p 61	N89-19733		
BCRS-4532/T0-2.7	p 50	N89-18740		
BMFT-01-QS-86090	p 15	N89-18948		
BMFT-01-QS-86174	p 30	A89-22586		
BMFT-01-QS-87033	p 15	N89-18948		
CNES-86-1227	p 31	A89-22598		
CNRS-ATP-0693	p 36	A89-30900		
DAAG29-80-C-0012	p 3	A89-22728		
DAAG29-85-K-0227	p 14	N89-18917		
	p 75	N89-19475		
DACA39-87-K-0022	p 54	A89-22649		
DACA76-85-C-0003	p 76	N89-19868		
DE-AC06-76RL-01830	p 57	N89-17375		
DE-AC09-76SR-00001	p 67	N89-17931		
	p 50	N89-17932		
DEN-E/5B/CON/935/2043	p 47	N89-19793		
DFG-SFB-133	p 31	A89-22594		
DI-14-12-0001-30340	p 37	N89-17357		
	p 37	N89-17358		
EPA-CR-814274-01-0	p 4	A89-27781		
ESA-6617/85-F-FL(SC)	p 44	N89-18841		
ESA-6635/86-HGE-1	p 72	N89-18893		
ESA-7088/87-NL-JG(SC)	p 73	N89-18913		
	p 75	N89-19483		
ESRIN-6297/86/HGE-II(SC)	p 32	A89-26442		
ESTEC-6483/85-NL-BI	p 45	N89-18910		
F19628-85-K-0018	p 29	A89-21798		
F19628-86-K-0025	p 25	N89-17933		
GSRN-1-7060-0450	p 8	N89-17339		
NAGW-0851	p 37	N89-15444		
NAGW-1165	p 48	A89-20771		
NAGW-1175	p 76	N89-19868		
NAGW-1344	p 47	N89-19102		
NAGW-290	p 64	A89-27990		
NAGW 374	p 5	A89-29409		
NAGW-465	p 64	A89-27991		
NAGW-949	p 28	N89-18935		
NAG5-270	p 54	A89-22649		
NAG5-271	p 6	A89-30266		
NAG5-414	p 31	A89-22876		
NAG5-459	p 19	N89-15476		
NAG5-486	p 12	N89-18846		
	p 14	N89-18918		
NAG5-814	p 19	N89-15476		
NAG5-842	p 24	N89-16199		
NAG8-063	p 48	A89-20771		
NASA TASK 161-10-06	p 66	A89-31947		
NASW-4066	p 23	A89-30271		
NAS5-28767	p 28	N89-18973		
NAS5-28769	p 49	A89-28033		
NAS5-28795	p 67	N89-16205		
	p 75	N89-19729		
NAS5-29373	p 67	N89-16205		
	p 75	N89-19729		
NAS7-100	p 73	N89-18921		
NAS7-923	p 64	A89-27990		
NAS7-934	p 64	A89-27990		
NAS8-33726	p 48	A89-20770		
NAS8-36547	p 68	N89-17981		
NATO-SA-9-9-03-0523/85	p 32	A89-26442		
NATO-0209/87	p 73	N89-18913		
NERC-F60/G6/12	p 26	N89-18818		
NERC-F60/96/12	p 61	N89-18956		
NERC-GR/3/6388	p 23	A89-29301		
NERC-GST/02/123	p 13	N89-18878		
NERC-GST/02/126	p 12	N89-18862		
	p 27	N89-18934		
NERC-GT4/86/TLS/47	p 11	N89-18822		
NGT-50103	p 18	N89-15476		
NOAA-MO-A01-78-00-4320	p 37	A89-32434		
NOAA-NA-84AAD00065	p 49	A89-32338		
NOAA-NA-85AADSG033	p 5	A89-29409		
NSC-75-0202-M008-21	p 48	A89-20771		
NSC-76-0202-M008-23	p 48	A89-20771		
NSERC-A-0766	p 18	A89-29371		
NSERC-A-1765	p 65	A89-29372		
NSERC-A-5252	p 5	A89-29373		
NSERC-A-8643	p 65	A89-29372		
NSF ATM-85-05558	p 3	A89-21740		
NSF ATM-87-05980	p 30	A89-22593		
NSF BSR-87-09242	p 28	N89-18935		
NSF DCR-86-04199	p 76	N89-19868		
NSF DPP-84-15203	p 62	A89-24022		
NSF EAR-80-25723	p 29	A89-21798		
NSF EAR-83-12651	p 23	A89-31755		
NSF EAR-83-13678	p 29	A89-21798		
NSF EAR-85-12724	p 22	A89-22632		
NSF EAR-86-07479	p 23	A89-31755		
NSF ECS-85-04381	p 54	A89-22649		
NSF ECS-85-07405	p 74	N89-18964		
NSF OCE-85-00669	p 30	A89-22592		
NSF OCE-85-15979	p 30	A89-22592		
NSF OCE-86-07962	p 32	A89-26438		
NSG-5265	p 19	N89-16207		
N00014-18-C-0295	p 40	N89-18747		
N00014-81-C-0295	p 40	N89-18744		
N00014-81-C-0915	p 46	N89-18942		
N00014-83-G-0126	p 30	A89-22586		
N00014-83-K-0258	p 54	A89-22649		
	p 47	N89-19792		
N00014-84-C-0832	p 64	A89-27990		
N00014-86-C-0469	p 40	N89-18744		
	p 46	N89-18943		
N00014-86-K-2001	p 37	A89-32434		
N00014-87-C-0418	p 46	N89-18942		
N00039-87-C-5301	p 33	A89-26643		
	p 43	N89-18837		
OMFB-7-12-0127	p 9	N89-18715		
RF PROJ. 761054/711055	p 19	N89-16207		
W-7405-ENG-48	p 57	N89-18204		

## Typical Report Number Index Listing

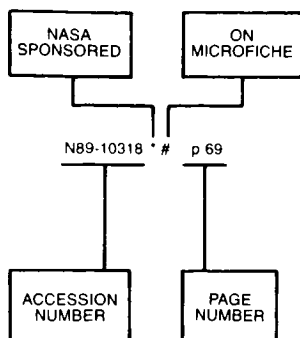


Listings in this index are arranged alphanumerically by report number. The page number indicates the page on which the citation is located. The accession number denotes the number by which the citation is identified. An asterisk (\*) indicates that the item is a NASA report. A pound sign (#) indicates that the item is available on microfiche.

ETN-89-93873	p 61	N89-19733	#
ETN-89-93874	p 16	N89-19734	#
ETN-89-93875	p 16	N89-19735	#
ETN-89-93900	p 20	N89-19736	#
ETN-89-93940	p 75	N89-19483	#
IAF PAPER 86-426	p 18	A89-24849	
IAF PAPER 87-136	p 65	A89-26329	
IAF PAPER 88-153	p 32	A89-24875	#
IEEE-88CH2497-6-VOL-2	p 69	N89-18836	#
IEEE-88CH2497-6-VOL-3	p 68	N89-18704	#
INPE-4637-PRE/1349	p 57	N89-17414	#
INPE-4653-PRE/1360	p 57	N89-15440	#
INPE-4708-PRE/1390	p 24	N89-15447	#
INPE-4709-PRE/1391	p 24	N89-15446	#
IOS-258	p 47	N89-19793	#
ISBN-92-63-10704	p 49	N89-17340	#
ISSN-0379-8566	p 68	N89-18704	#
ISSN-0379-8566	p 69	N89-18836	#
ISSN-0469-4236	p 20	N89-17935	#
LC-87-83254	p 68	N89-18704	#
LC-87-83254	p 69	N89-18836	#
MPL-U-42/87	p 31	A89-22876	*
NAS 1.15:100718	p 67	N89-16205	* #
NAS 1.15:100720	p 75	N89-19729	* #
NAS 1.15:101042	p 8	N89-17339	* #
NAS 1.26:183405	p 24	N89-16199	* #
NAS 1.26:183555	p 68	N89-17981	* #
NAS 1.26:184604	p 19	N89-15476	* #
NAS 1.26:184662	p 37	N89-15444	* #
NAS 1.26:184683	p 28	N89-18973	* #
NAS 1.26:184764	p 19	N89-16207	* #
NAS 1.26:184805	p 47	N89-19102	* #
NASA-CR-183405	p 24	N89-16199	* #
NASA-CR-183555	p 68	N89-17981	* #
NASA-CR-184604	p 19	N89-15476	* #
NASA-CR-184662	p 37	N89-15444	* #
NASA-CR-184683	p 28	N89-18973	* #
NASA-CR-184764	p 19	N89-16207	* #
NASA-CR-184805	p 47	N89-19102	* #
NASA-TM-100718	p 67	N89-16205	* #
NASA-TM-100720	p 75	N89-19729	* #
NASA-TM-101042	p 8	N89-17339	* #
NRL-MR-6259	p 37	N89-15309	#
OCS/MMS-87/0071-VOL-1	p 37	N89-17357	#
OCS/MMS-87/0071-VOL-2	p 37	N89-17358	#
OH-30	p 49	N89-17340	#
PB88-226048	p 37	N89-17357	#
PB88-226055	p 37	N89-17358	#
PNL-SA-15073	p 57	N89-17375	#
REPT-2021	p 16	N89-19735	#
REPT-89B00065	p 67	N89-16205	* #
REPT-89B00065	p 75	N89-19729	* #
SPIE-925	p 33	A89-27976	
UCRL-99730	p 57	N89-18204	#
USGS-OPEN-FILE-REPT-87-315	p 24	N89-16208	#
WMO-704	p 49	N89-17340	#
A-88309	p 8	N89-17339	* #
AD-A199536	p 37	N89-15309	#
AD-A200591	p 67	N89-16202	#
AD-A200958	p 25	N89-17933	#
AD-A201915	p 47	N89-19792	#
AD-A202220	p 20	N89-19731	#
AD-A202252	p 75	N89-19475	#
AFGL-TR-88-0204	p 25	N89-17933	#
AIAA PAPER 89-0817	p 54	A89-25595	* #
ARO-22851.1-GS	p 75	N89-19475	#
BCRS-87-18	p 52	N89-19732	#
BCRS-88-01	p 61	N89-19733	#
BCRS-88-03	p 16	N89-19734	#
BCRS-88-04	p 16	N89-19735	#
B8821606	p 19	N89-17371	#
CONF-8710161-2	p 57	N89-17375	#
CONF-8809220-1	p 50	N89-17932	#
CONF-8809220-2	p 67	N89-17931	#
CONF-8810243-1	p 57	N89-16204	#
DE89-001749	p 57	N89-17375	#
DE89-002872	p 57	N89-16204	#
DE89-004881	p 67	N89-17931	#
DE89-004882	p 50	N89-17932	#
DE89-005937	p 47	N89-18972	#
DFVLR-FB-85-49	p 57	N89-15442	#
DOE/ER-0402	p 47	N89-18972	#
DP-MS-88-152	p 50	N89-17932	#
DP-MS-88-153	p 67	N89-17931	#
ESA-CR(P)-2699	p 75	N89-19483	#
ESA-SP-284-VOL-2	p 69	N89-18836	#
ESA-SP-284-VOL-3	p 68	N89-18704	#
ESA-TT-975	p 57	N89-15442	#
ETN-89-92880	p 49	N89-17340	#
ETN-89-93243	p 69	N89-18836	#
ETN-89-93244	p 68	N89-18704	#
ETN-89-93326	p 19	N89-17371	#
ETN-89-93629	p 57	N89-15442	#
ETN-89-93711	p 47	N89-19793	#
ETN-89-93778	p 20	N89-17935	#
ETN-89-93872	p 52	N89-19732	#

# ACCESSION NUMBER INDEX

## Typical Accession Number Index Listing



Listings in this index are arranged alphanumerically by accession number. The page number listed to the right indicates the page on which the citation is located. An asterisk (\*) indicates that the item is a NASA report. A pound sign (#) indicates that the item is available on microfiche.

A89-20751	#	p 76	A89-20807	#	p 53	A89-22593	p	30	A89-28290	p	34	A89-32337	p	57
A89-20752	#	p 1	A89-20808	#	p 21	A89-22594	p	31	A89-28305	p	34	A89-32338	*	p 49
A89-20753	#	p 1	A89-20809	#	p 2	A89-22596	p	31	A89-28329	p	65	A89-32432	*	p 7
A89-20754	#	p 1	A89-20810	#	p 29	A89-22597	#	p 31	A89-28364	#	p 5	A89-32434	p	37
A89-20755	#	p 1	A89-20811	#	p 54	A89-22598	p	31	A89-28365	#	p 34			
A89-20756	#	p 1	A89-20812	#	p 54	A89-22622	#	p 62	A89-29064	p	55	N89-15309	#	p 37
A89-20757	#	p 1	A89-20813	#	p 17	A89-22632	p	22	A89-29066	p	55	N89-15439	#	p 23
A89-20758	#	p 1	A89-20814	#	p 2	A89-22639	#	p 19	A89-29070	p	65	N89-15440	#	p 57
A89-20759	#	p 1	A89-20815	#	p 2	A89-22647	*	p 22	A89-29073	p	56	N89-15442	#	p 57
A89-20760	#	p 2	A89-20816	#	p 54	A89-22649	*	p 54	A89-29074	p	56	N89-15444	#	p 37
A89-20761	#	p 2	A89-20817	#	p 21	A89-22728	p	3	A89-29075	p	34	N89-15446	#	p 24
A89-20762	#	p 2	A89-20818	#	p 48	A89-22876	*	p 31	A89-29301	*	p 23	N89-15447	#	p 24
A89-20763	#	p 2	A89-20819	#	p 2	A89-22877	*	p 22	A89-29371	#	p 18	N89-15459	#	p 67
A89-20764	#	p 52	A89-20820	#	p 21	A89-23431	*	p 3	A89-29372	#	p 65	N89-15476	#	p 19
A89-20765	#	p 52	A89-20821	#	p 54	A89-23433	p	31	A89-29373	#	p 5	N89-16199	#	p 24
A89-20766	#	p 16	A89-20822	#	p 3	A89-23438	*	p 31	A89-29374	#	p 5	N89-16202	#	p 67
A89-20767	#	p 52	A89-20823	#	p 21	A89-23464	*	p 62	A89-29375	#	p 65	N89-16204	#	p 57
A89-20768	#	p 48	A89-20824	#	p 17	A89-23590	p	32	A89-29409	*	p 5	N89-16205	#	p 67
A89-20769	#	p 2	A89-20825	#	p 21	A89-23645	p	54	A89-29410	p	5	N89-16207	#	p 19
A89-20770	#	p 48	A89-20826	#	p 3	A89-23646	p	32	A89-29411	p	6	N89-16208	#	p 24
A89-20771	#	p 48	A89-20827	#	p 21	A89-23663	p	3	A89-29412	p	6	N89-16886	#	p 67
A89-20772	#	p 48	A89-20828	#	p 21	A89-24022	p	62	A89-29415	p	6	N89-16887	#	p 67
A89-20773	#	p 2	A89-20829	#	p 21	A89-24442	#	p 19	A89-29433	p	65	N89-17339	#	p 8
A89-20774	#	p 48	A89-20923	p	3	A89-24649	p	48	A89-29435	p	65	N89-17340	#	p 49
A89-20775	#	p 52	A89-20925	p	29	A89-24651	#	p 17	A89-29436	p	65	N89-17357	#	p 37
A89-20776	#	p 48	A89-21249	p	54	A89-24849	p	18	A89-29437	p	18	N89-17358	#	p 37
A89-20777	#	p 48	A89-21250	p	17	A89-24872	*	p 32	A89-29726	p	35	N89-17371	#	p 19
A89-20778	#	p 48	A89-21397	p	76	A89-24873	*	p 4	A89-29729	p	35	N89-17375	#	p 57
A89-20779	#	p 20	A89-21410	p	62	A89-24875	#	p 32	A89-29730	p	35	N89-17414	#	p 57
A89-20780	#	p 20	A89-21612	p	3	A89-25595	#	p 54	A89-29731	p	35	N89-17910	#	p 24
A89-20781	#	p 20	A89-21740	*	p 3	A89-26178	p	62	A89-29732	p	35	N89-17915	#	p 25
A89-20782	#	p 52	A89-21798	p	29	A89-26181	p	32	A89-29763	#	p 35	N89-17922	#	p 58
A89-20783	#	p 20	A89-21892	*	p 17	A89-26397	#	p 22	A89-30019	p	35	N89-17930	#	p 8
A89-20784	#	p 20	A89-21931	p	17	A89-26398	#	p 62	A89-30114	p	35	N89-17931	#	p 67
A89-20785	#	p 28	A89-22000	*	p 29	A89-26399	#	p 63	A89-30116	p	23	N89-17932	#	p 50
A89-20786	#	p 28	A89-22066	p	17	A89-26438	*	p 32	A89-30118	p	23	N89-17933	#	p 25
A89-20787	#	p 28	A89-22210	p	29	A89-26442	p	32	A89-30119	p	23	N89-17935	#	p 20
A89-20788	#	p 28	A89-22213	p	17	A89-26443	p	33	A89-30120	p	36	N89-17981	#	p 68
A89-20789	#	p 29	A89-22214	p	62	A89-26444	p	33	A89-30121	p	49	N89-18074	#	p 68
A89-20790	#	p 52	A89-22215	p	21	A89-26843	*	p 63	A89-30122	p	36	N89-18075	#	p 58
A89-20791	#	p 52	A89-22216	p	22	A89-26844	#	p 33	A89-30123	p	56	N89-18076	#	p 37
A89-20792	#	p 17	A89-22217	p	22	A89-26846	p	33	A89-30239	p	56	N89-18077	#	p 37
A89-20794	#	p 52	A89-22218	p	22	A89-27630	p	18	A89-30252	p	49	N89-18078	#	p 8
A89-20795	#	p 61	A89-22221	p	3	A89-27753	*	p 63	A89-30257	p	36	N89-18079	#	p 8
A89-20796	*	p 53	A89-22223	p	22	A89-27779	*	p 63	A89-30258	p	36	N89-18100	#	p 58
A89-20797	#	p 53	A89-22224	p	30	A89-27781	p	4	A89-30259	p	36	N89-18111	#	p 58
A89-20798	#	p 53	A89-22225	p	62	A89-27783	p	54	A89-30260	p	36	N89-18112	#	p 8
A89-20799	#	p 53	A89-22249	p	3	A89-27785	p	18	A89-30261	p	49	N89-18113	#	p 8
A89-20800	#	p 53	A89-22316	p	19	A89-27786	p	18	A89-30262	p	6	N89-18114	#	p 8
A89-20801	#	p 53	A89-22583	p	30	A89-27788	p	18	A89-30263	p	18	N89-18115	#	p 9
A89-20802	#	p 2	A89-22584	p	30	A89-27789	*	p 55	A89-30264	*	p 6	N89-18116	#	p 9
A89-20803	#	p 29	A89-22585	*	p 30	A89-27933	p	63	A89-30265	p	6	N89-18117	#	p 38
A89-20804	#	p 29	A89-22586	p	30	A89-27934	p	63	A89-30266	*	p 6	N89-18118	#	p 38
A89-20805	#	p 29	A89-22587	*	p 30	A89-27935	p	63	A89-30267	p	6	N89-18119	#	p 38
A89-20806	#	p 53	A89-22592	p	30	A89-27937	p	55	A89-30268	p	7	N89-18120	#	p 38
						A89-27938	p	55	A89-30269	p	7	N89-18121	#	p 38
						A89-27941	p	33	A89-30270	p	7	N89-18122	#	p 38
						A89-27942	p	4	A89-30271	*	p 23	N89-18123	#	p 39
						A89-27944	p	4	A89-30900	p	38	N89-18124	#	p 9
						A89-27946	p	49	A89-30967	p	66	N89-18125	#	p 9
						A89-27976	p	33	A89-31020	p	66	N89-18126	#	p 9
						A89-27977	p	64	A89-31560	p	76	N89-18127	#	p 9
						A89-27980	p	33	A89-31755	p	23	N89-18128	#	p 10
						A89-27990	*	p 64	A89-31887	p	23	N89-18129	#	p 10
						A89-27991	*	p 64	A89-31888	p	58	N89-18130	#	p 10
						A89-27993	p	64	A89-31889	p	56	N89-18131	#	p 10
						A89-27995	p	34	A89-31890	p	7	N89-18132	#	p 10
						A89-27996	p	64	A89-31891	p	18	N89-18133	#	p 50
						A89-28003	p	34	A89-31892	p	7	N89-18134	#	p 39
						A89-28003	*	p 49	A89-31893	p	7	N89-18135	#	p 50
						A89-28034	p	34	A89-31894	p	7	N89-18136	#	p 39
						A89-28035	p	4	A89-31943	*	p 66	N89-18137	#	p 39
						A89-28036	p	55	A89-31946	*	p 66	N89-18138	#	p 39
						A89-28037	p	55	A89-31947	*	p 66	N89-18139	#	p 39
						A89-28038	p	64	A89-31948	*	p 66	N89-18140	#	p 50
						A89-28039	p	64	A89-31949	*	p 66	N89-18141	#	p 39
						A89-28126	p	23	A89-32108	p	36	N89-18142	#	p 39
						A89-28127	*	p 4	A89-32110	p	7	N89-18143	#	p 40
						A89-28128	*	p 4	A89-32334	p	66	N89-18144	#	p 40
						A89-28129	p	5	A89-32335	*	p 57	N89-18145	#	p 40
						A89-28130	p	5	A89-32336	p	7	N89-18146	#	p 40
						A89-28131	p	5				N89-18147	#	p 40
												N89-18148	#	p 76

N89-18749 #	p 40	N89-18882 #	p 13
N89-18750 #	p 76	N89-18883 #	p 13
N89-18751 #	p 68	N89-18884 #	p 71
N89-18752 #	p 76	N89-18885 #	p 71
N89-18753 #	p 68	N89-18886 #	p 71
N89-18754 #	p 68	N89-18887 #	p 71
N89-18755 #	p 68	N89-18888 #	p 71
N89-18757 #	p 69	N89-18889 #	p 71
N89-18759 #	p 58	N89-18890 #	p 71
N89-18760 #	p 58	N89-18891 #	p 71
N89-18761 #	p 58	N89-18892 #	p 72
N89-18763 #	p 59	N89-18893 #	p 72
N89-18764 #	p 59	N89-18894 #	p 60
N89-18765 #	p 41	N89-18895 #	p 14
N89-18766 #	p 41	N89-18896 #	p 60
N89-18768 #	p 50	N89-18897 #	p 60
N89-18769 #	p 51	N89-18898 #	p 61
N89-18770 #	p 51	N89-18899 #	p 14
N89-18772 #	p 10	N89-18900 #	p 61
N89-18773 #	p 11	N89-18901 #	p 14
N89-18774 #	p 11	N89-18902 #	p 14
N89-18775 #	p 51	N89-18905 * #	p 72
N89-18776 #	p 59	N89-18906 #	p 72
N89-18777 #	p 59	N89-18908 #	p 72
N89-18781 #	p 11	N89-18909 #	p 45
N89-18782 * #	p 41	N89-18910 #	p 45
N89-18783 #	p 41	N89-18911 #	p 72
N89-18784 #	p 41	N89-18913 #	p 73
N89-18785 #	p 41	N89-18914 #	p 73
N89-18786 #	p 41	N89-18917 #	p 14
N89-18787 #	p 42	N89-18918 * #	p 14
N89-18789 #	p 42	N89-18919 * #	p 15
N89-18790 #	p 59	N89-18920 #	p 15
N89-18791 #	p 25	N89-18921 * #	p 73
N89-18792 #	p 25	N89-18923 #	p 73
N89-18793 #	p 25	N89-18924 #	p 73
N89-18794 #	p 26	N89-18925 #	p 73
N89-18796 #	p 26	N89-18926 #	p 73
N89-18797 * #	p 42	N89-18928 #	p 74
N89-18799 #	p 42	N89-18929 #	p 27
N89-18800 * #	p 42	N89-18930 #	p 27
N89-18801 #	p 42	N89-18931 * #	p 27
N89-18802 #	p 43	N89-18932 #	p 27
N89-18803 #	p 43	N89-18933 #	p 27
N89-18804 #	p 43	N89-18934 #	p 27
N89-18805 #	p 43	N89-18935 * #	p 28
N89-18813 #	p 69	N89-18936 #	p 28
N89-18816 * #	p 77	N89-18937 #	p 51
N89-18817 #	p 43	N89-18938 #	p 45
N89-18818 #	p 26	N89-18939 #	p 46
N89-18821 #	p 59	N89-18940 #	p 46
N89-18822 #	p 11	N89-18941 #	p 46
N89-18824 #	p 60	N89-18942 #	p 46
N89-18825 #	p 11	N89-18943 * #	p 46
N89-18826 #	p 69	N89-18944 #	p 46
N89-18828 #	p 69	N89-18945 #	p 46
N89-18831 #	p 60	N89-18946 #	p 47
N89-18832 #	p 51	N89-18947 #	p 15
N89-18833 * #	p 19	N89-18948 #	p 15
N89-18836 #	p 69	N89-18949 #	p 15
N89-18837 #	p 43	N89-18950 #	p 15
N89-18838 #	p 43	N89-18951 #	p 16
N89-18839 #	p 44	N89-18952 #	p 74
N89-18840 #	p 44	N89-18954 #	p 74
N89-18841 #	p 44	N89-18956 #	p 61
N89-18842 #	p 69	N89-18957 #	p 61
N89-18843 #	p 11	N89-18958 #	p 74
N89-18844 #	p 12	N89-18960 #	p 74
N89-18845 * #	p 12	N89-18961 #	p 16
N89-18846 * #	p 12	N89-18964 #	p 74
N89-18848 #	p 12	N89-18966 #	p 16
N89-18849 #	p 60	N89-18972 #	p 47
N89-18850 #	p 69	N89-18973 * #	p 28
N89-18851 * #	p 70	N89-18984	p 51
N89-18853 #	p 70	N89-19039	p 74
N89-18854 #	p 70	N89-19079	p 75
N89-18855 #	p 70	N89-19102 * #	p 47
N89-18856 #	p 70	N89-19475 #	p 75
N89-18857 #	p 12	N89-19483 #	p 75
N89-18859 #	p 26	N89-19717	p 75
N89-18860 #	p 26	N89-19729 * #	p 75
N89-18861 #	p 26	N89-19731 #	p 20
N89-18862 #	p 12	N89-19732 #	p 52
N89-18863 #	p 27	N89-19733 #	p 61
N89-18869 #	p 44	N89-19734 #	p 16
N89-18870 #	p 44	N89-19735 #	p 16
N89-18871 #	p 44	N89-19736 #	p 20
N89-18872 #	p 45	N89-19792 #	p 47
N89-18874 #	p 45	N89-19793 #	p 47
N89-18875 #	p 45	N89-19868 * #	p 76
N89-18876 #	p 13		
N89-18877 #	p 70		
N89-18878 #	p 13		
N89-18879 #	p 13		
N89-18880 #	p 13		
N89-18881 #	p 13		

# AVAILABILITY OF CITED PUBLICATIONS

## IAA ENTRIES (A89-10000 Series)

Publications announced in *IAA* are available from the AIAA Technical Information Service as follows: Paper copies of accessions are available at \$10.00 per document (up to 50 pages), additional pages \$0.25 each. Microfiche<sup>(1)</sup> of documents announced in *IAA* are available at the rate of \$4.00 per microfiche on demand. Standing order microfiche are available at the rate of \$1.45 per microfiche for *IAA* source documents and \$1.75 per microfiche for AIAA meeting papers.

Minimum air-mail postage to foreign countries is \$2.50. All foreign orders are shipped on payment of pro-forma invoices.

All inquiries and requests should be addressed to: Technical Information Service, American Institute of Aeronautics and Astronautics, 555 West 57th Street, New York, NY 10019. Please refer to the accession number when requesting publications.

## STAR ENTRIES (N89-10000 Series)

One or more sources from which a document announced in *STAR* is available to the public is ordinarily given on the last line of the citation. The most commonly indicated sources and their acronyms or abbreviations are listed below. If the publication is available from a source other than those listed, the publisher and his address will be displayed on the availability line or in combination with the corporate source line.

Avail: NTIS. Sold by the National Technical Information Service. Prices for hard copy (HC) and microfiche (MF) are indicated by a price code preceded by the letters HC or MF in the *STAR* citation. Current values for the price codes are given in the tables on NTIS PRICE SCHEDULES.

Documents on microfiche are designated by a pound sign (#) following the accession number. The pound sign is used without regard to the source or quality of the microfiche.

Initially distributed microfiche under the NTIS SRIM (Selected Research in Microfiche) is available at greatly reduced unit prices. For this service and for information concerning subscription to NASA printed reports, consult the NTIS Subscription Section, Springfield, Va. 22161.

NOTE ON ORDERING DOCUMENTS: When ordering NASA publications (those followed by the \* symbol), use the N accession number. NASA patent applications (only the specifications are offered) should be ordered by the US-Patent-Appl-SN number. Non-NASA publications (no asterisk) should be ordered by the AD, PB, or other *report number* shown on the last line of the citation, not by the N accession number. It is also advisable to cite the title and other bibliographic identification.

Avail: SOD (or GPO). Sold by the Superintendent of Documents, U.S. Government Printing Office, in hard copy. The current price and order number are given following the availability line. (NTIS will fill microfiche requests, as indicated above, for those documents identified by a # symbol.)

(1) A microfiche is a transparent sheet of film, 105 by 148 mm in size containing as many as 60 to 98 pages of information reduced to micro images (not to exceed 26.1 reduction).

- Avail: BLL (formerly NLL): British Library Lending Division, Boston Spa, Wetherby, Yorkshire, England. Photocopies available from this organization at the price shown. (If none is given, inquiry should be addressed to the BLL.)
- Avail: DOE Depository Libraries. Organizations in U.S. cities and abroad that maintain collections of Department of Energy reports, usually in microfiche form, are listed in *Energy Research Abstracts*. Services available from the DOE and its depositories are described in a booklet, *DOE Technical Information Center - Its Functions and Services* (TID-4660), which may be obtained without charge from the DOE Technical Information Center.
- Avail: ESDU. Pricing information on specific data, computer programs, and details on ESDU topic categories can be obtained from ESDU International Ltd. Requesters in North America should use the Virginia address while all other requesters should use the London address, both of which are on the page titled ADDRESSES OF ORGANIZATIONS.
- Avail: Fachinformationszentrum, Karlsruhe. Sold by the Fachinformationszentrum Energie, Physik, Mathematik GMBH, Eggenstein Leopoldshafen, Federal Republic of Germany, at the price shown in deutschmarks (DM).
- Avail: HMSO. Publications of Her Majesty's Stationery Office are sold in the U.S. by Pendragon House, Inc. (PHI), Redwood City, California. The U.S. price (including a service and mailing charge) is given, or a conversion table may be obtained from PHI.
- Avail: NASA Public Document Rooms. Documents so indicated may be examined at or purchased from the National Aeronautics and Space Administration, Public Documents Room (Room 126), 600 Independence Ave., S.W., Washington, D.C. 20546, or public document rooms located at each of the NASA research centers, the NASA Space Technology Laboratories, and the NASA Pasadena Office at the Jet Propulsion Laboratory.
- Avail: Univ. Microfilms. Documents so indicated are dissertations selected from *Dissertation Abstracts* and are sold by University Microfilms as xerographic copy (HC) and microfilm. All requests should cite the author and the Order Number as they appear in the citation.
- Avail: US Patent and Trademark Office. Sold by Commissioner of Patents and Trademarks, U.S. Patent and Trademark Office, at the standard price of \$1.50 each, postage free. (See discussion of NASA patents and patent applications below.)
- Avail: (US Sales Only). These foreign documents are available to users within the United States from the National Technical Information Service (NTIS). They are available to users outside the United States through the International Nuclear Information Service (INIS) representative in their country, or by applying directly to the issuing organization.
- Avail: USGS. Originals of many reports from the U.S. Geological Survey, which may contain color illustrations, or otherwise may not have the quality of illustrations preserved in the microfiche or facsimile reproduction, may be examined by the public at the libraries of the USGS field offices whose addresses are listed in this Introduction. The libraries may be queried concerning the availability of specific documents and the possible utilization of local copying services, such as color reproduction.
- Avail: Issuing Activity, or Corporate Author, or no indication of availability. Inquiries as to the availability of these documents should be addressed to the organization shown in the citation as the corporate author of the document.



## **PUBLIC COLLECTIONS OF NASA DOCUMENTS**

**DOMESTIC:** NASA and NASA-sponsored documents and a large number of aerospace publications are available to the public for reference purposes at the library maintained by the American Institute of Aeronautics and Astronautics, Technical Information Service, 555 West 57th Street, 12th Floor, New York, New York 10019.

**EUROPEAN:** An extensive collection of NASA and NASA-sponsored publications is maintained by the British Library Lending Division, Boston Spa, Wetherby, Yorkshire, England for public access. The British Library Lending Division also has available many of the non-NASA publications cited in *STAR*. European requesters may purchase facsimile copy or microfiche of NASA and NASA-sponsored documents, those identified by both the symbols # and \* from ESA – Information Retrieval Service European Space Agency, 8-10 rue Mario-Nikis, 75738 CEDEX 15, France.

### **FEDERAL DEPOSITORY LIBRARY PROGRAM**

In order to provide the general public with greater access to U.S. Government publications, Congress established the Federal Depository Library Program under the Government Printing Office (GPO), with 50 regional depositories responsible for permanent retention of material, inter-library loan, and reference services. At least one copy of nearly every NASA and NASA-sponsored publication, either in printed or microfiche format, is received and retained by the 50 regional depositories. A list of the regional GPO libraries, arranged alphabetically by state, appears on the inside back cover. These libraries are *not* sales outlets. A local library can contact a Regional Depository to help locate specific reports, or direct contact may be made by an individual.

### **STANDING ORDER SUBSCRIPTIONS**

NASA SP-7041 and its supplements are available from the National Technical Information Service (NTIS) on standing order subscription as PB 89-903800 at the price of \$15.50 domestic and \$31.00 foreign. Standing order subscriptions do not terminate at the end of a year, as do regular subscriptions, but continue indefinitely unless specifically terminated by the subscriber.

## ADDRESSES OF ORGANIZATIONS

American Institute of Aeronautics and  
Astronautics  
Technical Information Service  
555 West 57th Street, 12th Floor  
New York, New York 10019

British Library Lending Division,  
Boston Spa, Wetherby, Yorkshire,  
England

Commissioner of Patents and  
Trademarks  
U.S. Patent and Trademark Office  
Washington, D.C. 20231

Department of Energy  
Technical Information Center  
P.O. Box 62  
Oak Ridge, Tennessee 37830

ESA-Information Retrieval Service  
ESRIN  
Via Galileo Galilei  
00044 Frascati (Rome) Italy

ESDU International  
P.O. Box 1633  
Manassas, Virginia 22110

ESDU International, Ltd.  
251-259 Regent Street  
London, W1R 7AD, England

Fachinformationszentrum Energie, Physik,  
Mathematik GMBH  
7514 Eggenstein Leopoldshafen  
Federal Republic of Germany

Her Majesty's Stationery Office  
P.O. Box 569, S.E. 1  
London, England

NASA Scientific and Technical Information  
Facility  
P.O. Box 8757  
B.W.I. Airport, Maryland 21240

National Aeronautics and Space  
Administration  
Scientific and Technical Information  
Division (NTT)  
Washington, D.C. 20546

National Technical Information Service  
5285 Port Royal Road  
Springfield, Virginia 22161

Pendragon House, Inc.  
899 Broadway Avenue  
Redwood City, California 94063

Superintendent of Documents  
U.S. Government Printing Office  
Washington, D.C. 20402

University Microfilms  
A Xerox Company  
300 North Zeeb Road  
Ann Arbor, Michigan 48106

University Microfilms, Ltd.  
Tylers Green  
London, England

U.S. Geological Survey Library  
National Center - MS 950  
12201 Sunrise Valley Drive  
Reston, Virginia 22092

U.S. Geological Survey Library  
2255 North Gemini Drive  
Flagstaff, Arizona 86001

U.S. Geological Survey  
345 Middlefield Road  
Menlo Park, California 94025

U.S. Geological Survey Library  
Box 25046  
Denver Federal Center, MS914  
Denver, Colorado 80225

# NTIS PRICE SCHEDULES

(Effective January 1, 1989)

## Schedule A STANDARD PRICE DOCUMENTS AND MICROFICHE

PRICE CODE	NORTH AMERICAN PRICE	FOREIGN PRICE
A01	\$ 6.95	\$13.90
A02	10.95	21.90
A03	13.95	27.90
A04-A05	15.95	31.90
A06-A09	21.95	43.90
A10-A13	28.95	57.90
A14-A17	36.95	73.90
A18-A21	42.95	85.90
A22-A25	49.95	99.90
A99	.	.
NO1	55.00	70.00
NO2	55.00	80.00

## Schedule E EXCEPTION PRICE DOCUMENTS AND MICROFICHE

PRICE CODE	NORTH AMERICAN PRICE	FOREIGN PRICE
E01	\$ 9.00	18.00
E02	11.50	23.00
E03	13.00	26.00
E04	15.50	31.00
E05	17.50	35.00
E06	20.50	41.00
E07	23.00	46.00
E08	25.50	51.00
E09	28.00	56.00
E10	31.00	62.00
E11	33.50	67.00
E12	36.50	73.00
E13	39.00	78.00
E14	42.50	85.00
E15	46.00	92.00
E16	50.50	101.00
E17	54.50	109.00
E18	59.00	118.00
E19	65.50	131.00
E20	76.00	152.00
E99	.	.

\*Contact NTIS for price quote.

### IMPORTANT NOTICE

NTIS Shipping and Handling Charges

U.S., Canada, Mexico — ADD \$3.00 per TOTAL ORDER

All Other Countries — ADD \$4.00 per TOTAL ORDER

Exceptions — Does NOT apply to:

ORDERS REQUESTING NTIS RUSH HANDLING  
ORDERS FOR SUBSCRIPTION OR STANDING ORDER PRODUCTS ONLY

NOTE: Each additional delivery address on an order  
requires a separate shipping and handling charge.

1. Report No. NASA SP-7041 (62)		2. Government Accession No.		3. Recipient's Catalog No.	
4. Title and Subtitle EARTH RESOURCES A Continuing Bibliography with Indexes (Issue 62)				5. Report Date July, 1989	
				6. Performing Organization Code	
7. Author(s)				8. Performing Organization Report No.	
9. Performing Organization Name and Address National Aeronautics and Space Administration Washington, DC 20546				10. Work Unit No.	
				11. Contract or Grant No.	
				13. Type of Report and Period Covered	
12. Sponsoring Agency Name and Address				14. Sponsoring Agency Code	
15. Supplementary Notes					
16. Abstract This bibliography lists 544 reports, articles and other documents introduced into the NASA scientific and technical information system between April 1 and June 30, 1989. Emphasis is placed on the use of remote sensing and geophysical instrumentation in spacecraft and aircraft to survey and inventory natural resources and urban areas. Subject matter is grouped according to agriculture and forestry, environmental changes and cultural resources, geodesy and cartography, geology and mineral resources, hydrology and water management, data processing and distribution systems, instrumentation and sensors, and economic analysis.					
17. Key Words (Suggested by Authors(s)) Bibliographies Earth Resources Remote Sensors			18. Distribution Statement Unclassified - Unlimited		
19. Security Classif. (of this report) Unclassified		20. Security Classif. (of this page) Unclassified		21. No. of Pages 148	22. Price * A07/HC

\*For sale by the National Technical Information Service, Springfield, Virginia 22161

# FEDERAL REGIONAL DEPOSITORY LIBRARIES

## **ALABAMA**

### **AUBURN UNIV. AT MONTGOMERY LIBRARY**

Documents Department  
Montgomery, AL 36193  
(205) 271-9650

### **UNIV. OF ALABAMA LIBRARY**

Documents Dept.-Box S  
University, AL 35486  
(205) 348-6046

## **ARIZONA**

### **DEPT. OF LIBRARY, ARCHIVES AND PUBLIC RECORDS**

Third Floor—State Cap  
1700 West Washington  
Phoenix, AZ 85007  
(602) 255-4121

### **UNIVERSITY OF ARIZONA LIB.**

Government Documents Dept.  
Tucson, AZ 85721  
(602) 621-6433

## **ARKANSAS**

### **ARKANSAS STATE LIBRARY**

One Capitol Mall  
Little Rock, AR 72201  
(501) 371-2326

## **CALIFORNIA**

### **CALIFORNIA STATE LIBRARY**

Govt. Publications Section  
P.O. Box 2037  
Sacramento, CA 95809  
(916) 324-4863

## **COLORADO**

### **UNIV. OF COLORADO LIB.**

Government Pub. Division  
Campus Box 184  
Boulder, CO 80309  
(303) 492-8834

### **DENVER PUBLIC LIBRARY**

Govt. Pub. Department  
1357 Broadway  
Denver, CO 80203  
(303) 571-2131

## **CONNECTICUT**

### **CONNECTICUT STATE LIBRARY**

Government Documents Unit  
231 Capitol Avenue  
Hartford, CT 06106  
(203) 566-7029

## **FLORIDA**

### **UNIV. OF FLORIDA LIBRARIES**

Library West  
Documents Department  
Gainesville, FL 32611  
(904) 392-0367

## **GEORGIA**

### **UNIV. OF GEORGIA LIBRARIES**

Government Reference Dept.  
Athens, GA 30602  
(404) 542-8949

## **HAWAII**

### **UNIV. OF HAWAII LIBRARY**

Govt. Documents Collection  
2550 The Mall  
Honolulu, HI 96822  
(808) 948-8230

## **IDAHO**

### **UNIV. OF IDAHO LIBRARY**

Documents Section  
Moscow, ID 83843  
(208) 885-6344

## **ILLINOIS**

### **ILLINOIS STATE LIBRARY**

Information Services Branch  
Centennial Building  
Springfield, IL 62756  
(217) 782-5185

## **INDIANA**

### **INDIANA STATE LIBRARY**

Serials Documents Section  
140 North Senate Avenue  
Indianapolis, IN 46204  
(317) 232-3686

## **IOWA**

### **UNIV. OF IOWA LIBRARIES**

Govt. Documents Department  
Iowa City, IA 52242  
(319) 353-3318

## **KANSAS**

### **UNIVERSITY OF KANSAS**

Doc. Collect—Spencer Lib.  
Lawrence, KS 66045-2800  
(913) 864-4662

## **KENTUCKY**

### **UNIV. OF KENTUCKY LIBRARIES**

Govt. Pub. Department  
Lexington, KY 40506-0039  
(606) 257-3139

## **LOUISIANA**

### **LOUISIANA STATE UNIVERSITY**

Middleton Library  
Govt. Docs. Dept.  
Baton Rouge, LA 70803  
(504) 388-2570

### **LOUISIANA TECHNICAL UNIV. LIBRARY**

Documents Department  
Ruston, LA 71272-0046  
(318) 257-4962

## **MAINE**

### **UNIVERSITY OF MAINE**

Raymond H. Fogler Library  
Tri-State Regional Documents  
Depository  
Orono, ME 04469  
(207) 581-1680

## **MARYLAND**

### **UNIVERSITY OF MARYLAND**

McKeldin Lib.—Doc. Div.  
College Park, MD 20742  
(301) 454-3034

## **MASSACHUSETTS**

### **BOSTON PUBLIC LIBRARY**

Government Docs. Dept.  
Boston, MA 02117  
(617) 536-5400 ext.226

## **MICHIGAN**

### **DETROIT PUBLIC LIBRARY**

Sociology Department  
5201 Woodward Avenue  
Detroit, MI 48202-4093  
(313) 833-1409

### **MICHIGAN STATE LIBRARY**

P.O. Box 30007  
Lansing, MI 48909  
(517) 373-1593

## **MINNESOTA**

### **UNIVERSITY OF MINNESOTA**

Government Pubs. Division  
409 Wilson Library  
309 19th Avenue South  
Minneapolis, MN 55455  
(612) 373-7870

## **MISSISSIPPI**

### **UNIV. OF MISSISSIPPI LIB.**

Documents Department  
University, MS 38677  
(601) 232-5857

## **MONTANA**

### **UNIV. OF MONTANA**

Mansfield Library  
Documents Division  
Missoula, MT 59812  
(406) 243-6700

## **NEBRASKA**

### **UNIVERSITY OF NEBRASKA - LINCOLN**

Love Library  
Documents Department  
Lincoln, NE 68588-0410  
(402) 472-2562

## **NEVADA**

### **UNIVERSITY OF NEVADA LIB.**

Govt. Pub. Department  
Reno, NV 89557-0044  
(702) 784-6579

## **NEW JERSEY**

### **NEWARK PUBLIC LIBRARY**

5 Washington Street  
Newark, NJ 07101-0630  
(201) 733-7812

## **NEW MEXICO**

### **UNIVERSITY OF NEW MEXICO**

Zimmerman Library  
Government Pub. Dept.  
Albuquerque, NM 87131  
(505) 277-5441

### **NEW MEXICO STATE LIBRARY**

Reference Department  
325 Don Gaspar Avenue  
Santa Fe, NM 87503  
(505) 827-3826

## **NEW YORK**

### **NEW YORK STATE LIBRARY**

Empire State Plaza  
Albany, NY 12230  
(518) 474-5563

## **NORTH CAROLINA**

### **UNIVERSITY OF NORTH CAROLINA AT CHAPEL HILL**

Davis Library  
BA/SS Documents Division  
Chapel Hill, NC 27515  
(919) 962-1151

## **NORTH DAKOTA**

### **UNIVERSITY OF NORTH DAKOTA**

Chester Fritz Library  
Documents Department  
Grand Forks, ND 58202  
(701) 777-4629  
In cooperation with North  
Dakota State Univ. Library

## **OHIO**

### **STATE LIBRARY OF OHIO**

Documents Department  
65 South Front Street  
Columbus, OH 43266-0334  
(614) 462-7051

## **OKLAHOMA**

### **OKLAHOMA DEPT. OF LIB.**

Government Documents  
200 NE 18th Street  
Oklahoma City, OK 73105  
(405) 521-2502, ext. 252

### **OKLAHOMA STATE UNIV. LIB.**

Documents Department  
Stillwater, OK 74078  
(405) 624-6546

## **OREGON**

### **PORTLAND STATE UNIV. LIB.**

Documents Department  
P.O. Box 1151  
Portland, OR 97207  
(503) 229-3673

## **PENNSYLVANIA**

### **STATE LIBRARY OF PENN.**

Government Pub. Section  
P.O. Box 1601  
Harrisburg, PA 17105  
(717) 787-3752

## **TEXAS**

### **TEXAS STATE LIBRARY**

Public Services Department  
P.O. Box 12927—Cap Sta.  
Austin, TX 78711  
(512) 475-2996

### **TEXAS TECH. UNIV. LIBRARY**

Govt. Documents Department  
Lubbock, TX 79409  
(806) 742-2268

## **UTAH**

### **UTAH STATE UNIVERSITY**

Merrill Library, U.M.C. 30  
Logan, UT 84322  
(801) 750-2682

## **VIRGINIA**

### **UNIVERSITY OF VIRGINIA**

Alderman Lib.—Public Doc.  
Charlottesville, VA 22903-2498  
(804) 924-3133

## **WASHINGTON**

### **WASHINGTON STATE LIBRARY**

Documents Section  
Olympia, WA 98504  
(206) 753-4027

## **WEST VIRGINIA**

### **WEST VIRGINIA UNIV. LIB.**

Documents Department  
Morgantown, WV 26506-6069  
(304) 293-3640

## **WISCONSIN**

### **MILWAUKEE PUBLIC LIBRARY**

814 West Wisconsin Avenue  
Milwaukee, WI 53233  
(414) 278-3065

### **ST. HIST. LIB. OF WISCONSIN**

Government Pub. Section  
816 State Street  
Madison, WI 53706  
(608) 262-4347

## **WYOMING**

### **WYOMING STATE LIBRARY**

Supreme Ct. & Library Bld.  
Cheyenne, WY 82002  
(307) 777-5919